

ÉCOLE DOCTORALE DES SCIENCES CHIMIQUES

Institut de Chimie, UMR 7177

THÈSE présentée par :

Fabian SCHLIMPEN

soutenue le : **16 décembre 2022**

pour obtenir le grade de : **Docteur de l'université de Strasbourg**

Discipline/ Spécialité : **Chimie**

**Synthesis of Propargylamines and
Derivatives through Copper Catalysis
Using Modified Zeolites**

THÈSE dirigée par :

M. PALE Patrick

M. CHASSAING Stefan

Professeur, Université de Strasbourg

Maître de Conférences, Université de Strasbourg

RAPPORTEURS :

M^{me} GOMEZ SIMON Montserrat

M. PRESTAT Guillaume

Professeure, Université Toulouse III – Paul Sabatier

Professeur, Université Paris Cité

INVITEE :

M^{me} BENETEAU Valérie

Maître de Conférences, Université de Strasbourg

To all those who cared. Thank you!

Acknowledgements

J'exprime ma gratitude à Professeure Montserrat Gómez, ainsi qu'au Professeur Guillaume Prestat de l'honneur qu'ils m'ont fait en acceptant d'être rapporteurs de cette thèse.

Je remercie mes (co-)directeurs de thèse, Patrick Pale, Stefan Chassaing, et Valérie Bénéteau, qui m'ont reçu dans leur laboratoire pendant ces trois années et m'ont donné leur confiance à mener à bien ce projet de thèse. J'ai saisi l'autonomie et l'espace que vous m'avez laissé pour grandir et pour découvrir de nouveaux horizons en chimie et pour me constituer un projet professionnel diversifié.

Je tiens aussi à remercier les autres permanents du laboratoire. Merci particulièrement à Jean-Marc pour l'opportunité de contribuer à l'enseignement des TPs. Cela fut un grand plaisir et une expérience très enrichissante! Merci à Auré pour les bons conseils et de m'avoir fait découvrir un peu les polyoxométallates dopés à l'or. J'aurais bien voulu y consacrer plus de temps.

Je souhaite également diriger tous mes remerciements aux doctorants du laboratoire, notamment Romain, Robin W., Loïc, Mathieu, Robin H., Andrés, Eliot, Xiaohui, pour les riches discussions sur la chimie, le partage de connaissances, le partage de bières artisanales (merci Loïc et vive la GrosLam Beer !), le partage de rigolades mais aussi de stress, et pour votre soutien en général. Merci pour rendre le labo un lieu vivant et de travail. Je vous souhaite une bonne continuation, beaucoup de force et un bon démarrage au nouvel arrivant, Pierre.

Merci aussi aux stagiaires Eliot, Ismayil et Eliott pour leurs contributions à ces travaux de thèse. Et puis bien sûr, Tun, Ehrenmann, pour avoir réalisé ton projet de master à mes côtés. Dat war mat Ofstand déi beschten Zäit an der soss leider oft geploter Aarbecht! Elo ass et endlech eriver! Et huet mir riesen Spaass gemaach mat dir ze schaffen, ze laachen an ze grübelen. Sinn ganz frou dat mir mat eiser gemeinsamer Aarbecht eng Publikatioun gepackt hunn, op déi hunn ech mech opmanst gefreet. Merci och fir déng Opmonterung. Wënschen dir alles Guddes an dat mer eis geschwënn engkéier gesinn!

Merci également à Ludovik pour ces contributions précieuses, à Delphine et Marc, ainsi qu'aux divers services d'analyses pour leur disponibilité et serviabilité.

Ich möchte mich ebenfalls herzlich bei den Professoren, Dozenten, und Betreuern bedanken, die mich im Laufe meines Studiums besonders geprägt haben. Danke für Ihr Engagement und die großartige Arbeit mit der Sie sicher nicht nur mich begeistert haben. Die Liste ist vermutlich länger, dennoch muss man irgendwo beginnen. Vielen Dank an Prof. Dr. Thorsten Bach, Dr.

Stefan Breitenlechner, Prof. Dr. Lukas Hintermann, Prof. Dr. Tobias Gulder, Prof. Dr. Stéphane Vuilleumier, Prof. Dr. Rainer Schobert, Dr. Pit Losch und Dr. Fabian Kallmeier.

Je souhaite un chaleureux merci à ma « famille adoptive » les écologues et botanistes du Laboratoire Image Ville Environnement, Eloïse Lenormand, Marion Martinez-Arnould ! Guillaume Jacek, Laurent Hardion, Etienne Chanez, la famille Audrey Muratet & François Chiron, pour leur accueil pendant les pauses de midi à l'Institut de Botanique, les rigolades et sorties alsaciennes (merci les tartes flambées amor Guigues !), les discussions sur toutes les thématiques (même sur de la chimie !), et enfin pour leur grand soutien morale.

Al final, y lamentablemente demasiado corto. Sin embargo, estoy seguro de que aquí no hacen falta muchas palabras. Muchas gracias a mi familia y a Armando por el enorme apoyo y amor en cada momento. Os quiero mucho.

I also thank the French Ministry of Research for a Ph.D. fellowship.

Table of Contents

Abbreviations	1
Preface	5
Part One. State of the Art	7
Thesis Objectives: Green Synthesis and Derivatisation of Propargylamines Using Metal-Doped Zeolites	8
Chapter I – Propargylamines	10
1. <i>Introduction</i>	11
2. <i>Synthesis of Propargylamines</i>	13
2.1. Base-Catalysed Imine Alkynylation	16
2.2. Metal-Catalysed Imine Alkynylation	17
2.3. Metal-Catalysed Carbonyl-Amine-Alkyne Coupling Reactions.....	19
2.4. Copper-Catalysed Cross-Dehydrogenative Coupling of Tertiary Amines	21
2.5. Metal-Catalysed Hydroamination/Protonation/Alkyne Addition (HPA)	22
3. <i>Synthetic Applications of Propargylamines</i>	23
3.1. Synthesis of Allenes.....	23
3.2. Synthesis of Five-Membered Heterocycles	25
3.2.1. 1,2,3-Triazoles	25
3.2.2. Imidazoles.....	26
3.2.3. Oxazolidin-2-ones and Oxazol-2-ones	27
3.2.4. Tetramic Acids	30
3.2.5. Thiazolidin-2-ones	31
3.3. Synthesis of Six-Membered Heterocycles	32
3.3.1. Pyridines	32
3.3.2. 1,6-Dihydropyridines	32
3.3.3. Piperazines and 1,2,3,4-Tetrahydropyrazines	33
3.3.4. 4-Amino-4 <i>H</i> -Pyranes	34
Chapter II – Zeolites	36
1. <i>Generalities</i>	37
1.1. Structure and Properties	37
1.2. Main Applications.....	39
1.2.1. Zeolites as Ion-Exchangers	39
1.2.2. Zeolites in Adsorption and Separation Processes.....	40
1.2.3. Zeolites in Catalysis	40
2. <i>From Natural to Metal-Loaded Tailor-Made Zeolites</i>	41
2.1. Natural Zeolites	41
2.2. <i>De novo</i> Synthesis of Zeolites	41
2.3. BRØNSTED Acidic Zeolites	42
2.4. Synthesis of Metal-Doped Zeolites.....	45
2.4.1. <i>via</i> Isomorphous Substitution.....	45
2.4.2. <i>via</i> Ion-Exchange and Related Strategies	46
2.4.3. <i>via</i> Encapsulation Techniques	48
2.5. Application of Zeolites in Organic Synthesis of Fine Chemicals	50
2.5.1. BRØNSTED Acidic Zeolites	50

2.5.2. Metal-Doped Zeolites	55
Part Two. Copper-Zeolite-Catalysed Syntheses of Propargylamines and Synthetic Applications.....	67
Chapter III – Synthesis of α-Tertiary Propargylamines via KA^2 and Related Coupling Reactions under Cu^I-USY Catalysis	68
1. <i>From A^3 to KA^2 Coupling Reaction – State of the Art</i>	69
1.1. Homogeneous and Heterogeneous A^3 Reaction	70
1.2. Homogeneous and Heterogeneous KA^2 Reaction	74
2. <i>Cu^I-USY-catalysed KA^2 Reaction with Terminal Alkynes.....</i>	79
2.1. Optimisation of Reaction Conditions	79
2.2. Up-scaling and Recyclability	82
2.3. Scope and Limitations	83
2.3.1. Amine Scope	83
2.3.2. Ketone Scope.....	86
2.3.3. Alkyne Scope	88
2.3.4. Limitations and Solutions	90
3. <i>Decarboxylative and Desilylative Cu^I-USY-catalysed KA^2 Reactions</i>	91
3.1. Decarboxylative KA^2 Reaction to Overcome Limitations	91
3.2. Optimisation of Reaction Conditions	92
3.3. Scope and Limitations	93
4. <i>Cascade and One-Pot Applications of KA^2(-Type) Reactions.....</i>	96
5. <i>Conclusion.....</i>	98
Chapter IV – Extension of the A^3/KA^2 Methodology Towards the Synthesis of γ-Amino-Ynamides from Terminal Ynamides.....	99
1. <i>Introduction</i>	100
2. <i>Synthesis of γ-Amino-Ynamides – State of the Art.....</i>	100
3. <i>Synthetic Applications of γ-Amino-Ynamides – State of the Art</i>	105
4. <i>Results and Discussion</i>	108
4.1. Preparation of Terminal Ynamides.....	108
4.1.1. Terminal Ynamides from 1,2-Dichloroenamides	108
4.1.2. Terminal Ynamides from TIPS-protected Ynamides	110
4.2. Optimisation of Reaction Conditions	112
4.2.1. Preliminary Results	112
4.2.2. Optimisation <i>via</i> Design of Experiments	113
4.2.3. Catalyst Screening	116
4.2.4. Catalyst Reusability and Stability.....	117
4.3. Scope and Limitations	118
4.3.1. Carbonyl Scope	118
4.3.2. Amine Scope	120
4.3.3. Ynamide Scope	124
4.3.4. Comparison with A^3/KA^2 Reactions and Mechanistic Rationale.....	126
5. <i>Conclusion.....</i>	128
Chapter V – Propargylamine Synthesis Involving Alkyne Hydroamination	129
1. <i>Introduction</i>	130
2. <i>Hydroamination-Protonation-Alkyne Addition (HPA) Reaction – State of the Art.....</i>	132
2.1. Anti-MARKOVNIKOV-selective HPA.....	132

2.2.	MARKOVNIKOV-selective HPA.....	133
3.	<i>Optimisation of the Cu^I-USY-Catalysed HPA Reaction</i>	139
3.1.	Preliminary Results.....	139
3.1.1.	Catalyst Screening	140
3.1.2.	Solvent Screening	142
3.2.	Optimisation <i>via</i> Design of Experiments	142
3.2.1.	First Factorial Screening Design: The Vital Few	142
3.2.2.	Further Optimisation Using a Central Composite Design	147
3.3.	Additive and Ligand Screenings.....	151
3.4.	Scope and Limitations	156
3.4.1.	Amine Scope	156
3.4.2.	Alkyne Scope	158
3.4.3.	Mechanistic Rationale Regarding the Hydroamination Regioselectivity.....	161
3.4.4.	Hot Filtration Test and Recyclability Study of Cu ^I -USY	163
4.	<i>Conclusion</i>	166
Chapter VI – Propargylamines as Precursors to 1,2-Dihydropyridines and their Applications.....		167
1.	<i>Introduction</i>	168
2.	<i>Methodologies for 1,2-Dihydropyridine Synthesis – State of the Art</i>	169
2.1.	Overview of Frequently Used Approaches.....	169
2.2.	The Case of Cycloisomerisation of 3- <i>aza</i> -1,5-Enynes.....	171
2.2.1.	Under Rhodium Catalysis	174
2.2.2.	Under Silver Catalysis	174
2.2.3.	Under Copper Catalysis	175
2.2.4.	Under Zinc Catalysis	178
2.2.5.	Under Metal-Free Conditions.....	180
3.	<i>Synthetic Applications of 1,2-Dihydropyridines – State of the Art</i>	181
4.	<i>Biological Relevance of 1,2-Dihydropyridines – State of the Art</i>	186
5.	<i>Synthesis of 1,2-Dihydropyridines from Propargylamines: Results and Discussion</i>	189
5.1.	Optimisation of 3- <i>aza</i> -1,5-Enyne Synthesis	189
5.2.	Evaluation of Cu ^I -USY as Cycloisomerisation Catalyst.....	193
5.2.1.	Optimisation of the Cycloisomerisation Conditions	193
5.2.2.	Effect of Enyne Substitution Degree and Catalyst Choice on the Cycloisomerisation: A Comparative Study	196
5.2.3.	Hot Filtration Test and Recyclability Study of Cu ^I -USY	198
5.3.	Scope and Limitations	199
5.3.1.	Amine Substituent	199
5.3.2.	Propargyl Substituent	201
5.3.3.	Alkyne Substituent.....	202
5.3.4.	Enamine Substitution Frame	204
5.4.	Cu ^I -USY-Catalysed Cascade 1,2-Dihydropyridine Synthesis	205
5.5.	Synthetic Applications of Spirocyclic 1,2-Dihydropyridines	208
5.5.1.	As Dienes in DIELS-ALDER Cycloaddition Reactions	208
5.5.2.	In Other Derivatisation Reactions.....	213
6.	<i>Conclusion</i>	216
General Conclusions and Perspectives		217
Experimental Part.		221
<i>General Information and General Procedures</i>		222

<i>Analytical Data of Compounds from Chapter III</i>	229
<i>Analytical Data of Compounds from Chapter IV</i>	253
<i>Analytical Data of Compounds from Chapter V</i>	279
<i>Analytical Data of Compounds from Chapter VI</i>	285
<i>Crystallographic Data</i>	322
References	325
Résumé en français	336

Abbreviations

∅	pore dimension	cod	cyclooctadiene
[M]	generic metal species	COF	covalent organic framework
(1,10)-phen	1,10-phenanthroline	conv.	conversion
2-MeTHF	2-methyl tetrahydrofuran	COSY	homonuclear correlation spectroscopy
3CR	three-component reaction	CPME	cyclopentyl methyl ether
4CR	four-component reaction	CuAAC	copper-catalysed azide–alkyne cycloaddition
A ³	aldehyde-amine-alkyne coupling	C.V.	coefficient of variation
Ac	acetyl	CVD	chemical vapour deposition
acac	acetylacetonate	Cy	cyclohexyl
AIE	aqueous ion-exchange	DABCO	1,4-diazabicyclo[2.2.2]octane
ANOVA	analysis of variance	DBU	1,8-diazabicyclo(5.4.0)undec-7-ene
aq.	aqueous	DCE	1,2-dichloroethane
Ar	generic aryl group	DCM	dichloromethane
ATA	allenation of terminal alkyne	DEC	diethyl carbonate
atm	atmosphere	DEPT	Distortionless enhancement by polarisation transfer
ATR	attenuated total reflection	df	degrees of freedom
AYA	aldehyde-ynamide-amine coupling	DHP	dihydropyridine
BET	Brunauer–Emmett–Teller theory	DIPEA	<i>N,N</i> -diisopropylethylamine
Bn	benzyl	DMAP	<i>N,N</i> -dimethylpyridin-4-amine
Boc	<i>tert</i> -butyloxycarbonyl	DMF	<i>N,N</i> -dimethylformamide
CA	cycloaddition	DMSO	dimethylsulfoxide
calcd	calculated	DoE	design of experiments
C _{aro}	aromatic carbon	dppf	bis(diphenylphosphino)ferrocene
cat.	catalyst	<i>dr</i>	diastereomeric ratio
Cbz	benzyloxycarbonyl	E	<i>entgegen</i>
CCDC	Cambridge crystallographic data centre	E ⁺	generic electrophile

EC	electrocyclisation	LDA	lithium diisopropylamide
ED	generic electron-donating group	LUMO	lowest unoccupied molecular orbital
<i>ee</i>	enantiomeric excess	M	Molar = mol dm ⁻³
EFAI	extra-framework aluminium	<i>m</i> -	<i>meta</i> -
eq.	molar equivalents	MCR	multicomponent reaction
ESI	electrospray ionisation	MOF	metal organic framework
EWG	generic electron-withdrawing group	MOR	Mordenite
FAU	faujasite	Ms	mesyl = methanesulfonyl
FAD	flavin adenine dinucleotide	MS (4 Å)	molecular sieves (4 Å)
HMBC	heteronuclear multiple bond correlation	MS (ESI-TOF)	Electrospray Ionisation Time-of-Flight (ESI-TOF) Mass Spectrometer
HMDS	hexamethyldisilazane	MW	microwave irradiation
HOMO	highest occupied molecular orbital	MO	mixed oxide
HPA	hydroamination/protonation/alkyne addition	NC	nano composite
HPLC	high performance liquid chromatography	n.i.	not indicated
HRMS	high-resolution mass spectrometry	n.d.	not determined
HSQC	heteronuclear single quantum correlation	n.r.	no reaction
I	generic intermediate	NBS	<i>N</i> -bromosuccinimide
ICP-AES	inductively coupled plasma – atomic emission spectroscopy	<i>n</i> -Bu	<i>normal</i> -butyl
IC ₅₀	half maximal inhibitory concentration	<i>n</i> -Hex	<i>normal</i> -hexyl
IE	ion-exchange	NMR	nuclear magnetic resonance spectroscopy
IPr	1,3-bis(2,6-diisopropylphenyl)imidazolidene	NOESY	nuclear Overhauser effect spectroscopy
<i>i</i> -Pr	<i>iso</i> -propyl	NP	nanoparticle
IR	infrared spectroscopy	NPM	<i>N</i> -phenylmaleimide
<i>J</i>	coupling constant	<i>n</i> -Pr	<i>normal</i> -Propyl
JohnPhos	(2-Biphenyl)di- <i>tert</i> -butylphosphine	Ns	nosyl = 4-nitrobenzenesulfonyl
KA ²	ketone-amine-alkyne coupling	Nuc	generic nucleophile
KYA	ketone-ynamide-amine coupling	NW	nanowire
L	ligand		

<i>o</i> -	<i>ortho</i> -	t	time
<i>p</i> -	<i>para</i> -	TBAF	tetrabutylammonium fluoride
PA	propargylamine	<i>t</i> -Am	<i>tert</i> -amyl = <i>tert</i> -pentyl
PEG	polyethylene glycol	TBDPS	<i>tert</i> -butyldiphenylsilyl
PG	generic protecting group	TBME	<i>tert</i> -butyl methyl ether
Ph	phenyl substituent	TBS	<i>tert</i> -butyldimethylsilyl
PhMe	toluene	<i>t</i> -Bu	<i>tert</i> -butyl
pK _a	acid dissociation constant	TCE	1,1,2-trichloroethylene
PMB	<i>para</i> -methoxybenzyl	TES	triethylsilyl
PMBS	<i>para</i> -methoxybenzenesulfonyl	Tf	trifluoromethanesulfonyl
PMP	<i>para</i> -methoxyphenyl	TFA	trifluoroacetic acid
ppm	parts per million	THF	tetrahydrofuran
PS	polystyrene	THP	tetrahydropyranyl
PTFE	polytetrafluoroethylene	THPy	tetrahydropyridine
Py	pyridine	TIPS	triisopropylsilyl
pyr	pyrrolidine	TLC	thin layer chromatography
qty	quantity	tmeda	<i>N,N,N',N'</i> -tetramethylethylenediamine
R	generic group	TMS	trimethylsilyl
rel	relative	Ts	tosyl = 4-methylbenzenesulfonyl
R _f	retardation factor	TS	transition state
<i>rr</i>	regioisomeric ratio	USY	ultra-stable Y zeolite
rt	room (ambient) temperature	XAES	X-ray induced Auger electron spectroscopy
SAR	silicon-to-aluminium ratio	Xantphos	4,5-bis(diphenylphosphino)-9,9-dimethylxanthene
SCIE	supercritical ion-exchange	XPS	X-ray photoelectron spectroscopy
SSA	specific surface area	XRD	X-ray diffraction
SSIE	solid-state ion-exchange	Z	<i>zusammen</i>
Std. Dev.	standard deviation	ZSM-5	Zeolite Socony Mobil-5
T	temperature (°C)		

Preface

In recent decades, metal-catalysed reactions have provided chemists with powerful tools for the construction of carbon-carbon or carbon-heteroatom bonds accessing molecular scaffolds of increased complexity. Out of convinced devotion to green chemistry, chemists increasingly focus on the development of atom- and step-economical procedures towards valuable molecules. Propargylamine, for instance, is a key compound class of great synthetic and therapeutic interest, finding diverse applications as versatile synthetic intermediates and as lead structures in drug design.

During the conceptualisation of sustainable synthetic processes, however, the negative environmental and economic impact of metal catalysts should not be neglected. The immobilisation of metal catalysts on solid supports addresses these shortcomings aiming at the design of recyclable catalysts. As a result, several materials have been investigated, among which are zeolites as inexpensive, stable, and benign natural or synthetic minerals.

The objective of this thesis lies in the development of greener procedures to synthesise and further derivatise propargylamines with the help of metal-doped zeolites as heterogeneous catalysts. The recyclability of the latter is scrutinised for the developed methodologies. This manuscript is divided into three parts.

Part One. State of the Art.

Chapter I introduces propargylamines, briefly addressing their unique chemical reactivity and major biological activities. Next, a comparative description of frequently used methods for their synthesis is given. Last follows a selection of synthetic applications to showcase the diversity of propargylamines as key building blocks towards value-added chemicals.

Due to their key role as heterogeneous catalysts in this work and far beyond, a detailed description of zeolites follows in **Chapter II**. In addition to BRØNSTED acidic zeolites, a particular focus will be set on the different preparative methods and properties of LEWIS acidic metal-loaded zeolites. Copper-loaded zeolites are dealt with more specifically, as this corresponds to the catalyst type applied to the methodologies developed in this thesis.

Part Two. Copper-Zeolite-Catalysed Syntheses of Propargylamines and Applications.

Chapters III and **IV** are dedicated to the synthesis of propargylamines *via* metal-catalysed carbonyl-alkyne-amine coupling reactions. More precisely, **Chapter III** deals with the application of our copper-zeolite in KA^2 reactions, whereas **Chapter IV** presents an unprecedented carbonyl-ynamide-amine coupling towards γ -amino-ynamides, an underexplored class of propargylamines.

Chapter V presents another cascade approach towards propargylamines, exploring our copper-zeolite in catalytic hydroaminations of terminal alkynes in the HPA reaction.

Chapter VI illustrates the potential of our copper-zeolite catalyst to synthesise complex targets, including 1-azaspirocycles, from propargylamines prepared in **Chapter III**. The synthesis of 1,2-dihydropyridines lies at the heart of **Chapter VI**.

Chapter VI is followed by the *Experimental Part*.

Part One. State of the Art.

On the properties, syntheses, and applications of propargylamines and zeolites.

Thesis Objectives: Green Synthesis and Derivatisation of Propargylamines Using Metal-Doped Zeolites

Propargylamines are of great interest to organic and medicinal chemists. Therefore, green synthetic procedures for their formation are required to meet today's expectations of a sustainable and responsible chemical industry. Since the foundation of the "Green Chemistry" concept by Paul ANASTAS and co-workers in 1998,^[1] the chemical community has become increasingly aware of the overall necessity for more economical and, above all, more sustainable chemical processes. Besides waste reduction, the design of shorter syntheses, and high atom efficiency, catalysis plays a key role in green synthesis.^[2] Transition metals are omnipresent in catalysis contributing significantly to a raised efficiency of organic syntheses, as will be exemplified in Chapter II for the synthesis and further derivatisation of propargylamines. It must nevertheless be stressed that there are major problems associated with the use of metals. The extraction of metals brings about serious environmental pollution and enormous energy consumption. Furthermore, metals represent limited resources with a tendency towards rising prices, thus resulting in higher production costs and consumer prices. Besides efforts in waste metal recovery, several strategies have emerged to reduce the amount of "new" metal resources consumed in metal-catalysed reactions. In the field of homogeneous catalysis, the focus mainly lies on the design of highly stable and active catalysts with great turnover numbers (TON) at catalyst loadings sometimes reaching the ppm range. Concerning heterogeneous catalysis, where these properties are greatly desired, heterogenisation of molecular catalysts pursues easy retrievability and recyclability of the metal catalyst. The economic and environmental profit *via* this approach must, however, be scrutinised for each application and is not given *per se*.^[3] Among others, the PALE research group has contributed to the establishment of immobilised (transition) metal catalysts.

Amid a large number of supports, silica, alumina,^[4] and (mesoporous) carbon^[5] represent frequently used materials. Despite their high specific surface areas (SSA), important chemical and thermal stabilities, as well as chemical inertness, the supported catalysts commonly suffer from metal leaching due to poor metal-support interactions. One strategy to solve this issue lies in the chemical derivatisation of the support's surface to introduce organic chains incorporating metal coordinating moieties, i.e., organic ligands. This finally results in mimicking homogeneous catalysis by immobilising the ligand rather than depositing the metal species directly on the support.^[6] Unfortunately, metal leaching is still an issue, and the more elaborate catalysts are costly. Similarly, such ligating moieties have been anchored on polymeric supports, such as polystyrene, which suffer from comparable drawbacks.^[7] Another approach to metal immobilisation is based on the inclusion of metal species in the voids of porous materials, such as clays

and zeolites.^[8] Both are aluminosilicates, yet the zeolitic three-dimensional and microporous networks are of greater stability compared to the clays' nano-scaled (inter)layers. Unfortunately, metal leaching is observed depending on the application. Metal-organic frameworks (MOFs),^[9] in turn, are highly porous molecular sieves akin to zeolites. They strongly bind metal ions as they are an integral part of the material's framework. Their high preparation cost (due to the use of immense amounts of metals, elaborate organic linkers and hazardous solvents) and reduced chemical stability compared to zeolites limits their use in liquid-phase catalytic applications. An emerging related material class, covalent organic frameworks (COFs), addresses these shortcomings.^[10] While this research area is still in its infancy, COFs are promising supports for metal complexes. Several other supported catalysts applied to the synthesis of propargylamines will also be mentioned in this section. In **Table 1**, a comparison of some key properties of three frequently used porous supports is given.

Table 1. Comparison of frequently used porous metal supports.

Support (S)	Chemical stability	Thermal stability	Pore size (nm)	SSA (m ² /g)	M-S interaction	Price range (€/g)
Mesop. C	High	High	~ 4	200-1000	Weak	> 2
Zeolites	High	High	~ 0.5-1	300-800	Medium	< 0.5
MOF	Moderate	High	~ 2	1000-10 000	High	> 10

Mesop.: mesoporous. C: carbon. M-S: metal-support.

It is inevitable that each class of material has advantages and disadvantages. Ideally, any support should be inherently safe, environmentally sound, stable, easy-to-handle and easy-to-recover. Its production should be cost-effective, have an acceptable environmental impact and be feasible at a large scale. Zeolites respond to these criteria and have already been proven versatile catalysts in organic synthesis (for details, see section II-2.5.). They are available at low cost and can be doped with (transition) metals through different techniques.^[11]

The objective of this thesis is to develop sustainable synthetic procedures to access propargylamines with the help of metal-loaded zeolites as solid-phase immobilised catalysts. Furthermore, the use of such catalysts in the derivatisation of propargylamines into other value-added scaffolds is targeted. The development of our synthetic procedures will be guided by Green Chemistry principles with a focus on atom- and step-economical transformations. As many organic solvents are of environmental and health concerns, solvent-free conditions or “greener” solvents will be used preferentially.

The next two chapters provide the reader with the properties, syntheses, and applications of propargylamines, as well as zeolites. Regarding the latter mainly their use as heterogeneous catalysts in organic synthesis will be highlighted.

Chapter I – Propargylamines

1. Introduction

Propargylamines, constituted of a carbon-carbon triple bond ($C\equiv C$) in β -position to an amino group (Figure 1), are of great interest in organic and medicinal chemistry.^[12] The presence of the propargylamine moiety in natural products and synthetic therapeutics (Figure 1a,b) is often indispensable for their bioactivities. Furthermore, propargylamines are relevant building blocks to access other attractive functionalities such as allenes or diverse *N*-heterocycles, thus constituting key intermediates in the synthesis of natural products and therapeutics.

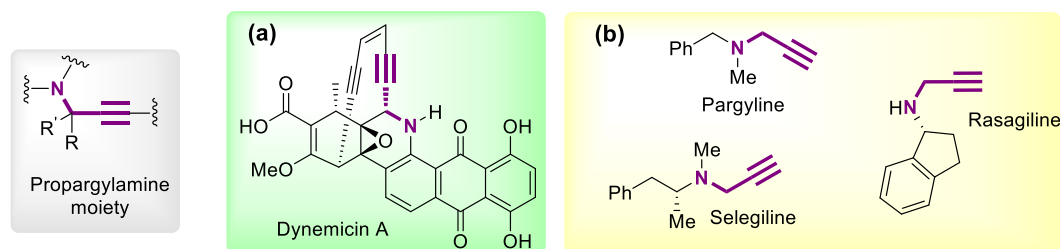


Figure 1. The propargylamine moiety and examples of (a) natural and (b) synthetic bioactive representatives.

In literature, two nomenclatures are used to define propargylamines regarding the substitution degree of their propargylic position (Figure 2a). Most frequently, the number of carbon-based substituents on the propargylic carbon, accompanied by the α -prefix, is used. As a result, unsubstituted, mono- or disubstituted propargylamines are called α -primary, α -secondary and α -tertiary, respectively. This more precise nomenclature is used throughout this manuscript. Alternatively, authors refer to secondary, tertiary, and quaternary propargylamines, including the amino group as a substituent of the propargyl carbon and omitting the α -prefix.

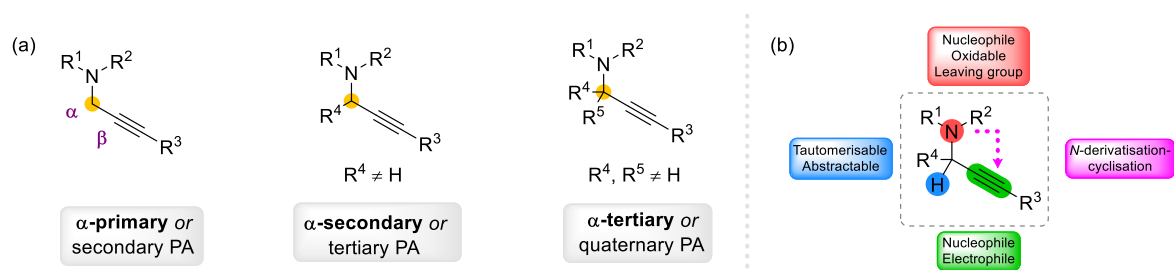
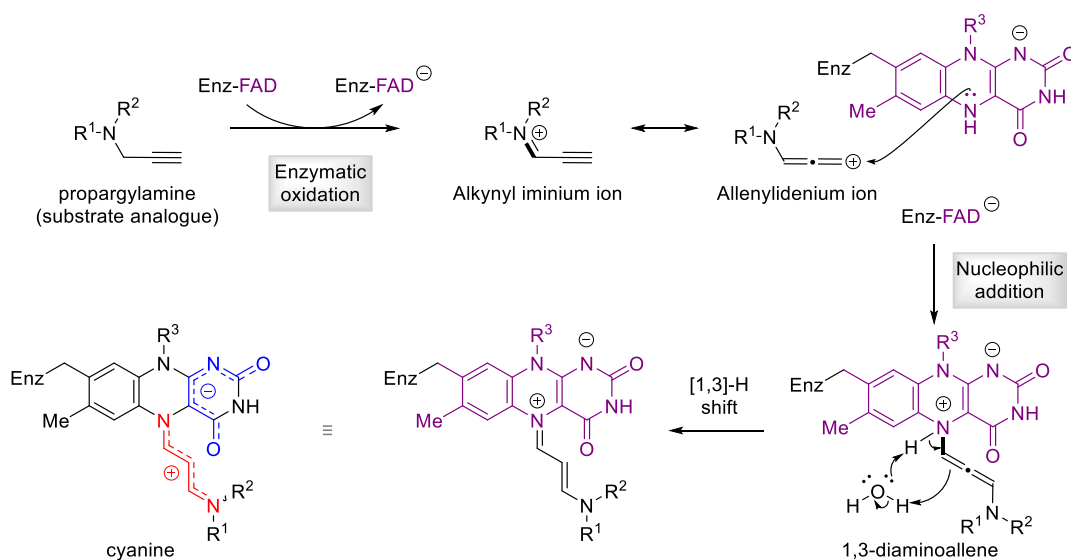


Figure 2. (a) Structural and (b) reactivity profiles of propargylamines (PA).

The simultaneous presence of the amine and alkyne functionality allows propargylamines to undergo a variety of chemical reactions (Figure 2b). While the amine frequently serves as a nucleophile in many transformations, it also has the potential to act as leaving group. Furthermore, the amine can be oxidised into *N*-oxides or oximes, which, in turn, can react in intramolecular cyclisations involving the alkyne moiety.^[13] In addition, the alkyne displays a π -LEWIS basic and nucleophilic character. Given its unique location between an amino and an alkynyl group, the propargylic position can also be involved in chemical transformations. A propargylic hydrogen, for instance, can be homo- or heterolytically abstracted or undergo tautomerisation to yield the corresponding allenylamine.

As mentioned above, their unique reactivity profile also significantly determines their biological activity. Several propargylamines, such as pargyline, rasagiline, and selegiline were shown to have neuroprotective properties acting as substrate analogues for monoamine oxidase (MAO) enzymes (**Figure 1b**).^[14] As a result, they are used to treat neurodegenerative diseases, such as PARKINSON and ALZHEIMER diseases. Regarding their mode of action, RAMSAY and co-workers recently proposed a general inactivation mechanism for such propargylamine-based MAO inhibitors (**Scheme 1**).^[15] Accordingly, FAD-mediated oxidation of the propargylamine to the corresponding alkynyl iminium ion enables a 1,4-addition of the reduced cofactor. This results in a covalent bond between the enzyme and the oxidised substrate analogue, yielding a 1,3-diaminoallene. With the help of a nearby water molecule, the latter undergoes a 1,3-prototropic rearrangement allowing the positive charge to be delocalised along a newly generated cyanine chain.



Scheme 1. Irreversible inactivation mechanism of MAO enzymes by propargylamines.^[15]

Enz: enzyme. FAD: flavin adenine dinucleotide. MAO: monoamine oxidase.

In recent years, medicinal chemists have paid increasing attention to the propargylamine moiety. This has resulted in the development of multi-target ligands/drugs by combining this structural motif with other well-established pharmacophores, aiming for faster and more efficient discovery of new lead structures for the treatment of multifactorial diseases. For instance, MAO and co-workers designed compound **A.1** displaying both AChE and MAO inhibitory properties as a lead structure toward novel anti-ALZHEIMER drugs (**Figure 3**).^[16] Pursuing the same goal, BAI and co-workers recently targeted the development of HDAC1/MAO-B dual inhibitors, such as **A.2** incorporating an aromatic hydroxamic acid onto pargyline-derived propargylamines.^[17] Both compounds showed promising inhibition activities.

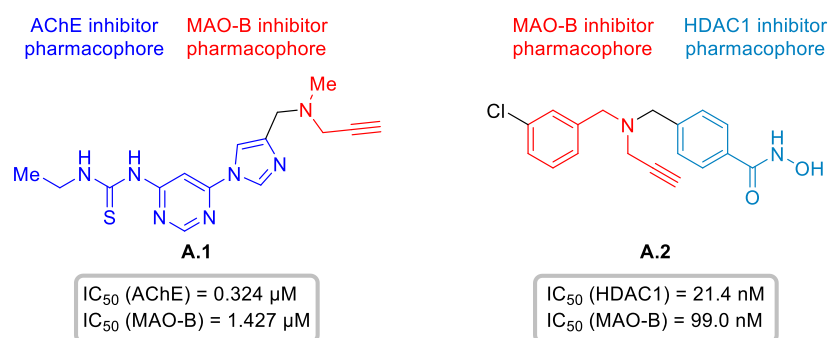
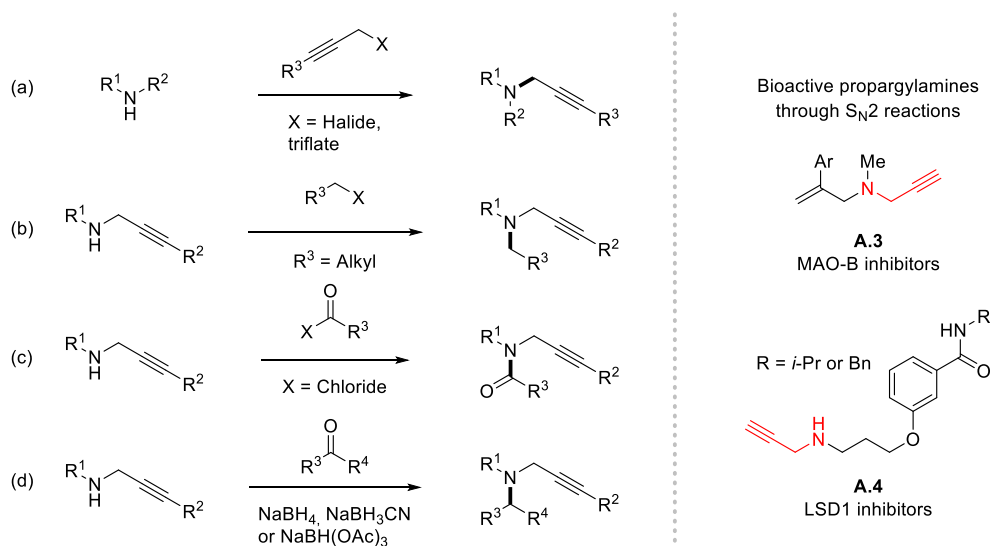


Figure 3. Propargylamine-based multi-target ligands against ALZHEIMER disease.^[16,17]
 AChE: Acetylcholinesterase. HDAC1: Histone deacetylase 1. MAO-B: monoamine oxidase B.

Given the great virtues of propargylamines, numerous research groups, including us, are highly interested in the synthesis of diverse propargylamines, but also to use them in further organic transformations. The following two sections aim to provide an overview of frequently used methods to synthesise propargylamines, as well as to showcase their utility as versatile building blocks to access relevant organic compounds through selected examples.

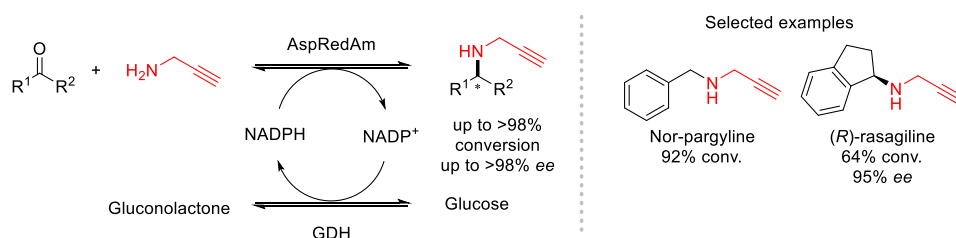
2. Synthesis of Propargylamines

Scheme 2 shows several fundamental organic transformations applied to the preparation of propargylamines. Nucleophilic substitution of amines with propargylic electrophiles (e.g., halides^[18,19] or triflates^[20]) represents a frequently used and simple approach towards propargylamines (**Scheme 2a**). Likewise, commercially available propargylamines can be derivatised by introducing novel functionalities, e.g., through *N*-alkylation or *N*-acylation (**Scheme 2b,c**). Such simple strategies have enabled the synthesis of valuable compounds and therapeutics, among which monoamine oxidase B (MAO-B) inhibitors **A.3**^[21] or inhibitors of lysine specific demethylase 1 (LSD1) **A.4**.^[22] As alkyl halides or related electrophiles often suffer from product selectivity issues due to multiple alkylations up to ammonium salt formation (MENSCHUTKIN reaction), reductive amination has become a prominent choice for *N*-alkylation (**Scheme 2d**). Accordingly, propargylamines are commonly prepared through reactions with aldehydes and ketones in the presence of boron-based hydride donors ($NaBH_4$, $NaBH_3CN$, or $NaBH(OAc)_3$) as reducing agents.^[23,24]



Scheme 2. Non-catalytic approaches for propargylamine synthesis and examples of simple bioactive propargylamines.

Such a monoalkylation of propargylamines *via* reductive amination can also be achieved through biocatalysis. TURNER and co-workers discovered a reductive aminase from *Aspergillus oryzae* (AspRedAm) which enabled a formal reductive amination of various primary and secondary amines with diverse aldehydes and ketones in the presence of NADPH (**Scheme 3**).^[25] The product scope includes propargylamines of therapeutical interest with attractive conversions and enantioselectivities such as Nor-pargyline and (*R*)-rasagiline. The NADPH cofactor is regenerated through the oxidation of sacrificial glucose by glucose dehydrogenase (GDH). A similar biocatalytic approach was recently published by ZHU and co-workers.^[26]



Scheme 3. Biocatalytic formal reductive amination to access propargylamines.^[25]

AspRedAm: reductive aminase from *Aspergillus oryzae*. NADPH: nicotinamide adenine dinucleotide phosphate. GDH: glucose dehydrogenase.

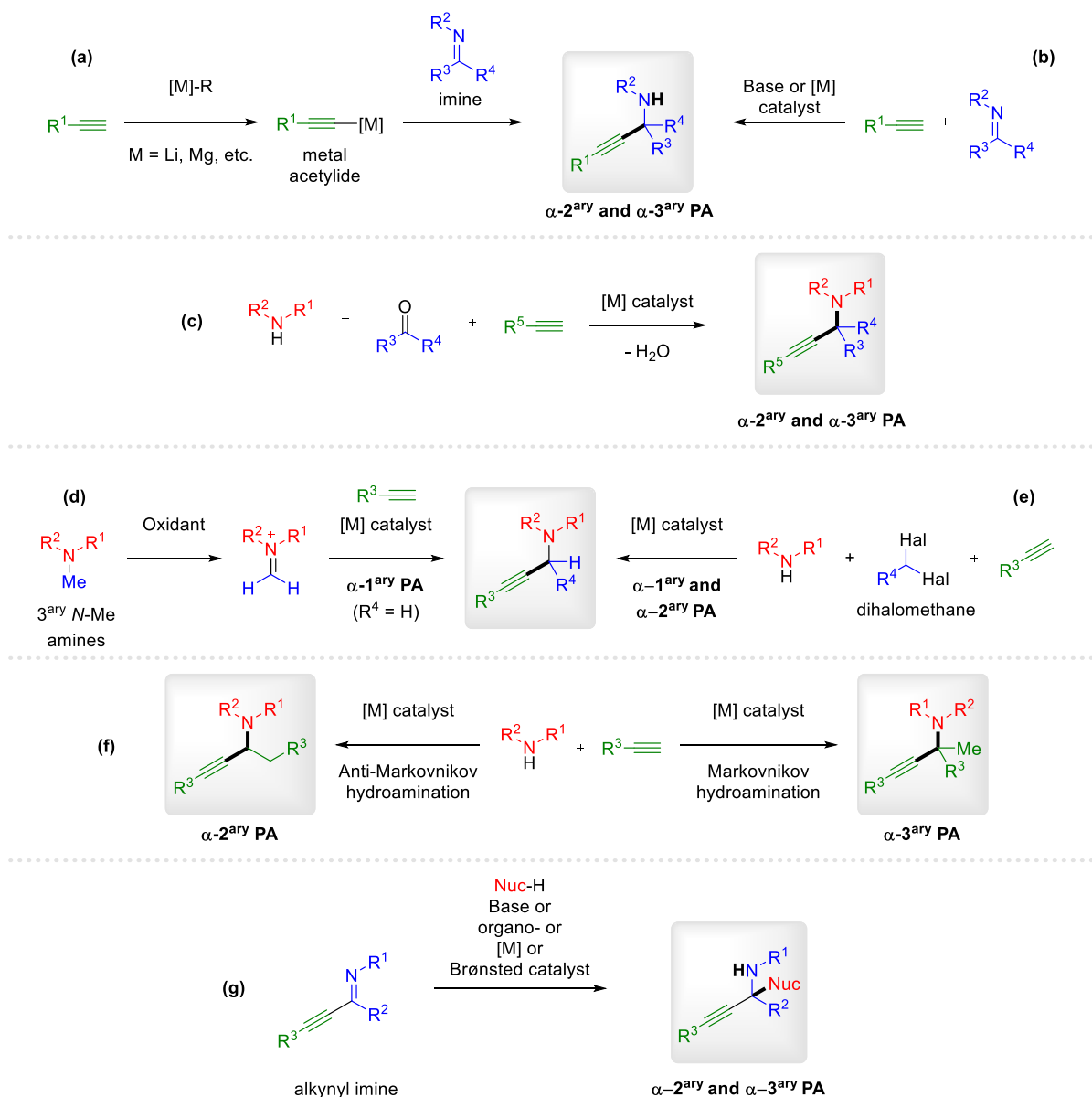
Owing to the significant gap in propargylamine scope when simply relying on the procedures mentioned above, the synthetic community has ever since reported new strategies to access these attractive targets. The most popular ones are summarised in **Scheme 4**. Not surprisingly, a vast majority relies on the imine/iminium ion functionality, whether as starting material or generated *in situ* through various strategies. These electrophiles are commonly trapped by metal acetylides which are for example generated with stoichiometric amounts of strong organometallic bases (**Scheme 4a**). The challenges associated with the preparation and handling of metal acetylides, the need for anhydrous conditions, and the preformation of the imine represent several drawbacks of this approach. Besides base-mediated alkynylations (**Scheme 4b**), the use of catalytic amounts of d-block metal complexes (e.g., Cu, Zn, Ni, Ag, Au, etc.) allowed to

partially overcome these limitations as the corresponding metal acetylides often display weaker basicities compared to alkali analogues (**Scheme 4b**).^[27] Beneficially, often no additional base is needed, and in some cases, the reaction even proceeded in water.^[28] Nevertheless, an additive-free multicomponent approach at practical temperatures was highly desirable from a green chemistry perspective. The A³ reaction, as coined by Li and co-workers describing the coupling of an amine, an aldehyde, and an alkyne, responds to these criteria (**Scheme 4c**). The concomitant one-pot formation of a C-C and C-N bond, producing water as the only by-product underlines the high atom and step economy of this method. Later, this methodology was also extended to the use of ketones giving rise to the KA² reaction. Both 3CRs are described in more detail in section III-1.

Complementary to an amine-carbonyl condensation approach, it is possible to generate iminium ions from tertiary *N*-methylamines through selective oxidation (**Scheme 4d**). The iminium intermediates undergo nucleophilic addition of a metal acetylide to afford α -primary propargylamines. Alternatively, such propargylamines can result from a less developed three-component reaction (3CR) which employs a dihalomethane compound as a formaldehyde replacement (**Scheme 4e**). This method is commonly referred to as AHA (amine-haloalkane-alkyne) coupling reaction. One more so-called “aldehyde replacement” strategy consists of a metal-catalysed hydroamination of alkynes to yield enamines (**Scheme 4f**). Their protonation affords the electrophilic iminium ion, which is trapped by a metal acetylide. In this manuscript, this approach is called HPA for hydroamination/protonation/alkyne addition and is covered in more detail in section V-2.

Another attractive method for propargylamine synthesis exploits alkynyl imines which react with various nucleophiles (**Scheme 4g**). The clear benefit of this approach is that it is not limited by the nucleophilicity of the incoming alkynyl nucleophile; thus, a complementary product scope is accessible compared to the previous methods described.

In the following, only a selection of literature reports on the synthesis of propargylamines based on several transformations shown in **Scheme 4** is presented due to the abundance of examples.

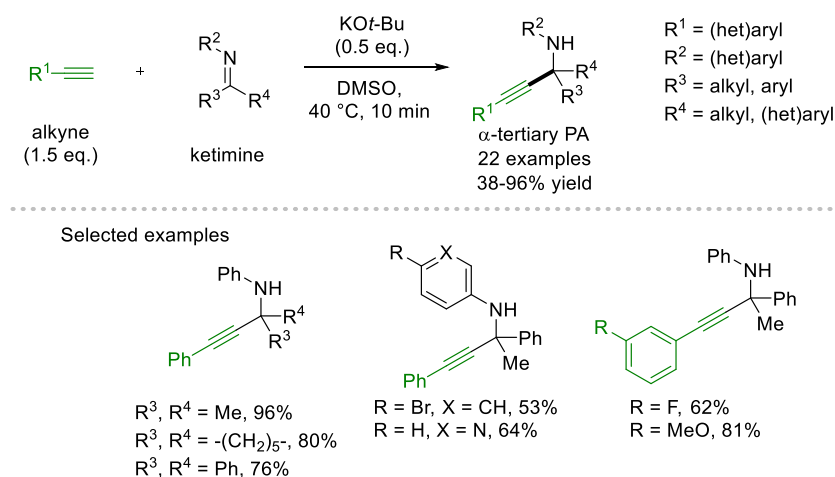


Scheme 4. From stoichiometric to catalysed approaches for propargylamine (PA) synthesis.

2.1. Base-Catalysed Imine Alkynylation

Following the strategy shown in [Scheme 4b](#), TROFIMOV and co-workers reported a $KOt\text{-Bu/DMSO}$ -catalysed addition of (hetero)aromatic terminal alkynes to various aniline-derived ketimines ([Scheme 5](#)).^[29] Although this approach requires the preformation of a ketimine, it represents a metal-free and highly efficient catalytic procedure to access α -tertiary propargylamines that are, to date, inaccessible or hard to form *via* a KA^2 reaction. In fact, a myriad of ketimines prepared from cycloaliphatic, but also linear aliphatic, as well as (di)aromatic ketones smoothly reacted to the corresponding propargylamines. Especially linear aliphatic and aromatic ketones are challenging substrates in the KA^2 reaction (for more details, see section III-1.2.). Nevertheless, this approach has significant limitations. Indeed, the amine scope includes exclusively primary anilines, while aliphatic amines (carrying methyl, allyl, or benzyl

substituents) are not reactive or lead to complex mixtures. Furthermore, aliphatic alkynes were shown to be incompatible.

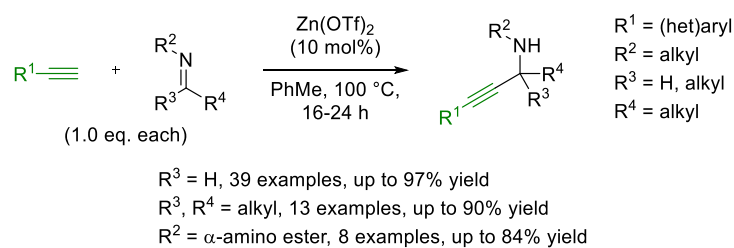


Scheme 5. *t*-BuOK-catalysed synthesis of aniline-derived propargylamines.^[29]

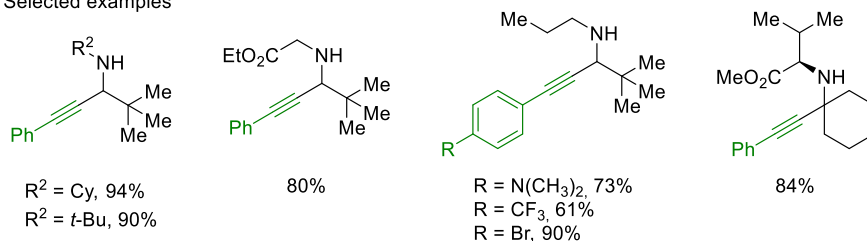
2.2. Metal-Catalysed Imine Alkynylation

Regarding the metal-catalysed alkynylation of imines (Scheme 4b), several procedures based on different d-block metals (e.g., Cu,^[30] Ag,^[31] Zn,^[32,33] Ir^[34] and Pd^[35]) have been reported. In the following section, only a selection of examples is given.

TEHRANI and co-workers reported a Zn(OTf)₂-catalysed synthesis of α -secondary and α -tertiary propargylamines from aldimines and ketimines, respectively (Scheme 6).^[32] Concerning α -tertiary propargylamines, they mainly focused on imines derived from linear ketones and primary aliphatic amines, among which several α -amino esters. As a result, this procedure offers a complementary scope to the KA² reaction, in which these represent challenging substrate classes (for more details, see section III-1.2.). Diversely functionalised aliphatic and aromatic alkynes were suitable coupling partners, while pyridinyl-based ketimines did not react. Compared to other catalytic systems, this protocol was however highly efficient with imines derived from sterically encumbered amines, such as cyclohexyl- and *t*-butylamine. Other attractive features include the use of equimolar amounts of coupling partners, the absence of an additional LEWIS acid for ketimine activation, and the product recovery through simple extraction without the need for further purification. The use of toluene as solvent nevertheless lowers the protocol's "green" character.

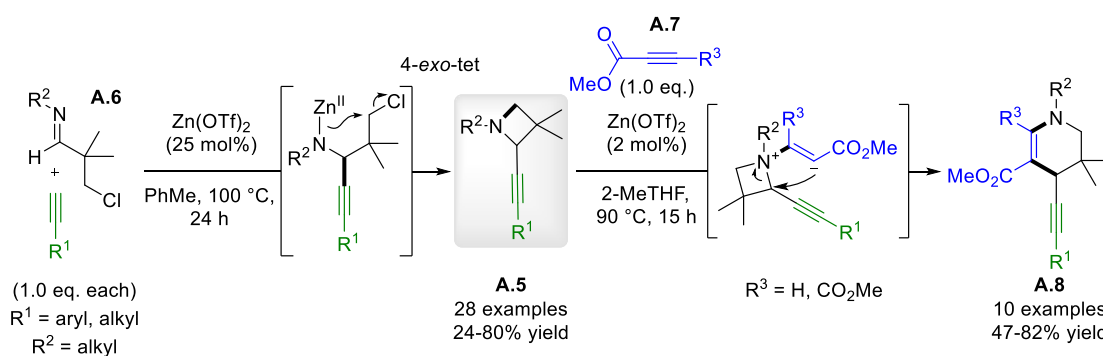


Selected examples



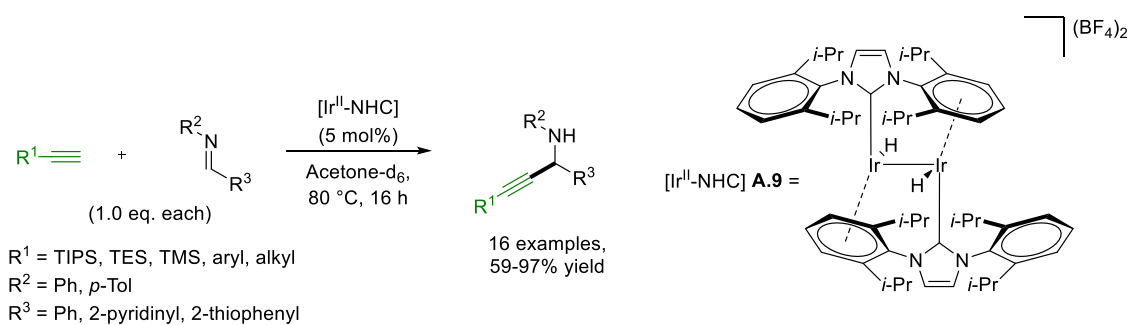
Scheme 6. Zn-catalysed synthesis of *N*-monoalkylated propargylamines.^[32]

Under similar conditions, the same authors prepared 2-alkynylazetidines **A.5** from β -chloro aldimines **A.6** through a cascade alkyne addition/intramolecular S_N2 reaction (**Scheme 7**).^[33] While only zinc(II) salts gave good yields and selectivities, high loadings were needed. The use of $\text{Zn}(\text{OTf})_2$ in 25 mol% was retained as a compromise in terms of lowest catalyst loading and high product yields. Various aliphatic amine components, including allyl, benzyl and α -secondary alkylamines were compatible, except for cyclopropylamine. Arylalkynes were generally more efficient than alkylalkynes. It is worth mentioning that azetidines **A.5** further underwent *aza*-MICHAEL addition/ring expansion with propiolates **A.7** to produce diverse and highly substituted tetrahydropyridines **A.8** in the presence of only 2 mol% of $\text{Zn}(\text{OTf})_2$. In this step, 2-MeTHF was used as a “greener” solvent alternative to toluene.



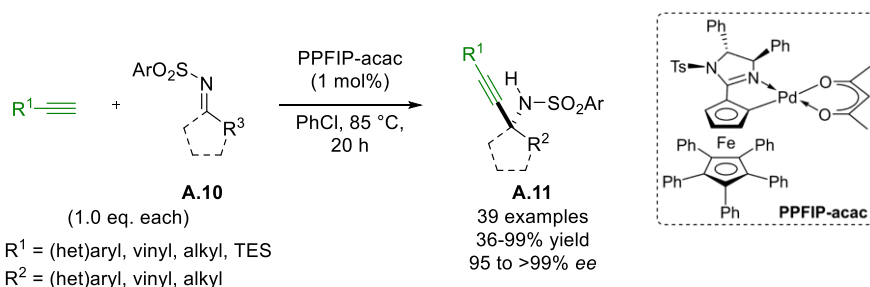
Scheme 7. Zn-catalysed synthesis of azetidine-based propargylamines.^[33]

The above presented Zn^{II} -based procedures are only effective with *N*-alkyl imines. ORO and co-workers have reported the use of a dimeric Ir^{II} -NHC complex **A.9** for the alkylation of *N*-aryl imines (**Scheme 8**).^[34] The iridium acetylide is believed to form through single-site oxidative addition of the alkyne at one of the iridium centres, thus affording a mixed Ir^{I} - Ir^{III} complex. Beneficially, the alkyne scope includes alkynylsilanes, aryl- and alkylalkynes, whereas imines were exclusively derived from aromatic aldehydes.



Scheme 8. Ir-catalysed synthesis of *N*-monoarylated propargylamines.^[34]

Complementary to existing methods, a direct and enantioselective palladium-catalysed alkyne addition to *N*-sulfonyl imines **A.10** to access *N*-sulfonyl propargylamines **A.11** was recently reported by PETERS and co-workers (Scheme 9).^[35] This catalytic system benefits from low catalyst loadings (0.01-1 mol%), high enantiomeric excesses from 95 to >99% *ee*, and a broad product scope with 36-99% yield from equimolar amounts of starting materials. A palladium-acetylide intermediate was detected *via* ESI-MS and is assumed to be generated with the help of catalytical acetylacetonate from the pre-catalyst PPFIP-acac.



Scheme 9. Enantioselective Pd-catalysed synthesis of *N*-sulfonylated propargylamines.^[35]

PPFIP: pentaphenylferrocenyl imidazoline palladacycle. acac: acetylacetonate. TES: triethylsilyl.

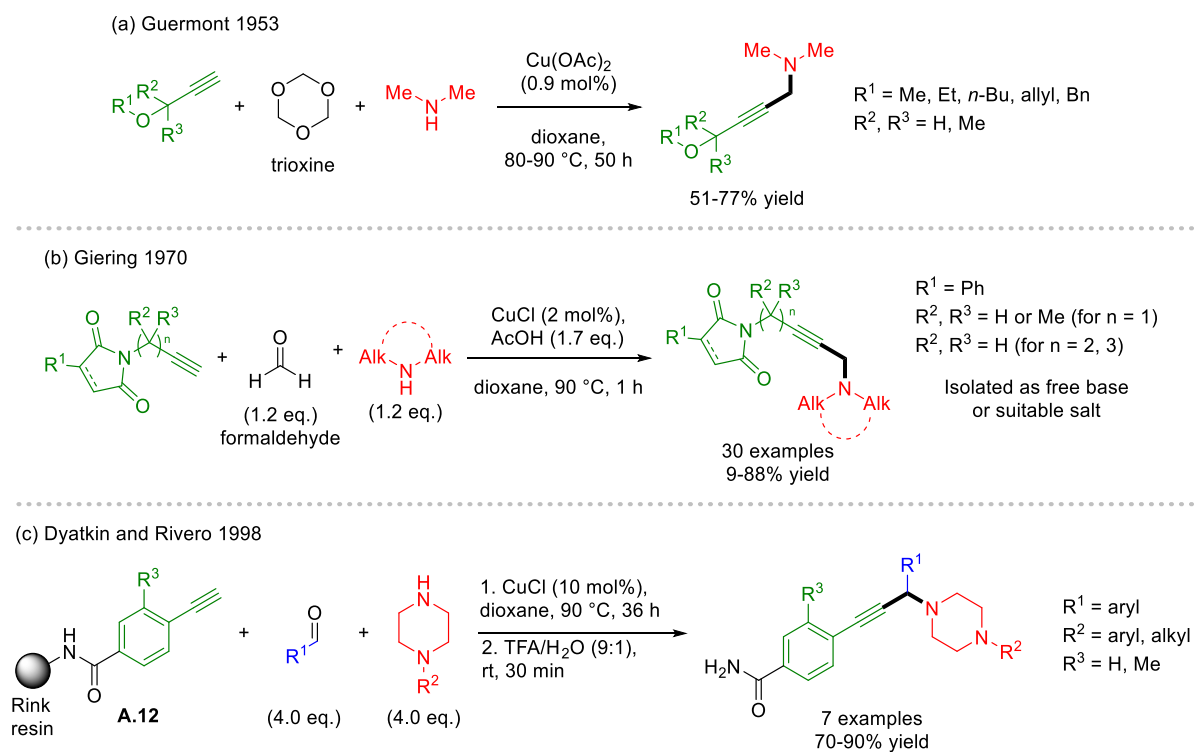
2.3. Metal-Catalysed Carbonyl-Amine-Alkyne Coupling Reactions

Several reactions fall under this category (Scheme 4c). It is not always easy to precisely define the origin of a name reaction. In the case of the A^3 reaction, some criteria need to be defined to distinguish between original pioneering contributions and the concrete emergence of the A^3 reaction. The use of a purely catalytic process, for instance, as well as the compatibility of the catalytic system with non-exclusive (para)formaldehyde, could represent such criteria. This section will only briefly discuss the preliminary work on this catalytic three-component methodology. A more detailed state of the art, as well as the remaining challenges for the A^3 reaction and its KA^2 extension, are described in section III-1.

The reports of GUERMONT in 1953^[36] and GIERING and co-workers in 1970^[37] represent the first examples of copper-catalysed 3CRs of formaldehyde (or trioxine), amines, and terminal alkynes to synthesise propargylamines (Scheme 10a,b). From these two reports, it is evident that copper(I) and copper(II) pre-catalysts are suitable for this transformation. Low copper loadings

of at most 2 mol% sufficed to give good yields in many cases but under GIERING's conditions a significantly faster coupling process was observed compared to GUERMONT's protocol.

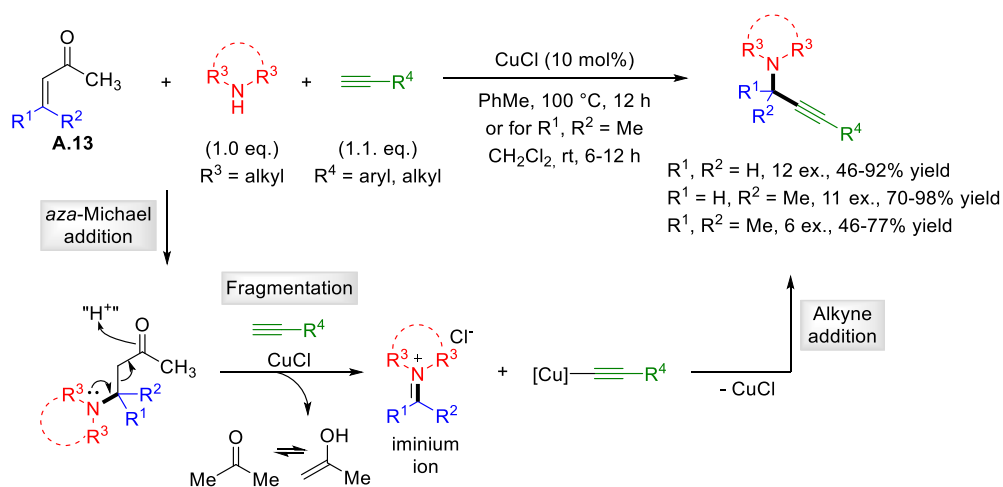
It is only nearly 30 years later that more functionalised aldehydes are exploited in this three-component methodology. In 1998, DAX and co-workers reported a solid-phase synthesis of propargylamines *via* a 3CR of terminal alkynes with resin-supported aldehydes or piperazines, respectively.^[38] While the scope included aromatic aldehydes allowing the incorporation of a propargylic substituent, this method relied on two equivalents of CuCl. In the same year, DY-ATKIN and RIVERO established a related but catalytic solid-phase system employing RINK resin-supported aromatic alkynes **A.12** and catalytic CuCl (10 mol%) (**Scheme 10c**).^[39] TFA-mediated cleavage yielded the propargylamines in 82 to above 95% purity. This protocol can thus be considered the first example of an A³ reaction. It is worth noting, that salicylaldehydes were shown to undergo metal-free A³ reactions with secondary cyclic amines and aromatic alkynes.^[40]



Scheme 10. Cu-catalysed 3CR of aldehydes, amines, and alkynes: from pioneering contributions^[36,37] to the first A³ reaction.^[39]

More recently, a novel catalytic 3CR of terminal alkynes, amines, and α,β -unsaturated ketones **A.13** has emerged (**Scheme 11**).^[41] This strategy is based on an *aza*-MICHAEL addition/fragmentation cascade process to generate the electrophilic iminium intermediate and is thus to be distinguished from the A³/KA² methodology. In fact, regarding the formation of α -tertiary propargylamines, this protocol is highly complementary circumventing the often challenging condensation of amines with aliphatic linear ketones. However, the authors only presented the use of mesityloxide leading to the corresponding *gem*-dimethyl propargylamines (**Scheme 11**,

$R^1, R^2 = \text{Me}$). Through a condensation (KA^2) approach, these products are described in poor yields, and based on excess acetone and high temperatures.^[42] Here, mesityloxide (**A.13** with $R^1, R^2 = \text{Me}$) can be employed in equimolar amounts and the reaction is performed at room temperature yielding six examples of *gem*-dimethyl propargylamines in 46-77% yield. Furthermore, α -primary and α -secondary propargylamines are accessible but the scope is not complementary to the corresponding A^3 procedures. In addition, the reaction conditions for these product classes are comparable to existing A^3 procedures and gave moderate to excellent yields (46-98%). It should also be stressed that this methodology is restricted to secondary amines, with diethylamine representing the only linear example. Examples based on α, β -unsaturated ketones **A.13** bearing an α -substituent was not presented.



Scheme 11. Aza-MICHAEL addition-based 3CR towards propargylamines.^[41]

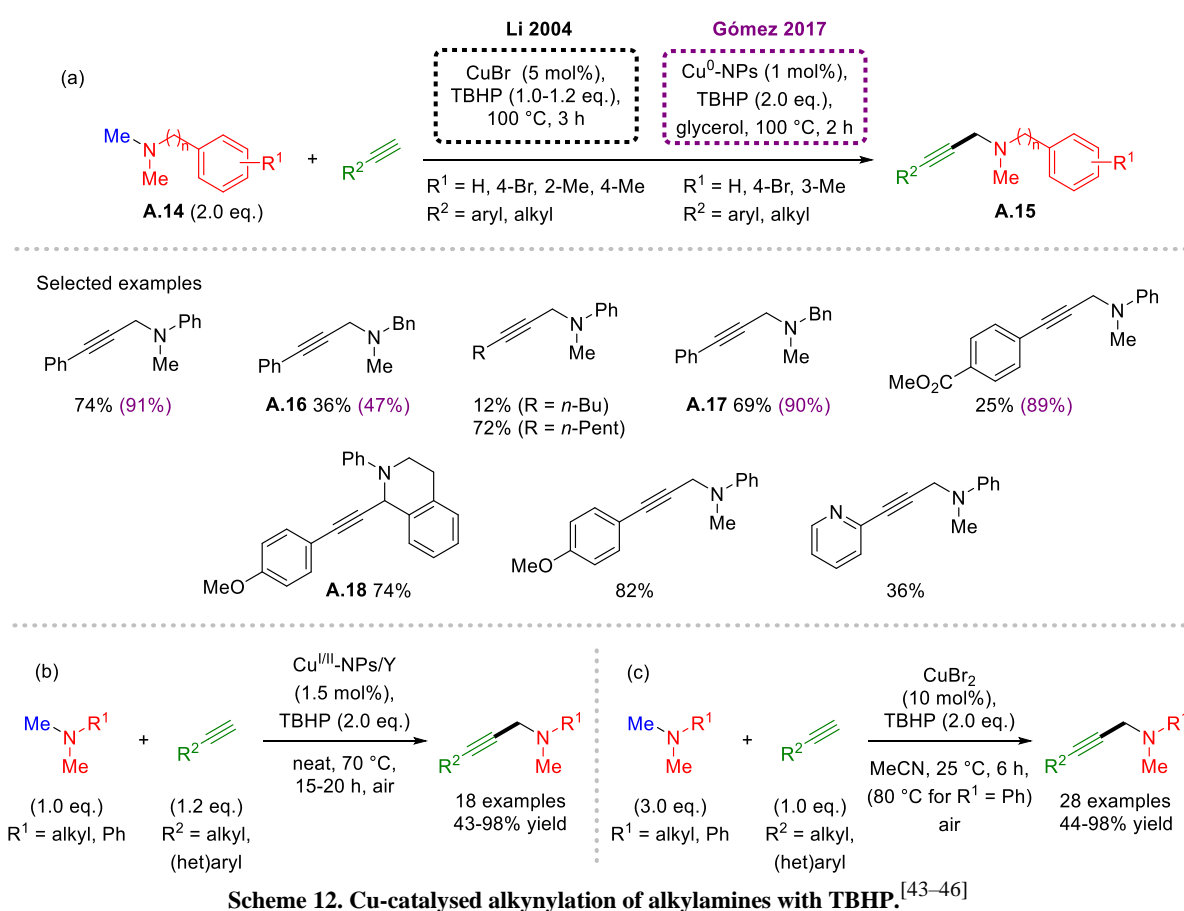
2.4. Copper-Catalysed Cross-Dehydrogenative Coupling of Tertiary Amines

Several research groups contributed to the development of the alkylation of tertiary methyl amines (Scheme 4d). In 2004, LI and co-workers developed a copper-catalysed oxidative alkylation of tertiary *N*-methyl anilines **A.14** with *tert*-butyl hydroperoxide (TBHP) as stoichiometric oxidant (Scheme 12a) to yield **A.15**.^[43] This protocol was also applicable to *N,N*-dimethyl benzylamine where alkylation preferentially occurred at the methyl rather than the benzyl position (\rightarrow **A.16** and **A.17**). Interestingly, in the absence of an *N*-methyl substituent, the benzyl position was selectively alkylated to give **A.18**.

ALONSO and co-workers achieved a large product scope using Cu^{II} nanoparticles (NPs) dispersed on Y zeolite (Scheme 12b).^[44] The procedure benefits from low catalyst loading (1.5 mol%), milder reaction temperature (70 vs. 100 °C), neat conditions, near equimolar amounts of the coupling partners, and catalyst reusability (seven runs with yields evolving from 93% to 80% yield).

In 2017, GÓMEZ and co-workers used another interesting approach based on Cu⁰ NPs in glycerol at only 1 mol% catalyst loading (Scheme 12a).^[45] The product scope included dimethyl aniline and benzylamine derivatives coupled to aromatic and aliphatic alkynes. Interestingly, the products were separated from the copper-glycerol phase through extraction without detecting a significant amount of copper in the extracts.

Recently, a very mild CuBr₂-based procedure was disclosed by XU and co-workers (Scheme 12c).^[46] A broad alkyne scope, including aliphatic and (hetero)aromatic derivatives, efficiently coupled with alkylamines at room temperature. Anilines were also shown to react but required a temperature of 80 °C. Nevertheless, the procedure relies on three equivalents of the amine component regardless of the amine class.



2.5. Metal-Catalysed Hydroamination/Protonation/Alkyne Addition (HPA)

This reaction refers to the approach presented in Scheme 4f. WEEDON and co-workers reported the anti-MARKOVNIKOV-selective HPA reaction of several secondary (morpholine, diethyl- and dimethylamine, 63-80% yield) and primary (*n*-butylamine, cyclohexylamine and benzylamines, 30-70% yield) amines with acetylene under CuCl catalysis (7 mol%) in 1949.^[47] The reactions were performed in autoclaves at temperatures ranging from 80-100 °C and acetylene pressures of about 14 bar. In 1961, KLEINSCHMIDT and KRUSE developed the MARKOVNIKOV-selective

HPA reaction utilising a bimetallic $\text{Zn}(\text{OAc})_2/\text{Cd}(\text{OAc})_2$ system. Again, drastic conditions (up to 120 °C and 38 bar) were needed and the substrate scope was limited to propyne with dimethyl- and diethylamine.^[48] More recent reports on HPA reactions performed under ambient pressure and larger product scopes will be described in section V-2.

3. Synthetic Applications of Propargylamines

Propargylamines represent highly versatile synthetic intermediates and their applications in organic synthesis are well-reviewed. In 2017, CASTAGNOLO and co-workers published an exhaustive review on the “synthesis and reactivity of propargylamines in organic chemistry.”^[12] Furthermore, CASTAGNOLO’s group recently highlighted the asymmetric synthesis of chiral propargylamines and their applications in “Methodologies in Amine Synthesis.”^[49] VAN DER EYCKEN’s^[50] and SHARMA’s^[51] groups contributed to summarising the use of propargylamines more specifically in the synthesis of heterocycles. Complementary, HUANG and co-workers focused primarily on the mechanisms underlying the organic transformations giving a classification into six categories depending on the reaction type.^[52]

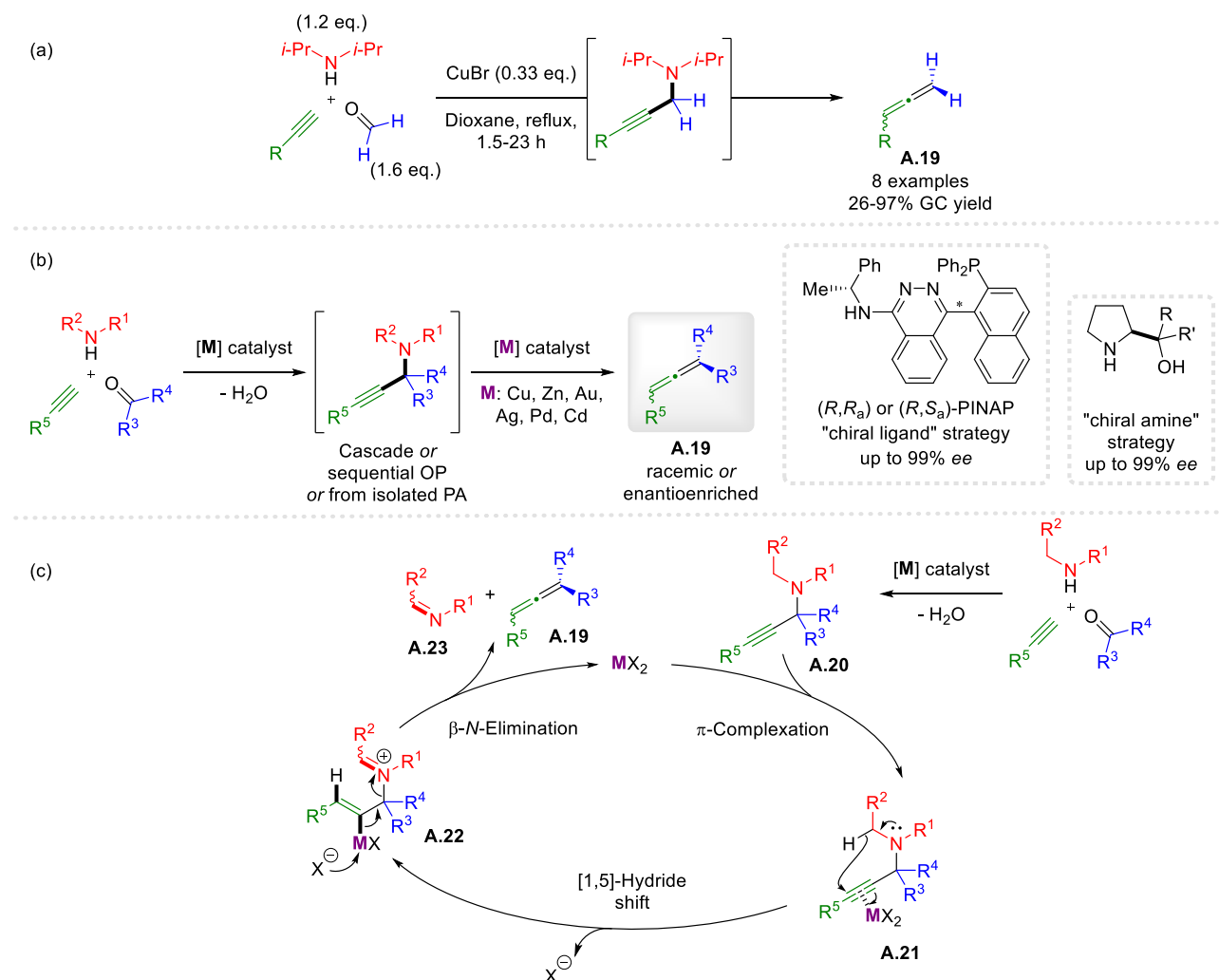
Synthetic applications presented in this part were selected because they showcase the versatile reactivity of propargylamines and/or due to the attractive “green” nature of the experimental conditions. Not surprisingly, many sequential or cascade procedures benefit from the unique simultaneous presence of the amine and alkyne moieties in propargylamines.

3.1. Synthesis of Allenes

Besides their numerous applications for the synthesis of heterocycles, propargylamines are also valuable precursors of allenes **A.19**. Historically, this was first observed in an impressive CuBr-catalysed cascade reaction between paraformaldehyde, diisopropylamine and terminal alkynes by CRABBÉ and co-workers in 1979 (**Scheme 13a**).^[53] This allenation from terminal alkynes (ATA reaction) was then extended to the use of aldehydes and ketones after more than 30 years, with pioneering contributions from MA and co-workers (**Scheme 13b**).^[54] Mechanistically, propargylamine **A.20** formation results from a metal-catalysed carbonyl-amine-alkyne coupling reaction (**Scheme 13c**). The subsequent allenation initiates through electrophilic activation of the alkyne upon π -complexation of the LEWIS acid (\rightarrow **A.21**). This lowers the activation energy barrier for a nitrogen-assisted [1,5]-hydride migration in a rate-determining step to yield organozinc compound **A.22**. The latter evolves through β -N elimination into allene **A.19** and imine **A.23**, along with the regeneration of the catalyst.^[55]

Interestingly, chiral allenes are accessible from chiral propargylamines through a centre-to-allene-axis chirality transfer. This is referred to as enantioselective ATA (EATA) reaction and

can be achieved through asymmetric catalysis using chiral ligands to form enantioenriched propargylamines or by starting from enantiopure amines with prolinol derivatives usually affording the highest enantiomeric excesses (up to 99% *ee*).



Scheme 13. Propargylamines as precursors of allenes.^[53–55]

PINAP: 4-[2-(diphenylphosphino)-1-naphthalenyl]-*N*-[1-phenylethyl]-1-phthalazinamine. OP: one-pot. PA: propargylamine.

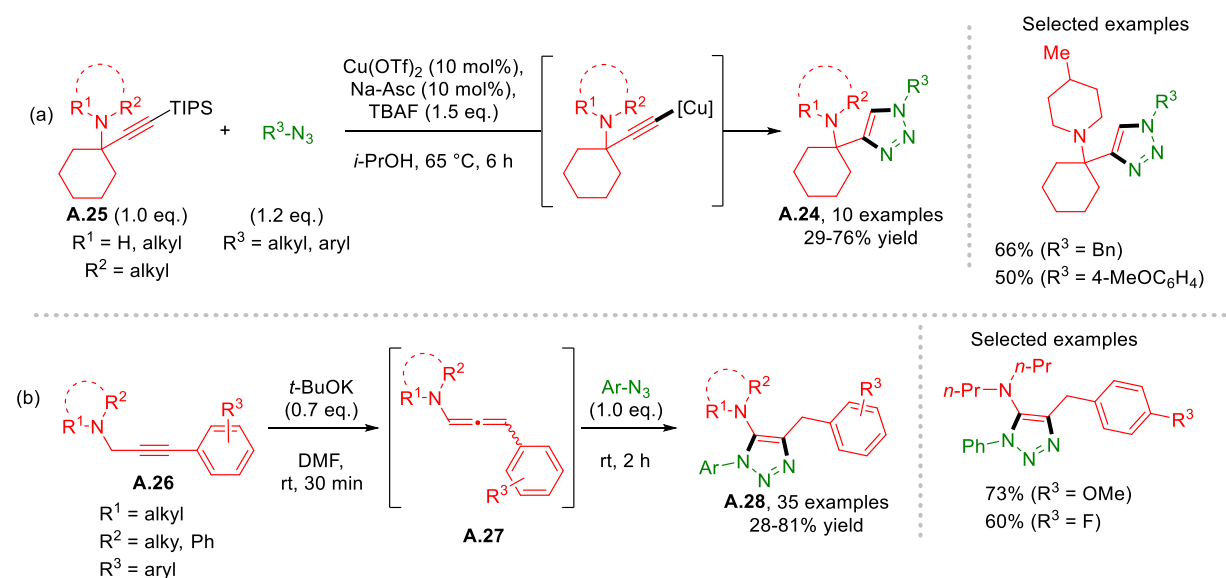
Although a cascade approach to allenes from simple starting materials is undoubtedly the most desirable strategy, it remains a highly challenging task. Often the propargylamine is formed in a first step and converted into the allene after isolation or in a sequential one-pot procedure. Metal salts and complexes derived from copper, zinc, and gold are frequently used but silver, palladium, and cadmium have also been reported for the allenation of propargylamines. Although highly attractive, the ATA reaction still presents several drawbacks. Most procedures rely on high catalyst loadings (up to 80 mol%), high temperatures (> 100 °C), and long reaction times (up to days), as well as limited functional group tolerance and poor to moderate conversions and yields.

3.2. Synthesis of Five-Membered Heterocycles

3.2.1. 1,2,3-Triazoles

The alkyne moiety in propargylamines has been utilised for the synthesis of amino-1,2,3-triazoles. LARSEN and co-workers, for instance, developed a cascade silyl deprotection/CuAAC reaction for rapid access to 1,2,3-triazoles **A.24** bearing α -tertiary amines in 4 position using “green” *i*-PrOH as solvent (Scheme 14a).^[56] The corresponding α -tertiary propargylamines **A.25** were produced in one step *via* KA² reaction. This represents thus an overall step- and atom-economical approach towards potentially therapeutically valuable core-structures.^[57,58]

Recently, WU and co-workers reported a complementary approach towards amino-1,2,3-triazoles starting from α -primary propargylamines **A.26** (Scheme 14b).^[59] Their one-pot procedure initiates with the base-catalysed isomerisation of the propargylamine into the corresponding allenylamine **A.27**. The latter is suggested to undergo an intermolecular cyclisation with the aromatic azide (ArN₃) to yield fully substituted 5-amino-1,2,3-triazoles **A.28**. While the reaction proceeded at room temperature, no “green” solvent alternative to DMF was mentioned.

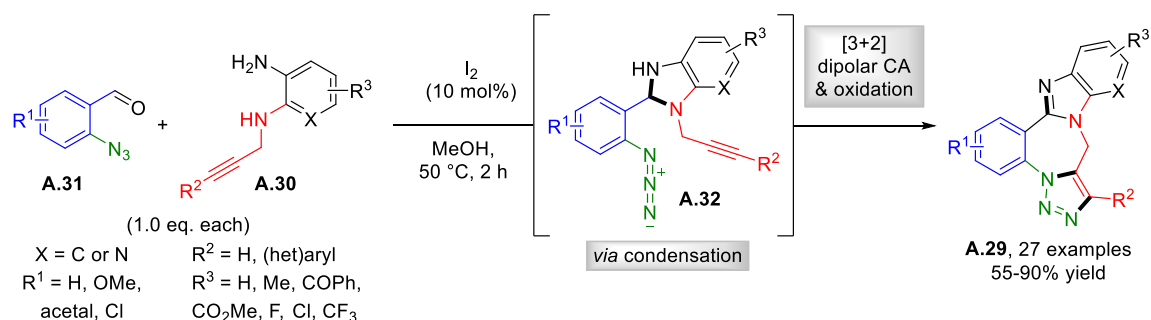


Scheme 14. Propargylamines as precursors of amino-1,2,3-triazoles.^[56,59]

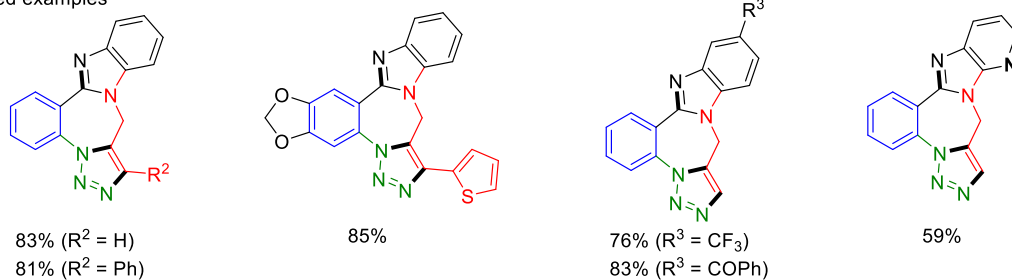
Na-Asc: sodium ascorbate. TBAF: tetrabutylammonium fluoride.

While the strategies above are exclusively based on the reactivity of the propargylamine's alkyne moiety, KUNDU and co-workers reported an attractive cascade reaction towards benzimidazotriazolobenzodiazepines **A.29** from *N*¹-alkyne-1,2-diamines **A.30** (Scheme 15). The latter underwent an iodine-catalysed condensation with *ortho*-azidobenzaldehydes **A.31** to yield hemiaminals **A.32**. Subsequent intramolecular [3+2] dipolar cycloaddition and aerobic oxidation produced numerous and diversely functionalised benzodiazepine-based polycycles **A.29** in good to excellent yields (50-90%). Rewardingly, this cascade reaction used equimolar amounts of both starting materials, and proceeded in MeOH (or similarly in EtOH) in two hours at mild

50 °C. Furthermore, the product scope generally reveals a satisfying performance for either electron-donating or -withdrawing groups for R¹ to R³. The compatibility of α -substituted propargylamines, and aliphatic alkynes was, however, not mentioned.



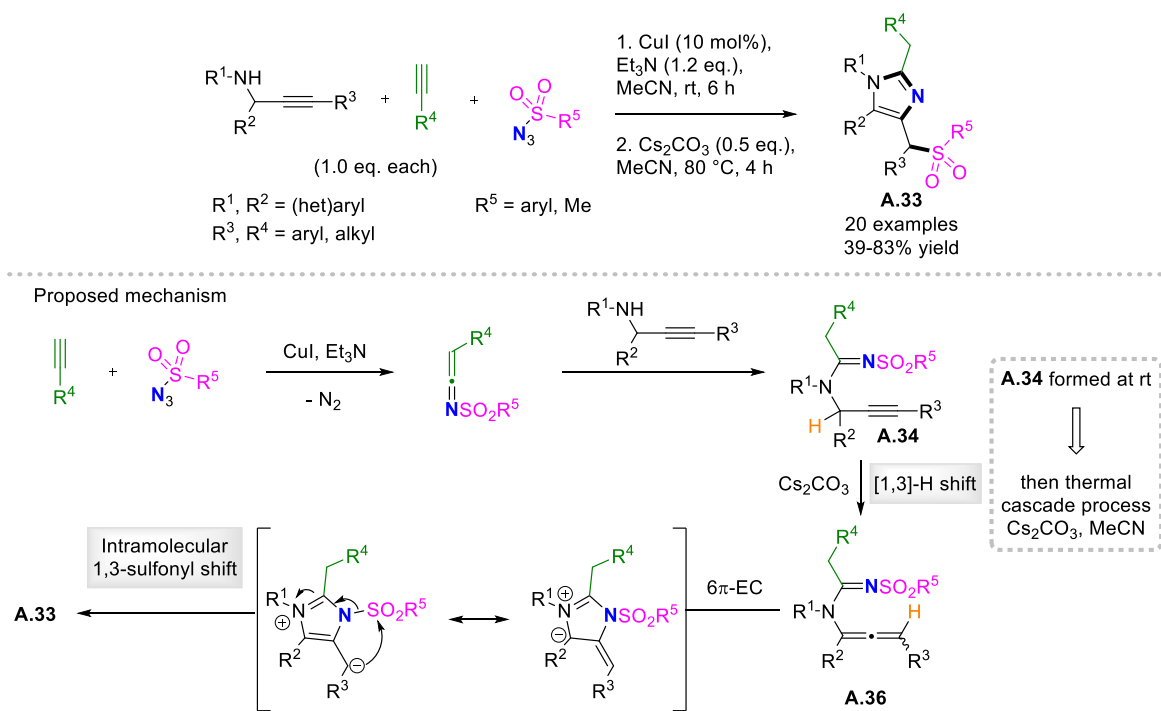
Selected examples



Scheme 15. Propargylamines as precursors of benzimidazotriazolobenzodiazepines **A.29**.^[60]

3.2.2. Imidazoles

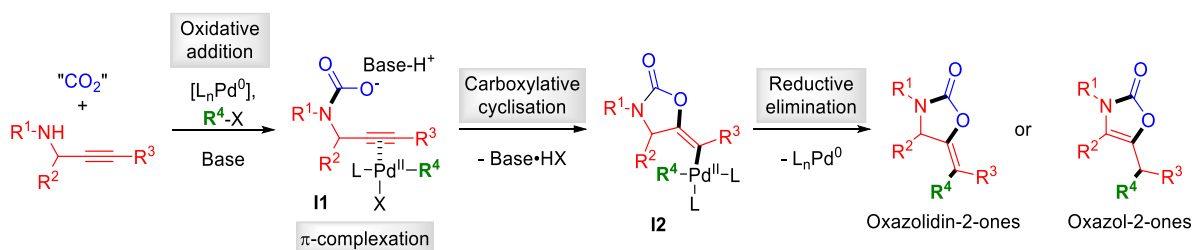
Apart from benzimidazoles, propargylamines represent appropriate precursors of additional imidazoles. In 2012, WANG and co-workers reported a sequential copper- and base-catalysed synthesis of fully substituted imidazoles **A.33** from α -secondary propargylamines, terminal alkynes and sulfonyl azides (R⁵SO₂N₃) (**Scheme 16**).^[61] Rewardingly, imidazoles **A.33** can be obtained in a one-pot procedure with the initiating 3CR providing *N*-sulfonylamidine **A.34** proceeding at room temperature. Unfortunately, dilute conditions in MeCN as an undesirable solvent were required due to the inherent instability of sulfonyl azides. Nevertheless, this protocol tolerated aromatic and aliphatic alkynes and amines, and used nearly equimolar amounts of each component. Mechanistically, the nucleophilic addition of the amine onto the sp carbon of the *in situ* generated *N*-sulfonylketenimine **A.35** yields *N*-sulfonylamidine **A.34**. Next, [1,3]-hydrogen shift gives the tautomeric allenylamine *N*-sulfonylamidine **A.36**. A 6 π -electrocyclisation (EC) with subsequent [1,3]-sulfonyl transfer finally leads to imidazole **A.33**. Cross experiments revealed the intramolecular nature of the [1,3]-sulfonyl shift.



Scheme 16. Propargylamines as precursors of fully substituted imidazoles.^[61] EC: electrocyclisation.

3.2.3. Oxazolidin-2-ones and Oxazol-2-ones

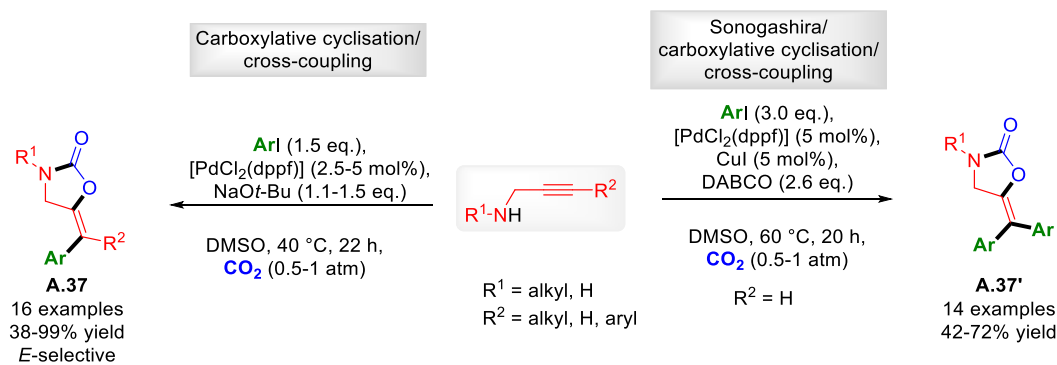
Reactions of propargylamines with electrophiles incorporating heteroatoms other than nitrogen afford mixed *N*-heterocycles. The carboxylative cyclisation of propargylamines with carbon dioxide, for instance, affords oxazolidin-2-ones and oxazol-2-ones (Scheme 17). This reaction commonly requires high temperature, pressure (e.g., supercritical CO₂) and/or strong promoting agents due to the high thermodynamic and kinetic stability of carbon dioxide. In the following, selected examples of milder cascade carboxylative cyclisation/cross-coupling reactions under palladium catalysis are presented (Scheme 17). The alkynophilicity of Pd^{II} facilitates the carboxylative cyclisation step *via* π -complex **I1**. The so-formed vinyl Pd^{II} species **I2** generates the oxazolidin-2-one through reductive elimination, regenerating the catalyst. In some cases, oxazolidin-2-ones then isomerise to the corresponding oxazol-2-ones.



Scheme 17. Propargylamines as precursors of oxazolidin-2-ones and oxazol-2-ones *via* carboxylative cyclisation/cross-coupling reaction cascade processes.

In 2016, NEVADO and co-workers presented two innovative palladium-catalysed MCRs using atmospheric CO₂ to access oxazolidin-2-ones **A.37** and **A.37'** from α -primary propargylamines and aryl iodides.^[62] Using 1.5 equivalents of aryl iodide in the presence of [PdCl₂(dppf)]/NaOt-Bu selectively afforded the desired oxazolidin-2-ones **A.37** in often high yields (Scheme 18,

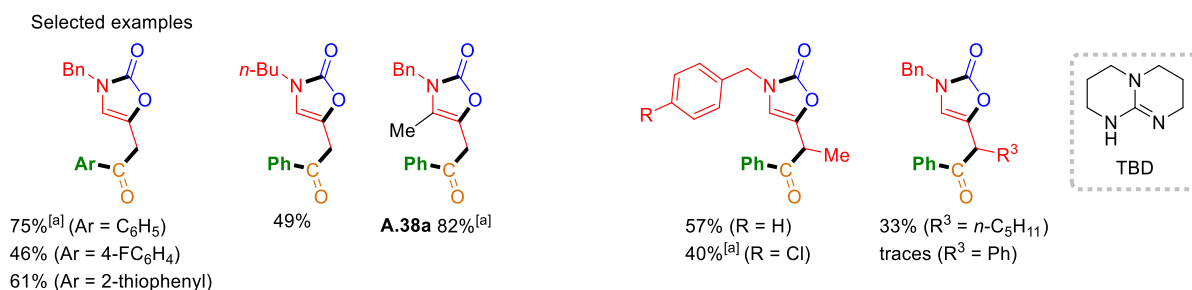
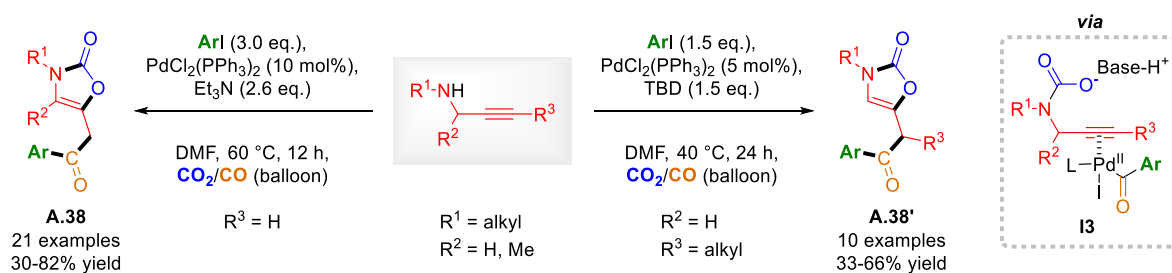
left). For propargylamines bearing a terminal alkyne, however, a SONOGASHIRA cross-coupling before the oxazolidin-2-one formation was observed, resulting in a mixture of mono- and diarylated products (**Scheme 18**, right). Increasing the aryl iodide equivalents, adding catalytic copper iodide, and employing sub-stoichiometric DABCO as a base then enabled selective access to the diaryl vinylidene products **A.37'**. Unfortunately, neither α -secondary nor α -tertiary propargylamines were included in the scope.



Scheme 18. Selective synthesis of mono- and diarylated oxazolidin-2-ones.^[62]
 dppf: bis(diphenylphosphino)ferrocene. DABCO: 1,4-diazabicyclo[2.2.2]octane.

Furthermore, HE and co-workers recently disclosed a 4CR of propargylamines, carbon dioxide, carbon monoxide, and aryl iodides (**Scheme 19**).^[63] Compared to the above-presented approaches, this strategy included an additional carbonylative step to afford an acylpalladium(II) intermediate **I3** prior to the carboxylative cyclisation. The resulting oxazolidin-2-ones isomerise to the corresponding oxazol-2-ones. Reaction conditions differ slightly depending on the absence (\rightarrow **A.38**, **Scheme 19**, left) or presence (\rightarrow **A.38'**, right) of an alkyne substituent in the propargylamine substrate.

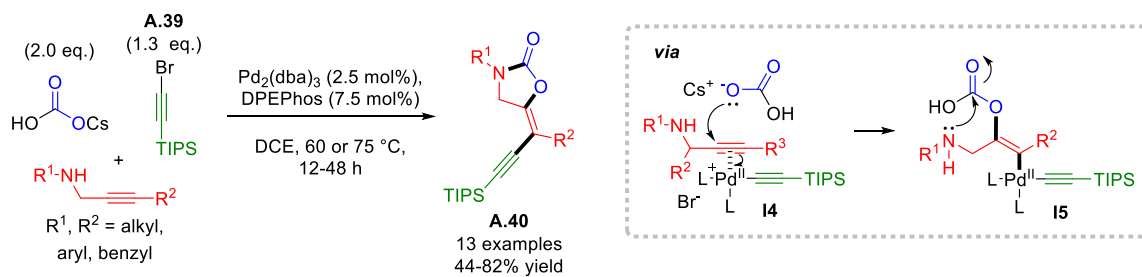
This transformation represents an attractive approach to incorporate two C₁ synthons in a single catalytic operation. Apart from this advantage, it is based on up to three equivalents of aryl iodide, relatively high catalyst loadings (5-10 mol%), and the use of DMF as an undesirable solvent. Regarding the product scope, mostly benzylamines were investigated but also other aliphatic amines were successful. Aromatic amines, however, were not mentioned. Unfortunately, an α -tertiary propargylamine failed to give the corresponding oxazolidin-2-one, whereas oxazol-2-one **A.38a** (R² = Me) was obtained in 82% yield from an α -secondary propargylamine. Apart from terminal alkynes, only aliphatic alkynes were found compatible.



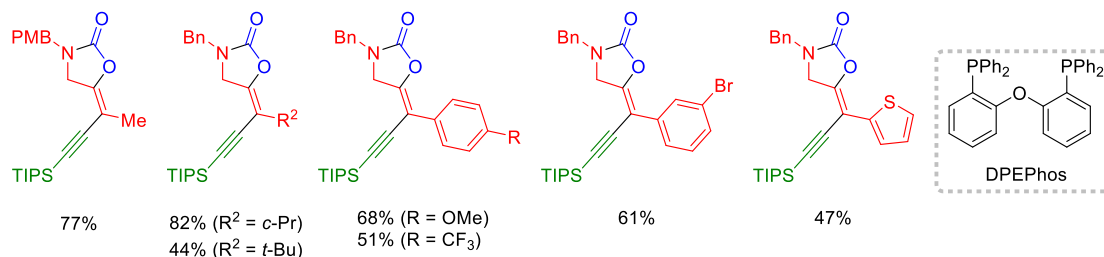
Scheme 19. Pd-catalysed four-component carboxylative cyclisation of propargylamines with aryl iodides, CO₂ and CO.^[63]

^[a] Yield estimated *via* ¹H NMR using 1,3,5-trimethoxybenzene as internal standard. TBD: 1,5,7-triazabicyclo[4.4.0]dec-5-ene.

Another important contribution was made by WASER and GREENWOOD replacing aryl iodides with (triisopropylsilyl)ethynyl bromide **A.39** as electrophile to access alkynyl oxazolidin-2-ones **A.40** (Scheme 20).^[64] Interestingly, caesium hydrogen carbonate was used as a solid and easy-to-handle carbon dioxide substitute. Rather than a thermal carbonate decomposition to liberate CO₂, the authors assume a site-selective nucleophilic addition of the hydrogen carbonate onto the π -activated alkyne **I4**. The oxazolidin-2-one is then generated through intramolecular condensation in vinyl complex **I5**. Regarding the substrate scope, α -primary propargylamines with aromatic and aliphatic alkyne substituents were employed. α -Secondary and α -tertiary propargylamines, however, were not compatible with this protocol. Furthermore, alkyl or aryl bromoalkynes were unsuccessful, resulting in (triisopropylsilyl)ethynyl bromide as the only suitable bromoalkyne.



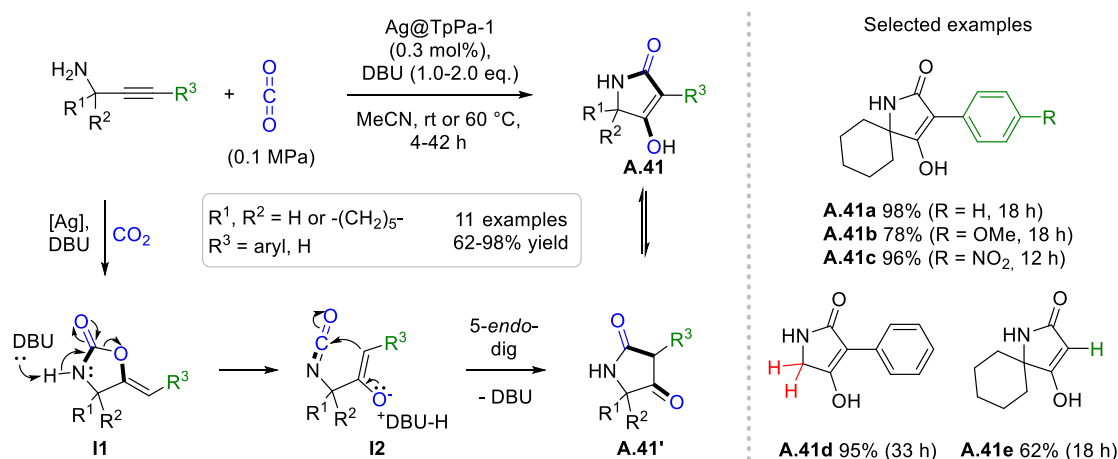
Selected examples



Scheme 20. Pd-catalysed carboxy-alkynylation of propargylamines.^[64]

3.2.4. Tetramic Acids

Depending on the catalytic system, the oxazolidin-2-ones formed from propargylamines *via* CO₂ fixation are further rearranged into tetramic acids. Accordingly, MANIRUL ISLAM and co-workers prepared tetramic acids **A.41** using silver nanoparticles dispersed on a covalent organic framework (TpPa-1) (**Scheme 21**).^[65] To confirm the heterogeneous nature of this catalytic system, the authors performed a hot filtration test, showing only minimal silver leaching in the ppm range. What is more, the catalyst was reused at least four times without a significant decrease in yield. Mechanistically, this is believed to proceed through DBU-mediated fragmentation of oxazolidin-2-one **II** to isocyanate **I2**. The latter then undergoes a 5-*endo*-dig cyclisation to pyrrolidine-2,4-dione **A.41'**, the tautomeric form of **A.41**. Regarding the alkyne substituent, various arylalkynes afforded the desired tetramic acids in high yields (see examples **A.41a-d**). A terminal alkyne was also tolerated under optimised conditions, albeit leading to tetramic acid **A.41e** in a lower 62% yield. In contrast, alkylalkynes are not reported and besides cyclohexyl, solely α -primary propargylamines are presented bearing primary amines (\rightarrow **A.41d** e.g.). It is worth mentioning, that α -primary propargylamines afforded high yields even at room temperature with one equivalent of DBU.

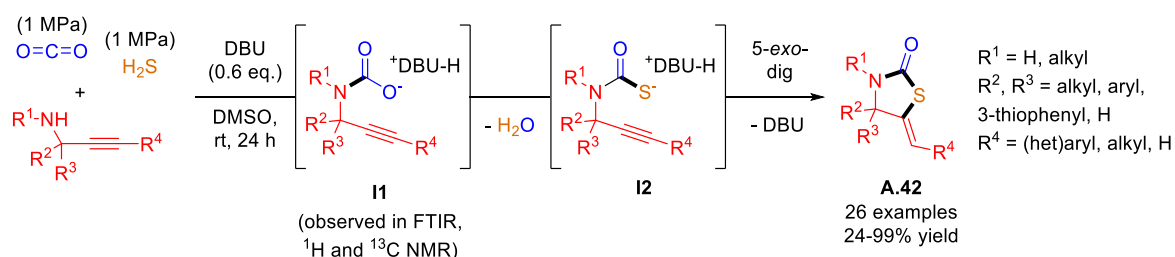


Scheme 21. Propargylamines as precursors of tetramic acids.^[65]

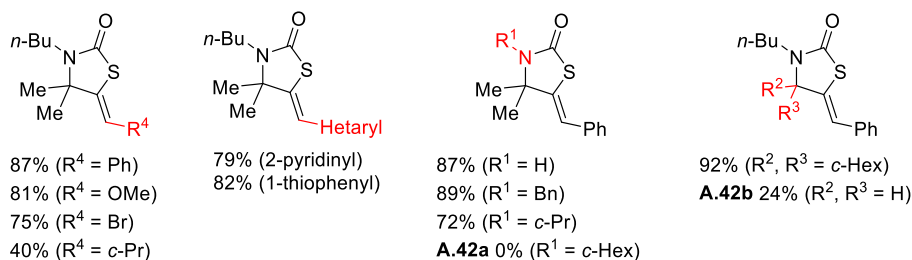
TpPa-1: Schiff-base polymer obtained from 1,3,5-triformylphloroglucinol (Tp) and 1,4-phenylenediamine (Pa-1).

3.2.5. Thiazolidin-2-ones

Thiazolidin-2-ones **A.42** represent another valuable class of five-membered heterocycles that can be derived from propargylamines. In 2022, ZHU and co-workers targeted this compound class establishing a DBU-catalysed 3CR involving carbon dioxide and hydrogen sulfide in an attractive way to process these waste gases (**Scheme 22**).^[66] NMR and FT-IR experiments enabled to elucidate the mechanism, which initiates with carbamate **I1** formation aided by DBU base. Next, the thiocarbamate **I2** is formed through *O/S*-exchange with H₂S, followed by a 5-*exo*-dig *S*-cyclisation to yield the thiazolidine-2-one **A.42**. The reaction was scalable to a multi-gram scale (10 mmol amine) and numerous diversely substituted propargylamines were compatible. Unfortunately, thiazolidine-2-one **A.42a** derived from a cyclohexylamine-based propargylamine did not react, probably due to its lower nucleophilicity. Furthermore, the use of aromatic amines was not reported. Whereas diversely functionalised α -tertiary and α -secondary propargylamines led to high yields, thiazolidine-2-one **A.42b** resulting from an α -primary propargylamine was isolated in a low 24% yield.



Selected examples



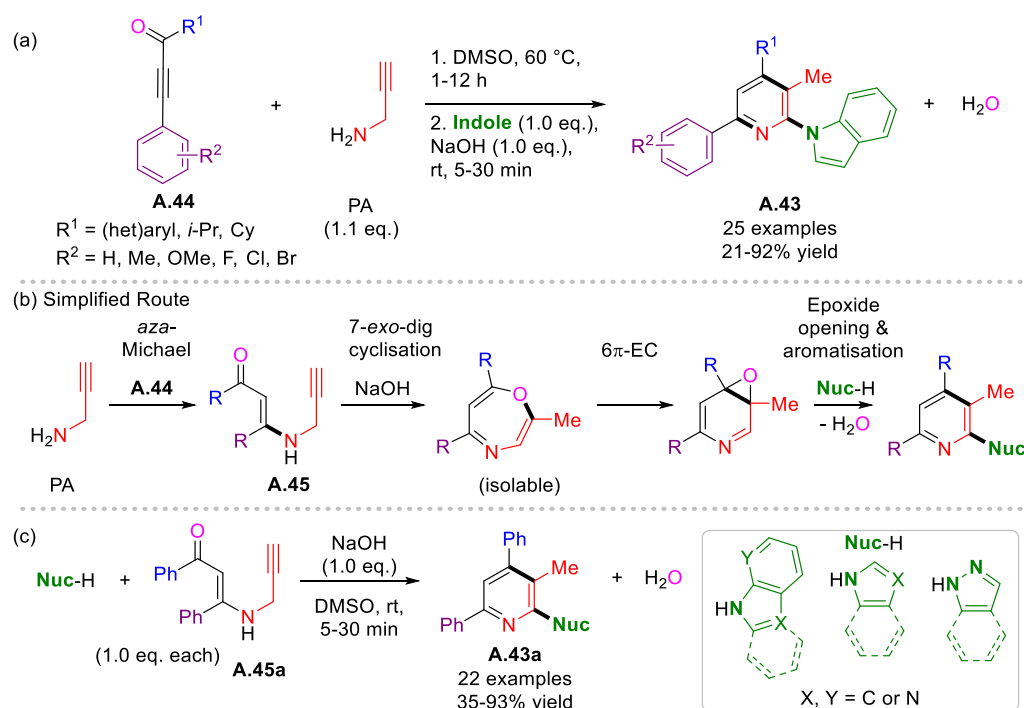
Scheme 22. Propargylamines as precursors of thiazolidin-2-ones.^[66]

3.3. Synthesis of Six-Membered Heterocycles

Propargylamines have been widely used as precursors for the synthesis of six-membered heterocycles, such as pyridines and their derivatives. Examples of piperazines and 4-amino-4*H*-pyranes will also be given in this section. Of course, many other six- or even higher-membered heterocycles have been prepared but are not included here.^[12]

3.3.1. Pyridines

As a noteworthy example, CUI and co-workers disclosed a base-mediated one-pot synthesis of tetrasubstituted pyridines **A.43** from ynones **A.44**, propargylamine (PA), and indole (**Scheme 23a**).^[67] First, PA is reacted with ynone **A.44** to give *N*-propargyl enaminone **A.45** via *aza*-MICHAEL addition in DMSO at 60 °C. Inexpensive NaOH then induces a cascade reaction including a 7-*exo*-dig cyclisation, a 6 π -electrocyclisation (EC), and a vinylogous epoxide ring opening as key steps (**Scheme 23b**). Furthermore, this cascade reaction was extended to various other *N*-heterocyclic nucleophiles starting from the pre-formed enaminone **A.45a** (**Scheme 23c**). While DMSO is considered a problematic solvent,^[68] this procedure nevertheless benefits from short reaction times at room temperature for the *N*-pyridylation step, satisfying atom economy and reagent stoichiometry, as well as a broad product scope.

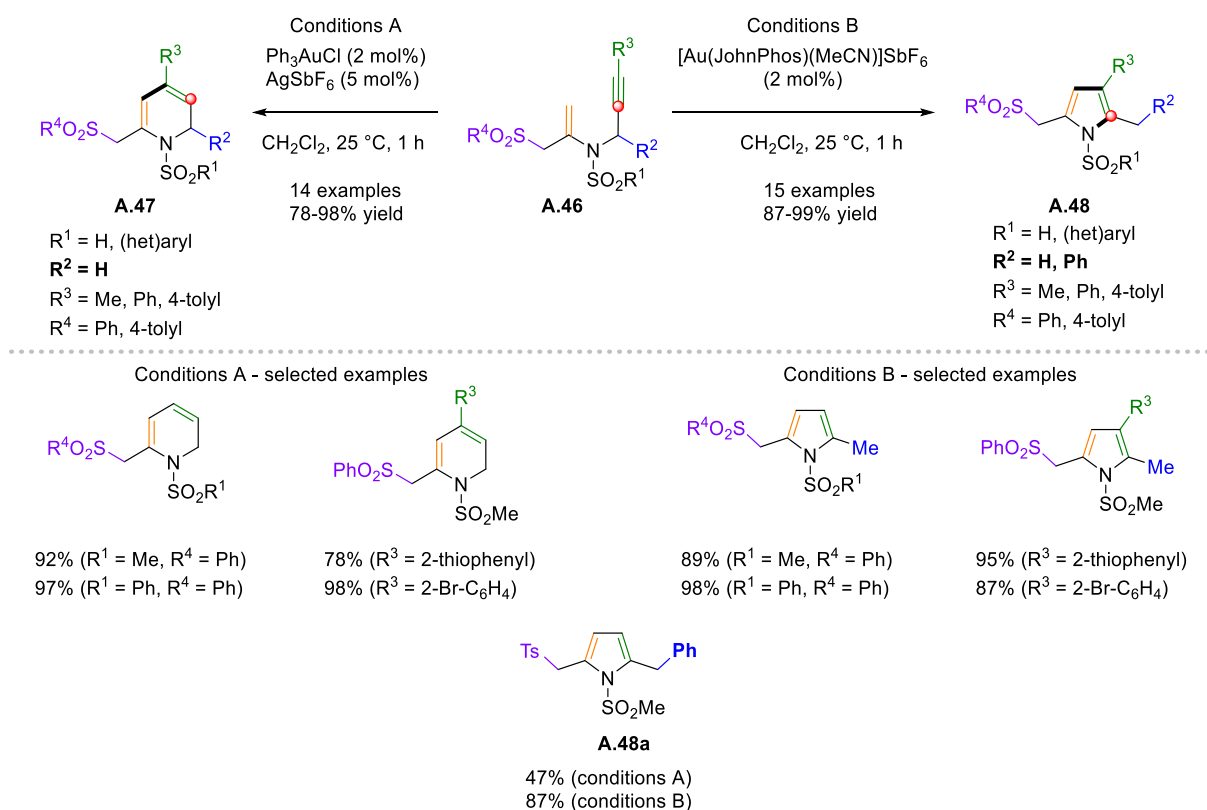


Scheme 23. Propargylamines as precursors of tetrasubstituted pyridines.^[67]

3.3.2. 1,6-Dihydropyridines

In **Scheme 23**, *N*-propargyl β -enaminones reacted to pyridines. MENON and co-workers, in turn, converted similar propargylamine-based 3-*aza*-1,5-enynes **A.46** into 1,6-dihydropyridines **A.47** through Au^I/Ag^I-catalysed cycloisomerisation (**Scheme 24**, left).^[69] The reaction proceeds

in CH₂Cl₂ at room temperature and several 1,6-dihydropyridines **A.47** were obtained in high yields (78-98%) in only one hour. Up to four diversity points were varied in the starting materials but the number of functional groups investigated is relatively limited and no clear electronic effects were observed. In addition, the scope includes only aromatic and terminal alkynes. Notably, divergent catalysis was observed shifting to ECHAVARREN's catalyst (Scheme 24, right). In this case, the corresponding pyrroles **A.48** were isolated in excellent yields (87-99%). It should nevertheless be stressed that catalyst control can be overwritten by the substitution frame of the enyne. Indeed, pyrrole **A.48a** (R² = Ph) was obtained in both optimised catalytic systems, with a superior yield using ECHAVARREN's catalyst (87% vs. 47%). For mechanistic details on both cycloisomerisation reactions, please see section VI-2.2.

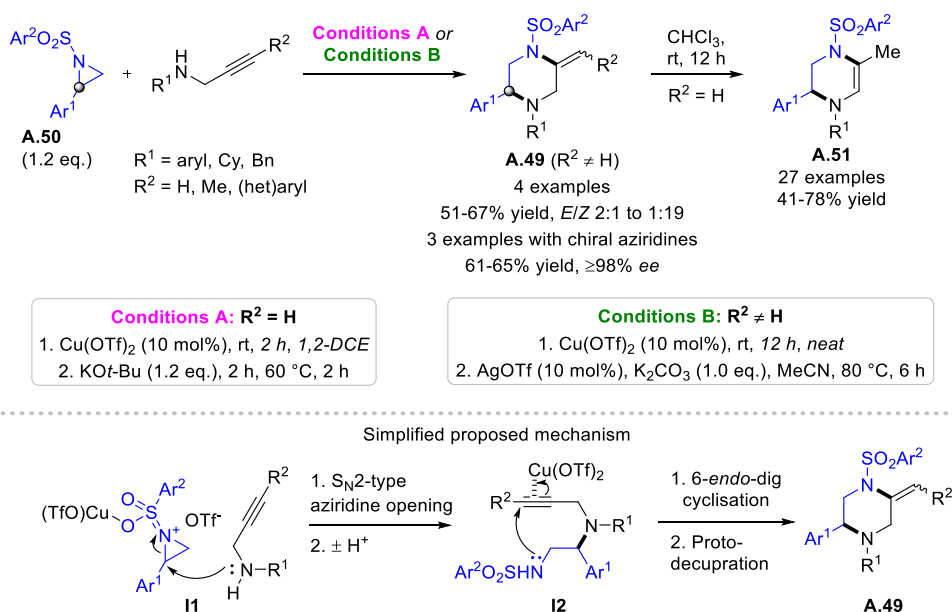


Scheme 24. Propargylamines as precursors of 1,6-dihydropyridines and pyrroles.^[69]

3.3.3. Piperazines and 1,2,3,4-Tetrahydropyrazines

In 2018, PUNNIYAMURTHY and co-workers reported the sequential one-pot copper-catalysed synthesis of piperazines **A.49** from *N*-sulfonylaziridines **A.50** and α -primary propargylamines (Scheme 25).^[70] With propargylamines lacking an alkyne substituent, the corresponding 1,2,3,4-tetrahydropyrazines **A.51** were formed through isomerisation in CHCl₃. Upon copper complexation to **I1**, nucleophilic aziridine ring opening proceeded at room temperature. The so-formed 6-yne-sulfonamide **I2** undergoes a 6-*endo*-dig hydroamination towards piperazines **A.49**. For unsubstituted alkynes, stoichiometric amounts of KO*t*-Bu sufficed to promote the hydroamination, whereas internal alkynes required the use of AgOTf/K₂CO₃ for electrophilic

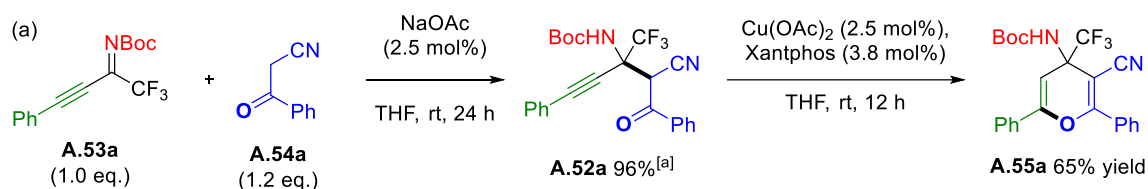
and nucleophilic activation. Most propargylamines are derived from anilines but aliphatic amine substituents were also compatible, albeit less efficient. Chiral, enantiopure aziridines were observed to produce the corresponding piperazines with high enantiomeric purities ($\geq 98\%$ *ee*). Mechanistically, this suggests a stereospecific S_N2 ring opening of the aziridine.



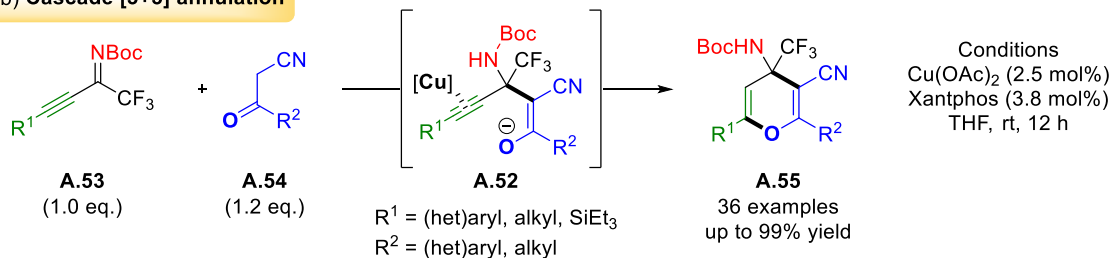
Scheme 25. Propargylamines as precursors of piperazines.^[70]

3.3.4. 4-Amino-4*H*-Pyranes

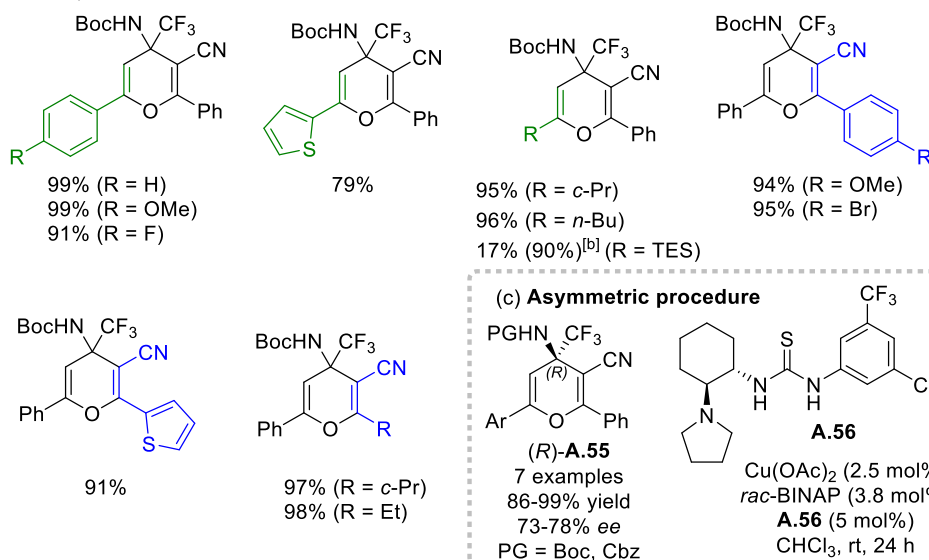
Recently, ZHANG and co-workers prepared propargylamine **A.52a** via a highly efficient and mild NaOAc-catalysed MANNICH-type reaction of alkynyl imine **A.53a** with cyano ketone **A.54a** (Scheme 26a).^[71] Interestingly, propargylamine **A.52a** underwent a regioselective 6-*endo*-dig *O*-cyclisation under copper catalysis, resulting in valuable 4-amino-4*H*-pyrane **A.55a** in 65% yield. Beneficially, this two-step procedure was extended into a cascade [3+3] annulation of α -CF₃ alkynyl ketimines **A.53** and α -cyano ketones **A.54** using copper salts with basic anions, in particular $Cu(OAc)_2$ (Scheme 26b). As a result, numerous diversely functionalised 4-amino-4*H*-pyranes **A.55** incorporating a quaternary CF₃-substituted carbon were produced in excellent yields. This protocol presents a broad functional group tolerance and proceeds with various alkynyl ketimines **A.53** and cyano ketones **A.54** with yields as high as 99%. In fact, diverse alkyl substituents (R^1) are compatible with this transformation. While mostly arylalkynes were examined with yields above 80%, 2-thiophenyl-, alkyl- and silylalkynes were also successful. Similarly, the ketone substituent (R^2) could represent functionalised (het)aryl or alkyl groups. Interestingly, the authors also set up asymmetric conditions using a chiral thiourea **A.56** as cocatalyst in the presence of racemic BINAP as copper ligand (Scheme 26c). Excellent yields of (*R*)-4*H*-pyranes (*R*)-**A.55** with good enantioselectivities (73-78% *ee*) were obtained.



(b) Cascade [3+3] annulation



Selected examples



Scheme 26. Propargylamines as precursors of highly functionalised 4-amino-4H-pyranes.^[71]

^[a] Obtained as a mixture of diastereoisomers and tautomers. ^[b] PPh₃ was used as ligand instead of Xantphos. PG: protecting group.

Chapter II – Zeolites

1. Generalities

Zeolites are naturally occurring minerals and were discovered in 1756 by the mineralogist Axel Frederik CRONSTEDT.^[72] CRONSTEDT observed that when heated, these minerals start boiling, due to the evaporation of adsorbed water molecules. Hence, he baptised them “zeolites” from the Greek word “*zeo-lithos*” (*zeo* for boiling and *lithos* for stone), which means "boiling stone". To date, there are about 40 natural zeolites reported, which are little used in chemistry except in some separation or adsorption processes of small molecules. Most zeolites are not of natural origin and there are currently more than 230 synthetic zeolites reported in the Atlas of Zeolite Structure Types published by the International Zeolite Association Structure Commission (IZA-SC).ⁱ IUPAC references the different zeolites with a three-letter code derived from their original name applying uniform rules (e.g., FAU for the faujasite topology among which exist zeolites X and Y).^[73]

1.1. Structure and Properties

Zeolites are highly organised, crystalline aluminosilicates mostly constituted of tetrahedral neutral silicate SiO_4 and negatively charged aluminate AlO_4^- units, also called T-members (**Figure 4a**). During the crystallisation process of the microporous zeolite framework, different morphologies are accessible depending on the relative assembling of second-order building units. Indeed, channel- or cage-type zeolites are produced depending on the conditions. The negatively charged three-dimensional framework incorporates charge-compensating cations, which can be of different natures (**Figure 4b**). In naturally occurring zeolites, the most abundant alkali or alkaline earth cations such as Na^+ , K^+ and Ca^{2+} are encountered. Furthermore, protons as the smallest possible cation or ammonium-loaded zeolites exist.

ⁱ <http://www.iza-structure.org/databases>

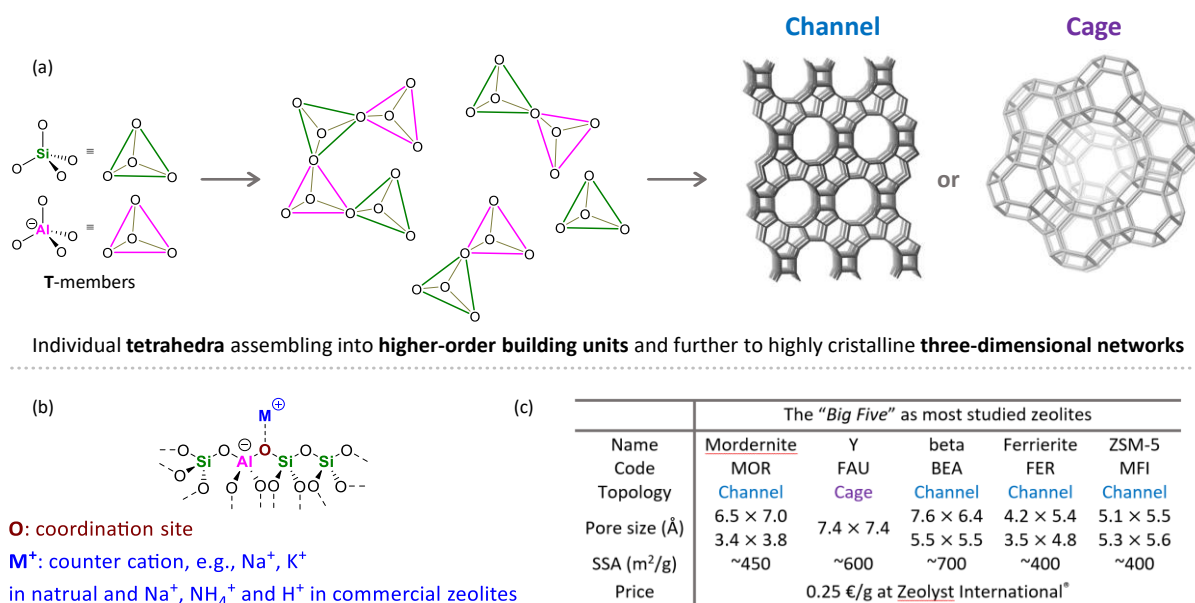


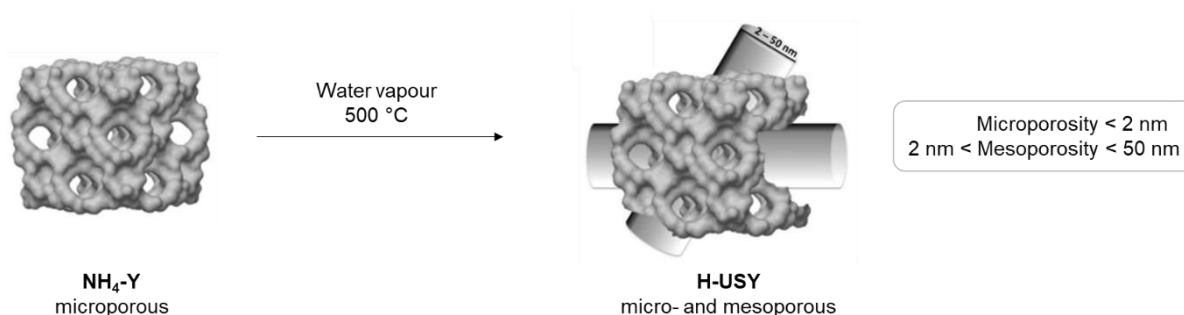
Figure 4. (a) Structural assembly of zeolites. (b) Simplified representation of the aluminosilicate framework. (c) Key properties of frequently used zeolites.

Figure 4c shows the key properties of the most studied zeolites. Besides pore shape, pore size, specific surface area (SSA), and Si/Al ratio (SAR) characterise zeolites. The SAR defines the number and density of negative charges present in the framework and repulsive COULOMB interaction requires a SAR > 1, which is known as the LOEWENSTEIN rule.^[74] The greater the Al-content, the more (BRØNSTED or LEWIS) acidic sites are available per mass unit. Depending on the SAR, zeolites are classified into three categories: i) low silica (or aluminium-rich) zeolites with SAR around 1, ii) intermediate silica zeolites with SAR ≈ 1.5 - 5, and high silica zeolites with SAR ≥ 10.

Microporosity (i.e., pore size $\phi < 20 \text{ \AA}$)^[75] is a unique property of zeolites and the pore size varies among the different zeolite types. While their microporous three-dimensional environment allows shape selectivity, this comes at the cost of limited mass transfer and restricted diffusivity increasing with the size of the guest molecules. In applications where these inconveniences become significant, the presence of higher-order porosity, such as meso- ($20 < \phi < 500 \text{ \AA}$) and macroporosity ($\phi > 500 \text{ \AA}$),^[75] could counteract in so-called complementary porous materials. This recent concept is described as hierarchical porosity.^[76,77] Meso- or macropores coexisting in microporous zeolites may facilitate both the access and the exit of molecules from active sites. As a result, reactants' and products' residence times on the shape-selective or catalytically active sites are reduced, thus limiting undesired side reactions. Nevertheless, an adequate equilibrium between the different porosities must be guaranteed, which in turn requires a highly controlled introduction of the complementary porosity, pore size, and abundance albeit preserving the overall stability of the framework.^[78,79] In fact, structural defects can arise depending on the method inducing complementary porosity producing less active

or shape-selective materials. Additionally, greater pores can also accommodate catalytically active sites and due to smaller confinement negatively impact the selectivity of the parent material.^[80] With exceeding pore size, molecule-surface interactions become negligible as the surface curvature flattens with greater pore size.

USY (ultra-stable Y) zeolite represents an example of a micro- and mesoporous zeolite. The mesoporosity is introduced by treating $\text{NH}_4\text{-Y}$ zeolite with water vapour at 500 °C (Scheme 27). This causes the partial dealumination of the framework producing mesopores. Fortunately, the faujasite topology and the crystallinity of the zeolite are not significantly altered. The superior performance of USY compared to its parent Y zeolite was for instance observed in industrially important processes, such as hydrocarbon conversions (e.g., cracking) and ammoxidation of ethane.^[81]



Scheme 27. Preparation of micro- and mesoporous H-USY through dealumination.

1.2. Main Applications

Zeolites are versatile materials that find a wide variety of applications due to their numerous attractive properties, such as their high specific surface area ($> 300 \text{ m}^2/\text{g}$) and their great adsorption and ion-exchange (IE) capacities. The three main applications in terms of tonnage use are their use as detergents, adsorbents and drying agents, as well as catalysts. Among these, detergents represent the largest contribution in terms of quantity, but about half of the zeolite market value is generated by their application as catalysts. Besides the previously mentioned characteristics of zeolites, this is due to their outstanding thermal and chemical stability. Consequently, zeolites often prove recyclable heterogeneous catalysts. This confers them numerous applications in industrial processes.

1.2.1. Zeolites as Ion-Exchangers

The negatively charged zeolite framework enables them to bind cations through electrostatic interactions. The reversibility of these interactions grants zeolites with a remarkable cation-exchange capacity. Indeed, they rapidly replaced phosphates which are known to promote eutrophication, as water softeners.^[82] Furthermore, zeolites proved efficient for the caption of

hazardous, radioactive isotopes, such as $^{137}\text{Cs}^+$ and were widely applied after the nuclear disasters in Chernobyl in 1986 and in Fukushima in 2011.

1.2.2. Zeolites in Adsorption and Separation Processes

Zeolites are largely used in adsorption and separation processes and are commonly referred to as molecular sieves. Since the 1950s zeolites allow to dry various gases and are also applied to the drying of organic solvents by adsorbing water molecules. Moreover, zeolites are “effective adsorbents in water and wastewater treatment”.^[83] The adsorption and separation properties of zeolites are directly dependent on their structural characteristics. More precisely, the form and the size of the pores, the hydrophobicity, and the nature of the charge-compensating cation are decisive factors, which can be modulated leading to highly selective materials for various applications.

1.2.3. Zeolites in Catalysis

Zeolites’ “sieving property” is also relevant in catalysis. Indeed, it influences the distribution of molecules as a function of their dimension, inducing the possibility of “shape selectivity”.^[84] Three main types of shape selectivity are listed below:

- **Reactant Shape Selectivity (RSS):** from a mixture of reactants, only those having compatible molecular dimensions to enter the zeolitic micropores have access to active sites. This selectivity is, for instance, exploited in the selective cracking of linear alkanes and alkenes over their branched isomers using zeolites with small pore dimensions.^[85]
- **Product Shape Selectivity (PSS):** a reaction occurring inside a zeolite that produces differently sized and shaped products sees its product distribution affected as a function of the zeolite’s pore dimensions. The preferential *para*-xylene formation through toluene alkylation with methanol over H-ZSM-5 zeolite is a noteworthy example.^[86]
- **Transition State Shape Selectivity (TSS):** similarly to the above-described selectivities, the confining zeolite micropores can favour a less bulky transition state over another e.g., leading to the selective formation of a particular diastereoisomer in cycloaddition reactions. Examples of such will be presented in section 3.3.2.

Besides their use in cracking,^[87] zeolites show great potential in the valorisation of bio-based materials. For instance, there is a rising interest to use zeolites in catalytic fast pyrolysis (CFP) of lignocellulosic biomass to produce aromatic hydrocarbons and olefins as fuels (or precursors).^[88] Both BRØNSTED and LEWIS acidic zeolites appear to be promising, with a particular emphasis on modified zeolites possessing additional mesoporosity to improve catalyst activity and lifespan. Yet, several challenges and limitations remain, such as the deciphering of catalyst deactivation mechanisms, robustness, and the recyclability of the zeolite catalysts. Furthermore,

and at the heart of this thesis, zeolites find numerous applications as catalysts in organic synthesis. Examples of protonic and metal-loaded zeolite catalysts are presented in section 3.3.

2. From Natural to Metal-Loaded Tailor-Made Zeolites

2.1. Natural Zeolites

Natural zeolites are found worldwide in intermediate and basic volcanic rocks. They almost invariably form secondarily, i.e., during the transformation of pyroclastic sediments in water-rich environments, at temperatures below 400 °C and pressures below 5 kbar. The formation of zeolites is essentially controlled by the soil composition, temperature, and pressure. Zeolites are formed when volcanic rocks react with aqueous solutions. The ratio of dissolved Si to Al and the pH of the solution are the main factors that determine which zeolites will crystallise. The formation of zeolites already starts at temperatures as low as 4 °C. As the temperature increases, different zeolites are formed. In turn, the pressure does not have a significant influence on the formation of zeolites. However, due to their porous structure, zeolites are generally only stable at pressures below 3-5 kbar. Zeolite deposits are known in almost all volcanic regions of the world, for example in the Deccan region of India, in Iceland, in the Eifel volcanic region, or on the Azores.

2.2. *De novo* Synthesis of Zeolites

It is important to mention that several million zeolite structures are theoretically possible and predicted to be stable.^[89] This highlights zeolites' great potential as tailor-made microporous materials for a myriad of applications. The great discrepancy with the actual number of reported zeolites, however, also shows that improvements in their preparation are still of relevance. As zeolites are crystallisation products, their relative stability is dependent on the lattice energy of their frameworks. The high number of possible zeolite structures remains on the highly combinatorial approach of the crystallisation process.

Zeolites are most commonly prepared *via* hydrothermal synthesis. The first hydrothermal synthesis was carried out by SAINTE-CLAIRE DEVILLE in 1862.^[90] This method, however, suffered from a lack of reproducibility. In 1948, BARRER reported the first reliable hydrothermal synthesis.^[91] Shortly after, industrialists prepared several new zeolites between 1950 and 1970. For instance, researchers MILTON and BRECK working for UNION CARBIDE synthesized the A,^[92,93] X;^[94,95] and Y^[96] zeolites. In 1961, BARRER discovered that the addition of an organic ammonium cation (originally tetramethylammonium) as a structuring agent during the crystallisation could influence the morphology of the zeolite.^[97] Following this seminal work, the MOBIL OIL company used various structuring agents (tetraethylammonium and tetrapropylammonium) to

synthesise the Beta^[98] and ZSM-5 zeolites,^[99] which are among the most commonly used zeolites today. Thanks to BARRER's discovery, a myriad of new zeolites has been prepared using diverse structuring agents and granted access to high-silica zeolites.^[100] Regardless of the type of zeolite prepared *via* hydrothermal synthesis, the same starting elements are required, namely a source of silicate (sodium silicate, tetraethoxysilane, ...), a source of aluminate (sodium aluminate, aluminium hydroxide, ...), water, a mineraliser (to solubilise silicates and aluminates) and a structuring agent (tetrapropylammonium, ...) (Figure 5). The different reagents are introduced in a precise order into an autoclave to form a gel. If needed, the autoclave is heated and set under pressure. Next, the zeolite is recovered by filtration and the structuring agent is then removed by calcination. By varying the source and the quantity of silicates and/or aluminates, the nature of the structuring agent, the type and concentration of the mineraliser, the order of addition of the reagents, the temperature, and the time in the autoclave, it is possible to access different morphologies of zeolites.^[100]

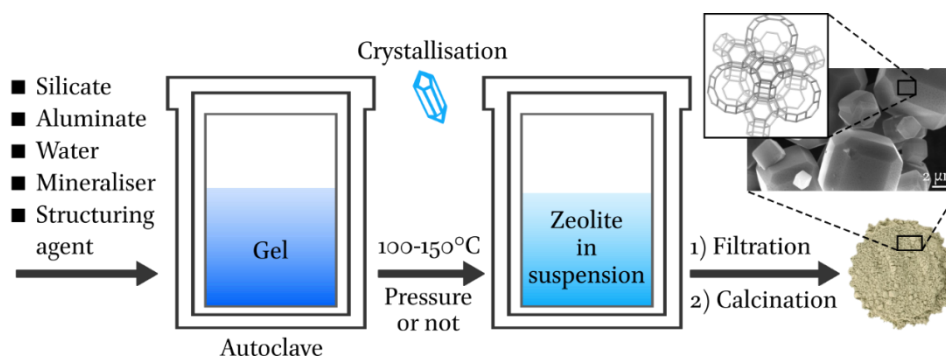


Figure 5. *De novo* synthesis of zeolites.

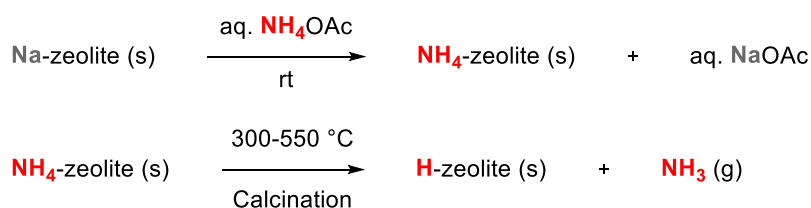
Generally, two families of mineralisers exist: alkali metal hydroxides and fluoride ions. Alkali metal hydroxides are the most common mineralisers and were applied to the first syntheses of zeolites. However, they require working at high pH, which can be problematic. Fluoride ions were introduced by FLANIGEN and PATTON in 1978.^[101] They allow to work at lower pH and to obtain larger zeolite crystallites with generally higher crystallinity.^[102] Nevertheless, the high toxicity and corrosivity of fluoride ions make this strategy less attractive for large-scale industrial applications.

2.3. BRØNSTED Acidic Zeolites

Depending on the silicate, aluminate, and mineralisers employed during the natural formation or the *de novo* synthesis of a zeolite, different alkali or earth alkaline cations are incorporated during the crystallisation of the zeolite network. In commercially available zeolites, these are frequently sodium ions. Such alkali- or earth alkaline-zeolites can undergo ion-exchange (IE) reactions to yield the corresponding ammonium form, NH₄-zeolites. Experimentally, this is typically achieved by consecutive multiple aqueous ion-exchange (AIE) reactions (see section

3.2.4. for details) in aqueous ammonium acetate (NH₄OAc) or nitrate (NH₄NO₃) solutions of defined concentration (Scheme 28, top).

From the NH₄-zeolites, it is possible to access the stronger protonic form, i.e., H-zeolites, through simple calcination causing the thermal removal of ammonia (Scheme 28, bottom). Typically, temperatures above 500 °C are employed with complete deammoniation after several hours. Given zeolites' great hydrothermal and chemical stability, the calcination can be performed under air. Nevertheless, in rare cases, procedures under inert atmosphere (e.g., He) or under vacuum have been described. In 2018, MOON and co-workers reported the optimisation of the deammoniation of an NH₄-Y zeolite under flowing helium.^[103] Their results show clear evidence that the material calcined at 400 °C for 24 h has a greater specific surface area along with a higher crystallinity compared to zeolites calcined at 500 or 600 °C. Prolonged heating at elevated temperatures thus causes a collapse of the crystalline structure. Furthermore, the authors observed *via* thermogravimetric analysis of the calcined materials that even at a calcination temperature of 300 °C, most of the ammonia is removed. These values, however, are likely to be dependent on the structural properties of each zeolite.



Scheme 28. Preparation of NH₄- and H-zeolites through cation-exchange.

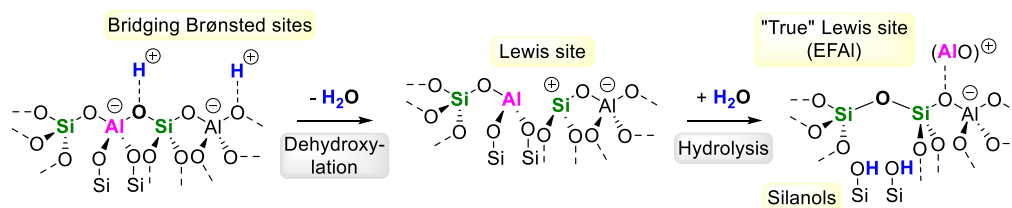
Beyond their preparation, zeolites can be described as solid acids. However, this constitutes different types of acidity, which must be defined more precisely. Roughly, a distinction can be made between BRØNSTED and LEWIS acidity, whereby several of these can be present. Furthermore, as with other mineral acids, not all zeolites are equally acidic. Thus, acidity is not only a function of nature (BRØNSTED and LEWIS) but also of the density and location of the acidic sites. Both also directly control acid strength.^[104] This will be explained in more detail for H-zeolites but similarities can be made for zeolites incorporating other metal cations.

Each topology has a characteristic Si-O-Al bond angle, which affects the lability of the H-zeolite bond in a Si-(OH)-Al constellation. This influences the partial charge and thus the acid strength of the corresponding material. With lower H-zeolite bond strengths, increased acidities result. Furthermore, however, the acid site density, depending on the intrinsic SAR, is also decisive for acidity. Therefore, zeolites with the same topology but different SAR can display different degrees of acidity. In general, the lower the aluminium content, the higher the acidity. Indeed, MORTIER argued that acid strength in Si-(OH)-Al groups is defined by the global electronegativity of the framework.^[105] The higher electronegativity of silicon compared to

aluminium (2.14 vs. 1.71, respectively on the SANDERSON's electronegativity scale), leads to an increased polarisation of the H-zeolite bond. However, as we all know from the example of hydrogen halides, not only the difference in electronegativities is crucial, but also the stability of the conjugate base defines the acid strength. In analogy to the weakly coordinating anions (WCA) principle, silicon-rich zeolites with high dispersion of aluminium show an improved charge delocalisation. Hence, silicon-rich zeolites behave as stabilised bases/anions resulting from stronger acids. Such zeolites could be considered soft like iodide, whereas aluminium-rich zeolites could be compared to hard fluoride.

It is also worth mentioning that the acidity of zeolites is also due to confinement effects.^[106] The spatially non-flat environment of the BRØNSTED acid sites is thought to have a reinforcing effect on the acidity.^[107] Based on this, the cavities of a zeolite (channels or cages) can be considered nanoreactors that maximise the interaction of reactants at specific acid sites. Whether zeolites act as “true” superacids is still under debate, but so-called “superacidic” behaviour was observed under certain temperatures, showing that zeolite acidity is also temperature-dependent.^[108]

In addition to BRØNSTED acidity, H-zeolites potentially possess LEWIS acid sites depending on their formation conditions or post-synthetic treatment. At elevated temperatures, bridging OH groups can undergo dehydroxylation, which generates three-fold coordinated aluminium, as well as a silylium cation, both possessing vacant coordination sites (Scheme 29, top). These so-called “LEWIS sites” can react with water causing the ejection of framework aluminium yielding now “true” LEWIS sites – commonly referred to as extra-framework aluminium (EFAI), which can be described as $(AlO)^+$ species acting as charge-balancing cations. Concomitantly, BRØNSTED acidic silanols (SiOH) emerge on the aluminium extraction sites. In the presence of water, “true” LEWIS acid sites can further evolve to mostly octahedral aluminium (IV or VI) hydroxide species generating an additional BRØNSTED acidity. Overall, up to three different BRØNSTED acid units are present in a zeolite, of which Si-(OH)-Al bridged hydroxyl groups show the highest acidity, followed by EFAI-bonded hydroxyl groups. Silanols can be considered weakly acidic akin to conventional silica.



Scheme 29. (top) Formation of “true” LEWIS acid sites.

All these types of BRØNSTED and LEWIS acid units can potentially be replaced by other cations through ion-exchange (IE) reactions. Importantly, they are not equally reactive as one might

imagine from their different acidities. Indeed, silanols are believed to exchange only at relatively high temperatures compared to stronger acid sites.^[109] The formation of d-block metal-exchanged zeolites *via* IE reactions will be discussed in section II-2.4.2.

2.4. Synthesis of Metal-Doped Zeolites

The term "metal-doped zeolites" includes a variety of materials differing in the structural and chemical properties of the metal component. This section introduces their underlying methods of preparation and will discuss their structural and reactivity properties. It is trivial to anticipate that the choice of method for the preparation of a metal-doped zeolite significantly defines the properties of the latter. It cannot be assumed that the same starting materials will lead to comparable materials *via* different preparation methods. Moreover, each of the methods is strongly influenced by the experimental parameters chosen, such as (i) the amount and nature of precursors, (ii) the zeolite topology, (iii) the temperature, and (iv) the use and the nature of solvents. Depending on the method, other factors may play a role.

In addition, different salts/complexes of the same cation are not equally suitable for each method. Furthermore, one method cannot always be transferred to another cation without further adjustments. The optimisation of a metal-doped zeolite is therefore a multi-step process involving many parameters. Once an optimised metal-doped zeolite catalyst was identified, it is not necessarily the catalyst of choice in all conceivable applications. It would therefore be desirable to have an arsenal of optimised zeolite catalysts for each cation and to re-evaluate their performance in every application.

2.4.1. *via* Isomorphous Substitution

A zeolite can be described as a silicate where some silicon atoms were replaced by aluminium, thus affording an aluminosilicate. Further substituting silicon or aluminium atoms in a zeolite framework for other elements has served as an inspiration for the design of several zeolite-type materials. This concept is called isomorphic substitution. Depending on the element, not only novel carrier materials but also catalysts can thus be created. The driving idea behind the isomorphic substitution of catalytically active elements into the zeolite framework was to reduce metal leaching and create catalytically active single metal sites. The incorporation of tetravalent Ti(IV) and Sn(IV), for instance, generates strong LEWIS acid sites exploitable in catalysis. Titanosilicates (TS) are prepared *via* a bottom-up approach using titanium alkoxide precursors, whereas tin-containing silicates result from the reaction of a dealuminated zeolite with SnCl₄ in a top-down approach. Such isomorphous substitution, however, is not going to be further discussed in this manuscript. An overview of such materials and their applications in sustainable chemistry was recently reviewed.^[110]

2.4.2. *via* Ion-Exchange and Related Strategies

One of the most frequently used strategies for the preparation of metal-doped zeolites is the exchange of extra-framework cations. A general distinction is made between a “wet” or “aqueous” (AIE) and a “solid-state” ion-exchange (SSIE) reaction and a comparison of both methods is given in **Table 2**. Related and more recent strategies are also presented in this section.

2.4.2.1. Aqueous and Solid-State Ion-Exchange Reactions

In an aqueous ion-exchange (AIE) or “wet exchange”, the incoming cation is present in a pH-controlled aqueous solution to handle the oxidation state and the solubility of the salt. A strongly acidic or basic pH could also lead to defects in the zeolite framework. Since zeolites are insoluble in water, this method is suitable to allow intimate contact of both precursors in suspension, while the resulting material can be easily filtered off from the excess solution. Beneficially, this strategy is feasible on a multigram lab-scale enabling the production of larger quantities. Nevertheless, AIE also counts with several shortcomings. In general, IE reactions represent thermodynamically reversible processes. In AIE, a one-time performance results in a partial exchange of the original cation for the desired one, rather than a quantitative reaction. If a high loading of the incoming cation is desired, this process must be repeated several times. This costs time and resources, and a large proportion of the cations in the solution usually turn into waste after filtration. Finally, the material obtained by filtration must also be washed and dried. The preparation of a zeolite catalyst *via* this method can therefore take several days or even weeks. Unfortunately, AIE reaction is not suitable for salts that are hardly or not at all soluble in water (or other solvents). Furthermore, the solvation shell of certain cations is too voluminous to penetrate the micropores of the zeolites at all, severely limiting the number of exchangeable cations *via* AIE.

Table 2. Comparison of aqueous (AIE) and solid-state ion-exchange (SSIE).

	Advantages	Drawbacks
AIE	<ul style="list-style-type: none">▪ easily scalable▪ common equipment required▪ milder T (rt to 100 °C)	<ul style="list-style-type: none">▪ pH control required▪ multiple consecutive operations for notable IE (days to weeks)▪ excessive metal use and waste generation▪ limited to soluble salts with small hydration shell▪ hydrated zeolite product recovered
SSIE	<ul style="list-style-type: none">▪ easily scalable▪ often single operation suffices▪ high exchange degrees▪ tuneable exchange degrees adapting reagent stoichiometry▪ waste reduction▪ frequently faster preparation than AIE	<ul style="list-style-type: none">▪ high temperatures (mostly > 300 °C)▪ usually under vacuum or inert atm▪ usually Soxhlet extraction after exchange▪ specified equipment required

Solid-state ion-exchange (SSIE) is most often defined by heating a solid mixture of a zeolite and a metal salt at a defined temperature ($> 300\text{ }^{\circ}\text{C}$). Both solids are mixed evenly for a specified time in a mortar or *via* ball milling. Heating can take place either under air, protective atmosphere (nitrogen or argon), or vacuum, which strongly influences the nature of the final metal species. In the presence of oxygen, the formation of metal oxides is commonly observed, some of which aggregate into nanoparticles. Under anaerobic conditions, on the other hand, redox processes can occur depending on the metal and oxidation state. In both cases, it is therefore possible that the metal is present in several stable oxidation states after the SSIE, which can be determined using spectroscopic methods.

The SSIE method has several advantages compared to the previously described AIE method (**Table 2**). It is commonly accepted that SSIE allows to displace the thermodynamic equilibrium of the IE reaction in favour of the desired zeolite material *via* evacuation of a volatile secondary product (e.g., hydrogen halides when metal halides and protonic zeolites are used). This, however, presupposes a complete exchange scenario, whereby in some cases a simple dispersion of the salt on the surface of the zeolites can also occur. Nevertheless, SSIE commonly leads to higher metal charges than AIE using the same starting materials. However, this is not true *per se*. Interestingly, significant differences in the reactivity of the final catalysts can nevertheless be observed. Catalysts prepared *via* SSIE are commonly more efficient, even in cases where the metal charge was comparatively low. Consequently, the distribution and localisation of the incoming cations strongly depend on the exchange strategy and the chosen parameters. It is therefore not surprising that the presence of water, depending on its amount, was found to strongly influence the SSIE.

It is indispensable to provide a precise experimental procedure for the preparation, but also for the characterisation of the metal-doped zeolites to allow reproducibility. ARMOR has published a proposal^[11] in this regard encompassing (i) the source and composition of the starting materials, (ii) the exact time-temperature diagram, (iii) the pH before and after IE, (iv) the stirring rate for AIE, (v) elemental analysis of final zeolite, (vi) the metal loading, etc.

In 2022, ERKEY and co-workers reported a novel IE reaction to produce copper-mordenite catalysts from copper(II) trifluoroacetylacetonate and H-MOR in supercritical CO_2 .^[111] This supercritical IE (SCIE) was carried out at $80\text{ }^{\circ}\text{C}$ for 72 h compared to SSIE, where temperatures are usually between 300 and $550\text{ }^{\circ}\text{C}$. However, it requires a specific and, above all, pressure-resistant apparatus (here up to 27.58 MPa). Their catalyst was examined in the stepwise direct methane to methanol (sDMTM) process and presented an improved methanol productivity by 16% compared to similarly loaded Cu^{II} -MOR catalysts (2.3 wt%) obtained from AIE. As for

SSIE, this suggests that the local environment of the incorporated copper ions by SCIE differs significantly from those obtained in an aqueous solution.

2.4.2.2. Chemical Vapour Deposition (CVD) and Ligand Exchange

A closely related method to SSIE for the preparation of metal-exchanged zeolites is chemical vapour deposition (CVD). In this method, the zeolites react with a volatile metal precursor (chloride, carbonyl, alkyl, etc.) under anhydrous conditions and at high temperatures. This results in a selective and stoichiometric reaction (acid-base or metathesis) of the zeolitic BRØNSTED acid sites with the metal precursor to produce defined monatomic catalysts. CVD enabled, for instance, the preparation of tin- (SnCl_4),^[112] rhenium- (CH_3ReO_3),^[113] gallium- ($\text{Ga}(\text{CH}_3)_3$),^[114] nickel- ($\text{Ni}(\text{C}_5\text{H}_5)_2$)^[115] and zinc-loaded (Et_2Zn)^[116] zeolites. The main difference to the SSIE method is usually determined by the spatial separation of both solid precursors. In fact, the volatile component is heated in another compartment and directed towards a depot containing the zeolite precursor with the help of a carrier gas or vacuum. Thus, there is initially no physical contact between the two solid precursors.

Closely related to CVD, the term “ligand exchange” can also be found in the literature. Here, defined metal complexes serve as precursors and undergo a ligand exchange, often due to a chemical reaction with the BRØNSTED acid zeolite. Interestingly, GATES and co-workers thus succeeded in preparing a whole range of noble transition metal zeolite catalysts (Rh,^[117] Ir,^[118] Pt^[119]) from commercially available alkyl, carbonyl, and acetoacetate precursors. Depending on the case, well-defined single-atom and cluster catalysts with different core contents could thus be prepared. In addition, GATES' group observed that the crystalline zeolite framework contributes significantly to the stabilisation of the metal complex unit and outperforms other amorphous supports such as silica-alumina phase. Presumably, this results in significantly higher sintering resistance, as demonstrated by a highly stable $\text{Ir}(\text{CO})_2/\text{H-Y}$ complex obtained from $[\text{Ir}(\text{acac})(\text{CO})_2]$.^[120]

The methods described above for the loading of metal species onto and into zeolite matrices often lead to a final zeolite catalyst, which is directly applied to a given catalytic procedure. Alternatively, the nature of the introduced metal species is further modified through post-synthetic techniques, e.g., the reduction of metal cations to metal nanoparticles. Nanoparticles in or on zeolites can, however, also be generated *via* techniques that are not relying on IE reactions.

2.4.3. *via* Encapsulation Techniques

Zeolites are commonly used as solid supports for metal nanoparticles (NPs). Metal@zeolite (Figure 6a) designates materials bearing nanoparticles inside the zeolite pore system,^[121] as

opposed to metal/zeolite (**Figure 6b**), where NPs are dispersed on the zeolite surface. An example of a Cu/Y was given in section I-2.4. in the catalytic preparation of propargylamines.^[44]

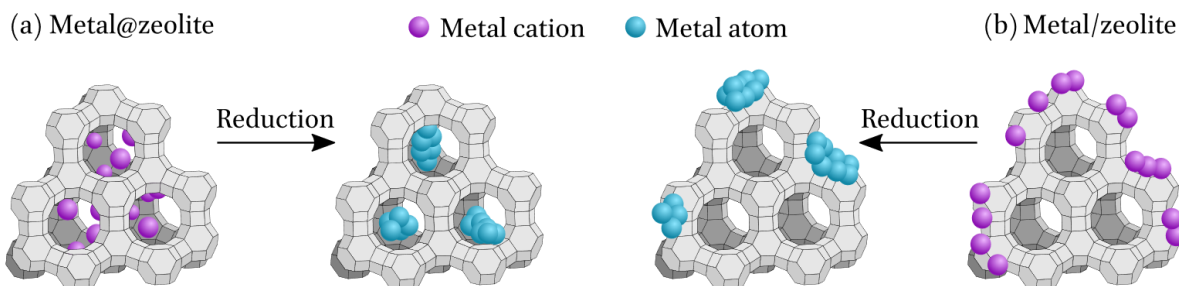


Figure 6. Metal@zeolite vs. metal/zeolite.

The formation of NPs inside the pores enables better control of their size and shape.^[122,123] This shape selectivity is partially controlled by the zeolite topology, while this property is absent in metal/zeolite materials.^[124] Furthermore, their mobility when incorporated in the zeolite network is greatly limited, which makes them more resistant to sintering and leaching.^[125] This allows their application in high-temperature procedures where sintering is often contributing to catalyst deactivation. Generally, different strategies to encapsulate NPs into zeolite channels and cages exist, namely post-synthetic,^[126,127] co-crystallisation^[123,127] and 2D to 3D transformation^[128] methods. A short description of the first two will be given below.

The post-synthetic approach represents the most frequently employed strategy and is based on the reduction of the metal species (**Figure 6**). Commonly, the latter are introduced through impregnation or IE of the charge-balancing cations.^[129] Next, the reduction is commonly performed using hydrogen gas at the lowest possible temperature to limit sintering.

As for co-crystallisation, this technique is especially suited in the case of small-pore zeolites.^[130] Due to smaller pore dimensions, IE can be more challenging, especially when the incoming cation presents an important hydration shell (AIE) or bulky counterions or ligands (other IE techniques). Co-crystallisation requires the formation and inclusion of NPs during the crystallisation of the zeolite matrix. In the final step, the metal precursors then merge into NPs upon calcination in a given atmosphere (e.g., air or H₂). Such catalysts, however, cannot accommodate molecules of dimensions commonly employed in organic synthesis. Nevertheless, they show great potential in other applications. YU and co-workers, for instance, obtained a Pd@S-1 (MFI) of outstanding activity in hydrogen production from formic acid under mild conditions.^[131] Given the excellent dispersion of Pd NPs well enclosed in the zeolite network, sintering was negligible, and the catalyst displayed an attractive recyclability.

It is worth mentioning that several strategies presented above for the metal-doped zeolites yet confer the possibility of concomitant existence of BRØNSTED and LEWIS acid sites. Beneficially, the design of multifunctional zeolites for tailor-made catalytic cascade processes is thus amenable based on strong metal–acid synergistic effects.^[132]

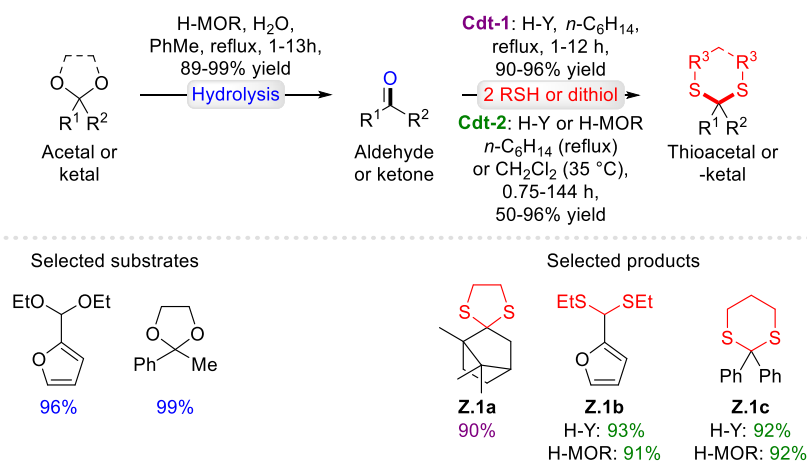
2.5. Application of Zeolites in Organic Synthesis of Fine Chemicals

2.5.1. BRØNSTED Acidic Zeolites

Zeolites possessing a proton as counterion are frequently referred to as acidic or protonic zeolites. They find wide applications as reusable heterogeneous stoichiometric reagents or even catalysts in organic transformations. They represent inherently safe substitutes for hazardous (super)acids, contributing to reducing plant corrosion, as well as waste reduction (e.g., salt formation). Their structural diversity in terms of topologies and pore dimensions, adjustable SAR, and acidity render screening or even designing of optimal catalysts possible. Besides their low cost, the possibility to regenerate their activity through calcination further reduces the production costs of a given industrial process. In organic chemistry, they are mostly known for their use in (de)protection reactions but also exhibited great efficacy in more advanced synthetic applications. In the following, a brief overview of concrete examples of acidic zeolites in the protection and deprotection of common functional groups is presented followed by intriguing examples of further synthetically valuable organic transformations.

2.5.1.1. Protecting Group Chemistry

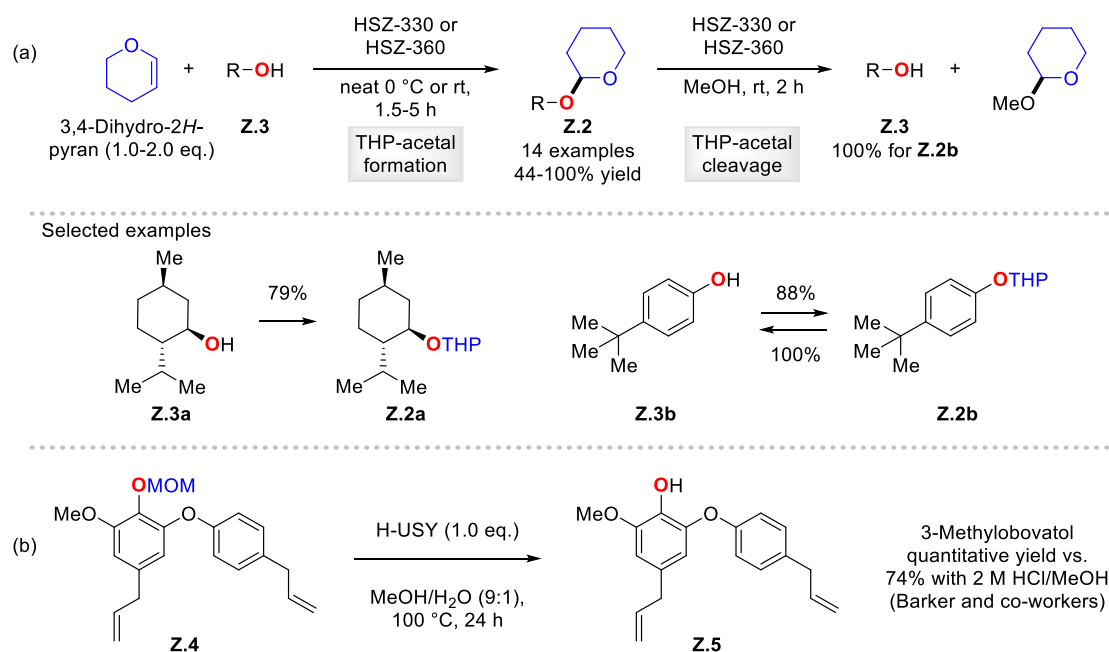
Acidic zeolites are attractive acidic reagents for the protection and deprotection of various carbonyl-derived functional groups (Scheme 30). REDDY and co-workers, for instance, successfully used H-MOR for the hydrolysis of various acetals and ketals in yields ranging from 89-99%.^[133] In addition, REDDY and co-workers developed an H-Y-promoted protocol for the preparation of diverse 1,3-dithiolanes (Cdt-1), such as **Z.1a**.^[134] While their conditions produced good yields and H-Y was regenerated and reused several times, the use of *n*-hexane is inconvenient for large-scale applications. In the following year, REDDY and co-workers proved H-Y and H-MOR to be efficient and reusable catalysts for the synthesis of cyclic and acyclic dithioacetals and -ketals (Cdt-2, cf. **Z.1b,c**).^[135] A wide scope of (un)saturated aliphatic and (hetero)aromatic, as well as sterically hindered carbonyl compounds, were successfully employed.



Scheme 30. Acetal or ketal hydrolysis and thioacetal and -ketal formation with protonic zeolites.^[133–135]

Various acidic zeolites of different morphologies were also applied to the preparation or cleavage of acetals (diacetates) from/to the corresponding aldehydes.^[136–138]

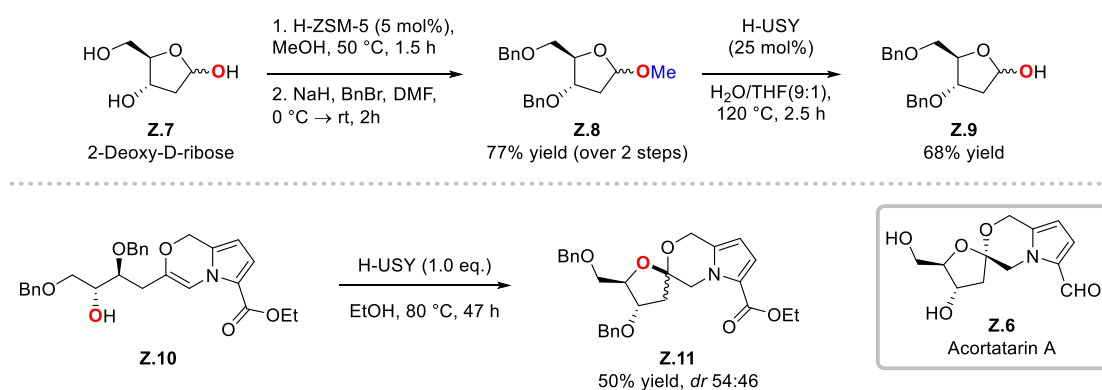
Furthermore, acidic zeolites are versatile reagents and catalysts in the (de-)protection of the hydroxy function. The latter is among the most abundant functional group in organic compounds and many protecting groups for their selective temporary or long-term preservation have emerged. For instance, several acidic zeolites, including H-beta,^[139] HSZ-330 or HSZ-360,^[140] were successfully applied to the formation and cleavage of tetrahydropyranyl (THP) acetals **Z.2** from/to alcohols **Z.3** (Scheme 31a). The solvent-free (\rightarrow **Z.2**) and mild conditions reported by BALLINI and co-workers are particularly attractive.^[140]



Scheme 31. (a) Formation and cleavage of THP acetals with protonic zeolites^[140] and (b) H-USY-mediated MOM deprotection for 3-methylobovatol synthesis.^[141]

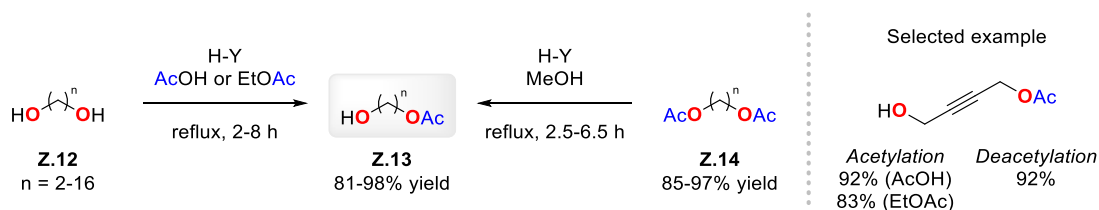
Similarly, stoichiometric H-USY enabled a highly chemoselective, last-step methoxymethyl (MOM) acetal deprotection in **Z.4** for the synthesis of the natural product 3-methylobovatol (**Z.5**) reported by CHASSAING and co-workers (Scheme 31b).^[141] This represented a relevant improvement in yield as compared to the use of 2 M HCl in MeOH^[142] and greatly simplified the procedure as the solid zeolite acid is simply filtered off after the reaction without the requirement for aqueous work-up.

Moreover, PALE's group applied acidic zeolites in several steps in the total synthesis of acortarin A (**Z.6**) (Scheme 32).^[143] 2-Deoxy-D-ribose (**Z.7**), for instance, was transformed quantitatively into the methyl acetal under anhydrous conditions using catalytic H-ZSM-5 in MeOH. After benzylation of the remaining hydroxyl groups, **Z.8** was selectively hydrolysed at the anomeric position with catalytic H-USY to yield **Z.9**. Furthermore, H-USY was later used stoichiometrically for the spiroketalisation of enamine **Z.10** yielding **Z.11** as key intermediate towards targeted **Z.6**.



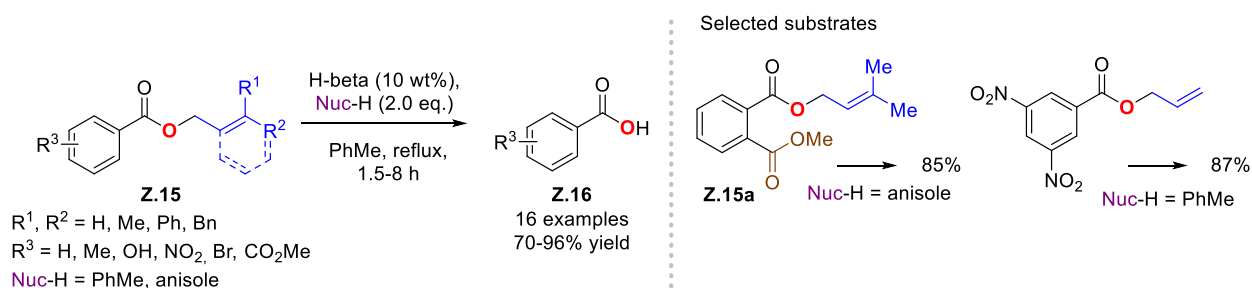
Scheme 32. Use of protonic zeolites in several steps for the synthesis of acortatarin A.^[143]

DAS and co-workers reported a highly selective monoacetylation of symmetric diols **Z.12** to **Z.13**, as well as the selective monodeacetylation of symmetric diacetates **Z.14** using H-Y zeolite in MeOH (**Scheme 33**).^[144] Unlike most procedures based on acetic anhydride, the authors used acetic acid (AcOH), or even more conveniently, neutral and non-corrosive EtOAc as the acetylating agent. This highly green procedure was applied to a broad range of saturated and unsaturated diols **Z.12** and diacetates **Z.14**. The zeolite was reused several times.



Scheme 33. Acidic zeolite-promoted monoacetylation of alcohols and monodeacetylation of diacetates.^[144,145]

The use of protonic zeolites for the selective cleavage of esters is not limited to acetates. In 2003, KUMAR and co-workers reported the highly selective deprotection of allylic(-like) esters **Z.15** catalysed by H-beta and providing the aromatic carboxylic acids **Z.16** in high yields (**Scheme 34**).^[146] Prenyl, allyl, cinnamyl, and benzyl esters among others were successfully converted while alkyl esters were tolerated (cf. **Z.15a**). Interestingly, the reaction is performed under anhydrous conditions with toluene acting as the nucleophile. Some substrates, however, require the addition of more electron-rich anisole.



Scheme 34. Selective deprotection of allylic and benzylic esters with recyclable H-beta.^[146]

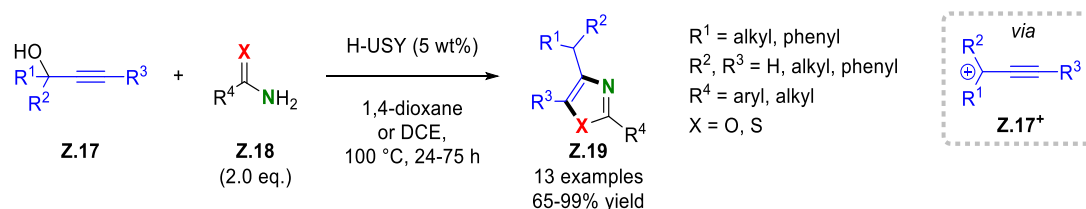
The overall advantage of all these procedures is that the acidic zeolites are commercially available, so no catalyst preparation is required. Furthermore, the acidic zeolites were reused several times giving consistently high yields. However, storage under anhydrous conditions or

activation through calcination before use is required as activity greatly depends on the amount of water adsorbed. Similarly, before the reuse of recovered materials, a brief calcination of several hours is required to re-establish a comparable activity.

2.5.1.2. Access to Nitrogenated Scaffolds

Acidic zeolites have proven versatile and competitive catalysts in more advanced organic synthesis. This section focuses on acidic zeolite catalysts applied to the preparation of nitrogen-containing scaffolds, illustrated by a selection of examples.

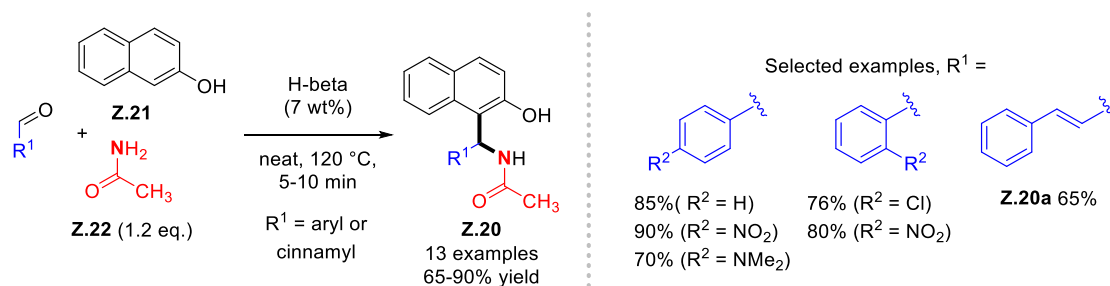
In 2015, CORMA and co-workers observed that H-USY enabled the dehydration of propargyl alcohols **Z.17** to the corresponding delocalised carbocations **Z.17⁺** under mild conditions (**Scheme 35**).^[147] According to them, the highly delocalised negative charge of the zeolite framework, acting as a macroanion, allows to stabilise **Z.17⁺** and thus further prolongs its lifetime. The addition of diverse nucleophiles, such as (thio)amides **Z.18** and phenols occurred with superior catalytic efficiency ($\text{TOF}_0 > 845 \text{ h}^{-1}$) as compared to significantly stronger homogeneous BRØNSTED or LEWIS acids. Several oxazoles and thiazoles **Z.19** were obtained from (thio)amides **Z.18** in high yields and presented significant inhibition percentages against a colon cancer cell line (Colo 320 KrasSL cells) at 0.2 μM concentration. Furthermore, recovered H-USY produced constant yields in five additional runs without intermediate reactivation. Nevertheless, this procedure is based on problematic solvents.



Scheme 35. Synthesis of oxazoles and thiazoles under H-USY catalysis.^[147]

MCRs, enabling the one-pot conversion of multiple educts into a product without intermediate isolation, are highly attractive from a green chemical viewpoint. Rewardingly, protonic zeolites were also shown to be efficient catalysts in such MCRs.

MAHERIA and co-workers, for instance, identified H-beta zeolite as an efficient catalyst for the synthesis of amidoalkyl naphthols **Z.20** through a MCR of 2-naphthol (**Z.21**), aromatic aldehydes, and acetamide (**Z.22**) (**Scheme 36**).^[148] This MANNICH-type reaction resembles the BETTI reaction. Near equimolar amounts of each coupling partner along with short reaction times and solvent-free conditions makes this an attractive green approach toward precursors of biologically relevant 1-aminomethyl-2-naphthols.

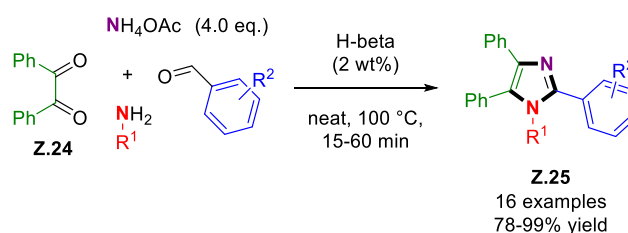


Scheme 36. H-beta-catalysed synthesis of amidoalkyl naphthols under solvent-free conditions.^[148]

The recovered H-beta was recycled for five runs maintaining a similar catalytic activity. XRD analysis of the recovered material revealed that crystallinity was retained as compared to a fresh sample. As for the scope, several functional groups on the aromatic aldehyde (halide, nitro, amine, etc.) were well tolerated. Generally, electron-rich aldehydes afforded slightly lower yields. Fortunately, cinnamyl aldehyde (\rightarrow **Z.20a**) could also be employed whereas aliphatic aldehydes failed to give the desired products. Competing enolisation of the latter might be a limiting factor. Other amine nucleophiles such as thiourea or aniline were unsuccessful.

In 2017, MAHERIA and co-workers applied similar conditions to a 4CR of benzil (**Z.24**), ammonium acetate NH_4OAc , aromatic aldehydes, and primary amines, either aromatic or aliphatic (**Table 3**).^[149] The desired tetrasubstituted imidazoles **Z.25** were generally produced in high yields using a catalytic amount of H-beta zeolite in the absence of solvent at 100 °C. Alternatively, EtOH was identified as an effective and green backup solvent in case of practical issues. Regarding the substrate scope, only the aromatic aldehyde and the amine component were varied. Several functional groups on the aromatic aldehyde (halide, nitro, hydroxyl, etc.) were well tolerated and no obvious electronic effects for the aldehyde component can be read from the product scope. As for the amine, benzylamine was systematically giving superior reaction rates and yields compared to aniline (Table 3, entries 1, 3, 5 vs. 2, 4, and 6).

Table 3. Synthesis of fully substituted imidazoles **Z.25** under H-beta catalysis.^[149]

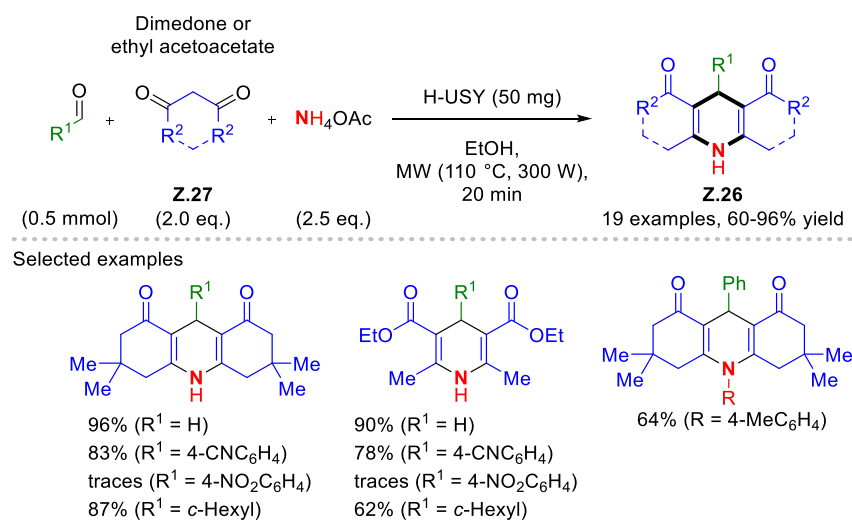


Entry	R ¹	R ²	Time (min)	Yield (%)
1	Bn	H	15	99
2	Ph	H	30	86
3	Bn	4-OH	20	93
4	Ph	4-OH	30	85
5	Bn	4-Cl-3-NO ₂	15	91
6	Ph	4-Cl-3-NO ₂	35	84

Beneficially, efficient recycling of H-beta was observed for up to six runs after drying and calcination under air at 550 °C after each run. Again, XRD analysis of the recovered material revealed that crystallinity was retained as compared to fresh H-beta. It is worth mentioning that other acidic zeolites were also examined revealing that for this application a low-to-moderate acidity combined with a higher SAR and surface area were optimal.

Recently, CORRÊA and co-workers demonstrated that H-USY can efficiently replace transition metal-based LEWIS acids, such as $\text{CuCl}_2 \cdot 2\text{H}_2\text{O}$ in the synthesis of 1,4-dihydropyridines **Z.26** (Scheme 37).^[150] Under microwave irradiation, an accelerated 3CR of different (hetero)aromatic and aliphatic aldehydes with a diketone **Z.27** (dimedone or ethyl acetoacetate) and ammonium formate afforded several 1,4-dihydropyridines **Z.26** in 60-96% yields. Other zeolite topologies in their protonic form (mordenite, ferrierite, ZSM-5, beta) were also effective in EtOH at 110 °C but afforded slightly lower yields.

The catalyst was easily recovered and recycled after calcination with a slow but progressive decrease in yield. Yet, its textural properties are greatly retained as shown by XRD and FTIR of adsorbed pyridine. Moreover, the specific surface area and acidic properties of the recovered protonic zeolite are comparable to fresh USY zeolite.



Scheme 37. H-USY-catalysed synthesis of 1,4-dihydropyridines.^[150]

2.5.2. Metal-Doped Zeolites

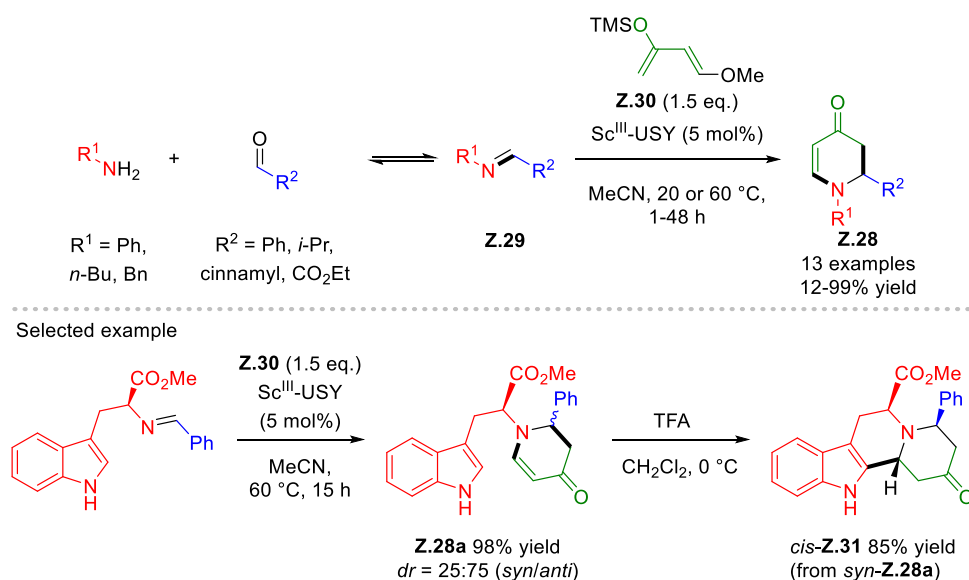
Before being applied to advanced organic synthesis, metal-doped zeolites have found applications in gas phase reactions, such as the FISCHER-TROPSCH process for the preparation of hydrocarbons from syngas, or NO_x reduction (e.g., using Fe, Co, Cu).^[151] Co^{II} -loaded zeolites also represent promising oxidation catalysts of alkenes, such as styrene and α -pinene.^[152] Among the metal-doped zeolites applied to organic transformations, copper examples are most frequently encountered. This section mostly focuses on the use of copper-loaded zeolites applied to organic synthesis as this is one of the main axes of this thesis work. Nevertheless, selected

examples of zeolite catalysts doped with other (transition) metals are also discussed. In general, the formation of nitrogen-containing compounds is shown preferentially. The catalysts' properties and their potential applications as a heterogeneous and recyclable catalyst are discussed.

2.5.2.1. Scandium

Scandium represents the first d-block metal ($[Ar] 3d^1 4s^2$) and is used in organic synthesis for its LEWIS acid properties. It was historically classified as a rare-earth element but is of similar earth abundance to cobalt. Nevertheless, Sc^{III} salts are comparatively expensive. The development of a heterogenised Sc^{III} catalyst is thus attractive from economical and green chemical viewpoints. In this context, PALE's group prepared a Sc^{III} -USY zeolite *via* SSIE reaction between H-USY and $Sc(OTf)_3$ at 450 °C.^[153] This zeolite was successfully applied in a MUKAIYAMA-aldol reaction,^[154] as well as two hetero-DIELS-ALDER reactions.^[155,156]

An *aza*-DIELS-ALDER reaction affording piperidinones **Z.28**, for instance, was disclosed in which imines **Z.29** act as dienophiles reacting with the electron-rich DANISHEFSKY diene **Z.30** (Scheme 38).^[156] The imine **Z.29** can be generated *in situ* but yields are often superior starting from pre-formed imines. This methodology was extended to enantiomerically pure amino acids to access mimics of natural alkaloids containing piperidinones, such as **Z.31**. Rewardingly, the Sc^{III} -USY zeolite maintained high product yields for ten runs, after which the recyclability study was ended.

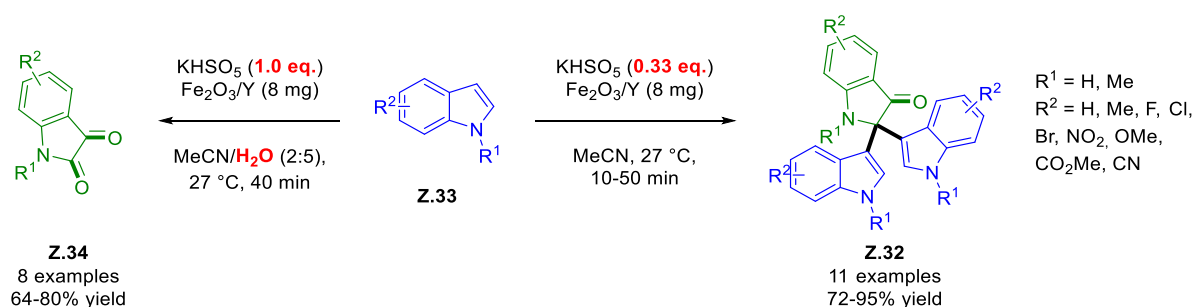


Scheme 38. Sc^{III} -USY-catalysed *aza*-DIELS-ALDER reaction towards piperidinones.^[156]

2.5.2.2. Iron

A low-cost and reusable iron oxide nanocatalyst supported on Y-zeolite was applied to the synthesis of C2 di-indolyl indolones **Z.32** under mild conditions (Scheme 39).^[157] The catalyst was prepared through base-induced precipitation of aqueous $Fe(NO_3)_3 \cdot 9H_2O$ on the Y-zeolite surface, followed by the formation of surface nanoparticles through heating at 327 °C for 12 h with

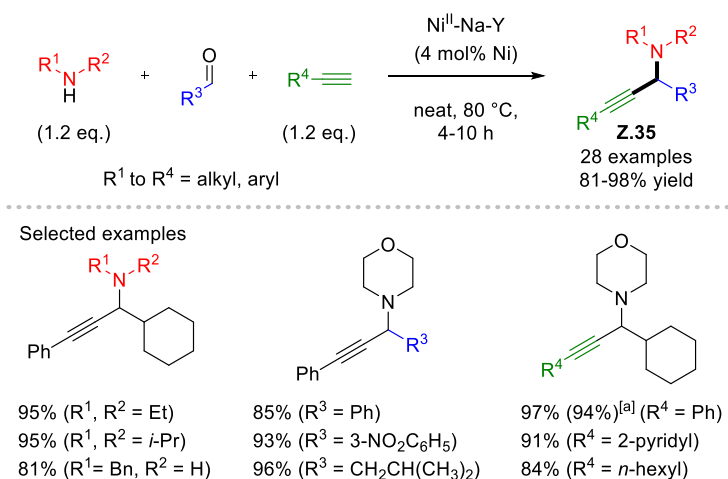
an average size of 2.36 nm. Products **Z.32** were obtained in short reaction times (10 to 50 min) and high yields (72-95%) through a C2-selective trimerisation of various indoles **Z.33**. From a comparison of different aluminosilicate supports, it was shown that a lower Si/Al ratio provided better selectivities for the C2 trimerised products **Z.32**. Beneficially, the catalyst was easily separated and reused up to five times without a decrease in yield when calcined before each run. A significantly reduced specific surface area (by about 70 m²/g), however, is believed to have induced a noteworthy drop in yield in the sixth run. Furthermore, the selective oxidation of diverse indoles **Z.33** into isatins **Z.34** was observed adjusting the water and oxidant proportions. Again, the reaction proceeded at room temperature in less than one hour.



Scheme 39. Synthesis of C2 di-indolyl indolones **Z.32** and isatins **Z.34** from indoles **Z.33**.^[157]

2.5.2.3. Nickel

In 2010, PITCHUMANI and co-workers prepared α -secondary propargylamines **Z.35** via Ni^{II}-Na-Y-catalysed A³ reactions (Scheme 40).^[158] The zeolite catalyst was prepared through AIE starting from Na-Y and NiSO₄•6H₂O but the exact procedure is not provided. Hence, the molecular nature of the catalytically active nickel species remains unknown. Interestingly, no leaching of nickel species was observed upon performing a SHELDON test and the same catalyst was reused for eight runs without a significant decrease in yield or reactivity. The A³ reaction was performed under solvent-free conditions at 80 °C in only four to ten hours using a slight excess of amine and alkyne at 4 mol% nickel loading. Rewardingly, the Ni^{II}-Na-Y zeolite presents a broad product scope with aromatic and aliphatic aldehydes, amines, and alkynes affording high to excellent product yields (81-98%). In contrast to most catalytic systems, enolisable and challenging aliphatic aldehydes gave superior results to aromatic aldehydes. Regarding the alkyne component, however, aromatic ones were superior to alkylalkynes, as commonly observed. Gratifyingly, various amines smoothly afforded the desired propargylamines **Z.35** in high yields. In fact, except for primary anilines, all amine classes are present in this product scope.

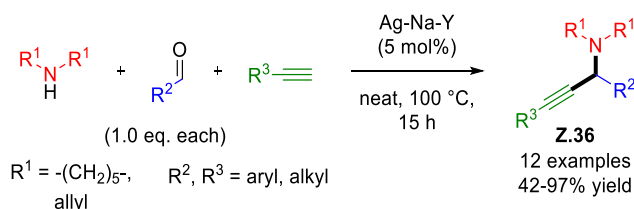


Scheme 40. Ni^{II}-Na-Y-catalysed A³ reaction for the synthesis of propargylamines.^[158]

^[a] Yield of gram-scale reaction (10 mmol aldehyde)

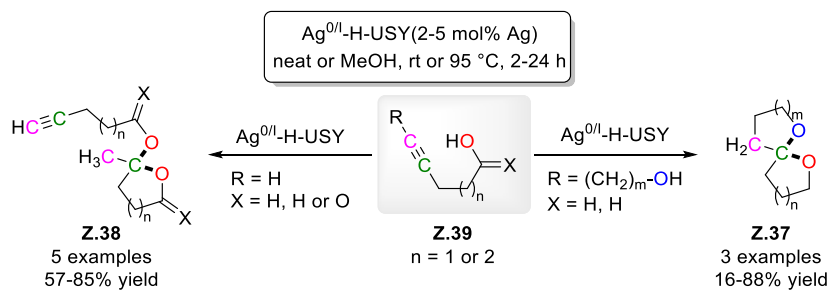
2.5.2.4. Silver

MAGGI and co-workers also studied the A³ reaction by applying Ag-Na-Y zeolite prepared *via* AIE to produce propargylamines **Z.36** (Scheme 41).^[159] Compared to analogously prepared Cu-Na-Y and Au-Na-Y zeolites, no further conversion after hot filtration of the reaction mixture was observed, suggesting that no silver cations leached into the solution. In terms of reaction conditions, scope, and performance, this protocol is similar to the protocols of most A³ catalytic systems (see section III-1 for more details). Rewardingly, recyclability with a total of four runs was observed using equimolar amounts of each component in the absence of solvent.



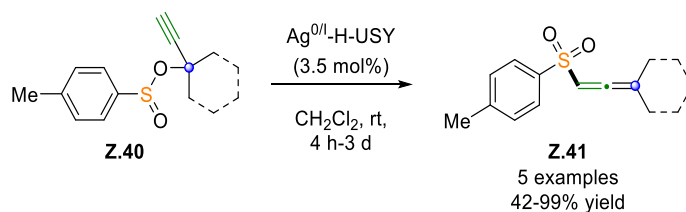
Scheme 41. Ag-Na-Y-catalysed A³ reaction for the synthesis of propargylamines.^[159]

PALE and co-workers group also established the synthesis of a silver-based bifunctional USY zeolite. Ag^{0/1}-H-USY was used as a heterogeneous catalyst for intramolecular spiroketalisation (→ **Z.37**) and intermolecular ketalisation (→ **Z.38**) of alkyne(di)ols **Z.39** (Scheme 42).^[160] Such spiroketals are found in various natural products^[161] and while other noble transition metals (Pd, Ir, Rh, and Au) were used in this transformation under homogeneous catalysis, this represented the first silver-based and heterogeneous approach. Beneficially, in most cases, the reaction proceeded under solvent-free conditions or in MeOH. Furthermore, the catalyst produced constant yields over five runs after calcination between each run.



Scheme 42. $\text{Ag}^{0\text{I}}\text{-H-USY}$ -catalysed (spiro)ketalisation of alkyne(di)ols **Z.39**.^[160]

This $\text{Ag}^{0\text{I}}\text{-H-USY}$ was also applied to the [2,3]-sigmatropic rearrangement of propargyl sulphinates **Z.40** into allenic sulphones **Z.41** by HAMPTON and HARMATA in 2015 (**Scheme 43**).^[162] Compared to their previous homogeneous conditions,^[163] the zeolite catalyst afforded similar yields, yet required longer reaction times. While catalyst recyclability was observed over three runs without a drop in yield, the reactivity further decreased. As the initial catalyst loading of the heterogeneous protocol was set higher (3.5 mol% vs. 2.0 mol%), there is no significant advantage of using the zeolite catalyst in this application.



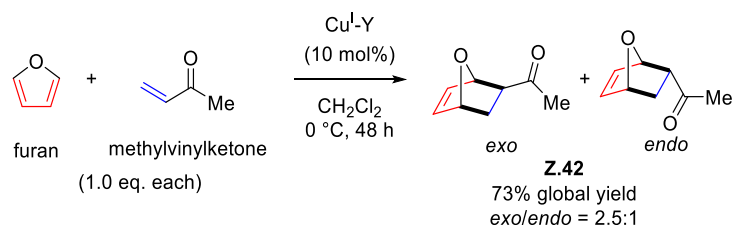
Scheme 43. Synthesis of allenic sulphones **Z.41** via [2,3]-sigmatropic rearrangement of propargyl sulphinates **Z.40**.^[162]

2.5.2.5. Copper

Copper-doped zeolites were first developed aiming for their use in depollution applications, particularly in the reduction of NO_x .^[164] Soon after, they gained great interest as heterogeneous catalysts in organic synthesis. Copper has a long history in organic synthesis and organometallic chemistry and novel examples of copper-facilitated (both stoichiometric and catalytic) reactions continue to be discovered.^[165–167] In fact, copper salts and complexes can act as oxidants, cross-coupling agents, and LEWIS acids. Compared to other commonly used elements sharing these properties, such as the other coinage metals silver and gold, as well as palladium and platinum, copper is an abundant base metal available at low cost and has significantly lower toxicity. Yet, copper compounds are potent LEWIS acids with a high affinity for π -bonds with carbon unsaturations, especially for alkynes.^[168] Indeed, various copper species promote catalytic transformations, such as cycloadditions, triple bond functionalisations with heteroatoms, and copper acetylide additions to electrophiles. Among others, PALE's group has further promoted the use of copper-doped zeolites in greener synthetic procedures toward advanced organic scaffolds. In the following, several applications classified by reaction type and catalysed by varying copper-based zeolites are discussed.

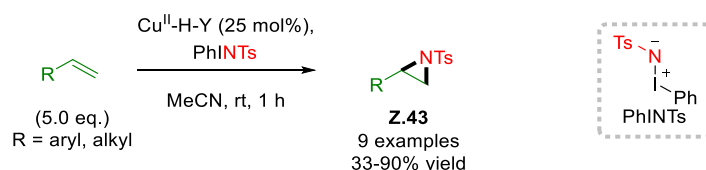
Copper Zeolites in Cycloadditions

To the best of our knowledge, the first application of copper-loaded zeolites in organic synthesis was reported in 1986 by IPAKTSCHI and co-workers performing Cu^I-Y-catalysed DIELS-ALDER reactions (Scheme 44).^[169] The catalyst was prepared in two steps. First, a Cu^{II}-Y zeolite was prepared through multiple AIE with Cu(OAc)₂ from the acidic H-Y. Next, Cu^{II}-Y was reduced under a flow of carbon monoxide at 300 °C to yield Cu^I-Y. Several dienes reacted with a series of acrylic and acetylenic dienophiles. DIELS-ALDER reactions are often delicate with furans as they are sensitive to ring openings in acidic aqueous media. The use of Cu^I-Y zeolite proved advantageous as it improved the yield of **Z.42** by 30% and operated at ambient pressure compared to standard conditions.^[170] Furthermore, a stereoselectivity in favour of the *exo*-isomer was observed (*exo/endo* = 2.5:1), whereas high-pressure conditions (15000 atm) lead to equivalent amounts of both isomers. This stereoselectivity might originate from the shape selectivity of the zeolite framework. At this time, no catalyst recyclability was investigated.



Scheme 44. Cu^I-Y-catalysed DIELS-ALDER reaction of furan and methylvinylketone.^[169]

In 1999, HUTCHINGS and co-workers^[171] reported a Cu^{II}-Y-catalysed synthesis of aziridines **Z.43** (Scheme 45) based on seminal works from a homogeneous Cu(OTf)₂-catalysed version developed by EVANS and co-workers.^[172] Using [*N*-(*p*-tolylsulfonyl)imino]phenyliodinane (PhI=NTs) as a nitrene donor, several terminal alkenes successfully led to the corresponding aziridines **Z.43** in a formal [2+1] cycloaddition.



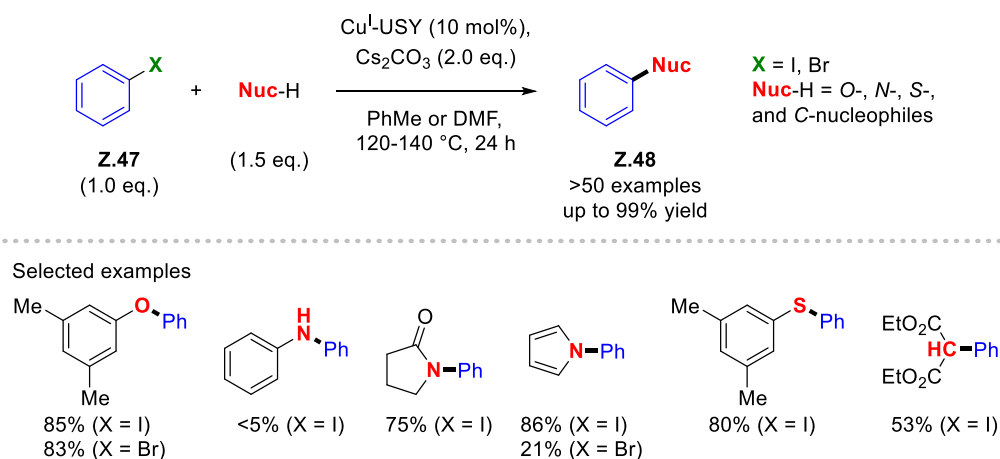
Scheme 45. Cu^I-Y-catalysed aziridination of alkenes.^[171]

The catalyst was prepared through AIE with Cu(OAc)₂ but calcined under air at 550 °C. The authors do not provide any analytical data of the catalyst. Thus, the nature of the copper species is unknown, and it cannot be excluded that (at least in part) copper oxide is present. A recyclability study showed a progressive decrease in catalytic activity, both in terms of yield and reaction rate. Interestingly, less than 0.5% of Cu^{II} ions were leached after each run, thus indicating that the decreased activity is due to catalyst deactivation. Indeed, its initial activity was re-established through calcination, suggesting that the build-up of water and/or organics caused the deactivation.

the recovery of a copper zeolite catalyst by applying an external magnet, SCHWAB and co-workers prepared a Cu^I-beta zeolite on γ -Fe₂O₃ microspheres (γ -Fe₂O₃-beta-Cu^I).^[182]

Copper Zeolites in Cross-Coupling Reactions

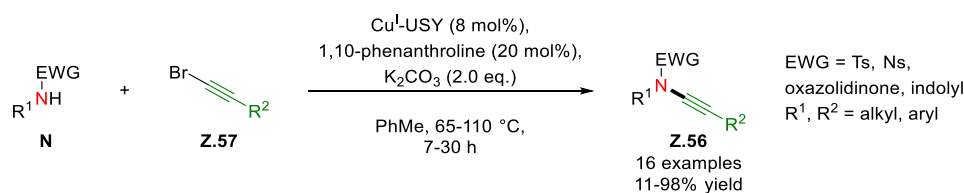
The first use of copper in organic synthesis dates back to the ULLMANN-GOLDBERG coupling reactions.^[183–185] It is nowadays an attractive method for the formation of C-C, C-N, C-S, and C-O bonds and often an alternative to conventional Pd- or Ni-based processes. It involves the cross-coupling of an aryl electrophile **Z.47** and a nucleophile (Nuc-H). A zeolitic version of this coupling reaction was developed by CHASSAING and co-workers for several *O*-, *S*-, *N*- and *C*-nucleophiles (**Scheme 47**).^[141,186] More than 50 coupling products **Z.48** were prepared using Cu^I-USY (10 mol%) in combination with Cs₂CO₃ in toluene or DMF without any ligand other than the zeolite framework. Unfortunately, greener solvents such as EtOH and water gave poor yields. Conveniently, the catalyst can be recycled five times without a decrease in yield.



Scheme 47. Cu^I-USY-catalysed ULLMANN-type coupling reaction.^[141,186]

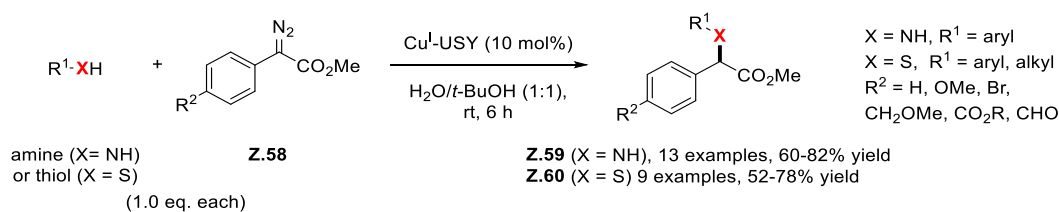
In 2017, PALE's group developed a Cu^I-USY-catalysed CHAN-LAM-type C-N coupling reaction between azoles **Z.49** or amides **Z.50** and various aromatic boronic acids **Z.51** in refluxing MeOH as green solvent (**Scheme 48**).^[187] Several *N*-arylation products **Z.52** and **Z.53** were obtained in 28-95% yield. In the original report dating back to 1998,^[188] the reaction was performed in CH₂Cl₂ using (sub-)stoichiometric amounts of an organic base, such as triethylamine and pyridine and no reaction occurred in MeOH. The Cu^I-USY-catalysed conditions, however, did not require any base additive, nor additional ligand and the reaction is run under air. Unfortunately, the zeolite catalyst maintained its original activity only for two runs, observing a drop in yield from the third run. This could at least partially be explained by some leaching of copper species into solution as evidenced by a SHELDON (hot filtration) test. It is however noteworthy that a significantly reduced conversion upon removal of the zeolite catalyst was observed under the optimised conditions.

ray fluorescence (XRF) analysis of the recovered zeolite material suggests that only about 1-2% of copper is lost after five runs.



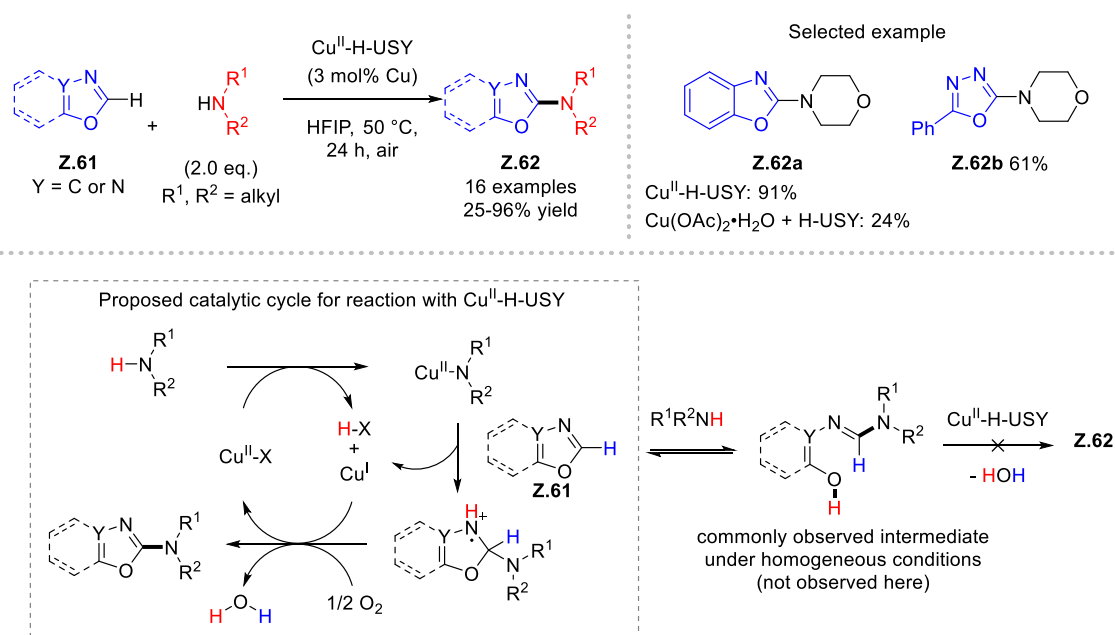
Scheme 50. Cu^I-USY-catalysed HSUNG coupling reaction towards ynamides.^[192]

In 2016, KWAK and co-workers performed N-H and S-H insertions into α -diazoesters **Z.58** to produce amines **Z.59** and thioethers **Z.60** in good yields (Scheme 51).^[193] Among the different zeolites tested, Cu^I-USY proved to be the most efficient. Interestingly, they did not observe the formation of double alkylation products for the N-H insertion, which is a known side reaction under homogeneous conditions.^[194] The authors explain this observation with the restricted pore dimension of Cu^I-USY, which disfavours the accommodation of another diazoester **Z.58** once the monoalkylated product **Z.59** is formed. Beneficially, the reaction is carried out using equimolar amounts of reagents in a H₂O/*t*-BuOH solvent mixture at room temperature, highlighting great green chemical features. Unfortunately, aliphatic amines were not successful, whereas aromatic and aliphatic thiols afforded the desired thioethers **Z.60**. The catalyst was recycled four times and maintained a satisfying activity (about 70-80% rate compared to a fresh sample). Thorough characterisation by X-ray diffraction (XRD), X-ray photoemission spectroscopy (XPS), and transmission electron microscopy (TEM) showed no significant change in zeolite crystallinity, copper location, or oxidation state compared to a fresh sample.



Scheme 51. Cu^I-USY-catalysed N-H and S-H insertions into α -diazoesters.^[193]

In 2020, DE VOS and co-workers reported the use of a Cu^{II}-H-USY zeolite catalyst on the cross-dehydrogenative coupling of azoles **Z.61** and secondary amines to 2-amino-azoles **Z.62** under aerobic conditions (Scheme 52).^[195] The reaction proceeded without the need of ligands or additives but proceeds in HFIP as an undesirable solvent and required two equivalents of the amine. The azole scope mostly covered benzoxazoles (e.g. \rightarrow **Z.62a**), but 5-phenyl-1,3,4-oxadiazole also afforded the desired coupling product **Z.62b**. As for the amine, only aliphatic secondary amines, including cyclic and linear examples, were compatible.



Scheme 52. Aerobic cross-dehydrogenative coupling of azoles **Z.61** and secondary amines with Cu^{II}-H-USY.^[195]

During their optimisation studies, the authors compared different zeolite topologies and applied zeolites with different SAR for the same topology. They noted that highly dealuminated, thus more hydrophobic zeolites gave superior yields. There could be several explanations, including a better evacuation of generated water molecules from catalytic sites, as well as a beneficial ratio between the LEWIS and BRØNSTED acid sites. Indeed, the BRØNSTED acid sites are believed to facilitate this azole amination, which presumably operates through a different mechanism than in zeolite-free protocols. It should however be highlighted that a SHELDON test revealed non-negligible copper leaching and that a noticeable drop in yield is observed upon reuse of recovered zeolite in a second run (from 91% to 42% yield). Yet, a great discrepancy in yield is observed comparing the use of Cu^{II}-H-USY catalyst to a simple mixture of the precursors Cu(OAc)₂·H₂O and H-USY (91% vs. 24%).

Among the above-presented organic reactions, many were catalysed by metal-Y and metal-USY zeolites. This is partially due to their great commercial availability but also because they frequently perform better in organic reactions thanks to the relatively great pore dimensions of such faujasite (FAU) zeolites (for details, see **Figure 4c** in section 3.1.1.). Given its large mesopores of about 40 Å in addition to its micropores (cavities of 12 Å), the hierarchical USY zeolite is particularly attractive in such applications (**Table 4**). Indeed, the mesoporous volume represents about one third of the total pore volume in USY zeolite, which allows the access of larger molecules. Furthermore, the chemical diffusion is enhanced, thus leading to faster conversions in organic reactions. Not surprisingly, USY represents a popular zeolite support for catalytically active metal species.

Table 4. Characteristics of a USY zeolite.

Pore aperture	Cage dimension	Average mesopore size	SSA	Microporous volume	Mesoporous volume	SAR
7.4 Å × 7.4 Å	12 Å	40 Å	600 m ² /g	0.235 cm ³ /g	0.1 cm ³ /g	2.9

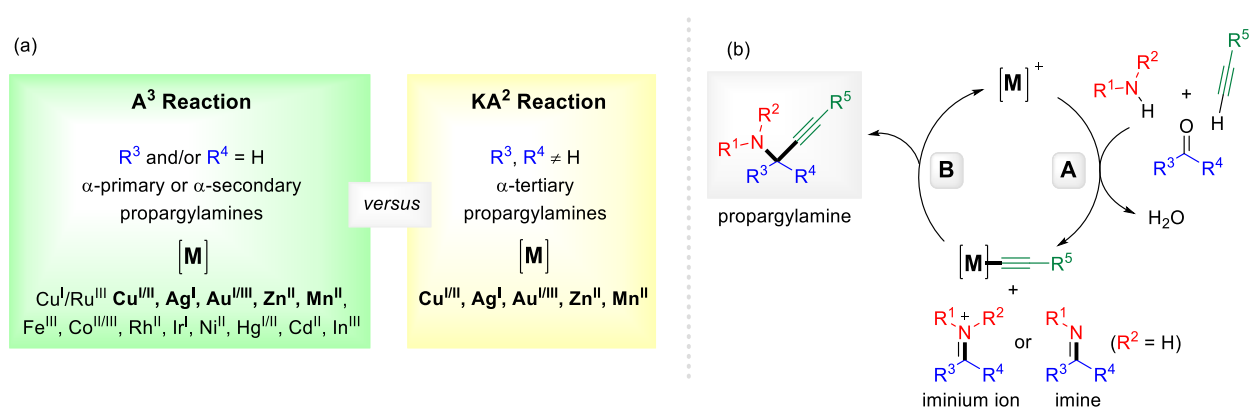
Data correspond to a selected example of H-USY obtained *via* calcination of commercial NH₄-USY (CBV500, Zeolyst International[®]). SSA: specific surface area. SAR: Si/Al ratio.

*Part Two. Copper-Zeolite-Catalysed Syntheses of Propargyl-
amines and Synthetic Applications.*

**Chapter III – Synthesis of α -Tertiary Propargylamines *via* KA^2
and Related Coupling Reactions under Cu^{I} -USY Catalysis**

1. From A³ to KA² Coupling Reaction – State of the Art

The A³ reaction is without doubt one of the most frequently studied C-H activation reactions (Scheme 53). This 3CR represents the metal-catalysed coupling of an aldehyde, amine, and terminal alkyne. Both key intermediates, i.e., the imine/iminium ion electrophile and the metal acetylide nucleophile, are formed in the same “pot” (Scheme 53b, step A). C-C bond formation through nucleophilic addition of the metal acetylide to the imine/iminium ion gives the propargylamine and regenerates the catalyst [M]⁺ (Scheme 53b, step B). Since the seminal contribution of DYATKIN and RIVERO^[39] at the end of the 20th century, it has turned into a bench-reaction for academic researchers to challenge and evaluate their innovative catalytic systems based on numerous transition metals. Not surprisingly, several groups have reviewed these contributions over the years.^[196–199] Various asymmetric protocols of this 3CR have been established as well, now known as the asymmetric A³ (AA³) reaction.^[200] In KOSTAKIS’ recent review,^[199] the authors shed light on the most frequently used classes of each component by exploiting a database containing 2376 A³ reaction entries. They revealed that aromatic alkynes and aldehydes are preferentially used over aliphatic ones, whereas primary anilines and aliphatic secondary amines are more commonly employed than primary aliphatic amines. These compounds represent the most active classes of each component affording the highest yields. Consequently, these classes are preferentially screened or might even represent the sole successful examples of a given catalytic system. Nevertheless, the number of different propargylamines made easily accessible through the A³ reaction is incredibly high. Consequently, creative and innovative contributions exploited the A³ reaction for diversity-oriented synthesis (DOS),^[201] and as a tool to access diverse heterocyclic compounds.^[202]



Scheme 53. (a) Comparison of A³ and KA² reactions and (b) their simplified catalytic cycle.

The KA² reaction, recently reviewed by VOUGIOUKALAKIS and co-workers,^[203] is a direct consequence of the extensive work on the A³ coupling reaction and consists of the 3CR of a ketone, an amine, and an alkyne to access α-tertiary propargylamines (Scheme 53). As for the A³ reaction, various transition metals (Cu^{III}, Ag^I, Au^{III}, Zn^{II} and Mn^{II}) catalyse this coupling reaction.

Compared to aldehydes, ketones display a reduced reactivity because of the additional substituent on the carbonyl carbon lowering its electrophilicity. Increased steric hindrance at the reaction centre, and electronic effects due to electron-rich substituents induce such lower reactivity. Consequently, most catalytic systems reported as efficient in the A^3 reaction gave only moderate yields when ketones were used instead of aldehydes.

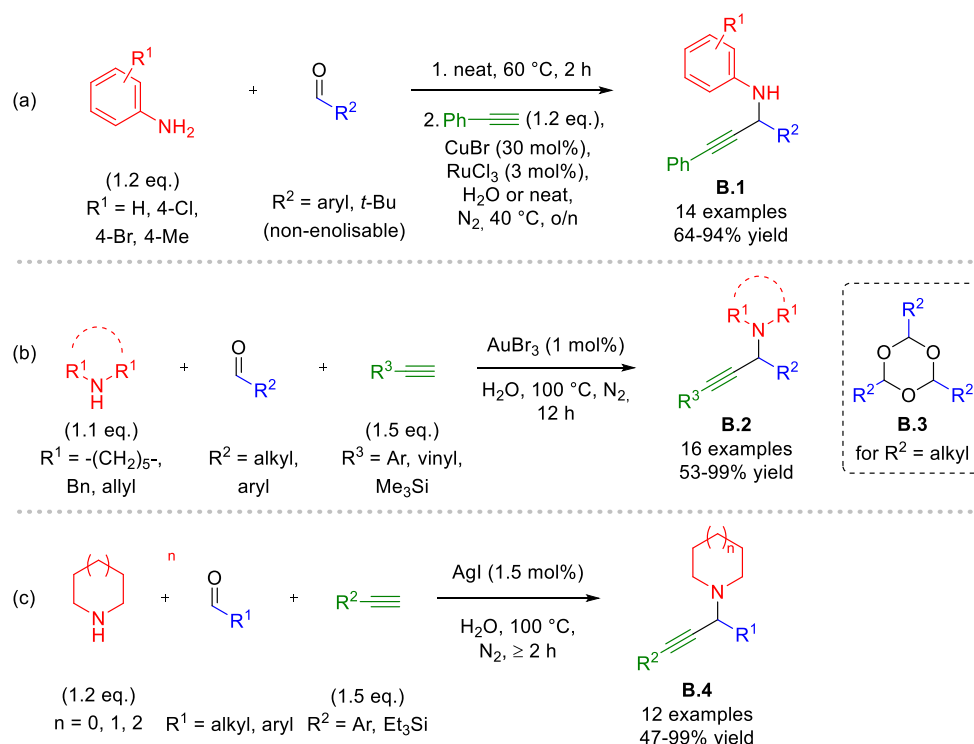
This introductory chapter aims to provide a non-exhaustive list of pioneering A^3 and KA^2 reports. Primarily, methods with broad product scopes or those that targeted highly challenging substrate classes will be presented. In addition, an emphasis on protocols' green chemical aspects will be given.

1.1. Homogeneous and Heterogeneous A^3 Reaction

Complementary to DYATKIN's and RIVERO's^[39] work, LI and co-workers described the use of CuBr/RuCl₃ for the efficient synthesis of primary aniline-derived α -secondary propargylamines **B.1** in 64-94% yield (Scheme 54a).^[204] It should, however, be highlighted that this represented a one-pot sequential procedure and not a cascade 3CR. The reaction was performed in water or under solvent-free conditions at mild reaction temperatures of 40-60 °C. Nevertheless, the use of an expensive Ru-based cocatalyst and a high catalytic loading of CuBr (30 mol%) in this homogeneous reaction increase the amount of waste, thus the *E* factor. Furthermore, the scope includes only non-enolisable aromatic aldehydes or pivalaldehyde.

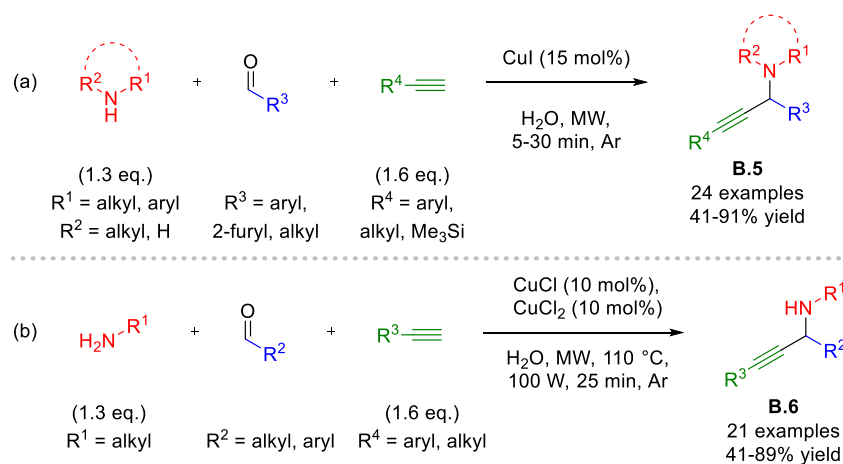
Next, LI's group proved that both Au^I and Au^{III} salts are efficient catalysts in the A^3 coupling reaction in 2003 (Scheme 54b).^[205] Beneficially, low catalyst loading (1 mol%) and water as the optimal solvent were applied. Nevertheless, heating to 100 °C for 12 h was required. The use of AuBr₃ (1 mol%) in water enabled to access α -secondary propargylamines **B.2** in good to excellent yields from piperidine, dibenzyl- or diallylamine, combined to a great diversity of aromatic and aliphatic aldehydes and alkynes. Primary aliphatic amines or anilines, however, were incompatible. Furthermore, a decreased reactivity of aliphatic aldehydes was observed, presumably due to their competing trimerisation to trioxines **B.3**. The occurrence of iminium-enamine equilibria with enolisable aldehydes could also explain their reduced reactivity.

To achieve better yields for aliphatic aldehydes, LI and co-workers established a Ag^I-based protocol (Scheme 54c).^[206] Using only 1 mol% of AgI in water (or organic solvents such as toluene and DMF) at 100 °C afforded the desired α -secondary propargylamines **B.4** with a wide scope of aldehydes and alkynes in good to excellent yields (47-99%). Remarkably, the unwanted trimerisation of aliphatic aldehydes was almost non-existent under these conditions. Unfortunately, this protocol is limited to cyclic secondary amines.



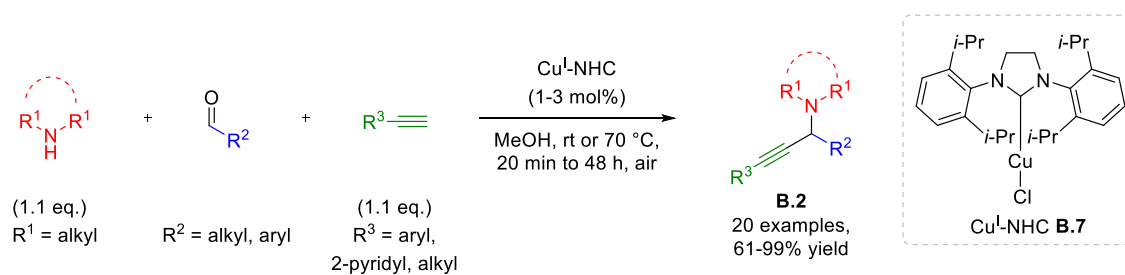
Scheme 54. (a) Cu/Ru-, (b) Au-, and (c) Ag-catalysed A³ reactions reported by LI and co-workers.^[204–206]

Despite all these seminal contributions, linear secondary and primary aliphatic amines remained challenging substrates for the multicomponent A³ reaction. Already in 2004, FAN and co-workers used microwave irradiation to accelerate the Cu^I-catalysed A³ reaction (**Scheme 55a**) to access α -secondary propargylamines **B.5**.^[207] Their catalytic system was successful with various substrate classes, including diethylamine, aniline, and *tert*-butylamine requiring maximum 30 minutes. Later, VAN DER EYCKEN and co-workers established similar conditions focussing particularly on secondary amine products under microwave irradiation (**Scheme 55b**).^[208,209] By combining CuCl/CuCl₂ in water, for instance, 21 propargylamines **B.6** from aliphatic primary amines, aryl- and alkylalkynes, and aliphatic aldehydes were obtained in 41-89% yield and only 25 minutes.^[209]



Scheme 55. Cu^I-catalysed A³ reactions under microwave activation.^[207–209]

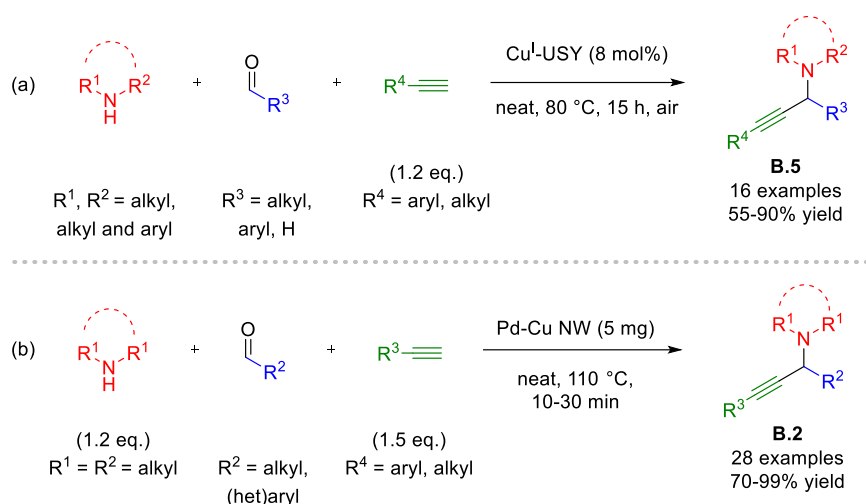
While most A^3 protocols operate at high reaction temperatures, NAVARRO and CHEN reported the use of a Cu^I -NHC complex **B.7** operating in MeOH at room temperature or 70 °C depending on the substrate combination (**Scheme 56**).^[210] Beneficially, near equimolar amounts of each component are used, and the reaction proceeds with low catalyst loadings within a few hours with aliphatic aldehydes.



Scheme 56. Cu^I -NHC-catalysed A^3 reaction.^[210]

The use of a supported metal catalyst could further increase the attractiveness and potential sustainability of the A^3 coupling reaction. In addition to the Ni -^[158] and Ag -loaded^[159] zeolite catalysts presented in section II-2.5.2., PALE and co-workers successfully employed Cu^I -loaded zeolites as reusable catalysts under solvent-free conditions.^[211] Cu^I -USY proved to be the best-performing catalyst among the copper zeolites screened at a copper loading of 8 mol%. Under solvent-free conditions at 80 °C, a diverse series of α -secondary propargylamines **B.5** were obtained in 55-90% yields. Secondary aromatic and aliphatic amines were successfully employed, combined with different aliphatic and aromatic aldehydes and alkynes. Furthermore, Cu^I -USY was recovered and reused four times without loss of activity when calcined before each run. After the fifth run, the yield was still good but significantly decreased.

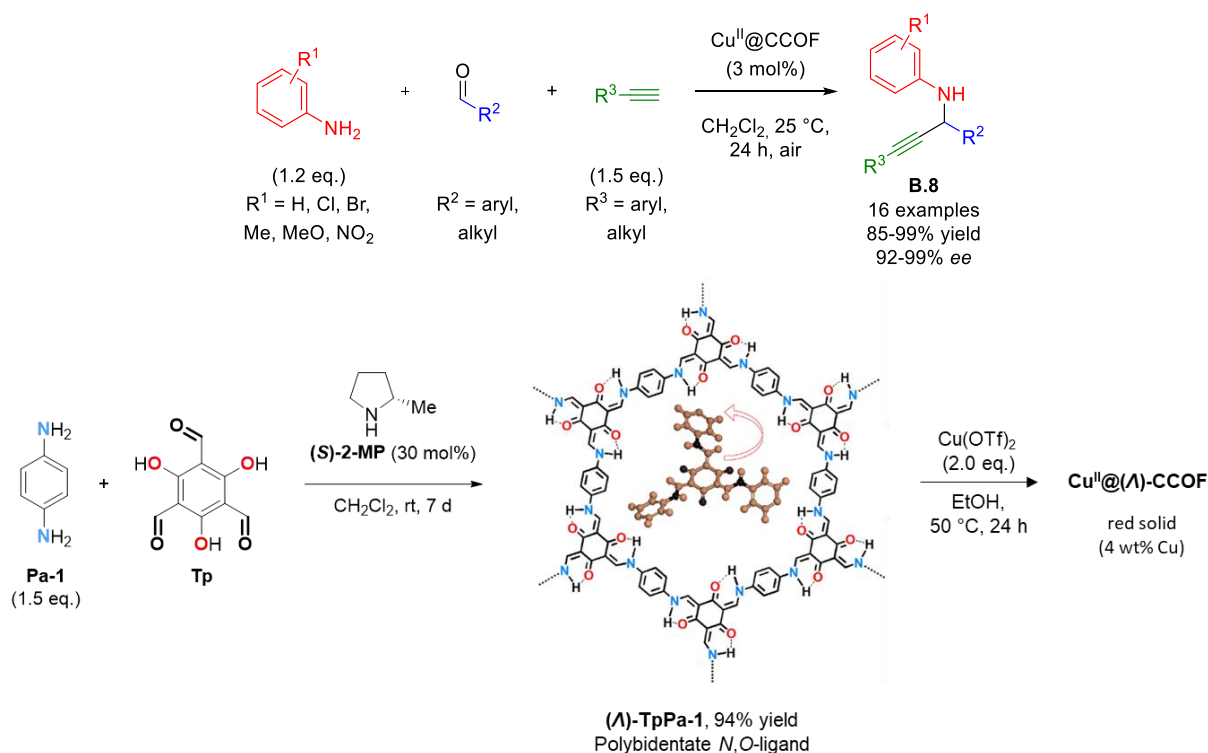
Recently, N. LI and co-workers developed the synthesis of bimetallic Pd-Cu nanowires which efficiently catalysed the solvent-free A^3 reaction to α -secondary propargylamines **B.2** in short times when heated to 110 °C.^[212] Interestingly, ICP-OES analysis indicated a leaching of less than 1 ppm of Pd and Cu after each run and the yield remained nearly unchanged for a total of five runs with recovered catalyst. Furthermore, a broad functional group tolerance was observed, and several substrate classes were efficient. Unfortunately, the scope does not include anilines, nor aliphatic primary amines.



Scheme 57. Heterogeneously-catalysed A³ reactions with (a) Cu^I-USY zeolite^[211] and (b) Pd-Cu nanowires (NW).^[212]

An outstanding example of an asymmetric A³ (AA³) reaction was recently disclosed by DONG and co-workers using supported copper(II) on a chiral TpPa-1-based covalent organic framework (Cu^{II}@CCOF) (**Scheme 58**).^[213] Chiral TpPa-1 COF represents a Schiff-base polymer obtained from 1,3,5-triformylphloroglucinol (Tp) and 1,4-phenylenediamine (Pa-1) using (*S*)-2-methylpyrrolidine (MP) as chiral organocatalyst. Their protocol presents numerous attractive features. The scope focused on α -secondary propargylamines **B.8** derived from primary anilines, and all products were obtained in high yields and *ee* ($\geq 92\%$). Aliphatic and aromatic alkynes and aldehydes were successful and several functional groups (halides, nitro, alkoxy) were well tolerated. Beneficially, the reaction proceeds at room temperature and low copper loading under air but requires CH₂Cl₂ as the solvent for good yields and enantioselectivities. Moreover, an aerogel was fabricated from the metal-doped CCOF and chitosan. Cu^{II}@(A)-CCOF@chitosan was then shaped into a fixed-bed reactor to perform scaled-up (20 mmol) AA³ reactions with consistently high yields and enantioselectivity over ten runs.

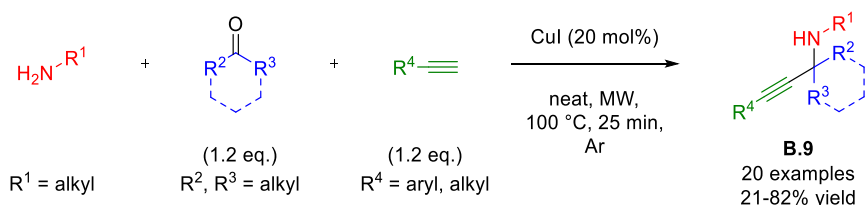
Other recent reports on supported catalysts for the A³ reaction include Ni-nanoparticles on graphene oxide^[214] and a magnetically recyclable triazine-based Cu-NNN-pincer complex.^[215]



Scheme 58. Mild asymmetric A^3 using a Cu^{II} -loaded chiral covalent organic framework (COF).^[213]

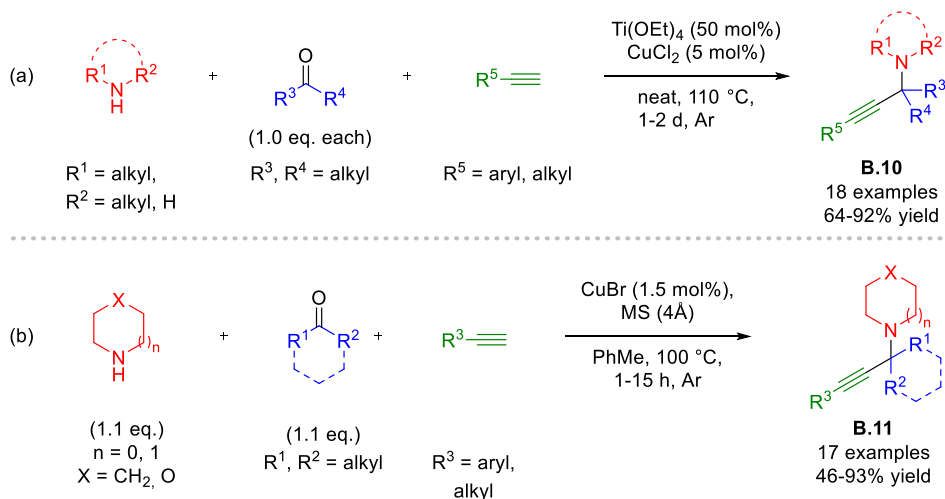
1.2. Homogeneous and Heterogeneous KA^2 Reaction

In 2010, VAN DER EYCKEN and co-workers coined the term KA^2 reaction and reported the first wide-ranging KA^2 protocol for the solvent-free and microwave-assisted synthesis of diverse α -tertiary propargylamines **B.9** (Scheme 59).^[42] Several primary aliphatic amines were reacted with cyclic aliphatic ketones and aryl- and alkylalkynes using CuI (20 mol%) as catalyst. From their product scope, it is evident that aliphatic alkynes are less efficient than aromatic ones. Furthermore, linear aliphatic (here acetone) and aromatic ketones (not mentioned) remained challenging coupling partners. There are steric and electronic reasons to explain the reduced reactivity of both ketone classes. Compared to ketimine/ketiminium intermediates from cyclic ketones, linear derivatives do not benefit from strain energy release upon nucleophilic addition of the metal acetylide.^[216,217] In aromatic ketones, the conjugation of the carbonyl and aryl groups induces a lower LUMO energy on the one hand but concomitantly reduces the energy level of the ketone on the other. Therefore, aromatic ketones are less reactive towards nucleophiles compared to linear aliphatic ketones. In the context of the KA^2 reaction, imine/iminium intermediate formation is thus more challenging with aromatic ketones. Moreover, the resulting imine/iminium intermediates again benefit from the electronic stabilisation through conjugation with the aromatic substituent, which hampers the nucleophilic addition of the metal acetylide.



Scheme 59. CuI-catalysed KA² reaction with primary amines under microwave irradiation.^[42]

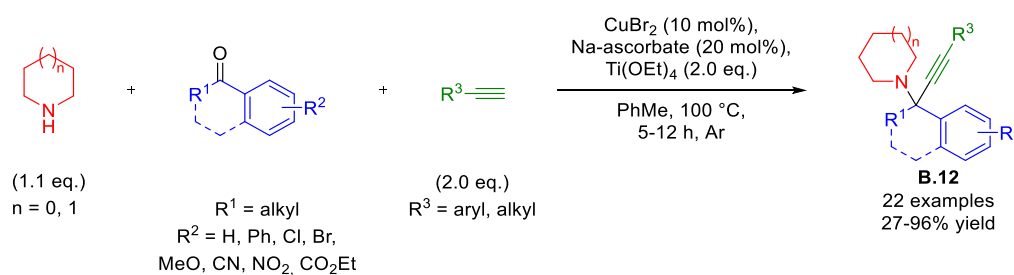
To overcome these limitations, LARSEN's and MA's groups scrutinised ways to promote ketimine formation and its electrophilic activation. In 2012, LARSEN and co-workers examined several LEWIS acids and/or dehydrating agents in the KA² reaction with linear aliphatic ketones to give **B.10** propargylamines.^[218] In the presence of CuCl₂ as catalyst, Ti(OEt)₄ (50 mol%) was the most efficient and afforded good yields with primary and secondary aliphatic amines, combined with alkyl- and arylalkynes (**Scheme 60a**). Aromatic ketones, however, remained unreactive. For primary amines, Ti(OEt)₄ presumably also enables electrophilic activation of the ketimine, as alkyne addition on pre-formed imine was observed to be less fast in its absence. Similar α -tertiary propargylamines **B.11** from linear aliphatic ketones were prepared by MA and co-workers (**Scheme 60b**).^[219] They used CuBr (1.5 mol%) and molecular sieves (MS, 300 mg/mmol) in hot toluene to afford good to high product yields in a few hours. Interestingly, the product scope was performed on 10 mmol scale and further up-scaling to 50 mmol was possible by replacing molecular sieves for a DEAN-STARK trap. Nevertheless, pyrrolidine led to significantly higher yields than morpholine and piperidine, whereas dibenzylamine and benzylamine were unsuccessful. The amine scope is therefore greatly limited.



Scheme 60. Additive-based KA² procedures for challenging aliphatic linear ketones using (a) Ti(OEt)₄^[218] or (b) molecular sieves (MS).^[219]

MA and co-workers also addressed the challenging aromatic ketones in 2016.^[220] Interestingly, a combination of CuBr₂, sodium ascorbate, and Ti(OEt)₄ afforded previously unattainable KA² products **B.12** (21 examples, 27-96% yield) from aromatic ketones bearing diverse functional groups, such as halides, nitro, ester, and alkoxy (**Scheme 61**). Rewardingly, besides aromatic

alkynes, hept-1-yne reacted smoothly, albeit requiring longer stirring. It is nevertheless worth mentioning that only pyrrolidine and piperidine were successfully employed, while acyclic secondary amines or primary amines were incompatible coupling partners. XPS and XAES analysis revealed the presence of a Cu^I-species from the reduction of CuBr₂ with sodium ascorbate. The exact nature of the catalytically active species remains however unknown.



Scheme 61. Cu-catalysed KA² reaction of challenging aromatic ketones.^[220]

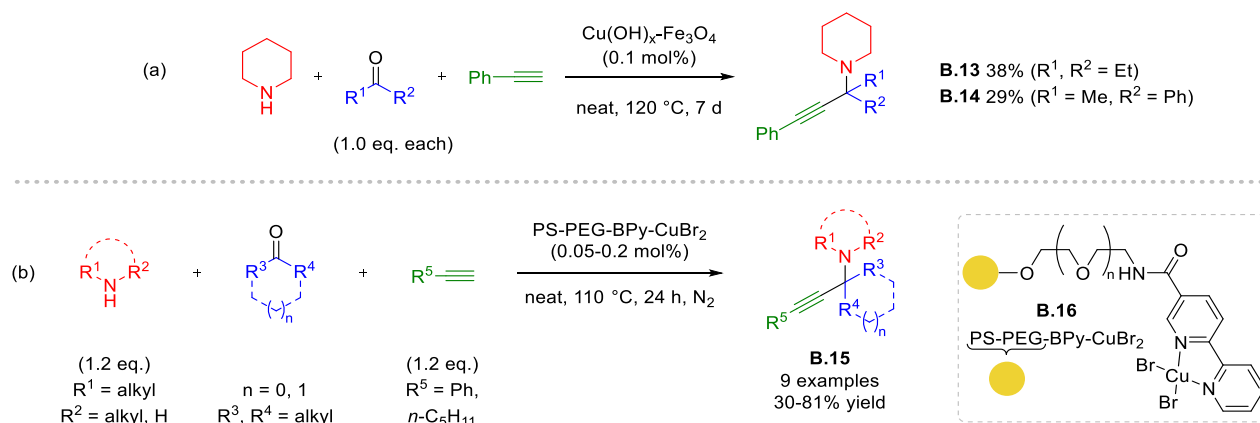
Unfortunately, the above-mentioned limitations have not been overcome by supported catalysts. Most protocols based on such catalysts show highly limited product scopes, such as the exclusive use of cyclic ketones and/or secondary cyclic aliphatic amines, as well as aromatic alkynes.^[221–224]

Nevertheless, some notable heterogeneous catalytic systems can be cited presenting a broader product scope, some “green” features, and sometimes a certain degree of recyclability. As for homogeneous examples, most protocols are based on copper.

Interestingly, the very first KA² reactions reported were performed under heterogeneous catalysis. RAMÓN and co-workers applied impregnated copper on magnetite as an easy-to-prepare and highly efficient catalyst in the A³ reaction leading to α -secondary propargylamines in up to quantitative yields in 2010.^[225] Shifting to 3-pentanone and acetophenone, the desired KA² products **B.13** and **B.14** were isolated in significantly lower yields (38% and 29%, respectively) after seven days at 120 °C (**Scheme 62a**). The catalyst loading, however, was set to only 0.1 mol%. To date, these product yields are highly competitive for an additive-free catalytic system. In fact, linear aliphatic and aromatic ketones represent the most challenging ketone classes in the KA² reaction. Moreover, the catalyst can conveniently be recovered using a magnet and its recyclability was established for ten runs without a significant drop in yield. Unfortunately, the authors have not screened the activity of their catalyst for additional ketones.

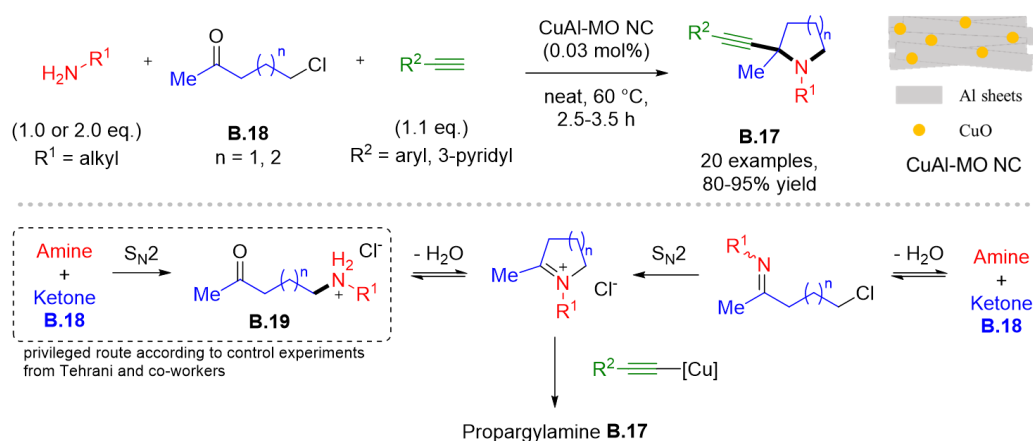
In 2019, UOZOMI and co-workers performed a solvent-free KA² reaction to propargylamines **B.15** with a polymer-supported Cu^{II}-bipyridine complex **B.16** using very low copper loadings of 0.05–0.2 mol% (**Scheme 62b**).^[226] While cyclic ketones reacted smoothly with cyclic secondary amines and phenylacetylene at 0.05 mol% copper loading, primary *n*-hexylamine, linear ketones or hept-1-yne required 0.2 mol% catalyst to give moderate to good yields. Unfortunately, compared to fast A³ reactions (1 h) under the same conditions, the KA² reaction was set

to 24 h, even at 110 °C. Given the small catalyst loadings, the authors did not perform a recyclability study. Furthermore, copper leaching was not commented.



Scheme 62. Heterogeneous copper-based catalysts in the KA² reaction featuring (a) impregnated copper on magnetite^[225] and (b) a polymer-supported Cu^{II}-bipyridine complex.^[226]
 PS-PEG: polystyrene-polyethylene glycol.

In 2019, RAWAT and co-workers prepared a CuAl-mixed oxide sheet-like nanocomposite (CuAl-MO NC), which they applied in a KA²-like 3CR towards 2-alkynylpyrrolidines and -piperidines **B.17** (Scheme 63).^[227] Mechanistically, a primary amine and ω -chloro ketone **B.18** generate a secondary ω -ammonium ketone **B.19**. The latter then undergoes intramolecular amine/ketone condensation to its iminium ion, which is trapped by the alkynyl copper nucleophile to yield **B.17**. This attractive MCR was initially reported by TEHRANI and co-workers with Cu₂O in MeCN.^[228,229] They observed that high yields can be achieved under solvent-free conditions, as reported by RAWAT's group. CuAl-MO NC enabled the synthesis of numerous 2-alkynylpyrrolidines and -piperidines **B.17** from primary aliphatic amines and arylalkynes at low copper loading (0.03 mol%) in several hours. Compared to TEHRANI's conditions, however, only a small number of functional groups were investigated and no alkylalkynes are presented. Several analytic techniques confirmed the stability of the nanoporous support, and recyclability was observed for a total of five runs starting from 0.09 mol% copper. ICP-OES analysis revealed a leaching of 1-7 and 0.2-0.6 ppm of copper and aluminium respectively throughout the recyclability study.



Scheme 63. Cu-catalyzed KA²-like reaction towards α -tertiary pyrrolidines and piperidines.^[227]

The following sections deal with the experimental results obtained with Cu^I-USY as supported catalyst in the KA² and related 3CRs. USY (ultra-stable Y) corresponds to a hierarchical faujasite zeolite possessing micro- and mesoporosity obtained *via* dealumination of Y zeolite (for details, see section II-1.1.). Following the seminal contribution of SLADE and co-workers on the preparation of Cu^I-Y zeolite through a solid-state ion-exchange reaction (SSIE, for details, see section II-2.4.2.) between H-Y and excess CuCl,^[109] Cu^I-USY was similarly prepared from H-USY and characterised by PALE's group in 2009.^[230] Rewardingly, the CuCl quantity was however reduced to equimolar amounts relative to the number of aluminate sites in USY zeolite. Accordingly, Cu^I-USY is prepared from a solid mixture of H-USY and CuCl, which is heated in a furnace under flowing nitrogen at 350°C for three days (Figure 7). The final copper loading as determined by ICP-AES is of ca. 3 mmol/g, which corresponds to an H-for-Cu exchange degree of ca. 80%. This suggests that about 20% of BRØNSTED acid sites remain but their chemical nature and locations are not precisely known. As we will see throughout the different synthetic methodologies studied in this manuscript, Cu^I-USY presented, however, an excellent tolerance for acid-labile groups, such as acetals and Boc-carbamates.

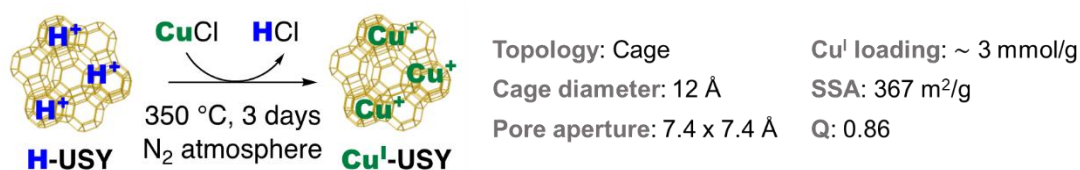


Figure 7. Preparation of Cu^I-USY *via* SSIE reaction and key properties.

SSA: specific surface area (660 m²/g in parent H-USY). Q: crystallinity (1.0 for parent H-USY).

It should be noted that additional copper- or other metal-loaded zeolites used throughout this thesis were prepared *via* the same procedure unless otherwise stated.

2. Cu^I-USY-catalysed KA² Reaction with Terminal Alkynes

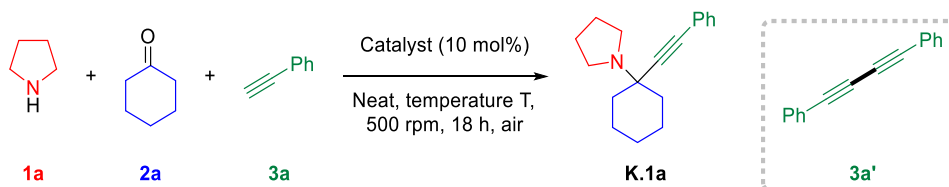
Motivated by its efficient use in the A³ reaction,^[211] we investigated the use of our Cu^I-USY zeolite as catalyst in the KA² reaction. To evaluate its potential compared to the above-presented heterogeneous KA² procedures, all substrate classes of the different coupling partners were examined.

2.1. Optimisation of Reaction Conditions

Initial investigations were conducted under conditions similar to the previously reported Cu^I-USY-catalysed A³ reaction conditions^[211] with pyrrolidine **1a**, cyclohexanone **2a**, and phenylacetylene **3a** as model coupling partners (Table 5, entry 1). Remarkably, these conditions gave the desired α -tertiary propargylamine **K.1a** in excellent yield. In addition, other transition metal-loaded zeolites were evaluated for this transformation. Zn^{II}-USY gave propargylamine **K.1a** in good 76% yield under identical conditions (entry 2), whereas Mn^{II}-USY gave a poor result (i.e., 34%, entry 3). Interestingly, Co^{II}-USY produced the desired KA² product **K.1a**, albeit in a modest 48% yield (entry 4). To the best of our knowledge, a Co-catalysed KA² reaction has not been reported to date. For all metal-exchanged USY zeolite catalysts, a complete conversion of cyclohexanone was observed *via* TLC and ¹H NMR, but undefined by-products were obtained. The use of CuCl alone (entry 5), or in combination with H-USY (entry 6), resulted in complete conversions, but with lower efficiency in terms of yield and chemoselectivity. These data show that the solid-state ion-exchange reaction generates a superior Cu^I-USY catalyst compared to a simple mixture of both precursors. As expected, control experiments showed that the KA² coupling process does not occur in the absence of any transition metal (entry 7) nor in the sole presence of the non-metalated zeolite precursors (i.e., NH₄-USY and H-USY, entries 8 and 9). Since Cu^I-USY emerged as the most promising catalyst, it was retained for further optimisation.

Subsequently, the influence of the reaction temperature was investigated (entries 10 and 11 vs. 1). Lowering the temperature to 60 °C led to a small but effective decrease in conversion and yield (entry 10). Higher temperature (110 °C) led to a comparably reduced yield despite the complete conversion of cyclohexanone, but due to the formation of by-products (entry 11). The effect of the alkyne amount was investigated next (entries 12 and 13 vs. 1). A low but progressive decrease in yield was observed when shifting from 1.5 to 1.3 (entry 12), and further to 1.0 equivalents (entry 13). This is explained by the formation of small amounts of the GLASER homocoupling product **3a'** as the reaction is run under air. Using 1.5 alkyne equivalents thus appears as a good compromise between yield and atom economy.

Table 5. Screening of catalysts, temperature, and alkyne equivalents for the KA² coupling reaction.^[a]



Entry	Catalyst	Alkyne eq.	T (°C)	Yield ^[b] K.1a (%)
1	Cu ^I -USY	1.5	80	92 (92) ^[c]
2	Zn ^{II} -USY	1.5	80	76 ^[d]
3	Mn ^{II} -USY	1.5	80	34 ^[d]
4	Co ^{II} -USY	1.5	80	48 ^[d]
5	CuCl	1.5	80	79 ^[d]
6	CuCl + H-USY	1.5	80	78 ^[d]
7	none	1.5	80	0
8	H-USY	1.5	80	0
9	NH ₄ -USY	1.5	80	0
10	Cu ^I -USY	1.5	60	83 ^[e]
11	Cu ^I -USY	1.5	110	81 ^[d]
12	Cu ^I -USY	1.3	80	86
13	Cu ^I -USY	1.0	80	82

^[a] Reactions run in a sealed tube with **1a** (1.0 mmol, 1. eq.), **2a** (1.0 eq.), **3a** (1.5 eq.), and catalyst (10 mol%), unless otherwise stated. ^[b] Yield estimated *via* ¹H NMR of the crude using 1,3,5-trimethoxybenzene as internal standard. ^[c] Yield of isolated product **K.1a**. ^[d] Complete conversion but formation of by-products. ^[e] Incomplete conversion.

While there is a clear environmental and economic advantage in using solvent-free conditions, numerous solvents were screened to identify a compatible, and at best “green”, alternative option in case of stirring or solubility issues (**Figure 8**). As already observed in several Cu^I-zeolite-catalysed organic reactions, toluene yielded the best result.^[186,192,231] Indeed, propargylamine **K.1a** was obtained with comparable efficiency to solvent-free conditions. While lower yields were obtained in MeCN, *n*-BuOAc, and ethylal (i.e., diethoxymethane) (75–83%), EtOAc and 2-MeTHF proved to be attractive „greener“ alternatives with similar efficiencies to toluene. Next, polar protic solvents were scrutinised. Performing the reaction in water still afforded propargylamine **K.1a** in 39% yield. EtOH and *n*-BuOH proved to be more efficient (55 and 83%, respectively). In both cases, complete conversion was achieved, although the formation of by-products still occurred.

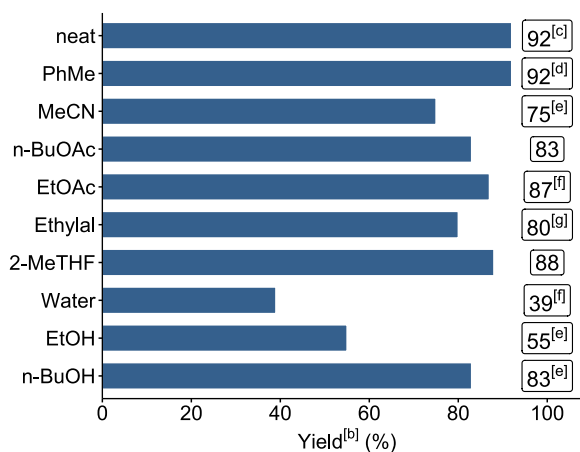
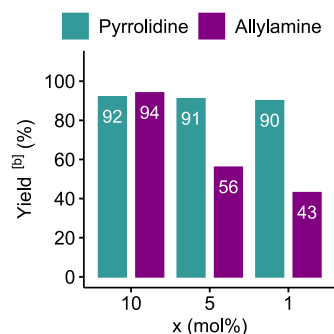
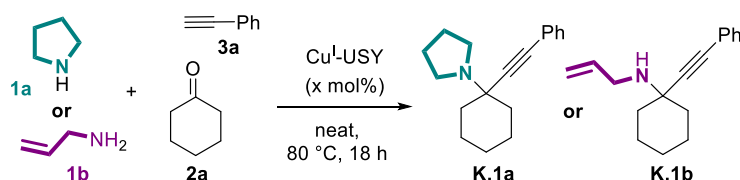


Figure 8. Solvent screening for the Cu^I-USY-catalysed KA² reaction.^[a]

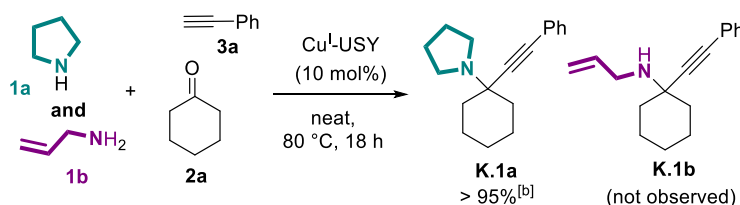
^[a] Reactions run in a sealed tube with **1a** (1.0 mmol, 1. eq. with a 1 M concentration), **2a** (1.0 eq.), **3a** (1.5 eq.) and Cu^I-USY (10 mol%), unless otherwise stated. ^[b] Yield estimated *via* ¹H NMR of the crude using 1,3,5-trimethoxybenzene as internal standard, unless otherwise stated. ^[c] Yield of isolated product **K.1a**. ^[d] 88% of isolated product. ^[e] Complete conversion but formation of by-products. ^[f] Incomplete conversion. ^[g] Diethoxymethane.

The effect of the catalyst loading was examined next. Since primary amines are known to be more challenging substrates, allylamine (**1b**) was also included as a primary model amine in this study. Both amines were used with cyclohexanone (**2a**) and phenylacetylene (**3a**) under the previously optimised conditions at different catalyst loadings (**Scheme 64a**). With 10 mol% Cu^I-USY, allylamine reacted smoothly to give the desired propargylamine **K.1b** with comparable efficiency to pyrrolidine (**1a**). While reducing the amount of catalyst to 1 mol% did not change the coupling efficiency for the secondary amine **1a**, a sharp decrease in conversion and yield was observed with allylamine (**1b**), as already observed with a Cu loading of 5 mol%. Based on these results, we decided to set the catalyst loading for the following studies to 10 mol% to apply standardised conditions, but also for practical and comparative reasons. To further illustrate the reactivity difference of both amines, the competition experiment summarised in **Scheme 64b** was realised. The concomitant addition of both amines resulted in the exclusive formation of propargylamine **K.1a** at the expense of **K.1b**. These findings reflect (i) the much higher nucleophilic reactivity of pyrrolidine compared to allylamine as reported elsewhere^[232,233] combined with (ii) the higher electrophilicity of the ketiminium intermediate formed from pyrrolidine compared to the ketimine intermediate from allylamine.

(a) Screening of Cu-loading^[a]



(b) Competition experiment^[c]



Scheme 64. (a) Screening of the catalyst loading and (b) competition experiment between pyrrolidine and allylamine. ^[a] Reactions run neat at $80\text{ }^{\circ}\text{C}$ in a sealed tube with pyrrolidine **1a** or allylamine **1b** (1.0 mmol, 1.0 eq.), cyclohexanone **2a** (1.0 eq.), phenylacetylene **3a** (1.5 eq.) and $\text{Cu}^{\text{I}}\text{-USY}$ (x mol%) with $x = 1, 5, 10$. ^[b] Yield estimated *via* ^1H NMR of the crude using 1,3,5-trimethoxybenzene as internal standard for $x = 1$ and 5 in A, and for B. ^[c] Reaction run neat at $80\text{ }^{\circ}\text{C}$ in a sealed tube with pyrrolidine **1a** and allylamine **1b** (1.0 mmol, 1.0 eq.), cyclohexanone **2a** (1.0 eq.), phenylacetylene **3a** (1.5 eq.) and $\text{Cu}^{\text{I}}\text{-USY}$ (10 mol%).

2.2. Up-scaling and Recyclability

First, the possibility for scale-up of our KA^2 procedure was evaluated for the model propargylamine **K.1a**. Under solvent-free conditions using 5 mol% of $\text{Cu}^{\text{I}}\text{-USY}$, a 10 mmol scale successfully yielded 2.1 g (82% yield) of **K.1a** after purification (**Figure 9**).

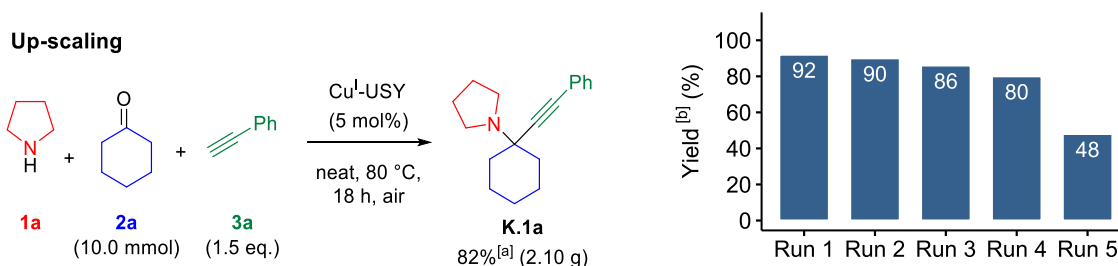


Figure 9. Up-scaling and recycling of $\text{Cu}^{\text{I}}\text{-USY}$ in the KA^2 benchmark reaction affording amine **K.1a**. ^[a] Isolated yield. ^[b] Yield estimated from crude mixtures *via* ^1H NMR using 1,3,5-trimethoxybenzene as internal standard.

In addition to their inexpensiveness, excellent thermal stability, ease of production and handling, zeolites are also environmentally friendly materials. As for other supported catalysts, the question of recovery and recyclability arises for metal-doped zeolites in each new process. For this reason, the recyclability of the $\text{Cu}^{\text{I}}\text{-USY}$ catalyst was investigated using the model reaction between cyclohexanone, pyrrolidine, and phenylacetylene (**Figure 9**). After each reaction run under the solvent-free conditions, the catalyst was recovered by filtration, washed, dried under vacuum, and used in the next run without reactivation. Since this procedure always involves some loss of material due to the mechanical recovery of the catalyst, this procedure was carried out with 10 mol % of $\text{Cu}^{\text{I}}\text{-USY}$. With this recycling procedure, a small, yet progressive loss of activity was observed from the first to the fourth run. However, on the fifth run, a significant

drop in product yield to 48% was observed, indicating an erosion of the catalytic activity. Compared to the related A³ reaction, however, no intermediate calcination of the recovered zeolite material was required to give similar recycling data.^[211] Considering that propargylamine **K.1a** can be produced in about 90% yield at 1 mol%, the time, energy, and resources required to recover the catalyst are not reasonable here.

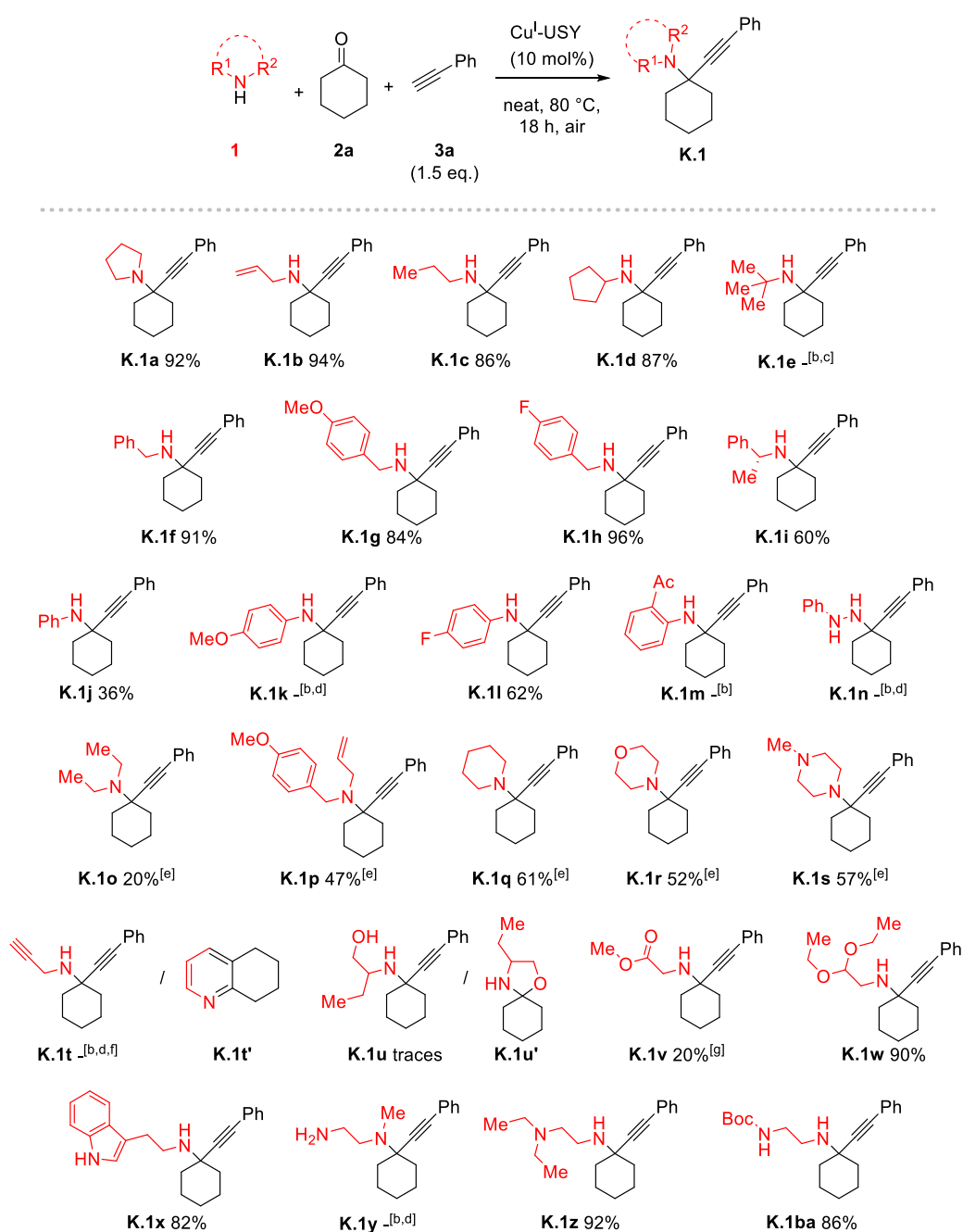
2.3. Scope and Limitations

Due to the promising yields, especially for the primary allylamine, we investigated the scope of this Cu^I-USY-catalysed KA² reaction.

2.3.1. Amine Scope

First, we investigated the amine scope (**Scheme 65**). Considering the reaction mechanism (**Scheme 53**), the amine may play a dual but possibly contradictory role in the reaction. On the one hand, more nucleophilic amines should allow easier access to the ketimine/ketiminium intermediate. On the other hand, the electronic and/or steric properties of the amine also define the electrophilicity of the resulting ketimine/ketiminium. Indeed, nucleophilic, and sterically hindered amines reduce the reactivity of these intermediates. Based on these mechanistic considerations, we first assessed the relevance of challenging primary amines as coupling partners, as they condense to less reactive ketimines.

Encouragingly, propargylamine **K.1c** was also formed in promising 84% yield, regardless of its low boiling point, as with allylamine (both at about 50 °C). Interestingly, switching to the bulkier α -secondary cyclopentylamine did not affect the coupling performance and still gave propargylamine **K.1d** in 87% yield. However, with *tert*-butylamine, the KA² product **K.1e** could not be obtained, probably due to steric effects. Benzylamines also proved to be efficient coupling partners and gave the corresponding propargylamines **K.1f-i** in good to excellent yields. Benzylamine gave **K.1f** in a high 91% yield, whereas the more electron-rich 4-methoxybenzylamine led to **K.1g** in a slightly lower 84% yield. Its electron-poor 4-fluoro analogue, however, furnished **K.1h** in 96% yield. As previously described by LARSEN and co-workers, the more electron-deficient the amine, the higher the yield of the KA² product.^[234] In contrast to cyclopentylamine, a pronounced steric influence was observed when (*R*)-(+)- α -methylbenzylamine was used. Indeed, amine **K.1i** was obtained in 60% yield as compared to 91% yield for **K.1f**.



Scheme 65. Amine scope of the Cu^{I} -USY-catalysed KA^2 reaction.^[a]

^[a] Reactions run neat at 80 °C in a sealed tube with cyclohexanone (**2a**, 1.0 mmol, 1.0 eq.), amine **1** (1.0 eq.), phenylacetylene (**3a**, 1.5 eq.) and Cu^{I} -USY (10 mol%), unless otherwise stated. ^[b] No traces of the expected KA^2 product were detected. ^[c] Almost no conversion was observed. ^[d] Complex mixture of unidentified difficult-to-purify products. ^[e] Formation of a by-product which will be discussed later in section III-2.3.4. ^[f] Reaction run with Cu^{I} -USY (1 mol%). ^[g] Reaction run in PhMe (0.5 M) with glycine methyl ester hydrochloride (1.0 mmol, 1.0 eq.) in the presence of NaHCO_3 (1.0 mmol, 1.0 eq.).

Although anilines are successful A^3 coupling partners,^[207,235,236] no successful example of KA^2 reactions has been reported so far, as anilines lead to complex reaction mixtures. Nevertheless, we investigated the suitability of anilines as coupling partners under our conditions (**Scheme 65**). Encouragingly, our catalytic conditions led to the aniline-derived propargylamine **K.1j**, albeit in a modest 36% yield. Again, electronic effects allowed tuning the KA^2 efficiency. The electron-deficient 4-fluoroaniline gave **K.1l** in an improved 62% yield, while the electron-rich 4-methoxyaniline led to a complex mixture in which no traces of the desired product **K.1k** were

detected. This is in agreement with the observations of other authors using other catalysts.^[237,238] As with benzylamines, the reaction was favoured by the use of arylamines with electron-withdrawing groups in the *para* position. Again, these electronic effects underline the key role of the ketimine intermediate, because the less nucleophilic the amine coupling partner was, the more reactive/electrophilic is the ketimine. Nevertheless, propargylamine **K.1m** could not be obtained because the acetyl group in *ortho* position completely prevented imine formation. Similar to electron-rich anilines, the strongly nucleophilic phenylhydrazine led to a complex mixture of unidentified, difficult-to-purify by-products without any traces of propargylamine **K.1n**.

In sharp contrast to pyrrolidine, other secondary amines gave the expected products **K.1o-s** in only low to moderate yields (**Scheme 65**). Although a complete conversion was observed for all examined amines, the concomitant formation of a by-product, which will be discussed later, hampered yields (**Scheme 68**). This resulted in hard-to-purify mixtures. Linear secondary amines generally exhibit reduced coupling efficiencies in the KA² and A³ reactions. Indeed, propargylamines **K.1o** and **K.1p** were obtained in low to moderate yields from diethylamine and *N*-allyl-*N*-(4-methoxybenzyl)amine (20% and 47%, respectively). Cyclic derivatives such as piperidine, morpholine, and *N*-methylpiperazine gave the desired KA² products **K.1q-s** in slightly higher but still moderate yields (52-61%).

To evaluate the functional group tolerance of our catalytic system, various primary amines carrying additional functional groups were included in the coupling process with cyclohexanone (**2a**) and phenylacetylene (**3a**). Propargylamine led to a complex mixture without traces of the desired product **K.1t**. Pyridine **K.1t'** was identified as one by-product, which arises from a cascade condensation/6-*endo*-dig cyclisation/aromatisation.^[239] 2-Aminobutanol yielded only trace amounts of the amine **K.1u**, due to competitive intramolecular nucleophilic scavenging of the iminium intermediate to give *N,O*-ketal **K.1u'**. VAN DER EYCKEN's report on the CuBr-catalysed A³ coupling reaction with α -amino ester hydrochlorides^[240] inspired us to employ glycine methyl ester with Cu^I-USY and NaHCO₃ in toluene to obtain amine **K.1v** in 20% yield. Interestingly, we demonstrated the suitability of amines bearing an acetal and an indole moiety. Indeed, the propargylamines **K.1w** and **K.1x** were obtained in high yields (90% and 82%, respectively). Unfortunately, *N*-methylethylenediamine failed to form the bis-nitrogenated KA² compound **K.1y**, demonstrating the unsuitability of mixed primary and secondary 1,2-diamines. Rewardingly, the bis-nitrogenated KA² analogues **K.1z** and **K.1ba** were obtained in high yield with *N,N*-diethyl- (92%), and *N*-Boc-ethylenediamine (86%), respectively.

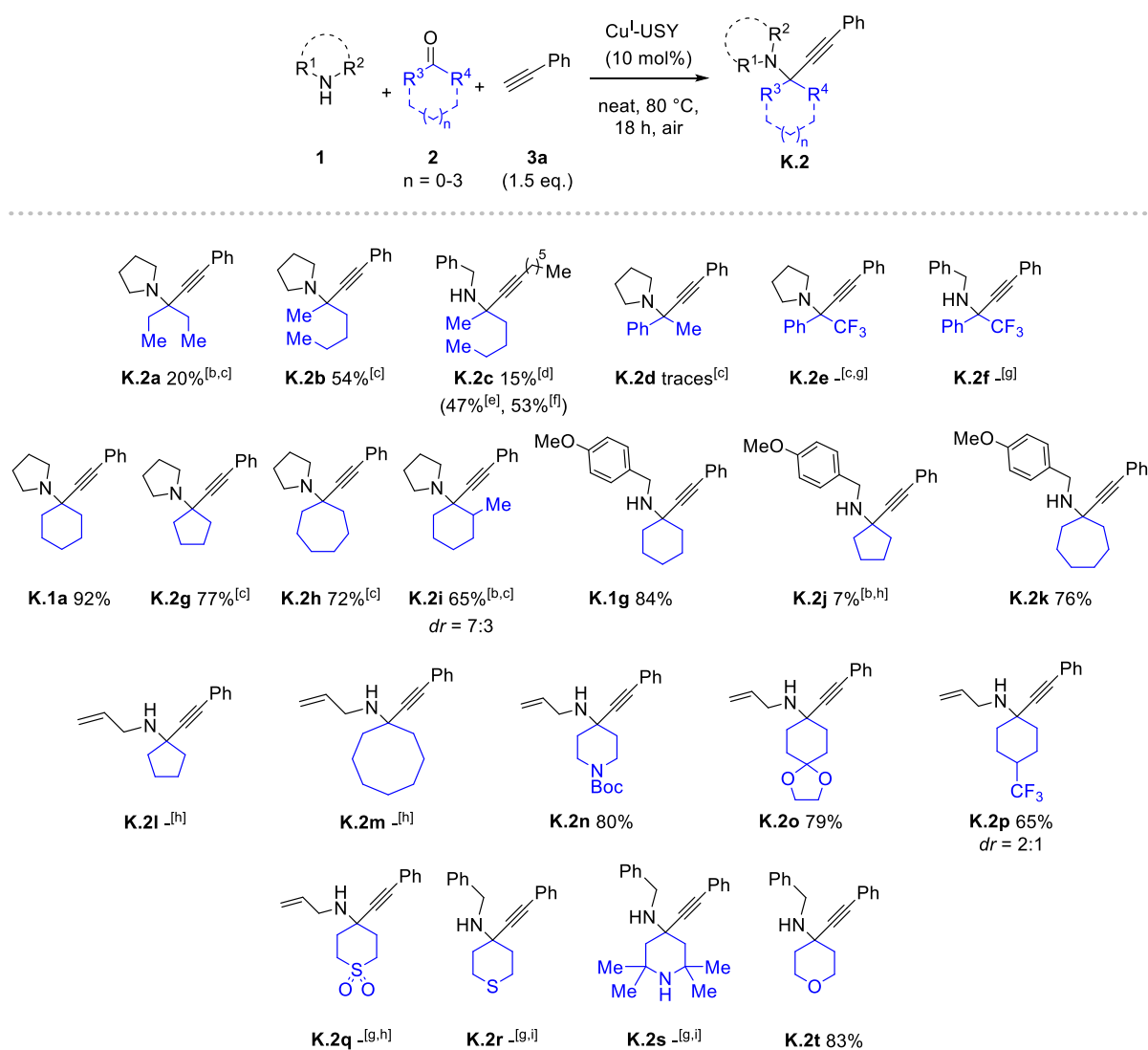
2.3.2. Ketone Scope.

In a second series of experiments, the ketone range was investigated (**Scheme 66**). Considering the reaction mechanism (**Scheme 53**), the more electrophilic the ketone, the more efficient the reaction is likely to be. Indeed, increased electrophilicity facilitates the condensation of the amine, as well as the nucleophilic addition of the copper acetylide to the more activated ketimine/ketiminium intermediate.

Since most KA² procedures published to date were predominantly limited to a small number of cyclic ketones, we investigated the compatibility of our Cu^I-USY system with the challenging linear aliphatic ketones. As expected, the linear aliphatic ketones, which do not release strain energy upon acetylide addition,^[217] proved less reactive. Compared to their cyclic analogues, propargylamines **K.2a,b** derived from pentan-3-one and prochiral hexan-2-one, respectively, were obtained in significantly lower yields (20% for **K.2a** and 54% for **K.2b** compared to 77% for **K.2g** and 92% for **K.1a**). Nevertheless, these results are still acceptable compared to previous additive-free reports with other catalysts. Similarly, propargylamine **K.2c**, which combines three challenging coupling components, i.e., a primary amine, linear ketone, and aliphatic alkyne, was formed in a low 15% yield under standard conditions. Interestingly, raising the temperature to 110 °C and doubling the catalyst loading resulted in a significant increase in yield (53%), allowing **K.2c** to be produced with similar efficiency to **K.2b**.

Next, we evaluated the potential of linear aromatic ketones as even more challenging coupling partners.^[220,238] Unfortunately, KA² coupling with acetophenone and 2,2,2-trifluoroacetophenone proved unsuccessful. In both cases, complex crude mixtures were obtained, containing only traces of the acetophenone-derived propargylamine **K.2d** and no traces of the 2,2,2-trifluoroacetophenone-derived products **K.2e,f**. Once again, the competing hydroamination pathway was predominant here.

Several cyclic aliphatic ketones were examined next. Besides cyclohexanone, cyclopentanone and cycloheptanone were employed in the KA² coupling with phenylacetylene and pyrrolidine. The corresponding propargylamines **K.2g,h** were efficiently obtained, yet a non-negligible ring size effect was observed (77% for **K.2g** and 72% for **K.2h** vs. 92% for **K.1a**). This finding is consistent with the electrophilicity profile of these cyclic ketones.^[217] Among these three ketones, cyclohexanone indeed displays the greatest electrophilicity, which is mainly due to the higher torsional strain released during nucleophilic additions to cyclohexanone, compared to cyclopentanone and cycloheptanone.^[216,217] Due to the increased steric hindrance, the switch from cyclohexanone to 2-methylcyclohexanone resulted in a drop in yield (92% for **K.1a** vs. 65% for **K.2i**). Interestingly, as for VOUGIOUKALAKIS' Zn(OAc)₂ system,^[237] a diastereomeric ratio of 7:3 was obtained. The Cu^I-USY catalyst, however, favoured the opposite diastereomer.



Scheme 66. Ketone scope of the Cu^I-USY-catalysed KA² reaction.^[a]

^[a] Reactions run neat at 80 °C in a sealed tube with ketone **2** (1.0 mmol, 1.0 eq.), amine **1** (1.0 eq.), phenylacetylene (**3a**, 1.5 eq.), and Cu^I-USY (10 mol%), unless otherwise stated. ^[b] Yield estimated *via* ¹H NMR analysis of hard-to-purify product mixture after purification using 1,3,5-trimethoxybenzene as internal standard. ^[c] Formation of a by-product which will be discussed later in section III-2.3.4. ^[d] Hex-1-yne was used instead of phenylacetylene. ^[e] Reaction performed at 110 °C instead of 80 °C. ^[f] Reaction performed at 110 °C instead of 80 °C, and with Cu^I-USY (20 mol%). ^[g] No traces of the expected KA² product were detected. ^[h] Complex mixture of unidentified difficult-to-purify products. ^[i] Almost no conversion of ketone.

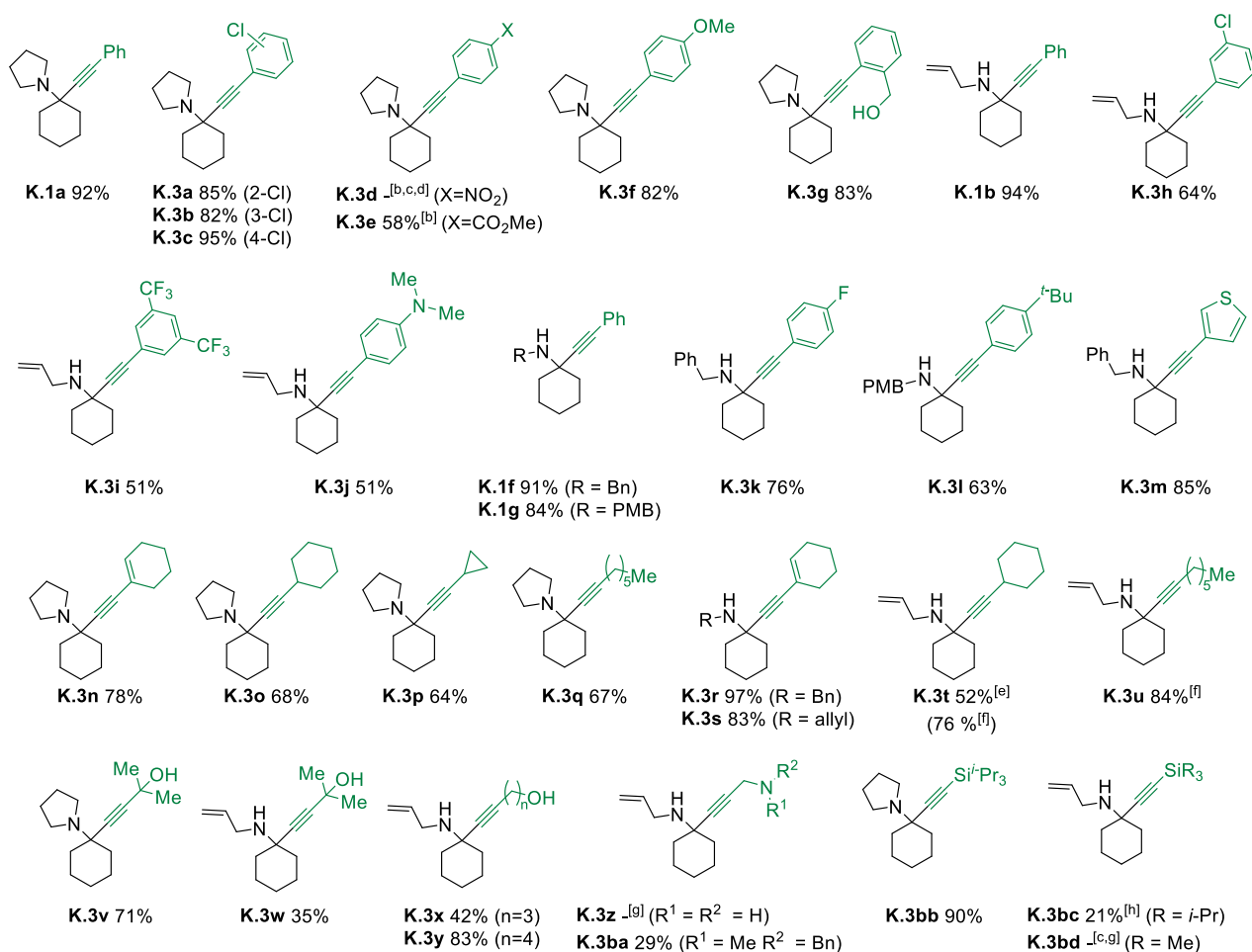
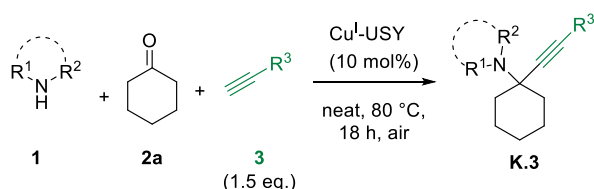
Shifting from pyrrolidine to 4-methoxybenzylamine led to propargylamines **K.1g** and **K.2k** with efficiencies corresponding to the electrophilicity of the corresponding ketones. The cyclopentanone-derived propargylamine **K.2j**, on the other hand, was obtained in very low yield as part of a complex mixture. A comparably complex result was observed with allylamine in combination with cyclopentanone (→ **K.2l**) and cyclooctanone (→ **K.2m**). In contrast, various functionalised six-membered (hetero)cyclic ketones gave reasonable coupling efficiencies. The good yields of propargylamines **K.2n,o** underlines again the compatibility of our catalytic conditions with acid-sensitive groups such as *tert*-butoxycarbonyl (Boc) in **K.2n** and 1,3-dioxolane ketal in **K.2o**. Interestingly, 4-(trifluoromethyl)cyclohexan-1-one led to a 2:1 mixture of two separable diastereomers of propargylamine **K.2p** in 65% yield. The X-ray crystal structure of a 1,2-dihydropyridine produced from the major diastereomer (for details, see section VI-5.3.2.)

showed that axial addition of the copper acetylide nucleophile was favoured over equatorial attack.

Sulphur-containing ketones did not yield the corresponding propargylamines **K.2q,r**, despite their greater electrophilicity compared to cyclohexanone.^[217] The sulphone derivative (\rightarrow **K.2q**) produced a complicated reaction mixture as a pitch-black, hardly soluble resin, while tetrahydro-4*H*-thiopyran-4-one led to partial formation of the corresponding imine, but not to propargylamine **K.2r**. Possibly, the thioether moiety leads to catalyst poisoning. A comparable result was obtained for piperidin-4-one, detecting no traces of **K.2s**. Fortunately, propargylamine **K.2t** was obtained in good 83% yield from tetrahydro-4*H*-pyran-4-one.

2.3.3. Alkyne Scope

In the KA² coupling reaction, the alkyne reactivity affects (i) the formation of the alkynyl copper nucleophile depending on its π -LEWIS basicity, and (ii) the ease of trapping the ketimine/ketiminium intermediate, thus the C-C bond formation. The nucleophilicity of the alkynyl copper intermediate is thought to have the greatest influence on reaction efficiency.^[203] With this in mind, different alkynes were scrutinised under our optimised conditions (**Scheme 67**). Most reactions were carried out using cyclohexanone as a model ketone in combination with pyrrolidine or allylamine as models for secondary and primary amines, respectively. Some additional examples based on primary benzylamines are also presented. The use of different terminal aromatic alkynes carrying either electron-withdrawing or electron-donating groups gave mixed results. Indeed, irrespective of the amine, it was found that the use of functionalised phenylacetylene derivatives led to yield diminution in most cases (see **K.3a,b** and **K.3d-g**). The isomeric chlorinated propargylamines **K.3a-c**, for instance, were isolated in 82-95% yield, with the 4-chloro product **K.3c** being the best result, possibly in parts due to steric reasons but electronic effects cannot be excluded. Unfortunately, 1-ethynyl-4-nitrobenzene resulted in a complex mixture of compounds in which no traces of propargylamine **K.3d** were detected. Competing hydroamination was predominantly observed due to the highly polarised triple bond. The less electron-withdrawing methyl ester, however, gave propargylamine **K.3e** in 58% yield. Electron-rich alkynes were investigated next. 1-Ethynyl-4-methoxybenzene delivered propargylamine **K.3f** in a slightly reduced yield (82% vs. 92% for **K.1a**), as already described in other KA² procedures. Similarly, propargylamine **K.3g**, bearing a 2-hydroxymethyl substituent, was obtained in a comparable 83% yield.



Scheme 67. Alkyne scope for the Cu^I-USY-catalysed KA² reaction.^[a]

^[a] Reactions run neat at 80 °C in a sealed tube with cyclohexanone (**2a**, 1.0 mmol, 1.0 eq.), amine **1** (1.0 eq.), alkyne (1.5 eq.) and Cu^I-USY (10 mol%), unless otherwise stated. ^[b] For practical reasons, reactions run in PhMe (1 M concentration of pyrrolidine and cyclohexanone). ^[c] No traces of the expected KA² product were detected. ^[d] Formation of a by-product which will be discussed later in section III-2.3.4. ^[e] Incomplete conversion after 18 h. ^[f] 24 h reaction for full conversion. ^[g] Complex mixture of compounds. ^[h] ¹H NMR yield estimated using 1,3,5-trimethoxybenzene as internal standard.

Concerning primary amines, larger variation in yields was often observed using functionalised phenylacetylene derivatives, depending on the electron-rich or electron-poor nature of the alkyne (**Scheme 67**). Nevertheless, many groups, such as Cl, F, CF₃, OH, NMe₂, were tolerated and the corresponding propargylamines **K.1b** and **K.3h-m** were isolated in good to very good yields (51-97%). Interestingly, the compatibility of 3-ethynylthiophene was also demonstrated giving **K.3m** in 85% yield.

Not surprisingly, the coupling efficiency decreased upon shifting from aryl- to alkylalkynes.^[203] Conjugated 1-ethynylcyclohex-1-ene proved to be the most efficient, regardless of the amine, leading to propargylamines **K.3n,r,s** in 78-97% yield. In the pyrrolidine series, the yield decreased with the number of π -bonds in the alkyne (cf. **K.1a** vs. **K.3n** vs. **K.3o**), while no effect

on either ring size or chain length was observed (**K.3o-q**). For allylamine, slower reactions were observed with aliphatic alkynes, inducing lower conversions. However, extending the reaction time to 24 h led to propargylamines **K.3t,u** in 76 and 84% yield, respectively.

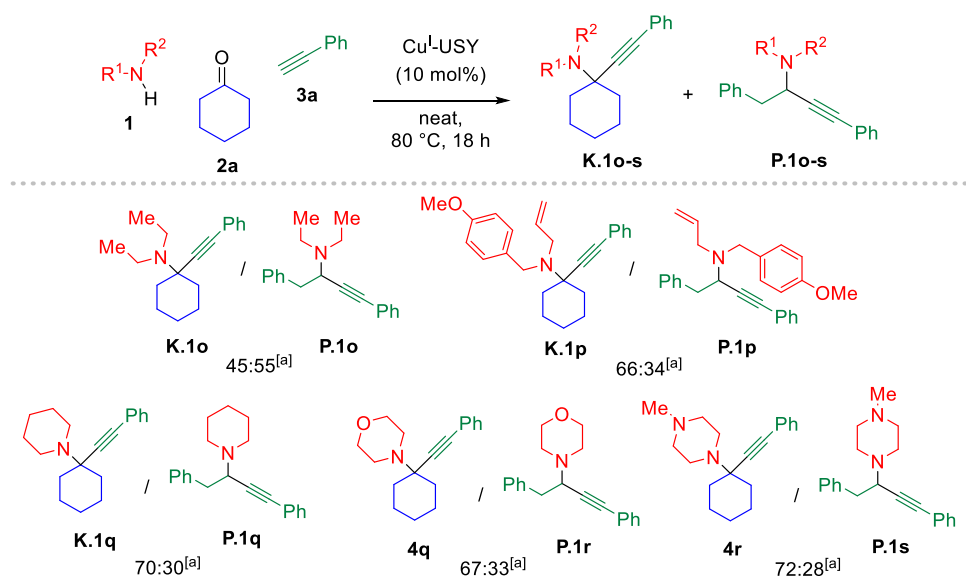
Aliphatic hydroxy-substituted alkynes gave the expected propargylamines **K.3v-y**, but with varying performances (**Scheme 67**). While 2-methylbut-3-yn-2-ol gave the pyrrolidine-derived product **K.3v** in 71% yield, its allylamine analogue **K.3w** was isolated in only half the yield. Surprisingly, pent-4-yn-1-ol and hex-5-yn-1-ol led to very different results. Propargylamine **K.3y** was obtained from hex-5-yn-1-ol in high 83% yield, whereas pent-4-yn-1-ol caused a dramatic drop in yield (42% for **K.3x**) due to the formation of unknown by-products. Although propargylamine (in the presence of 1 mol% Cu^I-USY) did not grant access to KA² product **K.3z**, its tertiary derivative pargyline (*N*-methyl-*N*-propargylbenzylamine) allowed the synthesis of **K.3ba** in 29% yield, which has an attractive 1,4-diamino-2-butyne moiety.

Furthermore, trimethylsilyl- and triisopropylsilylacetylene were investigated as coupling partners. While the trimethylsilyl group did not withstand the reaction conditions (cf. **K.3bd**), its bulkier triisopropyl analogue proved to be more robust. As a result, the pyrrolidine-derived propargylamine **K.3bb** was obtained in excellent and significantly higher yield than its allylamine equivalent **K.3bc** (90% vs. 21%) from triisopropylsilylacetylene. The coupling abilities of triisopropylsilylacetylene and 2-methylbut-3-yn-2-ol are of synthetic value due to the potentially easy access to the corresponding terminal alkynes using standard chemoselective deprotection conditions.

2.3.4. Limitations and Solutions

Overall, the Cu^I-USY-catalysed KA² procedure proved efficient at accessing a manifold of propargylamines bearing diverse functional groups. Primary amines reacted highly selectively, but sometimes incompletely. In sharp contrast, secondary amines, despite complete conversions, frequently led to hard-to-purify mixtures containing a non-negligible amount of a major by-product. The latter was difficult or impossible to separate from the desired KA² coupling product (see series **K.1o-s** in **Scheme 65** and **Scheme 68**). Careful analysis of the mixtures obtained after chromatographic purification, however, allowed the clear identification of the major by-products as α -secondary propargylamines **P.1o-s** (**Scheme 68**). Their formation suggests an alkyne hydroamination step instead of a ketone-amine condensation, making the ketone redundant.^[241] This represents another attractive, but here undesirable, cascade reaction. It is worth noting that diethylamine preferentially formed the α -secondary propargylamine **P.1o**, whereas the other secondary amines favoured the formation of the corresponding KA² products **P.1q-s** in an approximate 7:3 ratio. Surprisingly, this side reaction has not been reported in other KA²

publications, although, as we will see in Chapter V, both reactions are catalysed with the same transition metals, except for manganese. To solve this problem, we turned our attention to a decarboxylative approach of the KA² reaction employing alkynoic acids instead of terminal alkynes.



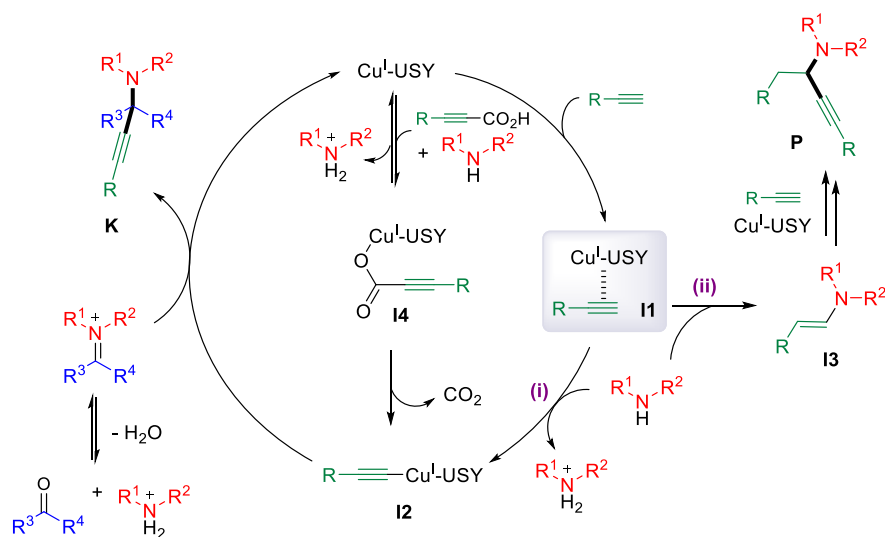
Scheme 68. Product distribution for the Cu^I-USY-catalysed KA² reaction involving secondary amines.

^[a] Ratios estimated from the crude mixtures *via* ¹H NMR.

3. Decarboxylative and Desilylative Cu^I-USY-catalysed KA² Reactions

3.1. Decarboxylative KA² Reaction to Overcome Limitations

By considering the probable mechanisms of the KA² and hydroamination/protonation/alkyne addition (HPA) reactions, it was possible to solve this chemoselectivity problem (Scheme 69). Both reactions presumably require the formation of the π -alkyne complex **I1**. Subsequently, the latter evolves either (i) into copper acetylide **I2** *via* amine-driven deprotonation and further to the desired KA² product **K** or (ii) undergoes hydroamination to give enamine intermediate **I3** and finally by-product **P**. The π -alkyne complex **I1** thus represents the cornerstone of both processes. To prevent hydroamination, and thus the formation of by-product **P**, it is necessary to limit or suppress the formation of **I1**. Therefore, we decided to explore a decarboxylative KA² approach^[242–244] that starts from alkynoic acids as the terminal alkyne surrogates and directly generates copper acetylide **I2** upon decarboxylation of complex **I4** instead of generating complex **I1**.



Scheme 69. Mechanistic rationalisation of the standard and decarboxylative KA² reactions.

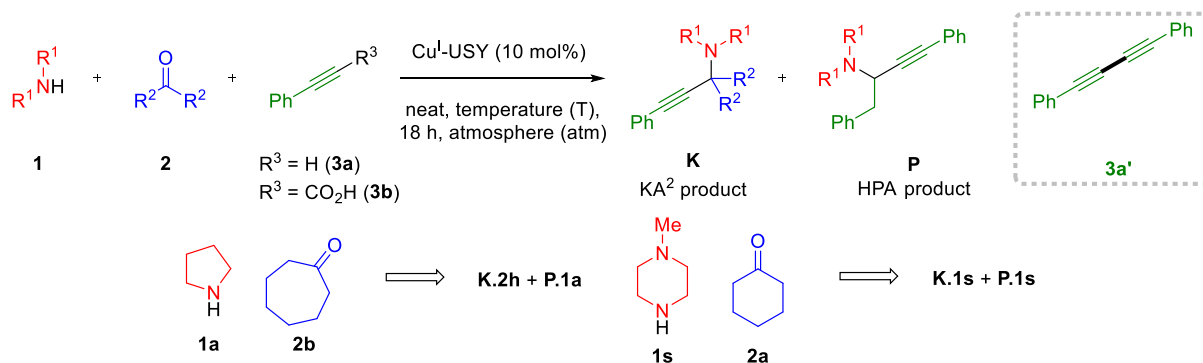
3.2. Optimisation of Reaction Conditions

The Cu^I-USY-catalysed decarboxylative KA² reaction conditions were optimised with the help of two different amine/ketone combinations: cycloheptanone (**2b**)/pyrrolidine (**1a**) and cyclohexanone (**2a**)/*N*-methylpiperazine (**1s**), together with phenylpropionic acid (**3b**). The results are summarised in **Table 6** and compared to our original KA² conditions with phenylacetylene (**3a**). Reacting cycloheptanone (**2b**), pyrrolidine (**1a**), and phenylacetylene (**3a**) under optimised KA² conditions produced product **K.2h** in 72% yield, together with the hydroamination product **P.1a** in ca. 10% (entry 1). Lowering the reaction temperature to 60 °C afforded the KA² product **K.2h** in high chemoselectivity yet in significantly reduced yield of 52% (entry 2). The reaction temperature was thus re-established to 80 °C, but phenylacetylene (**3a**) was replaced by phenylpropionic acid (**3b**). As a result, the yield of **K.2h** rose to 64%, even for equimolar amounts of each component, yet the high chemoselectivity was preserved (entry 3). Performing the reaction under an argon atmosphere with a slight excess of ketone, allowed for another increase in yield to 76% (entry 4). It is noteworthy that an alternative strategy, namely the increase of the ketone equivalents to quickly convert the amine by displacing the equilibrium towards the iminium ion, was examined. To keep it short, a larger excess of both ketone and alkyne was necessary to achieve a similar efficacy as for entry 4 (entry 5).

The cyclohexanone(**2a**)/*N*-methylpiperazine (**1s**) combination proved to be even more challenging (**Table 6**). Our optimised KA² conditions with phenylacetylene (**3a**) afforded a 58% yield of KA² product **K.1s** in an 82:18 ratio with the undesired HPA product **P.1s** (entry 6). Replacing Cu^I-USY with CuCl revealed that this chemoselectivity issue is not unique to our catalyst and is, in fact, even more pronounced for CuCl (entry 7). Yet, our decarboxylative conditions from entry 4 still yielded a mixture of amines, even with excess cyclohexanone (entry 8). Finally, reducing the reaction temperature to 60 °C induced excellent chemoselectivity

and gave KA² product **K.1s** in 58% yield (entry 9). From a mechanistic point of view, these findings suggest that the deprotonation of the π -complex **II** is greatly favoured over its hydroamination pathway at 60 °C (**Scheme 69**). The replacement of a terminal alkyne with an alkynoic acid, combined with a reduced reaction temperature could represent a solution to the KA²/HPA chemoselectivity issue even for challenging secondary amine/ketone combinations. To answer this, the scope of our decarboxylative KA² procedure was examined.

Table 6. Optimisation of the Cu^I-USY-catalysed decarboxylative KA² coupling reaction.^[a]



Entry	1	2	3	1:2:3	Atm	T (°C)	K/P	K Yield (%)
1	1a	2b	3a	1:1:1.5	Air	80	89:11	72 ^[b]
2	1a	2b	3a	1:1:1.5	Air	60	>99:1	52 ^[c]
3	1a	2b	3b	1:1:1	Air	80	>99:1	64 ^[c,d]
4	1a	2b	3b	1:1.2:1	Ar	80	>99:1	76 ^[b]
5	1a	2b	3a	1:2:1.5	Air	80	97:3	83
6	1s	2a	3a	1:1:1.5	Air	80	82:18	58 ^[b]
7 ^[e]	1s	2a	3a	1:1:1.5	Air	80	70:30	70 ^[c]
8	1s	2a	3b	1:1.5:1	Ar	80	89:11	66 ^[c]
9	1s	2a	3b	1:1.5:1	Ar	60	>99:1	58 ^[b]

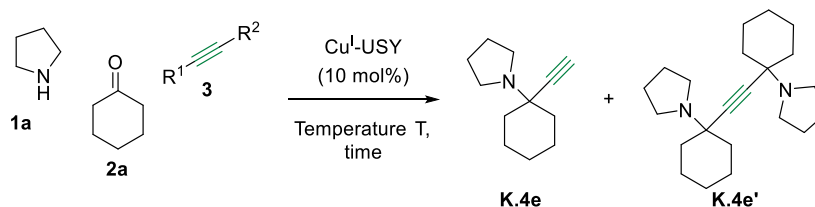
^[a] Reactions run neat in a sealed tube with ketone **2**, amine **1** (1.0 mmol, 1.0 eq.), terminal alkyne **3a** or alkynoic acid **3b**, and Cu^I-USY (10 mol%), unless otherwise stated. ^[b] Isolated yield. ^[c] Yield estimated *via* ¹H NMR of the crude product using 1,3,5-trimethoxybenzene as internal standard. ^[d] Significant amount of GLASER homocoupling product detected (**K.2h/3a'** 7:3). ^[e] Reaction run with CuCl (10 mol%) as catalyst. HPA: hydroamination-protonation-alkyne addition.

3.3. Scope and Limitations

Other challenging secondary amines were reacted with phenylpropionic acid under the conditions of entry 9 (**Scheme 70**). The previously investigated propargylamines **K.1p** and **K.1q-s** were now obtained in cleaner crude mixtures containing very few (or no) traces of α -secondary propargylamines **P.1o** and **P.1q-s**. This significantly facilitated their purification. More significantly, the piperidine- and morpholine-derived propargylamines **K.1q,r** were obtained in much higher yields than under KA² conditions with phenylacetylene (81 vs. 61% for **K.1q** and 79 vs. 52% for **K.1r**). Accordingly, the decarboxylative approach not only minimises the formation of the by-products **P.1q,r**, but also increases the KA² efficiency. Unfortunately, the difficult *N*-methylaniline remained a poor substrate, producing only traces of **K.4a**. To our delight, the

role of an ephemeral protecting group and thus minimises the second coupling process to **K.4e'**. As a result, the yield of **K.4e** significantly increased from 4 to 45% (entry 5 vs. entry 1). Switching from pyrrolidine to piperidine under the conditions of entry 5 allowed the preparation of 1-(1-ethynylcyclohexyl)piperidine **K.4f**, a propargylamine of biological importance as an AChE inhibitor, but in greatly reduced yield (**Scheme 70**).

Table 7. Screening of decarboxylative^[a] and desilylative^[b] KA² reaction conditions to access propargylamine **K.4e**.



Entry	R ¹	R ²	2a:1a:3	T (°C)	Time (h)	Yield K.4e (%)	Yield K.4e' (%)
1 ^[a]	H	CO ₂ H	1.5:1:1	60	18	4	30
2 ^[a]	H	CO ₂ H	1:1:1.5	80	18	22	27
3 ^[a]	H	CO ₂ H	1:1:1.5	40	60	9	n.d. ^[c]
4 ^[a]	H	CO ₂ H	1.5:1:1	rt then 35	40 then 24	25	0
5 ^[a]	CO ₂ H	CO ₂ H	1.5:1:1	60	18	45	n.d. ^[c]
6 ^[b]	H	SiMe ₃	1:1:1.5	80	18	54	26
7 ^[b]	H	SiMe ₃	1:1:1.5	rt then 35	40 then 24	30	0
8 ^[b]	H	SiMe ₃	1:1:1.5	40	60	58	0

^[a] Reactions run neat in a sealed tube with pyrrolidine (**1a**, 1.0 mmol, 1.0 eq.), cyclohexanone (**2a**, 1.0 or 1.5 eq.), alkynoic acid **3** (1.0 or 1.5 eq.) and Cu^I-USY (10 mol%) under argon. ^[b] Reactions run neat in a sealed tube with pyrrolidine (**1a**, 1.0 mmol, 1.0 eq.), cyclohexanone (**2a**, 1.0 eq.), trimethylsilylacetylene (R¹ = H, R² = SiMe₃, 1.5 eq.) and Cu^I-USY (10 mol%) under air. ^[c] not determined because part of a complex mixture with signal overlap.

Although useful, the decarboxylative approach still has some limitations. We thus envisioned an alternative strategy to access propargylamine **K.4e** through a selective and unprecedented cascade KA²/desilylation process using trimethylsilylacetylene (**3d**). Similar procedures were previously reported for its A³ analogue.^[245–247] LARSEN and co-workers have established a two-step KA²/desilylation procedure to access propargylamine-derived triazoles through CuAAC reaction.^[56] Under standard KA² conditions, **K.4e** was obtained in a promising 54% yield but the bispropargylamine **K.4e'** was also formed in non-negligible amounts (entry 6). This indicates that desilylation occurs, at least partially, before the completion of the KA² coupling, as confirmed by TLC analysis following the reaction progress. **K.4e'** was not detected when the reaction was run at room temperature (entry 7), nor at 40 °C yielding **K.4e** in improved 58% yield (entry 8). As for the decarboxylative approach, replacing pyrrolidine with piperidine, unfortunately, led to a drop in yield. Indeed, propargylamine **K.4f** was observed in a low 11% estimated yield (**Scheme 70**). It is worth mentioning that ZHANG and co-workers developed an efficient direct A³/KA²-type procedure to produce such α-secondary and α-tertiary terminal

propargylamines employing calcium carbide CaC_2 as alkyne component.^[248] Safety issues, such as the *in situ* formation of explosive Cu_2C_2 are worth mentioning.

These interesting results prompted us to check the generality of this Cu^{I} -USY-catalysed desilylative KA^2 reaction. The reaction of pyrrolidine (**1a**) and cyclohexanone (**2a**) with 1-phenyl-2-trimethylsilylacetylene was successful. In fact, under our standard KA^2 conditions, propargylamine **K.1a** was obtained with identical efficiency as compared to the reaction with phenylacetylene. Unfortunately, the scope of this desilylative approach could not be further explored for time reasons.

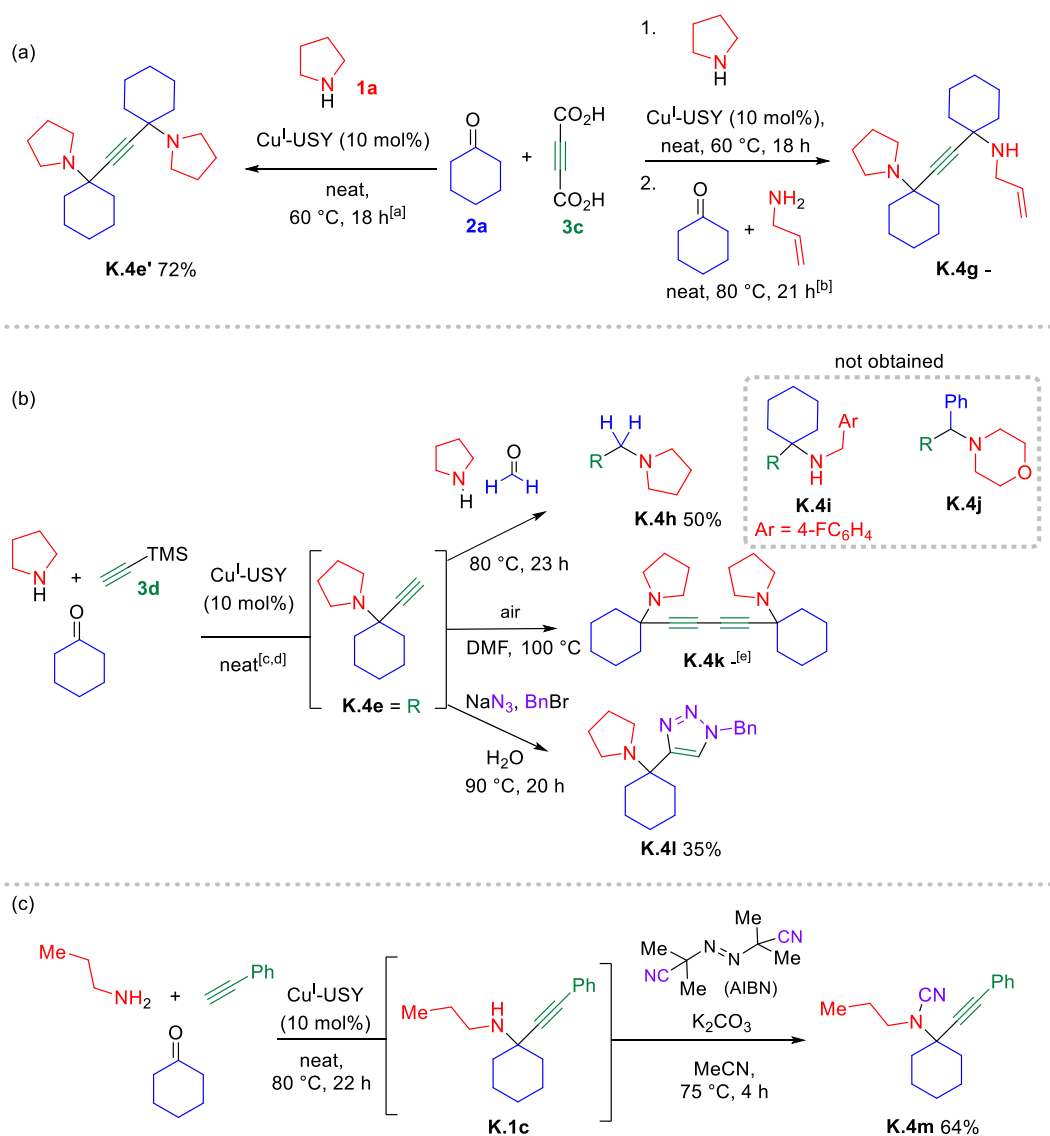
4. Cascade and One-Pot Applications of KA^2 (-Type) Reactions

Finally, several one-pot processes involving more than one Cu^{I} -USY-catalysed reaction and at least one KA^2 -type reaction as a key step were investigated (**Scheme 71**).

The deliberate and unprecedented synthesis of the symmetric bis- α,α' -tertiary-propargylamine **K.4e'** was efficiently achieved *via* a one-pot domino process of two decarboxylative KA^2 reactions from acetylenedicarboxylic acid (**3c**), pyrrolidine (**1a**), and cyclohexanone (**2a**) (**Scheme 71a**, left). This promising result led us to envisage the synthesis of dissymmetrical bispropargylamines. For this, a decarboxylative KA^2 reaction was performed to give **K.4e** and direct addition of cyclohexanone and allylamine (**1b**) was expected to produce the bis-propargylamine **K.4g**. Unfortunately, the latter was not detected and **K.4e** and **K.4e'** remained the major products within a complex mixture (**Scheme 71a**, right). Rewardingly, dissymmetric bispropargylamine **K.4h**, was successfully formed *via* a sequential one-pot desilylative KA^2/A^3 process using paraformaldehyde and pyrrolidine in the A^3 reaction step (**Scheme 71b**, top). When cyclohexanone and 4-fluorobenzylamine were used instead, the expected bispropargylamine **K.4i** was not obtained. As ketiminium ions resulting from aldehydes and secondary amines exhibit exalted electrophilicity, we selected the more favourable combination of benzaldehyde and morpholine. Unfortunately, bispropargylamine **K.4j** was not detected, leaving the first adduct propargylamine **K.4e** mostly unreacted. Not surprisingly, previous reports on decarboxylative A^3/A^3 cascade reactions solely allow to access bis- α,α' -primary-, or in reduced efficiency, bis- α -primary- α -secondary propargylamines.^[249,250]

Unfortunately, the attempt to convert in one-pot the terminal propargylamine **K.4e** into diyne **K.4k** through a Cu^{I} -USY-catalysed GLASER homocoupling reaction^[230] failed (**Scheme 71b**, centre). However, combining the KA^2 reaction with a CuAAC reaction^[179] proved to be feasible. Beneficially, the synthesis of triazole **K.4l** proceeded *via* a one-pot KA^2 /azide formation/ CuAAC process under favourable solvent-free conditions and then with water as solvent (**Scheme 71b**, bottom).

Besides the one-pot functionalisation of the reactive alkyne moiety, a sequential one-pot Cu^I-USY-catalysed KA²/*N*-cyanation^[251] process was envisaged as a rapid route to valuable cyanamides (**Scheme 71c**).^[252,253] Rewardingly, this sequence produced cyanamide **K.4m** in 64% overall yield. It is worth noting that **K.4m** is the first example of an α-tertiary propargyl cyanamide.



Scheme 71. Applications involving Cu^I-USY-catalysed KA²-(type) reactions.

^[a] Reaction run neat in a sealed tube with pyrrolidine (**1a**, 1.0 mmol, 1.0 eq.), cyclohexanone (**2a**, 3.0 eq.), acetylenedicarboxylic acid (**3c**, 2.0 eq.) and Cu^I-USY (10 mol%) under argon. ^[b] Reaction run neat at 60 °C for 18 h in a sealed tube with pyrrolidine (**1a**, 1.0 mmol, 1.0 eq.), cyclohexanone (**2a**, 1.0 eq.), acetylenedicarboxylic acid (**3c**, 1.0 eq.) and Cu^I-USY (10 mol%) under argon, then addition of cyclohexanone (**2a**, 1.0 eq.) and allylamine (**1b**, 1.0 eq.) followed by stirring at 80 °C for 21 h under argon. ^[c] For **K.4h**, reaction run neat in a sealed tube for 60 h at 40 °C. ^[d] For **K.4k** and **K.4l**, reaction run neat in a sealed tube for 18 h at 80 °C. ^[e] Complete conversion but only formation of degradation products without traces of the expected diyne **K.4k**.

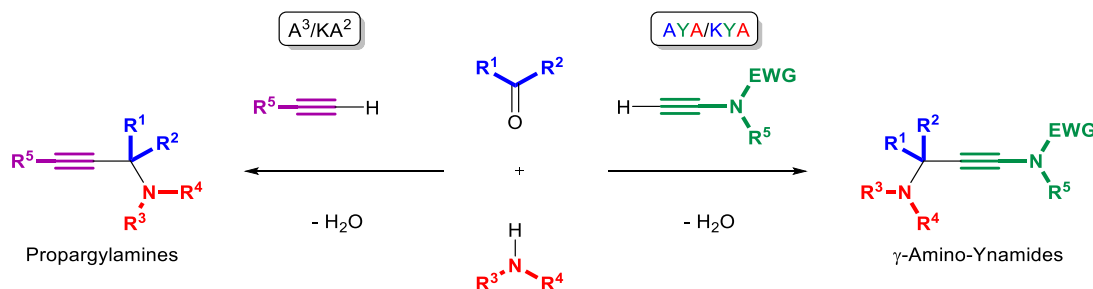
5. Conclusion

In this study, Cu^I-USY was shown to be an efficient and easy-to-handle supported copper(I) catalyst in solvent-free KA² and related reactions. These 3CRs enabled the one-pot coupling of amines, ketones, and alkyne-based nucleophiles. Recovered Cu^I-USY was reused several times, but a progressive erosion of the catalytic activity was observed, as well as partial copper leaching. Compared to other reported catalysts with temperatures ≥ 100 °C, the valuable α -tertiary propargylamines were formed under milder conditions, i.e., at temperatures ranging from 60-80 °C in most cases. Our procedures are based on near equimolar amounts of each coupling partner and show a large tolerance of functional groups (e.g., amino, halide, acetal, carbamate, ether, hydroxy, ester, etc.). Remarkably, numerous challenging aliphatic primary amines afforded high yields in our Cu^I-USY-catalysed KA² reaction with terminal alkynes. Furthermore, the coupling with unprecedented anilines was shown feasible but further efforts are required to extend their scope. In contrast to literature reports, we identified a competing alkyne hydroamination pathway with secondary amines, affording α -secondary propargylamines. This side reaction was bypassed through a decarboxylative KA² reaction using alkynoic acids as surrogates for terminal alkynes at a milder temperature, i.e., 60 °C. A major benefit of the decarboxylative approach was the incorporation of short-chained alkyne moieties through easy handling of their liquid or solid alkynoic acid surrogates compared to highly volatile acetylenes. Furthermore, the feasibility to access attractive α -tertiary propargylamines having a terminal alkyne moiety through Cu^I-USY-catalysed decarboxylative and desilylative KA² reactions was shown. Further optimisation of reaction conditions is nevertheless needed to extend the product scope. It might also be of interest to investigate the potential of Cu^I-USY in the related 3CR with calcium carbide as a cost-efficient carbon source.^[248] Although Cu^I-USY enables a broad substrate scope compared to most supported, but also many homogeneous catalysts, the main limitations of the KA² coupling reaction could not be overcome. Indeed, aliphatic acyclic secondary amines, and secondary anilines, as well as linear aliphatic ketones gave the propargylamines in low yields. More importantly, aromatic ketones proved unsuitable coupling partners using our Cu^I-USY procedures. On the other hand, Cu^I-USY was successfully employed in several one-pot procedures exploiting the reactivity of the propargylamine scaffold in further copper-catalysed transformations.

Chapter IV – Extension of the A³/KA² Methodology Towards the Synthesis of γ -Amino-Ynamides from Terminal Ynamides

1. Introduction

The A^3/KA^2 reactions are undoubtedly powerful MCRs for the atom- and step-economical preparation of diverse propargylamines. In the previous section, we saw that in addition to terminal alkynes, their alkynoic acid and alkynylsilane analogues can be used in this 3CR methodology. In some cases, this allowed a more direct and/or chemoselective access to certain propargylamines. Yet, these alkyne surrogates *in situ* evolve to the same metal acetylide as for the terminal alkyne, thus resulting in the same product. The use of structurally different alkyne surrogates, featuring at least one additional functionality, is especially fascinating as it paves the way towards various valuable product classes through a multicomponent approach. Among the various possibilities, we reasoned that the use of terminal ynamides as alkyne surrogates in the A^3/KA^2 methodology would represent a simple and beneficially greener route towards γ -amino-ynamides (Scheme 72). Indeed, this so-far underexplored class of propargylamines is commonly prepared through multi-step sequences involving hazardous and problematic chemicals, as will be described in section 2.2. As ynamides display greater nucleophilicity than alkynes (higher N parameters),^[254] the carbon-carbon bond formation step might be facilitated. Yet, their inherent electrophilic character at the ynamide α -carbon requires a catalytic system that guarantees adequate control of the chemoselectivity for the desired γ -amino-ynamides.



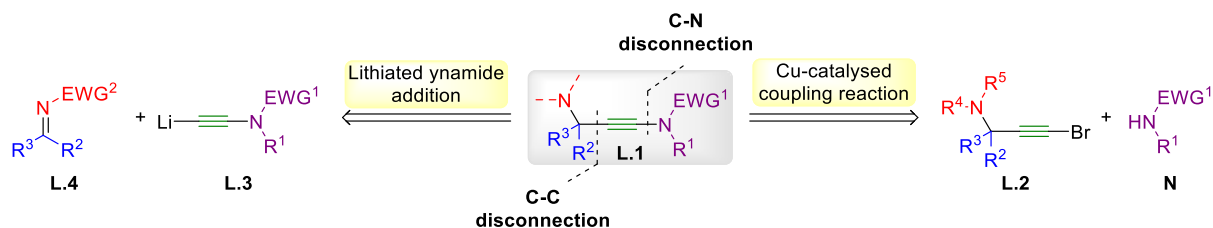
Scheme 72. Extending the carbonyl-alkyne-amine coupling methodology to the synthesis of γ -amino-ynamides.

On this basis, this section will start with a literature overview of the state of the art in γ -amino-ynamide synthesis, as well as their synthetic applications. The development of a novel Cu^I-USY-catalysed carbonyl-ynamide-amine coupling reaction will then be described. In analogy to the A^3/KA^2 nomenclature, we have coined the corresponding ynamide-based coupling reactions as AYA, standing for aldehyde-ynamide-amine, and KYA for ketone-ynamide-amine.

2. Synthesis of γ -Amino-Ynamides – State of the Art

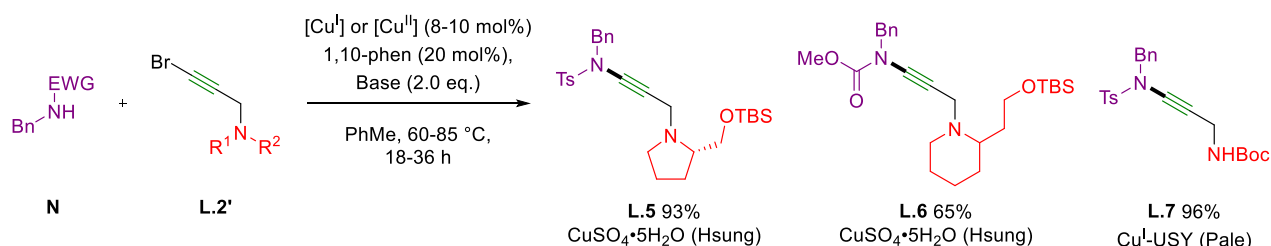
From 2006 to 2014, γ -amino-ynamides **L.1** had been accessible through two retrosynthetic strategies, namely a C-N or a C-C disconnection approach (Scheme 73). In the C-N disconnection strategy, the propargylamine moiety is previously established and a transition metal-catalysed C-N coupling reaction of the corresponding bromoalkyne **L.2** and N -nucleophile **N**

generates the ynamide **L.1** (Scheme 73, right). Alternatively, the C-C disconnection approach involves the nucleophilic addition of a metalated ynamide **L.3** (usually M = Li) onto a nitro-generated electrophile, typically an imine **L.4** (Scheme 73, left).



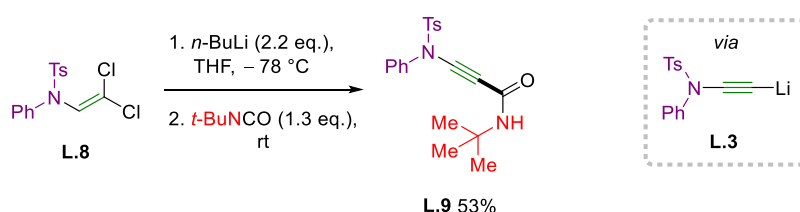
Scheme 73. Major retrosynthetic approaches to access γ -amino-ynamides **L.1**.

To the best of our knowledge, HSUNG and co-workers were the first to report γ -amino-ynamides during their seminal work on the copper-catalysed C-N coupling of diverse *N*-nucleophiles **N** and bromoalkynes **L.2'**.^[255] Their vast ynamide product scope included two examples of α -primary γ -amino-ynamides incorporating a pyrrolidine (**L.5**) or piperidine (**L.6**) motif (Scheme 74). This novel transformation was successfully heterogenised by PALE and co-workers who reported a Cu^I-USY-catalysed synthesis of ynamides in 2014 under similar conditions.^[192] As acyclic carbamates were inactive under the Cu^I-USY coupling conditions, the selective synthesis of γ -amino-ynamide **L.7** was possible in high 96% yield (Scheme 74).



Scheme 74. Synthesis of γ -amino-ynamides through copper-catalysed C-N coupling reactions.^[192,255]

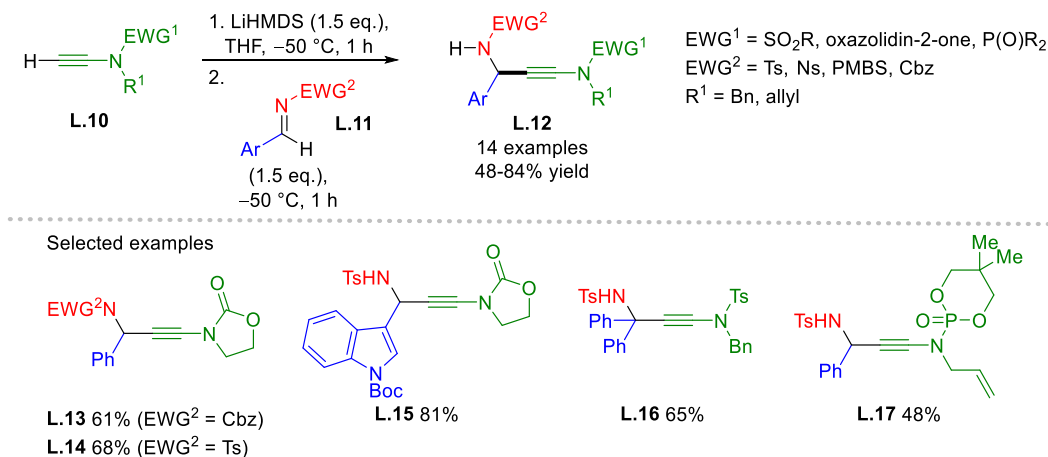
Regarding the C-C disconnection approach, the first γ -amino-ynamide scaffold was reported by SAA and co-workers during their investigation on the nucleophilic addition of lithiated ynamides **L.3** to various electrophiles at room temperature (Scheme 75).^[256] **L.3** was generated *in situ* from a β,β -dichloroenamide **L.8** using 2.2 equivalents of *n*-butyllithium. γ -Amino-ynamide **L.9** was obtained in 53% yield employing *t*-butyl isocyanate as electrophile.



Scheme 75. Synthesis of γ -amino-ynamide **L.9** from a lithiated ynamide and *t*-butyl isocyanate.^[256]

While all these reports represented isolated examples of γ -amino-ynamides among wider product scopes, HSUNG and co-workers more specifically addressed their preparation in 2013 (Scheme 76).^[257] Unlike SAA, HSUNG's group started from the preformed ynamide **L.10**, which

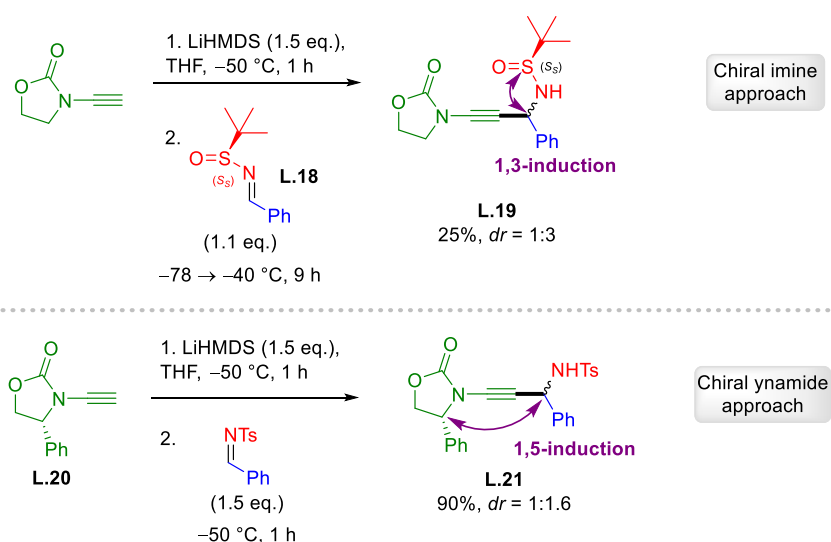
was deprotonated with lithium bis(trimethylsilyl)amide (LiHMDS) at $-50\text{ }^{\circ}\text{C}$. The so-formed lithiated ynamide **L.3** was then trapped with an activated aromatic imine **L.11** bearing an electron-withdrawing group (EWG) to afford the γ -amino-ynamide **L.12**. The ynamide scope includes oxazolidinone (**L.13-15**), tosyl sulfonamide (**L.16**) and phosphoramidate (**L.17**) derivatives. Regarding the imine electrophile **L.11**, the EWG corresponds mostly to sulfonyl (e.g., **L.14-17**), including the nosyl group, but also one carboxybenzyl (Cbz) carbamate example (**L.13**). Besides phenyl, the aryl group includes heteroaromatics (**L.15**) and two examples of α -tertiary γ -amino-ynamides were obtained in good yields (**L.16**).



Scheme 76. Synthesis of γ -amino-ynamides from lithiated ynamides and activated imines.^[257]

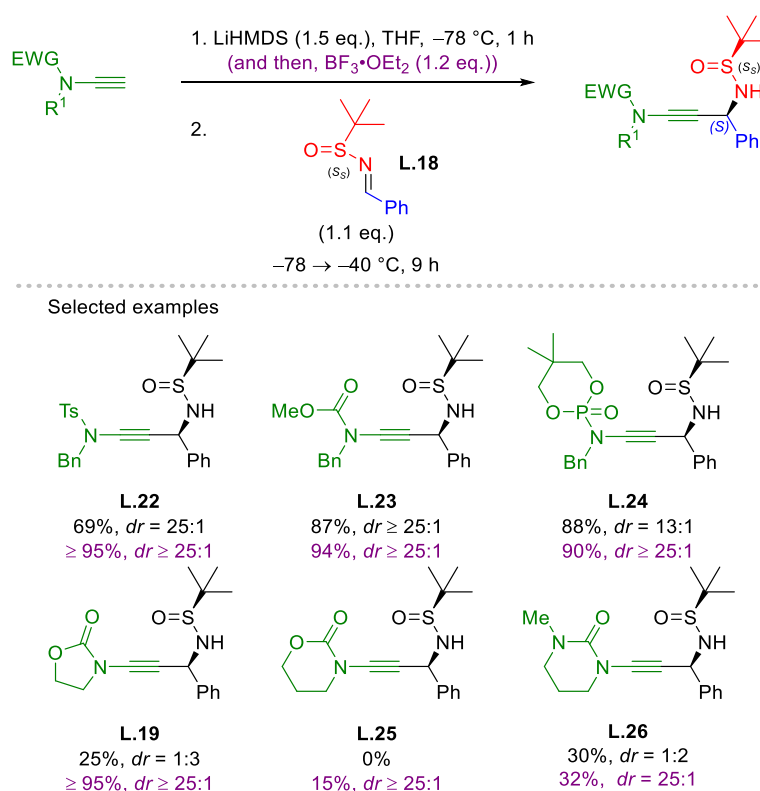
PMBS: *para*-methoxybenzenesulfonyl. Cbz: carboxybenzyl.

In the following years, HSUNG and co-workers explored approaches towards chiral γ -amino-ynamides through diastereoselective nucleophilic addition of lithiated ynamides onto imines (**Scheme 77**).^[258,259] Imines bearing a chiral EWG, or ynamides carrying a chiral auxiliary were explored leading to 1,3- or 1,5-asymmetric induction, respectively. The use of ELLMAN-DAVIS *N-t*-butanesulfinyl imine **L.18** with a chiral sulphur centre led to superior asymmetric induction as in **L.19** (*dr* \sim 1:3), as compared to the use of an EVANS-type chiral oxazolidinone ynamide **L.20** to give **L.21** (*dr* \sim 1:1.6).



Scheme 77. Diastereoselective synthesis of chiral γ -amino-ynamides.^[258,259]

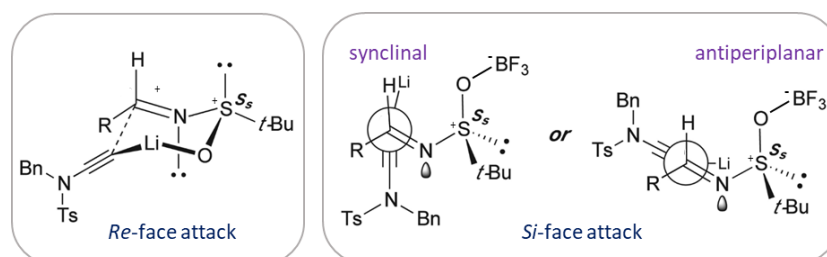
However, the reaction proved to be much more efficient with sulfonamide-, acyclic carbamate- and phosphoramidate-based ynamides in terms of yield and diastereoselectivities (L.22-L.24). A selection of the product scope is shown in Scheme 78.



Scheme 78. Representative scope of the diastereoselective synthesis of chiral γ -amino-ynamides from ELLMAN-DAVIS *N*-*t*-butanesulfinyl imines.^[258,259]

Strikingly, a unique reversal of stereoselectivity was observed by adding $\text{BF}_3 \cdot \text{OEt}_2$ and its extent was dependent on the number of equivalents used (0.5–2.0 eq.). This selectivity switch was rationalised by a change from a ZIMMERMAN-TRAXLER-type chelation transition state (TS) to an open-TS induced by a competitive complexation of the sulfinyl oxygen to $\text{BF}_3 \cdot \text{OEt}_2$ (Scheme 79). This supposedly leads to a *Si*-face addition of the lithium ynamide in contrast to

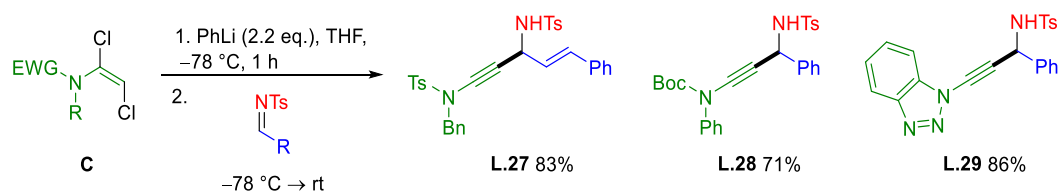
the *Re*-face addition in the chelation-TS, yielding the opposite absolute configuration at the new stereocentre. Similar observations were made by POISSON and co-workers during the examination of the analogous addition of lithiated ynol-ethers to such chiral imines.^[260] The free rotation around the N-S bond in the open-TS, however, arises the question of whether this model suffices to explain the high diastereoselectivity observed. Beneficially, yields and diastereoselectivities greatly improved ($\geq 25:1$).



Scheme 79. Representation of the chelation-TS (left) and the open-TS (right) leading to opposite diastereoisomers.

During these studies, the authors also extended the ynamide scope now including oxazolidinanone- (**L.25**) and tetrahydropyrimidinone-substituted (**L.26**) γ -amino-ynamides.^[259] Interestingly, **L.25** was not obtained in the absence of $\text{BF}_3 \cdot \text{OEt}_2$, whereas the analogous oxazolidinone **L.19** and tetrahydropyrimidinone **L.26** products were obtained in low yields. Even in the presence of $\text{BF}_3 \cdot \text{OEt}_2$, the product yields remain low for **L.25,26**. This suggests that the terminal ynamides follow the same nucleophilicity trend as their substituted analogues, previously established by MAYR and co-workers.^[254] Accordingly, oxazolidinone-based ynamides are weaker nucleophiles than *N*-tosyl ynesulfonamides. Oxazolidinanone- and tetrahydropyrimidinone-based ynamides may be less nucleophilic than their oxazolidinone analogues and/or less stable under HSUNG's conditions.

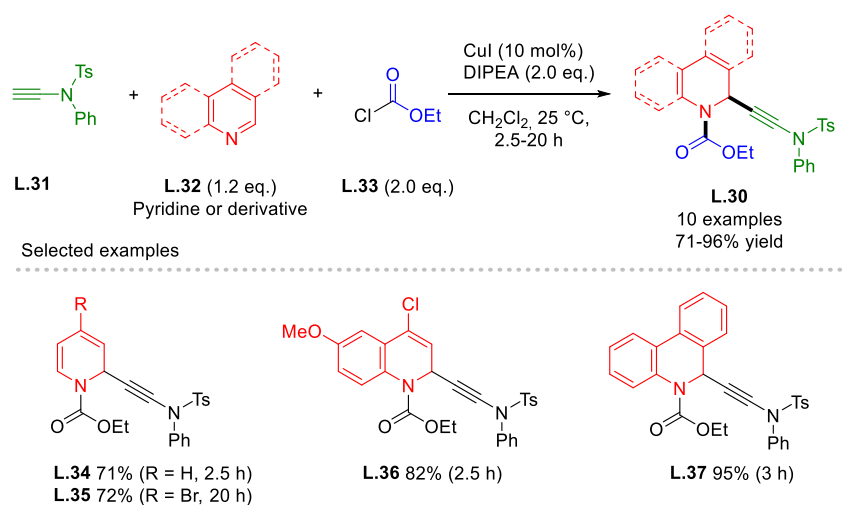
In 2015, ANDERSON and co-workers reported the synthesis of diverse ynamides starting from α,β -dichloroenamides **C** (**Scheme 80**).^[261] Complementary to HSUNG's scope, they included a cinnamyl-derived imine (\rightarrow **L.27**), a Boc-protected ynamide (\rightarrow **L.28**), as well as a benzotriazole-based ynamide (\rightarrow **L.29**). All were obtained in good yields (71-86%).



Scheme 80. Synthesis of γ -amino-ynamides from α,β -dichloroenamides **C** and *N*-tosyl-imines.^[261]

While these seminal contributions opened access to a manifold of γ -amino-ynamides, the highly basic and nucleophilic nature of the lithiated ynamides limits the number of tolerated functional groups. The development of milder and ideally catalytic methods towards this ynamide class would provide more economical and sustainable access to a larger number of products.

In this context, WOLF and co-workers developed the first catalytic approach to γ -amino-ynamides **L.30** derived from ynesulfonamide **L.31**, *N*-heterocycles **L.32** and ethyl chloroformate (**L.33**) via a REISSERT-type reaction in 2014 (Scheme 81).^[262] Their protocol is attractive from a green chemical viewpoint as it represents a 3CR, which is performed at room temperature and based on catalytic amounts of a rather cheap base metal salt. Unfortunately, the reactions were run in CH₂Cl₂, and no alternative solvents were mentioned. As for the scope of each component, the *N*-heterocycle **L.32** was varied most. Several functionalised pyridines and quinolines, as well as phenanthridine were used to give **L.34-L.36** 71-95% yield. Pyridines with an unsubstituted *para*-position sometimes afforded a mixture of 1,2- and 1,4-regioisomers, always in favour of the desired 1,2-isomer. Furthermore, isoquinolines and acridine were reported to afford selective 1,2-addition but were converted slowly. Regarding the ynamide scope, only ynesulfonamide **L.31** was shown, although the authors claim to observe smooth reactions with yne-carbamates and indole-derived ynamides. Strikingly, ethyl chloroformate (**L.33**) could not be replaced by its methyl or benzyl derivative, with poor conversions observed with the latter. To the best of our knowledge, these products have yet not been investigated in organic synthesis but given their multiple functionalities (ynamide, 1,2-dihydropyridine, alkene, 1,*n*-enynes, carbamate), several applications are imaginable.

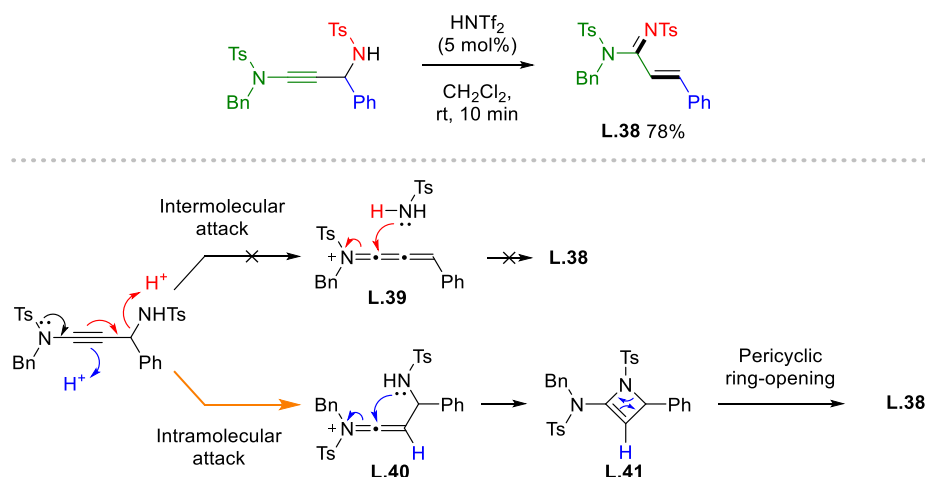


Scheme 81. Cu-catalysed synthesis of γ -amino-ynamides through a REISSERT-type 3CR.^[262]

3. Synthetic Applications of γ -Amino-Ynamides – State of the Art

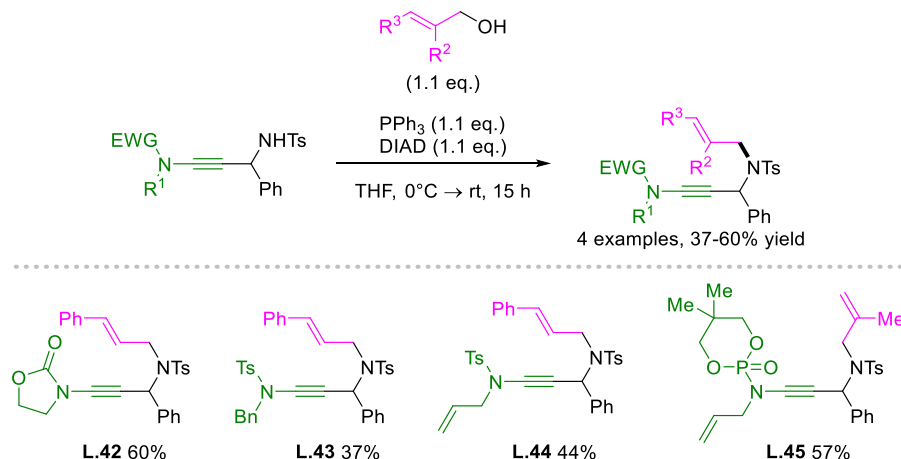
Thanks to the great interest of the organic chemical community in ynamides, they are nowadays involved in a myriad of transformations to access original molecular scaffolds. γ -Amino-ynamides can more generally be described as alkyl-substituted ynamides. It is of course conceivable that many of the already existing, but also future synthetic methodologies involving such internal ynamides are also transferable to γ -amino-ynamides. As for applications involving γ -amino-ynamides, HSUNG and co-workers were again pioneers.

They observed that some of their products were not stable on silica gel and cleanly rearranged into the corresponding amidines **L.38** (Scheme 82).^[257] This *aza*-MEYER-SCHUSTER reaction could deliberately be performed with catalytic triflimide (HNTf₂) at room temperature. Using a mixture of two differently decorated γ -amino-ynamides, no crossover products were detected in ¹H NMR, nor LC-MS. Consequently, the authors suggest that instead of forming allenylidene iminium ion **L.39**, the ynamide selectively protonates at the β -carbon, thus affording vinylidene iminium ion **L.40**. Intramolecular nucleophilic trapping at the α -carbon then affords 2-azetine **L.41** which undergoes a pericyclic ring opening to yield the amidine **L.38**.



Scheme 82. *aza*-MEYER-SCHUSTER rearrangement of γ -amino-ynamides to α,β -unsaturated amidines **L.38**.^[257]

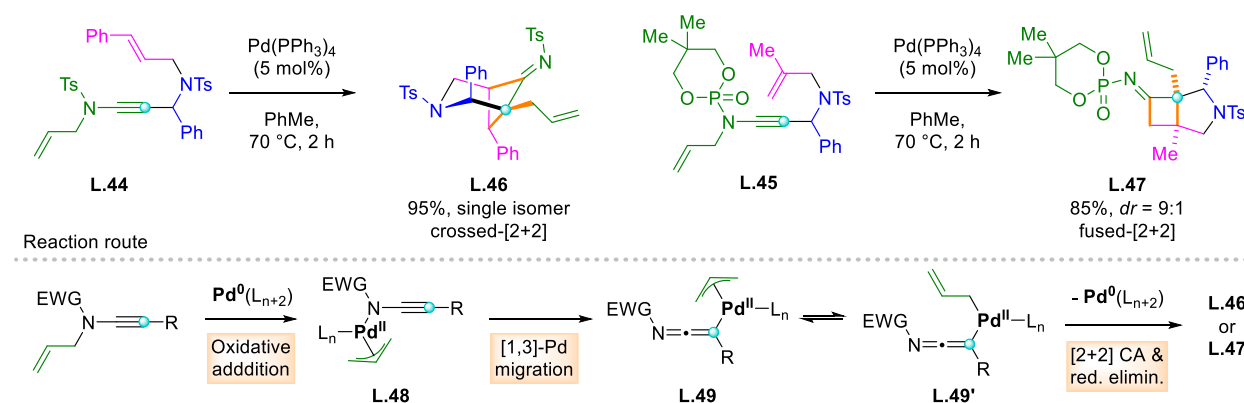
Furthermore, *N*-allylation of various γ -amino-ynesulfonamides was achieved under typical MITSUNOBU conditions to afford 1,6-enynes **L.42-L.45** in 37 to 60% yield (Scheme 83).^[257]



Scheme 83. Synthesis of 1,6-enynes via *N*-allylation of γ -amino-ynamides under MITSUNOBU conditions.^[257]

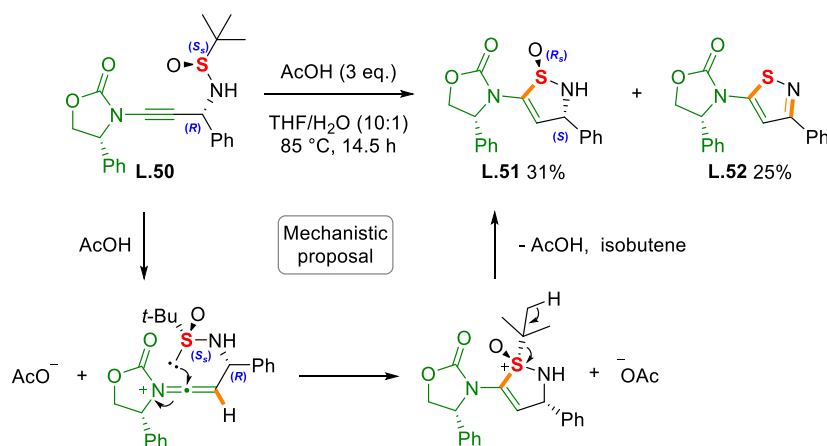
Ynamides **L.44** and **L.45** bearing an allyl substituent could further be derivatised under Pd⁰-catalysis into original *N*-heterocycles **L.46** and **L.47**, respectively (Scheme 84).^[257] Oxidative addition of Pd⁰ into the activated *N*-allyl bond affords Pd^{II}-allyl complex **L.48**. [1,3]-Palladium migration onto the electron-rich ynamide β -carbon gives ketenimine **L.49**. Next, highly stereoselective tandem [2+2] cycloaddition, followed by reductive elimination of the Pd^{II}-allyl complex efficiently yields the corresponding crossed (**L.46**) or fused cycloadduct (**L.47**). These

conditions were previously established by HSUNG and co-workers for the analogous γ -allyl enol ether ynamides.^[263]



Scheme 84. Pd-catalysed [2+2] cycloadditions towards *N*-heterocycles.^[257] Newly formed bonds are indicated in orange.

HSUNG and co-workers further discovered a novel acid-promoted 5-*endo*-dig cyclisation involving their chiral γ -sulfinamide-ynamides, such as **L.50** (Scheme 85).^[258,259] The regioselective cyclisation implies the sulphur atom with a concomitant loss of the *t*-butyl group affording a mixture of 2,3-dihydroisothiazole (*S*)-oxide **L.51** and isothiazole **L.52**. The latter is likely to stem from dehydration of **L.51** but always represented the minor product. Strikingly, the X-ray structure of **L.51** revealed that an inversion at the *S*-centre had occurred, hinting towards the mechanism shown in Scheme 85. Unfortunately, this transformation was restricted to oxazolidinone derivatives and only led to low product yields.



Scheme 85. Acid-promoted synthesis of 2,3-dihydroisothiazole (*S*)-oxides and isothiazoles.^[258,259] Newly formed bonds are indicated in orange.

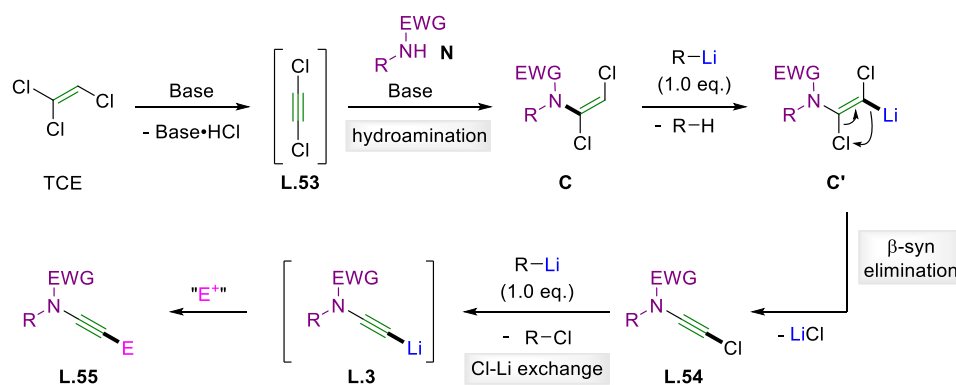
4. Results and Discussion

4.1. Preparation of Terminal Ynamides

Before discussing the optimisation of the AYA/KYA reaction conditions, this section briefly presents the methods for the synthesis of the terminal ynamides used in this study. A more complete overview of the numerous strategies to access terminal ynamides is given in the review article by WOLF and co-workers.^[264]

4.1.1. Terminal Ynamides from 1,2-Dichloroenamides

First, we envisaged a two-step approach which was reported by KERWIN and co-workers in 2002^[265] and was further improved by ANDERSON and co-workers in 2015 (Scheme 86).^[261] In this method, dichloroacetylene **L.53** acts as a two-carbon synthon, which is generated *in situ* from trichloroethylene (TCE) upon reaction with a base. Base-mediated addition of *N*-nucleophiles **N** yields the corresponding 1,2-dichloroenamides **C** (mostly as the *E*-diastereomers). Treatment of enamides **C** with strong organolithium bases (e.g., PhLi or *n*-BuLi) induces alkene lithiation to **C'**, followed by β -*syn* elimination of lithium chloride towards the chloroenamide **L.54**.ⁱⁱ The latter then undergoes a chlorine-lithium exchange to give the lithiated ynamide **L.3**, which is quenched with an electrophile (E^+) to afford ynamide **L.55**. Protic quenching ($E^+ = H^+$) of the reaction mixture yields the corresponding terminal ynamide.



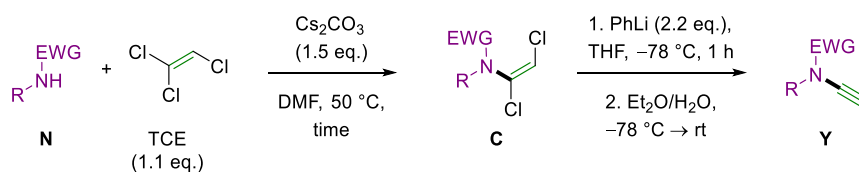
Scheme 86. Two-step synthesis of ynamides **L.55** via 1,2-dichloroenamides **C**.^[261]

This method is attractive because of its relatively short sequence and the generally good overall yields observed, even on a multi-gram scale. On the other hand, it presents numerous disadvantages from a green chemical viewpoint (hazardous solvents and chemicals). Nevertheless, several terminal ynamides were prepared using the procedure established by ANDERSON and co-workers and the results are summarised in Table 8.^[261] Various sulfonamide-derived 1,2-dichloroenamides **C.1-4** were obtained in good to excellent yields (70-95%) except for the 4-

ⁱⁱ This mechanistic proposal is based on the seminal work of POISSON and co-workers on the preparation of analogous ynamides from the corresponding dichloroenol ethers.^[266]

nosyl compound **C.5** (entries 1-4 vs. 5). This is most likely due to unoptimised reaction work-up conditions (poor solubility of **C.5** in EtOAc and CH₂Cl₂) as ANDERSON and co-workers report its formation in 84% yield^[261] albeit on a significantly lower scale (ca. 0.7 mmol in ref.^[261] vs. ca. 10 mmol here). Furthermore, oxazolidine-2-one, benzotriazole, and imidazole afforded the targeted 1,2-dichloroenamides **C.6-8** in good yields (56-72%, entries 6-8).

Table 8. Synthesis of terminal ynamides **Y** from 1,2-dichloroenamides **C**.^[261]



Entry	N	Time (min)	Yield ^[a] C (%)	Yield ^[a] Y (%)
1		100	C.1 95	Y.1 95
2		140	C.2 83	Y.2 68
3		120	C.3 90	Y.3 71
4		90	C.4 70	Y.4 0 ^[b]
5		360	C.5 39	Y.5 0 ^[c]
6		100	C.6 72	Y.6 0 ^[c]
7		60	C.7 56	Y.7 0 ^[c]
8		120	C.8 66	Y.8 0 ^[b,d]

^[a] Isolated yield. ^[b] Complex crude mixtures observed due to degradation. ^[c] Mostly unreacted 1,2-dichloroenamides recovered.

^[d] *n*-BuLi was used instead of PhLi.

Next, the terminal ynamides were generated using phenyllithium (PhLi), followed by an aqueous quench. While tosylated 1,2-dichloroenamides **C.1-3** gave the corresponding ynesulfonamides **Y.1-3** in good to excellent yields (68-95%, entries 1-3), the mesyl- and 4-nosyl derivatives **C.4** and **C.5** proved to be poor substrates (entries 4 and 5). Mesyl-dichloroenamide **C.4** underwent degradation (entry 4), whereas its 4-Ns-analogue **C.5** was mainly unreactive (entry 5). Oxazolidin-2-one- and benzotriazole-derived enamides **C.6** and **C.7** did not react (entries 6 and 7), while the imidazole analogue **C.8** underwent degradation (entry 8).

4.1.2. Terminal Ynamides from TIPS-protected Ynamides

Due to the limitations of the previous method, the copper-catalysed HSUNG coupling reaction of electron-deficient amines and (bromoethynyl)triisopropylsilane **L.56** was used complementarily for the preparation of terminal ynamides (**Table 9**).^[255] Generally, this reaction presents a broad functional group tolerance. Furthermore, the applicability of Cu^I-USY as a heterogeneous catalyst in this reaction was previously reported by PALE's group.^[192] Thus, most of the HSUNG coupling reactions were performed under Cu^I-USY catalysis, illustrating here the suitability of (bromoethynyl)triisopropylsilane **L.56** with this catalytic system. Additional examples with HSUNG's original CuSO₄•5H₂O-based catalytic system are also reported.^[255] The reactions with sulfonamides **N.4,5**, and **9** run with both catalytic systems illustrate the efficiency of Cu^I-USY in this coupling reaction (entries 1-3), resulting in notably higher yields for ynamides **H.1** and **H.3** compared to CuSO₄•5H₂O (entries 1 and 3). Sulfonamides **N.10** and **N.11** were also compatible, but **N.11** underwent Boc-deprotection under HSUNG's conditions to give **H.5** in moderate 45% yield (entry 5). Interestingly, pyrrolidin-2-one (**N.12**) afforded **H.6** in only half the yield than **H.7** derived from its more nucleophilic carbamate analogue oxazolidine-2-one (**N.6**) (entry 6 vs. 7). This is due to partial degradation observed during the long reaction time of nine days for **N.12** (entry 6). Moreover, the vinylogous indole-based ynamide **H.8** was isolated in 87% yield, whereas otherazole-based ynamines **H.9** and **H.10** from benzotriazole (**N.7**) and imidazole (**N.8**) were not obtained due to an overall lack of reactivity under the investigated conditions.

Next, the terminal ynamides were prepared by TBAF-mediated desilylation (**Table 9**). In general, good to high yields (51-88%) were observed with short reaction times, even at -40 °C. The TIPS-protected pyrrolidin-2-one derivative **H.6**, however, reproducibly required several hours and ynamide **Y.12** was obtained in poor 27% yield (entry 6). Yet TLC indicated a rather clean conversion, suggesting that the terminal ynamide degrades upon aqueous work-up, possibly *via* hydration to its imide. Indeed, a much smaller crude quantity than expected was recovered, whereas ¹H NMR spectrum of the crude mainly showed the desired product **Y.12**.

Table 9. Synthesis of terminal ynamides via HSUNG coupling/TBAF deprotection.^[a]

Entry	N	T (°C)	Time	Yield ^[b] H (%)	Time	Yield ^[b] Y (%)
1		90/85	2 d/4 d	H.1 85 (80) ^[c] /66	5 min	Y.5 84
2		60/60	18 h/18 h	H.2 99 (95) ^[c] /99	90 min	Y.4 81
3		65/65	21 h/21 h	H.3 80/44	30 min	Y.9 51
4		65	18 h	H.4 89	15 min	Y.10 62
5		85-95	13 d	H.5 45 ^[d]	1 h ^[e]	Y.11 87
6		85-105	9 d	H.6 43 ^[f]	2 h	Y.12 27
7		110	60 h	H.7 82	12 min	Y.6 88
8		90	2 d	H.8 87	15 min	Y.13 60
9		90-120	7 d	H.9 0 ^[g]	-	Y.7 -
10		90	3 d	H.10 0 ^[h]	-	Y.8 -

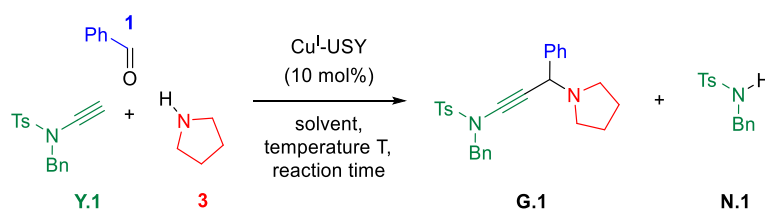
^[a] Values indicated in pink refer to reactions run with Cu^I-USY, while blue stands for CuSO₄·5H₂O. ^[b] Isolated yields. ^[c] Isolated yield obtained shifting from 0.5 mmol to 5 mmol scale. ^[d] Yield obtained for the ynamide bearing the unprotected indole moiety due to Boc-deprotection under operating conditions. ^[e] Left to warm to -10 °C over 1 h after 10 min at -40 °C due to slow conversion. ^[f] Degradation observed. ^[g] No conversion was observed at 90 °C and degradation occurred at higher temperatures up to 120 °C; compound **Y.7** not reported in the literature. ^[h] No conversion observed.

4.2. Optimisation of Reaction Conditions

4.2.1. Preliminary Results

We were interested in assessing the feasibility of direct catalytic access to γ -amino-ynamides in a three-component carbonyl-ynamide-amine coupling reaction. Initial investigations were conducted under conditions similar to our previously reported Cu^I-USY-catalysed A³ and KA² reaction conditions,^[211,267] with benzaldehyde (**4a**), *N*-ethynylsulfonamide **Y.1**, and pyrrolidine (**1a**) as model coupling partners (**Table 10**). Heating these three reagents in toluene/MeCN (1:1) at 80 °C for three hours furnished the expected γ -amino-ynamide **G.1** in a promising isolated yield (entry 1), along with sulfonamide **N.1** as the major product (i.e., 35% yield for **G.1** vs. 59% yield for **N.1**). **N.1** was not observed in the ¹H NMR spectrum of the crude mixture but is thought to result from the decomposition of an unidentified and unstable by-product during column chromatography on silica gel. Shifting to solvent-free conditions and performing the reaction at 90 °C resulted in complete consumption of ynamide but afforded only trace amounts of ynamide **G.1**. Sulfonamide **N.1** was again obtained as the major product after column chromatography (entry 2). Lowering the reaction temperature dramatically improved the coupling efficiency. In fact, running the reaction at 40 °C under solvent-free conditions (entry 3) afforded **G.1** in 83% yield. Last, “green” solvents were evaluated, anticipating potential solubility, or stirring issues. Stirring for two hours at room temperature, followed by one hour at 40 °C in 2-MeTHF gave **G.1** in good 61% yield. Interestingly, EtOAc competes with the coupling efficiency under neat conditions, even at 30 °C using equimolar amounts of each component (entry 5). Beneficially, the reaction proved to be faster in this solvent (30 min vs. 2 h).

Table 10. Preliminary optimisation studies for multicomponent γ -amino-ynamide synthesis.^[a]



Entry	Solvent	T (°C)	Time (h)	Yield G.1 (%)	Yield N.1 (%)
1	PhMe/MeCN (1:1)	80	3	35 ^[b]	59 ^[b]
2	none	90	1	Traces	43 ^[b]
3	none	40	2	83 ^[c]	.. ^[d]
4	2-MeTHF	rt then 40	2 then 1	61 ^[c]	.. ^[d]
5 ^[e]	EtOAc	30	0.5	82 ^[c]	.. ^[d]

^[a] Reactions run in a sealed tube under an argon atmosphere using benzaldehyde (**4a**, 1.4 eq.), pyrrolidine (**1a**, 1.1 eq.), ynamide **Y.1** (1.0 eq., at 0.13 M concentration) and Cu^I-USY (10 mol%) unless otherwise stated. ^[b] Isolated yield after purification by column chromatography. ^[c] Estimated yield by ¹H NMR of crude using 1,3,5-trimethoxybenzene as internal standard. ^[d] **N.1** not observed in the crude. ^[e] Equimolar amounts of each component were used.

4.2.2. Optimisation *via* Design of Experiments

Following these preliminary findings, the solvent-free AYA reaction between 1, **Y.1**, and 3 was used as a bench reaction for further optimisation studies *via* Design of Experiments (DoE).

To identify the most important variables influencing the γ -amino-ynamide yield, a typical fractional factorial design (FFD) was selected. The effect of temperature (A), catalyst loading (B), aldehyde equivalents (C), stirring rate (D), stirring bar type (E), and reaction time (F) were studied in a 2^{6-3} FFD, yielding a total of eight parallel experiments. **Table 11** shows the low and high levels for each variable.

Table 11. The investigated variables for the AYA reaction and their respective ranges.

Variable	Name	Units	Type	Min	Max	Mean	Std. Dev.
A	Temperature	°C	Numeric	30	60	45	16.04
B	Catalyst loading	mol%	Numeric	3	10	6.5	3.74
C	Aldehyde qty	eq.	Numeric	1.0	1.5	1.25	0.2673
D	Stirring rate	rpm	Numeric	200	600	400	213.81
E	Stirring bar	-	Categoric	Small	Big	-	-
F	Reaction time	min	Numeric	60	120	90	32.07

Table 12 shows the design matrix listing the standard (std) run numbers,ⁱⁱⁱ as well as the actual run number order together with the estimated ¹H NMR yields (%) of γ -amino-ynamide **G.1** (the recorded response) determined using 1,3,5-trimethoxybenzene as internal standard.

Table 12. Design matrix.

Std	Run	A (°C)	B (mol%)	C (eq.)	D (rpm)	E	F (min)	Yield G.1 (%)
1	1	30	3	1.0	600	Big	120	86
6	2	60	3	1.5	200	Big	60	59
4	3	60	10	1.0	600	Small	60	63
5	4	30	3	1.5	600	Small	60	86
2	5	60	3	1.0	200	Small	120	78
7	6	30	10	1.5	200	Small	120	84
3	7	30	10	1.0	200	Big	60	79
8	8	60	10	1.5	600	Big	120	83

Preliminary model selection was performed based on the half-normal probability plot and PARETO chart. Generally, the further a variable lies on the right side of the line, the greater its influence on the studied response. On the other side, variables laying close or on the line have little to no impact on the studied response (here: yield of AYA product **G.1**). Two models that

ⁱⁱⁱ Standard run numbers are given for completeness and are independent from the actual run number order. Each standard run number corresponds to a specific design point and is inherent to each design.

differ only in the inclusion or exclusion of the stirring rate variable (D) were identified (Figure 10). Indeed, when included, variable D exceeds the t-value limit in the PARETO chart, however, significantly lies below the BONFERRONI limit. Consequently, the model excluding stirring rate (D) was retained preferentially. Nevertheless, both models show that temperature (A) displays the greatest impact on the ynamide yield, followed by the reaction time (F). In addition, the interaction term of both variables, AF, significantly affected the ynamide yield. Considering our data set, the variables catalyst loading (B), aldehyde equivalents (C), and stirring bar type (E) do not have significant effects on the ynamide yield within the investigated ranges. Table 13 gives the analysis of variance (ANOVA) of the polynomial model including the variables temperature (A) and reaction time (F), as well as their interaction term AF. In addition, Table 14 outlines the corresponding Fit Statistics.

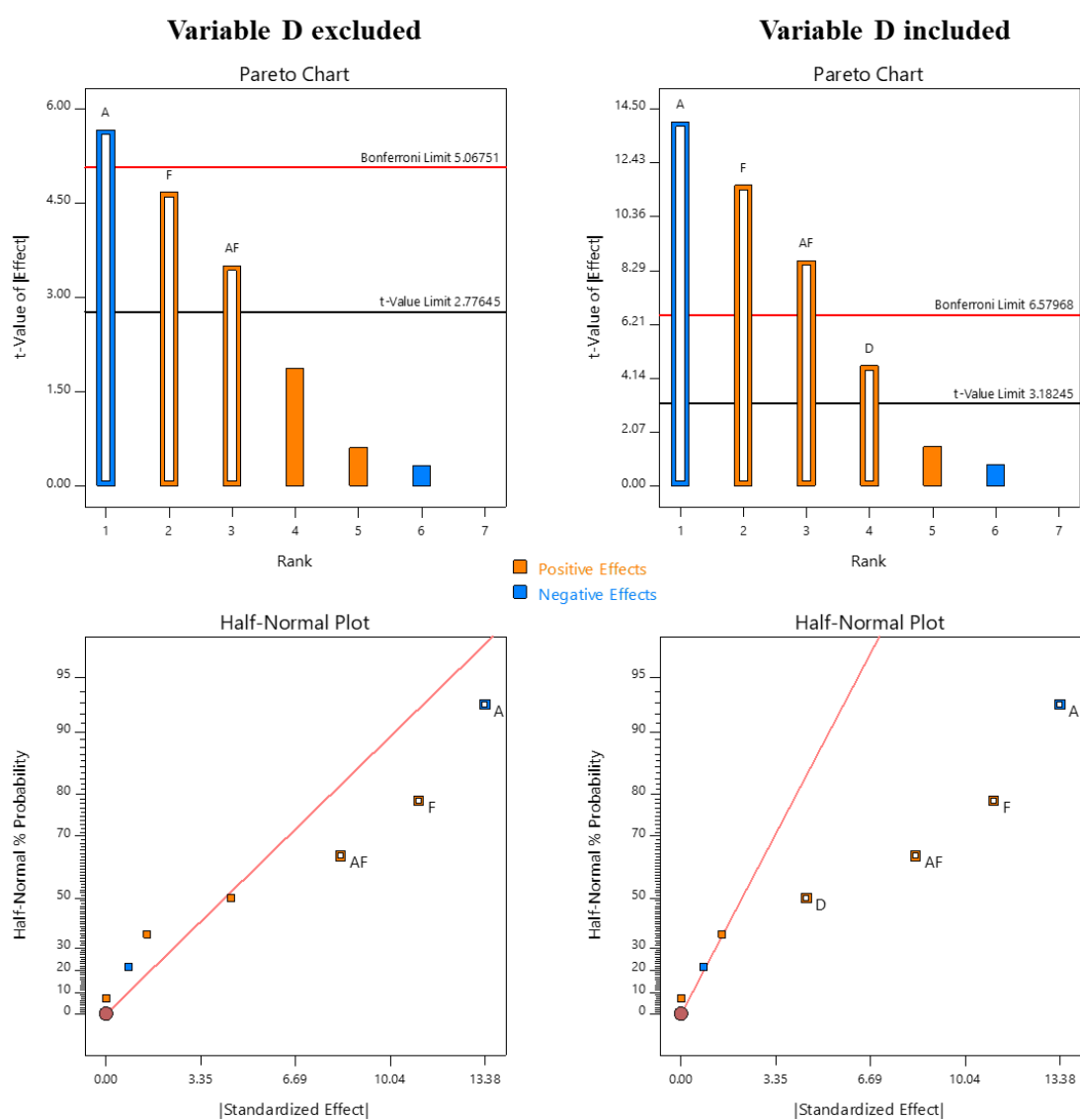


Figure 10. Pareto charts and half normal plots with variable D excluded or included.

Table 13. ANOVA for selected factorial model.

Source	Sum of Squares	df	Mean Square	F-value	p-value	
Model	739.48	3	246.49	22.08	0.0060	significant
A-Temperature	358.12	1	358.12	32.08	0.0048	
F-Reaction time	244.13	1	244.13	21.87	0.0095	
AF	137.24	1	137.24	12.29	0.0248	
Residual	44.65	4	11.16			
Cor Total	784.13	7				

Table 14. Fit Statistics.

Std. Dev.	Mean	C.V. %	R ²	Adjusted R ²	Predicted R ²	Adequate Precision
3.34	77.17	4.33	0.9431	0.9004	0.7722	10.3408

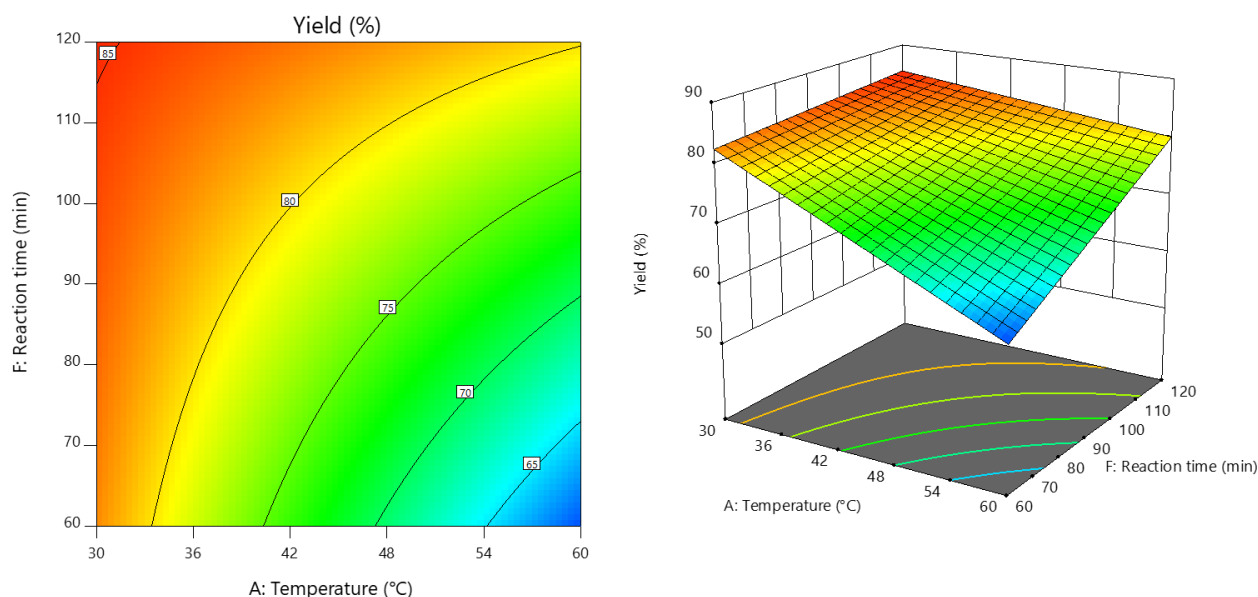
Accordingly, the coded equation for the selected model is:

$$\text{Yield (\%)} = 77.17 + (-6.69 \times A) + 5.52 \times F + 4.14 \times AF \quad (\text{Equation 1})$$

Its actual equation is:

$$\begin{aligned} \text{Yield (\%)} = & 117.95 + (-1.27 \times \text{Temperature}) + (-0.23 \times \text{Reaction time}) \\ & + 0.01 \times \text{Temperature} \times \text{Reaction time} \quad (\text{Equation 2}) \end{aligned}$$

yielding the graphical representation shown in **Figure 11**.

**Figure 11. Contour plot and response surface.**

Actual variables: catalyst loading (B): 3 mol%. Aldehyde qty (C): 1.0 eq. Stirring rate (D): 600 rpm. Stirring bar (E): big.

In conclusion, temperature (A) and reaction time (F) were identified as the critical variables to afford ynamide in high yield. This is in concordance with our preliminary observations mentioned above. As the optimal settings for those variables are likely to depend on the substrate combination, no further optimisation studies *via* DoE were performed. The retained values for the other variables are summarised in **Table 15**. The reaction temperature was set to 30 °C, and

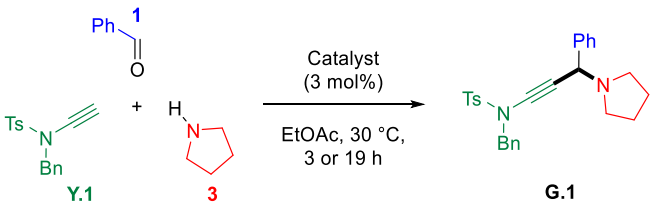
the reaction progress was monitored using thin-layer chromatography until the starting materials were completely converted. The catalyst loading (B) was set to its lowest investigated level, i.e., 3 mol%, and the same type of reactor and magnetic stirrer (E) was used throughout the entire scope. Although not statistically significant in this brief study, the number of aldehyde equivalents (C) and the stirring rate (D), were positively correlated with **G.1** yield. Nonetheless, we used equimolar amounts of all coupling partners and set the stirring rate to the highest investigated value (i.e., 600 rpm).

Table 15. Optimised AYA conditions.

A: Temperature	B: Catalyst loading	C: Aldehyde qty	D: Stirring Rate	E: Stirring bar
30 °C	3 mol%	1.0 eq.	600 rpm	Small

4.2.3. Catalyst Screening

With the optimised conditions in hand, the potential of additional catalysts in the AYA reaction was investigated in EtOAc to allow rigorous stirring in each case (**Table 16**). First, three USY zeolites doped with metal cations (Cu^{II} , Zn^{II} and Mn^{II}) known to catalyse the A^3 and KA^2 reaction of classical alkynes were evaluated. Cu^{I} -USY stood out as the best catalyst under these conditions, affording 88% conversion after three hours and excellent selectivity for γ -aminoynamide **G.1** (entry 1 vs. entries 2-4). Despite nearly complete conversion after 19 hours, switching to its oxidised Cu^{II} -form resulted in a dramatic drop in yield (entry 2). In addition to reduced chemoselectivity for ynamide **G.1**, the recovered crude mass after filtration was surprisingly low. Comparably low yields were obtained with Mn^{II} - and Zn^{II} -USY (entries 3 and 4 vs. 2), but unlike Cu^{II} -USY, the lower yields are primarily due to significantly lower conversions when compared to Cu^{I} -USY (entries 3 and 4 vs. 1). Next, copper halides, also proved as effective catalysts in A^3/KA^2 reactions, were examined. Despite full conversions, CuCl , CuBr and CuI gave ynamide **G.1** in poor yields due to the formation of numerous unidentified by-products (entries 5-7). It is unclear whether this is related to the presence of nucleophilic halides which could perform a nucleophilic addition onto π -activated ynamide **Y.1**.^[268,269] Last, control experiments confirmed that neither the presence of H-USY (entry 6) nor the absence of catalyst promoted the coupling reaction (entry 7). As a result, Cu^{I} -USY proved to be by far the best catalyst to promote this novel 3CR and was thus used to further investigate its scope and limitations.

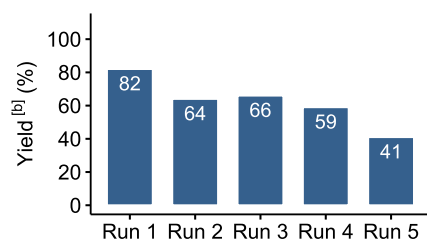
Table 16. Catalyst screening for the synthesis of γ -amino-ynamide G.1.^[a]

Entry	Catalyst	Time (h)	Yield ^[b] G.1 (%)	Conv. ^[b] (%)
1	Cu ^I -USY	3	84	88
2	Cu ^{II} -USY	19	21 ^[c]	95
3	Zn ^{II} -USY	3	31 ^[d]	46
4	Mn ^{II} -USY	3	16 ^[d]	23
5	CuCl	3	32 ^[c]	100
6	CuBr	3	13 ^[c]	100
7	CuI	3	32 ^[c]	100
8	H-USY	19	0 ^[e]	0 ^[e]
9	none	19	0 ^[e]	0 ^[e]

^[a] Reactions run in a sealed tube with benzaldehyde (**4a** 1.0 eq. with a 0.85 M concentration), ynamide **Y.1** (1.0 eq.), and pyrrolidine (**1a**, 1.0 eq.). ^[b] Yield and conversion estimated by ¹H NMR of the crude using 1,3,5-trimethoxybenzene as internal standard. ^[c] Formation of several unidentified by-products. ^[d] Selective but slow conversion. ^[e] No conversion was observed, and no **G.1** was detected after 19 h.

4.2.4. Catalyst Reusability and Stability

Next, the stability and recyclability of the Cu^I-USY catalyst were investigated using the benchmark reaction of benzaldehyde (**4a**), *N*-ethynylsulfonamide **Y.1**, and pyrrolidine (**1a**) (Figure 12). For practical reasons, the catalyst loading was set to 10 mol%. After each reaction, the catalyst was separated from the crude mixture through decantation after centrifugation, washed several times with EtOAc, and then directly employed in the next run. Figure 12 shows a notable decrease in yield starting from the second run (82% vs. 64%). Up to the fourth run, however, the yield varies little (59-66%) before dropping to 41% in the fifth run. It should be noted

**Figure 12. Catalyst recycling study.^[a]**

^[a] Reactions run for model reaction forming **G.1** under conditions from Table 16 – entry 1, using 10 mol% of Cu^I-USY. ^[b] Yield estimated from crude mixtures via ¹H NMR using 1,3,5-trimethoxybenzene as internal standard. The conversions from Run 1 to 5 were as follows: 100%, 79%, 82%, 77%, 67%.

that the reaction time was kept constant and that the decreased yields are due to lower conversions. The chemoselectivity, however, remained significantly high throughout the study and thus superior to the other catalysts screened (see Table 16). These findings, together with a green colouring of the reaction mixture, which loses in intensity throughout the runs, suggested the leaching of copper cations. To verify this hypothesis, a filtration test was performed under optimal conditions (i.e., 3 mol% of Cu^I-USY running the reaction at 30 °C

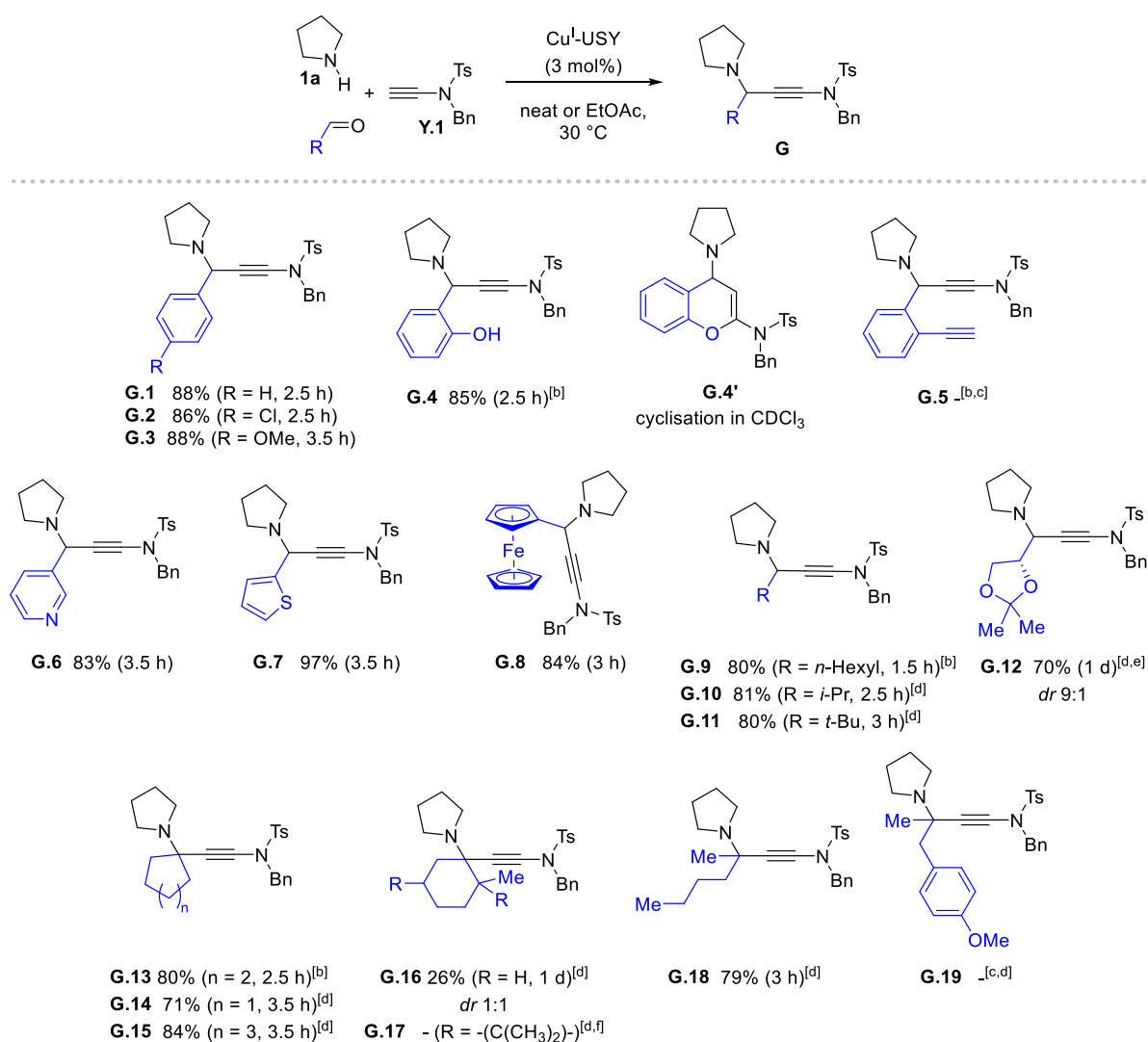
in EtOAc). Indeed, complete conversion of the starting materials was observed after Cu^I-USY

was filtered off, albeit at a lower rate. The copper zeolite possibly acts as a “reservoir” of copper cations, which form an active catalyst in solution affording γ -amino-ynamide **G.1** in high chemoselectivity compared to copper halides. Such leaching phenomena are common with coordinating substrates and intermediates (e.g., amine and ynamide here), and were previously observed in the Cu^I-USY-catalysed synthesis of ynamides.^[192] Yet, XPS analysis revealed that the copper ions present on the surface of the recovered Cu^I-USY zeolite remained at their +I oxidation state. The remarkable chemoselectivity under Cu^I-USY catalysis motivated us to further develop this novel 3CR.

4.3. Scope and Limitations

4.3.1. Carbonyl Scope

First, the potential of the AYA reaction was investigated by reacting several aldehydes with pyrrolidine (**1a**) and ynesulfonamide **Y.1** (**Scheme 87**). 4-Chloro- and 4-methoxybenzaldehyde reacted similarly to benzaldehyde (**4a**), yielding the desired γ -amino-ynamides **G.2** and **G.3** in comparable yields (86-88%) with little electronic influence. Salicylaldehyde selectively yielded the AYA product **G.4** in 85% yield. Interestingly, stirring the crude product in CDCl₃ overnight resulted in an intramolecular 6-*endo*-dig cyclisation to give benzopyrane **G.4'**. Strikingly, no cyclisation was observed from purified **G.4** in CDCl₃, suggesting that besides the solvent, leached copper might be decisive for the cyclisation reaction to occur. Surprisingly, a fresh sample of Cu^I-USY did not result in a clean conversion to benzopyrane **G.4'**. In sharp contrast to salicylaldehyde, 2-ethynylbenzaldehyde produced a complex reaction mixture with no traces of the desired product **G.5**. Rewardingly, heteroaryl aldehydes, namely 3-pyridinecarboxaldehyde and 2-thiophenecarboxaldehyde, as well as organometallic ferrocenecarboxaldehyde, proved to be suitable coupling partners, yielding **G.6-G.8** in high to excellent yields (84-97%) with consistently short reaction times. Next, we turned our attention to aliphatic aldehydes which displayed comparable coupling efficiency in the AYA reaction. Indeed, γ -amino-ynamides **G.9-G.11** were isolated in comparably high yields from linear *n*-heptanal (cf. **G.9** in 80%) or branched 2-methylpropanal and 2,2-dimethylpropanal (cf. **G.10** in 81% and **G.11** in 80%, respectively). Notably, the use of chiral 2,3-*O*-isopropylidene-glyceraldehyde resulted in a substrate-controlled asymmetric synthesis of γ -amino-ynamide **G.12** in 70% and good diastereoselectivity (*dr* 9:1).



Scheme 87. Carbonyl scope of the Cu^I-USY-catalysed AYA/KYA reactions.^[a]

^[a] Reactions run solvent-free at 30 °C in a sealed tube using benzaldehyde (**4a**) or cyclohexanone (**2a**) (1.0 eq.), an ynamide (1.0 eq.), pyrrolidine (**1a**, 1.0 eq.) and Cu^I-USY (3 mol%), unless otherwise stated. ^[b] Reaction performed in EtOAc (at 0.85 M concentration). ^[c] Complex mixture of unidentified by-products. ^[d] Reaction performed in EtOAc (0.85 M) adding molecular sieves (4 Å, 300 mg/mmole). ^[e] Reaction was set up at 0 °C and left to warm to rt overnight. ^[f] No conversion of the corresponding ketone was observed.

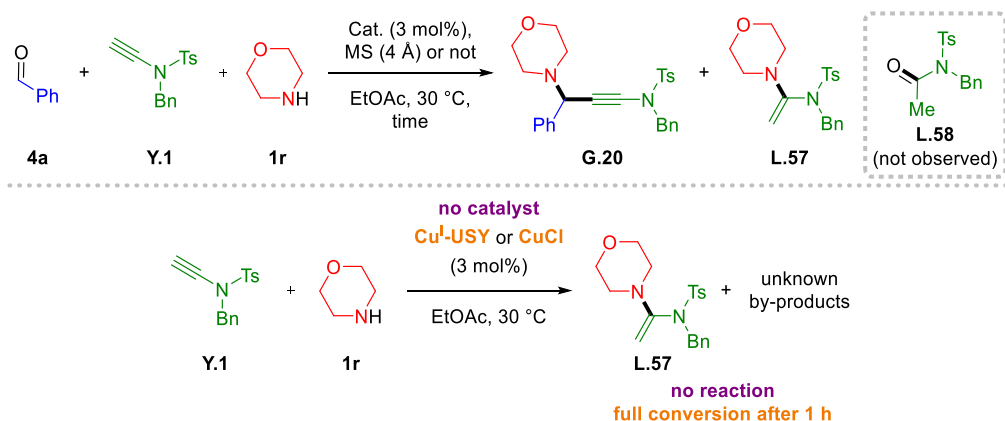
Encouraged by these promising results, we investigated the suitability of ketones as more difficult coupling partners to pave the way for the KYA approach (Scheme 87). As is the case for related KA² reactions, cyclohexanone was observed to be an efficient coupling partner, with no need to change the optimised solvent-free reaction conditions. The expected KYA product **G.13** was obtained in comparable yield (80%) and reaction time undoubtedly thanks to the beneficial strain energy release upon nucleophilic additions involving this cyclic ketone and its iminium form.^[217] In the presence of molecular sieves, less reactive cyclopentanone and cycloheptanone yet afforded ynamides **G.14** and **G.15** in similar yields. Increasing the steric hindrance on the cyclic ketone, however, had a non-negligible negative effect on the efficiency of the KYA coupling reaction. Shifting from cyclohexanone to 2-methylcyclohexanone resulted in a significant decrease in yield (80% for **G.13** vs. 26% for **G.16**), whereas the more hindered (+)-camphor did not react under our conditions (no traces of **G.17**). Notably, **G.16** was obtained as a 1:1

mixture of both diastereoisomers, whereas diastereoselectivity was demonstrated in related KA² reactions.^[42,203,267] As for acyclic aliphatic ketones, hexan-2-one afforded γ -amino-ynamide **G.18** smoothly in 79% yield in the presence of molecular sieves. In sharp contrast, even at 55 °C, 4-methoxyphenylacetone did not provide the desired KYA product **G.19**, most likely due to the high stability of the resulting conjugated enamine,^[270] which prevents the coupling from taking place.

4.3.2. Amine Scope

Next, the compatibility of other secondary amines in the AYA reaction with benzaldehyde (**4a**) and ynesulfonamide **Y.1** was examined. Shifting from pyrrolidine to morpholine in EtOAc gave the desired ynamide **G.20** in 55% isolated yield, along with ketene aminal **L.57** (Table 17, entry 1). ¹H NMR analysis showed a significant amount of unreacted benzaldehyde (**4a**) (**G.20/4a** 60:40) and a **G.20/L.57** ratio of 67:33. In a control experiment, omitting benzaldehyde and Cu^I-USY, morpholine and ynamide **Y.1** did however not react. Adding 3 mol% of Cu^I-USY or CuCl then resulted in the complete conversion of ynamide **Y.1** in one hour. During the reaction, and before complete ynamide consumption, an additional unidentified product forms, while no hydrolysis of the ketene aminal **L.57** to amide **L.58** was observed. Compared to CuCl, Cu^I-USY afforded a cleaner crude mixture, similar to the observation made during the catalyst screening (for details, see Table 16).

Table 17. Evaluation of the AYA reaction with morpholine.^[a]



Entry	4 Å MS (mg/mmol)	Catalyst	G.20/4a ^[b]	G.20/L.57 ^[b]	Yield ^[c] G.20 (%)
1	-	Cu ^I -USY	60:40	67:33	55%
2	100	Cu ^I -USY	81:19	85:15	n.d.
3	300	Cu ^I -USY	93:7	100:0	85%
4	-	Sc ^{III} -Cu ^I -USY	51:49	58:42	45%

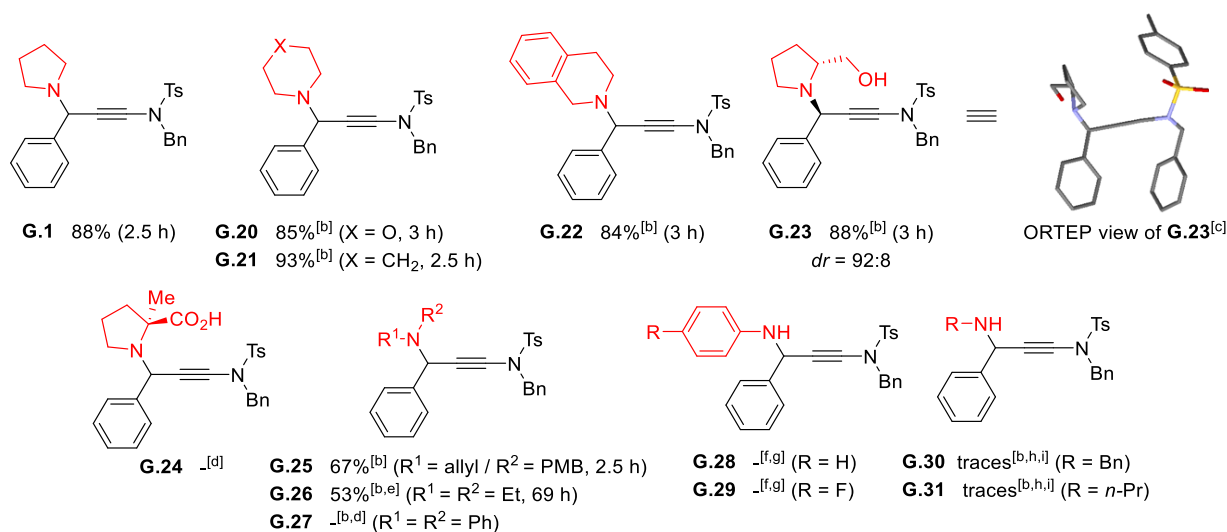
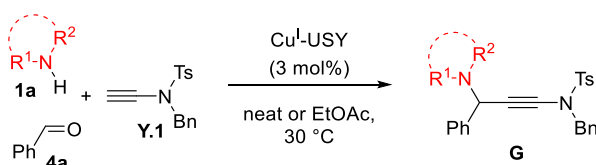
^[a] Reactions run in EtOAc (at 0.85 M concentration) at 30 °C in a sealed tube using equimolar amounts of each component and Cu^I-USY (3 mol%), unless otherwise stated. ^[b] Ratios were determined from crude mixtures *via* ¹H NMR. ^[c] Yield estimated from crude mixtures *via* ¹H NMR using 1,3,5-trimethoxybenzene as internal standard.

As ketene aminal **L.57** results from a formal hydroamination of morpholine onto ynamide **Y.1**, molecular sieves were added to accelerate the condensation of morpholine onto benzaldehyde, and to prevent the direct adduct formation to ketene aminal **L.57** (Table 17, entries 2 and 3). With 300 mg/mmol of molecular sieves, no ketene aminal **L.57** was observed, and **G.20** was isolated in 85% yield (entry 3). Additionally, bimetallic Sc^{III}-Cu^I-USY, possessing highly oxophilic scandium cations for carbonyl activation, was evaluated but resulted less efficient than Cu^I-USY (entry 4 vs. 1).

Following this short optimisation with morpholine, most reactions during the investigation of the amine scope were conducted in the presence of molecular sieves (Scheme 88).

In general, cyclic secondary amines such as pyrrolidine, morpholine, piperidine, and tetrahydroisoquinoline provided high to excellent yields (84-93%) of the desired AYA products **G.1** and **G.20- G.22**. Next, the potential of amine-controlled stereoselective AYA reactions was investigated using chiral amines. (*R*)-Prolinol efficiently formed the expected γ -amino-ynamide **G.23** with high diastereoselectivity (*dr* = 92:8) under standard conditions and without further optimisation. Crystallising **G.23** via slow evaporation from a CH₂Cl₂/Et₂O solution yielded fine pale-yellow needles, whose X-ray analysis (CCDC2155844) confirmed the structure and absolute configuration of this chiral γ -amino-ynamide. It is worth noting that the revealed diastereoselectivity is similar to that reported in related A³ reactions involving (*R*)-prolinol as the chiral component.^[271] In contrast, the AYA coupling was ineffective with α -methyl-L-proline as the chiral amine (\rightarrow **G.24**), most likely due to solubility and/or reactivity issues. Regarding secondary acyclic amines, coupling efficiencies were generally lower. *N*-Allyl-4-methoxybenzylamine, for instance, gave the desired ynamide **G.25** at a slightly lower yield along with an unidentified by-product. *N,N*-Diethylamine, on the other hand, reacted cleanly but much slower than its cyclic analogue pyrrolidine (cf. 53% for **G.26** after 69 hours vs. 88% for **G.1** after 2.5 hours). Finally, the less nucleophilic *N,N*-diphenylamine (\rightarrow **G.27**) did not react at all.

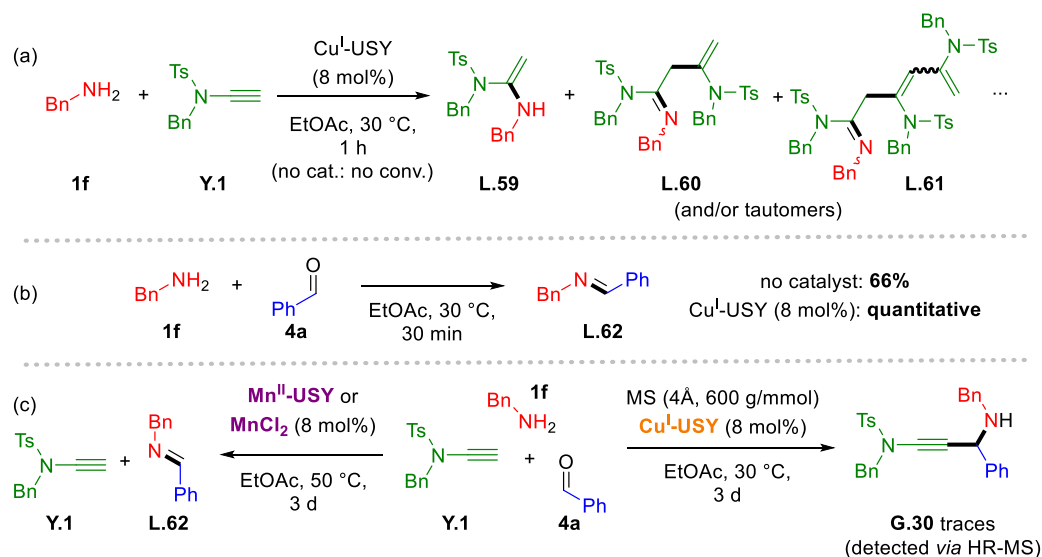
AYA reactions with primary amines were found to be even more challenging (Scheme 88). The reaction with aniline (\rightarrow **G.28**), for instance, stalled at the imine intermediate. A similar result was obtained for 4-fluoroaniline (\rightarrow **G.29**), along with small amounts of the amide resulting from the hydration of starting ynamide **Y.1** and other unidentified by-products. Aliphatic primary amines, such as benzylamine and *n*-propylamine, resulted in complex mixtures containing only trace amounts of the AYA products **G.30** and **G.31** along with ynamide-derived oligomers, rendering benzaldehyde (**4a**) futile.



Scheme 88. Amine scope of the Cu^I-USY-catalysed AYA reaction.^[a]

^[a] Reactions run solvent-free at 30 °C in a sealed tube using benzaldehyde (**4a**) or cyclohexanone (**2a**) (1.0 eq.), an ynamide (1.0 eq.), pyrrolidine (**1a**, 1.0 eq.) and Cu^I-USY (3 mol%), unless otherwise stated. ^[b] Reaction performed in EtOAc (with 0.85 M concentration) adding molecular sieves (4 Å, 300 mg/mmol). ^[c] CCDC2155844. ^[d] No conversion of the corresponding amine was observed. ^[e] Incomplete conversion with **G.26/Y.1** = 7:3. ^[f] Reaction performed in EtOAc (0.85 M). ^[g] Corresponding imine was observed as the major product. ^[h] Traces of desired product detected. ^[i] Complex mixture of unidentified by-products.

This prompted us to examine the reaction between ynamide **Y.1** and benzylamine under similar conditions in EtOAc at 30 °C (**Scheme 89**). As with morpholine, no reaction occurred in the absence of Cu^I-USY. Yet the addition of benzylamine to a suspension of ynamide **Y.1** and Cu^I-USY in EtOAc instantaneously initiated the conversion of ynamide **Y.1**. After one hour, TLC analysis revealed a multitude of product spots, and a white precipitate is obtained. MS analysis confirmed the formation of ynamide-derived oligomers (**L.60** and **L.61**), probably resulting from ketene aminal **L.59**. Although imine **L.62** formation from benzaldehyde (**4a**) and benzylamine under the same conditions was rather efficient (complete conversion in 30 min), the use of up to 600 mg/mmol of molecular sieves in EtOAc only decelerated the degradation of the reaction mixture (**Scheme 89c**, right). The desired γ -amino-ynamide **G.30** was obtained in trace amounts allowing its detection in HR-MS. Shifting from Cu^I-USY to Mn^{II}-USY or MnCl₂ with reaction temperatures up to 50 °C did only result in imine **L.62** without conversion of ynamide **Y.1** (**Scheme 89c**, left).



Scheme 89. Control experiments for the reaction of benzylamine with (a) ynamide **Y.1** and (b) benzaldehyde, and (c) further attempts for the 3CR with benzylamine.

To avoid the proposed hydroamination pathway, a two-step approach starting from pre-formed imines and trapping them with the ynamide partner was thus envisioned (Table 18). Stirring *N*-benzylaldimine and ynamide **Y.1** under AYA conditions, still afforded a complex mixture without traces of the targeted **G.30** (entry 1). Ynamide **Y.1** was entirely consumed, whereas most of the aldimine remained unreacted and traces of benzaldehyde (**4a**) were observed. Possibly, the partial hydrolysis of imine **L.62** generated benzylamine, which induced the hydroamination/oligomerisation path. Adding Et₃N (1.0 eq.) to assist the formation of copper acetylide afforded a similar result (entry 2). Copper acetylide formation thus was not considered to be the limiting step, but rather the nucleophilic addition itself. As a result, the use of stoichiometric LEWIS acid additives for electrophilic imine activation was envisaged. Interestingly, BF₃•OEt₂ induced a complete conversion of ynamide **Y.1** in two hours but aldimine **L.62** remained the major product and no traces of ynamide **G.30**, nor benzaldehyde (**4a**) were detected (entry 3). The use of Ti(OEt)₄, in turn, demonstrated the feasibility of this alternative two-step approach (entry 4).^[218] Nevertheless, ynamide **G.30** was isolated in low 17% yield after six days. Unfortunately, shifting to *N*-phenylbenzaldimine **L.63**, no conversion was observed unless the reaction was heated to 50 °C. Yet, under such conditions, a complex mixture was obtained (entry 5). Our additive-free Cu^I-USY-based catalytic system is thus restricted to aliphatic secondary amines. Despite our efforts to show the accessibility of γ -amino-ynamides bearing aliphatic secondary amines *via* a two-step approach, further improvement is needed to achieve satisfying results.

Table 18. Attempts towards a bimolecular catalytic synthesis of γ -amino-ynamides from pre-formed imines.

L.62 (R = Bn)
 L.63 (R = Ph)
 (2.0 eq.)

Y.1

$\text{Cu}^{\text{I}}\text{-USY (8 mol\%)}$,
 additive or not
 $\text{EtOAc, 30 }^\circ\text{C}$

G.30 (R = Bn)
 G.31 (R = Ph)

Entry	R	Additive (1.0 eq.)	Time	Yield (%)	Conversion Y.1 (%)
1	Bn	-	1 d	0 ^[a]	
2	Bn	Et ₃ N	1 d	0 ^[a]	
3	Bn	BF ₃ •OEt ₂	2 h	0 ^[a]	100
4	Bn	Ti(OEt) ₄	6 d	17 ^[b]	
5 ^[c]	Ph	Ti(OEt) ₄	1 d	0 ^[d]	

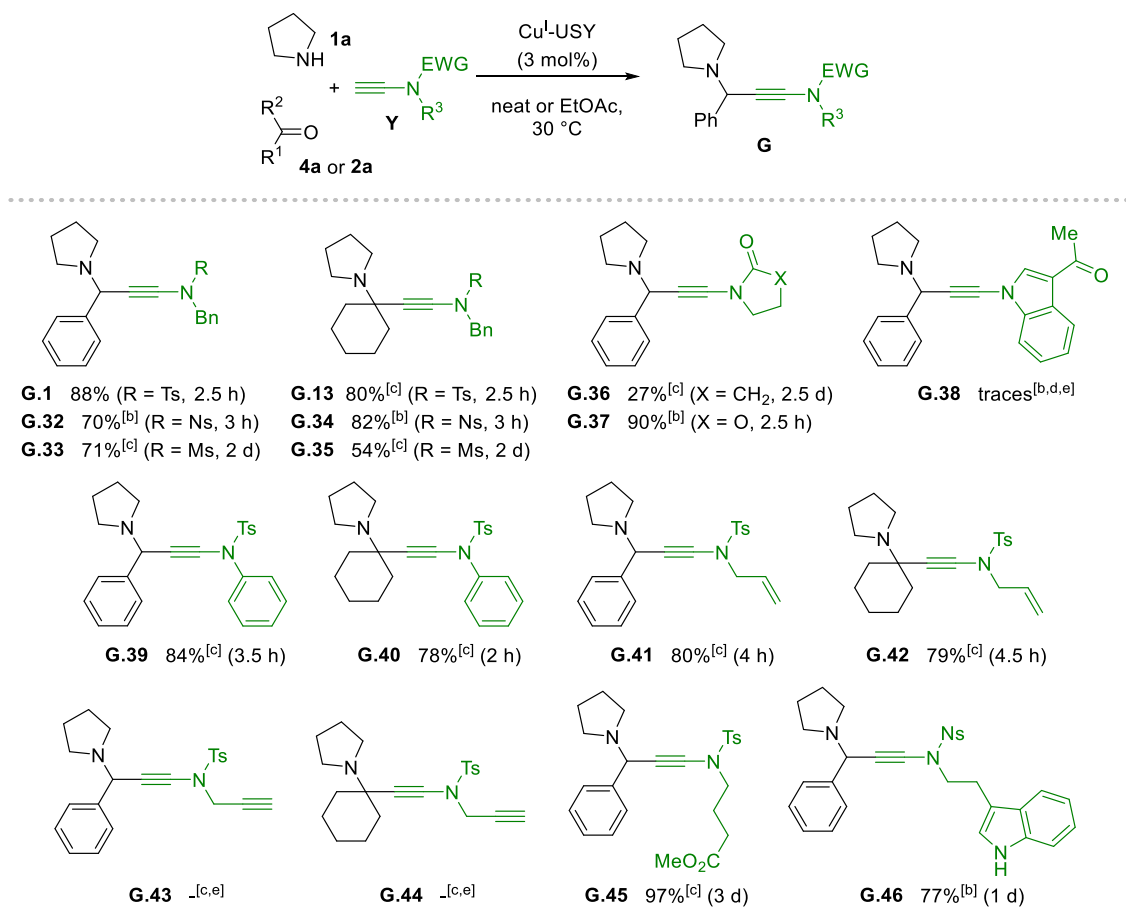
^[a] Aldimine **L.62** was observed as the major product in the crude mixture, without traces of terminal ynamide **Y.1**, nor product **G.30**. ^[b] Isolated yield. ^[c] Reaction run at 50 °C. ^[d] Complex mixture of unidentified products.

4.3.3. Ynamide Scope

In a final series of experiments, the terminal ynamide partner was varied (**Scheme 90**).

First, we examined the impact of the electron-withdrawing group on the ynamide nitrogen atom. For this, tosyl, mesyl and nosyl sulfonyl groups were tested and found to be amenable in AYA/KYA reactions with moderate to high yields of the corresponding γ -amino-ynamides **G.1** and **G.13** and **G.32-G.35**. Nonetheless, the nature of the sulfonyl group proved to have a significant influence on reaction efficiencies and kinetics. While tosylated AYA/KYA products **G.1** and **G.13** were formed in 2.5 hours, it took several days to achieve full conversions to mesyl analogues **G.33** and **G.35** isolated in lower yields. Nosyl derivatives **G.32** and **G.34**, however, formed at comparable rates and yields by adding molecular sieves. In the absence of molecular sieves, several by-products among which mainly the hydrated form of the nosylated starting ynamide **Y.5** were observed, thus showing the relevance of using molecular sieves. In addition to sulfonamides, our conditions afforded lactam **G.36** in low 27% yield after 2.5 days. In sharp contrast, carbamate **G.37** was isolated in excellent 90% yield in 2.5 h from the more nucleophilic 2-oxazolidinone-derived terminal ynamide **Y.6**. The vinylogous indole-derived product **G.38**, however, only formed in small amounts and could not be isolated in pure form. In fact, the reaction mixture started to degrade before a notable conversion of the starting materials was reached. Last, diverse amino group substituents in *N*-tosyl-ynamides were scrutinised. Besides the benzyl group, phenyl and allyl groups were also well tolerated, resulting in γ -amino-ynamides **G.39-G.42** in 78-84% yield. The propargylamine-derived ynamide **Y.9**, however, was incompatible with our catalytic system, impeding the formation of products **G.43** and **G.44**. Beneficially, other functional groups, such as methyl ester and unprotected indole,

were highly compatible, resulting in the corresponding γ -amino-ynamides **G.45** and **G.46** in 97% and 77% yield, respectively.



Scheme 90. Ynamide scope of the Cu^{I} -USY-catalysed AYA/KYA reactions.^[a]

^[a] Reactions run solvent-free at 30 °C in a sealed tube using benzaldehyde (**4a**) or cyclohexanone (**2a**) (1.0 eq.), an ynamide (1.0 eq.), pyrrolidine (**1a**, 1.0 eq.) and Cu^{I} -USY (3 mol%), unless otherwise stated. ^[b] Reaction performed in EtOAc (with 0.85 M concentration) adding molecular sieves (4 Å, 300 mg/mmol). ^[c] Reaction performed in EtOAc (0.85 M). ^[d] Traces of desired product detected. ^[e] Complex mixture of unidentified by-products.

4.3.4. Comparison with A³/KA² Reactions and Mechanistic Rationale

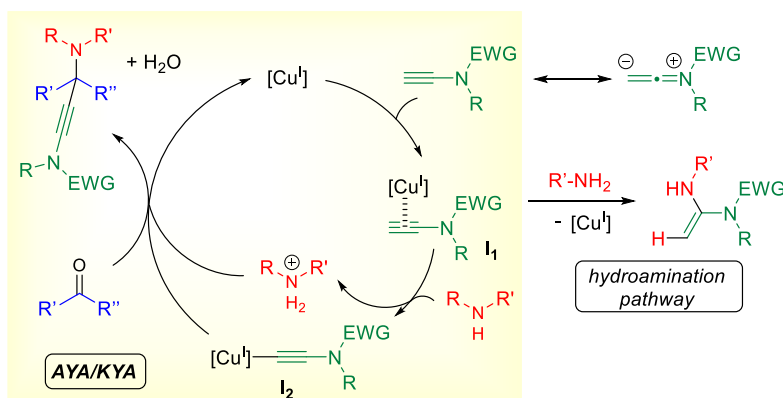
At this point, it is possible to compare the novel AYA/KYA reactions to their preceding A³ and KA² versions (Table 19), especially with the Cu^I-USY-based catalytic systems.^[211,267] As for the Cu^I-USY-catalysed A³ and KA² reactions, a broad functional group tolerance was observed allowing for the preparation of functionalised propargylamines. Nonetheless, several discrepancies regarding the substrate scope exist and merit to be stressed.

Table 19. Comparison between Cu^I-USY-catalysed AYA/KYA and A³/KA² reactions.

	AYA/KYA	A ³ /KA ²
Optimised temperature	30 °C	80 °C
Reaction time	< 5 h ^[a]	≥ 15 h
Catalyst loading	3 mol%	8-10 mol%
Challenging substrates	Primary aliphatic amines, ^[b] anilines ^[c]	Secondary aliphatic amines, ^[d] linear ketones ^[e]
Competing pathway	Hydroamination with primary aliphatic amines	Hydroamination with secondary aliphatic amines ^[d]

^[a] Observed in most cases. ^[b] Were not evaluated in the Cu^I-USY-catalysed A³ reaction^[211] but examples evaluated in the AYA reaction were highly efficient in KA² reaction. ^[c] Were not evaluated in the Cu^I-USY-catalysed A³ reaction but showed low-to-moderate performance in KA² reaction. ^[d] Other than pyrrolidine. ^[e] Cu^I-USY-catalysed KA² reaction with such substrates however not performed in presence of molecular sieves.

The comparison of reaction times (2-5 vs. 15-18 h) and optimal temperatures (30 vs. 80 °C) unequivocally demonstrates that a significant rate acceleration is achieved shifting from terminal unactivated alkynes to terminal ynamides. In the A³ and KA² reactions, the addition of the metal acetylide nucleophile to the imine electrophile is generally believed to be the rate-determining step (Scheme 91).^[234] Yet, the formation rate of the metal acetylide, presumably through deprotonation of the π -complexed alkyne, should also be considered. In the case of terminal ynamides, the delocalised non-binding nitrogen electron pair greatly enriches the π -system of the carbon-carbon triple bond, despite the σ -electron-withdrawing effect of the “amide” group. As a result, ynamides are better π -nucleophiles compared to terminal alkynes (see *N* parameters)^[254], and thus may be the corresponding copper acetylides. In addition, it is highly likely that this enhanced π -nucleophilicity favours the formation of the π -ynamide complex **I1** and thus accelerates the formation of the copper acetylide intermediate **I2**. Yet the increased electron density on the terminal ynamide carbon might also disfavour the deprotonation, possibly making it the rate-determining step. WATSON and co-workers, however, observed a kinetically enhanced copper acetylide formation with aryl ynamines and 3-ethynyloxazolidin-2-one (**Y.6**) in comparison to unactivated alkynes in copper-catalysed CuAAC reactions.^[272,273]



Scheme 91. Mechanistic proposal for the copper-catalysed AYA/KYA reactions.

It should also be noted that formal hydroamination of the π -complex **II** was observed for the KA^2 (see section III-2.3.4.) and the AYA/KYA reactions. In both cases, this likely results from a competition between hydroamination and imine/iminium ion formation. The tendencies, however, are dependent on the amine class and differ for both processes. This is not surprising as the alkyne components in both methods display inherently different reactivity profiles. Regarding the KA^2 reaction, involving unactivated alkynes, hydroamination was exclusively observed with secondary aliphatic amines under optimised conditions. In both methods, it was observed that pyrrolidine showed an increased “ease” to undergo the condensation/coupling pathway compared to other secondary amines. Primary aliphatic amines, however, were not nucleophilic enough to undergo the unfavourable hydroamination reaction with unactivated alkynes. In sharp contrast, π -ynamide complexes were found to be sufficiently reactive to undergo adduct formation with such less nucleophilic primary amines. Regarding secondary amines, chemoselectivity for the AYA reaction was restored using molecular sieves, whereas primary amines still followed the hydroamination pathway. Given their lower nucleophilicity, this could, in parts, originate from a less favourable condensation reaction. Yet the main limitation seems to be the insufficient electrophilicity of the resulting imine, which is not trapped by copper acetylide intermediate **I2**.

5. Conclusion

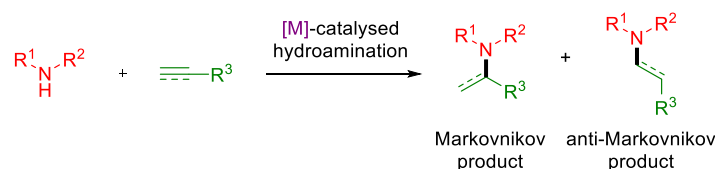
In conclusion, a successful extension of the carbonyl-alkyne-amine 3CR methodology was achieved using terminal ynamides as alkyne surrogates under mild Cu^I-USY catalysis. The so-called AYA/KYA reactions represent the first one-pot synthesis of γ -amino-ynamides from aliphatic amines. Recovered Cu^I-USY was reused several times, but a progressive erosion of the catalytic activity was observed, as well as partial copper leaching. Nevertheless, consistently high chemoselectivity for the γ -amino-ynamides was observed throughout the recycling study, whereas classical copper halides as catalysts induced decomposition under homogeneous conditions. Moreover, the Cu^I-USY-based system offers a wide product scope tolerating a myriad of functional groups (e.g., heteroaromatic, halide, acetal, carbamate, ether, hydroxy, ester, sulfonyl, lactam, oxazolidinone, etc.). In addition, the Cu^I-USY-catalysed AYA/KYA reactions are based on equimolar amounts of each component, proceed under mild conditions (i.e., 30 °C, neat or EtOAc as benign solvent) with low copper loading (3 mol%) and in generally short reaction times (mostly < 5 h). Water further being the only by-product formed, AYA/ KYA processes thus emerge as powerful energy-, atom- and step-economical methods to access γ -amino-ynamides, in great accordance with Green Chemistry principles. However, further efforts are needed to extend this methodology to challenging primary amines and aniline.

Chapter V – Propargylamine Synthesis Involving Alkyne Hydroamination

Cu^I-USY-Catalysed Hydroamination/Protonation/Alkyne Addition Reaction

1. Introduction

Hydroamination describes the direct addition of an amine to a carbon-carbon multiple bond, such as an alkene, allene, or alkyne. Hydroamination is highly desirable for the synthesis of *N*-containing compounds thanks to its complete atom economy and often relies on easily available starting materials. It is therefore not surprising that countless reports on hydroamination are published and summarised relentlessly. In contrast to alkenes, which afford alkylamines upon hydroamination, alkynes result in enamines, which can undergo further transformations. Undoubtedly, this renders alkyne hydroamination an attractive tool for the facile and rapid construction of more complex molecules in multicomponent reactions or (sequential) one-pot strategies. In many hydroamination processes, however, arises the question of regioselectivity. Amine addition can proceed through MARKOVNIKOV or anti-MARKOVNIKOV selectivity giving rise to two regioisomers (**Scheme 92**).

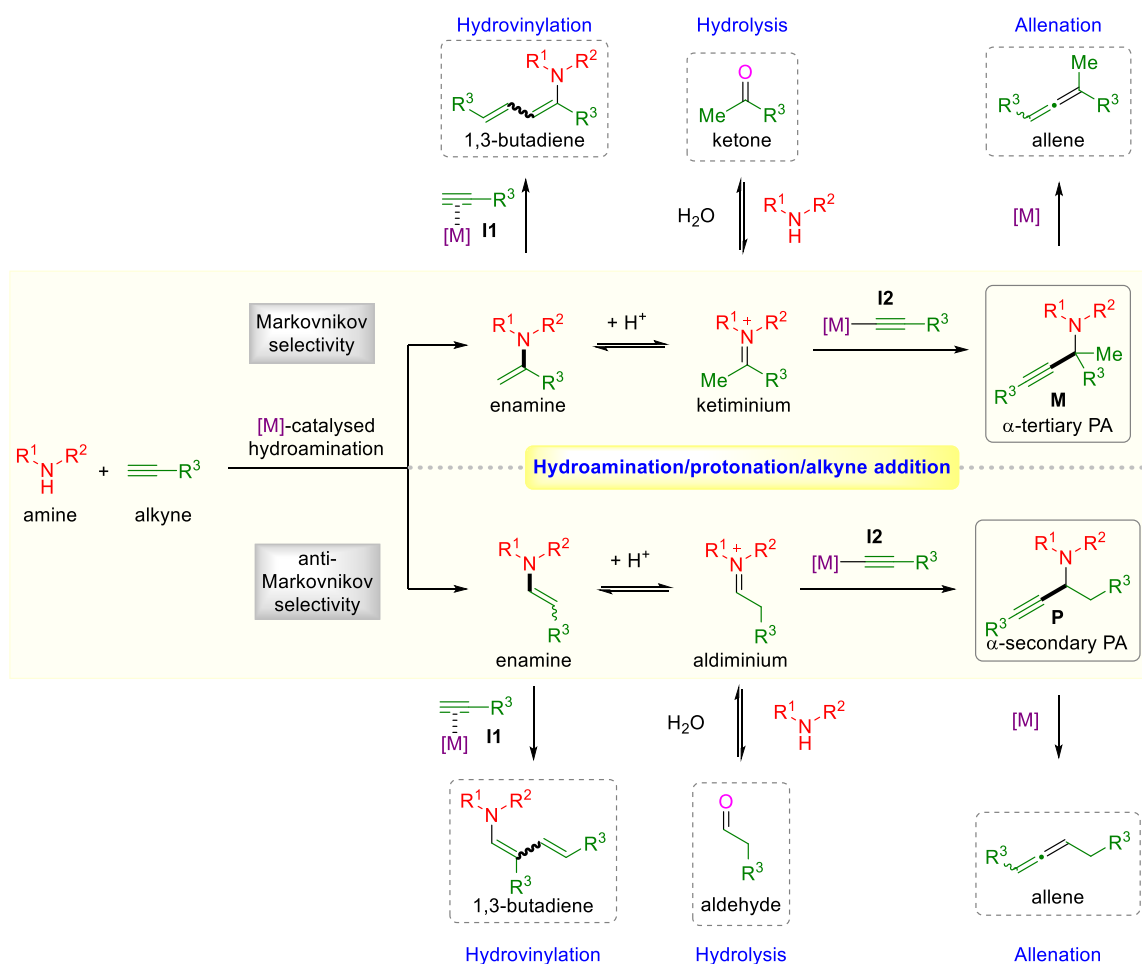


Scheme 92. Metal-catalysed MARKOVNIKOV and anti-MARKOVNIKOV hydroamination of alkenes and alkynes.

As both, the amine and the π system of the carbon-carbon multiple bond(s) are electron-rich, it often requires a catalyst to enable their otherwise kinetically and thermodynamically disfavoured direct coupling. While some protocols for base-mediated alkyne hydroamination have been developed,^[274] this reaction commonly proceeds through metal catalysis. Many metals have been described in catalytic hydroaminations of alkynes, from alkali metals to early and late transition metals, as well as lanthanides.^[275–278] As for other metal-based catalytic organic transformations, the use of abundant and inexpensive metals, also referred to as “base metals”, is highly desirable.^[279] Furthermore, base metal salts and complexes tend to be less moisture- and air-sensitive, and display a reduced oxophilicity compared to alkali metals and lanthanides. Consequently, they are easier to handle and possess improved functional group tolerance.

Besides the 3CRs discussed in chapters II and III based on the coupling of carbonyls, amines, and alkyne nucleophiles, propargylamines are accessible *via* a hydroamination-alkyne addition procedure. In this approach, the alkyne plays an ambivalent role replacing the carbonyl electrophile, while also acting as the nucleophile in the alkyne addition step. It is however important to note that besides the requirement to efficiently control regioselectivity, chemoselectivity must be guaranteed as several products can arise from the initially formed enamine(s) (**Scheme 93**). Their protonation to a ketiminium (MARKOVNIKOV) or aldiminium (anti-MARKOVNIKOV) intermediate, followed by nucleophilic addition of metal acetylide **12** gives the desired

propargylamines **M** and **P**, respectively. In the presence of water, an equilibrium between the iminium intermediates and their corresponding carbonyls establishes, which most likely slows down the overall conversion. In addition, 1,3-butadienes can result from nucleophilic enamine addition onto π -complex **I1**, thus representing a hydrovinylation of the terminal alkyne. Another possible side reaction consists in the previously described formation of allenes from propargylamines (for details, see section I-3.1.), more particularly for cyclic secondary amines.



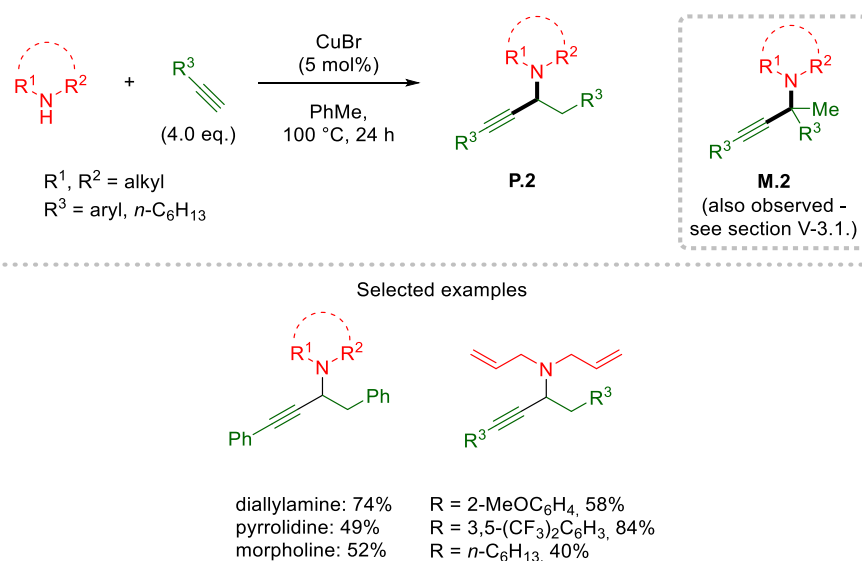
Scheme 93. Possible products resulting from the hydroamination of amines and terminal alkynes.

It requires a highly chemoselective catalytic system to efficiently afford propargylamines. We investigated the use of different metal-exchanged zeolites for the hydroamination-protonation-alkyne addition (HPA) cascade reaction. The following section provides an overview of the currently established protocols towards α -secondary and -tertiary propargylamines through HPA reaction depending on the relative regioselectivity of the hydroamination step.

2. Hydroamination-Protonation-Alkyne Addition (HPA) Reaction – State of the Art

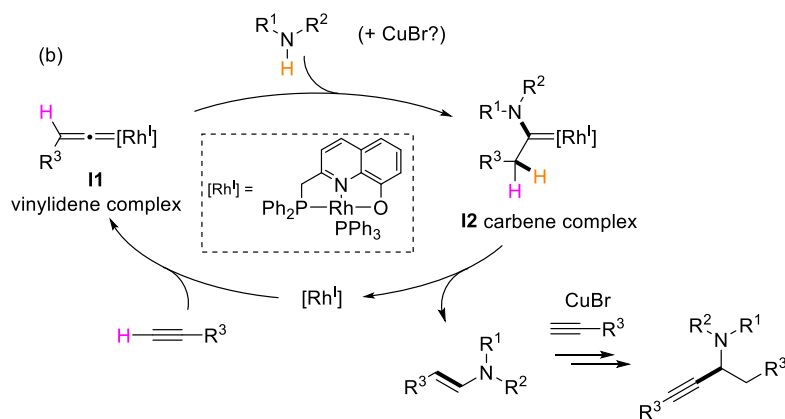
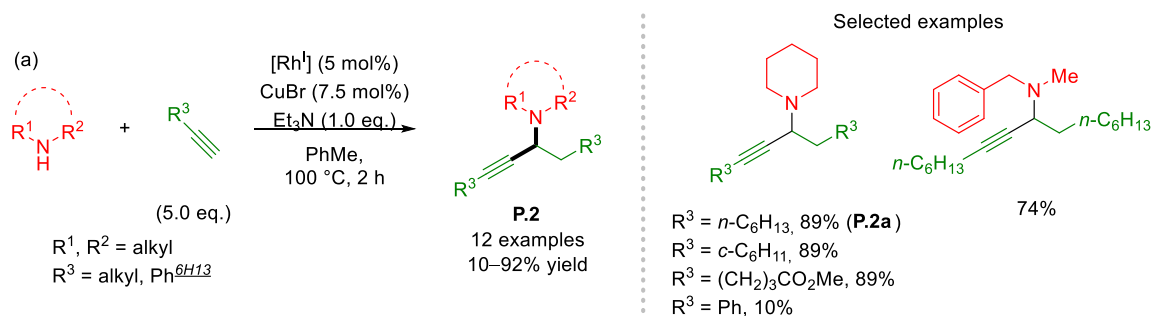
2.1. Anti-MARKOVNIKOV-Selective HPA

Following the first high-pressure HPA reports mentioned in section I-2.5., LI and co-workers established a CuBr-based HPA procedure under ambient pressure in toluene at 100 °C (**Scheme 94**).^[241] Under their conditions, formation of the anti-MARKOVNIKOV propargylamines **P.2** were reported but as we will see later in section V-3.1., the MARKOVNIKOV isomers **M.2** also formed in non-negligible amounts. Other copper(I) and (II) salts, among which CuI, CuCl₂, and CuBr₂, as well as AuI were shown to be active catalysts in this transformation but afforded lower yields. Their procedure relied on four equivalents of alkyne, which increases its *E* factor. The scope included cyclic secondary aliphatic amines and diallylamine. Apart from 1-octyne, arylalkynes were examined which led to superior yields. Interestingly, the reaction proceeded smoothly with electron-rich and -deficient arylalkynes, whereas methoxy substituents caused non-negligible drops in yield.



Scheme 94. CuBr-catalysed anti-MARKOVNIKOV HPA reaction.^[241]

A highly regioselective anti-MARKOVNIKOV HPA reaction was reported by TAKANO and co-workers in 2017 using a Cu^I/Rh^I bimetallic system (**Scheme 95**).^[280] The high anti-MARKOVNIKOV selectivity for the hydroamination was attributed to the regioselective amine addition onto Rh^I-vinylidene complex **II**, leading to α -aminocarbene **I2**. Indeed, in the absence of the Rh-catalyst, 1-octyne and piperidine preferentially produced the MARKOVNIKOV isomer **M.2a**, albeit in a low 16% NMR yield, together with 4% of its anti-MARKOVNIKOV isomer **P.2a**. Moreover, omitting CuBr did not solely impede the formation of propargylamine but also yielded only trace amounts of enamine suggesting a synergistic effect of both metals in the hydroamination.

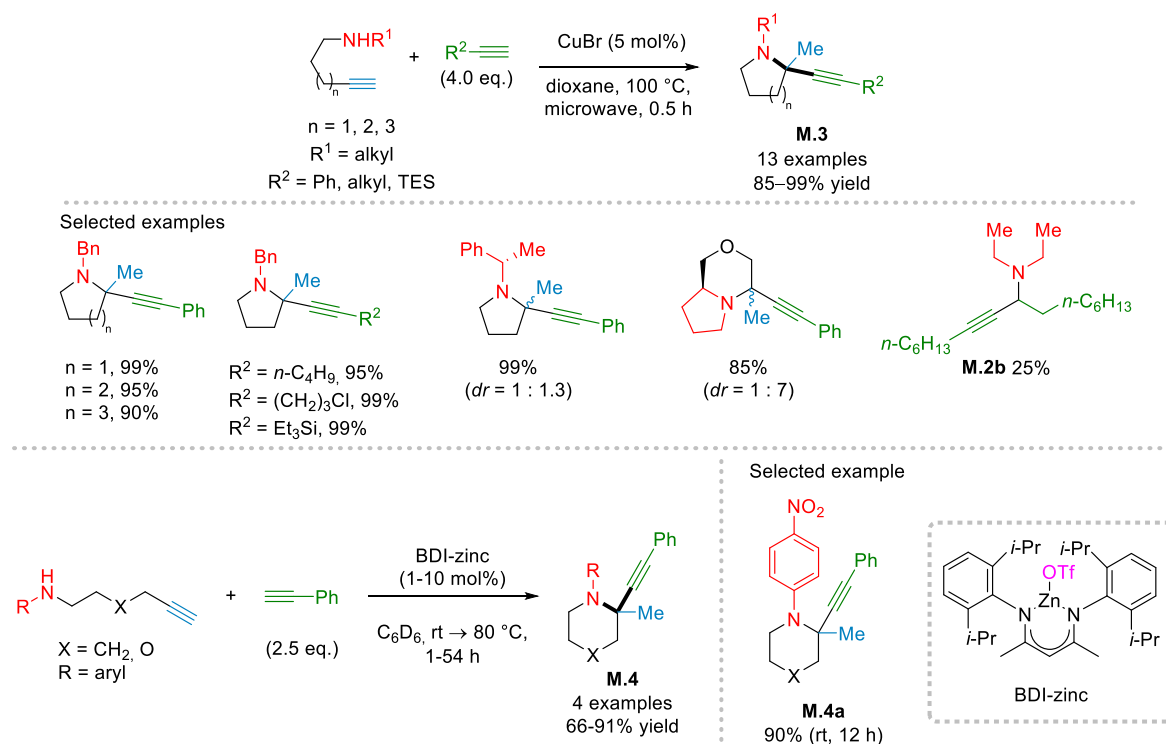


Scheme 95. (PNO) Rh^I /CuBr-catalysed anti-MARKOVNIKOV HPA reaction.^[280]

Assets of this catalytic system are the tolerance of several functional groups (nitrile, ester, acetal), the short reaction time, and the high yields observed with more challenging substrates such as linear secondary amines and sterically encumbered ethynylcyclohexane. Nevertheless, the necessity of an expensive rhodium co-catalyst and the use of five alkyne equivalents drastically reduce its economic interest. Furthermore, arylalkynes as observed for phenylacetylene (**3a**) represent poor substrates, strongly limiting the product scope.

2.2. MARKOVNIKOV-Selective HPA

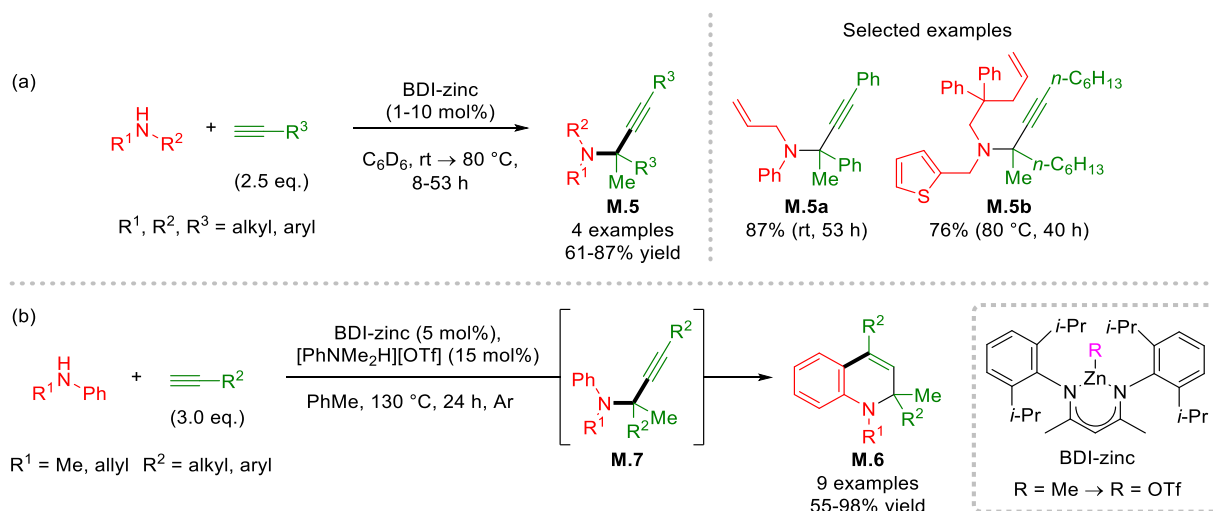
The MARKOVNIKOV-selective HPA reaction represents an attractive alternative to the KA² reaction to access α -tertiary propargylamines. In 2010, HAMMOND and co-workers exploited an intramolecular MARKOVNIKOV HPA reaction toward various five- to seven-membered *N*-heterocycles **M.3** (pyrrolidines, piperidines, azepine, and morpholine)^[281] with complete regioselectivity following BALDWIN's rules^[282] (Scheme 96a). This efficient procedure benefits from greatly reduced reaction times (30 min) when performed under microwave irradiation with high product yields of 85–99%. Unfortunately, three-, four- and eight-membered rings were inaccessible. Short-chained aminoalkynes led to complex reaction mixtures instead of the corresponding aziridine or azetidone, while the attempt to access azocanes afforded the intermolecular anti-MARKOVNIKOV HPA product. The latter was also observed reacting diethylamine with 1-octyne resulting in propargylamine **M.2b** in a low 25% yield. It is noteworthy that this procedure again relied on a non-negligible excess of alkyne.



In the same year, BLECHERT and co-workers disclosed a β -diiminate (BDI)-zinc complex-catalysed intramolecular MARKOVNIKOV-selective HPA reaction to *N*-heterocycles **M.4** (Scheme 96b).^[283] Complementary to HAMMOND's scope, their catalyst converted aniline derivatives, such as **M.4a**. Interestingly, even strongly deactivated amines afforded the desired product in high yields, sometimes even at room temperature. Unfortunately, such zinc complexes are not bench-stable due to their water sensitivity: Therefore, reactions were performed in sealed NMR tubes under an inert atmosphere. It is worth noting that in the absence of an external alkyne, amines underwent chemoselective hydroamination to give the corresponding cyclic enamines.^[284]

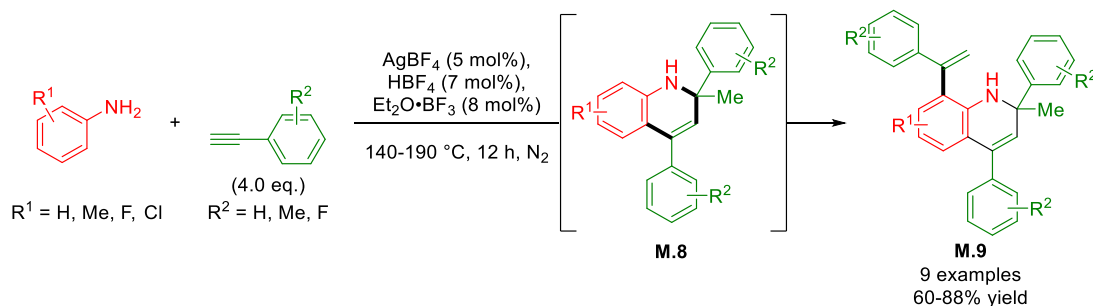
Nevertheless, the BDI-zinc catalyst was also efficient in the intermolecular MARKOVNIKOV HPA reaction, converting aromatic and aliphatic amines (Scheme 97a). Good to high yields were obtained for propargylamines **M.5** and the alkyne equivalents were set to 2.5. Intermolecular alkyne hydroamination was preferred over intramolecular alkene hydroamination for amine substrates bearing alkenes (cf. **M.5a**). Overall, the substrate scope covered exclusively acyclic secondary amines but operated well with both, aryl- and alkylalkynes (cf. **M.5a,b**).

In 2012, BLECHERT and co-workers extended their BDI-zinc-catalysed MARKOVNIKOV HPA reactions towards the synthesis of 1,2-dihydroquinoline derivatives **M.6** (Scheme 97b) employing [PhNHMe₂][OTf] as a co-catalyst at 130 °C.^[285] The aromatic propargylamines **M.7** resulting from the HPA reaction undergo a LEWIS acid-catalysed intramolecular hydroarylation in a 6-*endo*-dig fashion.



Scheme 97. BDI-zinc-catalysed intermolecular MARKOVNIKOV HPA reactions (a) towards α -tertiary propargylamines^[283] and (b) to access α -tertiary 1,2-dihydroquinolines in a cascade approach.^[285]

A similar cascade reaction was established by LI and co-workers for primary anilines and arylalkynes under LEWIS and BRØNSTED acid catalysis (**Scheme 98**).^[286] In contrast to BLECHERT's procedure, the 1,2-dihydroquinoline **M.8** resulting from intramolecular hydroarylation, next undergoes MARKOVNIKOV- and site-selective hydroarylation with a second terminal alkyne equivalent to deliver 1,2-dihydroquinoline **M.9**. Electron-withdrawing and -donating groups can be tolerated on both, the alkyne and aniline, but drastic reaction temperatures of 140-190 °C were required.

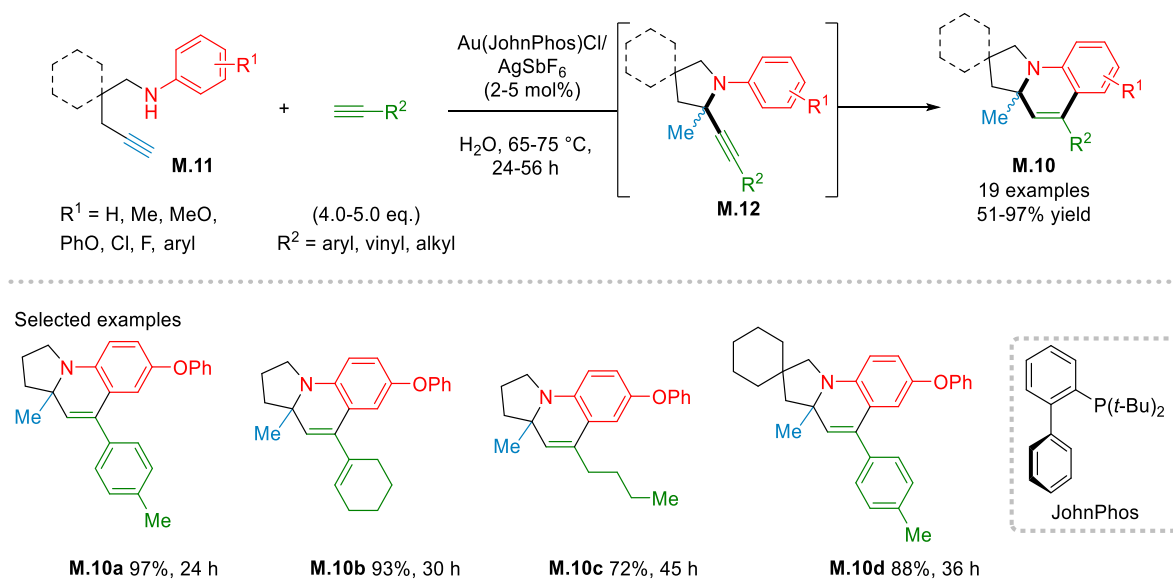


Scheme 98. Synthesis of 1,2-dihydroquinolines from primary anilines.^[286]

CHE and co-workers produced similar results under Au^I-NHC catalysis for the reaction of primary aromatic amines and indolamine with terminal aryl- and alkylalkynes at 150 °C under microwave irradiation.^[287]

In 2008, the same group reported a Au^I-catalysed synthesis of diversely substituted pyrrolo[1,2-*a*]quinolines **M.10** from 1-amino-4-alkynes **M.11** (**Scheme 99**).^[288] Intramolecular HPA reaction leads to aromatic 2-ethynylpyrrolidine **M.12**, which upon intramolecular 6-*endo*-dig hydroarylation delivers the polycyclic **M.10**. In sharp contrast to the previously mentioned related cascade reactions, this transformation proceeded at milder 75 °C in water. Nevertheless, long reaction times and four to five equivalents of terminal alkynes were used. Although aromatic and vinylic alkynes afforded the highest yields (cf. **M.10a,b**), aliphatic alkynes were also

compatible (cf. **M.10c**). Rewardingly, original spirocyclic pyrrolo[1,2-*a*]quinolines, such as **M.10d**, were obtained in high yields.



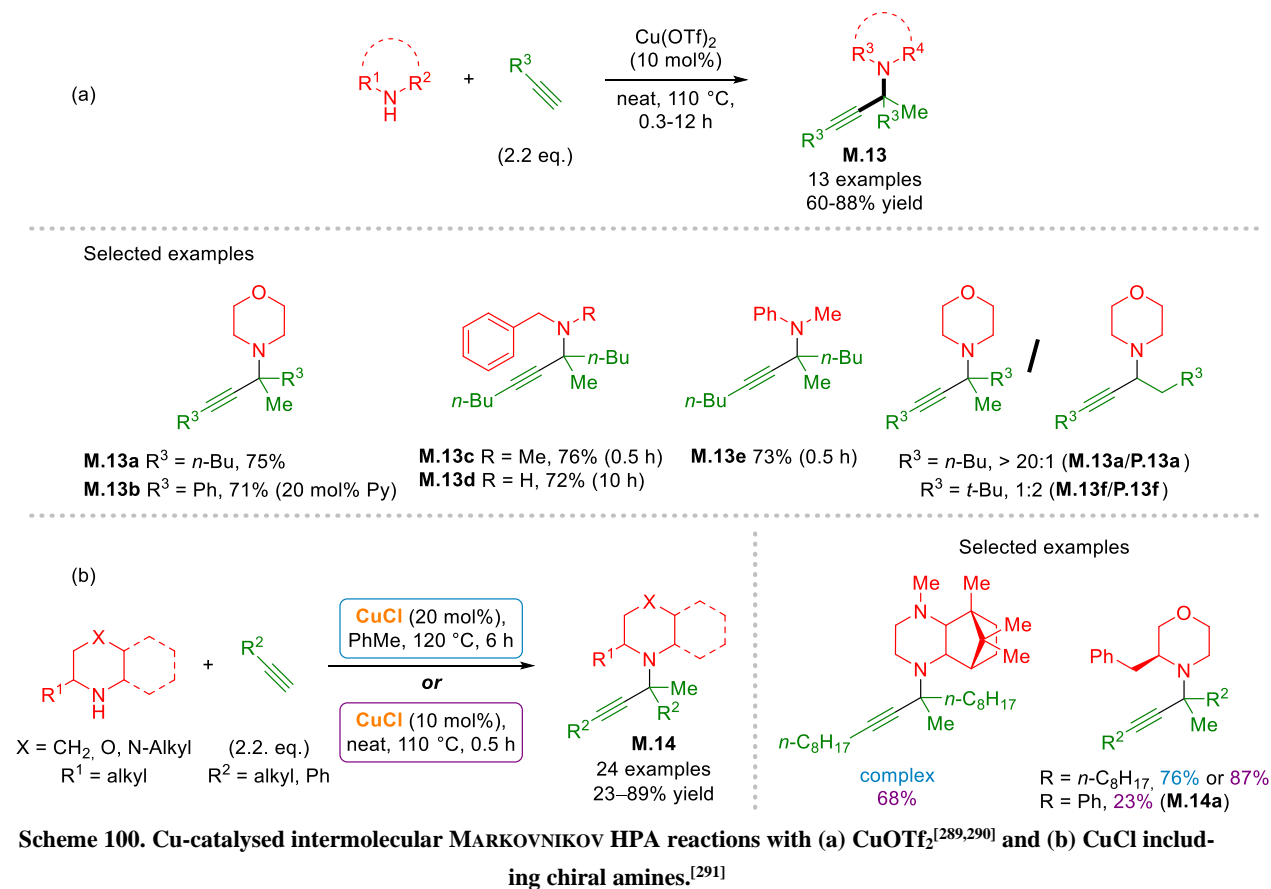
Scheme 99. Au^I-catalysed synthesis of pyrrolo[1,2-*a*]quinolines from 1-amino-4-alkynes.^[288]

In 2013, LARSEN and co-workers then disclosed a Cu(OTf)₂-catalysed intermolecular MARKOVNIKOV-selective HPA reaction under solvent-free conditions (**Scheme 100a**).^[289] Interestingly, propargylamines derived from every amine class, except for primary anilines, were reported. Secondary amines and anilines reacted fastest and afforded the highest yields (cf. **M.13a-c** and **M.13e**). Nevertheless, primary benzylamines produced good yields with prolonged reaction times (cf. **M.13d**). Indeed, this represents the only report on the use of primary amines under (close to) ambient pressure conditions (hexyne b.p. 71 °C). Regarding the alkyne, diverse aliphatic substrates were successful. With phenylacetylene (**3a**), however, pyridine was added in 20 mol% to afford a satisfying product yield of **M.13b** (71%). Its exact role, however, remains unclear and is further discussed in section V-3.3. Fortunately, the alkyne equivalents (2.2 eq.) were set lower than in previous reports.

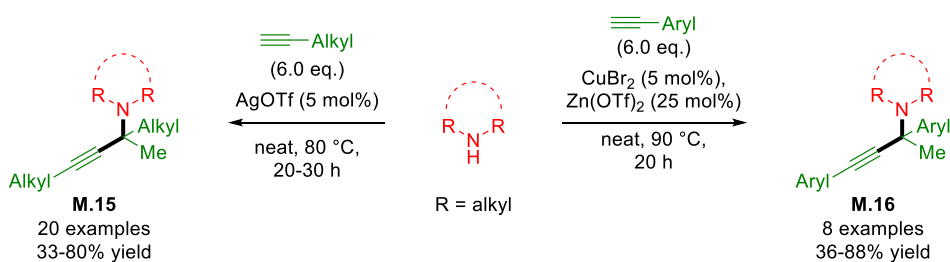
In 2015, LARSEN's group further showed that the regioselectivity significantly varies depending on the bulkiness of the aliphatic alkyne substituent (**Scheme 100a**).^[290] Reacting morpholine with 1-hexyne, greatly favoured the MARKOVNIKOV product **M.13a**, whereas *t*-butyl acetylene preferentially underwent the anti-MARKOVNIKOV HPA reaction to **P.13f**. Furthermore, kinetic studies revealed the reaction to be of first order for the amine, alkyne, and copper.

In 2016, PERIASAMY and co-workers also reported the MARKOVNIKOV-selective intermolecular HPA reaction (**Scheme 100b**).^[291] They established two CuCl-based catalytic systems to access α -tertiary propargylamines **M.14** differing mostly in catalyst loading and the presence or absence of toluene as solvent. The solvent-free conditions gave faster conversions but, in most cases, comparable yields were obtained. In contrast to LARSEN's protocol, only cyclic secondary amines were included. Rewardingly, chiral enantiopure amines led to diastereomerically

pure propargylamines in up to 89% yield. A broad functional group tolerance for the alkyne component was observed. Nevertheless, only alkylalkynes proved efficient, whereas phenylacetylene afforded low yields (cf. **M.14a**).



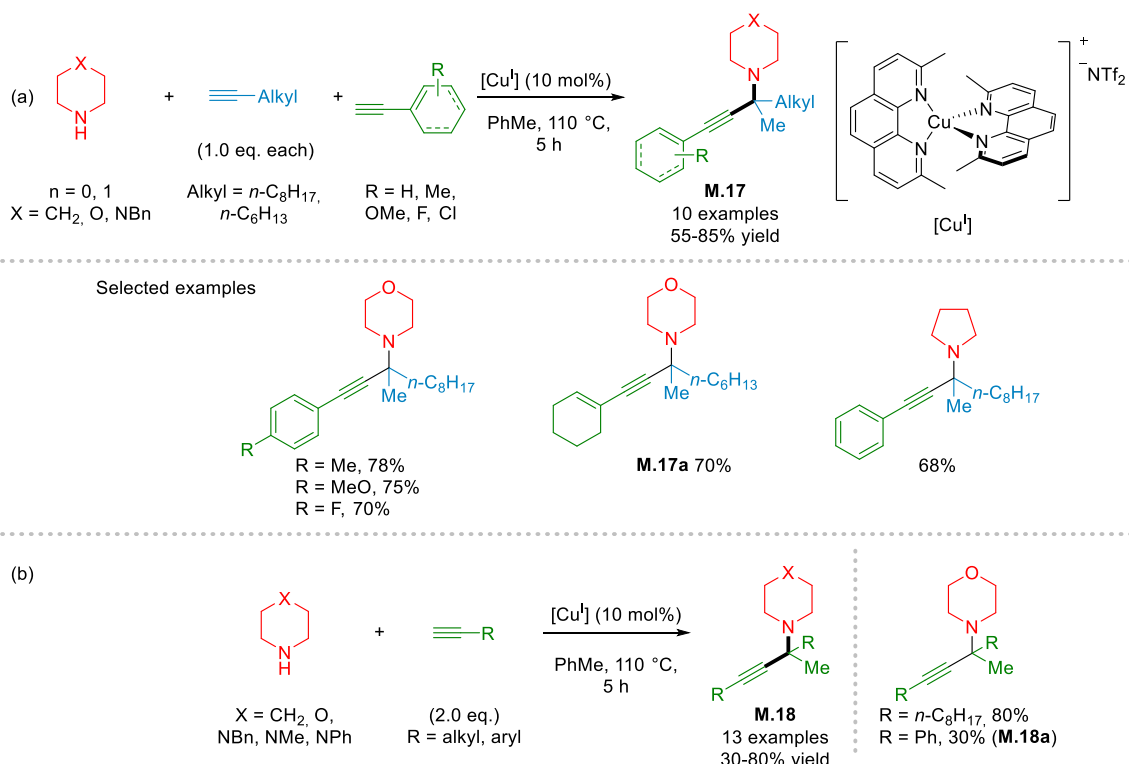
Besides copper and zinc, WEIMIN and co-workers reported the use of AgOTf (5 mol%) for the solvent-free intermolecular MARKOVNIKOV HPA reaction with aliphatic alkynes yielding α -tertiary propargylamines **M.15** (Scheme 101, left).^[292] The reactions were performed at milder 80 °C but a total of six alkyne equivalents were used. The amine scope included cyclic and linear secondary aliphatic amines, whereas primary ones were unreactive. Unfortunately, the examined alkylalkynes did not incorporate additional functional groups, thus the relative group tolerance of this protocol remains unclear. As for LARSEN and PERIASAMY, phenylacetylene led to unsatisfactory yield. Consequently, the authors suggested an alternative bimetallic $\text{CuBr}_2/\text{Zn(OTf)}_2$ catalytic system to form α -tertiary propargylamines **M.16** (Scheme 101, right). It is noteworthy that Zn(OTf)_2 alone did not catalyse the HPA reaction, whereas only CuBr_2 led to low yields. A comparable amine scope was observed, and 4-fluoro- and 4-methoxyphenylacetylene led to moderate yields.



Scheme 101. Intermolecular MARKOVNIKOV HPA reactions with alkylalkynes (left) or arylalkynes (right).^[292]

A seminal contribution to the HPA reaction was recently achieved by KIM and co-workers with an unprecedented 3CR towards α -tertiary propargylamines **M.17** starting from an amine, an aliphatic, and an aromatic alkyne (Scheme 102a).^[293] A cationic Cu^I-bis(1,10-phenanthroline) complex in toluene favoured the MARKOVNIKOV hydroamination of the aliphatic alkyne over the aromatic one. The latter reacted to the corresponding copper acetylide nucleophile to produce α -tertiary propargylamines **M.17**. This suggests that hydroamination of aliphatic alkynes is notably faster with this catalytic system. Furthermore, the use of oct-1-yne and a cyclic vinyl alkyne afforded the corresponding propargylamine **M.17a** with the same chemoselectivity and 70% yield. Another attractive feature of this protocol is the use of equimolar amounts of each component.

The authors also performed the intermolecular MARKOVNIKOV-selective HPA reaction to yield propargylamines **M.18**, mainly from aliphatic alkynes (Scheme 102b). As for previous catalytic systems, phenylacetylene afforded a low yield (cf. **M.18a**). It should be noted that both procedures presented in Scheme 102 featured exclusively cyclic secondary amines.

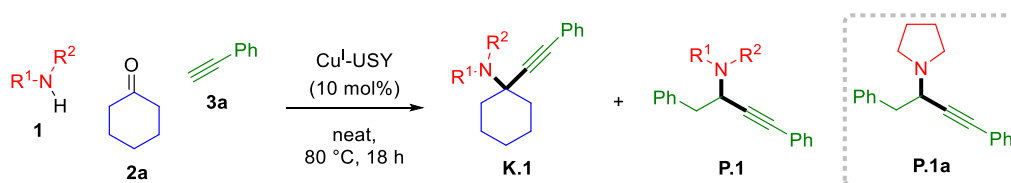


Scheme 102. (a) Novel Cu^I-catalysed MARKOVNIKOV-selective HPA-based 3CR and (b) intermolecular MARKOVNIKOV HPA reaction towards α -tertiary propargylamines.^[293] Tf₂N⁻: trifluoromethanesulfonimide.

3. Optimisation of the Cu^I-USY-Catalysed HPA Reaction

3.1. Preliminary Results

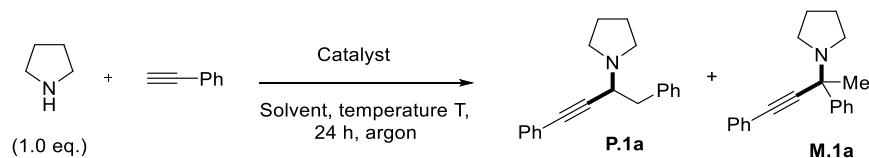
While investigating Cu^I-USY as catalyst in the KA² coupling reaction, we observed the formation of α -secondary propargylamines **P.1** via an HPA reaction depending on the substrate combination (Scheme 103, for more details, see Scheme 68 p. 90). Given our general interest in propargylamines and the academic and industrial importance of hydroamination procedures, we decided to explore this challenging cascade reaction. For this, pyrrolidine (**1a**) and phenylacetylene (**3a**) were selected as model substrates targeting propargylamine **P.1a**, previously reported by LI and co-workers.^[241] To date, no supported catalyst has been used to catalyse the HPA reaction.



Scheme 103. Competing HPA reaction under Cu^I-USY-catalysed KA² conditions.

First, the optimised conditions from LI's group were applied to evaluate the potential of the Cu^I-USY-catalysed HPA reaction and to compare its performance to the originally reported CuBr system (Table 20).

Hence, pyrrolidine (**1a**) and phenylacetylene (**3a**) (4.0 eq.) were stirred at 100 °C in toluene during 24 h at 5 mol% catalyst loading (entries 1 and 2). In both cases, the desired α -secondary propargylamine **P.1a** was obtained in a mixture with its α -tertiary isomer **M.1a**, among other by-products. Regarding their combined yield and the regioisomeric ratio, Cu^I-USY gave a similar result to CuBr. To our delight, reducing the catalyst loading from 5 to 2.5 mol% and running the reaction under solvent-free conditions with 2.5 equivalents of alkyne resulted in a superior 69% yield and an improved regioisomeric ratio of 8:2 (entry 3). At 1 mol% Cu^I-USY loading, however, the yield was nearly cut in half without alteration of the isomer proportion (entry 4 vs. 3). Likewise, the phenylacetylene (**3a**) quantity was observed to have a strong impact on the HPA yield. Indeed, shifting from 2.5 to 2.25 equivalents lessened the yield from 69 to 54% (entry 5 vs. 3). In contrast, a slight increase in temperature to 110 °C led to a comparable yield but notably worsened the selectivity for the anti-MARKOVNIKOV isomer **P.1a** (entry 6 vs. 3).

Table 20. Preliminary results for the Cu^I-USY-catalysed HPA reaction.^[a]

Entry	Cat. (mol%)	Solvent	Alkyne eq.	T (°C)	Yield ^[b] 1 (%)	P.1a/M.1a ^[c]
1	CuBr (5)	PhMe	4.0	100	52 ^[d]	30:70
2	Cu ^I -USY (5)	PhMe	4.0	100	50 ^[e]	25:75
3	Cu ^I -USY (2.5)	neat	2.5	100	69	20:80
4	Cu ^I -USY (1)	neat	2.5	100	39	25:75
5	Cu ^I -USY (2.5)	neat	2.25	100	54	30:70
6	Cu ^I -USY (2.5)	neat	2.5	110	69	35:65

^[a] Reactions run in a Schlenk tube under an argon atmosphere for 24 h. ^[b] Yield estimated from the crude mixtures *via* ¹H NMR using 1,3,5-trimethoxybenzene as internal standard, unless otherwise stated. ^[c] Determined from the crude mixtures *via* ¹H NMR. ^[d] 49% isolated yield reported for **P.1a** by Li and co-workers. ^[e] Isolated yield.

3.1.1. Catalyst Screening

Prior to further optimisation, several catalysts were screened in the solvent-free benchmark HPA reaction under the conditions of entry 3 in **Table 20** (**Figure 13**).

With CuBr, a slightly improved yield of 59% was observed, while the formation of the anti-MARKOVNIKOV isomer **P.1a** was less favoured compared to entry 1 in **Table 20**. In the case of heterogenised metal catalysts based on porous supports, such as zeolites, catalysis can occur inside the porous network. As previously described on page 40 in section II-1.2.3., a chemical reaction in a confined environment is subjected to certain types of selectivities that directly impact the reaction outcome. In the case of the HPA reaction, zeolites of different topologies might afford varying chemo- and regioselectivities depending on their product and transition state selectivities. Complementary to the cage-type Cu^I-USY (7.4 × 7.4 Å pore aperture), two channel-type zeolites of smaller pore dimensions, namely Cu^I-MOR (6.5 × 7.0 Å) and Cu^I-ZSM-5 (5.1 × 5.5 Å), were applied in the benchmark HPA reaction. Only small differences in yield were observed (62-70% with USY > MOR > ZSM-5), while the regioselectivity remains close to 65:35 for all three zeolites (**Figure 13**). This suggests that pore shapes and dimensions did not play a key role in the HPA reaction. Perhaps catalysis does not (exclusively) take place inside the zeolite since the pore dimensions of the two channel-type zeolites Cu^I-MOR and Cu^I-ZSM-5 are significantly lower compared to Cu^I-USY. Furthermore, the molecular dimensions of the HPA products likely exceed the pore dimensions of the purely microporous MOR and ZSM-5 frameworks, in contrast to the micro- and mesoporous USY zeolite. A surface reaction with exchanged and/or adsorbed copper species, including agglomerates, and/or leaching of copper leading to homogeneous catalysis could alternatively be at play.

The progressive decrease in yield from USY (SAR = 2.9) to MOR (SAR = 10.3) to ZSM-5 (SAR = 25.0), however, follows an increased silicon content in the respective zeolite. The increasing number and density of [AlO₄] induces a greater negative charge of the zeolite framework, which induces a stronger electron-donating capacity to the Cu⁺ ions. This is believed to increase the energy level of their HOMO, hence the capacity for π -back-donation of electron density from Cu⁺ to π^* antibonding orbitals of the C \equiv C in phenylacetylene (**3a**).^[294] As a result, π -complex formation, which represents a key step in the HPA reaction, would be facilitated with Al-rich USY, compared to the MOR and ZSM-5.

Nevertheless, the density of the copper sites, but also the quantity used of each zeolite catalyst (adapted to 2.5 mol% Cu) could be the source of such discrepancies. Therefore, a less charged Cu^I-USY-04 zeolite (0.4 eq. of CuCl were used in the SSIE procedure) of identical SAR was prepared. At the usual 2.5 mol% copper loading, the HPA products were obtained in a reduced 51% yield in a near 1:1 ratio. Differences in HPA performance can thus not solely be explained by changes in the SAR of the zeolite support.

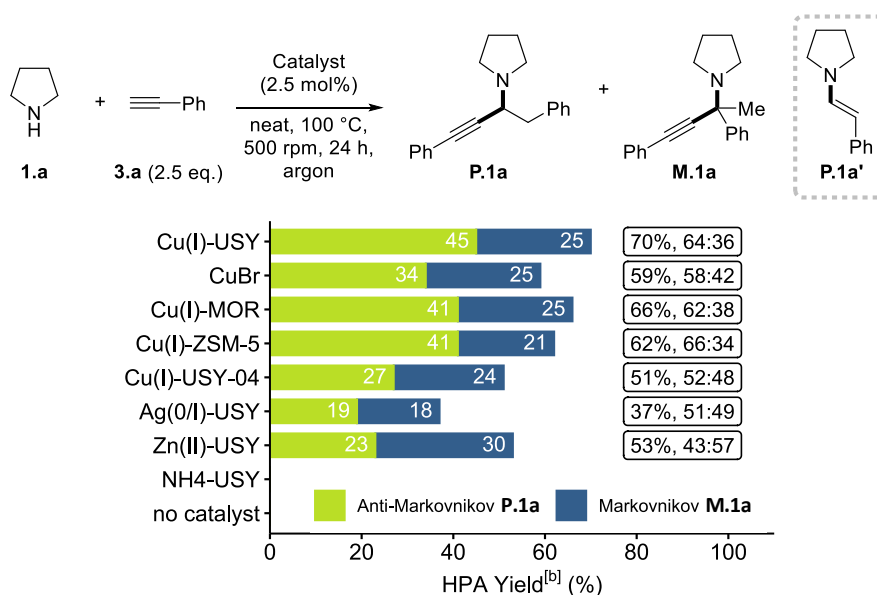


Figure 13. Catalyst screening for HPA reaction.^[a-c]

^[a] Reactions run in a sealed tube under an argon atmosphere. ^[b] Yield estimated from crude mixtures *via* ¹H NMR using 1,3,5-trimethoxybenzene as internal standard. ^[c] The regioisomeric ratios **P.1a**/**M.1a** were determined from the crude mixtures *via* ¹H NMR.

In addition to copper-based catalytic systems, we evaluated Ag^{0/I}- and Zn^{II}-USY as these transition metals have also been reported in HPA reactions with secondary amines (Figure 13). With Ag^{0/I}-USY, a moderate HPA yield of 37% was observed. In fact, (*E*)-enamine **P.1a'** represented the major product in 63% yield resulting from the *anti*-MARKOVNIKOV hydroamination of phenylacetylene (**3a**). Zn^{II}-USY, in turn, slightly favoured the formation of the MARKOVNIKOV HPA isomer **M.1a** (57:43), but again a lower HPA yield was observed compared to Cu^I-

USY (53% vs. 70%). Cu^I-USY thus gave the most promising performance for the targeted HPA reaction, whereas NH₄-USY or no catalyst led to no conversion of the starting materials.

3.1.2. Solvent Screening

Next, the effect of different solvents on the efficiency of the Cu^I-USY-catalysed HPA reaction was screened (Figure 14). Although toluene is the most common solvent for this transformation, a non-negligible drop in yield to 55% and a near 1:1 ratio of both isomers was observed. In polar aprotic MeCN, the conversion was negatively affected, resulting in a low 30% yield. Next, the reaction was evaluated in several “green” solvents. While polar protic *i*-PrOH led to a poor conversion, an interesting 93:7 isomeric ratio was observed.^{iv} Shifting to EtOAc led to a superior 57% yield and restored the regioisomeric ratio observed under neat conditions. Interestingly, 2-MeTHF and ethylal, afforded comparable results to the solvent-free conditions.

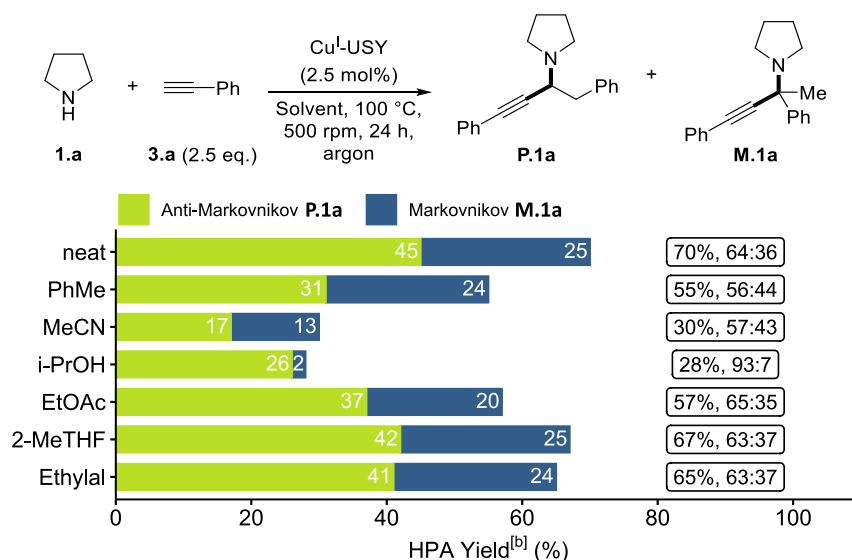


Figure 14. Screening of different solvents in HPA reaction.^[a-c]

^[a] Reactions run in a sealed tube under an argon atmosphere. ^[b] Yield estimated from crude mixtures *via* ¹H NMR using 1,3,5-trimethoxybenzene as internal standard. ^[c] The regioisomeric ratios P.1a/M.1a were determined from the crude mixtures *via* ¹H NMR.

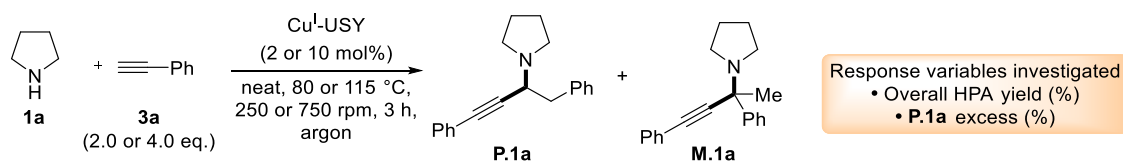
3.2. Optimisation *via* Design of Experiments

3.2.1. First Factorial Screening Design: The Vital Few

Following the preliminary findings, a typical 2⁵⁻² (eight experiments) fractional factorial design (FFD) was performed to scrutinise the effects of temperature (variable A), catalyst loading (B), and alkyne quantity (C) on the HPA yield and the regioisomeric ratio. Given the use of a supported catalyst, the stirring rate (D), as well as the type of stirring bar (E) were also evaluated. Table 21 shows the investigated ranges, i.e., the low and high levels for each variable.

Table 21. Investigated variables in an FFD for the HPA reaction and their respective ranges.

^{iv} The negative impact of *i*-PrOH on the HPA yield was, however, already observed adding it in 20 mol% relative to pyrrolidine (51% vs. 70% neat), whereas the isomeric ratio dropped to 72:27.



Variable	Name	Units	Type	Min.	Max.	Mean
A	Temperature	°C	Numeric	80	115	97.5
B	Catalyst load	mol%	Numeric	2	10	6
C	Alkyne qty	eq.	Numeric	2	4	3
D	Stirring	rpm	Numeric	250	750	500
E	Stirring bar	-	Categorical	Small	Big	-

Table 22 shows the design matrix with the collected data for each run. All experiments were run in parallel and the response variables, i.e., the combined HPA yield (%) for **P.1a** and **M.1a**, and the excess of the anti-MARKOVNIKOV regioisomer **P.1a**, were determined from the crude mixtures *via* ^1H NMR. **P.1a** excess was calculated using **Equation 3**. Hence, a negative percentage corresponds to an excess of the MARKOVNIKOV isomer **M.1a**. It should be noted that the reaction time was kept universal for all runs and that low HPA yields at lower temperatures are also due to incomplete conversions of the starting materials and reaction intermediates.

$$\text{P. 1a excess (\%)} = \frac{\text{Yield(P. 1a)} - \text{Yield(M. 1a)}}{\text{Yield(P. 1a)} + \text{Yield(M. 1a)}} \times 100 \quad (\text{Equation 3})$$

Table 22. FFD design matrix.

Std	Run	A (°C)	B (mol%)	C (eq.)	D (rpm)	E	HPA Yield (%)	P.1a excess (%)
5	1	80	2	4	750	S	24	57
2	2	115	2	2	250	S	42	-6
3	3	80	10	2	250	B	55	61
4	4	115	10	2	750	S	15	-21
1	5	80	2	2	750	B	27	55
7	6	80	10	4	250	S	49	57
6	7	115	2	4	250	B	78	3
8	8	115	10	4	750	B	60	-10

S: small. B: big.

Response 1: HPA yield

Regarding the overall yield in HPA isomers, the half-normal probability plot and PARETO chart were analysed for preliminary model selection (**Figure 15**). It should, however, be noted that the following conclusions are drawn on a limited number of runs. Considering this data set, the variables stirring rate (D), stirring bar (E), alkyne equivalents (C), and temperature (A) influence the overall HPA yield, while the catalyst loading, within the range of 2 to 10 mol%, does

not have a significant effect. More precisely, stirring rate (D) has the largest, but negative, effect on the yield. Consequently, a lower stirring rate is beneficial in the Cu^I-USY-catalysed HPA reaction. In contrast, stirring bar (E), alkyne equivalents (C), and temperature (A) correlate positively with HPA yield. While temperature (A) does not exceed the BONFERRONI limit, its inclusion in the model resulted in an overall better model fit.

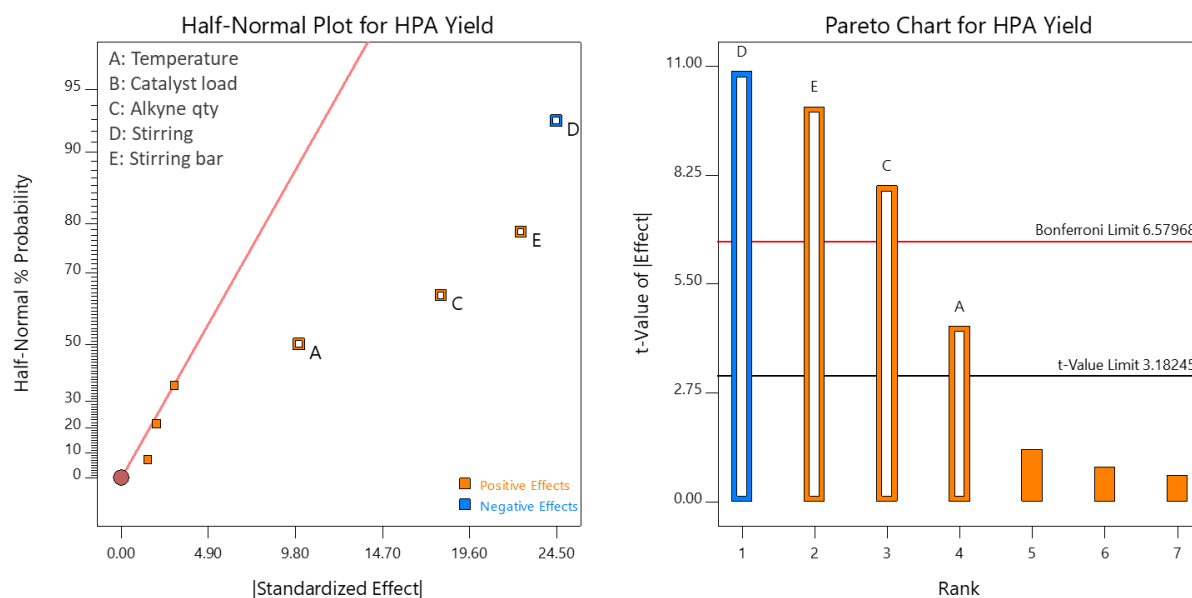


Figure 15. Half-normal plot and PARETO chart for HPA yield.

Model selection resulted in Equation 4 (coded variables) and Equation 5 (actual variables, with E = big).

$$\text{HPA yield (\%)} = 43.75 + 5.0 \times A + 9.0 \times C - 12.25 \times D + 11.25 \times E \quad (\text{Equation 4})$$

$$\text{HPA yield (\%)} = 24.64 + 0.29 \times A + 9.0 \times C - 0.05 \times D \quad (\text{Equation 5})$$

Graphically this translates into a plane (Figure 16) as no variable interaction terms, nor curvature can be deduced from this reduced FFD design.

A summary of the analysis of variance (ANOVA) for the selected quadratic model is given in Table 23. The ANOVA statistics on the preliminary model confirm the statistical significance of the overall model and its terms (variables A, C, D, and E) as their p-values < 0.05. Model terms with p-values > 0.1 indicate that they are not significant. The model F-value of 75.27 implies the significance of the model. There is only an 0.24% chance (p-value = 0.0024) that an F-value this large could occur due to noise.

The fit statistics (Table 24) show a high adjusted R²-value of 0.9770 and a predicted R² of 0.9298, which means both R²-values are in reasonable agreement. Furthermore, the adequate precision (a measure of signal-to-noise ratio) of 25.7860 indicates an adequate signal for the navigation of the selected design space.

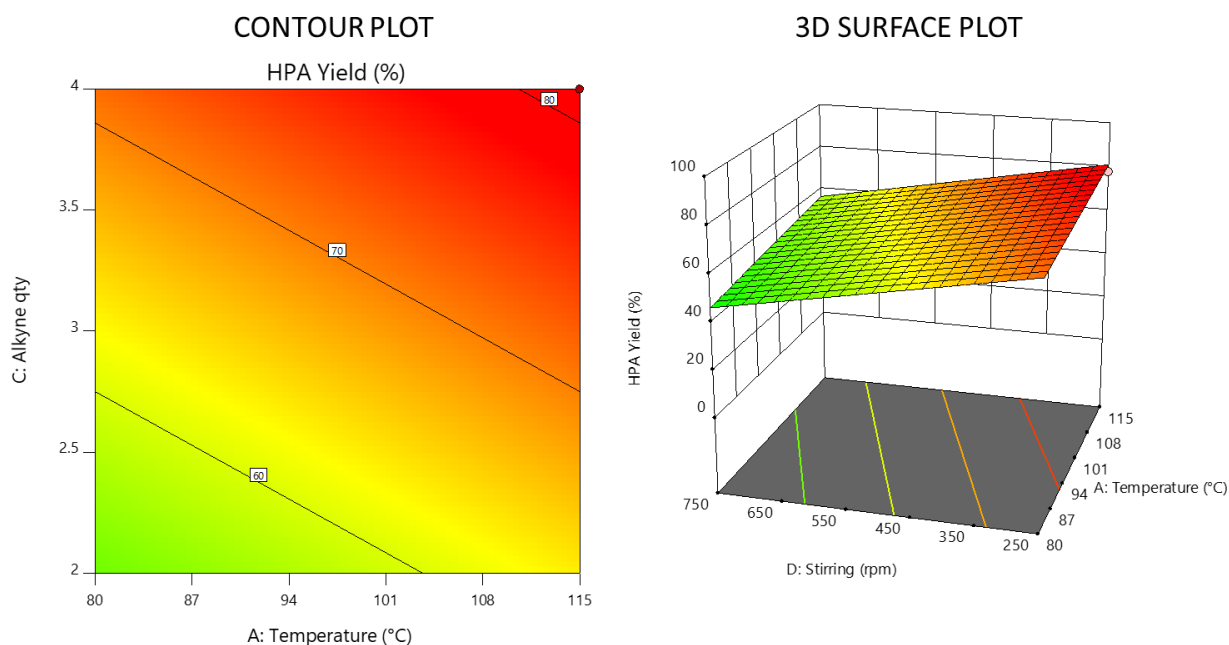


Figure 16. Contour Plot and 3D surface of the factorial model for HPA yield.
 Variable Settings: B: Catalyst load = 2 mol%. C: Alkyne qty = 4 eq. E: Stirring bar = Big.

Table 23. ANOVA for the selected factorial model for HPA yield.

Source	Sum of Squares	df	Mean Square	F-value	p-value	
Model	3061.00	4	765.25	75.27	0.0024	significant
A-Temperature	200.00	1	200.00	19.67	0.0213	
C-Alkyne qty	648.00	1	648.00	63.74	0.0041	
D-Stirring	1200.50	1	1200.50	118.08	0.0017	
E-Stirring Bar	1012.50	1	1012.50	99.59	0.0021	
Residual	30.50	3	10.17			
Cor Total	3091.50	7				

Table 24. Fit statistics for the selected factorial model for HPA yield.

Std. Dev.	Mean	C.V. %	R ²	Adjusted R ²	Predicted R ²	Adequate Precision
3.19	43.75	7.29	0.9901	0.9770	0.9298	25.7860

Response 2: Excess of the anti-MARKOVNIKOV Product P.1a

Following the same procedure as for the HPA yield, preliminary model selection was done based on the half-normal probability plot and the PARETO chart. Accordingly, only temperature (A) was found to significantly affect the ratio of both HPA products, greatly exceeding both statistical limits. The very strong negative correlation indicates that, at least within the range of 80 to 115 °C, the abundance of MARKOVNIKOV regioisomer **M.1a** increases with higher temperatures.

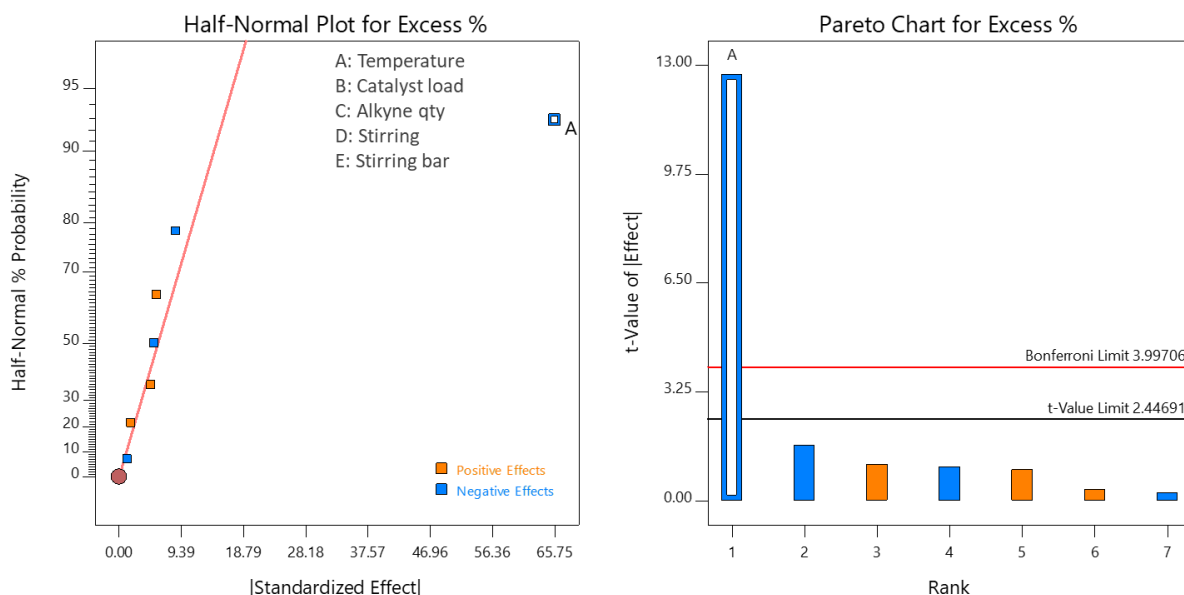


Figure 17. Half-normal plot and PARETO chart for P.1a excess.

Model selection resulted in Equation 6 (coded variables) and Equation 7 (actual variables) and Figure 18 shows the corresponding model graphs.

$$\text{P. 1a excess (\%)} = 24.50 - 32.87 \times A \quad (\text{Equation 6})$$

$$\text{P. 1a excess (\%)} = 207.66 - 1.88 \times A \quad (\text{Equation 7})$$

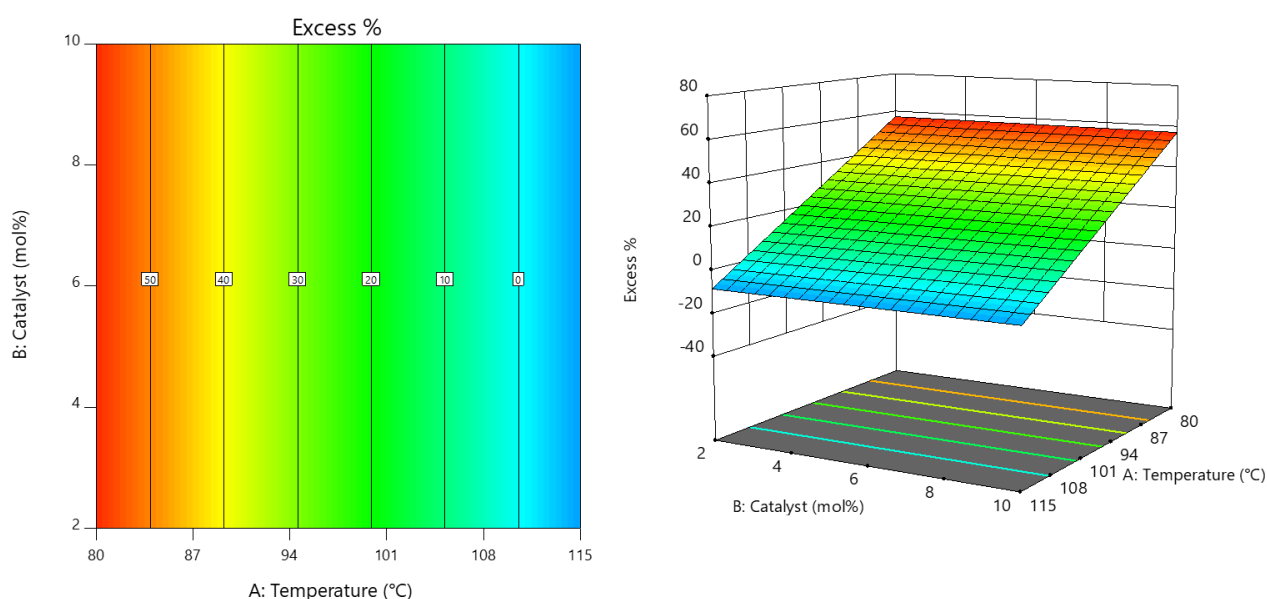


Figure 18. Contour Plot and 3D surface of the factorial model for P.1a excess.

Rewardingly, the ANOVA statistics (Table 25) stated a highly significant model with only a 0.01% chance that an F-value this large could result from noise. The fit statistics (Table 26) show a high adjusted R^2 -value of 0.9583 and a predicted R^2 of 0.9365, which means both R^2 -values are in reasonable agreement. Furthermore, the adequate precision of 17.9939 indicates a reliable signal-to-noise ratio.

Table 25. ANOVA for the selected factorial model for P.1a excess.

Source	Sum of Squares	df	Mean Square	F-value	p-value	
Model	8646.11	1	8646.11	161.89	< 0.0001	significant
A-Temperature	8646.11	1	8646.11	161.89	< 0.0001	
Residual	320.44	6	53.41			
Cor Total	8966.56	7				

Table 26. Fit statistics for the selected factorial model for P.1a excess.

Std. Dev.	Mean	C.V. %	R ²	Adjusted R ²	Predicted R ²	Adequate Precision
7.31	24.50	29.83	0.9643	0.9583	0.9365	17.9939

To conclude, the above 2⁵⁻² FF screening design showed that the variables A (temperature), B (stirring bar), C (alkyne quantity) and D (stirring) significantly affect the HPA yield. In contrast, the regioisomeric ratio of both HPA products seems to be mostly temperature-controlled. As a result, the best-performing stirring bar type was retained, while the catalyst loading was set to a low value of 2.5 mol%. For the following optimisation, a central composite design (CCD) was envisaged for which the investigated ranges of variables A and D were adjusted. The reaction temperature was set from 80 to 140 °C to evaluate the effect of higher temperatures on the chemoselectivity but also to scrutinise if the MARKOVNIKOV isomer can be formed preferentially. As low stirring rates afforded higher HPA yields, the range of the stirring rate was set from 50 to 250 rpm.

3.2.2. Further Optimisation Using a Central Composite Design

Based on the previous FFD screening results, further optimisation of the reaction conditions was conducted with a central composite design (CCD), based on response surface methodology (RSM). **Table 27** shows the evaluated variables, namely temperature (A), alkyne quantity (C), and stirring (D). Their respective coded low (-1) and high (+1) levels, as well as their minimum (- α) and maximum (+ α) values, are given. It should be noted that a stirring rate of 18 rpm (corresponding to - α setting for variable D in **Table 27**) is technically impossible with our equipment. Nevertheless, CCD designs are relatively robust to missing data points. Therefore, the effect of one missing entry on the overall “goodness” of the design and the final model was judged neglectable. **Table 28** shows the design matrix with the collected data for each run.

Table 27. Investigated variables in a CCD for the HPA reaction and their respective ranges.

Var.	Name	Unit	Min. (- α)	Max. (+ α)	Low (-1)	High (+1)	Mean	Std. Dev.
A	Temp.	°C	71	149	80	140	110	23.30
C	Alkyne qty	eq.	1.68	4.32	2.00	4.00	3.00	0.777
D	Stirring	rpm	18	280	50	250	150	77.68

All investigated variables are of numeric type.

Table 28. CCD design matrix.

Std	Block	Run	A (°C)	C (eq.)	D (rpm)	HPA Yield (%)	P.1a Excess (%)
1	Factorial	1	80	2	50	12	75
2	Factorial	2	140	2	50	29	-13
9	Factorial	3	110	3	150	80	12
5	Factorial	4	80	2	250	17	61
7	Factorial	5	80	4	250	13	62
8	Factorial	6	140	4	250	49	-19
10	Factorial	7	110	3	150	72	17
11	Factorial	8	110	3	150	69	14
6	Factorial	9	140	2	250	25	-4
3	Factorial	10	80	4	50	8	68
4	Factorial	11	140	4	50	53	-9
12	Factorial	12	110	3	150	74	22
19	RSM	13	110	3	150	82	20
15	RSM	14	110	1.68	150	31	9
18	RSM	15	110	3	282	76	26
20	RSM	16	110	3	150	74	19
17	RSM	17	110	3	18	- ^a	- ^a
13	RSM	18	71	3	150	13	69
16	RSM	19	110	4.32	150	71	15
14	RSM	20	149	3	150	33	6

^a No data available.

Response 1: HPA Yield

By applying multiple regression analysis on the experimental data (**Table 28**), the response variable “HPA Yield” and the test variables were related by the quadratic **Equation 8** (coded variables) and **Equation 9** (actual variables).

$$\text{HPA yield (\%)} = 75.66 + 11.61 \times A + 8.03 \times C + 7.0 \times AC - 31.84 \times A^2 - 15.64 \times C^2 \quad (\text{Equation 8})$$

$$\text{HPA yield (\%)} = -482.87 + 7.47 \times A + 76.19 \times C + 0.23 \times AC - 0.04 \times A^2 - 15.64 \times C^2 \quad (\text{Equation 9})$$

Accordingly, the HPA yield is described by the terms A (temperature), C (alkyne quantity), AC, A², and C², whereas the stirring rate (D) did not significantly affect the HPA yield (F-value < 0.001, p-value = 0.99) within the evaluated range. The significance of AC reveals an interaction between variables A and C. In other words, by varying one variable, the effect on the HPA yield depends on the setting of the other. Furthermore, the significant quadratic terms

A^2 and C^2 indicate the existence of curvature. Indeed, **Figure 19** shows the contour plot and the 3D surface plot, representing a bell-shaped surface.

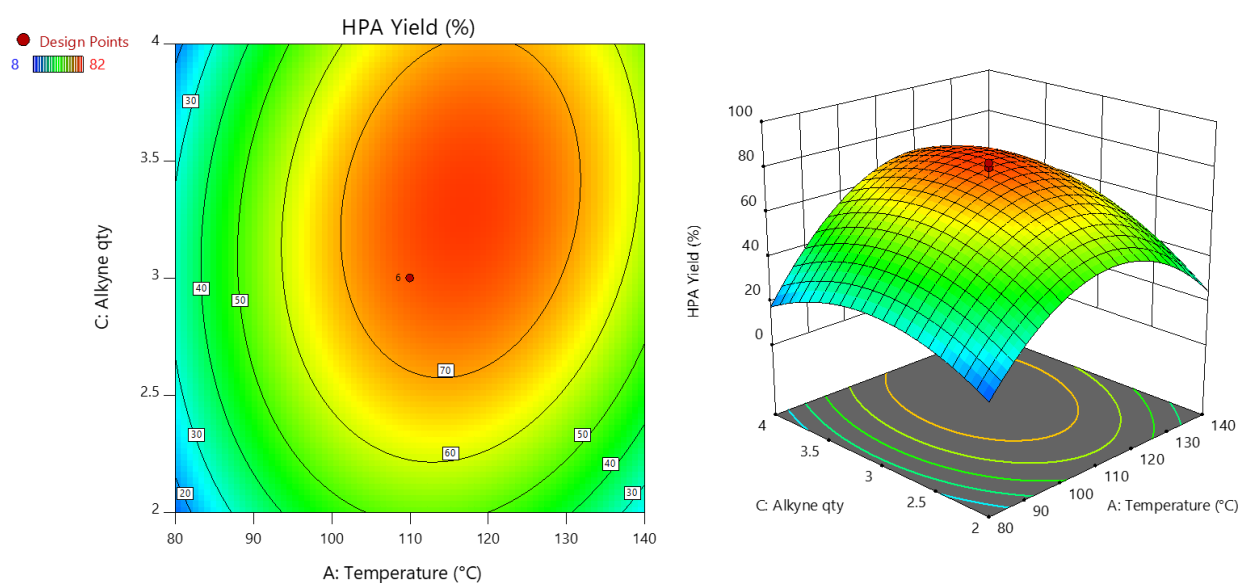


Figure 19. Contour Plot and 3D surface of the quadratic model for HPA yield.

A summary of the analysis of variance (ANOVA) for the selected quadratic model is given in **Table 29**. The ANOVA statistics confirm the statistical significance of the quadratic model (p-values < 0.05). Furthermore, the lack of fit F-value of 1.86 and the associated p-value of 0.2877 implies an insignificant lack of fit of the model relative to the pure error. In other words, the model explains well the experimental data.

The fit statistics (**Table 30**) show an acceptable adjusted R^2 -value of 0.9645 and a predicted R^2 of 0.8607, which means both R^2 -values are in reasonable agreement as the difference is less than 0.2. Furthermore, the adequate precision of 18.8231 indicates a reliable signal-to-noise ratio.

Table 29. ANOVA for the reduced quadratic model for HPA yield.

Source	Sum of Squares	df	Mean Square	F-value	p-value	
Block	710.05	1	710.05			
Model	12374.91	5	2474.98	65.12	< 0.0001	significant
A-Temperature	1545.01	1	1545.01	40.65	< 0.0001	
C-Alkyne qty	738.71	1	738.71	19.44	0.0009	
AC	392.00	1	392.00	10.31	0.0075	
A^2	6918.10	1	6918.10	182.03	< 0.0001	
C^2	1668.32	1	1668.32	43.90	< 0.0001	
Residual	456.07	12	38.01			
Lack of Fit	359.33	8	44.92	1.86	0.2877	not significant
Pure Error	96.74	4	24.19			
Cor Total	13541.03	18				

Row 17 of **Table 28** was ignored for this analysis because no data was available.

Table 30. Fit statistics for the selected reduced quadratic model for HPA yield.

Std. Dev.	Mean	C.V. %	R ²	Adjusted R ²	Predicted R ²	Adequate Precision
6.16	46.42	13.28	0.9645	0.9496	0.8607	18.8231

Response 2: Excess of the anti-MARKOVNIKOV Product P.1a

Regarding the **P.1a** excess, the results are less clear-cut. Forward and backward model selection resulted in the inclusion of the terms A and A². Accordingly, only temperature would have a significant influence on the ratio of both HPA isomers. The ANOVA (**Table 31**) states an overall significant model described by **Equations 10** and **11**. Nevertheless, the lack of fit (p-value = 0.047) is also significant, even if close to the threshold of p-value > 0.05. Yet the fit statistics (**Table 32**) show a high adjusted R²-value of 0.9459, which is in reasonable agreement with the predicted R² of 0.8650. Furthermore, the adequate precision of 22.0989 indicates a reliable signal-to-noise ratio. Still, this model should be interpreted with caution.

Furthermore, one must bear in mind that the **P.1a** excess percentage is not a direct measure of the hydroamination regioselectivity but is calculated from the ratio of the HPA isomers. This ratio is, however, greatly dependent on the chemoselectivity of the reaction for each condition, as the hydroamination products, i.e., the enamines, can undergo several reaction pathways leading to various by-products or remain unreacted in the reaction mixture (for details, see **Scheme 93**). Furthermore, differences in product stability of the HPA products would also affect their relative ratio. Therefore, the same analysis was applied to the combined yields of anti-MARKOVNIKOV- and MARKOVNIKOV-derived products, respectively. The so-obtained model resulted in a very similar graphical representation. Consequently, the same general conclusion can be drawn, i.e., anti-MARKOVNIKOV hydroamination is kinetically favoured and predominant at lower temperatures. Roughly, the anti-MARKOVNIKOV amine **P.1a** dominates over its isomer at temperatures below 125 °C.

Table 31. ANOVA for the reduced quadratic model for P.1a excess.

Source	Sum of Squares	df	Mean Square	F-value	p-value	
Block	0.4657	1	0.4657			
Model	14407.78	2	7203.89	105.42	< 0.0001	significant
A-Temperature	13498.83	1	13498.83	197.54	< 0.0001	
A ²	908.95	1	908.95	13.30	0.0024	
Residual	1025.04	15	68.34			
Lack of Fit	967.78	11	87.98	6.15	0.0471	significant
Pure Error	57.26	4	14.31			
Cor Total	15433.28	18				

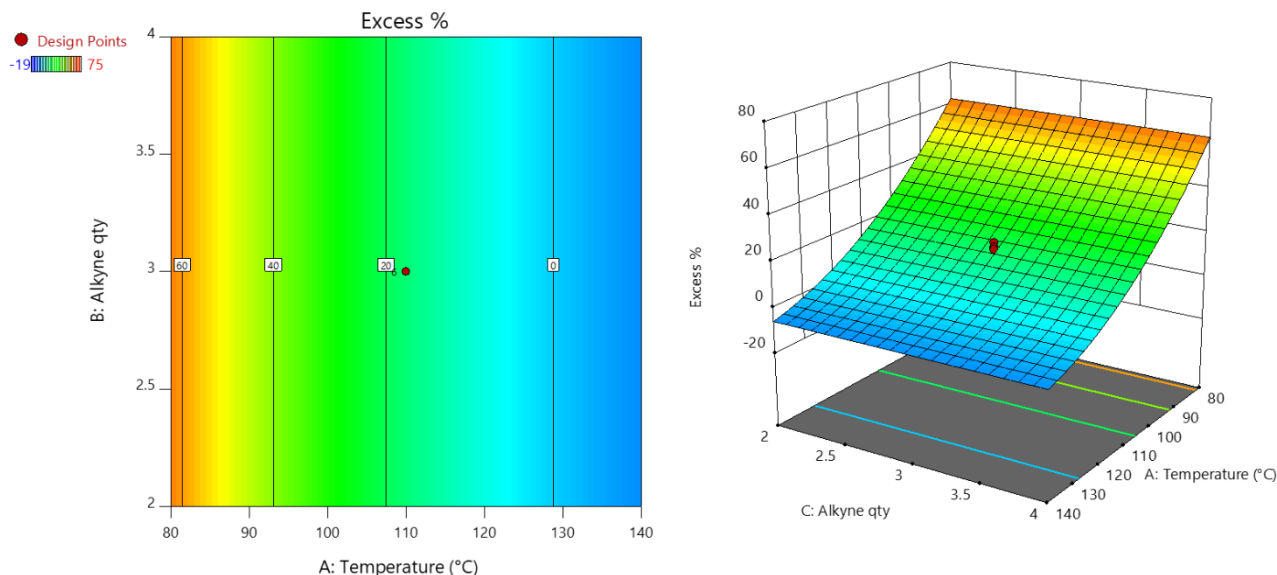
Row 17 of **Table 28** was ignored for this analysis because no data was available.

Table 32. Fit statistics for the reduced quadratic model for P.1a excess.

Std. Dev.	Mean	C.V. %	R ²	Adjusted R ²	Predicted R ²	Adequate Precision
8.27	23.71	34.86	0.9336	0.9247	0.8326	23.8128

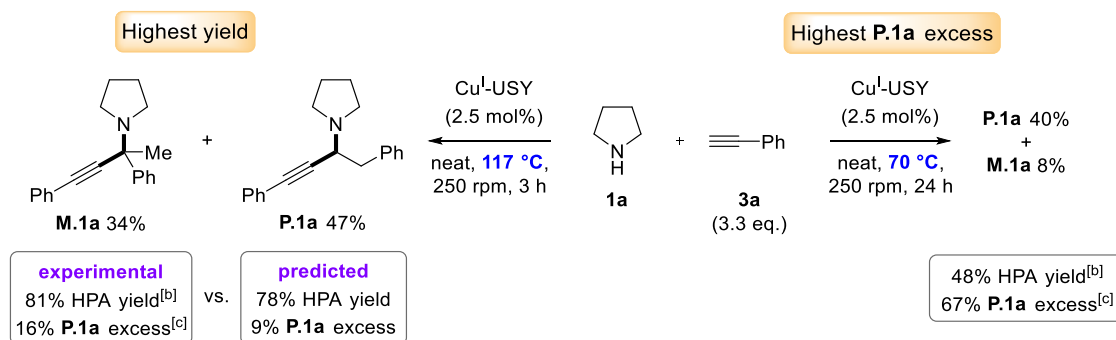
$$\mathbf{P.1a} \text{ excess (\%)} = 17.03 - 34.31 \times A + 11.43 \times A^2 \quad (\text{Equation 10})$$

$$\mathbf{P.1a} \text{ excess (\%)} = 296.58 - 3.94 \times A + 0.01 \times A^2 \quad (\text{Equation 11})$$

**Figure 20. Contour plot and 3D surface of the reduced quadratic model for P.1a excess.**

3.3. Additive and Ligand Screenings

After optimising the conditions through DoE, two experiments were conducted to test the validity of our models. First, conditions targeting maximal HPA yield were employed (**Scheme 104**, left). The models predicted 78% HPA yield and 9% **P.1a** excess are in reasonable agreement with the experimental results (i.e., 81% HPA yield, 16% **P.1a** excess or **P.1a/M.1a** 58:42). Then, we aimed for high **P.1a** excess (**Scheme 104**, right). In this case, the reaction was performed at 70 °C, although this temperature is not covered by the model. Yet, a **P.1a** excess of ca. 60% would be expected at 80 °C, whereas a slightly higher excess was expected and observed at 70 °C (67% **P.1a** excess). These findings are in agreement with the conclusions drawn from the models for the Cu^I-USY-catalysed HPA reaction between pyrrolidine (**1a**) and phenylacetylene (**3a**). Given the opposite effect of temperature on the HPA yield and the regioisomeric ratio, a satisfying yield of either of the regioisomers **P.1a** or **M.1a** (> 60%) combined with a good selectivity ($\geq 75:25$, i.e., 50% excess) cannot be achieved, without further adjustment of the catalytic system. Therefore, the potential of additives and ligands to enhance the performance of the Cu^I-USY-catalysed HPA reaction was scrutinised.



Scheme 104. Model confirmation runs.^[a]

^[a] Reactions run solvent-free with pyrrolidine (**1a**, 1.0 mmol, 1.0 eq.), phenylacetylene (**3a**, 3.3 eq.), Cu^I-USY (2.5 mol%) under argon. ^[b] Yields were estimated *via* ¹H NMR using 1,3,5-trimethoxybenzene as internal standard. ^[c] Isomeric ratios of **P.1a** and **M.1a** were determined from crude mixtures *via* ¹H NMR to calculate the **P.1a** excess.

Indeed, LARSEN and co-workers observed that the use of 20 mol% of pyridine led to an improved yield in their Cu(OTf)₂-catalysed HPA reaction between morpholine and phenylacetylene (**3a**).^[289,290] Likewise, TAKANO and co-workers obtained superior yields in their Rh^I/Cu^I-based HPA reactions of aliphatic alkynes and secondary amines adding triethylamine (1.0 eq.).^[280] Pyridine and triethylamine could act as copper ligands and/or as BRØNSTED bases participating in proton shuttles. The exact role of these additives was however not further investigated. Interestingly, DATKA and co-workers, observed through IR spectroscopy that co-adsorption of pyridine and acetylene in Cu^I-exchanged zeolites induced a small shift of the C≡C band to a lower frequency ($\Delta\nu = 2 \text{ cm}^{-1}$) than without pyridine.^[294] This suggests that pyridine binds to Cu⁺ ions and enhances their electron-donor properties in the π -back-bonding to the acetylene π^* orbitals. As a result, the π -complex formation should be facilitated, enhancing the HPA reaction. A comparable effect is also conceivable for other copper-based catalysts. Based on these previous reports, several additives were examined in the Cu^I-USY-catalysed HPA reaction of pyrrolidine (**1a**) and phenylacetylene (**3a**) (Figure 21). Their influence on the chemoselectivity for the HPA reaction and the regioisomeric ratio **P.1a**/**M.1a** was scrutinised. Aliphatic tertiary amines, namely triethylamine (TEA) and *N,N*-diisopropylethylamine (DIPEA) both gave superior yields and regioselectivities for **P.1a** compared to the additive-free conditions (67% excess vs. 69% for TEA or 77% for DIPEA). DIPEA is slightly less basic and sterically more hindered than TEA, which rather excludes its capacity to coordinate copper cations but might also affect its ability to intervene in deprotonation and proton shuttle scenarios in confined spaces. Shifting to aromatic amines, *N,N*-dimethylpyridin-4-amine (DMAP) caused a significant drop in conversion perhaps due to catalyst poisoning. Pyridine, on the other hand, allowed for a sharp increase in yield to 77% and overall improved chemo- and regioselectivity. Considering such strongly contrasting results with DMAP and pyridine, as well as their significantly lower basicity compared to aliphatic tertiary amines, copper coordination is likely to influence the reaction outcome with such aromatic amines. Lowering the pyridine charge to

20 mol% still had the same, but attenuated, effect on the yield and regioselectivity but slightly worsened the chemoselectivity compared to using one equivalent.

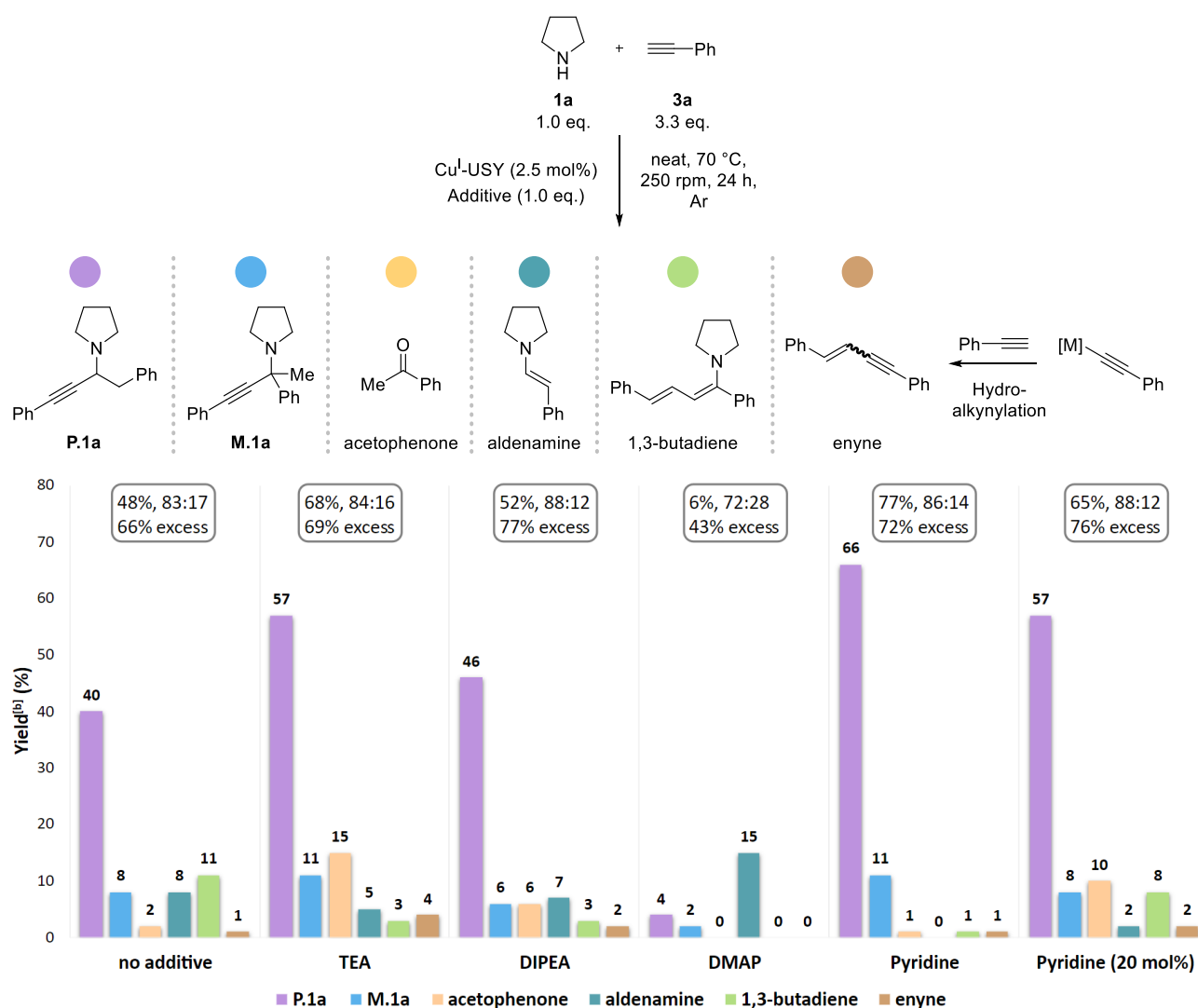


Figure 21. Screening of organic base additives in HPA reaction.^[a,c]

^[a] Reactions run solvent-free with pyrrolidine (**1a**, 1.0 mmol, 1.0 eq.), phenylacetylene (**3a**, 3.3 eq.), Cu^I-USY (2.5 mol%) and additive (1.0 eq.) at 70 °C, 250 rpm, 24 h under argon, unless otherwise stated. ^[b] Yields were estimated *via* ¹H NMR using 1,3,5-trimethoxybenzene as internal standard. ^[c] Isomeric ratios of **P.1a** and **M.1a** were determined from crude mixtures *via* ¹H NMR. TEA: triethylamine. DIPEA: *N,N*-diisopropylethylamine. DMAP: *N,N*-dimethylpyridin-4-amine. Approximate pK_a values for the conjugate acids of TEA (9.0), DIPEA (8.5), and pyridine (3.3) in DMSO.^[295]

Among the literature reports presented in section V-2., several HPA catalytic systems are not based on simple metal salts but on metal complexes. In addition to Zn^{II}-^[283] Rh^I/Cu^I^[280] and Au^I-based^[288] systems, KIM's cationic Cu^I-bis(1,10-phenanthroline) complex can be cited.^[293] As for metal cation-exchanged zeolites, the zeolitic framework can be considered a counteranion and/or a polyoxygenated macroligand. Nevertheless, the presence of an additional ligand can significantly exalt the activity of a zeolite catalyst. For instance, in the Cu^I-USY-catalysed synthesis of ynamides *via* a HSUNG-type coupling reaction, only the addition of *N,N'*-dimethyl-1,2-ethanediamine or 1,10-phenanthroline as ligands led to full conversions and high yields.^[192] With other common copper ligands, or omitting a ligand, Cu^I-USY failed to convert the starting materials.

We thus evaluated the effect of numerous ligands on the chemo- and regioselectivity using the HPA benchmark reaction under solvent-free conditions (**Figure 22**). While most of the ligands led to an increased HPA yield (**Li.2,4,6,8-11**), several others significantly reduced the HPA efficiency (**Li.1,3,5**, and **7**). The results show that tertiary amines **Li.2,4** led to a notable yield improvement compared to the ligand-free conditions, similar to the result obtained for triethylamine as additive (see **Figure 21**). On the other hand, sterically demanding tertiary amines **Li.1,3** were less efficient. No ligand enabled to increase the regioselectivity for the anti-MARKOVNIKOV isomer **P.1a**, nor allowed to overwrite the inherent regioselectivity of the ligand-free Cu^I-USY system. The best results in terms of chemo- and regioselectivity in favour of the α -secondary propargylamine **P.1a** were obtained with ligands **Li.2,6** and **11**. The findings, however, do not allow us to draw a general conclusion on what ligand class is best suited for this transformation.

To conclude, ligands **Li.2,6,9** and **11** led to promising HPA yields in the reaction of pyrrolidine (**1a**) and phenylacetylene (**3a**). The use of one equivalent of pyridine as additive afforded the best chemoselectivity and regioisomeric ratio. For practical reasons, the scope of the Cu^I-USY-catalysed HPA reaction was thus further investigated with pyridine as additive. Yet the beneficial effects of these ligands remain interesting, especially considering the small amounts used (5 mol% vs. 1.0 eq. of pyridine). Although commonly employed, pyridine can in fact not be considered “green”. Additional ligands could be screened in the future, and more particularly chiral ligands might enable the synthesis of enantioenriched propargylamines *via* an unprecedented asymmetric HPA reaction.

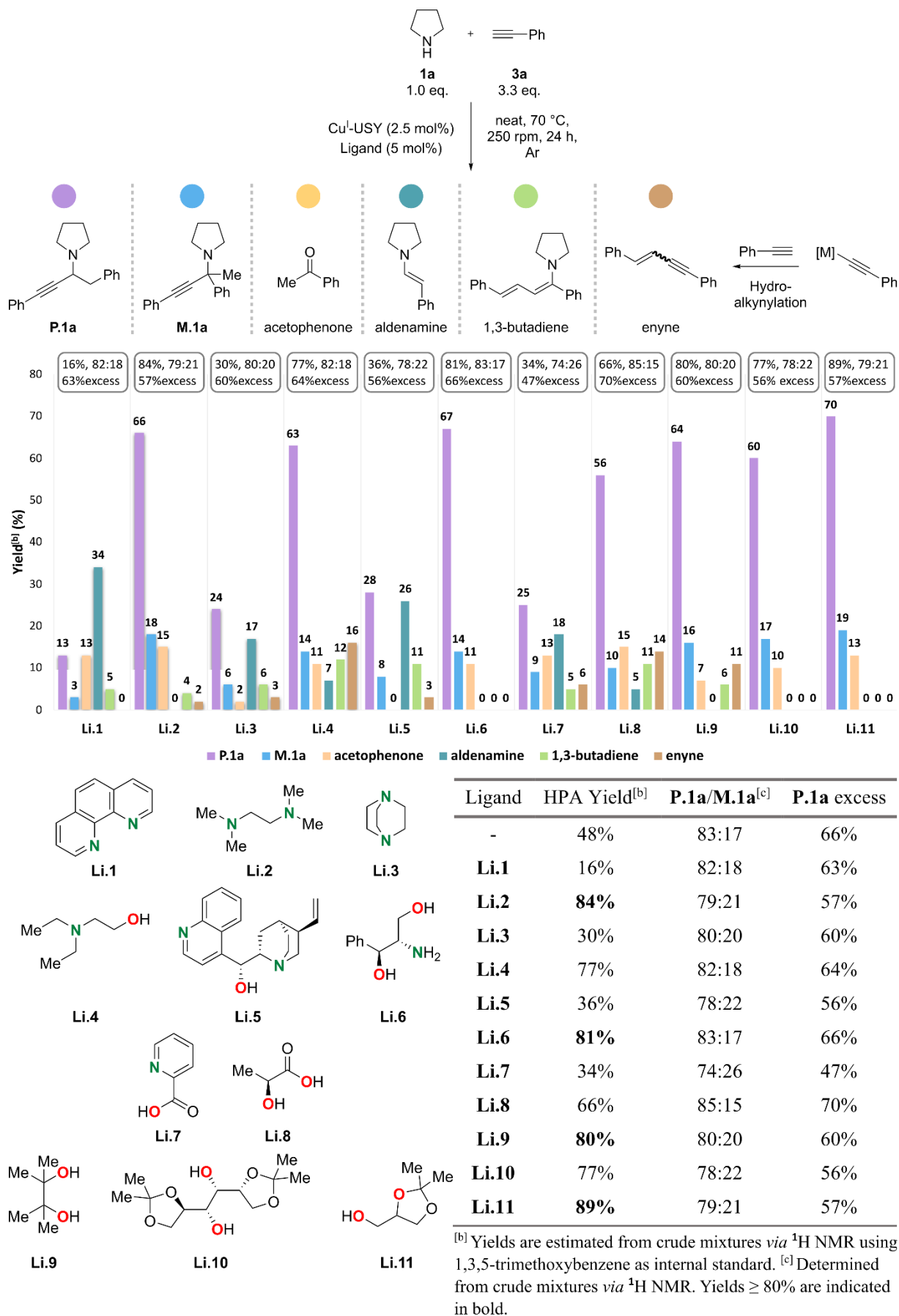


Figure 22. Ligand screening in model HPA reaction.^[a]

^[a] Reactions run solvent-free with pyrrolidine (**1a**, 1.0 mmol, 1.0 eq.), phenylacetylene (**3a**, 3.3 eq.), Cu^I-USY (2.5 mol%), and ligand (5 mol%) at 70 °C and 250 rpm for 24 h under argon.

3.4. Scope and Limitations

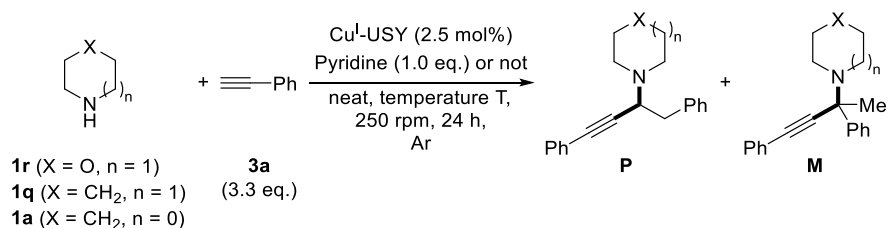
The scope of the solvent-free Cu^I-USY-catalysed HPA reaction was investigated next, starting with the amine component.

3.4.1. Amine Scope

The optimisation studies showed that the use of pyridine leads to an improved HPA reaction for pyrrolidine (**1a**) and phenylacetylene (**3a**) at 70 °C. Whether this also applies to other cyclic amines was investigated next. **Table 33** shows the results for morpholine (**1r**) and piperidine (**1q**) with phenylacetylene (**3a**).

For the reaction of morpholine (**1r**) at 70 °C, the addition of pyridine resulted in a higher selectivity for the anti-MARKOVNIKOV product **P.1r** (entry 2 vs. 1). The yield, on the other hand, remained comparatively moderate at 47% instead of 45%. Increasing the reaction temperature to 80 °C produced **P.1r** in an improved 57% yield and a further enhancement in the regioselectivity to 98:2 (entry 3).

Table 33. Evaluation of the effect of pyridine in the HPA reaction of phenylacetylene (3a**) with secondary amines.**



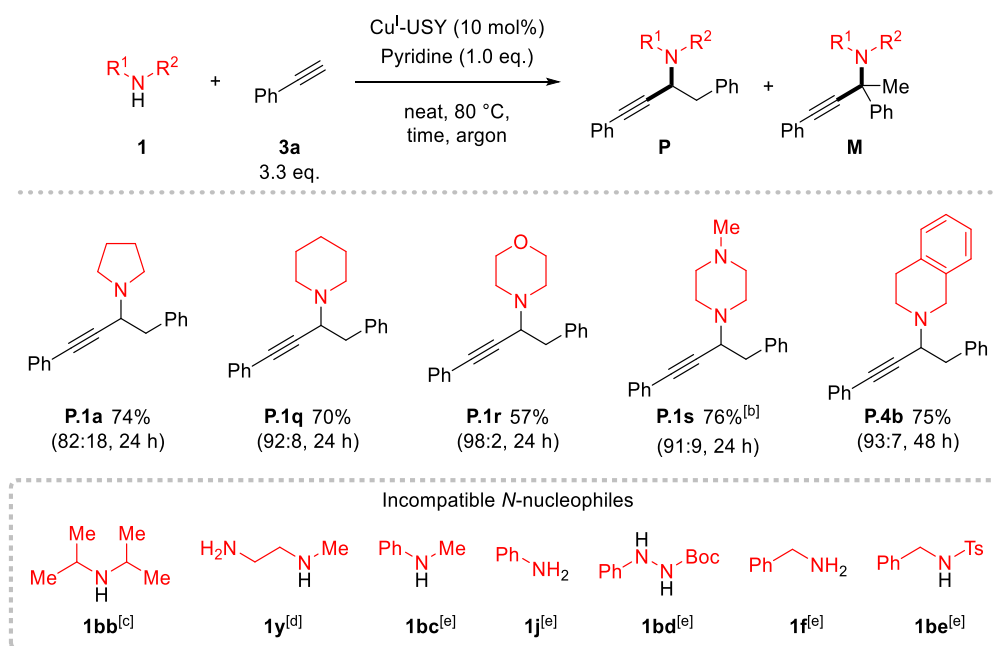
Entry	Amine 1	Pyridine	T (°C)	P	Yield P ^[a] (%)	P/M ^[b]
1	Morpholine (1r)	-	70	P.1r	45	73:27
2	Morpholine (1r)	+	70	P.1r	47	91:9
3	Morpholine (1r)	+	80	P.1r	57	98:2
4	Piperidine (1q)	-	80	P.1	46 ^[c]	96:4
5	Piperidine (1q)	+	80	P.1	70	92:8
6	Pyrrolidine (1a)	+	70	P.1a	66 ^[c]	86:14
7	Pyrrolidine (1a)	+	80	P.1a	74	82:18

^[a] Isolated yield, unless otherwise stated. ^[b] Determined from crude mixtures *via* ¹H NMR. ^[c] Yield estimated from crude mixtures *via* ¹H NMR using 1,3,5-trimethoxybenzene as internal standard.

Shifting to piperidine (**1q**), and in the absence of pyridine, the anti-MARKOVNIKOV product **P.1q** was obtained in 46% yield like in the reaction with morpholine (**1r**) (entry 4 vs. 1). Interestingly, an already high preference for the anti-MARKOVNIKOV product **P.1q** was observed (96:4). The addition of pyridine further enhanced the yield of **P.1q** to 70% but caused a slight decline in its excess (entry 5 vs. 4). Since an increased HPA yield was achieved at 80 °C without a strong deterioration of the regioselectivity, pyrrolidine (**1a**) was also examined under these conditions (entry 7). Rewardingly, a noticeable increase in yield from 66% at 70 °C (entry 6) to 74% at 80 °C was observed for propargylamine **P.1a**.

Comparing the yields for propargylamines **P.1a** and **P.1q,r** at 80 °C and in the presence of pyridine (i.e., entries 7, 5 and 3), our findings suggest that the higher the nucleophilicity of the amine, the better the HPA yield.^[233] To draw a conclusion, the amine scope needs however to be further investigated.

Additional amines were evaluated in the HPA reaction with phenylacetylene (**3a**) under solvent-free conditions (**Scheme 105**). Interestingly, *N*-methylpiperazine (**1s**) yielded the best result of all cyclic secondary amines investigated. Running the reaction at 70 °C without addition of pyridine gave propargylamine **P.1s** in good 76% yield and high selectivity (91:9). Tetrahydroisoquinoline, as cyclic benzylic amine, was also efficient yielding propargylamine **P.4b** in 75%. Several amines could however not be converted to the desired propargylamines under our conditions. With sterically hindered diisopropylamine (**1bb**), no conversion was observed at up to 110 °C, whereas even higher temperature led to degradation. It is worth noting that such sterically demanding amines have not been reported in other HPA protocols. Not surprisingly, *N*^l-methylethane-1,2-diamine (**1y**) reacted unselectively to produce a complex mixture. As for the KA² reaction, other 1,2-diamines, bearing one tertiary or a protected amine, might offer a suitable alternative.



^[a] Reactions run solvent-free with an amine **1** (1.0 mmol, 1.0 eq.), phenylacetylene (**3a**, 3.3 eq.), pyridine (1.0 eq.), and Cu^I-USY (2.5 mol%) at 80 °C under argon, unless otherwise stated. Isolated yields of **P** are indicated, and the isomeric ratios of **P/M** were determined from crude mixtures *via* ¹H NMR. ^[b] Reaction run at 70 °C without addition of pyridine. ^[c] No conversion was observed at up to 110 °C, whereas even higher temperature led to degradation. ^[d] Complex mixture without unambiguous detection of the desired product. ^[e] No conversion was observed at 100 °C.

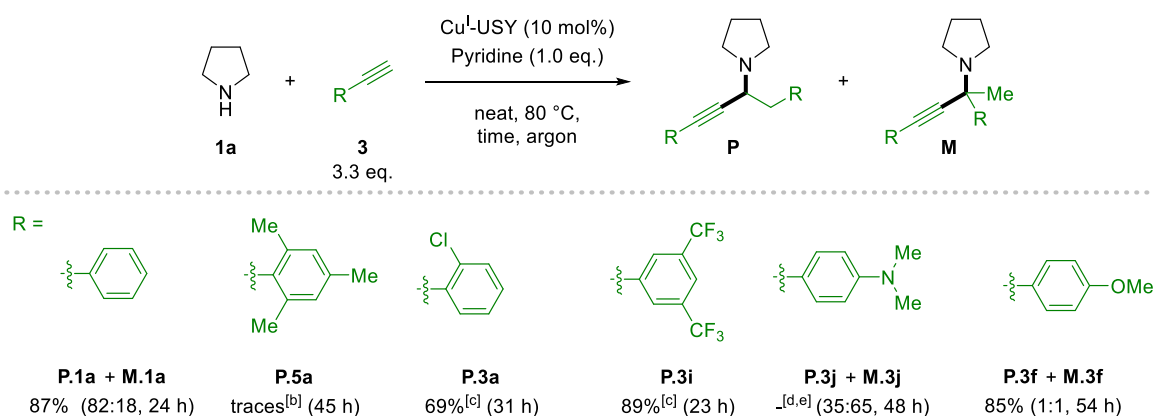
Reported intermolecular HPA versions with aromatic alkynes feature exclusively secondary aliphatic amines, except for BLECHERT's Zn-BDI complex which was compatible with *N*-phenyl-*N*-allylamine (for details, see **M.5a** in **Scheme 97a**). This has led us to investigate the

compatibility of additional *N*-nucleophiles. Unfortunately, *N*-methylaniline (**1bc**) and aniline (**1j**) were unreactive using our Cu^I-USY conditions at temperatures up to 100 °C. Likewise, hydrazine **1bd**, benzylamine (**1f**), and sulfonamide **1be** did not react with phenylacetylene (**3a**). As LARSEN and co-workers^[289,290] reported the reaction of *N*-methylaniline and benzylamine with hex-1-yne using catalytic Cu(OTf)₂, these substrate combinations were also tested with Cu^I-USY at 100 °C, but without success. When applying their optimised procedure with Cu(OTf)₂, the desired propargylamines were however not detected.

Additional secondary amines should be investigated to complete the amine scope. Particularly the reactivity of acyclic secondary amines could be compared to their cyclic analogues (e.g., diethylamine vs. pyrrolidine), especially as they are underrepresented in current HPA reports.

3.4.2. Alkyne Scope

A preliminary alkyne scope was started next. Shifting from phenylacetylene to the di-*ortho*-substituted 2-ethynyl-1,3,5-trimethylbenzene produced only trace amounts of the anti-MARKOVNIKOV isomer **P.5a**. This highlights the effect of sterics on the ability of Cu^I-USY to ensure electrophilic activation of the alkyne *via* π -complexation. The presence of a single *ortho*-chlorine substituent in 1-chloro-2-ethynylbenzene, however, was well tolerated and led to anti-MARKOVNIKOV isomer **P.3a** in 69% yield. Furthermore, 1-ethynyl-3,5-bis(trifluoromethyl)benzene reacted smoothly to propargylamine **P.3i** in 89% yield. Interestingly, such electron-deficient aromatic alkynes led exclusively to the anti-MARKOVNIKOV propargylamines. The inherent regioselectivity observed for the hydroamination with phenylacetylene (**3a**) thus seems to be exalted for electron-poor arylalkynes (for details, see section V-3.4.3.). Moreover, propargylamines **P.3a** and **P.3i** formed in similar reaction times to phenylacetylene (**3a**) (23-31 h).



Scheme 106. Preliminary results for Cu^I-USY-catalysed HPA reaction with aromatic terminal alkynes.

^[a] Reactions run solvent-free with pyrrolidine (**1a**, 0.35, 0.7 or 1.0 mmol, 1.0 eq.), an alkyne (**3a**, 3.3 eq.), pyridine (1.0 eq.), and Cu^I-USY (2.5 mol%) at 80 °C under argon, unless otherwise stated. Total isolated HPA yields are indicated and, where applicable, the isomeric ratios of **P/M** were determined from crude mixtures *via* ¹H NMR. ^[b] Poor conversion was observed and formation of **M.5a** cannot be completely excluded although not unambiguously detected *via* ¹H NMR. ^[c] Only the corresponding anti-MARKOVNIKOV HPA product **P** was formed. ^[d] Poor conversion was observed at 80 °C and the indicated ratio was obtained after 48 h at 100 °C. ^[e] Complex mixture due to degradation at 100 °C.

To further investigate the electronic effects in aromatic alkynes, electron-rich derivatives were examined next. The strong π -electron-donating 4-*N,N*-dimethylamino group hardly led to any conversion at 80 °C after four days. This could be due to several reasons. The electrophilic activation provided through complexation of Cu^I-USY might simply be insufficient at 80 °C for such an electron-rich alkyne to enable the nucleophilic addition of pyrrolidine. Furthermore, the 4-*N,N*-dimethylamino group might act as a ligand and poison the catalyst, or a combination of both is conceivable. Increasing the reaction temperature to 100 °C, however, resulted in progressive degradation of the reaction mixture. Therefore, the reaction was stopped after two days. Nevertheless, ¹H NMR analysis of the crude mixture revealed the preferred formation of the MARKOVNIKOV HPA product **M.3j** over its α -secondary isomer **P.3j** (**P.3j**/**M.3j** = 35:65).

The 4-methoxy analogue further supported the opposite electronic effect observed with electron-rich arylalkynes compared to their electron-poor analogues. 1-Ethynyl-4-methoxybenzene converted slowly to **P.3f** and **M.3f** (54 h vs. 24 h with phenylacetylene (**3a**)) but gave a satisfying 85% HPA yield. Compared to the reaction with phenylacetylene (**3a**), **P.3f** and **M.3f** were obtained in a 1:1 mixture. This suggests that the stronger the electron-donating effect of the *para*-substituent (cf. Hammett parameters^[296]), the greater the proportion of the MARKOVNIKOV HPA isomer **M**.^v

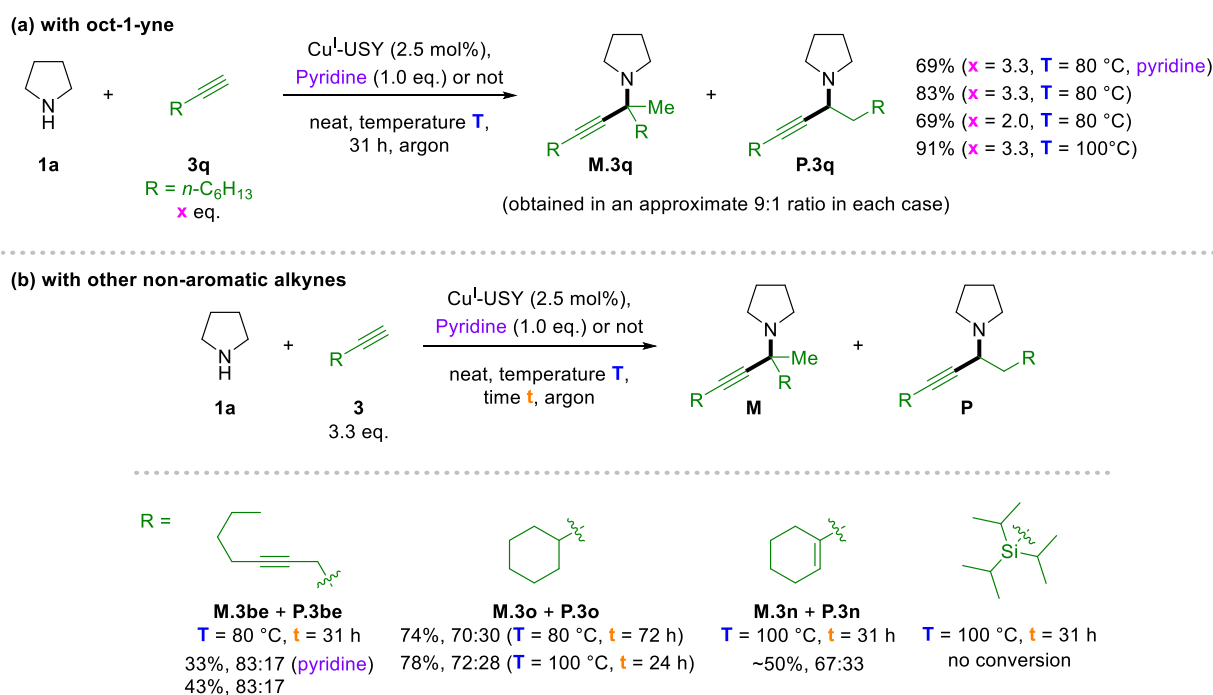
Our optimised conditions were next applied to oct-1-yne (**3q**) to evaluate the compatibility of aliphatic alkynes (**Scheme 107a**). Interestingly, opposite hydroamination regioselectivity was observed leading to a preferred formation of the MARKOVNIKOV HPA product **M.3q** over its isomer **P.3q** (ca. 93:7) in a combined 69% yield. Although the yield is noticeably lower than for the reaction with phenylacetylene (**3a**) (69% vs. 87%), the discrepancy in yield between both aliphatic and aromatic alkynes is not as large as with other reported catalytic systems.^[241,280,290–292] Interestingly, by omitting pyridine in the HPA reaction of pyrrolidine and oct-1-yne (**3q**), the HPA yield increased to 83%, without altering the regioisomer ratio. Nevertheless, similar to the results obtained with phenylacetylene (**3a**), a decrease in yield was observed when using only two oct-1-yne (**3q**) equivalents (69% vs. 83%). Therefore, the alkyne equivalents were also kept at 3.3 for aliphatic alkynes. A rise in temperature to 100 °C, and omitting pyridine, led to an enhanced 91% combined yield. Such a positive effect of temperature on the HPA yield was also observed with phenylacetylene (**3a**). In sharp contrast, the regioisomeric ratio remained unvaried for the reaction with oct-1-yne (**3q**). Indeed, a 93:7 ratio (i.e. 86% excess of **M.3q**) was estimated for the reactions at 80 and 100 °C. For comparison, a drop

^v Similar results can be deduced from the thesis work of J. BAHRI on the one-pot hydroamination/reduction of aromatic alkynes with secondary aliphatic amines.^[297]

from ca. 63% to 29% **P.1a** excess is predicted by our model when shifting from 80 to 100 °C for the reaction of pyrrolidine (**1a**) and phenylacetylene (**3a**).

Similar to the findings with oct-1-yne (**3q**), omitting pyridine led to a higher yield in the reaction with deca-1,5-diyne (**3be**) (33% vs. 43%) (**Scheme 107b**). Further changes of the catalytic system did not lead to an improvement in yield. Indeed, the use of a higher 10 mol% Cu^I-USY loading or the addition of one equivalent of triethylamine (cf. TAKANO's conditions^[280]) led to similar results. Not surprisingly, only the terminal alkyne was observed to undergo hydroamination, showing the tolerance of internal alkynes under these conditions.

To study the effect of increasing steric bulk of the aliphatic alkyne substituent, ethynylcyclohexane (**3o**) was used next (**Scheme 107b**). The highest HPA yield (78%) was achieved at 100 °C under additive-free conditions. It is important to note that the MARKOVNIKOV isomer **M.3o** still represented the major product but in a significantly reduced preference compared to the reaction with oct-1-yne (**3q**) (72:28 vs. 93:7 at 100 °C). This increasing proportion of the anti-MARKOVNIKOV propargylamine **P.3o** due to greater steric bulk of the cyclohexyl substituent is in agreement with the findings from LARSEN and co-workers.^[290] Shifting to 1-ethynylcyclohex-1-ene (**3n**) produced a more complex and hard-to-purify mixture. It is estimated that the HPA products **M.3n** and **P.3n** were obtained in about 50% yield and in a 67:33 ratio. Not surprisingly, sterically demanding (triisopropylsilyl)acetylene did not react under our Cu^I-USY HPA conditions.



Scheme 107. Preliminary results for Cu^I-USY-catalysed HPA reaction with aliphatic terminal alkynes.

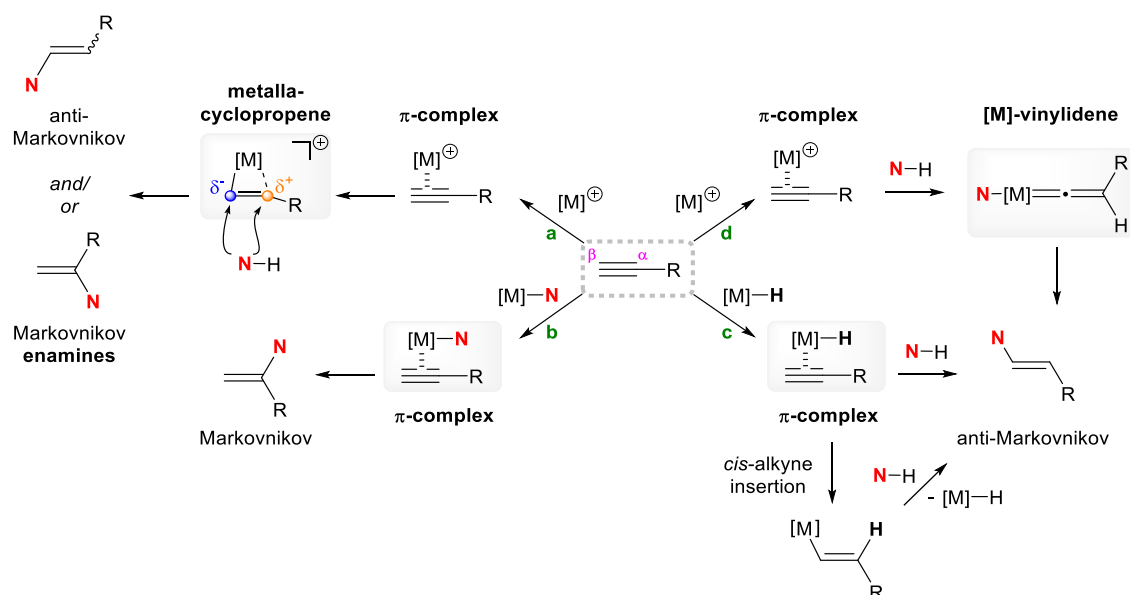
^[a] Reactions run solvent-free with pyrrolidine (**1a**, 1.0 mmol, 1.0 eq.), an alkyne **3** (3.3 eq.), pyridine if indicated (1.0 eq.), and Cu^I-USY (2.5 mol%) at the indicated temperature under argon. Total isolated HPA yields are indicated, and the isomeric ratios of P/M were determined from crude mixtures *via* ¹H NMR.

In contrast to previously reported HPA procedures, our conditions are compatible with aromatic and aliphatic alkynes. The efficiencies, however, vary significantly depending on the substrate combination and both the amine and alkyne scope need to be further investigated. The question of functional group tolerance also needs to be addressed.

Based on the preliminary observations during the scope investigation, a mechanistic proposal to account for the varying regioselectivity in the hydroamination step will be discussed in the next section.

3.4.3. Mechanistic Rationale Regarding the Hydroamination Regioselectivity

Several mechanisms have been proposed for alkyne hydroamination, i.e., the first step in the HPA cascade reaction. Generally, the mechanism is defined by the combination of catalyst(s), substrates, and reaction conditions. GOOßEN and co-workers presented a classification into four categories depending on the initiating steps (Scheme 108).^[277] In **path a** (top left), the alkyne and LEWIS acid form a π -complex which further evolves into a metallacyclopropene. The latter undergoes a nucleophilic addition by the *N*-nucleophile (simplified as N-H) to give the corresponding enamines. **Path b** and **c** (bottom left and right) initiate through the formation of a metal-nitrogen (M-N) or metal-hydrogen bond (M-H), respectively. Subsequent π -complexation and *cis*-selective alkyne insertion yields the enamines. In **path d** (top right), the initial η^2 - π -complex evolves into a η^1 -vinylidene complex. Nucleophilic addition of N-H on $M=C_\beta$ then affords the anti-MARKOVNIKOV enamine.



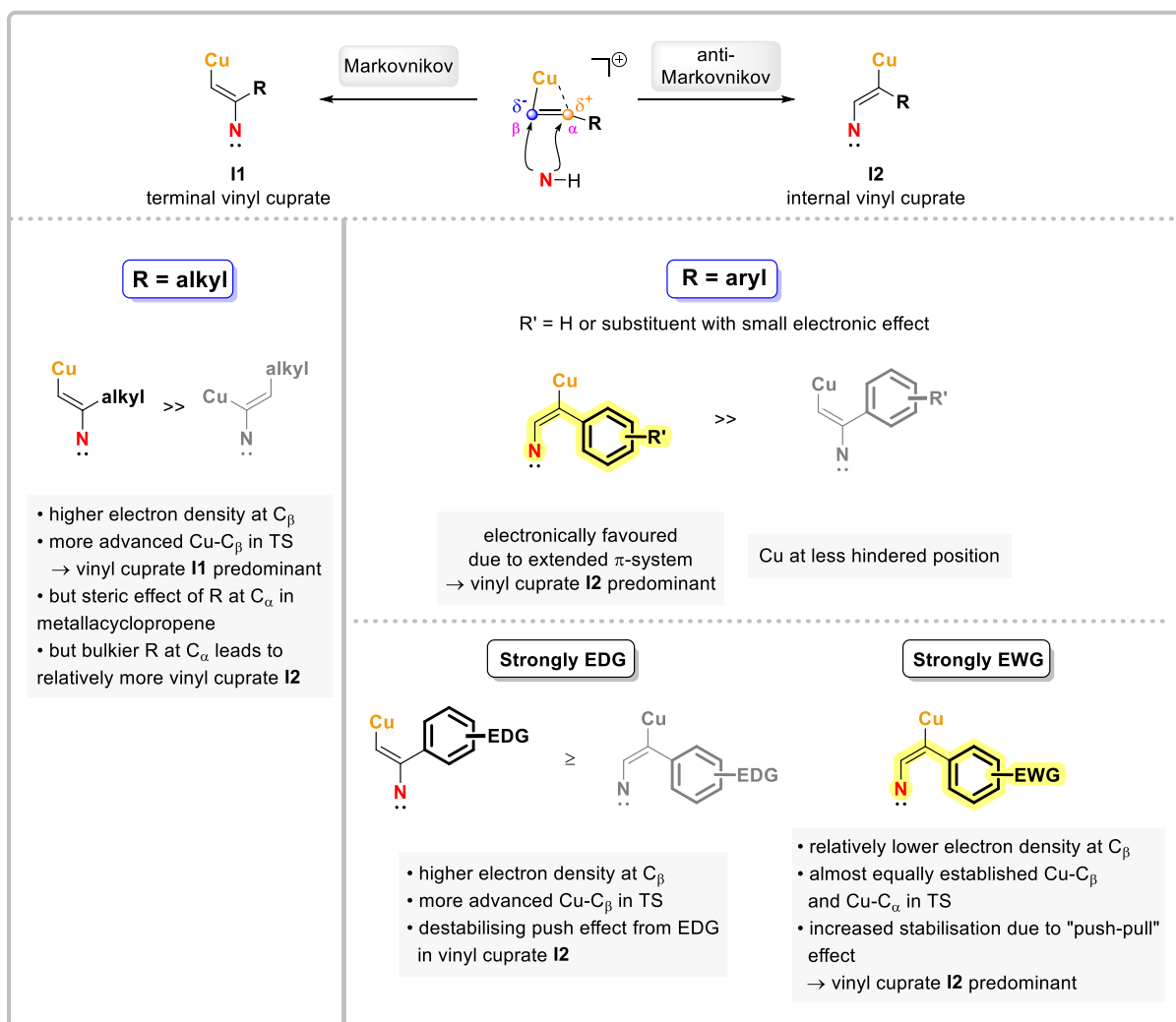
Scheme 108. Proposed mechanisms for metal-catalysed hydroamination of alkynes.

Few reports on alkyne hydroaminations, and more particularly in the case of HPA reactions provide any mechanistic rationalisation, except for TAKANO's Rh^I/Cu^I system (Scheme 95).^[280] They surmise the formation of a rhodium-vinylidene complex, which led exclusively to anti-MARKOVNIKOV hydroamination as shown in **path d** (Scheme 108, top right). However, they

predominantly used aliphatic alkynes which under our Cu^I-USY-based conditions afforded preferentially the MARKOVNIKOV isomer. Furthermore, to the best of our knowledge, a comparable copper vinylidene complex formed from such terminal alkynes has not been documented. Regarding **path c**, alkyne insertion into a metal-hydride bond also seems unlikely with basic amine nucleophiles and in the absence of a hydride transfer reagent (e.g., silane). Similarly, hydroamination *via path b* was described for anilines and amides rather than aliphatic amines. Formation of the metal-amido complex involves Rh, Ir, Pt and Pd complexes and is often believed to result from oxidative addition of the metal complex into the N-H bond. Furthermore, **path b** and **c** are sensitive to the steric hindrance of the R substituent with the metal complex inclined to sit on the less hindered position. Consequently, the greater the steric bulk of R, the higher the MARKOVNIKOV selectivity, contrary to the results observed with Cu^I-USY for aliphatic alkynes.

We thus surmise the Cu^I-USY-catalysed alkyne hydroamination to proceed *via path a*. The presumed mechanism needs to account for the varying regioselectivities observed depending on the substrate class. From the metallacyclopropene intermediate, it can be deduced that the metal cation shows a stronger interaction with C_β bearing a partial negative charge (**Scheme 109**). Steric considerations moreover suggest that, upon nucleophilic addition, copper is generally inclined to go to the less hindered carbon. Accordingly, formation of the vinyl cuprate **I1** *via* MARKOVNIKOV hydroamination would be preferred. This likely represents the more stable vinyl cuprate intermediate. Nevertheless, increased bulkiness of the alkyne substituent renders the nucleophilic addition on the C_α carbon more challenging, which is why the proportion of anti-MARKOVNIKOV isomer **I2** augments. This is in accordance with our results obtained for aliphatic alkynes, shifting for instance from oct-1-yne to ethynylcyclohexane.

For aromatic alkynes, however, continuous conjugation of the nitrogen lone pair with the styryl system in the internal vinyl cuprate **I2** likely contributes significantly to its stabilisation compared to **I1**.^[298,299] Accordingly, in the case of phenylacetylene, the activation energy required for the anti-MARKOVNIKOV hydroamination is significantly lower, thus the formation of complex **I2** is favoured. In analogy to “push-pull” systems, EWGs on the aryl ring could exalt this electronic effect, allowing to further stabilise **I2**. What is more, the EWG impacts the partial charge distribution on C_α and C_β. The partial negative charge on C_β is likely to decrease, which facilitates nucleophilic addition on this position. The combination of these effects could explain the selective formation of anti-MARKOVNIKOV HPA products **P.3a** and **P.3i**.



Scheme 109. Electronic and steric effects on the hydroamination regioselectivity.

In contrast, the “push” effect of an EDG could counteract the resonance-based stabilisation in vinyl cuprate **I2** and might increase the negative partial charge on the C_β carbon. Depending on the electron-donating capacity of the substituent, formation of the MARKOVNIKOV-derived vinyl cuprate **I1** possibly represents the preferred hydroamination route. Accordingly, the strongly π-electron-donating 4-*N,N*-dimethylamino substituent favoured the formation of the MARKOVNIKOV HPA isomer **M.3j**.

It can however not be excluded that aromatic and aliphatic alkynes operate *via* different mechanisms. Mechanistic investigations in addition to further examination of the substrate scope are needed to draw a conclusion.

3.4.4. Hot Filtration Test and Recyclability Study of Cu^I-USY

To evaluate the leaching of copper cations in the Cu^I-USY-catalysed HPA reaction of pyrrolidine (**1a**) and phenylacetylene (**3a**), a hot filtration test was performed from a suspension in EtOAc at 80 °C. **Figure 23** shows the HPA yields and the regioisomeric ratios for the filtered reaction compared to two non-filtered reference reactions running for seven and twenty-four hours, respectively. Filtration over a PTFE membrane under air afforded a particle-free but

light green solution, suggesting the presence of dissolved copper species. Stirring the filtrate at 80 °C to complete 24 hours, indeed, resulted in further conversion of the starting materials compared to the reaction stopped after seven hours (31% vs. 16% yield). Nevertheless, the reaction containing Cu^I-USY for 24 h gave a slightly higher yield of 40%. This discrepancy, however, could result from the use of additional EtOAc during the filtration step, resulting in more dilute conditions for the filtered run.

As for the AYA reaction (see p. 117), copper leaching is believed to originate from the coordination of the amine starting materials but potentially also the propargylamine products, competing with the copper-zeolite interaction. The contribution of coordinating reaction intermediates (e.g., π -complexes and copper acetylides) is also conceivable. It is noteworthy that EtOAc which was used here as solvent for practical reasons, is not believed to cause the leaching of active copper species. To verify this, a suspension of Cu^I-USY in EtOAc was heated to 100 °C for three hours and then filtered over a PTFE membrane. Adding pyrrolidine (**1a**) and phenylacetylene (**3a**) to the filtrate did not afford any conversion at 80 °C.

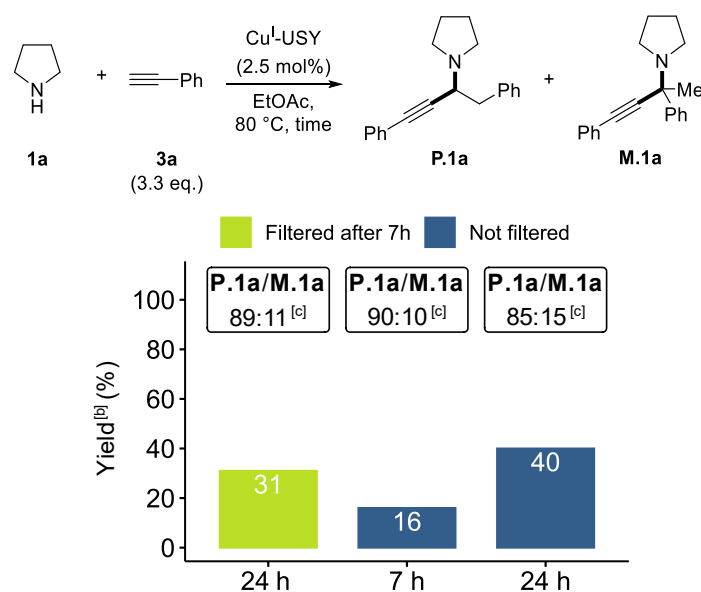


Figure 23. SHELDON test for Cu^I-USY-catalysed HPA reaction in EtOAc.

^[a] Reactions run with pyrrolidine (**P.1a**, 1.0 mmol, 1.0 eq.), phenylacetylene (**3a**, 3.3 eq.), and Cu^I-USY (2.5 mol%) in EtOAc at 80 °C under argon. ^[b] Yields (**P.1a**+**M.1a**) were estimated from crude mixtures *via* ¹H NMR using 1,3,5-trimethoxybenzene as internal standard. ^[c] Regioisomeric ratios **P.1a**/**M.1a** were determined from crude mixtures *via* ¹H NMR.

The stability and recyclability of the Cu^I-USY catalyst was investigated under solvent-free conditions using pyrrolidine (**1a**) and phenylacetylene (**3a**) (Figure 24). For practical reasons, the catalyst loading was set to 10 mol%. After each reaction, the catalyst was separated from the crude mixture through decantation after centrifugation, washed several times with CH₂Cl₂ and then dried under vacuum before being used in the next run without intermediate reactivation. Surprisingly, the second run afforded an increased yield (from 67% in run 1 to 81% in run 2), while the regioisomeric ratio remained unchanged (close to 8:2). This improved performance

of the recovered Cu^I-USY zeolite was observed up to run six, after which the recyclability study was ended for practical reasons.

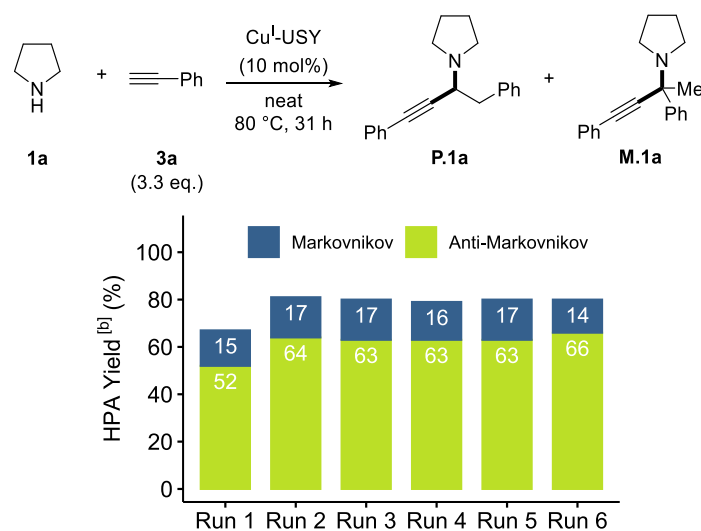


Figure 24. Recyclability study of Cu^I-USY in the HPA reaction.^[a]

^[a] Reactions run neat with pyrrolidine (**P.1a**, 1.0 mmol, 1.0 eq.), phenylacetylene (**3a**, 3.3 eq.), and Cu^I-USY (10 mol%) at 80 °C under argon. The recovered Cu^I-USY was washed with CH₂Cl₂ and dried under vacuum before being used in the next run. ^[b] Yields (**P.1a**+**M.1a**) were estimated from crude mixtures *via* ¹H NMR using 1,3,5-trimethoxybenzene as internal standard.

The hot filtration test and the recycling data could hint at a “release and catch” (also “boomerang”) process.^[300] In this scenario, the catalyst might operate in solution under the reaction conditions (as suggested by the SHELDON test results) but once the reaction mixture is cooled down, the copper cations (partially) return to the zeolite support. In this case, a better recyclability compared to a leaching scenario without a return of the catalyst would be expected. This should be investigated in the future. Nevertheless, it needs to be stressed that the catalyst loading for this recycling study was set four times higher than under optimised conditions.

Yet, neither the higher catalyst loading, nor a “release and catch” process accounts for the improved catalytic activity of the recovered Cu^I-USY. In a way, one could consider the fresh Cu^I-USY sample as a “pre-catalyst” that after a first run leads to a modified but catalytically enhanced material that requires to be further characterised. During the reaction, Cu^I-USY undergoes a colour change. The initially brown powder turns bright yellow, a colour typically observed for copper acetylides, including (phenylethynyl)copper derivatives.^[301] Upon recovery of the zeolite and washing with CH₂Cl₂, the colour persists. The presence of certain copper-alkyne species on and/or inside the recovered zeolite can therefore not be excluded.

Given the superior HPA yields and/or regioisomeric ratios observed with pyridine as additive in reactions involving phenylacetylene (**3a**), it would be interesting to investigate the effect of pyridine on the recycling potential of Cu^I-USY and whether a similar enhanced catalytic performance is observed for the recovered zeolite material.

4. Conclusion

In this chapter, Cu^I-USY was evaluated as catalyst in the hydroamination/protonation/alkyne addition (HPA) reaction involving secondary aliphatic amines and terminal alkynes. This transformation was initially observed as a side reaction under our Cu^I-USY-catalysed KA² reaction conditions discussed in chapter III.

The reaction conditions were optimised with the aid of experimental designs based on the reaction between pyrrolidine and phenylacetylene. Our study revealed that both regioisomers, i.e., MARKOVNIKOV and anti-MARKOVNIKOV, were accessible and that the overall yield was competitive with reported homogeneous conditions. Interestingly, we identified a significant impact of the stirring rate and the type of stirring bar on the overall HPA yield. In addition, temperature and alkyne equivalents were found to be critical variables to achieve high yields. The regioisomeric ratio in the reaction of pyrrolidine and phenylacetylene, however, was mainly temperature-controlled, with a decreasing selectivity for the anti-MARKOVNIKOV product with increasing temperature. This highlights an opposite effect of temperature on the HPA yield and the excess of the anti-MARKOVNIKOV product in the model reaction.

Preliminary investigations of the substrate scope have shown that the regioisomeric ratio further varies depending on the electronic properties of the aromatic alkyne. Indeed, strongly electron-withdrawing groups allowed a selective access to the anti-MARKOVNIKOV regioisomer, whereas electron-donating substituents induce an increasing proportion of the MARKOVNIKOV-derived propargylamine.

Unlike most current HPA procedures, which are limited to either aromatic or aliphatic alkynes, the Cu^I-USY system converted a series of aromatic and aliphatic alkynes. The latter preferentially produced the MARKOVNIKOV-derived propargylamines. This regioselectivity difference is believed to emerge from electronic and steric effects.

A SHELDON test evidenced that under our reaction conditions, catalysis takes place in solution. Nevertheless, a recyclability study showed that the recovered Cu^I-USY zeolite had an enhanced catalytic activity compared to a fresh Cu^I-USY sample. Starting from the second run and up to run six, i.e., the end of the recycling study, a noticeably higher and stable HPA yield was observed, whereas the regioisomeric ratio remained unchanged. Further experiments and characterisation of the recovered zeolite material are required to explain these intriguing findings and whether a “release and catch” scenario is operating.

In addition to these perspectives, the potential of our Cu^I-USY conditions for the synthesis of valuable *N*-heterocycles (e.g., α -tertiary pyrrolidines and piperidines) *via* intramolecular HPA reactions could be examined.^[281]

Chapter VI – Propargylamines as Precursors to 1,2-Dihydropyridines and their Applications

Cu^I-USY-Catalysed Cycloisomerisation of Propargylamine-Derived 3-*aza*-1,5-Enynes

1. Introduction

Amid nitrogen heterocycles, pyridine and its derivatives occupy without doubt a special place. In fact, pyridine is among the most abundant component of pharmaceuticals.^[302] Consequently, the synthesis of pyridines and related structures has attracted relentless attention. Upon removal of one of the unsaturations in pyridine, three possible double bond dihydropyridine (DHP) isomers arise, namely 1,4-dihydropyridine, 1,2- (or 1,6-)dihydropyridine, and 2,3-dihydropyridine (**Figure 25**). 1,4-Dihydropyridines are found in numerous bioactive compounds, such as calcium-channel blockers,^[303] as well as in the universal biological reducing agent nicotinamide adenine dinucleotide (NADH). The 2,3- and 1,2- (or 1,6-) congeners, however, are less explored. To simplify, 1,2- and 1,6-dihydropyridines will be referred to as 1,2-dihydropyridines, regardless of their substitution and corresponding numbering following IUPAC rules.

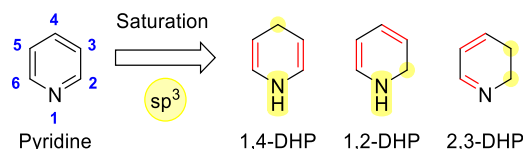
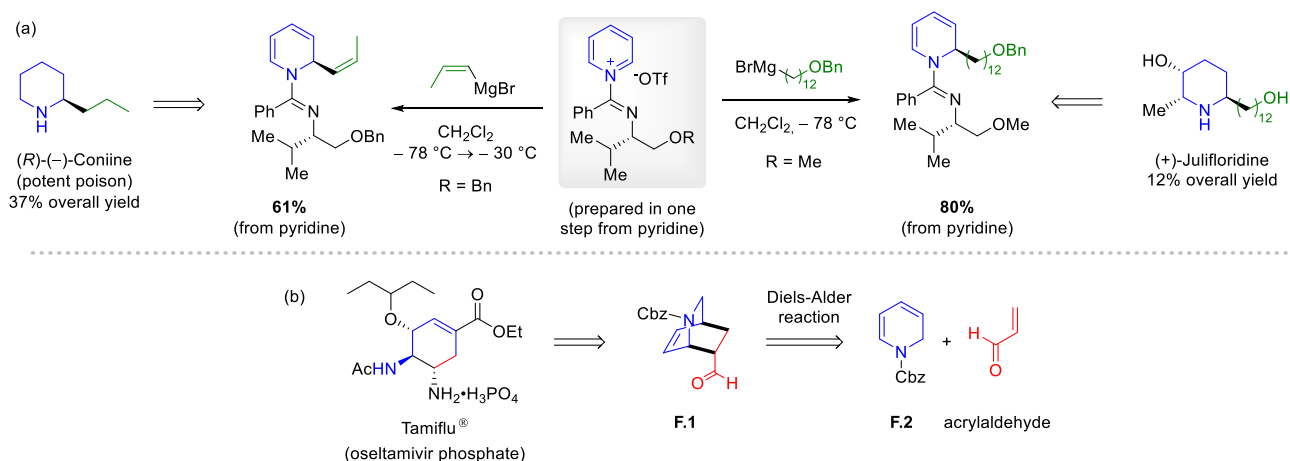


Figure 25. Pyridine and its dihydropyridine (DHP) isomers.

Nevertheless, several 1,2-dihydropyridines constituted key intermediates in the synthesis of natural products, such as (*R*)-(-)-coniine^[304] and (+)-julifloridine (**Scheme 110a**).^[305] Moreover, such dihydropyridines represent well-established precursors to give bicyclo[2.2.2]octanes, commonly referred to as isoquinuclidines, through [4+2] cycloadditions with various dienophiles. In fact, the influenza A and B drug oseltamivir phosphate (Tamiflu[®]) is prepared from isoquinuclidine **F.1**, which was formed through a DIELS-ALDER reaction of 1,2-dihydropyridine **F.2** with acrylaldehyde (**Scheme 110b**).^[306]



Scheme 110. Synthesis of (a) natural products (*R*)-(-)-coniine^[304] and (+)-julifloridine^[305], as well as (b) Tamiflu[®]^[306] from 1,2-dihydropyridines.

This chapter provides the reader with a broad but non-exhaustive overview of synthetic methodologies to prepare 1,2-dihydropyridines and provides examples of their recent synthetic and

therapeutical applications. In addition, experimental results on the synthesis of 1,2-dihydropyridines will be discussed.

2. Methodologies for 1,2-Dihydropyridine Synthesis – State of the Art

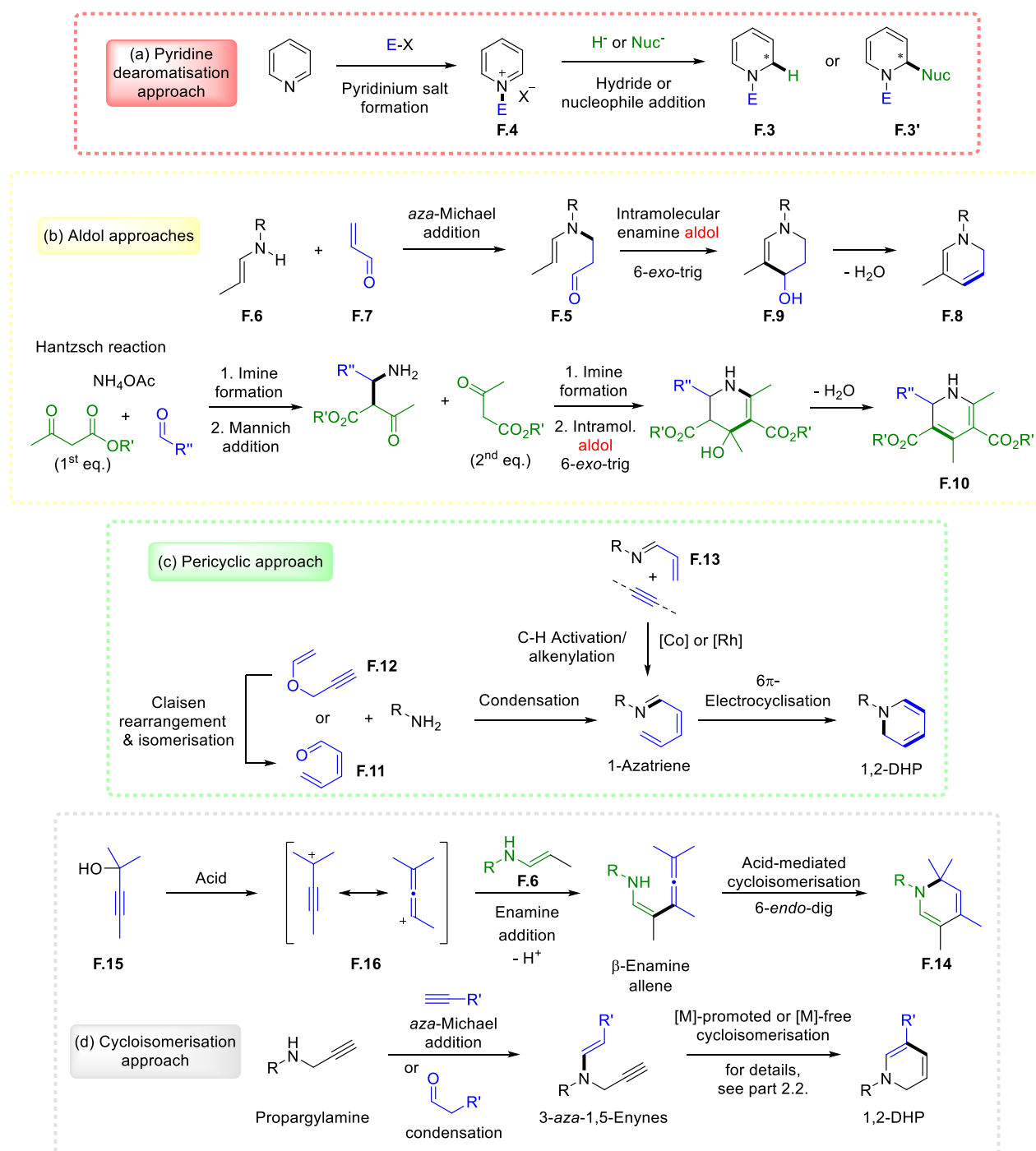
2.1. Overview of Frequently Used Approaches

Numerous synthetic procedures dealing with the synthesis of 1,2-dihydropyridines up to 2017 are summarised in the reviews from SILVA and co-workers^[307] and SINGH and co-workers.^[303] **Scheme 111** represents a selection of the most frequently used approaches to generate this scaffold. In the following, a brief literature overview is presented, which by no means, covers the overwhelming breadth of methods for the preparation of 1,2-dihydropyridines. Cited examples also include more recent reports not covered in above-mentioned reviews.

Various 1,2-dihydropyridines **F.3** and **F.3'** are accessible through the dearomatisation of pyridines (**Scheme 111a**). The reduction of pyridinium salts **F.4** using hydride donors (\rightarrow **F.3**), such as NaBH₄, was pioneered by FOWLER and co-workers.^[308] Since then, efforts for highly chemoselective and mild protocols have been made to allow the tolerance of sensitive functionalities (e.g., carbonyl, ester, nitriles, etc.).^[309] Besides chemoselectivity, it is essential to control the regioselectivity of the hydride addition. C3-Substituted pyridines, for instance, might afford a mixture of 1,2-, 1,4- and 1,6-dihydropyridines, and their relative ratio depends on the reaction conditions and the hydride source. Pyridinium salts can be generated through *N*-alkylation, but also through *N*-acylation or *N*-sulfonylation using stronger electrophiles, such as chloroformates or sulfonyl chlorides. The latter afford 1,2-dihydropyridines bearing electron-withdrawing groups on the nitrogen, largely contributing to their air stability. Closely related to the hydride reduction is the addition of diverse nucleophiles to pyridinium salts **F.4**.^[310] This often represents a method of choice for the preparation of more functionalised and elaborate 1,2-dihydropyridines **F.3'**. However, the same regioselectivity concerns apply. Interestingly, the use of chiral *N*-substituents can afford enantioselective nucleophilic additions, as shown in **Scheme 110a** for the synthesis of natural piperidines.^[311]

In addition to the derivatisation of pyridines, 1,2-dihydropyridines can also be constructed from acyclic precursors in bimolecular or MCRs (**Scheme 111b**). The six-membered azacycle is commonly formed *via* an aldol reaction as a key step. A simple approach consists in generating a β -enaminocarbonyl intermediate **F.5** *via* an *aza*-MICHAEL addition of enamines **F.6** onto unsaturated carbonyl acceptors **F.7**. Subsequent intramolecular enamine aldol reaction and dehydration then yield 1,2-dihydropyridine **F.8** *via* aminoalcohol **F.9**.^[312] Interestingly, asymmetric

organocatalytic protocols exist based on the generation of chiral unsaturated iminium ions from the MICHAEL acceptor and a chiral secondary amine.^[313]



Scheme 111. Frequently used synthetic approaches to construct the 1,2-dihydropyridine core.

Furthermore, the HANTZSCH reaction, which originally served to synthesise 1,4-dihydropyridines, sometimes affords a mixture of both isomers and even exclusively generates 1,2-dihydropyridines **F.10** depending on the reaction conditions (Scheme 111b).^[314,315]

Another major approach towards 1,2-dihydropyridines is the 6π -electrocyclisation of 1-azatrienes (Scheme 111c). This pericyclic approach heavily relies on the accessibility of 1-azatrienes and their capability to exist in the *s-cis* conformation. 1-Azatrienes are accessible from primary amines and 2,4-dienals **F.11**.^[316] The latter can also arise from propargylic enol ethers

F.12 through a CLAISEN [3,3]-sigmatropic rearrangement.^[317,318] Moreover, the low valent cobalt-^[319] or rhodium-catalysed^[320] annulation of α,β -unsaturated imines **F.13** and internal alkynes proceeds through a 6π -electrocyclisation of the *in situ* formed 1-azatrienes. In this strategy, the performance of the cyclisation reaction often greatly depends on the steric bulk of the nitrogen substituent. The smaller the *N*-substituent, the higher the relative cyclisation rate.

Furthermore, several approaches based on a cycloisomerisation reaction as a key step have been reported. The synthesis of 1,2-dihydropyridines **F.14**, for instance, can be accomplished from propargylic alcohols **F.15** and enamines under LEWIS^[321,322] or BRØNSTED^[323] acid promotion or catalysis. Enamine **F.6** aldol addition onto an allenyl cation **F.16** affords a β -enamine allene that undergoes a formal 6-*endo*-dig cyclisation. Depending on the protocol, the enamine is pre-formed, or the reaction proceeds as a MCR. Beneficially, this strategy gives access to 1,2-dihydropyridines **F.14** incorporating an α -tertiary amine moiety. The cycloisomerisation of diverse 3-*aza*-1,5-enynes also represents a widely used strategy to access 1,2-dihydropyridines. Such enynes can be pre-formed or generated *in situ* from propargylamines through an *aza*-MICHAEL addition or condensation approach. Different procedures exist based on electronically and structurally varying 3-*aza*-1,5-enynes and the mode of activation. Indeed, various transition metal-catalysed procedures, but also thermal or electrophilic activation-based approaches are described in the literature.

In this thesis, the focus lies on the cycloisomerisation of propargylamine-derived 3-*aza*-1,5-enynes. This strategy is discussed in more detail in the following section.

2.2. The Case of Cycloisomerisation of 3-*aza*-1,5-Enynes

There are several mechanistic proposals for the cycloisomerisation of 3-*aza*-1,5-enynes towards 1,2-dihydropyridines. It is often not obvious which mechanism is effective, however, depending on the substitution frame of the enyne, not all are eligible. **Scheme 112** provides an overview of the hypothesised reaction pathways to 1,2-dihydropyridines, as well as competitive pathways resulting in five-membered isomeric ring systems. Several contributions have shown that in addition to the reaction conditions (e.g., the catalyst or solvent),^[69,324] their substitution frame defines the product selectivity for the cycloisomerisation.^[69,324,325] Although metal-free conditions have been reported,^[326,327] most procedures rely on carbophilic (transition) metal π -LEWIS acid catalysts. Accordingly, π -complex **I1** can be considered a shared intermediate for these transformations.

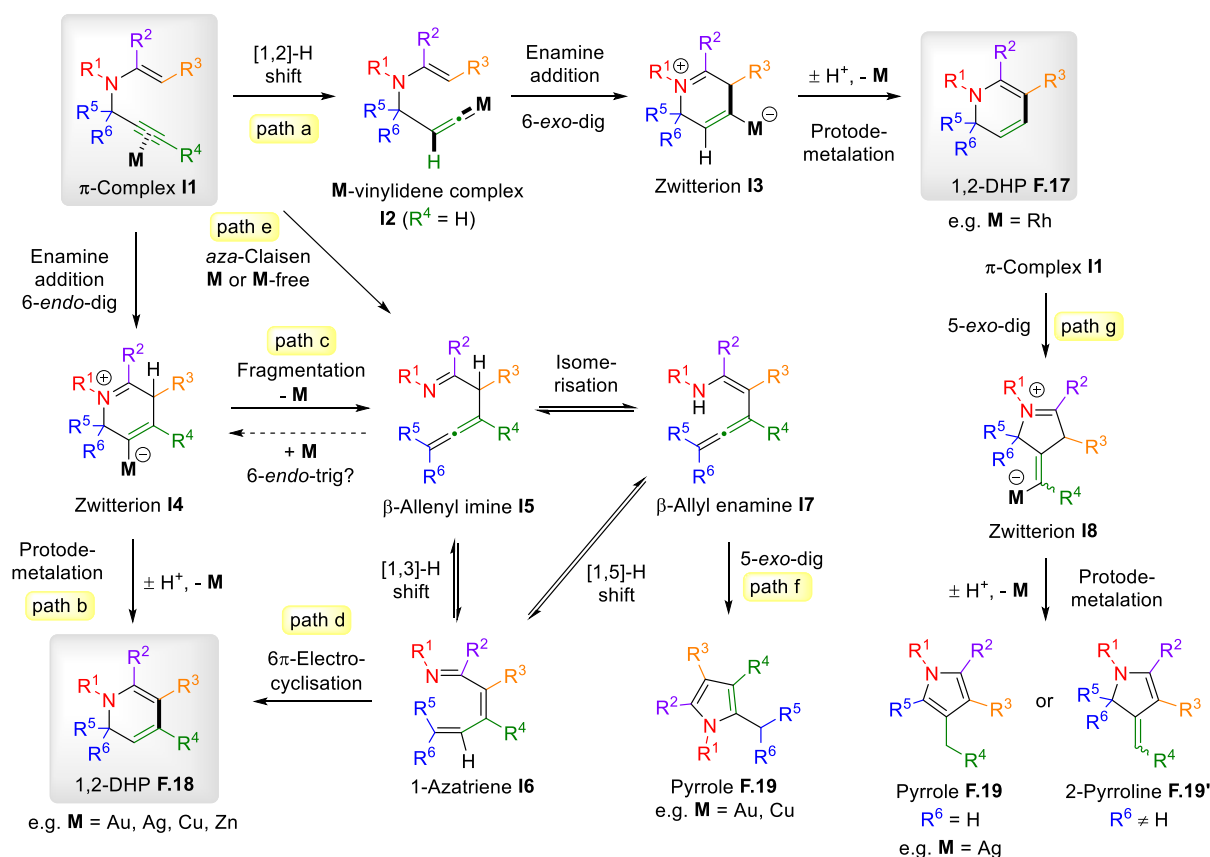
In metal-catalysed cycloisomerisations of 3-*aza*-1,5-enynes lacking an alkyne substituent, metals that tend to form metal vinylidene complexes, such as rhodium, are believed to follow **path a**. Starting from **I1**, metal vinylidene complex **I2** forms through [1,2]-hydrogen shift of the

acetylenic proton. 6-*exo*-dig cyclisation *via* the intramolecular nucleophilic addition of the enamine onto the vinylidene α -carbon then generates zwitterion **I3**. Deprotonation and subsequent protodemetalation yield the dihydropyridine **F.17** and regenerate the metal catalyst.

This mechanism is, however, not satisfactory for metals that are usually not discussed to form vinylidene complexes or in the case of 3-*aza*-1,5-enynes bearing internal alkynes. In addition to **path a**, additional routes were thus proposed. Indeed, π -complex **I1** could undergo a 6-*endo*-dig cyclisation towards zwitterion **I4**. Following **path b**, 1,2-dihydropyridine **F.18** is formed upon deprotonation and protodemetalation, regenerating the catalyst. Moreover, it is also conceivable that zwitterion **I4** undergoes a GROB-like fragmentation to β -allenyl imine **I5** (**path c**). The latter can evolve into 1-azatriene **I6**, which, as previously described, leads to 1,2-dihydropyridines **F.18** through 6π -electrocyclisation (**path d**). This presupposes that fragmentation of zwitterion **I4** proceeds faster than its deprotonation. POUR and co-workers surmised that this depends on the relative stability of the formed imine **I5**, which is determined by the nature of R^2 .^[328] Accordingly, $R^2 \neq H$ promotes fragmentation, i.e., the formation of ketimines compared to aldimines. Yet, β -allenyl imine **I5** can also arise from an *aza*-CLAISEN rearrangement (**path e**). The latter is commonly proposed in thermal procedures^[326,327] but could also be metal-catalysed similar to what is observed for propargyl vinyl ether analogues.^[329,330] To the best of our knowledge, the existence of **I5** from 3-*aza*-1,5-enynes in cycloisomerisation reactions towards dihydropyridine **F.18** has never been proven. The fact that this path is proposed is because in certain cases the formation of pyrrole **F.19** is observed (**path f**) as a by-product or even exclusively. Indeed, pyrrole **F.19** could arise from a 5-*exo*-dig cyclisation of allyl enamine **I7**. It is worth noticing that **I7** could also form *via* [1,5]-hydrogen shift from 1-azatriene **I6**.

Moreover, there is at least theoretically another route towards 1,2-dihydropyridine **F.18** from β -allenyl imine **I5**. Indeed, LEWIS acid activation of the allene moiety could induce a 6-*endo*-trig cyclisation yielding zwitterion **I4**. This has, for instance, been suggested in the synthesis 2*H*-pyrans from propargyl vinyl ethers^[330] but has not been discussed for the analogous 3-*aza*-1,5-enynes. Unfortunately, in most literature reports, the cycloisomerisation mechanism is not known. Given the possible hydrogen shifts and equilibria shown in **Scheme 112**, deuterium experiments are often inconclusive.

It is also worth noting that π -complex **I1** could alternatively evolve into the five-membered zwitterion **I8** through a 5-*exo*-dig cyclisation (**path g**). With enynes derived from α -primary and α -secondary propargylamines, this would lead to pyrroles **F.19**,^[325] whereas α -tertiary analogues would provide 2-pyrrolines **F.19'**.



Different types of 3-*aza*-1,5-enynes which vary in their substitution frame have been used in cycloisomerisation reactions to access 1,2-dihydropyridines. As aforementioned their substitution frame greatly modulates their reactivity for a given set of conditions. Accordingly, and to provide more clarity, it might be helpful to regroup enynes with similar structural features. By way of example, **Figure 26** proposes a classification of 3-*aza*-1,5-enynes reported to give 1,2-dihydropyridines into three types (**A-C**). For the sake of brevity, this section only discusses the use of type **B** enynes to synthesise 1,2-dihydropyridines as this corresponds to the enyne type exploited during this thesis work.

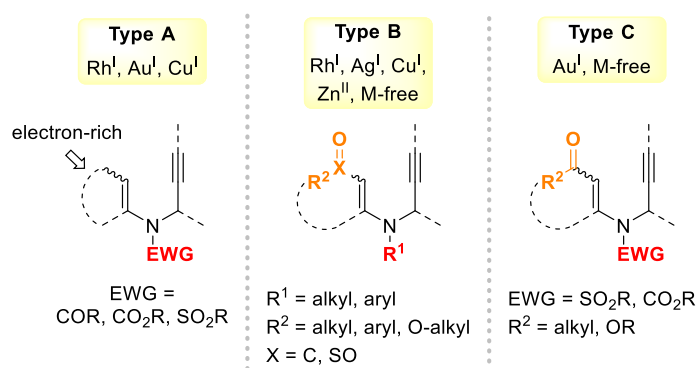


Figure 26. Different types of 3-*aza*-1,5-enynes reported in cycloisomerisation reactions.

In analogy to their propargylamine precursors, the 3-*aza*-1,5-enynes (in the following often simply “enynes”) will be denoted as α -primary, α -secondary, and α -tertiary enynes depending

on their number of propargylic substituents (**Figure 27**). Upon cycloisomerisation, the C2 position in the 1,2-dihydropyridines will be defined as α -carbon, applying the same nomenclature accordingly. As a result, an α -tertiary propargylamine, for instance, represents the starting material to an α -tertiary enyne, the latter cycloisomerising into an α -tertiary 1,2-dihydropyridine.

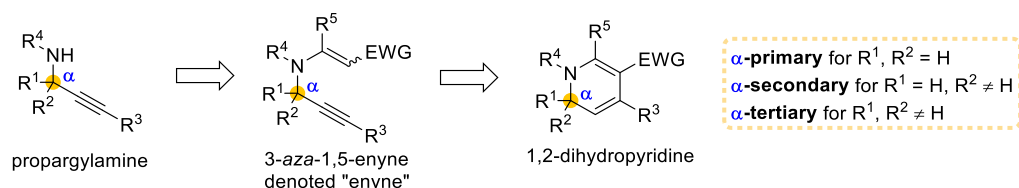
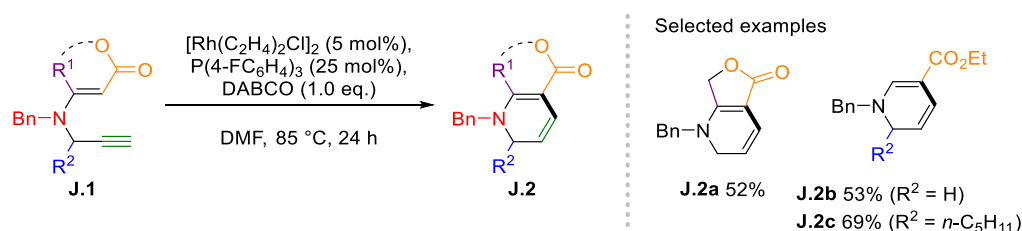


Figure 27. Defining the nomenclature for 3-aza-1,5-enynes and 1,2-dihydropyridines in this work.

2.2.1. Under Rhodium Catalysis

KIM and LEE were among the first to report the cycloisomerisation of 3-aza-1,5-enynes to yield six-membered heterocycles in 2006 (**Scheme 113**).^[331] Enynes **J.1** of type **B** were among the substrates investigated and afforded α -primary and α -secondary 1,2-dihydropyridines **J.2a-c** in 52-69% yield. The reaction proceeded with a combination of $[\text{Rh}(\text{C}_2\text{H}_4)_2\text{Cl}]_2$ (5 mol%) and $\text{P}(4\text{-FC}_6\text{H}_4)_3$ (25 mol%) phosphine ligand in DMF. The addition of a stoichiometric amount of 1,4-diazabicyclo[2.2.2]octane (DABCO) led to better yields. The base is believed to favour proton shuttling, thus accelerating the regeneration of the rhodium catalyst. Enynes of type **B** required a reaction temperature of 85 °C. Mechanistically, this transformation could initiate with the formation of a rhodium vinylidene complex, i.e., follow **path a** shown in **Scheme 112**.



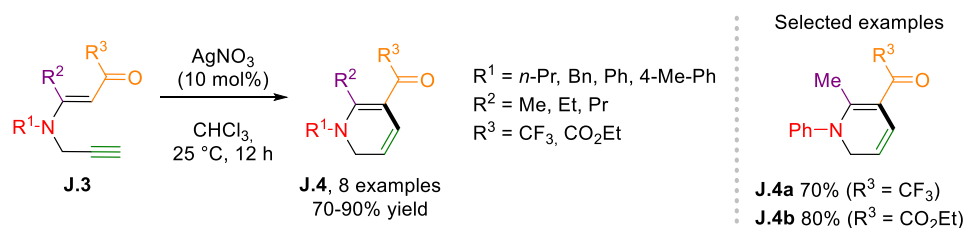
Scheme 113. Rhodium-catalysed synthesis of 1,2-dihydropyridines.

This catalytic system presents several disadvantages. First, rhodium represents a precious, thus rare metal and five equivalents (relative to rhodium) of commercial but costly phosphine ligand are required. Last, the compatible solvents DMF and DMSO are high-boiling and from a green chemical viewpoint undesirable solvents for large-scale applications.

2.2.2. Under Silver Catalysis

In 2013, BONACORSO and co-workers^[325] reported the first silver-catalysed cycloisomerisation of type **B** enynes **J.3** to give α -secondary dihydropyridines **J.4** using AgNO_3 (10 mol%) in CHCl_3 at room temperature (**Scheme 114**). Their enyne scope mostly featured CF_3 ($=R^3$)-derived enamino-carbonyls (e.g., \rightarrow **J.4a**), except for aniline-derived enaminoester **J.4b**. In general, the substrate scope included aliphatic, as well as aromatic amine substituents. Moreover,

enynes featured aliphatic R² substituents on the enamine α -carbon, but no example included a propargylic or alkyne substituent. Conveniently, reactions were performed on a 5 mmol scale, proving that this procedure is amenable on a gram scale. Nevertheless, the reaction needed to be run in the absence of light under a nitrogen atmosphere to maintain catalytic activity. It is worth noting that isolation of the α -primary 1,2-dihydropyridines **J.4** was achieved when column chromatography was performed under a nitrogen atmosphere. Nevertheless, product degradation occurred when the 1,2-dihydropyridines were left in solution. Under pure form, a relative stability of five days was observed under air.



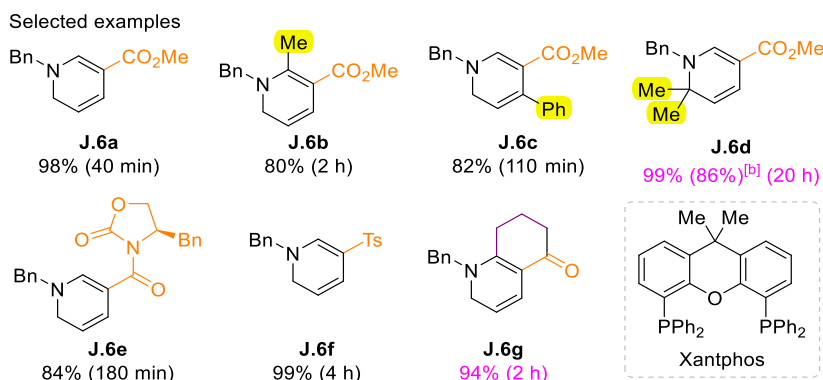
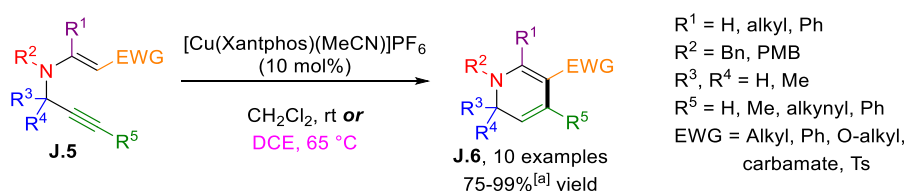
Scheme 114. Ag^I-catalysed 6-*endo*-dig cycloisomerisation of α -primary 3-*aza*-1,5-enynes **J.3**.

Besides the mild character of this procedure, the use of an easy-to-handle and stable base metal catalyst operating in green solvent would be highly desirable.

2.2.3. Under Copper Catalysis

In 2015, OGURI and co-workers investigated the use of several cationic cuprous complexes for the chemoselective 6-*endo*-dig cyclisation of enynes **J.5** to 1,2-dihydropyridines **J.6** (Scheme 115).^[332] Among the screened complexes, [Cu(Xantphos)(MeCN)]PF₆ was shown to afford the best result compared to complexes equipped with other diphosphine ligands. For comparison, the authors tested a combination of CuCl and Xantphos, which afforded almost no conversion compared to all cationic complexes examined. This shows the beneficial reactivity of such cationic complexes under such cycloisomerisation conditions.

The product scope included benzylamine-derived 1,2-dihydropyridines. The electron-withdrawing group (EWG) represented mostly esters (**J.6a-d**), but amides (**J.6e**) and an aryl sulfone (**J.6f**) were observed to react efficiently in CH₂Cl₂ at room temperature. Despite the necessity to heat β -enaminoketone-derived enynes in DCE at 65 °C, they afforded excellent product yields above 90% (cf. **J.6g**). Introducing an additional α -enamine substituent R¹ did not alter the chemoselectivity using the same catalyst. Indeed, 1,2-dihydropyridine **J.6b** and **J.6g** were obtained in very good yields, while CUI and co-workers isolated pyrroles from comparable enynes employing Cu₂O (20 mol%) in DCE.^[333]

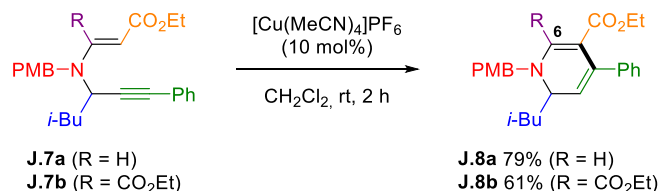


Scheme 115. Enyne cycloisomerisation to 1,2-dihydropyridines using a cationic Cu^{I} -Xantphos complex.^[332]

^[a] Yields estimated from crude mixtures *via* ^1H NMR analysis using 4-nitrobenzonitrile as internal standard, unless otherwise stated. ^[b] Isolated yield after purification over silica gel. Xantphos: 4,5-bis(diphenylphosphino)-9,9-dimethylxanthene. DCE: 1,2-dichloroethane.

Furthermore, the product scope featured an α -tertiary 1,2-dihydropyridine **J.6d**, which in contrast to α -primary 1,2-dihydropyridines is oxidation-stable and was isolated in 86% yield. It is noteworthy that the *gem*-dimethyl substituent increases the steric hindrance around the alkyne π -system, thus rendering its electrophilic activation through π -complexation more difficult. Consequently, a higher reaction time and temperature of 65 °C were required compared to α -primary enynes. Likewise, π -complexation is potentially retarded with internal alkynes but the cycloisomerisations still proceeded at room temperature and in good yields (**J.6c** vs. **J.6a**).

In continuation of the work by OGURI and co-workers,^[332] PESHKOV's group reacted enyne **J.7a** (with $\text{R} = \text{H}$) with $[\text{Cu}(\text{MeCN})_4]\text{PF}_6$ in CH_2Cl_2 at room temperature without adding any ligand (**Scheme 116**).^[334] Gratifyingly, 1,2-dihydropyridine **J.8a** was obtained in 79% yield, pointing out the competitiveness of this ligand-free catalytic system for type **B** enynes. Furthermore, enyne **J.7b** ($\text{R} = \text{CO}_2\text{Et}$) obtained from diethyl acetylene dicarboxylate, gave 1,2-dihydropyridine **J.8b** carrying a C6-substituent in 61% yield, complementary to OGURI's scope.



Scheme 116. Ligand-free Cu -catalysed synthesis of 1,2-dihydropyridines **J.8**.^[334]

To go further, PESHKOV and co-workers were the first to report a cascade *aza*-MICHAEL addition/cycloisomerisation reaction of α -secondary propargylamine **J.9a**, with ethyl buta-2,3-dienoate (**J.10**) to yield tetrasubstituted 1,2-dihydropyridine **J.11a** (**Table 34**). This approach enabled the incorporation of a C6-methyl substituent in **J.11a**. Unfortunately, $[\text{Cu}(\text{MeCN})_4]\text{PF}_6$ in

CH₂Cl₂ at room temperature did not produce **J.11a** in satisfying yield (entry 1). Although a promising conversion of propargylamine **J.9a** was observed after six hours, the selectivity was moderate and a significant amount of unreacted enyne **J.12a** remained. Shifting to CuBr in toluene at 90 °C gave a substantial enhancement producing dihydropyridine **J.11a** in 66% yield (entry 2). Moreover, adding an equivalent of an organic base (entries 3 and 4) further improved the yields with up to 76% of isolated **J.11a** using pyridine (entry 4). The authors assumed that the base promotes the *aza*-MICHAEL addition of propargylamine onto ethyl buta-2,3-dienoate (**J.10**), hence improving the overall efficiency of this cascade reaction. Since pyridine is also a suitable copper ligand, an effect on the electronic properties of the catalytically active species should also not be ruled out.

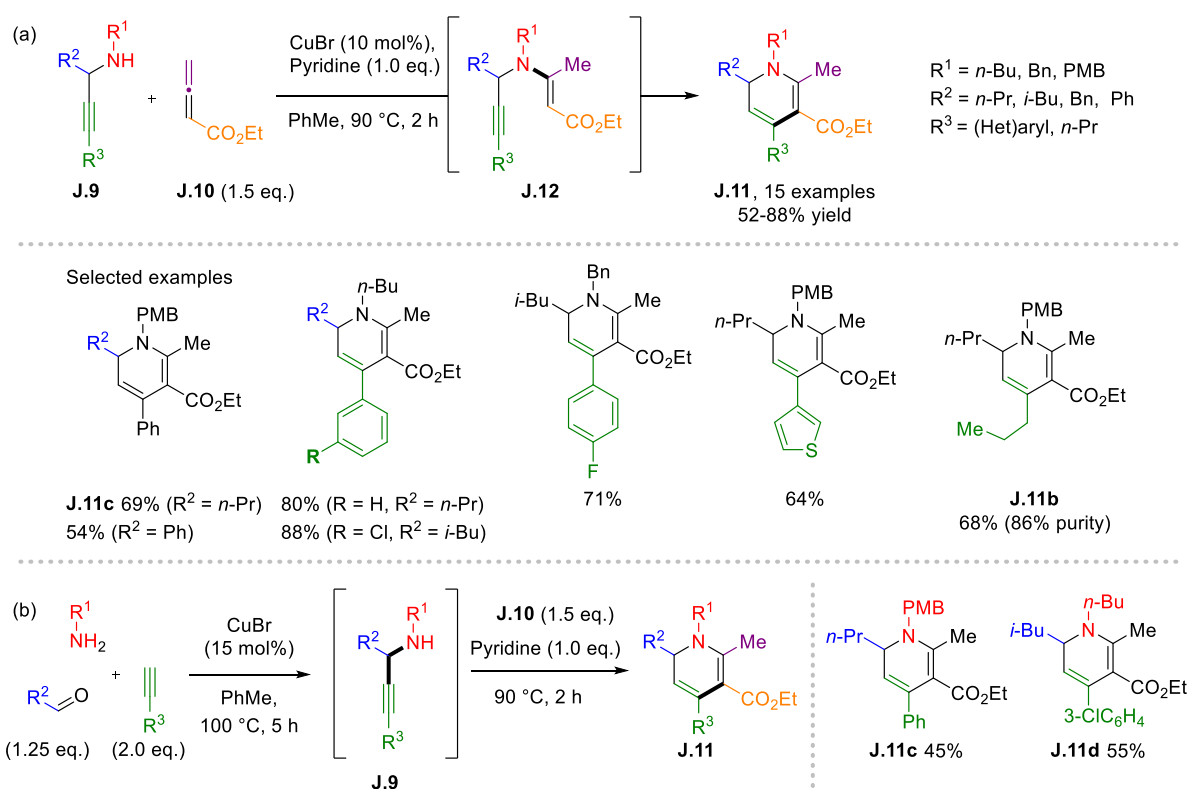
Table 34. Optimisation of the copper-catalysed cascade synthesis of 6-methyl-1,2-dihydropyridine J.11a (a selection).^[334]

Entry	x (eq.)	Cat.	Base	Conc. (M)	Temp. (°C)	Conv. of PA (%)	Yield ^[a] (%)	
							DHP	EN
1 ^[b]	1.2	[Cu(MeCN) ₄]PF ₆	-	0.1	rt	90	30	37
2 ^[c]	1.5	CuBr	-	0.4	90	100	66	-
3 ^[c]	1.5	CuBr	Et ₃ N	0.4	90	100	74	-
4 ^[c]	1.5	CuBr	Py	0.4	90	100	78 ^[d]	-

^[a] Yield estimated from the crude *via* ¹H NMR analysis using 3,4,5-trimethoxybenzaldehyde as internal standard. ^[b] Reaction run in CH₂Cl₂ for 6 h. ^[c] Reaction run in PhMe for 2 h. ^[d] 76% isolated yield at a 0.5 mmol scale. PMB: *para*-methoxybenzyl. Py: pyridine.

In total, the product scope of this cascade reaction comprises 15 examples in 52-88% yield starting from α -secondary propargylamines **J.9** (Scheme 117a). Regarding the product, scope *n*-propyl and *i*-butyl propargylic substituents gave better yields than benzyl or phenyl. All the aliphatic amine components investigated (*n*-butyl, benzyl and *p*-methoxybenzyl) afforded consistently good yields. Substrates bearing (hetero)aromatic alkynes selectively led to 1,2-dihydropyridines in good yields, whereas a sole aliphatic example (**J.11b**) was obtained in a complex mixture with hard-to-separate and unidentified by-products.

Last, a one-pot sequential A³ coupling/*aza*-MICHAEL addition/cycloisomerisation sequence was examined affording 1,2-dihydropyridines **J.11c,d** in 45 and 55% yield (Scheme 117b).



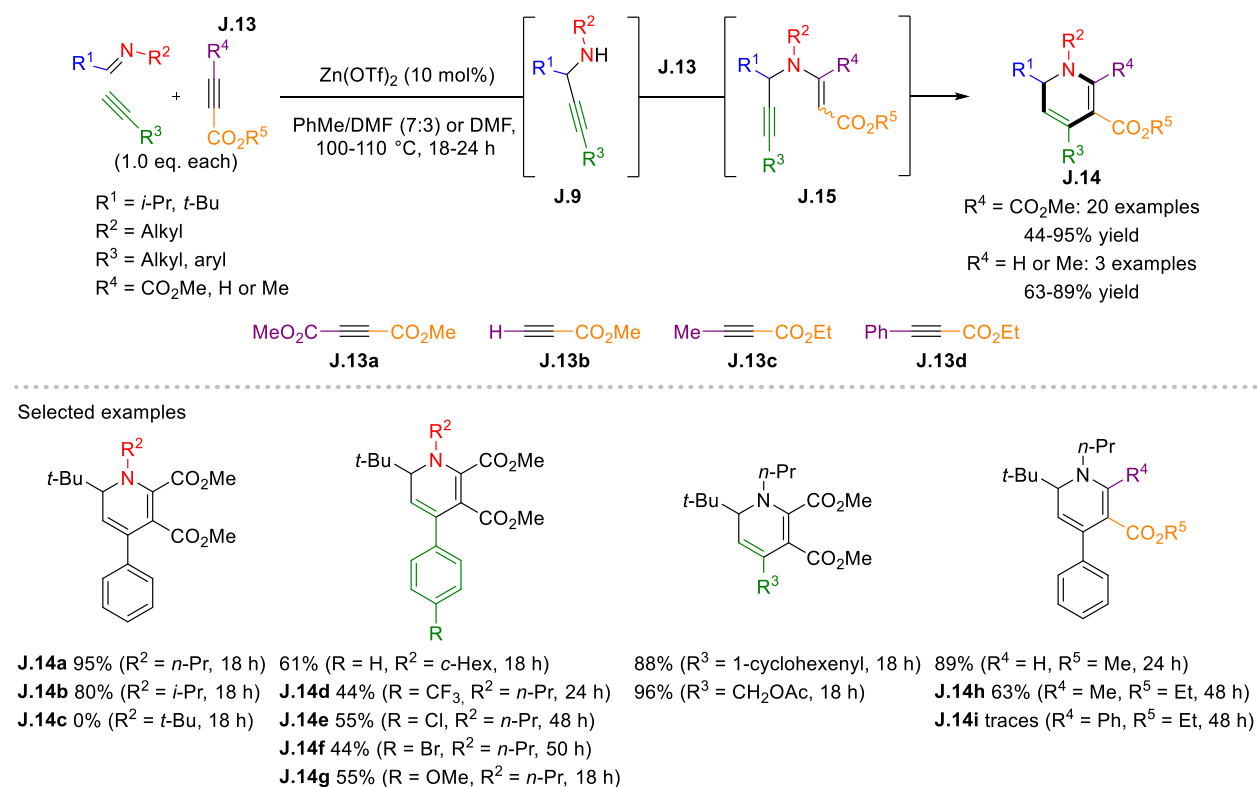
Scheme 117. (a) Cu-catalysed synthesis of 6-methyl-1,2-dihydropyridines from α -secondary propargylamines and ethyl buta-2,3-dienoate (**J.10**). (b) One-pot sequential Cu-catalysed A³/aza-MICHAEL addition/cycloisomerisation reaction for the synthesis of 6-methyl-1,2-dihydropyridines.^[334]

2.2.4. Under Zinc Catalysis

In 2018, TEHRANI and co-workers reported an attractive novel 3CR between aldimines, unactivated terminal alkynes, and propiolates **J.13** to access α -secondary 1,2-dihydropyridines **J.14** (**Scheme 118**).^[335] This cascade reaction starts with a metal-catalysed alkyne addition to pre-formed aldimines yielding the corresponding propargylamine **J.9**. The latter, bearing a secondary amine, nucleophilically adds onto propiolate **J.13** to give an intermediate type **B** enyne **J.15**. This *aza*-MICHAEL addition could also be possibly catalysed by the LEWIS acid. Finally, a 6-*endo*-dig selective metal-catalysed cycloisomerisation furnishes the 1,2-dihydropyridine **J.14**. A 7:3 toluene/DMF mixture as solvent resulted in the best outcome in terms of yield and cleanliness of the crude mixture. Furthermore, $\text{Zn}(\text{OTf})_2$ proved to be more efficient than zinc halides, while $\text{Cu}(\text{OTf})_2$ and CuBr_2 gave moderate to good yields. Similar to typical KA^2 reaction conditions, the reaction required elevated temperatures of 100-110 °C.

Regarding the substrate scope, solely aldimines derived from branched aliphatic aldehydes gave the corresponding 1,2-dihydropyridines. Aldimines derived from *n*-butyraldehyde, and benzaldehyde, for instance, yielded complex mixtures, whereas the use of ketimines was not reported. The amine substituent scope includes α -primary and α -secondary aliphatic amines (cf. **J.14a,b**), while an *N*-*t*-butylamine-derived aldimine (\rightarrow **J.14c**) was unsuccessful. The increased steric

hindrance most likely impeded the *aza*-MICHAEL addition. More functionalised amines or aniline-derived imines were not included.



Scheme 118. Zn-catalysed 3CR of aldimines and alkynes towards α -secondary 1,2-dihydropyridines **J.14**.^[335]

Regarding the alkyne scope, electron-rich and -poor aromatic and aliphatic alkynes were efficient coupling partners. It is worth highlighting that poorly nucleophilic 1-ethynyl-4-(trifluoromethyl)benzene, however, gave **J.14d** in moderate 44% yield. Furthermore, the 4-Cl or 4-Br analogues were also less efficient (**J.14e,f** 44-55%). Their lower nucleophilicity might render the metal acetylide addition less efficient. Additionally, the so-formed propargylamine incorporates a less LEWIS basic alkyne moiety, which could complicate the π -complexation of the LEWIS acid, thus potentially retarding the cycloisomerisation. Dihydropyridines **J.14e** and **J.14f** indeed required more than twice the reaction time. In contrast, electron-rich arylalkynes converted faster, but also resulted in moderate yields, such as dihydropyridine **J.14g**.

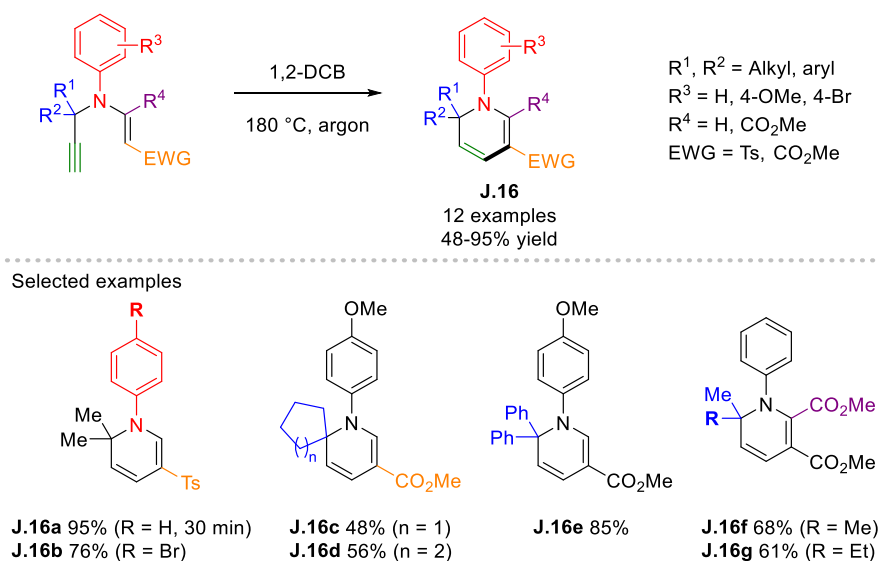
Besides dimethyl acetylenedicarboxylate (**J.13a**), terminal **J.13b** and methyl- or phenyl-substituted **J.13c,d** propiolates were investigated. Their lower reactivity required the use 1.5 equivalents of propiolate performing the reaction in DMF at 110 °C. Under these conditions, ethyl 2-butynoate (**J.13c**) gave 1,2-dihydropyridine **J.14h** in 63% yield in 48 hours. Ethyl phenylpropiolate (**J.13d**), in contrast, produced 1,2-dihydropyridine **J.14i** only in trace amounts, possibly due to the increased steric hindrance of the phenyl substituent.

Overall, this catalytic transformation benefits from several advantages such as its three-component approach, the use of equimolar amounts of each component for most examples, and the application of a base metal catalyst. Although $\text{Zn}(\text{OTf})_2$ resulted in superior yields, significantly

cheaper ZnCl₂ also led to promising results. Unfortunately, no alternative and “greener” but equally efficient solvent system has been identified to bypass the undesirable toluene/DMF mixture.

2.2.5. Under Metal-Free Conditions

In 2020, VARALA and co-workers established a thermal procedure for the synthesis of aniline-derived α -tertiary 1,2-dihydropyridines **J.16**. The reaction proceeded best in 1,2-dichlorobenzene (1,2-DCB) at 180 °C in 30 minutes for dihydropyridine **J.16a** (Scheme 119).^[327]



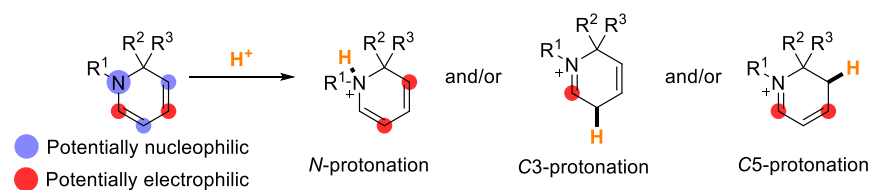
Scheme 119. Thermal enyne cycloisomerisation in 1,2-DCB towards 1,2-dihydropyridines **J.16**.

The authors assume that the reaction proceeds *via* an *aza*-CLAISEN rearrangement/electrocyclisation sequence^[336] but no mechanistic studies were carried out. Unfortunately, the optimised conditions were incompatible with α -primary and α -secondary enynes due to product degradation. In total, 12 examples of α -tertiary 1,2-dihydropyridines **J.16** were prepared in yields ranging from 48-95%. Importantly, the substrate scope includes exclusively enynes carrying terminal alkynes leading to 1,2-dihydropyridines lacking a C4 substituent. Furthermore, three different electrophiles, namely ethynyl *p*-tolyl sulfone (\rightarrow **J.16a,b**), methyl propiolate (\rightarrow **J.16c-e**), and dimethyl acetylene dicarboxylate (DMAD) (\rightarrow **J.16f,g**), were used to prepare the enyne starting materials. Dihydropyridines obtained from DMAD were isolated in lower yields compared to analogous dihydropyridines prepared from methyl propiolate. While for the open-chain propargyl substituents, as well as for most aniline derivatives, no clear electronic trend can be read from the product scope, it is noticeable that cyclopentyl and cyclohexyl gave spirocyclic 1,2-dihydropyridines **J.16c,d** in reduced yields (48-56%). The authors, however, mention that electron-withdrawing substituents on the aniline moiety, such as the nitro group, were unsuccessful, which might explain the noticeably lower yield in dihydropyridine **J.16b** carrying a deactivating 4-bromo substituent.

3. Synthetic Applications of 1,2-Dihydropyridines – State of the Art

As previously mentioned, 1,2-dihydropyridines find numerous applications in organic synthesis. In this section, a range of synthetic applications is presented to illustrate their diverse reactivity. Since the formation of α -tertiary 1,2-dihydropyridines has not been a focus for a long time, their synthetic applications are less developed. Nevertheless, selected examples of innovative and more recent synthetic applications of α -tertiary 1,2-dihydropyridines, including spirocyclic derivatives, are highlighted in this section.

In 2021, ELLMAN and co-workers published an account on the use of 1,2-dihydropyridines in attractive synthetic transformations to access diversely functionalised tetrahydropyridines and piperidines.^[337] Before having a look at some of these applications, it is worth discussing the reactivity of dihydropyridines towards electrophiles. In fact, 1,2-dihydropyridines possess three potential nucleophilic sites (**Scheme 120**). In addition to the two competing C3 and C5 positions, the nitrogen atom, especially when carrying an electron-rich alkyl or aryl group, could also act as a nucleophile. Considering a protonation scenario, three isomeric cations can result, each displaying a different distribution of the carbon unsaturations, thus displaying different reactivities towards potential nucleophiles.

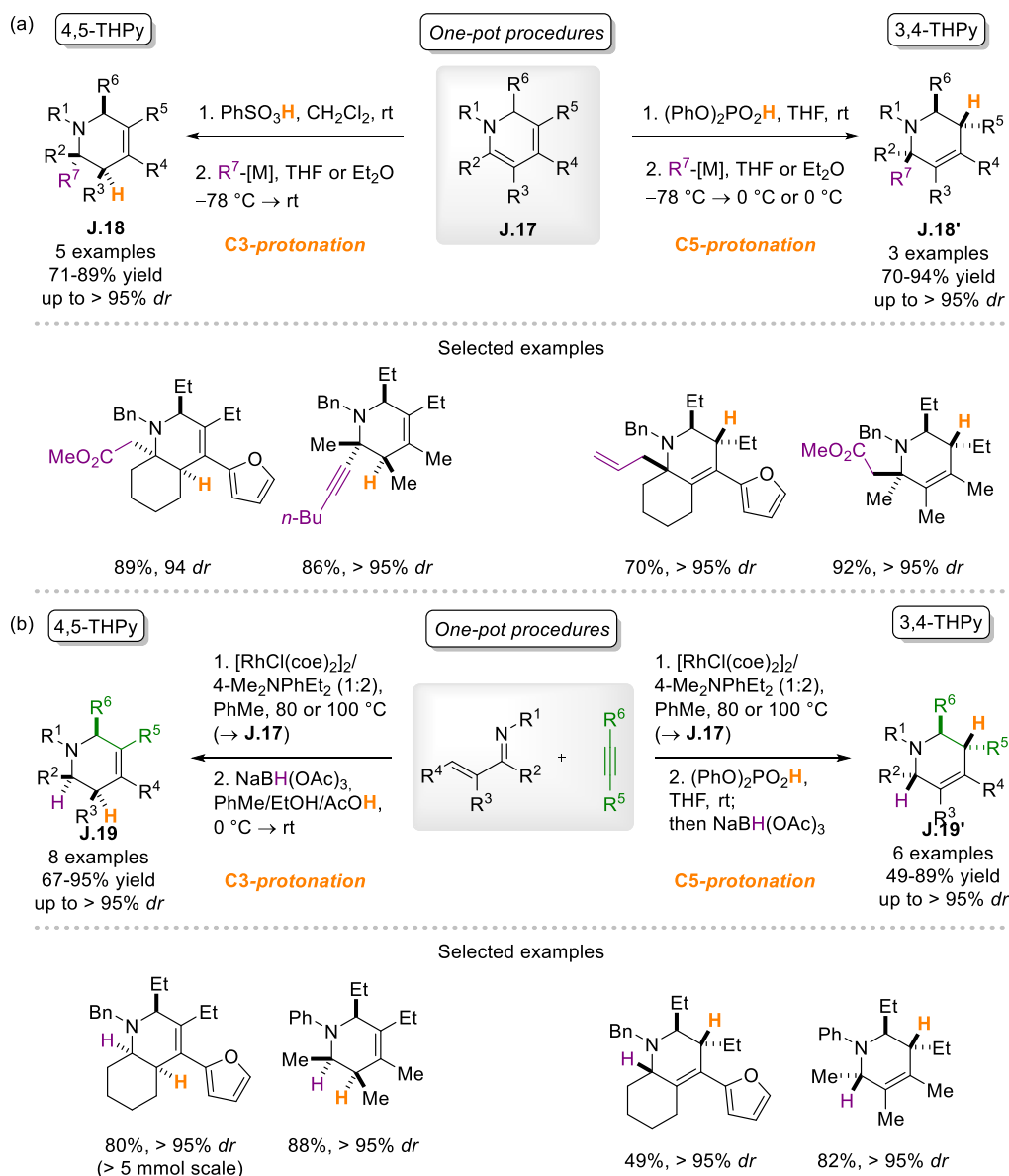


Scheme 120. 1,2-Dihydropyridine protonation leads to three possible isomeric cations.

ELLMAN and co-workers observed that site-selective C-protonation can be achieved depending on the acid strength. They observed kinetic protonation at C3 (or α) position using a mild acid such as acetic acid followed by *in situ* reduction preventing equilibration, or by using a strong sulphonic acid (e.g., benzenesulphonic acid PhSO₃H), leading to irreversible protonation. Acids with an intermediate strength that allow equilibration, e.g., diphenyl phosphate (PhO)₂PO₂H, afford the thermodynamic iminium ion through C5- (or γ -) protonation. Its greater stability results from the remaining double bond resonance.

Being able to control the regioselectivity of the protonation step, ELLMAN and co-workers established highly selective protocols towards diverse tetrahydropyridines (THPyS) (**Scheme 121**). Nucleophilic trapping of the iminium ion from dihydropyridines **J.17** with organometallic reagents, for instance, delivered 4,5- and 3,4-THPyS **J.18** and **J.18'** bearing a quaternary carbon in a one-pot approach (**Scheme 121a**)^[338]. In addition, the dihydropyridine **J.17** formation *via* Rh^I-catalysed C-H alkenylation/electrocyclisation was directly coupled to the reduction of the

corresponding iminium ions to 4,5- and 3,4-THPyS **J.19** and **J.19'** using $\text{NaBH}(\text{OAc})_3$ ^[338,339] (**Scheme 121b**). Rewardingly, very good yields and high diastereoselectivities were achieved.

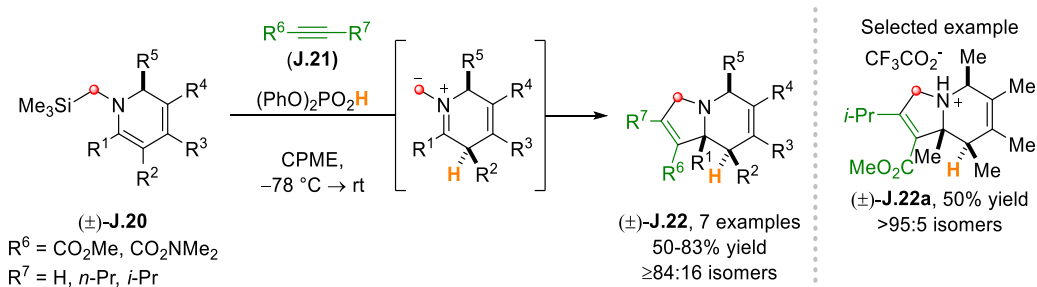


Scheme 121. Synthesis of tetrahydropyridines (THPyS) *via* (a) one-pot protonation/nucleophilic addition^[338] and *via* (b) one-pot Rh^{I} -catalysed C–H alkenylation/electrocyclisation/protonation/reduction.^[338,339]

Beyond proton as an electrophile for iminium ion generation, the authors established a similar one-pot sequence using alkyl triflates and halides as alkylating agents. Subsequent hydride reduction or carbon nucleophile addition enabled the generation of up to two new quaternary carbons with controlled diastereoselectivity.^[340]

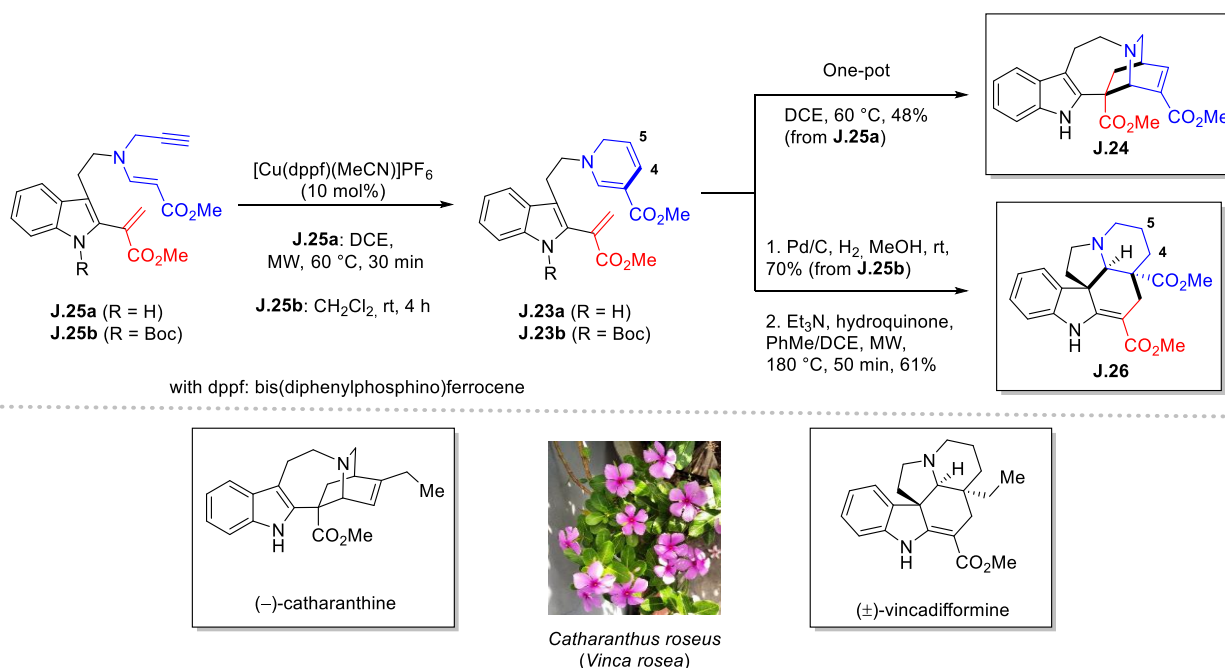
In addition, 1,2-dihydropyridines **J.20** derived from (trimethylsilyl)methylamine were found to generate azomethine ylides after protonation with $(\text{PhO})_2\text{PO}_2\text{H}$ in cyclopentyl methyl ether (CPME) (**Scheme 122**).^[341] Subsequent [3+2] cycloaddition with activated alkyne dipolarophiles **J.21** generated original indolizidines **J.22** that were isolated as their triflic acid salts. The authors developed additional fascinating transformations from their 1,2-dihydropyridines, but

also from the produced tetrahydropyridines,^[337] which are not further discussed in this manuscript.



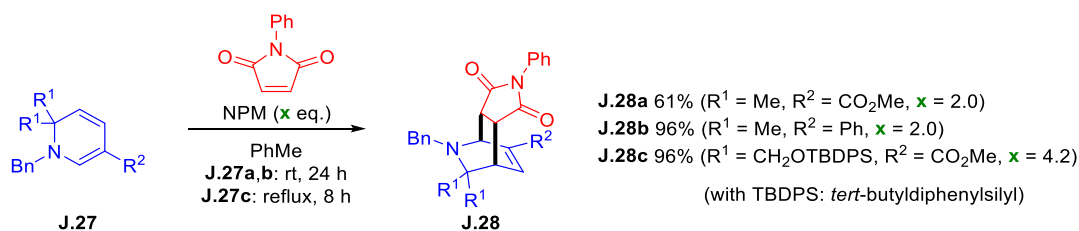
Scheme 122. Indolizidine synthesis via [3+2] cycloaddition of *in situ* formed azomethine ylides and alkynes.^[341]

Another common application of 1,2-dihydropyridines is their use as dienes in DIELS-ALDER [4+2] cycloadditions.^[342,343] In 2014, OGURI and co-workers made excellent use of this reactivity in a biogenetically inspired [4+2] cycloaddition of α -primary 1,2-dihydropyridine **J.23a** ($R = \text{H}$) to access *iboga*-type compound **J.24** (**Scheme 123**, top).^[344] Rewardingly, **J.24** was obtained in a cascade sequence from the corresponding enyne **J.25a** in 48% yield. Their catalytic system was also applied to the asymmetric total synthesis of (-)-catharanthine, a natural alkaloid from *Catharanthus roseus* (**Scheme 123**, bottom). Moreover, 1,2-dihydropyridine **J.23b** ($R = \text{Boc}$) was regioselectively hydrogenated on the more electron-rich C4-C5 double bond to give the corresponding isolable tetrahydropyridine in 70% yield from enyne **J.25b** (**Scheme 123**, top). Next, microwave-assisted heating in the presence of triethylamine and hydroquinone (to prevent polymerisation) caused thermal Boc deprotection, enabling [4+2] cyclisation towards *aspidosperma*-type compound **J.26**. (±)-Vincadifformine was prepared based on this strategy (**Scheme 123**, bottom).



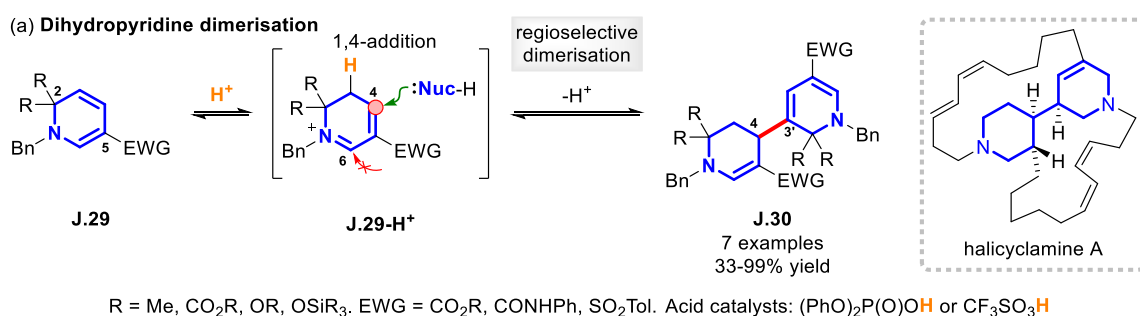
Scheme 123. Bio-inspired syntheses of *iboga*- and *aspidosperma*-type alkaloids.^[344]

Furthermore, OGURI and co-workers examined the capacity of α -tertiary 1,2-dihydropyridines **J.27** to act as dienes in DIELS-ALDER [4+2] cycloadditions with *N*-phenylmaleimide (NPM) as activated dienophile (**Scheme 124**).^[345] Dihydropyridine **J.27a** afforded isoquinuclidine **J.28a** in 61% yield at room temperature. Shifting from the electron-withdrawing ester in C5 position to a phenyl affords a richer diene **J.27b**. As expected, an enhanced [4+2] cycloaddition efficiency was observed and led to isoquinuclidine **J.28b** in excellent 96% yield. Interestingly, increasing the steric hindrance in C2 position, had a significant effect on the ease of cycloaddition. In fact, dihydropyridine **J.27c** was refluxed in toluene using a greater excess of NPM to produce isoquinuclidine **J.28c** in 96% yield. In all cases, only the formation of the favoured *endo*-isomer is described.

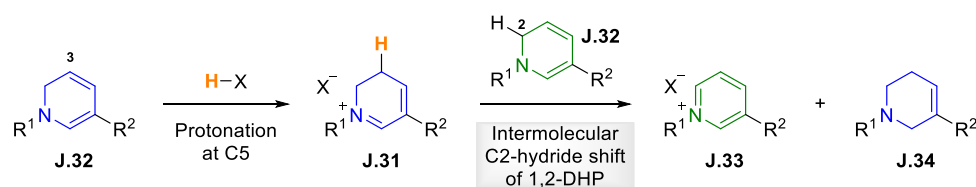


Scheme 124. DIELS-ALDER reactions of α -tertiary 1,2-dihydropyridines with *N*-phenylmaleimide.^[345]

In addition, OGURI and co-workers studied the BRØNSTED acid-catalysed regio- and chemoselective dimerisation of α -tertiary 1,2-dihydropyridines **J.29** to access bis-nitrogenated cores **J.30** present in manzamine alkaloids (e.g. halicyclamine A) (**Scheme 125a**).^[345] Typically, such biomimetic dimerisations were performed from pre-formed iminium salts **J.31** (**Scheme 125b**) and required sacrificial 1,2-dihydropyridine **J.32** or another hydride reagent such as NaBH_4 . This novel approach elegantly circumvents the necessity of an additional hydride source. The α -tertiary character of the dihydropyridine substrates was essential for the excellent regio- and chemoselectivities. In fact, disproportionation of the iminium ions **J.31** is commonly observed, yielding the corresponding pyridinium ion **J.33** and tetrahydropyridine **J.34** (**Scheme 125b**). The absence of a C2 hydrogen, however, impedes disproportionation *via* C2-hydride shift. Importantly, the ester functionality on the C5 position was crucial to assure regioselective C3-protonation, as well as the site-selective nucleophilic addition on the C4 position for C-C bond formation.

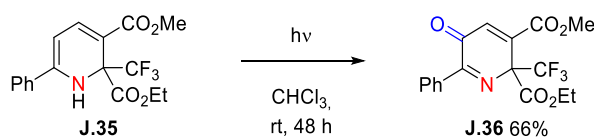


(b) **Dihydropyridine disproportionation**



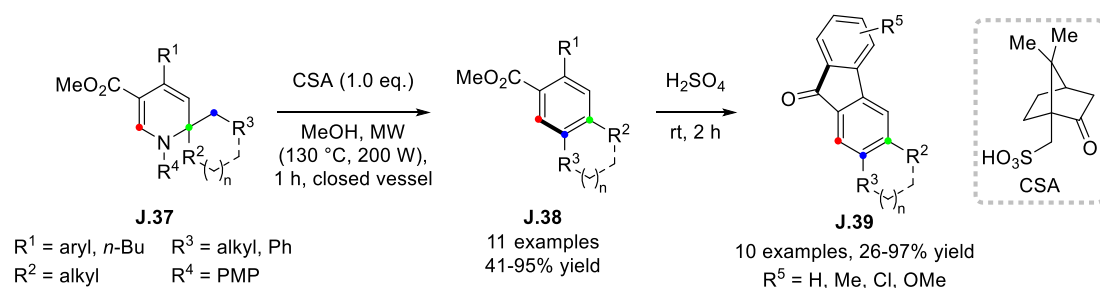
Scheme 125. (a) BRÖNSTED acid-catalysed dimerisation of α -tertiary 1,2-dihydropyridines; (b) disproportionation reaction of 1,2-dihydropyridines.^[345]

In contrast to often oxidation-labile α -primary 1,2-dihydropyridines, α -tertiary 1,2-dihydropyridines are generally quite stable under air. NOVIKOV and co-workers, however, observed that 1,2-dihydropyridine **J.35**, bearing a free amino group, undergoes slow aerobic oxidation to 5-pyridone **J.36** in CHCl₃ under light.^[346] The role of light was not further commented.

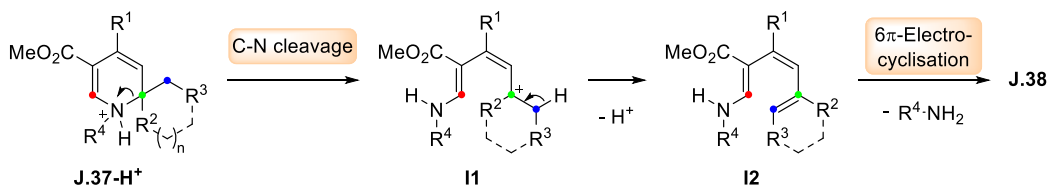


Scheme 126. Aerobic oxidation of 1,2-dihydropyridine **J.35** to 5-pyridone **J.36**.^[346]

Another compound class accessible from 1,2-dihydropyridines are benzoic esters. They are key industrial building blocks to produce value-added chemicals and materials. In 2016, TEJEDOR and co-workers showed that α -tertiary 1,2-dihydropyridines **J.37**^[318] afford polysubstituted benzoic esters **J.38** under microwave irradiation using camphor sulfonic acid (CSA) in MeOH as green solvent (**Scheme 127**, top).^[347] Interestingly, spirocyclic 1,2-dihydropyridines led to annulated bicyclic benzoic esters in 58-95% yield. Mechanistically, this transformation is believed to initiate through site-selective *N*-protonation of dihydropyridine **J.37**, enabling C-N bond activation and cleavage (**Scheme 127**, bottom). The latter requires the formation of a stabilised carbocation **I1**, which is ensured with α -tertiary 1,2-dihydropyridines. Generation of an enamine triene **I2** through proton elimination, followed by 6 π -electrocyclisation and amine elimination delivers the benzoic ester **J.38**. Beneficially, benzoic esters bearing an aromatic R¹ group were further derivatised into fluorenones **J.39** using sulphuric acid.



Proposed mechanism



Scheme 127. Preparation of benzoic esters **J.38** and fluorenones **J.39** from α -tertiary 1,2-dihydropyridines **J.37**.^[347]

4. Biological Relevance of 1,2-Dihydropyridines – State of the Art

In contrast to 1,4-dihydropyridines, which have repeatedly served as core structures for blockbuster drugs, their 1,2-dihydropyridine isomers are less associated with biological activities. Nevertheless, several reports on biologically active 1,2-dihydropyridines can be found in literature possessing diverse bioactivities, such as anti-ulcer ($X = \text{N-CN}$ or N-NO_2)^[348] or anti-cancer ($X = \text{NH}$ or O , e.g., compound **J.40**^[349])^[349–351] activities (**Figure 28**). A prominent example of a natural bioactive dihydropyridine is huperzine A (**Figure 28**), a sesquiterpene alkaloid, known as reversible acetylcholinesterase (AChE) inhibitor.^[352] Huperzine A is currently commercialised as a nutrient supplement and believed to act as a cognitive enhancer beneficially affecting memory and concentration. Yet, these compounds feature varying $C_{\text{sp}2}$ -heteroatom-based functional groups in the C2 position. Examples of 1,2-dihydropyridines incorporating a saturated $C_{\text{sp}3}$ -carbon in C2 position, however, are rare and have only emerged in recent years. Bioactive compounds based on this rather underexplored but promising core will be the focus of this part revealing their potential as anti-viral and antiproliferative agents among other bioactivities.

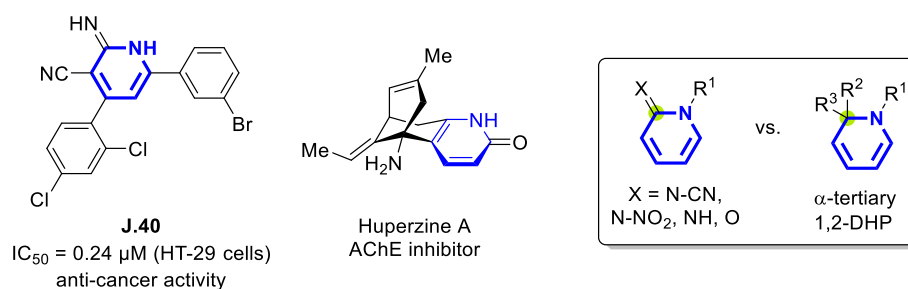
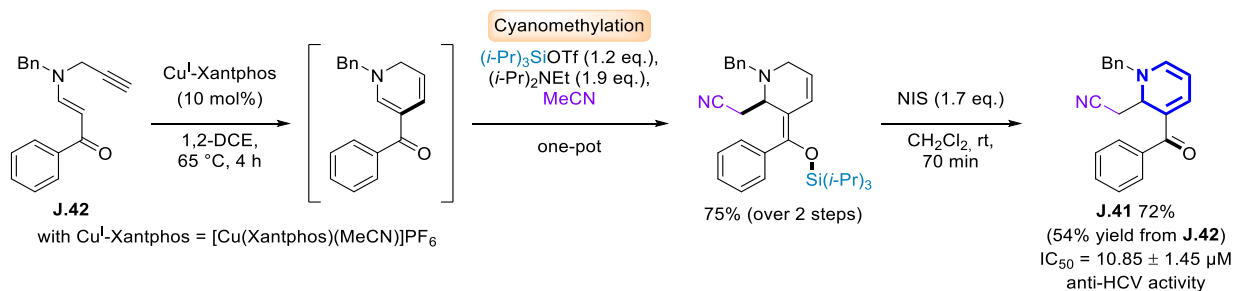


Figure 28. **J.40** and huperzine A as examples of $C_{\text{sp}2}$ -based bioactive 1,2-dihydropyridines compared to α -tertiary derivatives.

IC_{50} : minimal compound concentration required to produce 50% inhibition *in vitro*.

As first example, OGURI and co-workers evaluated in 2017 the anti-hepatitis C virus (HCV) activity of 1,2-dihydropyridine **J.41** and observed a promising IC₅₀ value of 10.85 ± 1.45 μM (**Scheme 128**).^[353] HCV infections frequently cause liver cirrhosis and hepatocellular carcinoma. This represents a non-negligible threat to public health worldwide and to date there is no vaccine available. Most currently approved anti-HCV agents operate upon protein inhibition but are prone to the emergence of drug resistance and rely on costly multi-step syntheses. Dihydropyridine **J.41**, in contrast, is obtained in three steps from propargylamine **J.42** in 54% yield.



Scheme 128. Synthesis of the first anti-HCV active 1,2-dihydropyridine **J.41**.^[353]

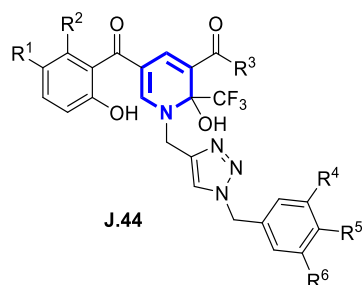
Furthermore, BOSICA and co-workers evaluated the antiproliferative activity of several HANTZSCH-like 1,2-dihydropyridines **J.43** against six human solid tumour cell lines (**Table 35**).^[315] Growth inhibition-50 (GI₅₀) concentration values were determined for several of their synthetic compounds and cisplatin (CDDP) as a reference drug. Among the compounds screened, **J.43a-e** protruded with a GI₅₀ value < 7 μM and with a great competitiveness compared to CDDP for all cell lines, especially for T-47D and WiDr cells. However, no control, i.e., non-tumour human cell line was included in the study. Thus, no selectivity indexes to evaluate the impact of their compounds on “healthy” cells were given.

Table 35. Antiproliferative activity of 1,2-dihydropyridines **J.43a-e** against human tumour cell lines.

Compound	Cell line					
	A549	HBL-100	HeLa	SW1573	T-47D	WiDr
J.43a	14 ± 3.1	19 ± 3.0	12 ± 4.5	22 ± 1.2	17 ± 3.6	17 ± 1.2
J.43b	5.1 ± 0.3	4.8 ± 0.4	2.7 ± 0.5	5.6 ± 1.0	4.0 ± 0.3	3.3 ± 0.5
J.43c	43 ± 14	42 ± 6.2	26 ± 4.0	49 ± 12	33 ± 5.1	41 ± 9.6
J.43d	18 ± 4.9	20 ± 0.9	22 ± 6.6	18 ± 6.8	22 ± 2.1	18 ± 1.6
J.43e	16 ± 6.7	16 ± 3.5	4.9 ± 1.0	11 ± 1.7	15 ± 1.9	19 ± 3.3
CDDP	4.9 ± 0.2	1.9 ± 0.2	1.8 ± 0.5	2.7 ± 0.4	17 ± 3.3	23 ± 4.3

GI₅₀ values < 10 μM are indicated in bold. Data given represent the average over two independent replicates. CDDP: cisplatin.

Recently, RAJU and co-workers synthesised a series of 1*H*-1,2,3-triazolyl-1,2-dihydropyridines **J.44** and evaluated their bioactivity profile (Scheme 129).^[354] Some compounds showed potent antiproliferative activity against HeLa cell line, as well as promising free radical scavenging (DPPH, ABTS^{•+}), α -glucosidase inhibitory, and anti-inflammatory activities.

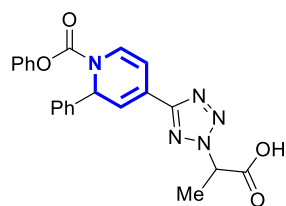


Antiproliferative activity against HeLa: IC₅₀ up to 4.18 μ M
 DPPH scavenging: SC₅₀ up to 9.28 μ g/mL
 ABTS^{•+} scavenging: SC₅₀ up to 7.03 μ g/mL
 α -Glucosidase inhibition: IC₅₀ up to 28.58 μ g/mL
 Anti-inflammatory activity: IC₅₀ up to 1.52 μ g/mL

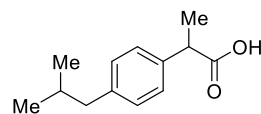
Scheme 129. Antiproliferative, free radical scavenging, anti-hyperglycaemic, and anti-inflammatory active 1*H*-1,2,3-triazolyl-1,2-dihydropyridines J.44.^[354]

IC₅₀: minimal compound concentration required to produce 50% inhibition *in vitro*. SC₅₀: sample concentration reducing the concentration of the compound to be scavenged to half of its initial value. DPPH: 1,1-diphenyl-2-picrylhydrazyl; ABTS: 2,2'-azino-bis(3-ethylbenzothiazoline-6-sulphonic acid).

KNAUS and KUMAR also reported anti-inflammatory activities for several 1,2-dihydropyridines bearing tetrazoles in the C4 position. Scheme 130 shows the inflammatory inhibition percentage of the most potent compound **J.45** compared to ibuprofen.^[355]



J.45 (75 mg/kg oral dose)
 % inhibition (3 h): 69.2 \pm 0.2
 % inhibition (5 h): 75.3 \pm 3.0

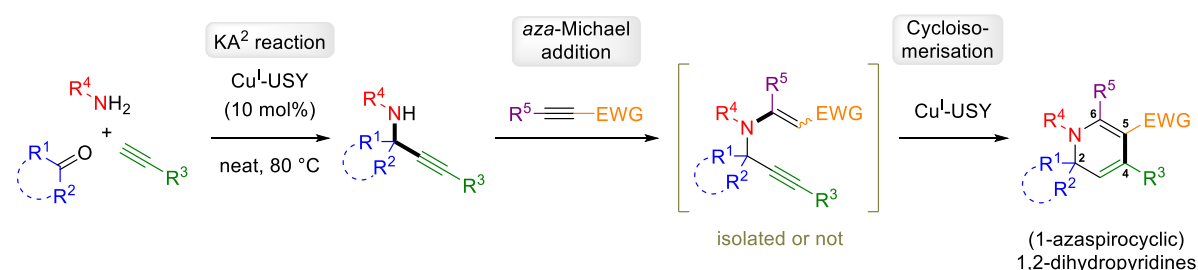


Ibuprofen (100 mg/kg oral dose)
 % inhibition (3 h): 44
 % inhibition (5 h): 52

Scheme 130. Anti-inflammatory activity of 1,2-dihydropyridine J.45 vs. ibuprofen for the same biological model.^[355]

5. Synthesis of 1,2-Dihydropyridines from Propargylamines: Results and Discussion

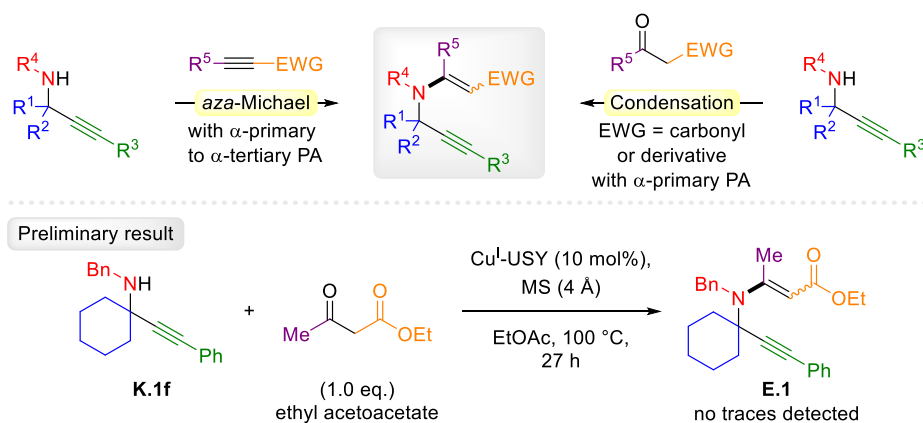
Given their therapeutic and synthetic interest, we targeted the synthesis of 1,2-dihydropyridines. As previously described in section I-3.3.2., this scaffold can be accessed from propargylamines *via* the cycloisomerisation of an 3-*aza*-1,5-enyne (Scheme 131). Complementary to most existing procedures, we primarily aimed at the formation of α -tertiary 1,2-dihydropyridines, and more particularly focussed on 1-azaspirocyclics. Conveniently, the propargylamine precursors are easily accessible through the Cu^I-USY-catalysed KA² reaction (for details, see section III-2.) with primary amines, allowing for three diversification points. In the following sections, the results of the enyne formation and cycloisomerisation reaction will be presented and discussed.



Scheme 131. Envisaged synthetic strategy to 1,2-dihydropyridines.

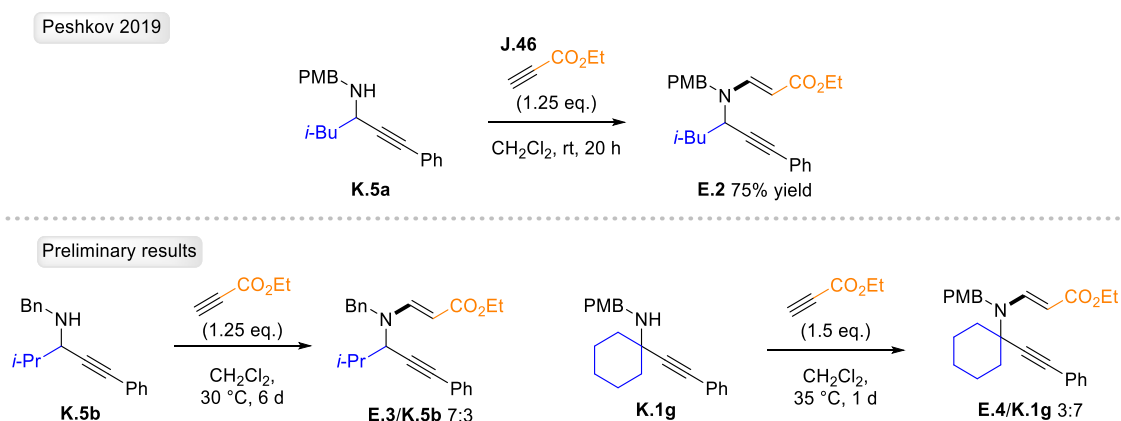
5.1. Optimisation of 3-*aza*-1,5-Enyne Synthesis

The generation of 3-*aza*-1,5-enynes from our α -tertiary propargylamines was envisaged through *aza*-MICHAEL addition using different alkyne-based MICHAEL acceptors (Scheme 132, top). It is worth mentioning that 3-*aza*-1,5-enynes are also commonly accessed through condensation of the amine with β -dicarbonyl compounds,^[332,356] including their use in cycloisomerisations into 1,2-dihydropyridines.^[357] This strategy has however only been reported with α -primary propargylamines, whereas their α -tertiary analogues are likely to be challenging substrates due to the steric hindrance around the nitrogen atom. Indeed, a preliminary test reaction with propargylamine **K.1f** and ethyl acetoacetate failed to give enyne **E.1** (Scheme 132, bottom). Electrophiles based on reactive C_{sp}-hybridised carbons, in turn, react more easily with such α -tertiary amines. Nevertheless, harsher conditions compared to the reaction with α -primary and α -secondary analogues are often needed.



Scheme 132. Synthesis of 3-aza-1,5-enynes via an aza-MICHAEL reaction or condensation approach.

As first illustration, PESHKOV and co-workers reported the synthesis of α -secondary enyne **E.2** in 75% isolated yield from propargylamine **K.5a** and ethyl propiolate (**J.46**) in CH_2Cl_2 at room temperature (Scheme 133, top).^[334] These conditions were thus used as a starting point and applied to structurally comparable, albeit slightly more sterically hindered, propargylamine **K.5b** (Scheme 133, bottom). Surprisingly, we observed an incomplete conversion after six days affording the desired enyne **E.3** in a 7:3 mixture with amine **K.5b**. Hence, such mild conditions seem to be inefficient, even with certain α -secondary propargylamines. Not surprisingly, a poor conversion of α -tertiary amine **K.1g** into enyne **E.4** was observed under similar conditions.

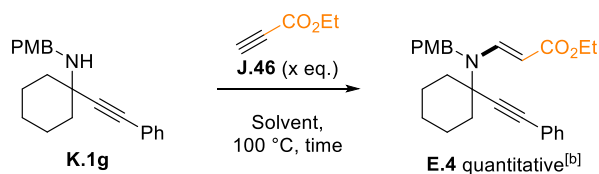


Scheme 133. First evaluation of aza-MICHAEL reaction conditions to access 3-aza-1,5-enynes.

Following these unsuccessful preliminary tests, the aza-MICHAEL addition was briefly evaluated under varying conditions using propargylamine **K.1g** and ethyl propiolate (**J.46**) (Table 36). Employing a large excess of **J.46** in MeCN at 100 °C afforded enyne **E.4** quantitatively and without the need for purification, yet requiring two hours for completion (entry 1). Switching to DCE with two equivalents of **J.46** also afforded a clean and complete reaction after 20 hours (entry 2). Under solvent-free conditions, four equivalents of **J.46** were needed to fully convert amine **K.1g** in 30 hours at 100 °C (entry 3). This suggested that the presence of a solvent is beneficial, which might be related to the volatility of ethyl propiolate (**J.46**). Refluxing solvent thus allows to “wash down” **J.46** that condensed on the flask walls above the reaction mixture, thus ensuring contact between both reagents. To replace DCE with a “greener”

alternative, EtOAc was evaluated next (entry 4). Rewardingly, under identical conditions, enyne **E.4** was obtained in comparable efficiency. Shifting to EtOH as a protic solvent, the reaction rate was drastically enhanced, affording enyne **E.4** in only 10 minutes in satisfying purity (entry 5). Similarly, *n*-BuOH and *t*-AmOH were found superior compared to the evaluated aprotic solvents (entries 6 and 7, respectively). Aiming to improve the economy of the *aza*-MICHAEL reaction, amine **K.1g** and ethyl propiolate (**J.46**) were used in near equimolar amounts in EtOH. This resulted, however, in significantly longer reaction time (from minutes to hours), which was solved by shifting to shorter reactors to prevent the condensation of propiolate above the solvent's "reflux front line" (entry 8). The faster conversion observed with protic solvents might originate from a stabilisation of the intermediate oxyanion *via* hydrogen bonding. Enhanced conversions in EtOH and *n*-BuOH (25 min) could arise from the greater H-donating abilities of these alcohols as compared to *t*-AmOH (60 min).^[358]

Table 36. Optimisation of the *aza*-MICHAEL reaction towards 1,5-enyne **E.4.^[a]**



Entry	Solvent	J.46 (eq.)	Time
1	MeCN	21.0	2.5 h
2	DCE	2.0	20 h
3	neat	4.0	30 h
4	EtOAc	2.0	21 h
5	EtOH	2.0	10 min
6	<i>n</i> -BuOH	2.0	25 min
7	<i>t</i> -AmOH	2.0	60 min
8 ^[c]	EtOH	1.05	15 min

^[a] Reaction run in an 8 mL sealed tube at 1 M concentration on a 0.2 mmol scale relative to amine **K.1g**, unless otherwise stated.

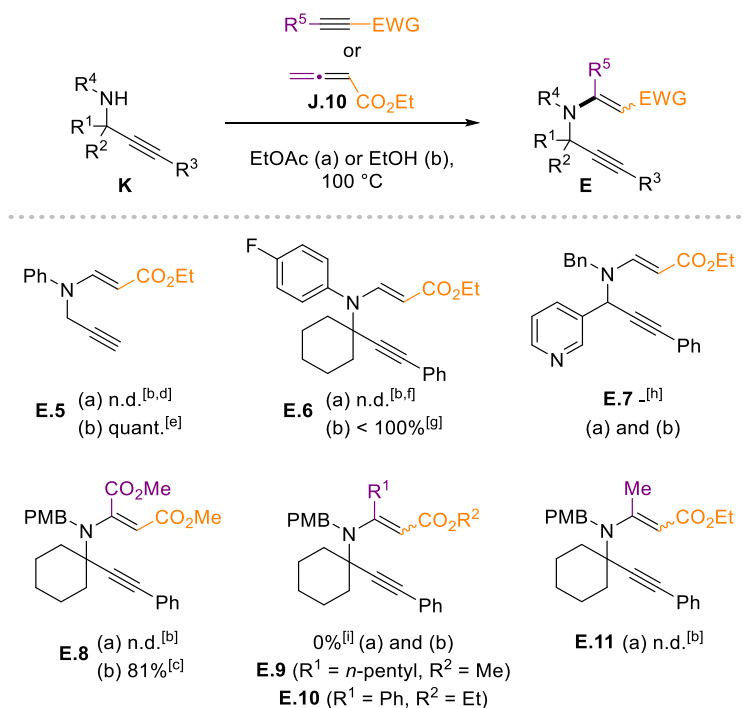
^[b] Complete conversion was observed in each case without the detection of by-products via ¹H NMR. ^[c] Reaction run in a 3 mL sealed tube at 1 M concentration.

It should be noted that several enynes were already prepared using the conditions from entry 4 in EtOAc and engaged in the cycloisomerisation reaction (discussed in section VI-5.2.), meanwhile, the optimisation of the enyne formation was continued in parallel. As the scope of successfully produced enynes can be deduced from the dihydropyridine scope shown in section VI-5.2., only particular examples are presented in [Scheme 134](#).

Indeed, certain enynes were obtained with improved chemoselectivity in EtOH (entry 8) compared to EtOAc (entry 4). Aniline-derived propargylamines, for instance, were found to be challenging compared to aliphatic analogues. A propargylamine derived from aniline, for instance, did not convert to enyne **E.5** at room temperature, while heating to 50 °C in EtOAc led

to partial degradation. In EtOH, however, the targeted enyne **E.5** was obtained in satisfying purity within five hours. Not surprisingly, producing the sterically and electronically deactivated 4-fluoro-aniline-derived enyne **E.6** was even more difficult. In EtOAc at 100 °C, the progressive addition of a total of 12 equivalents of **J.46** over two weeks was needed to give full conversion. In sharp contrast, **E.6** formed much cleaner and faster running the reaction for 18 hours in EtOH. Nevertheless, small amounts of an unidentified by-product were still observed. Unfortunately, the pyridine motif was completely incompatible with both reaction conditions resulting in rapid degradation of the propargylamine and no traces of the desired enyne **E.7**.

Next, disubstituted propiolates were tested with propargylamine **K.1g** in the perspective of tetrasubstituted 1,2-dihydropyridines bearing a C5 substituent. Using dimethyl acetylene dicarboxylate (DMAD) in EtOAc gave a complex mixture of enyne **E.8** and several unknown by-products requiring two days to reach full conversion of **K.1g**. Fortunately, in EtOH, the reaction was complete within five minutes and enyne **E.8** was obtained in a cleaner crude mixture. Purification over silica gel afforded **E.8** in high 81% yield. The use of alkyl- or aryl-substituted propiolates, however, completely impeded *aza*-MICHAEL addition in EtOAc and EtOH, leading to no traces of enynes **E.9** and **E.10**. Furthermore, allenolate **J.10** was evaluated in EtOAc at 100 °C but resulted in a complex mixture containing enyne **E.11**, traces of the corresponding dihydropyridine and several unknown by-products.



Scheme 134. Overview of challenging enyne syntheses.^[a]

^[a] Reactions were run in sealed tubes at 1 M concentration. 2.0 eq. and 1.05 eq. of electrophile were used in EtOAc or EtOH, respectively, unless otherwise stated. ^[b] Product formation observed but present in a complex mixture due to by-product formation. ^[c] Isolated yield. ^[d] No conversion of propargylamine was observed at room temperature, then heated to 50 °C. ^[e] Determined from crude mass due to satisfying ¹H NMR spectrum. ^[f] 12.0 eq. of ethyl propiolate (**J.46**) were used and the reaction was stirred for 14 d. ^[g] Presence of a small amount of unknown by-product. ^[h] Degradation without detection of enyne **E.7**. ^[i] No conversion observed using 5.0 eq. of propiolates.

5.2. Evaluation of Cu^I-USY as Cycloisomerisation Catalyst

With suitable conditions for enyne formation in hand, the cycloisomerisation conditions were optimised next.

5.2.1. Optimisation of the Cycloisomerisation Conditions

To begin, reported metal-free procedures were evaluated to perform the cycloisomerisation of enyne **E.4** into dihydropyridine **D.1a** (Table 37). VARALA's thermal conditions^[327] (for details, see section VI-2.2.5.), i.e., stirring enyne **E.4** in 1,2-dichlorobenzene (DCB) at 180 °C, unfortunately did not give any conversion (entry 1). Likewise, heating enyne **E.4** in MeOH^[326] to up to 100 °C did not yield dihydropyridine **D.1a** (entry 2). The lack of reactivity of **E.4** under these conditions most likely arises from its different substitution frame compared to the 3-*aza*-1,5-enynes originally used in these procedures.

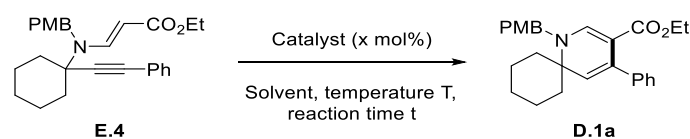
Consequently, we turned our attention to transition metal catalysts, starting with copper as the most represented metal for the cycloisomerisation of this enyne class. Indeed, heating enyne **E.4** in EtOAc at 100 °C in the presence of Cu(OTf)₂ (10 mol%) afforded dihydropyridine **D.1a**, albeit in 30 hours and with unsatisfying chemoselectivity (42% yield) (entry 3). [Cu(MeCN)₄][PF₆] (5 mol%), in turn, proved to be very active leading to a fast conversion of enyne **E.4** in 1,2-dichloroethane (DCE) at 100 °C (entry 4). Unfortunately, the reaction mixture starts to degrade after two hours, before reaching full conversion of enyne **E.4** (entry 5). Reducing the reaction temperature to 65 °C still afforded a reasonable conversion (95% after 15 hours) but led to a moderate 49% yield (entry 5). Shifting to Cu₂O (20 mol%) in DCE at 80 °C resulted in an improved yield of 73% in a comparable time (entry 6).

Aiming to establish an efficient procedure based on a supported catalyst, conditions reported by OGURI and co-workers^[332] were employed, replacing their cationic [Cu(Xantphos)(MeCN)][PF₆] complex (10 mol%) with a Cu^I-USY/Xantphos combination at the same catalyst loading in DCE at 65 °C (entry 7). Unfortunately, no conversion was observed, similar to their observation using CuCl/Xantphos. Likewise, replacing CuBr with Cu^I-USY in PESHKOV's Cu^I/pyridine system in toluene at 90 °C^[334] resulted in only trace amounts of dihydropyridine **D.1a** (entry 8). Remarkably, running the reaction in DCE at 100 °C under ligand- and additive-free conditions, Cu^I-USY (10 mol%) efficiently delivered dihydropyridine **D.1a** in high 90% yield (entry 9). In sharp contrast, Ag^{0/I}-USY did not give any conversion under similar conditions (entry 10).

Since our research group is also interested in the preparation and catalytic applications of metal-doped polyoxometalates,^[359] this class of materials was briefly evaluated here. While Ag₂H₂SiW₁₂O₄₀ (5 mol% Ag) gave a complex mixture (entry 11), [P₂W₁₈O₆₂]⁶⁻

[Au(IPr)MeCN]⁺[H⁺]₅ (5 mol%) yielded dihydropyridine **D.1a** in 84% in only 30 min in DCE at 100 °C (entry 12). In comparison, using twice the catalyst loading for Au(JohnPhos)NTf₂ resulted in a notably lower reaction rate and yield (5 h, 72%) (entry 13). Shifting to AuCl₃ (10 mol%) led to poor conversion (67% after 30 h) and a low 7% yield of dihydropyridine **D.1a** partially due to the hydrolysis of enyne **E.4** (entry 14). Although [P₂W₁₈O₆₂]⁶⁻[Au(IPr)MeCN]⁺[H⁺]₅ outperformed Cu^I-USY in the cycloisomerisation of enyne **E.4** in terms of reaction rate (30 min vs. 21 h), its residual BRØNSTED acidity was incompatible with acid-sensitive substrates. Consequently, the optimisation was pursued with Cu^I-USY as the catalyst.

Table 37. Evaluation of cycloisomerisation conditions to yield dihydropyridine D.1a.



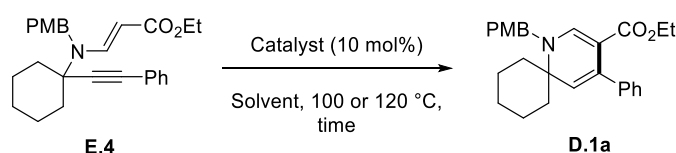
En-try	Catalyst (x)	Sol-vent	T (°C)	t (h)	Conv. ^[b] (%)	Yield ^[b] D.1a (%)
1	none	DCB	180	2.5	0	0
2	none	MeOH	100	16	0	0
3	Cu(OTf) ₂ (10)	EtOAc	100	30	100	42 ^[c]
4	[Cu(MeCN) ₄]PF ₆ (5)	DCE	100	2	n.d. ^[d]	n.d. ^[c]
5	[Cu(MeCN) ₄]PF ₆ (5)	DCE	65	15	95 ^[e]	49 ^[c]
6	Cu ₂ O (20)	DCE	80	17	100	73
7	Cu ^I -USY (10)/Xantphos (10)	DCE	65	22	0	0
8	Cu ^I -USY (10)/pyridine (1.0 eq.)	PhMe	90	15	n.d.	< 5%
9	Cu ^I -USY (10)	DCE	100	21	100	90 ^[f]
10	Ag ^{0/I} -USY (10)	EtOAc	100	23	0	0
11	Ag ₂ H ₂ SiW ₁₂ O ₄₀ (5, Ag)	DCE	100	2	n.d.	n.d. ^[c]
12	[P ₂ W ₁₈ O ₆₂] ⁶⁻ [Au(IPr)MeCN] ⁺ [H ⁺] ₅ (5, Au)	DCE	100	0.5	100	84 ^[f]
13	[Au(JohnPhos)]NTf ₂ (10)	DCE	100	5	100	72
14	AuCl ₃ (10)	DCE	100	30	67 ^[g,h]	7 ^[i]

^[a] Reactions run in a sealed tube at 83 mM concentration under argon. ^[b] Estimated from the crude mixture *via* ¹H NMR using 1,3,5-trimethoxybenzene as internal standard, unless otherwise stated. ^[c] Formation of unidentified by-products observed. ^[d] **D.1a**/**E.4** = 7:3. ^[e] **D.1a**/**E.4** = 91:9. ^[f] Isolated yield. ^[g] Partial enamine hydrolysis affording the corresponding propargylamine **K.1g**. ^[h] **D.1a**/**E.4** = 82:18. ^[i] Estimated 33% of enyne **E.4** remained unreacted. Conv.: conversion. DCB: 1,2-dichlorobenzene. n.d.: not determined. DCE: 1,2-dichloroethane.

Following the promising yield of dihydropyridine **D.1a** in DCE (Table 37, entry 9), a solvent screening was performed to identify a “greener” alternative (Table 38). Interestingly, for alcoholic solvents, conversions and yields improved with increasing lipophilicity of the solvent (EtOH < *n*-BuOH < *t*-AmOH, entries 2-4). In fact, EtOH led to incomplete conversion and a poor 38% yield after 30 hours at 100 °C (entry 2), whereas enyne **E.4** was fully consumed in *n*-BuOH but afforded a mixture of dihydropyridine **D.1a** and its *n*-butyl ester derivative in a combined 59% yield (entry 3). To avoid transesterification, *t*-AmOH, as a sterically hindered but

“green” solvent was evaluated. Rewardingly, dihydropyridine **D.1a** was obtained in improved 77% yield with a reduced reaction time of 21 hours (entry 4). Yet, this yield was notably lower than for the reaction in DCE (entry 1). Shifting to diethyl carbonate (DEC), however, resulted in a drop in yield to 63% (entry 5) and complicated product separation due to its high boiling point. Fortunately, running the reaction in EtOAc brought about the desired result. Dihydropyridine **D.1a** was isolated in 94% yield, thus outperforming undesired DCE (entry 6 vs. 1). Nevertheless, more than a day was needed to reach full conversion. Therefore, the reaction temperature was increased to 120 °C, which gave dihydropyridine **D.1a** in five hours but caused a notable decrease in yield to 82% (entry 7). As for the HPA reaction (for details, see section V-3.1.1.), our analogously prepared Cu^I-MOR zeolite, possessing a channel- instead of USY’s cage-type framework, yielded a comparably good but inferior result under identical conditions giving dihydropyridine **D.1a** in 87% yield (entry 8).

Table 38. Optimisation of copper-zeolite-catalysed cycloisomerisation of enyne **E.4 towards dihydropyridine **D.1a**.^[a]**



Entry	Catalyst	Solvent	Time (h)	Conv. ^[b] (%)	Yield ^[b] D.1a (%)
1	Cu ^I -USY	DCE	21	100	90 ^[c]
2	Cu ^I -USY	EtOH	30	88 ^[d]	38
3	Cu ^I -USY	<i>n</i> -BuOH	30	100	34 ^[e]
4	Cu ^I -USY	<i>t</i> -AmOH	21	100	77
5	Cu ^I -USY	DEC	30	100	63
6	Cu ^I -USY	EtOAc	30	100	94 ^[c]
7	Cu ^I -USY	EtOAc ^[f]	5	100	82
8	Cu ^I -MOR	EtOAc	30	94 ^[g]	87
9	CuCl	EtOAc	30	95 ^[g]	75
10	H-USY	EtOAc	24	n.d. ^[h,i]	0
11	none	EtOAc	18	0	0

^[a] Reactions run in a sealed tube at 83 mM concentration under argon. ^[b] Estimated from the crude mixture *via* ¹H NMR using 1,3,5-trimethoxybenzene as internal standard, unless otherwise stated. ^[c] Isolated yield. ^[d] **D.1a/E.4** = 77:23. ^[e] 25% yield of dihydropyridine bearing *n*-butyl ester observed. ^[f] Reaction run at 120 °C. ^[g] **D.1a/E.4** = 94:6. ^[h] Incomplete conversion. ^[i] Partial enamine hydrolysis affording the corresponding propargylamine **K.1g**. DCE: 1,2-dichloroethane. DEC: diethyl carbonate.

Furthermore, **D.1a** was obtained in 75% yield using CuCl (entry 9) which represents the copper precursor for our Cu^I-loaded zeolites. This shows the superiority of the metal-exchanged zeolite catalysts in this cycloisomerisation, as previously observed in the KA² and AYA/KYA reactions. Control experiments showed that neither the parent H-USY zeolite (entry 10), nor the absence of a catalyst (entry 11) in EtOAc at 100 °C promote enyne cycloisomerisation. In the

case of H-USY, however, partial enamine hydrolysis was observed, suggesting that the remaining protons in Cu^I-USY are not accessible, or not acidic enough to cause this side reaction.

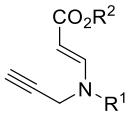
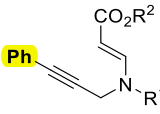
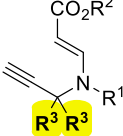
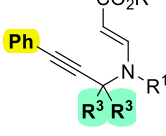
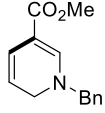
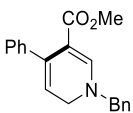
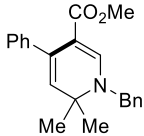
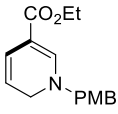
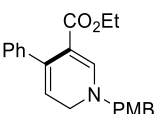
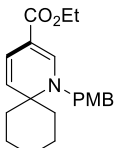
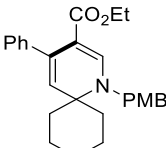
5.2.2. Effect of Enyne Substitution Degree and Catalyst Choice on the Cycloisomerisation: A Comparative Study

This section discusses the effect of the substitution frame of several 3-*aza*-1,5-enynes of type **B** (for details, see section VI-2.2.) regarding their performance in Cu^I-catalysed cycloisomerisation reactions. For this, some results obtained in the [Cu(Xantphos)(MeCN)]PF₆-catalysed cycloisomerisation reported by OGURI and co-workers are selected and summarised in **Table 39**.^[332] In addition, we performed a comparable series under Cu^I-USY zeolite catalysis to compare our catalyst to a more labour-intensive and sensitive cationic copper complex (**Table 39**).

Under OGURI's conditions, α -primary enyne **E.12**, lacking an alkyne substituent, underwent cycloisomerisation at room temperature to give 1,2-dihydropyridine **D.1b** in excellent 98% yield in 40 minutes. Substituting the alkyne with a phenyl group, thus increasing the steric hindrance around the alkyne LEWIS base, potentially renders π -complexation more difficult. Indeed, enyne **E.13** required more than double the reaction time than enyne **E.12** but still reacted at room temperature. The estimated yield of 1,2-dihydropyridine **D.1c**, however, was also found to be notably lower (82% vs. 98%). Introducing a *gem*-dimethyl propargyl substituent leading to α -tertiary enyne **E.14** probably further complicated π -complexation. As a result, stirring at 65 °C for 20 hours was necessary for cycloisomerisation. Nevertheless, α -tertiary dihydropyridine **D.1d** was obtained in 86% isolated yield.

As for OGURI's catalytic system, enyne **E.15** reacted at room temperature using our Cu^I-USY catalyst in EtOAc. Contrary to the short reaction times reported with [Cu(Xantphos)(MeCN)]PF₆, Cu^I-USY gave 75% conversion after 17 hours and led to a mixture of 1,2- and 1,4-dihydropyridines **D.1e**. Shifting to enyne **E.16** bearing a phenyl alkyne substituent required a temperature rise. While no conversion was observed at 50 °C, heating to 78 °C caused degradation, thus dihydropyridine **D.1f** was not obtained. To study the influence of the propargyl substituent independently from the substitution of the alkyne moiety, enyne **E.17** was progressively heated starting from room temperature. Heating to 78 °C was required, resulting in near full conversion after 42 hours. In contrast to enyne **E.16**, the corresponding dihydropyridine **D.1g** was obtained in 87% yield. Substitution of the alkyne or propargyl position thus caused a similar effect on the reactivities of the respective enynes **E.16** and **E.17** for the Cu^I-USY system. The α -tertiary character in **E.17**, however, conferred a chemoselective reaction affording exclusively the 1,2-dihydropyridine **D.1g** compared to α -primary enyne **E.15**.

Table 39. Evaluation and comparison of differently substituted enynes in Cu^I-catalysed cycloisomerisation reactions.

General Structure				
Catalytic System				
	E.12 (Oguri) E.15 (this work)	E.13 (Oguri) E.16 (this work)	E.17 (this work)	E.14 (Oguri) E.4 (this work)
OGURI [Cu ^I -Xantphos] (10 mol%) CH ₂ Cl ₂ or DCE			-	
	D.1b 98% ^[a] rt, 40 min	D.1c 82% ^[a] rt, 2 h		D.1d 99% ^[a] (86%) ^[b] 65 °C, 20 h
This work Cu ^I -USY (10 mol%) EtOAc				
	1,2-D.1e/1,4-D.1e (74:26) 75% conversion ^[c] rt, 17 h	D.1f - 78 °C, degradation	D.1g 87% ^[a] 78 °C, 42 h	D.1d 100 °C, 26 h ^[a] DHP 94%

^[a] Yield estimated from crude mixture *via* ¹H NMR using 4-nitrobenzonitrile as internal standard. ^[b] Isolated yield. ^[c] Conversion estimated from the crude mixtures *via* ¹H NMR using 1,3,5-trimethoxybenzene as internal standard. [Cu-Xantphos] refers to [Cu(Xantphos)(MeCN)]PF₆.

Last, the cycloisomerisation of enyne **E.4** was investigated at 78 °C and 100 °C in EtOAc to evaluate the effect of the phenyl alkyne substituent in addition to the cyclohexyl motif. As expected, **Figure 29** shows that cycloisomerisation to dihydropyridine **D.1a** is very slow at 78 °C, resulting in only 9% conversion after ten hours compared to an advanced 74% at 100 °C.

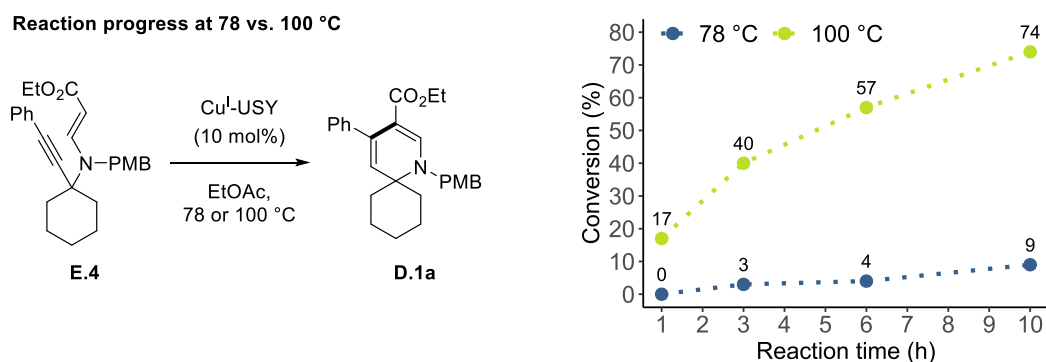


Figure 29. Reaction monitoring at 78 and 100 °C for the Cu^I-USY-catalysed cycloisomerisation of enyne E.4.

To conclude, Cu^I-USY was generally observed to be less active than cationic [Cu(Xantphos)(MeCN)]PF₆. In addition, OGURI's catalyst is reported to give a regio- and chemoselective 6-*endo*-dig cyclisation with α -primary 3-*aza*-1,5-enynes towards 1,2-dihydropyridines. Nevertheless, Cu^I-USY might offer a thermostable, easy-to-prepare, easy-to-handle, and reusable alternative for α -tertiary 3-*aza*-1,5-enynes operating in EtOAc as recommended solvent.

5.2.3. Hot Filtration Test and Recyclability Study of Cu^I-USY

A SHELDON test was conducted for enynes **E.4** and **E.15** setting up a reaction under optimised conditions in EtOAc at 100 °C and a 10 mol% Cu^I-USY loading. In both cases, no further conversion was observed after the zeolite catalyst was filtered off. As an example, **Figure 30a** shows the conversions of α -tertiary enyne **E.4** and the proportions of dihydropyridine **D.1a** for the filtered reaction compared to two non-filtered reference reactions running for seven and 48 hours, respectively. Our findings suggest that there is no evidence for the leaching of catalytically active copper species under our reaction conditions.

The recyclability of Cu^I-USY was evaluated in the cycloisomerisation reaction of enyne **E.4** (**Figure 30b**). After each reaction, the mixture was centrifuged, and the supernatant was decanted. The zeolite was washed three times with EtOAc, centrifuged and the supernatant was decanted. Recovered Cu^I-USY was then directly employed in the next run without reactivation. Gratifyingly, dihydropyridine **D.1a** was obtained in a constantly high 94% yield in 26 hours until the third run. In the fourth run, the recycled catalyst afforded **D.1a** with equally high chemoselectivity even though a slightly prolonged reaction time (31 h) was required to achieve complete conversion. This indicates a small but noticeable erosion of the catalytic activity, perhaps due to coke formation.^[360]

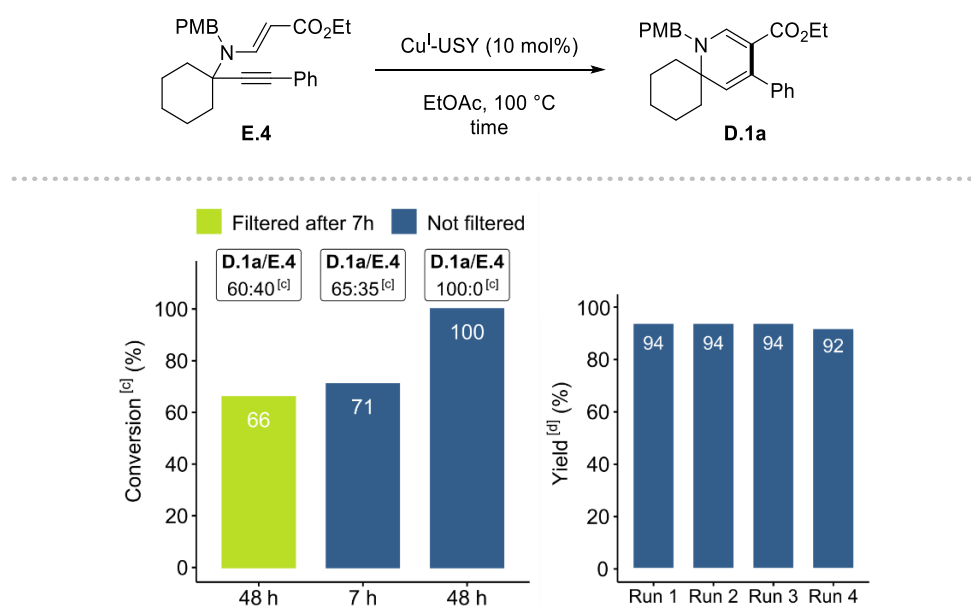
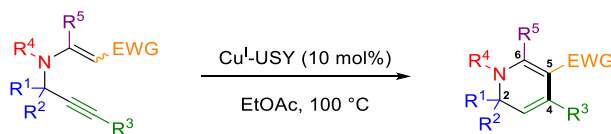


Figure 30. Hot filtration test^[a] (left) and recyclability study^[b] (right) for the Cu^I-USY-catalysed cycloisomerisation of enyne **E.4** to dihydropyridine **D.1a**.

^[a] Reactions run with 10 mol% catalyst in EtOAc (at 0.3 M concentration) at 100 °C for indicated time. ^[b] Reactions run with 10 mol% catalyst in EtOAc (1 M) at 100 °C for 26 h (run 1 to 3). For run 4, 83% conversion was observed after 26 h and 31 h afforded full conversion. ^[c] Conversions and **D.1a** to **E.4** proportions were determined from the crude mixtures *via* ¹H NMR. The estimated yields from left to right were as follows: 60%, 66% and 92%. ^[d] Yield estimated from crude mixtures *via* ¹H NMR using 1,3,5-trimethoxybenzene as internal standard.

5.3. Scope and Limitations

With the optimised conditions in hand, the scope and limitations of this cycloisomerisation procedure were scrutinised. The enynes synthesised for this purpose were characterised and used without intermediate purification unless otherwise stated. All diversification points in the enyne were varied throughout the scope to unravel their respective influence on the efficiency of the cycloisomerisation reaction (Scheme 135). The electronic properties and the size of the amine substituent were changed. Moreover, enynes bearing different propargylic substituents, including α -primary to -tertiary examples, were employed, resulting in different C2 substituents in the dihydropyridines. Furthermore, the nature of the alkyne moiety was varied to evaluate the scope of the C4 substitution in dihydropyridines. The enamine frame was also modified, resulting in dihydropyridines with different C5/C6 substituents.



Scheme 135. Diversification points examined during the scope study.

5.3.1. Amine Substituent

First, we evaluated the influence of the amine substituent on the efficiency of our cycloisomerisation protocol (Scheme 136).

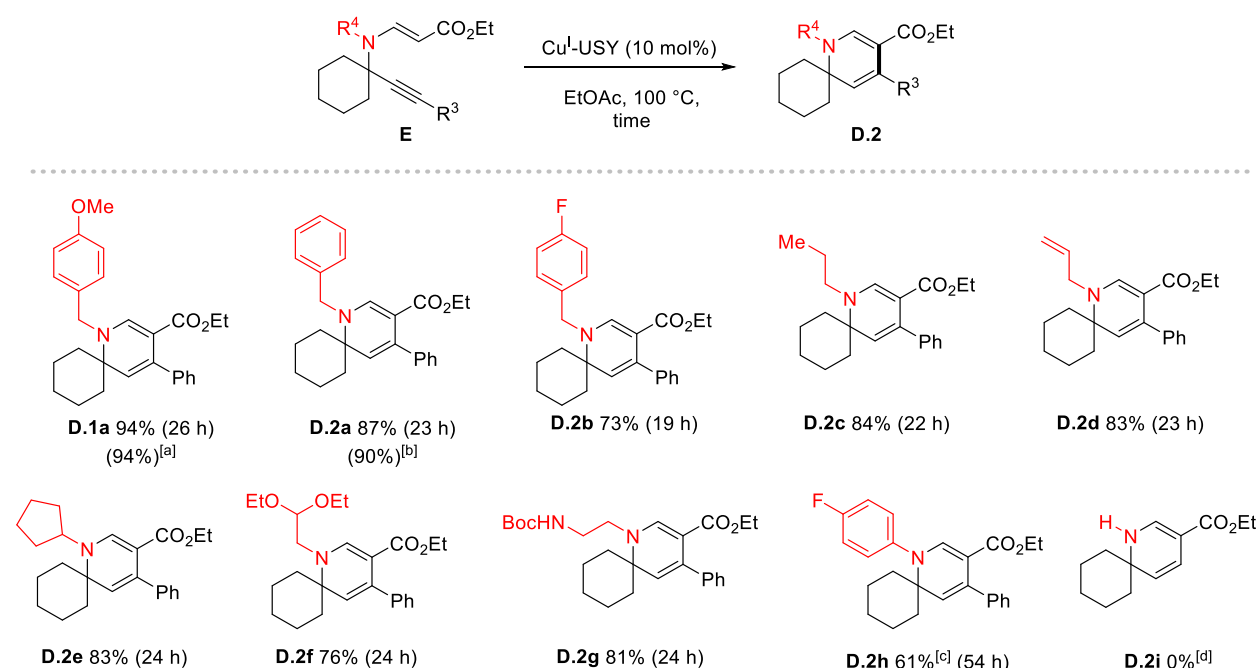
Evaluating a series of benzylamines, a progressive decrease in yield was observed depending on the electronic properties of the aryl ring. In fact, when shifting from 4-methoxybenzylamine to benzylamine and 4-fluorobenzylamine, the yield of the corresponding dihydropyridines evolved from 94% (**D.1a**) to 87% (**D.2a**) to 73% (**D.2b**) yield, respectively. From a mechanistic viewpoint, this could be rationalised by a stronger σ -donating amine substituent facilitating the nucleophilic addition of the enamine β -carbon onto the alkyne-metal π -complex in a 6-*endo*-dig fashion. This could hint towards the Cu^I-USY-catalysed cycloisomerisation reaction following **path b** or **c** with zwitterion **I4** as key intermediate as presented in Scheme 112. Fortunately, the cycloisomerisation was equally efficient on gram-scale for dihydropyridine **D.1a**. Moreover, it is worth mentioning that the *aza*-MICHAEL addition/cycloisomerisation sequence is equally efficient when performed as a sequential one-pot procedure, i.e., without intermediate solvent evaporation. For this, the enyne formation step is run with equimolar amounts of propargylamine and propiolate. In this way, dihydropyridine **D.2a** was obtained in 90% estimated yield.

Besides benzylamines, other aliphatic amine-derived enynes efficiently led to the desired dihydropyridines in good yields. Examples include *n*-propyl- and allyl-derived dihydropyridines **D.2c** and **D.2d**, obtained in a comparable yield to the benzylamine analogue **D.2a**. The presence

of a branched aliphatic amine with increased steric hindrance, such as cyclopentylamine, did not negatively impact the cycloisomerisation. Indeed, dihydropyridine **D.2e** was isolated in 83% yield. Furthermore, amines bearing acid-sensitive functional groups such as acetals and Boc-carbamates were compatible with our conditions, producing dihydropyridines **D.2f** and **D.2g** in comparable yields and reaction times (76% for **D.2f**, 81% for **D.2g**).

Next, aniline derivatives were scrutinised, which we believed more challenging due to the delocalisation of the nitrogen electron lone pair in the π -system of the aromatic substituent. Remarkably, the strongly deactivating 4-fluorophenyl substituent still afforded dihydropyridine **D.2h** in promising 61% yield. Nevertheless, a prolonged reaction time of 54 hours was required compared to the aliphatic examples, such as the 4-fluorobenzylamino analogue **D.2b**.

Next, the compatibility of an unsubstituted, i.e., free NH, was examined. Unfortunately, the reaction mixture started degrading without detecting traces of the desired dihydropyridine **D.2i** leaving mostly unreacted starting material behind. To the best of our knowledge, no successful cycloisomerisation example of a similar 3-*aza*-1,5-enyne bearing a free N-H moiety has been reported in the literature. Overall, our results suggest that a certain enamine nucleophilicity is a prerequisite for the successful cycloisomerisation reaction under Cu^I-USY catalysis.



Indicated yields correspond to isolated yields obtained over two steps starting from the corresponding propargylamines, unless otherwise stated. General reaction conditions: reactions run in a sealed tube in EtOAc (1 M) at 100 °C using 10 mol% of Cu^I-USY catalyst for the indicated time. [a] Isolated yield obtained starting from 1.0 g of the corresponding enyne in a reaction run under standard conditions. [b] Estimated yield for a sequential one-pot *aza*-MICHAEL addition/cycloisomerisation sequence using ethyl propiolate (**J.46**, 1.0 eq.) in EtOAc to form the corresponding enyne. [c] 10% of the corresponding propargylamine isolated. [d] Reaction run in a degassed EtOAc solution at 78 °C leading to the degradation of the enyne starting material.

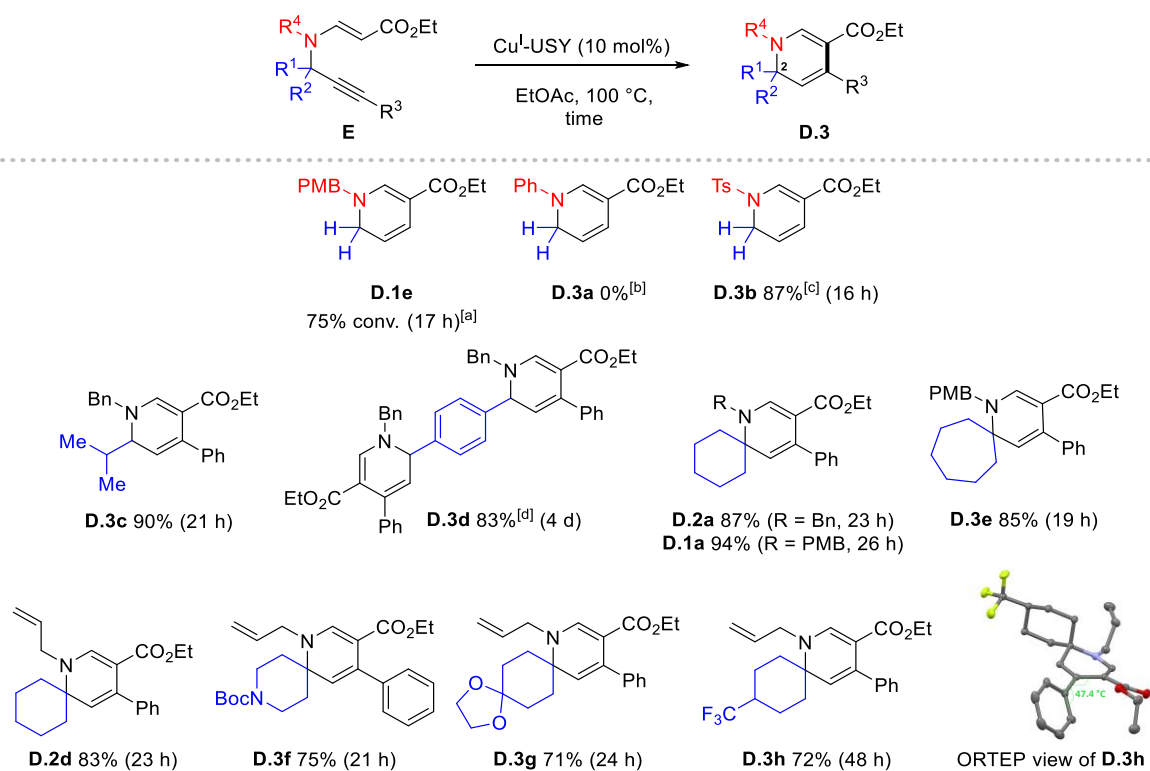
5.3.2. Propargyl Substituent

In a second set of experiments, the effect of the enyne propargyl substituent, i.e., the C2 substituent in the dihydropyridine product, was investigated (Scheme 137).

In the absence of any propargyl substituent and unlike dihydropyridine **D.1e** incorporating a 4-methoxybenzylamino substituent, its aniline analogue **D.3a** did not form at room temperature, stressing again the deactivating effect of aromatic amines. Heating the reaction mixture to 40 °C, however, initiated the slow but progressive degradation of the corresponding enyne, which is in line with the findings of VARALA and co-workers.^[327] Replacing the aniline substituent with a tosyl group restored the chemoselectivity, yielding 1,2-dihydropyridine **D.3b** in 87%. A temperature rise to 120 °C was nevertheless necessary, highlighting the strongly deactivating effect of the tosyl compared to its 4-methoxybenzylamine analogue (→ **D.1e**). Rewardingly, the corresponding pyrrole, possibly resulting from a competing *aza*-Claisen rearrangement/*5-exo*-dig cyclisation, as sometimes observed with other catalytic systems,^[69,324] was not detected.

α -Secondary enynes were evaluated next under Cu^I-USY catalysis. Rewardingly, dihydropyridine **D.3c** bearing an *i*-propyl substituent was isolated in a similar yield to the analogous cyclohexyl-substituted dihydropyridine **D.2a**. Moreover, our conditions afforded bis-dihydropyridine **D.3d** in good 83% yield. Yet the reaction required four days for completion, possibly due to the low solubility of the starting material in EtOAc. Whereas the *i*-propyl substituted dihydropyridine **D.3c** proved stable, bis-dihydropyridine **D.3d** degraded with time.

Next, we turned our attention again towards the synthesis of intriguing 1-azaspirocyclic dihydropyridines. Shifting from cyclohexyl to cycloheptyl caused a small reduction in yield (85% for **D.3e** vs. 94% for **D.1a**). The greater steric hindrance of the seven-membered ring possibly makes π -complexation more challenging, thus lowering the cycloisomerisation efficiency. Furthermore, dihydropyridines **D.3f-h** bearing functionalised six-membered rings were obtained in good yields. The acid-labile Boc-carbamate and 1,2-ethanediol-ketal in dihydropyridines **D.3f,g** were well tolerated, achieving 75% and 71% yield, respectively. Nevertheless, their yields are slightly reduced compared to **D.2d** (83% yield). Strikingly, the formation of dihydropyridine **D.3h** equipped with a trifluoromethyl group required double the reaction time but was isolated in a comparable 72% yield. The X-ray crystal structure of **D.3h** revealed that the C4 phenyl substituent is tilted rather than being conjugated to the enamine π -system.



Scheme 137. Scope of the dihydropyridine C2 substituent.

Indicated yields correspond to isolated yields obtained over two steps starting from the corresponding propargylamines, unless otherwise stated. General reaction conditions: reactions run in a sealed tube in EtOAc (1 M) at 100 °C using 10 mol% of Cu^I-USY catalyst for the indicated time. ^[a] Performed at rt and product **D.1e** obtained as major isomer in a mixture with the corresponding 1,4-dihydropyridine (74:26). ^[b] Reaction run in a degassed EtOAc solution with no conversion observed at rt and degradation starting from 40 °C. ^[c] Yield estimated from crude mixtures *via* ¹H NMR using 1,3,5-trimethoxybenzene as internal standard because compound **D.3b** degrades under air and was not isolated. ^[d] Unstable product which degrades upon storage.

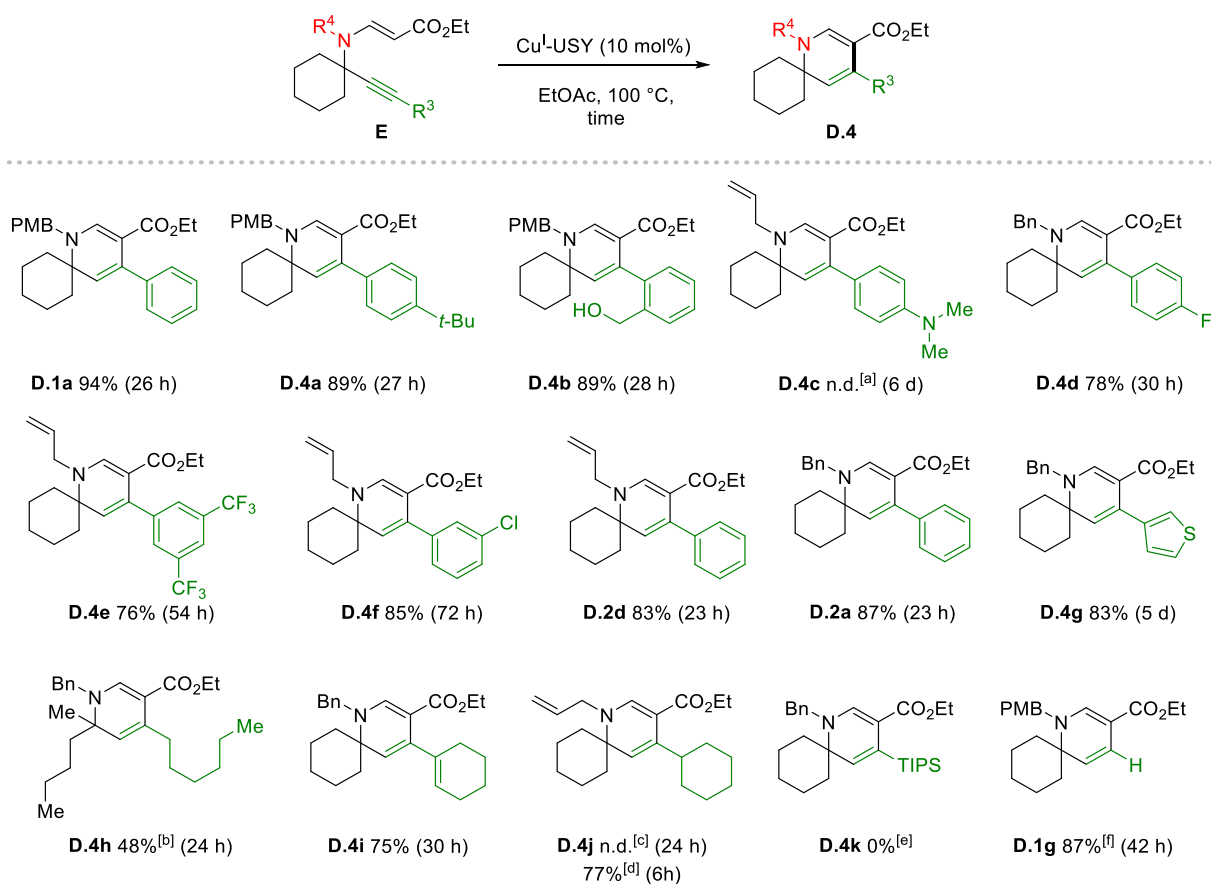
5.3.3. Alkyne Substituent

Next, we investigated the scope of the alkyne substituent starting with more functionalised arylacetylene derivatives compared to dihydropyridine **D.1a** (Scheme 138).

The presence of electron-rich 4-*t*-butyl or 2-hydroxymethyl substituents gave the corresponding dihydropyridines **D.4a,b** in comparable yield and time (89%, 27-28 h). The presence of the strongly electron-donating 4-*N,N*-dimethylamino substituent, however, led to an incomplete conversion after six days (enyne/**D.4c** = 4:96). While the crude spectrum shows dihydropyridine **D.4c** as the major product, the latter was found to be unstable on silica and aluminium oxide impeding its isolation. Besides electronic effects, the capability of the dimethylaniline to act as LEWIS base might contribute to the long reaction time observed if catalyst poisoning phenomena are at play.

Electron-withdrawing groups (EWGs), namely 4-fluoro, 3,5-bis(trifluoromethyl) and 3-chloro substituents were well tolerated leading to the corresponding dihydropyridines **D.4d-f** in 76-85% yield. While dihydropyridine **D.4f** was obtained in a comparable yield to its phenylacetylene analogue **D.2d** (85% for **D.4f** vs. 83% for **D.2d**), three times the reaction time was required for full conversion. Similarly, the fluorine-based EWGs induced longer reaction times, and a

small but noticeable decrease in yield compared to phenylacetylene analogues is observed (i.e., **D.4d** vs. **D.2a** and **D.4c** vs. **D.2d**).



Indicated yields correspond to isolated yields obtained over two steps starting from the corresponding propargylamines, unless otherwise stated. General reaction conditions: reactions run in a sealed tube in EtOAc (1 M) at 100 °C using 10 mol% of Cu^I-USY catalyst for the indicated time. ^[a] Incomplete conversion with enyne/**D.4c** 4:96 observed after six days. **D.4c** could not be isolated due to degradation on deactivated silica gel and aluminium oxide. ^[b] Yield estimated after column chromatography *via* ¹H NMR using 1,3,5-trimethoxybenzene as internal standard due to inseparable by-products; ^[c] Obtained as a hard-to-purify mixture with no estimated yield determined. ^[d] **D.4j** isolated in 77% yield running the reaction with Au(JohnPhos)NTf₂ (5 mol%) in 1,2-DCE at 100 °C for 6 h. ^[e] Reaction run at 125 °C. ^[f] Reaction run at 78 °C.

A heteroaryl substituent was evaluated next. 3-Thiophenyl-derived dihydropyridine **D.4g** was isolated in a comparable yield to its phenylacetylene analogue **D.2a** (83% vs. 87%), even though the reaction took five times longer to reach full conversion. Thiophene is a rather weak LEWIS base, suggesting here an electronic effect.

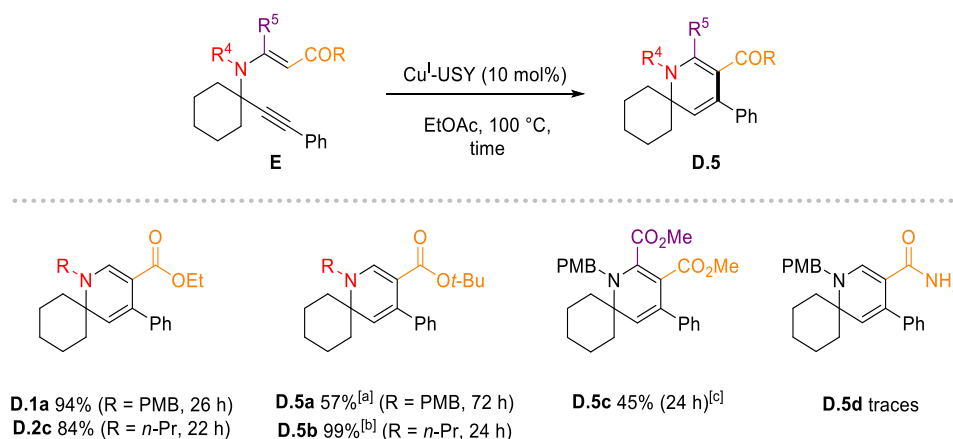
Regarding 3-*aza*-1,5-enynes possessing aliphatic alkyne substituents, this enyne class is generally less represented in current literature reports. PESHKOV and co-workers, however, observed that switching from aromatic alkynes to an *n*-propyl substituted alkyne provided a complex and hard-to-purify mixture of the desired dihydropyridine and unidentified by-products using their CuBr/pyridine system.^[334] Similarly, our conditions gave dihydropyridine **D.4h** (bearing an *n*-hexyl) in a hard-to-purify mixture with a moderate 48% yield, whereas a vinyl alkyne substituent reacted smoothly to give dihydropyridine **D.4i** in 75% yield. Shifting to its saturated cyclohexyl analogue **D.4j** worsened the chemoselectivity, yet the corresponding enyne was fully

converted in an ordinary reaction time of 24 hours. As PESHKOV's procedure also relied on a copper catalyst, we presumed that another transition metal might afford a more selective reaction to afford dihydropyridine **D.4j** in good yield. Indeed, Au(JohnPhos)NTf₂, which was identified as an active catalyst for the cycloisomerisation of model enyne **D.1a**, selectively produced **D.4j** in 77% yield.

Next, we further increased the bulkiness of the alkyne substituent using a triisopropylsilyl group. This entirely impeded cycloisomerisation even at 125 °C with no traces of dihydropyridine **D.4k** detected. In contrast, an enyne bearing a terminal alkyne afforded dihydropyridine **D.1g** in 87% yield after two days, even at 78 °C (for more details on the effect of the alkyne substituent on the ease of cycloisomerisation, see section VI-5.2.2).

5.3.4. Enamine Substitution Frame

Last, a small number of enamine substituents were compared (Scheme 139). Shifting from ethyl to *t*-butyl ester led to a clean formation of dihydropyridine **D.5a**. Nevertheless, **D.5a** was isolated in 57% yield, due to some loss suspected from partial *t*-butyl ester deprotection during column chromatography. Strikingly, for the *N*-propyl analogue, a faster reaction was observed, and fortunately, no purification was required giving dihydropyridine **D.5b** in excellent yield. When an additional ester functionality was introduced on the enamine α -carbon, the cycloisomerisation reproducibly afforded a more complex reaction outcome. In fact, dihydropyridine **D.5c** was isolated in a moderate 45% yield. An even more complex result was obtained when the ester functionality was replaced by a primary amide. The targeted dihydropyridine **D.5d** was only obtained in trace amounts, despite the complete conversion of the corresponding enyne.



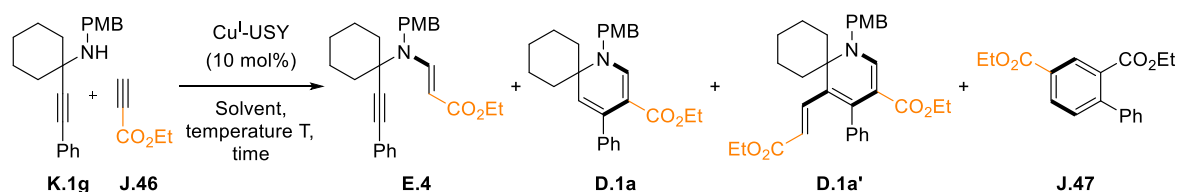
Scheme 139. Scope of the dihydropyridine C5/C6 substituent.

Indicated yields correspond to isolated yields obtained over two steps starting from corresponding propargylamines, unless otherwise stated. General reaction conditions: reactions run in a sealed tube in EtOAc (1 M) at 100 °C using 10 mol% of Cu^I-USY catalyst for the indicated time. ^[a] Product loss during column chromatography due to suspected *t*-butyl ester cleavage, followed by degradation. ^[b] Crude yield. ^[c] Reaction run from purified enyne.

5.4. Cu^I-USY-Catalysed Cascade 1,2-Dihydropyridine Synthesis

Aiming for an increased step economy, we further evaluated a direct approach to spirocyclic 1,2-dihydropyridines by performing the enyne formation/cycloisomerisation reactions in a single cascade operation. For this, propargylamine **K.1g** and ethyl propiolate **J.46** were used as model substrates, employing Cu^I-USY as catalyst (Table 40). First, propargylamine **K.1g** and excess ethyl propiolate **J.46** (8.0 eq.) were heated in a series of different solvent conditions (EtOAc, DCE, *t*-AmOH^{vi} and under solvent-free conditions, entries 1-4). The reaction mixtures were analysed *via* TLC and ¹H NMR spectroscopy after six hours. In each case, significant amounts of unreacted propargylamine **K.1g** remained, while several by-products were detected. Among the latter, dihydropyridine **D.1a'** and isophthalate **J.47** were identified and their proportions are given in Table 40 (entries 1-4).

Table 40. Optimisation of the Cu^I-catalysed cascade synthesis of dihydropyridine **D.1a** from propargylamine **K.1g**.^[a]



Entry	J.46 (eq.)	Solvent	T (°C)	t (h)	Yield D.1a ^[b] (%)	D.1a / E.4 ^[c]	D.1a / D.1a' / J.47 ^[c]
1	8	neat	100	6	n.d.	7:3	23:53:24
2	8	DCE	100	6	n.d.	1:1	53:31:26
3	8	EtOAc	100	6	n.d.	7:3	71:18:11
4	8	<i>t</i> -AmOH	100	6	n.d.	8:2	63:16:21
5	2	EtOAc	100	23	42	1:0	74:13:13
6	1	EtOAc	100	42	58 ^[d]	8:2	1:0:0
7	1	<i>t</i> -AmOH	100	24	91	1:0	1:0:0
8	1	<i>t</i> -AmOH	120	2.5	32 ^[g]	4:6	1:0:0
9	1	<i>t</i> -AmOH	120	2.5 ^[e]	73 ^[f]	9:1	1:0:0
10	1	<i>t</i> -AmOH	110	10 ^[e]	78	1:0	1:0:0

^[a] Reactions run in a sealed tube at 83 mM concentration for entries 2-4, and 1 M for entries 5-10. ^[b] Yield estimated from crude mixtures *via* ¹H NMR using 1,3,5-trimethoxybenzene as internal standard. ^[c] Ratios were determined from crude mixtures *via* ¹H NMR. ^[d] Traces of amine **K.1g** and 17% yield of **E.4** observed. ^[e] Reaction run under microwave irradiation. ^[f] 10% yield of **E.4** observed. ^[g] 47% yield of **E.4** observed. n.d.: not determined.

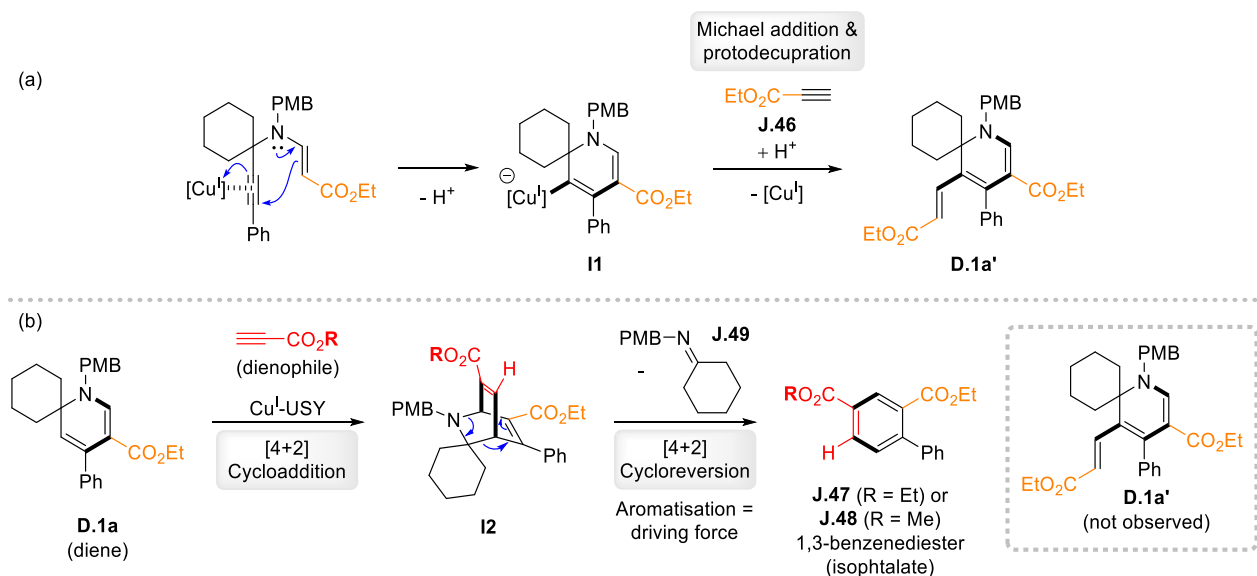
The formation of by-products **D.1a'** and **J.47** involves a second equivalent of ethyl propiolate (**J.46**) and a mechanistic rationalisation is given in Scheme 140. Dihydropyridine **D.1a'** is believed to form from vinylcuprate **II** *via* MICHAEL addition,^{vii} before protodecupration, as it was not observed starting from dihydropyridine **D.1a** (Scheme 140a). This highlights the

^{vi} Cu^I-USY is believed to activate ethyl propiolate (**J.46**) *via* LEWIS acid catalysis as the enol ether resulting from the *O*-MICHAEL addition of *t*-AmOH onto **J.46** was formed in Table 40 entry 4, but not in the absence of Cu^I-USY.

^{vii} It cannot be excluded that Cu^I-USY assists the expected MICHAEL addition reaction.

involvement of vinylcuprate **II** as a key intermediate in the 1,2-dihydropyridine synthesis as presented in [Scheme 112](#).

On the other hand, **D.1a** might act as a diene in a [4+2] cycloaddition with ethyl propiolate (**J.46**) to give isoquinuclidine **I2** ([Scheme 140b](#)). Driven by aromatisation, **I2** yields isophtalate **J.47** via [4+2] cycloreversion. The involvement of two dihydropyridine equivalents to form isophtalate **J.47** was ruled out using methyl propiolate, leading to isophtalate **J.48** incorporating two different ester groups and the detection of ketimine **J.49** via $^1\text{H NMR}$.



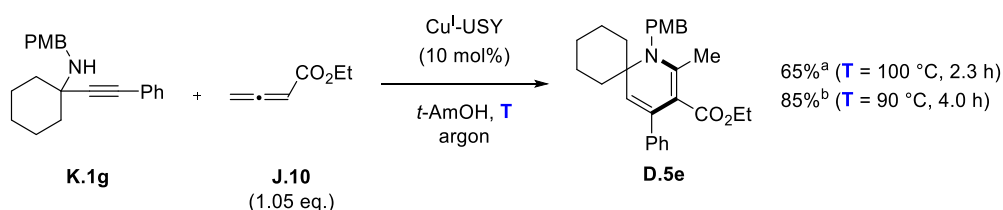
Scheme 140. Proposed mechanistic rationalisation for the emergence of by-products **D.1a'** and **J.47**.

To avoid the formation of by-products, only two equivalents of ethyl propiolate (**J.46**) were added to the reaction. This led to the complete conversion of amine **K.1g** after 23 hours in EtOAc at 100 °C (entry 5). Yet, dihydropyridine **D.1a** was formed in a moderate 42% yield as part of a complex mixture (**D.1a/D.1a'/J.47** 74:13:13). Shifting to equimolar amounts of amine **K.1g** and ethyl propiolate (**J.46**) further improved the chemoselectivity for dihydropyridine **D.1a** which was produced in 58% yield (vs. 94% for the two-step procedure), without detecting the known by-products **D.1a'** and **J.47** (entry 6). Nevertheless, traces of starting **K.1g**, along with 17% of uncyclised enyne **E.4** remained after 42 hours in EtOAc at 100 °C.

These preliminary results showed that the desired cascade synthesis of dihydropyridines is possible, but some conditions need to be met to achieve a selective reaction. In general, ethyl propiolate (**J.46**) should only be added in one equivalent. In addition, the fastest possible conversion of **J.46** into the corresponding enyne should be assured to reduce the formation of by-products. In fact, alcoholic solvents, such as EtOH, *n*-BuOH and *t*-AmOH, were observed to give accelerated *aza*-MICHAEL additions. However, the solvent must also guarantee an efficient Cu^I-USY-catalysed cycloisomerisation reaction. *t*-AmOH meets these criteria (see [Table 38](#), entry 4) and indeed made it possible to deliver dihydropyridine **D.1a** in high 91% yield in 24 hours (entry 7). Running the reaction at 120 °C revealed an accelerating effect under

microwave irradiation compared to conventional heating, forming dihydropyridine **D.1a** in 73% vs. 32% after 2.5 hours (entry 9 vs. 8). ^1H NMR analysis of both crude mixtures, however, revealed the emergence of a so-far unidentified by-product. The latter was still observed, although to a lesser extent, at 110 °C, resulting in dihydropyridine **D.1a** in 78% yield under microwave irradiation for ten hours (entry 10). It is noteworthy that no significant rate acceleration was achieved under microwave irradiation at 100 °C compared to conventional heating. To date, the conditions from entry 7 thus represent the conditions of choice for the Cu^{I} -USY-catalysed cascade synthesis of 1,2-dihydropyridines. The scope of this procedure, however, still needs to be evaluated.

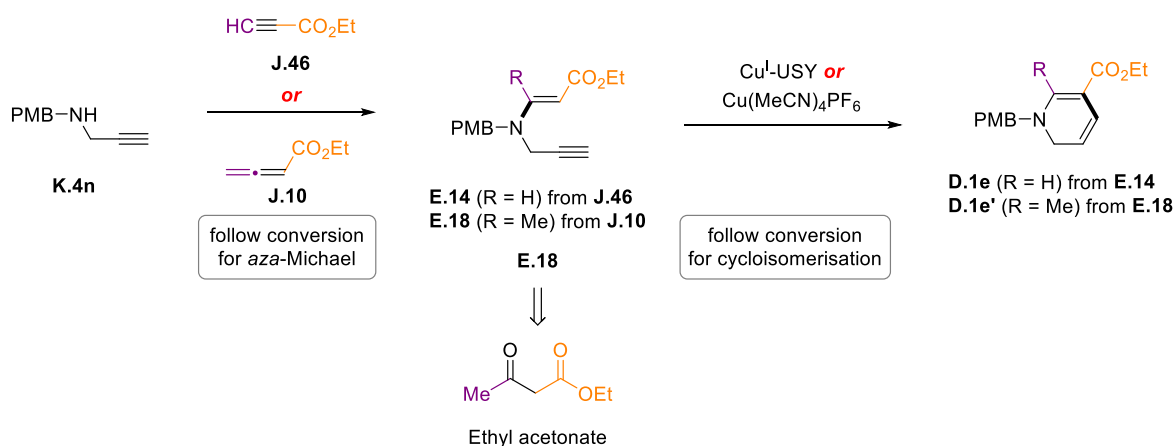
Nevertheless, an extension of this procedure towards C6-methylated 1,2-dihydropyridines from propargylamines and allenolate **J.10**, as established by PESHKOV and co-workers,^[334] was examined (**Scheme 141**). Interestingly, the reaction of propargylamine **K.1g** was faster with allenolate **J.10** than ethyl propiolate (**J.46**). In fact, dihydropyridine **D.5e** was obtained in 65% yield in only 2.3 h (140 min) with full conversion of propargylamine **K.1g** observed. Lowering the reaction temperature to 90 °C resulted in a superior 85% yield of **D.5e**, maintaining a reasonable reaction time of four hours.



Scheme 141. Cascade *aza*-MICHAEL addition/cycloisomerisation of propargylamine **K.1g** and allenolate **J.10**.

^[a] Yield estimated from the crude mixture *via* ^1H NMR using nitromethane as internal standard. ^[b] Isolated yield.

For now, the origin of this reactivity difference between ethyl propiolate (**J.46**) and ethyl buta-2,3-dienoate (**J.10**) is not well understood. As a perspective, both reactions of this cascade process could be investigated individually. For instance, the conversion of propargylamine **K.4n** in the respective *aza*-MICHAEL addition reactions with both electrophiles could be monitored *via* TLC, HPLC and/or ^1H NMR (**Scheme 142**). Likewise, the cycloisomerisation reactions of the corresponding enynes **E.15** and **E.18** could be followed to compare the reaction times. In case the *aza*-MICHAEL reaction conditions do not provide enyne **E.18** in satisfying yield, an alternative preparation from propargylamine **K.4n** and ethyl acetate can be envisaged.



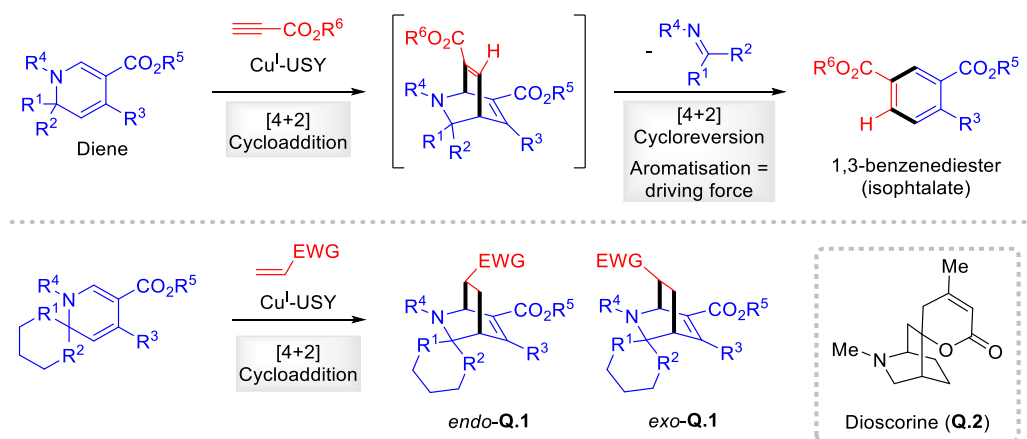
Scheme 142. Envisaged perspective to rationalise the faster dihydropyridine formation with allenolate J.10 vs. propiolate J.46.

5.5. Synthetic Applications of Spirocyclic 1,2-Dihydropyridines

In section VI-3., several intriguing synthetic applications of dihydropyridines were presented, yet few examples involved α -tertiary ones. These are, however, particularly interesting for the synthesis of valuable α -tertiary amines. Therefore, a preliminary investigation of the synthetic potential of our spirocyclic dihydropyridines to access unprecedented 1-azaspirocyclic α -tertiary amines was initiated in this thesis.

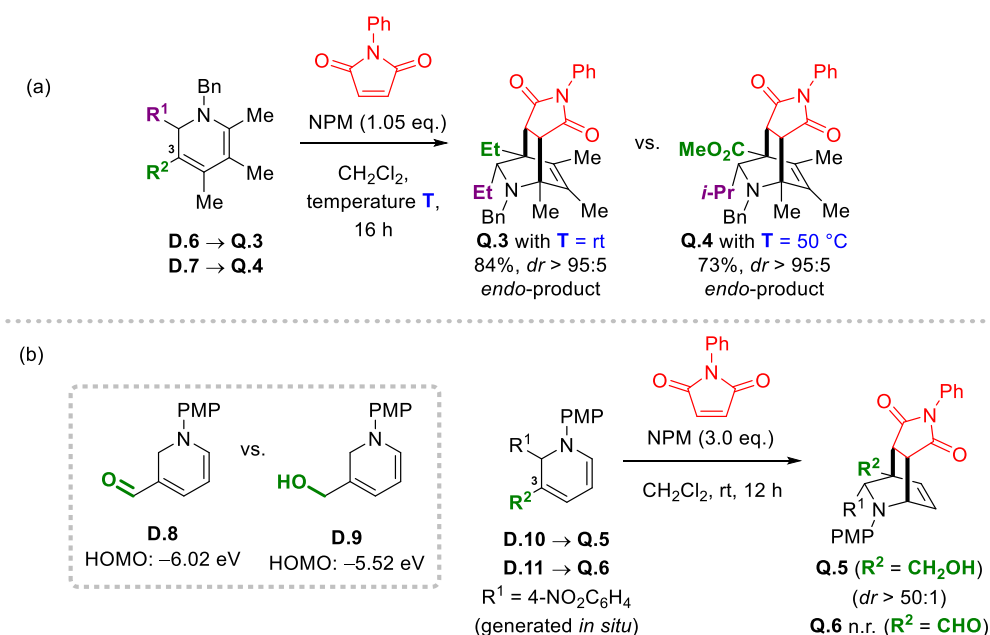
5.5.1. As Dienes in DIELS-ALDER Cycloaddition Reactions

During the optimisation studies for the cascade synthesis of 1,2-dihydropyridines, the latter were observed to act as dienes in the DIELS-ALDER reaction with propiolates to give isophthalates (**Scheme 143**, top). We reasoned that the [4+2] cycloaddition (CA) of such 1-azaspirocyclic 1,2-dihydropyridines with activated alkenes allows for the preparation of unprecedented spirocyclic isoquinuclidines **Q.1** (**Scheme 143**, bottom). As for existing procedures discussed below, we mainly or exclusively expect the formation of the *endo*-diastereoisomer. To the best of our knowledge, very few examples of spirocyclic isoquinuclidines have been reported. A noteworthy example is dioscorine (**Q.2**). This natural alkaloid is a neurotoxin produced as a defence metabolite by several tropical yams of the *Dioscorea* genus.



Scheme 143. 1,2-Dihydropyridines as dienes in DIELS-ALDER reactions: from isophthalates to spirocyclic isoquinuclidines **Q.1**.

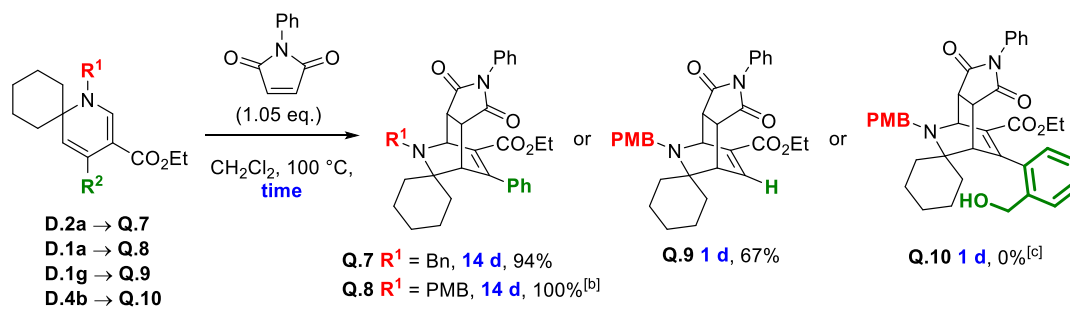
Looking at current literature reports, however, revealed that the targeted [4+2] cycloaddition would be no easy task. ELLMAN and co-workers, for instance, reported the synthesis of highly substituted isoquinuclidines from the corresponding 1,2-dihydropyridines and various dienophiles.^[361] Most of their dihydropyridines reacted with *N*-phenylmaleimide (NPM) at room temperature to give the corresponding isoquinuclidines in high yields (e.g. **D.6** → **Q.3**). By contrast, push-pull dihydropyridine **D.7**, bearing an electron-withdrawing C3 ester group in direct conjugation with the diene π -system, was heated to 50 °C to give **Q.4** (Scheme 144a). What is more, KUMAR and co-workers showed that shifting from a C3 aldehyde (**D.8**) to the corresponding primary alcohol (**D.9**) substituent should result in an electron-rich diene, reflected by a higher HOMO energy level (Scheme 144b).^[343] This shift is believed to have enabled the DIELS-ALDER reaction of dihydropyridine **D.10** with NPM at room temperature yielding **Q.5**, whereas push-pull **D.11** did not convert to **Q.6** under the same conditions. As shown in Scheme 124 in section VI-3, similar observations were made by OGURI and co-workers.^[345] Furthermore, they showed that the size of the C2 substituent in 1,2-dihydropyridines significantly affects the ease of cycloaddition. In all cases, these groups reported highly diastereoselective reactions, describing solely the *endo*-product. Given that our 1-azaspirocyclic 1,2-dihydropyridines combine the presence of an ester group in conjugation with the enamine functionality, and a sterically encumbering C2 substituent, they were considered attractive but challenging dienes.



Scheme 144. DIELS-ALDER reactions of push-pull 1,2-dihydropyridines with *N*-phenylmaleimide (NPM).^[343,361]

To start our investigation, the DIELS-ALDER reaction of dihydropyridine **D.2a** and NPM (1.05 eq.) was placed under ELLMAN's conditions at 50°C in CH_2Cl_2 . Not surprisingly, the reaction proceeded very sluggishly, so the temperature was risen to 100°C (Scheme 145). Even at this high temperature, cycloaddition proceeded at a slow pace but highly selectively, affording isoquinuclidine **Q.7** in 94% yield after 14 days, observing a single diastereoisomer. Shifting to dihydropyridine **D.1a** bearing a slightly electron-rich 4-methoxybenzylamine, did not improve the reaction kinetics but a similar promising yield for **Q.8** was observed. This low reactivity of dihydropyridines **D.2a** and **D.1a** is most likely not exclusively due to the electronic deactivation caused by the C3 ester functionality. The C4 phenyl substituent in our dihydropyridines is believed to significantly hinder the approach of the dienophile as expected from the X-ray crystal structure of dihydropyridine **D.3h** (cf. Scheme 137). In fact, the C4 phenyl substituent is not conjugated to the enamine moiety of the dihydropyridine core and adopts an oblique position to avoid the ester group.

We thus decided to scrutinise the effect of the C4 substituent on the reactivity of 1-azaspirocyclic dihydropyridines in the DIELS-ALDER reaction with *N*-phenylmaleimide (NPM) (Scheme 145). Indeed, under identical conditions, dihydropyridine **D.1g** (with $R^2 = \text{H}$) was fully converted to isoquinuclidine **Q.9** in 24 hours. The isolated yield, however, dropped to 67%, although a satisfying crude mixture was obtained. Furthermore, dihydropyridine **D.4b** bearing an additional *ortho* 2-hydroxymethyl substituent on the C4 aryl was evaluated. In this case, no conversion to **Q.10** was observed after 24 hours at 100°C , nor at 120°C , further supporting the impact of sterics in such cycloadditions.



Scheme 145. Effect of the C4 substituent on the ease of DIELS-ALDER CA.^[a]

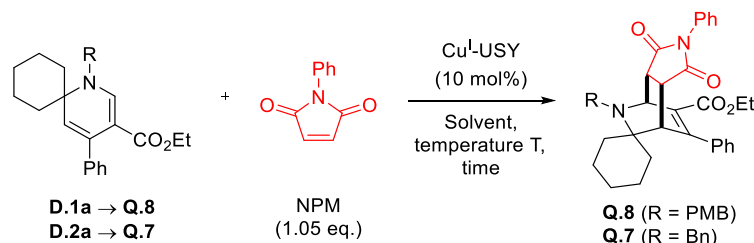
^[a] Reactions run at 0.1 M concentration in a sealed tube with isolated yields indicated, unless otherwise stated. ^[b] Yield estimated from crude mixtures *via* ¹H NMR using 1,3,5-trimethoxybenzene as internal standard. ^[c] No conversion observed, nor at 120 °C.

Motivated by these promising first results, we aimed to further optimise the DIELS-ALDER reaction (**Table 41**). To reduce the long reaction times observed, we investigated whether Cu^I-USY can act as catalyst through LEWIS acidic dienophile activation. Indeed, (transition) metal-loaded zeolites, among which copper examples, were employed as catalysts in DIELS-ALDER reactions in the past.^[153,362] Gratifyingly, Cu^I-USY drastically accelerated the [4+2] CA. Indeed, adding Cu^I-USY (10 mol%) to CH₂Cl₂ at 100 °C quantitatively yielded isoquinuclidine **Q.8** after 46 h compared to 14 days under catalyst-free conditions (entry 2 vs. 1). To substitute undesired CH₂Cl₂ for a “greener” solvent and in view of an extension to a one-pot dihydropyridine synthesis/[4+2] CA, the reaction was next run in *t*-AmOH (entry 3). This resulted in a slightly reduced 90% yield of **Q.8** after six days to reach complete conversion. To reduce the reaction time, the temperature was increased to 150 °C using the analogous dihydropyridine **D.2a** in superheated *t*-AmOH (entry 4). Rewardingly, isoquinuclidine **Q.7** formed in high 95% yield within seven hours. While *t*-AmOH/EtOAc (1:1) better solubilised the starting materials at room temperature and the lower boiling point of EtOAc (78 °C vs. 101 °C for *t*-AmOH) could accentuate the superheating effect, no improvement compared to using only *t*-AmOH was observed (entry 5). Further increasing the reaction temperature to 200 °C, in contrast, provided isoquinuclidine **Q.7** in 35 min in 97% estimated yield (entry 6). Such drastic conditions, however, cause a pressure build-up of about 20 bar. This represents a potential safety concern or requires special equipment. In addition, more labile/reactive functional groups might not withstand such conditions, resulting in a limited product scope. Furthermore, a visual change in the zeolite aspect was observed. In case of an incomplete conversion of dihydropyridine **D.2a** (entries 5 and 6), the mixture was heated again under the same conditions for one hour but showed no significant reaction progress. This possibly indicates the deactivation of the catalyst under such drastic conditions.

Therefore, additional solvents were evaluated in the [4+2] CA of dihydropyridine **D.2a** and NPM heating close to their respective boiling points in sealed tubes. Toluene is commonly employed in DIELS-ALDER reactions involving 1,2-dihydropyridines,^[342] although it is not a

desirable solvent. Indeed, toluene led to a similar result compared to CH₂Cl₂, producing isoquinuclidine **Q.7** in 91% yield after 30 hours at 110 °C (entry 7). Running the reaction in *n*-BuOAc or cyclopentyl methyl ether (CPME), two high-boiling “green” solvents, afforded **Q.7** in good yields but with a slightly reduced efficiency (entries 8 and 9).

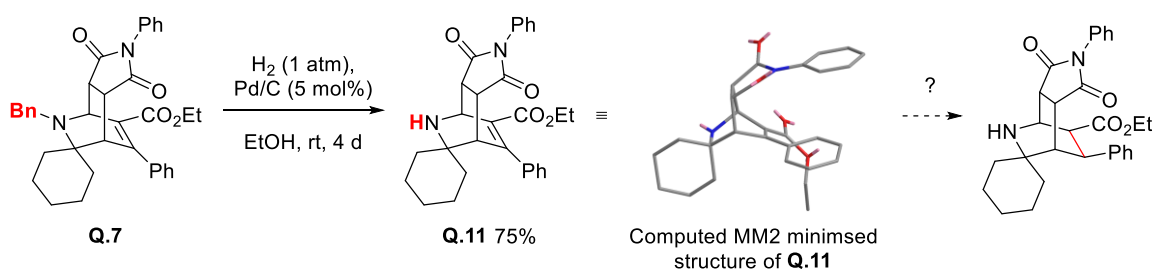
Table 41. Optimisation of Cu^I-USY-catalysed DIELS-ALDER reaction towards spirocyclic isoquinuclidines.^[a]



Entry	Solvent	D	R	T (°C)	Time	Yield ^[b] (%)
1 ^[c]	DCM	D.1a	PMB	100	14 d	100 ^[d]
2	DCM	D.1a	PMB	100	2 d	100 ^[d] (90) ^[e]
3	<i>t</i> -AmOH	D.1a	PMB	100	6 d	90 ^[d]
4	<i>t</i> -AmOH	D.2a	Bn	150	7 h	95 ^[f,g]
5	<i>t</i> -AmOH/EtOAc (1:1)	D.2a	Bn	150	7 h	95 ^[f,h]
6	<i>t</i> -AmOH	D.2a	Bn	200	35 min	97 ^[f]
7	PhMe	D.2a	Bn	110	30 h	91 ^[d]
8	<i>n</i> -BuOAc	D.2a	Bn	125	30 h	84 ^[d]
9	CPME	D.2a	Bn	105	110 h	85 ^[d]

^[a] Reactions run in a sealed tube at 0.5 M concentration in the presence of Cu^I-USY (10 mol%), unless otherwise stated. ^[b] Estimated yields from crude mixtures *via* ¹H NMR using an internal standard, unless otherwise stated. ^[c] Reaction run without Cu^I-USY. ^[d] Yield estimated using 1,3,5-trimethoxybenzene. ^[e] Isolated yield. ^[f] Yield estimated using nitromethane. ^[g] ¹H NMR ratio **Q.7/D.2a** = 94:6. ^[h] ¹H NMR ratio **Q.7/D.2a** = 9:1.

It is worth noting that deprotection conditions were evaluated to access isoquinuclidines bearing an unprotected amino group. Rewardingly, hydrogenolysis at room temperature and ambient H₂ pressure using Pd/C (5 mol%) produced isoquinuclidine **Q.11** in 75% yield (**Scheme 146**). Not surprisingly, the electron-poor and sterically hindered C-C double bond in the isoquinuclidine core was not hydrogenated under such mild conditions, in contrast to a more electron-rich and accessible example reported in the literature.^[343] Nevertheless, it could be an interesting challenge to identify suitable hydrogenation conditions, and to investigate the influence of the cyclohexyl substituent on its diastereoselectivity (**Scheme 146**). Indeed, the phenyl ring of the succinimide moiety shields the upper side, which should greatly favour the hydrogenation from below. The C4 phenyl and C2 cyclohexyl substituents, however, might complicate the contact between the substrate and the hydrogenation catalyst.



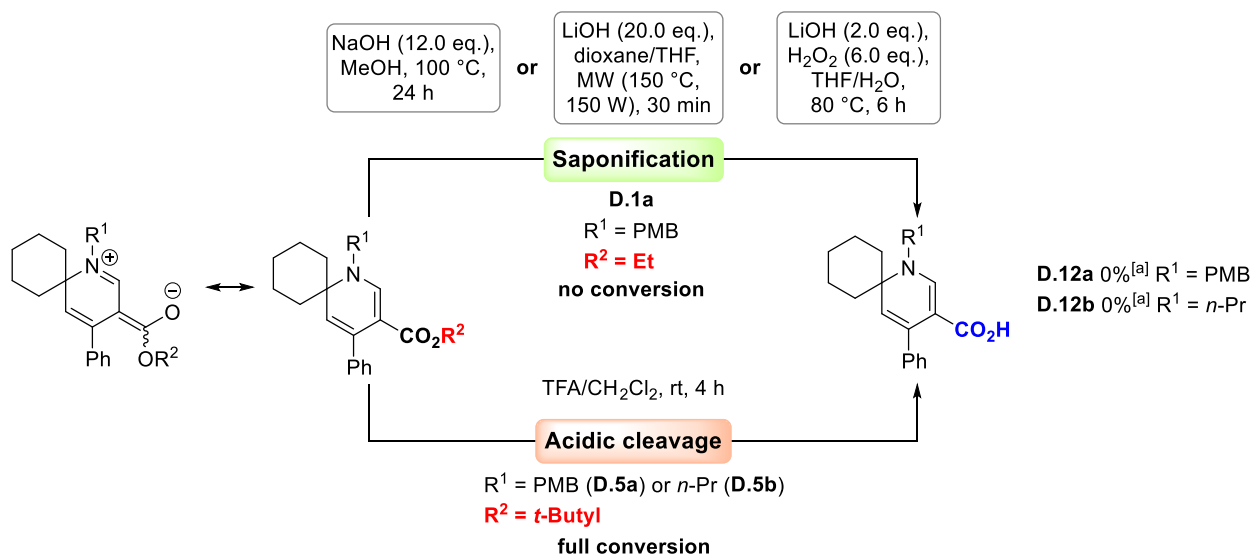
Scheme 146. Synthesis of *N*-unsubstituted isoquinuclidine **Q.11**.

5.5.2. In Other Derivatisation Reactions

Beyond their use as dienes in DIELS-ALDER reactions to form isoquinuclidines, other scaffolds through chemical derivatisations of our spirocyclic dihydropyridines were targeted.

In contrast to 3-piperidinecarboxylic acid derivatives reported to have diverse biological properties,^[363] the corresponding unsaturated dihydropyridines have not been described in the literature. We reckoned that the selective generation of the carboxylic acid in our dihydropyridines might thus be of interest to exploit their potential bioactivities and to allow further chemical derivatisation. First, saponification of ethyl ester in dihydropyridine **D.1a** was examined under various conditions (Scheme 147, top). It quickly became clear that classical mild conditions are ineffective. In fact, the mesomeric structure of **D.1a** shows that the delocalisation of the nitrogen lone pair strongly increases the electron density around the carbonyl carbon, which drastically reduces its electrophilicity. This is further intensified by the σ -donating amine substituent. Even harsher conditions, such as excess aqueous NaOH in MeOH at 100 °C or excess aqueous LiOH in dioxane/THF at 150 °C were ineffective. Likewise, *in situ* generation of highly nucleophilic lithium hydroperoxide^[364] was unsuccessful. No conversion was observed in each case, testifying of the great stability of 1,2-dihydropyridine **D.1a**.

Alternatively, the syntheses of carboxylic acids **D.12a** and **D.12b** were attempted through TFA-mediated deprotection of the corresponding *t*-butyl esters **D.5a** and **D.5b** (Scheme 147, bottom). Indeed, both esters were completely converted in a few hours at room temperature and TLC showed the formation of a significantly more polar compound. In both cases, however, the yellow organic solution recovered after work-up turned into a dark brown viscous oil upon solvent evaporation leading to complex mixtures. It is unclear whether the carboxylic acids **D.12a** and **D.12b** were selectively formed in excess TFA. In fact, OGURI and co-workers^[345] recently showed that push-pull dihydropyridines can be protonated with diphenyl phosphate ($pK_a \approx 1.9$ ^[365]). As TFA is slightly more acidic ($pK_a \approx 0.3$), protonation, in addition to ester cleavage, might have occurred leading to an instable salt.



Scheme 147. Attempts to synthesise 1,2-dihydropyridines **D.12a,b** bearing carboxylic acids.

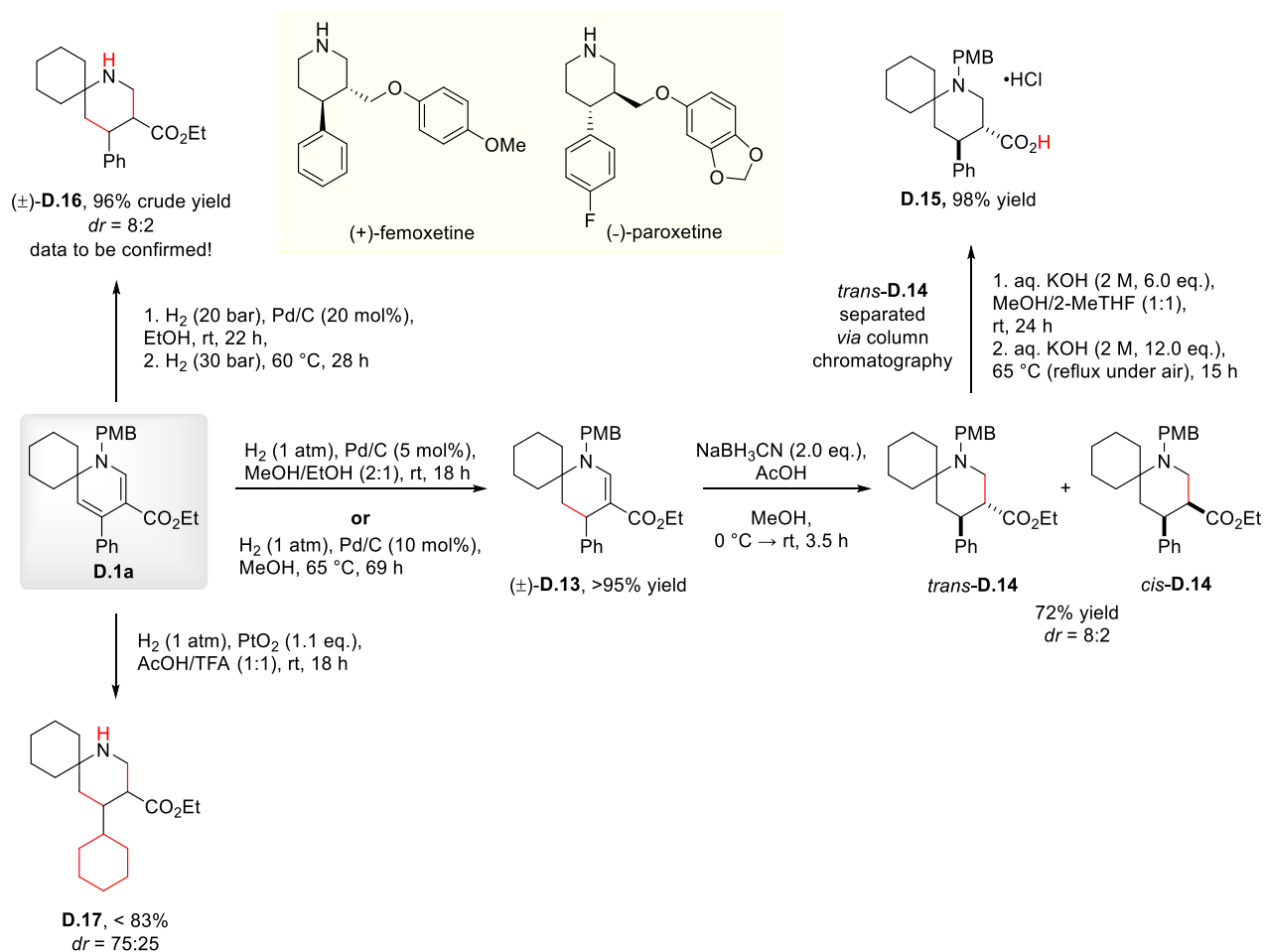
^[a] TLC showed spot-to-spot conversions with TFA/CH₂Cl₂, but complex crude mixtures were obtained upon solvent evaporation for R¹ = PMB and *n*-Pr. TFA: trifluoroacetic acid.

Subsequently, we started exploring other possibilities to derivatise our dihydropyridines through partial or complete saturation of the dihydropyridine core (**Scheme 148**).

Using classical Pd/C (5-10 mol%) hydrogenation conditions at ambient pressure, tetrahydropyridine **D.13** was obtained quantitatively without observing the deprotection of the methoxybenzyl moiety, even at 65 °C and under prolonged heating. Next, NaBH₃CN/AcOH enabled enamine reduction yielding ethyl piperidine-3-carboxylate **D.14** in 72% yield as a mixture of both diastereoisomers (*dr* = 8:2). A pure fraction of the major diastereoisomer was isolated and converted into 3-piperidinecarboxylic acid **D.15** through saponification. After acidic aqueous work-up, the chloride salt of **D.15** was easily recovered through trituration in excellent 98% yield.

Moreover, piperidine-3-carboxylate ester **D.16** was obtained through one-pot hydrogenation of both double bonds and hydrogenolysis of the PMB (4-methoxybenzylamino) group using H₂ (up to 30 bar) and Pd/C (20 mol%) at up to 60 °C. Although the reaction conditions still need to be optimised, this represents a promising first result as such C4 aryl-substituted derivatives are attractive precursors to pharmacologically relevant 4-arylpiperidines, such as (+)-femoxetine and (-)-paroxetine (Paxil[®], Seroxat[®]).^[366] These two 4-arylpiperidines are known serotonin reuptake inhibitors used to treat depression and panic disorders. A step-economical sequence towards spirocyclic analogues is conceivable from the preliminary results presented here.

Interestingly, in the presence of stoichiometric PtO₂ in AcOH/TFA, PMB hydrogenolysis and complete hydrogenation of dihydropyridine **D.1a**, including the C4 phenyl group, was achieved at room temperature. Although piperidine **D.17** was obtained as the main product (*dr* = 75:25), the presence of a small amount of an unidentified by-product does not allow to determine a precise yield, thus considered to be below 83%.



Scheme 148. Derivatization of dihydropyridine D.1a through saturation of the dihydropyridine core.

6. Conclusion

In this study, we demonstrated the potential of Cu^I-USY as an efficient, ligand-free catalyst for the cycloisomerisation of 3-*aza*-1,5-enynes towards attractive 1,2-dihydropyridines. Especially noteworthy is that the synthesis of 3-*aza*-1,5-enynes was achieved *via* a highly “green” *aza*-MICHAEL addition starting from equimolar amounts of propargylamines and propiolates in EtOH. This represents a full atom-economic and simple method to generate such enynes. Rewardingly, their Cu^I-USY-catalysed cycloisomerisation proceeded in benign EtOAc as compared to reported methods relying on hazardous solvents (DCE, toluene, benzene, etc.). Remarkably, a large tolerance of functional groups (e.g., amino, halide, acetal, carbamate, ether, hydroxy, ester, etc.) was observed. Nevertheless, long reaction times (ca. 24 h in most cases) at 100 °C were needed with sterically hindered enynes derived from α -tertiary propargylamines. Yet beneficially, in most cases, highly attractive 1-azaspirocyclic 1,2-dihydropyridines were generated in good to excellent yields. A hot filtration test suggests the heterogeneity of this catalytic system and the recovered Cu^I-USY was used in four runs with consistently high activity. Further structural (e.g., XRD and BET) and spectroscopic analyses (ICP-AES) of this recovered zeolite material are needed to scrutinise its stability and determine its remaining copper loading. Excitingly, the enyne formation/cycloisomerisation sequence was successfully extended into a cascade process under Cu^I-USY catalysis in benign *t*-AmOH. The product scope of this procedure, and the potential recyclability of Cu^I-USY, however, still need to be investigated.

Furthermore, this study provides first encouraging results for the DIELS-ALDER reaction of spirocyclic 1,2-dihydropyridines with *N*-phenylmaleimide. This challenging [4+2] cycloaddition was significantly accelerated under Cu^I-USY catalysis and afforded unprecedented spirocyclic isoquinuclidines, possibly allowing the exploration of new chemical space. Although the compatibility of *t*-AmOH with the Cu^I-USY-catalysed [4+2] CA has been demonstrated, further optimisation of the catalytic system is desired to reduce the reaction time and temperature. This could also include the examination of other catalysts.

General Conclusions and Perspectives

High thermal and chemical stability

Easy recovery and recyclability

Facile large-scale production

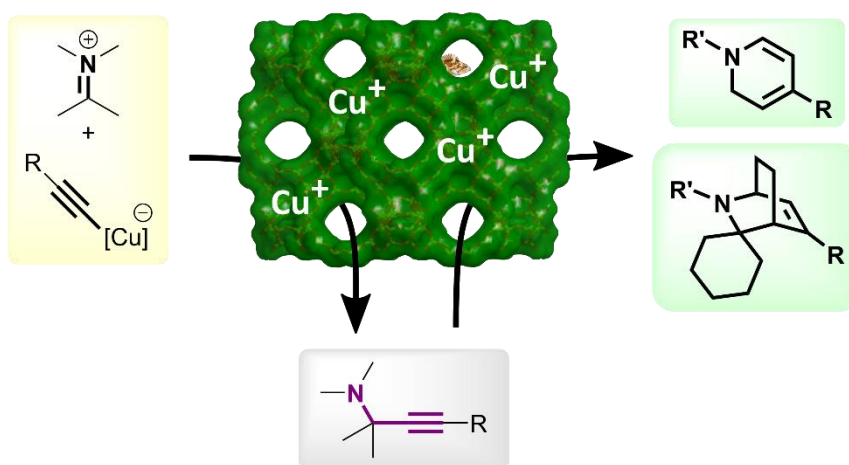
Insoluble in most solvents

Commercially available

Environmentally benign

Universal support

Safe to handle



Catalysis



Safer Solvents

Waste Prevention



Renewable Feedstock

Atom Economy



Short Synthesis

The objective of this thesis work was to synthesise propargylamines and derivatives by applying metal-loaded zeolites as heterogeneous catalysts. For this, Cu^I-USY, a cage-type hierarchical zeolite, was prepared through a solid-state ion-exchange reaction. The latter produced structurally diverse propargylamines through various catalytic methods and displayed varying reusability schemes depending on the application. The propargylamines formed also served as starting materials for more complex target compounds. Thus, the main objectives of this thesis could be fulfilled.

Part One provided a non-exhaustive but wide-ranging state of the art regarding the two main axes of this thesis, namely propargylamines (**Chapter I**) and zeolites (**Chapter II**). Without doubts, propargylamines represent a key compound class in organic and medicinal chemistry, thus asking for responsible production methods to meet today's expectations of sustainable chemistry. The suitability of zeolites, as established, safe, and potentially reusable heterogeneous catalysts were scrutinised for such greener processes in *Part Two*.

Overall, Cu^I-USY was shown to be an efficient catalyst for the synthesis of propargylamines and their derivatisation, operating under highly desirable neat or benign solvent conditions.

In **Chapter III**, a myriad of α -tertiary propargylamines could be produced through Cu^I-USY-catalysed KA² and related coupling reactions with terminal alkynes, alkynoic acids, and alkynylsilanes under solvent-free conditions. Rewardingly, compared to frequently used copper halides, Cu^I-USY produced the desired propargylamines at mild temperatures of 60-80 °C. With pyrrolidine as a representative secondary amine, catalyst loadings as low as 1 mol% gave high yields.

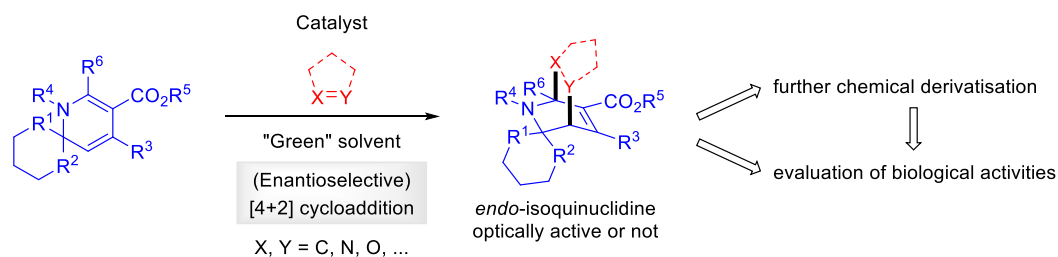
Motivated by these results, this 3CR methodology was extended to the use of terminal ynamides as alkyne surrogates in the unprecedented cascade synthesis of γ -amino-ynamides (**Chapter IV**). Interestingly, Cu^I-USY was particularly efficient for the chemoselective conversion of such sensitive terminal ynamides, whereas copper halides led to complex mixtures. Compared to the related 3CRs with terminal alkynes, the reactions proceeded at mild 30 °C, low catalyst loadings (3 mol%), and short reaction times but were also compatible with benign solvents (EtOAc) or neat conditions.

In **Chapter V**, Cu^I-USY was established as an efficient hydroamination catalyst, enabling propargylamine formation through HPA reaction at 2.5 mol% copper loading. To date, the Cu^I-USY-catalysed HPA reaction is limited to aliphatic secondary amines, whereas aromatic and aliphatic alkynes are suitable coupling partners. Regioisomeric ratios of the MARKOVNIKOV- and anti-MARKOVNIKOV products are governed mostly by electronic effects for aromatic alkynes, and steric effects for aliphatic alkynes.

The synthetic potential of propargylamines was shown in **Chapter VI**. More precisely, propargylamines carrying secondary amines were further derivatised into 1,2-dihydropyridines through an enyne formation/cycloisomerisation sequence. Gratifyingly, Cu^I-USY allowed the access to numerous 1-azaspirocyclic scaffolds in good to high yields in “green” EtOAc. The potential to extend the two-step procedure into a cascade reaction was further demonstrated using benign *t*-AmOH as solvent. Promising preliminary results showed the potential of these dihydropyridines as dienes in DIELS-ALDER reactions towards unprecedented spirocyclic isoquinuclidines. Other product classes, such as spirocyclic piperidines and nipecotic acids were also produced.

Regarding catalyst stability, Cu^I-USY could be reused in several runs for the applications presented in **Chapters III** to **VI**. However, a progressive erosion of its catalytic activity was observed. In contrast to the cycloisomerisation of 3-*aza*-1,5-enynes to 1,2-dihydropyridines, partial copper leaching under our conditions was evidenced for the propargylamine syntheses. Not surprisingly, less strongly coordinating motifs, such as enamides, thus seem to have beneficial repercussions on the potential recyclability of Cu^I-USY. Indeed, the cycloisomerisation led to the most promising recycling profile.

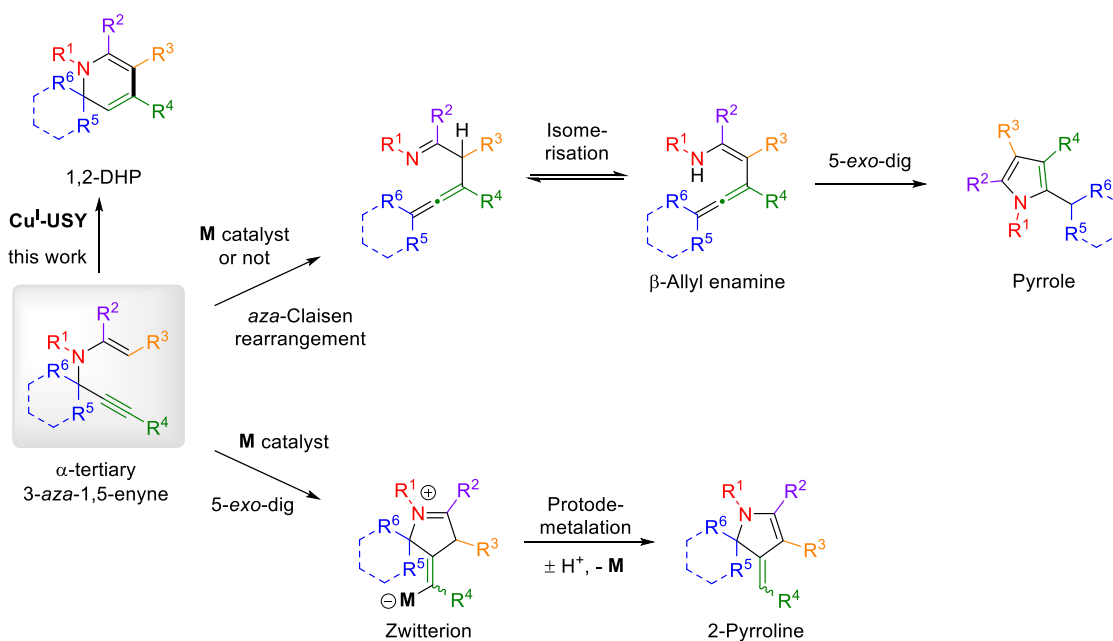
Following the preliminary results described herein, further optimising and extending the use of spirocyclic dihydropyridines as dienes in DIELS-ALDER cycloadditions towards novel isoquinuclidines seems a promising prospect (**Scheme 149**). After further optimisation with *N*-phenylmaleimide, keeping Green Chemistry principles in mind, other dienophiles should therefore be evaluated. In the context of the constant demand for innovative and highly three-dimensional lead structures,^[367] the resulting compounds could be screened for their biological activities. The elaboration of enantioselective DIELS-ALDER reaction conditions would of course be of particular significance in a medicinal chemistry context.



Scheme 149. 1,2-Dihydropyridines as molecular platform towards highly three-dimensional

Furthermore, a simple and green procedure towards 3-*aza*-1,5-enynes was disclosed in this thesis work in **Chapter VI**. As already mentioned, besides serving as precursors to 1,2-dihydropyridines (**Scheme 150**, top left), these intermediates could also provide access to other attractive scaffolds depending on the reaction conditions. Five-membered heterocycles, either

pyrroles *via* an *aza*-CLAISEN rearrangement/*5-endo-dig* cyclisation cascade process (Scheme 150, top right), or 2-pyrrolines *via* a direct *5-exo-dig* cyclisation (Scheme 150, bottom right) are noteworthy examples. To our knowledge, the latter has in fact only been described once under silver catalysis for a single example of a 3-*aza*-1,5-enyne structurally related to our substrates.^[325] Consequently, the synthetic and biological potential of the resulting compounds is largely unexplored. Future efforts could contribute to the identification of suitable conditions to prepare these intriguing heterocycles.



Scheme 150. Product divergence from easily accessible 3-*aza*-1,5-enynes.

Experimental Part.

General Information and General Procedures

All starting materials were purchased and used as received, unless otherwise stated. Deuterated solvents CDCl_3 , CD_2Cl_2 , CD_3CN and CD_3OD were purchased from Euriso-Top and dried over molecular sieves (4 Å) prior to use. Solvents were purchased from commercial sources and purified according to the standard procedure and freshly distilled under argon prior to use if necessary. CH_2Cl_2 , toluene, CH_3CN , MeOH and Et_2O were dried by passing through activated alumina under a positive pressure of argon using GlassTechnology GTS100 devices. Anhydrous reactions were carried out in flame-dried glassware and under an inert argon atmosphere, using standard Schlenk techniques. Anhydrous THF was obtained from distillation over sodium. Evaporation of solvents was conducted under reduced pressure at temperatures equal to or less than 40 °C using a rotary evaporator.

Reactions were monitored by thin-layer chromatography carried out on silica (silica gel 60 F₂₅₄, Merck) or alumina (aluminum oxide 60 F₂₅₄, Merck) plates using UV-light, KMnO_4 , vanillin (especially for carbonyls) and ninhydrine (for amines and imines) stains for visualisation. Column chromatographies were performed on (deactivated) silica gel 60 (40-63 µm, Merck) using cyclohexane/EtOAc mixtures as eluents, unless otherwise stated.

IR spectra were recorded neat on a Bruker Alpha II Fourier transform spectrometer. Wave numbers (ν) are given in cm^{-1} .

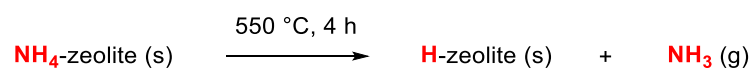
NMR spectra were recorded on Bruker Avance III spectrometer operating at specified power (Bruker Corporation, Billerica, MA, USA). ^1H and ^{13}C NMR spectra were recorded at 300, 400 or 500 MHz for ^1H and 126 MHz for ^{13}C NMR experiments at 298 K. ^{19}F NMR spectra were recorded at 282 MHz or 471 MHz on a 500 MHz spectrometer (equipped with a CP BBO 500S1 BBF-H-D-05 Z probe) at 298 K and are referenced externally to CFCl_3 in CDCl_3 at 0.00 ppm. Chemical shifts (δ) and coupling constants (J) are given in parts per million (ppm) and Hertz (Hz), respectively. Chemical shifts (δ) are reported relative to the residual solvent as an internal standard (CDCl_3 : $\delta = 7.26$ ppm for ^1H and $\delta = 77.16$ ppm for ^{13}C). Data are presented as follows: chemical shift (δ), multiplicity (standard abbreviations), coupling constants (J), integration, assignment (where possible). The signal multiplicity is described according to the following abbreviations: s (singlet), bs (broad singlet), d (doublet), t (triplet), q (quartet), quint (quintet), sept (septet), and m (multiplet). Assignments were determined based on chemical shifts, multiplicities and coupling constants. Carbon multiplicities were determined by DEPT135 experiments and are described according to the following abbreviations: CH (primary carbon), CH_2 (secondary carbon), CH_3 (tertiary carbon) and C_q (quaternary carbon). COSY, HSQC, HMBC and NOESY experiments were sometimes used to fully interpret spectra for related compounds. Further abbreviations and symbols were used to assign ^1H and ^{13}C NMR signals: H_{aro} or C_{aro} for an aromatic proton or carbon, respectively; \equiv for a triple bond; = for a double bond; $\text{C}_{q-\text{Ph}}$ for a quaternary carbon of a phenyl group. If more than one H or C is given in the assignment, the atom in question is italicised, e.g., in CH_2CH_3 the ^{13}C signal is assigned to the carbon of the methyl group.

Low- (MS) and high-resolution mass spectra (HRMS) data were recorded on a micrOTOF spectrometer (Bruker Corporation, Billerica, MA, USA) equipped with an orthogonal electrospray interface (ESI) or with atmospheric pressure chemical ionisation (APCI). The parent ions $[\text{M}+\text{H}]^+$, $[\text{M}+\text{Na}]^+$, $[\text{M}+\text{K}]^+$ are indicated. Mass spectra were obtained from the “Service de Spectroscopie de Masse” of the Fédération de Chimie “Le Bel” (FR2010).

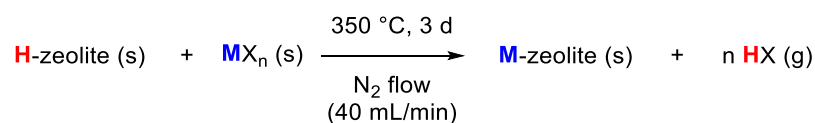
$\text{Ag}^{0/\text{I}}\text{-USY}^{[160]}$ was used as provided.

▪ General Procedure A: Preparation of Metal-Doped Zeolites *via* SSIE

(a) Calcination



(b) SSIE



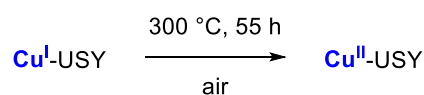
Metal-zeolites were prepared according to the solid-state ion-exchange (SSIE) reaction procedure reported by LOUIS and co-workers in 2009.^[230] Commercial NH₄-zeolite (purchased from Zeolyst International[®]) was loaded into an oven and then heated at 550 °C for 4 h to give the corresponding H-zeolite. So-formed H-zeolite (1.0 g) and metal halide (MX_n, 1.0 eq. related to the number of H-zeolite protons for monovalent cations or 0.5 eq. for divalent cations, unless otherwise stated) were ground by mortar and pestle for 5 min under air to give an intimate H-zeolite/metal halide mixture. This mixture was then loaded into a tubular glass reactor which was sealed and connected to a flow manifold. H-zeolite/metal halide was heated in a furnace to 350 °C (35 °C/min) under flowing nitrogen (40 mL/min) and the temperature was kept constant for three days affording the expected metal-zeolite. The latter was stored under argon atmosphere prior to use.

Table S1. The metal-loaded zeolites (M-zeo) were prepared following the general procedure above.

M-zeo	NH ₄ -zeo	NH ₄ -zeo acidic sites	MX _n	MX _n eq.	MX _n quantity	M-zeo aspect
Cu ^I -USY	CBV 500	3.8 mmol/g	CuCl	1.0	376 mg	brown
Cu ^I -USY 04	CBV 500	3.8 mmol/g	CuCl	0.4	150 mg	pale-brown
Cu ^I -MOR	CBV 21A	1.48 mmol/g	CuCl	1.0	146 mg	pale-brown
Cu ^I -ZSM-5	CBV 5524G	0.86 mmol/g	CuCl	1.0	85 mg	pale-brown
Mn ^{II} -USY	CBV 500	3.8 mmol/g	MnCl ₂ •4H ₂ O	0.5	476 mg	pale pink
Co ^{II} -USY	CBV 500	3.8 mmol/g	CoCl ₂ •6H ₂ O	0.5	452 mg	dark blue
Zn ^{II} -USY	CBV 500	3.8 mmol/g	ZnCl ₂	0.5	256 mg	white
Sc ^{III} -Cu ^I -USY	CBV 500	3.8 mmol/g	Sc(OTf) ₃ CuCl	0.05 0.8	94 mg 301 mg	brown-green

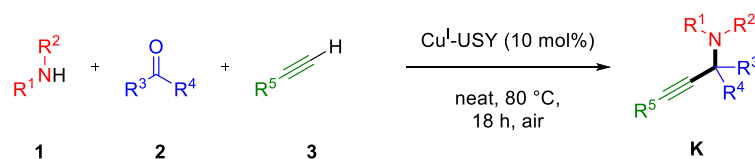
CuCl and Sc(OTf)₃ were purchased from Sigma-Aldrich[®] (> 99% purity). MnCl₂•4H₂O and CoCl₂•6H₂O were purchased from Merck[®] (> 99% purity). ZnCl₂ was purchased from Sigma-Aldrich[®] (anhydrous, free-flowing, Redi-Dri[™], reagent grade, ≥ 98%).

▪ Preparation of Cu^{II}-USY



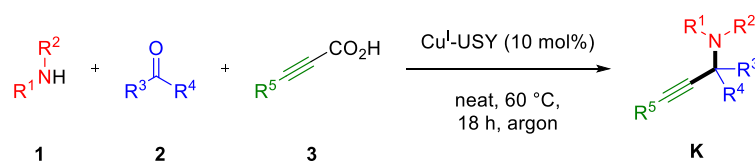
Cu^I-USY, as prepared according to the General Procedure A, was heated in a furnace under air at 300 °C for 55 h to give Cu^{II}-USY as a pale blue powder.

- General Procedure B: Synthesis of Propargylamines *via* KA² Reaction with Terminal Alkynes



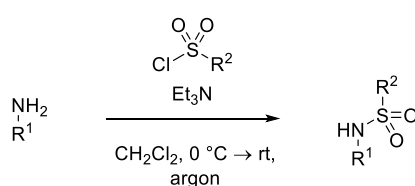
Ketone (1.0 eq., 1.0 mmol), alkyne (1.5 eq. 1.5 mmol) and Cu^I-USY (36 mg, 10 mol%) were successively added to a screw cap tube (10 mL) and stirred at rt and 500 rpm for 15 min. Next, amine (1.0 eq., 1.0 mmol) was added, and the mixture was progressively heated to 80 °C within 45 min and left to stir at 80 °C for 18 h. Once cooled to rt, the reaction mixture was diluted with EtOAc or CH₂Cl₂ (2 mL), filtered over celite, and washed with EtOAc or CH₂Cl₂ (3 × 20 mL). The filtrate was concentrated under reduced pressure and the crude product was purified by flash chromatography over silica gel using cyclohexane/EtOAc or CH₂Cl₂/MeOH.

- General Procedure C: Synthesis of Propargylamines *via* Decarboxylative KA² Reaction with Alkynoic Acids



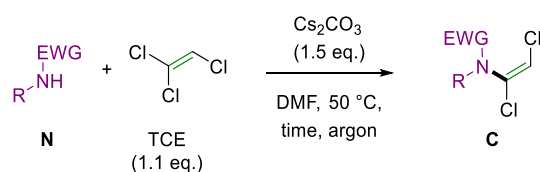
Ketone (1.5 eq., 1.5 mmol), propiolic acid (1.0 eq. 1.0 mmol) and Cu^I-USY (36 mg, 10 mol%) were successively added to a screw cap tube (10 mL) and stirred at rt and 500 rpm for 15 min. Next, amine (1.0 eq., 1.0 mmol) was added, and the mixture was flushed with argon before being progressively heated to 60 °C within 30 min and left to stir at 60 °C for 18 h. Once cooled to rt, the reaction mixture was diluted with EtOAc or CH₂Cl₂ (2 mL) and neutralised with saturated aq. NaHCO₃ (2 mL). The mixture was then filtered over celite and washed with EtOAc or CH₂Cl₂ (3 x 20 mL). The org. phase was washed with saturated aq. NaHCO₃ (10 mL) and brine (10 mL), then dried over Na₂SO₄, filtered, and concentrated under reduced pressure. The crude product was purified by flash chromatography over silica gel using cyclohexane/EtOAc or CH₂Cl₂/MeOH.

- General Procedure D: Sulfonylation of Amines



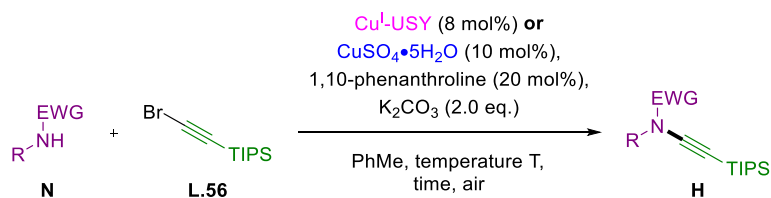
To an ice-cold solution of primary amine (1.0 eq.) and Et₃N (2.0 eq.) in dry CH₂Cl₂ (0.2 M) was added the corresponding sulfonyl chloride (1.1 eq.) in small portions and the mixture was stirred at room temperature until completion as indicated by thin layer chromatography. The reaction was then quenched with water (30 mL/10 mmol amine) and the aq. phase was extracted with CH₂Cl₂ (3 × 20 mL). The combined org. phases were dried over Na₂SO₄, filtered and the solvent was removed under reduced pressure. If necessary, the crude product was purified *via* column chromatography using silica gel or *via* recrystallisation.

▪ General Procedure E: Synthesis of 1,2-Dichloroenamides



Amide **N** (1.0 eq.) and powdered Cs₂CO₃ (1.5 eq.) were given into a flame-dried Schlenk flask equipped with a stirring bar. After three cycles of high vacuum evacuation and argon backfill of the flask, DMF (0.75 mL/mmol of amide substrate) was added and degassed for 5 minutes with argon. Next, the suspension was heated to 50 °C followed by a dropwise addition of trichloroethylene (TCE, 1.1 eq.) over 5 to 10 minutes. The resulting mixture was stirred at 50 °C until completion, as analysed by TLC. The mixture was cooled to room temperature and then partitioned between EtOAc and water (ca. EtOAc/H₂O 2:1). Next, the org. layer was separated and further washed three times with water, and once with brine. The org. layer was then dried over Na₂SO₄, filtered, and the solvent was removed under reduced pressure. The crude mixtures were purified by column chromatography over silica gel using cyclohexane/EtOAc if necessary.

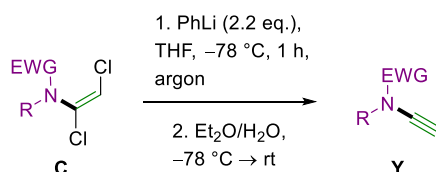
▪ General Procedure F: Synthesis of TIPS-Protected Ynamides



To a solution of 1-bromo-2-(triisopropylsilyl)acetylene (**L.56**, 1.1 eq.) in toluene (0.5 M) were successively added amide **N** (1.0 eq.), K₂CO₃ (2.0 eq.), CuSO₄•5H₂O (10 mol%) (homogeneous)^[255] or Cu^I-USY (8 mol%) (heterogeneous)^[192] and 1,10-phenanthroline (20 mol%). The vial was capped under air, then placed into a pre-heated aluminium block (60-110 °C) and stirred at 600 rpm until completion of the reaction. Next, the reaction mixture was filtered over celite,

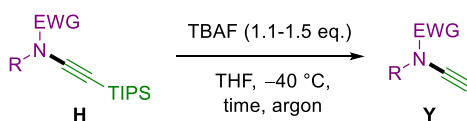
washed with EtOAc or CH₂Cl₂ and the solvent was removed under reduced pressure. The crude mixtures were purified by column chromatography over silica gel using cyclohexane/EtOAc.

▪ General Procedure G: Synthesis of Terminal Ynamides from 1,2-Dichloroenamides



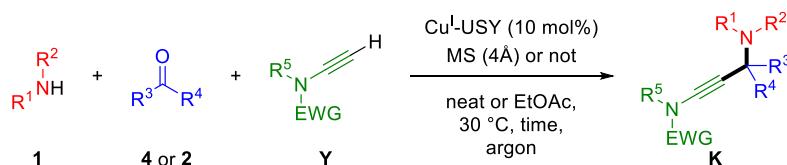
To a solution of 1,2-dichloroenamide (1.0 eq.) in freshly distilled THF (10 mL/mmol enamide) was added phenyllithium solution (1.9 M in Bu₂O, 2.2 eq.) dropwise over 2-10 min under vigorous magnetic stirring at -78 °C. After completion (ca. 1 h at -78 °C), the mixture was quenched with Et₂O/H₂O (1:1) at -78 °C and left to warm to room temperature. The two phases were separated, and the aq. layer was extracted with Et₂O (3×). The combined org. layers were washed once with saturated aq. brine, dried over Na₂SO₄ and the solvent was removed under reduced pressure. The crude mixtures were purified by column chromatography over silica gel using cyclohexane/EtOAc with 1% NEt₃.

▪ General Procedure H: Desilylation of TIPS-protected Ynamides



To a solution of silylated ynamide **H** (1.0 eq.) in freshly distilled THF (1 M) was added TBAF (1 M in THF, 1.1 eq.) dropwise over 2-3 min under vigorous magnetic stirring at -40 °C. After completion, the mixture was quenched with EtOAc/H₂O (1:1) and left to warm to room temperature. The two phases were separated, and the aq. layer was extracted with EtOAc (3×). The combined org. layers were washed once with saturated aq. brine, dried over Na₂SO₄ and the solvent was removed under reduced pressure. The crude mixtures were purified by column chromatography over silica gel using cyclohexane/EtOAc with 1% NEt₃.

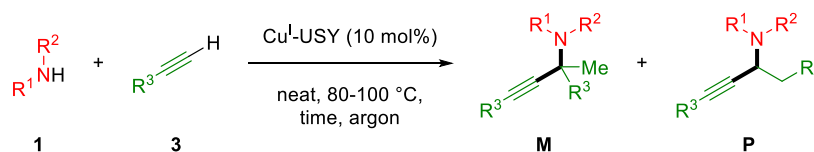
▪ General Procedure I: Synthesis of γ -Amino-Ynamides *via* AYA/KYA



Aldehyde or ketone (1.0 eq.), amine (1.0 eq.), terminal ynamide (1.0 eq.), Cu^I-USY (3 mol%), and MS (4 Å, 75 mg/250 μmol if indicated) were added to a 10 mL screw cap tube. When needed, EtOAc (0.15 mL/250 μmol) is added and the tube is flushed with argon before sealing.

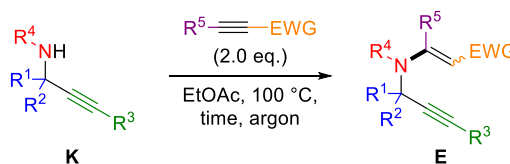
The tube is placed into a pre-heated aluminium block at 30 °C and stirred until completion of starting material at 600 rpm. Next, the mixture was diluted with EtOAc (2 mL), filtered over celite and the residue was washed with EtOAc. The crude product was purified by column chromatography over silica gel cyclohexane/EtOAc with 1% NEt₃.

▪ General Procedure J: Synthesis of Propargylamines *via* HPA Reaction



Cu^I-USY (9 mg, 2.5 mol%), amine (1.0 mmol, 1.0 eq.), alkyne (3.3 mmol, 3.3 eq.) and pyridine (if indicated, 1.0 eq.) were successively added to a screw cap tube (10 mL) equipped with a stirring bar. The tube was flushed with inert gas (argon) for 15 s before sealing. Next, the tube was placed into a pre-heated aluminium block at the indicated temperature and stirred at 250 rpm for the indicated time. Once cooled to room temperature the reaction mixture was diluted with EtOAc (2 mL) and filtered over a short celite pad in a Pasteur pipette. The residue was washed with EtOAc (10 mL) and the solvent was removed under reduced pressure. The crude was purified over silica gel, unless otherwise stated.

▪ General Procedure K: Synthesis of 3-*aza*-1,5-Enynes in Ethyl Acetate



Activated alkyne (2.0 eq.) was added to a solution of propargylamine (1.0 eq.) in EtOAc (1 M) in a screw cap tube (10 mL) equipped with a stirrer. The reaction flask was briefly flushed with argon (10 s) before sealing. Next, the mixture was placed into a pre-heated aluminium block at 100 °C and 500 rpm and stirred until completion. All volatiles were removed under reduced pressure and the crude product was used without further purification unless otherwise stated.

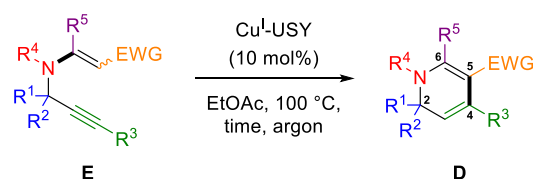
▪ General Procedure L: Synthesis of 3-*aza*-1,5-Enynes in Ethanol



Activated alkyne (1.05 eq.) was added to a solution of propargylamine (1.0 eq.) in EtOH (1 M) in a screw cap tube (3 mL) equipped with a stirrer. The reaction flask was briefly flushed with argon (10 s) before sealing. Next, the mixture was placed into a pre-heated aluminium block at

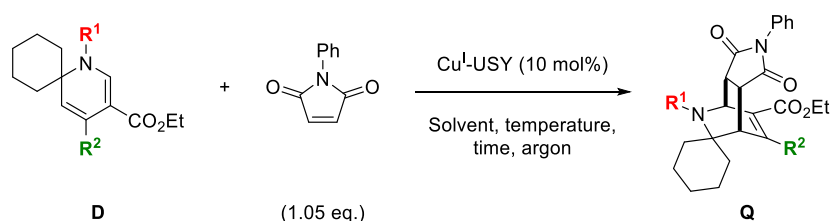
100 °C and 500 rpm and stirred until completion. All volatiles were removed under reduced pressure and the crude product was used without further purification unless otherwise stated. N.B.: A short reactor which is entirely surrounded by the heating source is crucial for the speed of the reaction with methyl and ethyl propiolate for volatility reasons. Otherwise, condensation of the latter on the reactor flask wall renders them partially inaccessible, impeding complete conversion of the amine. Alternatively, a greater excess of activated alkyne, as for the reaction in EtOAc can be used.

▪ General Procedure M: Synthesis of 1,2-Dihydropyridines *via* Cycloisomerisation



Cu^I-USY (10 mol% of copper species) was added to a solution of enyne in EtOAc (1 M) in a screw cap tube (10 mL) equipped with a stirrer. The reaction flask was briefly flushed with argon (10 s) before sealing. Next, the mixture was placed into a pre-heated aluminium block at 100 °C and 500 rpm and stirred until completion. The zeolite catalyst was filtered off through a short pad of celite and the residue was washed several times with EtOAc. Finally, the solvent was removed under reduced pressure and the crude product was purified *via* column chromatography over silica gel or aluminium oxide using an appropriate gradient of cyclohexane/EtOAc eluent.

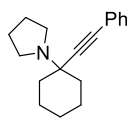
▪ General Procedure N: Synthesis of Isoquinuclidines *via* DIELS-ALDER Reaction



Cu^I-USY (10 mol%) is added to a solution (at 0.5 M concentration relative to **D**) of dihydropyridine **D** (1.0 eq.) and *N*-phenylmaleimide (1.05 eq.) in a screw cap tube equipped with a stirrer. The reaction flask was briefly flushed with argon (10 s) before sealing. Next, the mixture was placed into a pre-heated aluminium block at the desired temperature and 500 rpm. At the end of the reaction, the zeolite catalyst was filtered off through a short pad of celite and the residue was washed several times with EtOAc. The solvent was removed under reduced pressure and the yield was estimated *via* ¹H NMR of the crude using an appropriate internal standard, unless otherwise stated.

Analytical Data of Compounds from Chapter III

1-(1-(Phenylethynyl)cyclohexyl)pyrrolidine (K.1a) (CAS: 835654-21-2)^[219]



Chemical Formula: C₁₈H₂₃N
Molecular Weight: 253,3890

Following the General Procedure A, the title compound **K.1a** was isolated as an orange oil (233 mg, 0.92 mmol). Yield 92%.

R_f = 0.37 (SiO₂, cyclohexane/EtOAc 7:3).

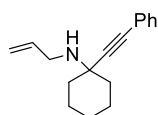
ATR-FTIR (neat) ν = 3299, 3082, 3056, 3025, 2937, 2917, 2857, 1596, 1490, 1464, 1443, 1285, 1117, 1028, 946, 787, 735 cm⁻¹.

¹H NMR (500 MHz, CDCl₃) δ = 7.47 – 7.39 (m, 2H, H_{aro}), 7.32 – 7.26 (m, 3H, H_{aro}), 2.83 – 2.77 (m, 4H, 2 × NCH₂), 2.08 – 2.00 (m, 2H, 2 × NC_qCH₂), 1.82 – 1.77 (m, 4H, 2 × NCH₂CH₂), 1.73 – 1.60 (m, 5H), 1.53 (td, *J* = 11.7, 4.6 Hz, 2H), 1.30 – 1.18 (m, 1H) ppm.

¹³C NMR (126 MHz, CDCl₃) δ = 131.9 (C_{aro}H), 128.3 (C_{aro}H), 127.8 (C_{aro}H), 123.8 (C_q), 90.6 (C≡), 86.2 (C≡), 59.5 (NC_q), 47.2 (NCH₂), 38.1 (CH₂), 25.9 (CH₂), 23.6 (CH₂), 23.2 (CH₂) ppm.

MS (ESI-TOF, + mode) *m/z* (rel intensity) 254.19 (100), 183.12 [C₁₄H₁₅]⁺.

N-Allyl-1-(phenylethynyl)cyclohexan-1-amine (K.1b) (CAS: 2414088-65-4)



Chemical Formula: C₁₇H₂₁N
Molecular Weight: 239,3620

Following the General Procedure A, the title compound **K.1b** was isolated as a yellow oil (225 mg, 0.94 mmol). Yield 94%.

R_f = 0.45 (SiO₂, cyclohexane/EtOAc 7:3).

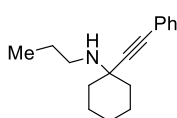
ATR-FTIR (neat) ν = 3080, 3062, 2930, 2855, 1643, 1598, 1489, 1444, 1292, 1158, 1070, 915, 691 cm⁻¹.

¹H NMR (300 MHz, CDCl₃) δ = 7.46 – 7.40 (m, 2H, H_{aro}), 7.34 – 7.27 (m, 3H, H_{aro}), 6.00 (ddt, *J* = 17.3, 10.2, 6.0 Hz, 1H, CH=CH₂), 5.23 (dq, *J* = 17.2, 1.7 Hz, 1H, CH=CH₂), 5.09 (dq, *J* = 10.2, 1.4 Hz, 1H, CH=CH₂), 3.46 (dt, *J* = 6.1, 1.5 Hz, 2H, NCH₂), 2.00 – 1.91 (m, 2H, 2 × NC_qCH₂), 1.74 – 1.58 (m, 5H), 1.51 – 1.39 (m, 4H), 1.33 – 1.17 (m, 1H) ppm.

¹³C{¹H} NMR (126 MHz, CDCl₃) δ = 137.5 (CH), 131.8 (CH), 128.4 (CH), 127.9 (CH), 123.7 (C_q), 115.9 (CH=CH₂), 93.3 (C≡), 84.9 (C≡), 55.1 (NC_q), 46.5 (NCH₂), 38.4 (CH₂), 26.0 (CH₂), 23.2 (CH₂) ppm.

HRMS (ESI-TOF, + mode) *m/z* calcd for C₁₇H₂₂N 240.1747, found 240.1746 [M+H]⁺.

1-(Phenylethynyl)-N-propylcyclohexan-1-amine (K.1c) (CAS: 2173012-03-6)^[32]



Chemical Formula: C₁₇H₂₃N
Molecular Weight: 241,3780

Following the General Procedure A, the title compound **K.1c** was isolated as a yellow oil (208 mg, 0.86 mmol). Yield 86%.

R_f = 0.25 (SiO₂, cyclohexane/EtOAc 7:3).

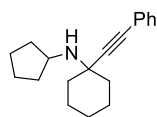
ATR-FTIR (neat) ν = 3081, 3056, 3032, 2929, 2854, 1598, 1489, 1460, 1443, 1289, 1126, 911, 753, 689, 534 cm⁻¹.

¹H NMR (500 MHz, CDCl₃) δ = 7.45 – 7.40 (m, 2H, H_{aro}), 7.34 – 7.27 (m, 3H, H_{aro}), 2.76 (t, *J* = 7.2 Hz, 2H, NCH₂), 1.98 – 1.90 (m, 2H, 2 × NC_qCH₂), 1.73 – 1.61 (m, 5H), 1.53 (h, *J* = 7.3 Hz, 2H, CH₂CH₃), 1.46 – 1.38 (m, 2H), 1.28 – 1.18 (m, 1H), 0.96 (t, *J* = 7.4 Hz, 3H, CH₃) ppm.

¹³C{¹H} NMR (126 MHz, CDCl₃) δ = 131.8 (C_{aro}H), 128.3 (C_{aro}H), 127.8 (C_{aro}H), 123.9 (C_q), 93.8 (C≡), 84.5 (C≡), 55.1 (NC_q), 45.4 (NCH₂), 38.4 (CH₂), 26.1 (CH₂), 24.0 (CH₂), 23.2 (CH₂), 12.2 (CH₃) ppm.

MS (ESI-TOF, + mode) *m/z* (rel intensity) 242.19 (20) [M+H]⁺, 183.12 (100) [C₁₄H₁₅]⁺.

N-Cyclopentyl-1-(phenylethynyl)cyclohexan-1-amine (K.1d) (CAS: 2743452-44-8)



Chemical Formula: C₁₉H₂₅N
Molecular Weight: 267,4160

Following the General Procedure A, the title compound **K.1d** was isolated as a yellow oil (233 mg, 0.87 mmol). Yield 87%.

R_f = 0.48-0.33 (SiO₂, cyclohexane/EtOAc 7:3).

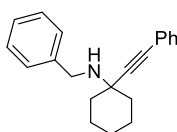
ATR-FTIR (neat) ν = 3058, 2930, 2854, 1598, 1489, 1443, 1342, 1290, 1157, 1122, 1069, 1027, 939, 753, 689 cm⁻¹.

¹H NMR (300 MHz, CDCl₃) δ = 7.41 – 7.34 (m, 2H, H_{aro}), 7.30 – 7.22 (m, 3H, H_{aro}), 3.43 (quint, *J* = 7.6 Hz, 1H, NCH), 1.99 – 1.84 (m, 4H), 1.68 – 1.09 (m, 14H) ppm.

¹³C{¹H} NMR (126 MHz, CDCl₃) δ = 131.7 (C_{aro}H), 128.4 (C_{aro}H), 127.8 (C_{aro}H), 124.0 (C_q), 94.6 (C \equiv), 84.4 (C \equiv), 55.5 (NCH), 55.4 (NC_q), 39.3 (CH₂), 35.8 (CH₂), 25.9 (CH₂), 24.3 (CH₂), 23.3 (CH₂) ppm.

HRMS (ESI-TOF, + mode) *m/z* calcd for C₁₉H₂₆N 268.2060, found 268.2070 [M+H]⁺.

N-Benzyl-1-(phenylethynyl)cyclohexan-1-amine (K.1f) (CAS: 1227795-08-5)^[42]



Chemical Formula: C₂₁H₂₃N
Molecular Weight: 289,4220

Following the General Procedure A, the title compound **K.1f** was isolated as a yellow solid (263 mg, 0.91 mmol). Yield 91%.

R_f = 0.35 (SiO₂, cyclohexane/EtOAc 9:1).

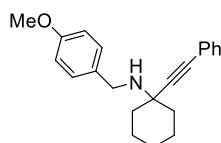
ATR-FTIR (neat) ν = 3299, 3082, 3056, 3025, 2937, 2917, 1596, 1490, 1443, 1285, 1117, 1028, 946, 787, 735 691 cm⁻¹.

¹H NMR (300 MHz, CDCl₃) δ = 7.49 – 7.38 (m, 4H, H_{aro}), 7.36 – 7.29 (m, 5H, H_{aro}), 7.30 – 7.18 (m, 1H, H_{aro}), 3.99 (s, 2H, NCH₂), 2.04 – 1.94 (m, 2H, 2 × NC_qCH₂), 1.77 – 1.52 (m, 7H), 1.36 – 1.19 (m, 1H) ppm.

¹³C{¹H} NMR (126 MHz, CDCl₃) δ = 141.2 (C_q), 131.8 (C_{aro}H), 128.6(4) (C_{aro}H), 128.6(0) (C_{aro}H), 128.4 (C_{aro}H), 127.9 (C_{aro}H), 127.0 (C_{aro}H), 123.8 (C_q), 93.7 (C \equiv), 84.9 (C \equiv), 55.5 (NC_q), 48.2 (NCH₂), 38.3 (CH₂), 26.1 (CH₂), 23.2 (CH₂) ppm.

MS (ESI-TOF, + mode) *m/z* (rel intensity) 290.19 (50) [M+H]⁺, 183.12 (100) [C₁₄H₁₅]⁺, 108.08 (15) [C₇H₁₀N]⁺.

N-(4-Methoxybenzyl)-1-(phenylethynyl)cyclohexan-1-amine (K.1g) (CAS: 1227794-87-7)^[42]



Chemical Formula: C₂₂H₂₅NO
Molecular Weight: 319,4480

Following the General Procedure A, the title compound **K.1g** was isolated as a yellow oil (268 mg, 0.84 mmol). Yield 84%.

R_f = 0.45 (SiO₂, cyclohexane/EtOAc 7:3).

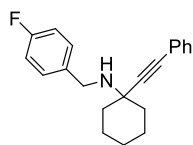
ATR-FTIR (neat) ν = 3310, 3079, 3058, 3032, 2996, 2929, 2852, 2852, 2834, 1611, 1598, 1585, 1510, 1442, 1172, 1034, 822 cm⁻¹.

¹H NMR (400 MHz, CDCl₃) δ = 7.49 – 7.43 (m, 2H, H_{aro}), 7.35 – 7.28 (m, 5H, H_{aro}), 6.90 – 6.82 (m, 2H, 2 × OC_qCH_{aro}), 3.92 (s, 2H, NCH₂), 3.80 (s, 3H, CH₃), 2.02 – 1.93 (m, 2H, 2 × NC_qCH₂), 1.78 – 1.61 (m, 5H), 1.57 – 1.47 (m, 2H), 1.35 – 1.20 (m, 2H) ppm.

¹³C{¹H} NMR (126 MHz, CDCl₃) δ = 158.7 (CH₃OC_q), 133.4 (C_q), 131.8 (C_{aro}H), 129.8 (C_{aro}H), 128.4 (C_{aro}H), 127.9 (C_{aro}H), 123.8 (C_q), 114.0 (C_{aro}H), 93.8 (C \equiv), 84.8 (C \equiv), 55.4(4) (OCH₃), 55.4(3) (NC_q), 47.6 (NCH₂), 38.4 (CH₂), 26.1 (CH₂), 23.2 (CH₂) ppm.

MS (ESI-TOF, + mode) *m/z* (rel intensity) 320.20 (100) [M+H]⁺, 183.12 (80) [C₁₄H₁₅]⁺, 121.07 (50) [C₈H₉O]⁺.

N-(4-Fluorobenzyl)-1-(phenylethynyl)cyclohexan-1-amine (K.1h) (CAS: 2320511-46-2)^[237]



Chemical Formula: C₂₁H₂₂FN
Molecular Weight: 307,4124

Following the General Procedure A, the title compound **K.1h** was isolated as a yellow oil (295 mg, 0.96 mmol). Yield 96%.

R_f = 0.68 (SiO₂, cyclohexane/EtOAc 7:3).

ATR-FTIR (neat) ν = 3080, 3054, 2930, 2853, 1600, 1508, 1489, 1443, 1219, 1114, 824, 753, 689 cm⁻¹.

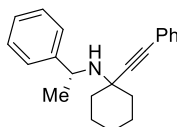
¹H NMR (300 MHz, CDCl₃) δ = 7.50 – 7.42 (m, 2H, H_{aro}), 7.40 – 7.28 (m, 5H, H_{aro}), 7.05 – 6.96 (m, 2H, H_{aro}), 3.94 (s, 2H, NCH₂), 2.02 – 1.92 (m, 2H, 2 × NC_qCH₂), 1.78 – 1.61 (m, 5H), 1.57 – 1.46 (m, 2H), 1.34 (s, 1H), 1.32 – 1.23 (m, 1H) ppm.

¹⁹F{¹H} NMR (282 MHz, CDCl₃) δ = -116.3 ppm.

¹³C{¹H} NMR (126 MHz, CDCl₃) δ = 162.0 (d, ¹J_{C-F} = 244.3 Hz, FC_q), 137.0 (d, ⁴J_{C-F} = 3.2 Hz, NCH₂C_q), 131.8 (C_{aro}H), 130.1 (d, ³J_{C-F} = 7.9 Hz, FC_qCHCH), 128.4 (C_{aro}H), 128.0 (C_{aro}H), 123.7 (C_q-Ph), 115.3 (d, ²J_{C-F} = 21.2 Hz, FC_qCH), 93.6 (C≡), 84.9 (C≡), 55.4 (NC_q), 47.5 (NCH₂), 38.4 (CH₂), 26.0 (CH₂), 23.1 (CH₂) ppm.

MS (ESI-TOF, + mode) *m/z* (rel intensity) 308.18 (25) [M+H]⁺, 183.12 (100) [C₁₄H₁₅]⁺.

(R)-N-(1-Phenylethyl)-1-(phenylethynyl)cyclohexan-1-amine (K.1i) (CAS: 2320511-45-1)^[237]



Chemical Formula: C₂₂H₂₅N
Molecular Weight: 303,4490

Following the General Procedure A, the title compound **K.1i** was isolated as a yellow oil (182 mg, 0.60 mmol). Yield 60%.

R_f = 0.72 (SiO₂, cyclohexane/EtOAc 7:3).

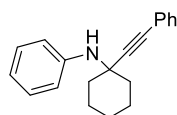
ATR-FTIR (neat) ν = 3331, 3081, 3060, 3024, 2929, 2854, 1598, 1489, 1445, 1343, 1290, 1115, 1070, 952, 754, 690 cm⁻¹.

¹H NMR (300 MHz, CDCl₃) δ = 7.43 – 7.33 (m, 4H, H_{aro}), 7.31 – 7.12 (m, 6H, H_{aro}), 4.30 (q, *J* = 6.7 Hz, 1H, NCH), 1.93 – 1.84 (m, 1H), 1.71 – 1.61 (m, 2H, 2 × NC_qCH₂), 1.61 – 1.40 (m, 6H), 1.37 (d, *J* = 6.7 Hz, 3H, CH₃), 1.19 – 1.03 (m, 2H) ppm.

¹³C{¹H} NMR (126 MHz, CDCl₃) δ = 148.6 (C_q), 131.7 (C_{aro}H), 128.3(4) (C_{aro}H), 128.3(1) (C_{aro}H), 127.8 (C_{aro}H), 126.9 (C_{aro}H), 126.5 (C_{aro}H), 123.9 (C_q), 94.2 (C≡), 84.6 (C≡), 56.1 (NC_q), 53.8 (NCH), 39.9 (CH₂), 38.8 (CH₂), 26.9 (CH₃), 25.8 (CH₂), 23.3 (CH₂), 23.1 (CH₂) ppm.

MS (ESI-TOF, + mode) *m/z* (rel intensity) 304.21 (50) [M+H]⁺, 183.12 (100) [C₁₄H₁₅]⁺, 122.09 (25) [C₈H₁₂N]⁺.

N-(1-(Phenylethynyl)cyclohexyl)aniline (K.1j) (CAS: 2243957-86-8)^[29]



Chemical Formula: C₂₀H₂₁N
Molecular Weight: 275,3950

Following the General Procedure A, the title compound **K.1j** was isolated as a pale brown solid (99 mg, 0.36 mmol). Yield 36%.

R_f = 0.78 (SiO₂, cyclohexane/EtOAc 7:3).

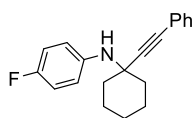
ATR-FTIR (neat) ν = 3362, 3080, 3054, 3027, 2970, 2928, 2854, 1598, 1489, 1434, 1318, 1254, 1157, 1070, 975, 743, 690, 553 cm⁻¹.

¹H NMR (300 MHz, CDCl₃) δ = 7.44 – 7.37 (m, 2H, H_{aro}), 7.31 – 7.26 (m, 3H, H_{aro}), 7.23 – 7.13 (m, 2H, H_{aro}), 7.05 – 6.99 (m, 2H, H_{aro}), 6.78 (tt, *J* = 7.3, 1.1 Hz, 1H, *p*-H_{aro}), 3.71 (bs, 1H, NH), 2.33 – 2.21 (m, 2H, 2 × NC_qCH₂), 1.85 – 1.57 (m, 6H), 1.38 – 1.22 (m, 2H) ppm.

¹³C{¹H} NMR (126 MHz, CDCl₃) δ = 145.7 (C_q), 131.7 (C_{aro}H), 128.9 (C_{aro}H), 128.3 (C_{aro}H), 128.0 (C_{aro}H), 123.6 (C_q), 118.7 (C_{aro}H), 117.1 (C_{aro}H), 92.2 (C≡), 85.6 (C≡), 53.2 (NC_q), 38.9 (CH₂), 25.8 (CH₂), 22.9 (CH₂) ppm.

MS (ESI-TOF, + mode) *m/z* (rel intensity) 276.17 (15) [M+H]⁺, 183.12 (100) [C₁₄H₁₅]⁺.

4-Fluoro-N-(1-(phenylethynyl)cyclohexyl)aniline (K.1l) (CAS: 2743452-48-2)



Chemical Formula: C₂₀H₂₀FN
Molecular Weight: 293,3854

Following the General Procedure A, the title compound **K.1l** was isolated as a pale orange solid (182 mg, 0.62 mmol). Yield 62%.

R_f = 0.52 (SiO₂, cyclohexane/EtOAc 7:3).

ATR-FTIR (neat) ν = 3364, 3084, 3062, 3035, 2969, 2856, 1596, 1503, 1440, 1290, 1214, 111, 915, 820, 757, 692 cm⁻¹.

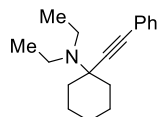
¹H NMR (300 MHz, CDCl₃) δ = 7.42 – 7.34 (m, 2H, H_{aro}), 7.32 – 7.27 (m, 3H, H_{aro}), 7.03 – 6.95 (m, 2H, H_{aro}), 6.94 – 6.85 (m, 2H, H_{aro}), 3.54 (bs, 1H, NH), 2.26 – 2.13 (m, 2H, 2 × NC_qCH₂), 1.79 – 1.52 (m, 7H), 1.37 – 1.24 (m, 1H) ppm.

¹⁹F{¹H} NMR (282 MHz, CDCl₃) δ = –125.4 ppm.

¹³C{¹H} NMR (126 MHz, CDCl₃) δ = 157.3 (d, ¹J_{C-F} = 238.1 Hz, FC_q), 141.7 (d, ⁴J_{C-F} = 2.3 Hz, NC_{q-aro}), 131.7 (C_{aro}H), 128.4 (C_{aro}H), 128.1 (C_{aro}H), 123.4 (C_{q-Ph}), 119.7 (d, ³J_{C-F} = 7.4 Hz, FC_qCHCH), 115.3 (d, ²J_{C-F} = 22.1 Hz, FC_qCH), 92.2 (C≡), 85.7 (C≡), 54.1 (NC_q), 38.9 (CH₂), 25.7 (CH₂), 23.0 (CH₂) ppm.

HRMS (ESI-TOF, + mode) *m/z* calcd for C₂₀H₂₁FN 294.1653, found 294.1650 [M+H]⁺.

N,N-Diethyl-1-(phenylethynyl)cyclohexan-1-amine (K.1o) (CAS: 2191418-95-6)^[368]



Chemical Formula: C₁₈H₂₅N
Molecular Weight: 255,4050

Following the General Procedure A, the title compound **K.1o** was isolated in 20% yield (51 mg, 0.20 mmol). Following the General Procedure C, the title compound **K.1o** was isolated in 31% yield as a yellow oil (79 mg, 0.31 mmol).

R_f = 0.58 (SiO₂, cyclohexane/EtOAc 7:3).

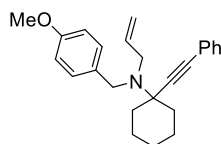
ATR-FTIR (neat) ν = 3080, 3056, 2928, 2855, 1598, 1489, 1444, 1344, 1228, 1155 948, 754, 690 cm⁻¹.

¹H NMR (500 MHz, CDCl₃) δ = 7.45 – 7.35 (m, 2H, H_{aro}), 7.31 – 7.22 (m, 3H, H_{aro}), 2.76 (q, *J* = 7.2 Hz, 4H, 2 × CH₂CH₃), 2.11 – 2.01 (m, 2H, 2 × NC_qCH₂), 1.74 – 1.55 (m, 5H), 1.52 – 1.39 (m, 2H), 1.29 – 1.14 (m, 1H), 1.10 (t, *J* = 7.2 Hz, 6H, 2 × CH₃) ppm.

¹³C{¹H} NMR (126 MHz, CDCl₃) δ = 131.6 (C_{aro}H), 128.3 (C_{aro}H), 127.7 (C_{aro}H), 124.1 (C_q), 93.2 (C≡), 85.2 (C≡), 59.5 (NC_q), 42.9 (NCH₂), 37.3, (CH₂) 25.9 (CH₂), 23.4 (CH₂), 15.0 (CH₃) ppm.

MS (ESI-TOF, + mode) *m/z* 256.20 (45) [M+H]⁺, 183.12 (100) [C₁₄H₁₅]⁺.

N-Allyl-N-(4-methoxybenzyl)-1-(phenylethynyl)cyclohexan-1-amine (K.1p) (CAS: 2743452-50-6)



Chemical Formula: C₂₅H₂₉NO
Molecular Weight: 359,5130

Following the General Procedure A, the title compound **K.1p** was isolated as a yellow oil (169 mg, 0.47 mmol). Yield 47%.

R_f = 0.75 (SiO₂, cyclohexane/EtOAc 7:3).

ATR-FTIR (neat) ν = 3064, 3032, 2995, 2930, 2853, 2833, 1611, 1598, 1585, 1509, 1442, 1292, 1241, 1036, 913, 816, 690 cm⁻¹.

¹H NMR (500 MHz, CDCl₃) δ = 7.49 – 7.42 (m, 2H, H_{aro}), 7.36 – 7.26 (m, 5H, H_{aro}), 6.87 – 6.81 (m, 2H, 2 × OC_qCH_{aro}), 6.02 (ddt, *J* = 16.7, 10.1, 6.4 Hz, 1H, CH=CH₂), 5.04 (dq, *J* = 17.2 Hz, 1.6, 1H, CH=CH₂), 5.01 – 4.97 (m, 1H, CH=CH₂), 3.81 (s, 2H, NCH₂ benzyl), 3.80 (s, 3H, CH₃), 3.37 – 3.32 (m, 2H, NCH₂ allyl), 2.14 – 2.07 (m, 2H, 2 × NC_qCH₂), 1.77 – 1.52 (m, 7H), 1.30 – 1.18 (m, 1H) ppm.

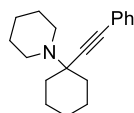
¹³C{¹H} NMR (126 MHz, CDCl₃) δ = 158.3 (CH₃OC_q), 137.7 (CH), 134.1 (C_q), 131.8 (CH), 129.6 (CH), 128.4 (CH), 127.8 (CH), 124.0 (C_q), 115.9 (CH=CH₂), 113.5 (CH), 92.6 (C≡),

85.5 (C≡), 59.7 (NC_q), 55.4 (OCH₃), 52.3(9) (NCH₂), 52.3(6) (NCH₂), 37.7 (CH₂), 25.8 (CH₂), 23.3 (CH₂) ppm.

MS (ESI-TOF, + mode) *m/z* (rel intensity) 360.24 (100) [M+H]⁺, 178.13 (30) [C₁₁H₁₆NO]⁺.

HRMS (ESI-TOF, + mode) *m/z* calcd for C₂₅H₃₀NO 360.2322, found 360.2322 [M+H]⁺.

1-(1-(Phenylethynyl)cyclohexyl)piperidine (K.1q) (CAS: 330593-87-8)^[237]



Chemical Formula: C₁₉H₂₅N
Molecular Weight: 267,4160

Following the General Procedure A, the title compound **K.1q** was isolated in 61% yield (163 mg, 0.61 mmol). Following the General Procedure C, the title compound **K.1q** was isolated in 81% yield as a yellow oil (217 mg, 0.81 mmol).

R_f = 0.48 (SiO₂, cyclohexane/EtOAc 7:3).

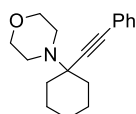
ATR-FTIR (neat) ν = 3081, 2978, 2927, 2852, 2795, 1598, 1489, 1468, 1442, 1292, 1156, 1095, 965, 753, 689 cm⁻¹.

¹H NMR (500 MHz, CDCl₃) δ = 7.47 – 7.43 (m, 2H, H_{aro}), 7.32 – 7.27 (m, 3H, H_{aro}), 2.68 (bs, 4H), 2.16 – 2.03 (m, 2H, 2 × NC_qCH₂), 1.77 – 1.69 (m, 2H), 1.69 – 1.57 (m, 7H), 1.53 – 1.41 (m, 4H), 1.28 – 1.21 (m, 1H) ppm.

¹³C{¹H} NMR (126 MHz, CDCl₃) δ = 131.9 (C_{aro}H), 128.3 (C_{aro}H), 127.8 (C_{aro}H), 123.9 (C_q), 91.0 (C≡), 86.2 (C≡), 59.4 (NC_q), 47.3 (NCH₂), 35.9 (CH₂), 26.8 (CH₂), 25.9 (CH₂), 24.9 (CH₂), 23.3 (CH₂) ppm.

MS (ESI-TOF, + mode) *m/z* 268.20 (100) [M+H]⁺, 183.12 (40) [C₁₄H₁₅]⁺.

4-(1-(Phenylethynyl)cyclohexyl)morpholine (K.1r) (CAS: 164264-99-7)^[237]



Chemical Formula: C₁₈H₂₃NO
Molecular Weight: 269,3880

Following the General Procedure A, the title compound **K.1r** was isolated in 52% yield (140 mg, 0.52 mmol). Following the General Procedure C, the title compound **K.1r** was isolated in 79% yield as a pale yellow solid (213 mg, 0.79 mmol).

R_f = 0.69 (SiO₂, cyclohexane/EtOAc 7:3).

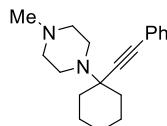
ATR-FTIR (neat) ν = 3056, 2929, 2852, 2817, 1597, 1489, 1452, 1269, 1117, 973, 754, 690 cm⁻¹.

¹H NMR (500 MHz, CDCl₃) δ = 7.45 – 7.39 (m, 2H, H_{aro}), 7.31 – 7.22 (m, 3H, H_{aro}), 3.78 – 3.71 (m, 4H, 2 × OCH₂), 2.73 – 2.67 (m, 4H, 2 × NCH₂), 2.06 – 1.95 (m, 2H, 2 × NC_qCH₂), 1.75 – 1.66 (m, 2H), 1.65 – 1.55 (m, 3H), 1.51 – 1.42 (m, 2H), 1.30 – 1.19 (m, 1H) ppm.

¹³C{¹H} NMR (126 MHz, CDCl₃) δ = 131.8 (C_{aro}H), 128.3 (C_{aro}H), 127.9 (C_{aro}H), 123.5 (C_q), 89.9 (C≡), 86.6 (C≡), 67.6 (CH₂O), 59.0 (NC_q), 46.8 (NCH₂), 35.6 (CH₂), 25.8 (CH₂), 22.9 (CH₂) ppm.

MS (ESI, + mode) *m/z* 270.18 (65) [M+H]⁺, 183.12 (100) [C₁₄H₁₅]⁺.

1-Methyl-4-(1-(phenylethynyl)cyclohexyl)piperazine (K.1s) (CAS: 1312712-39-2)^[369]



Chemical Formula: C₁₉H₂₆N₂
Molecular Weight: 282,4310

Following the General Procedure A, the title compound **K.1s** was isolated in 57% yield (161 mg, 0.57 mmol). Following the General Procedure C, the title compound **K.1s** was isolated in 58% yield as a yellow oil (164 mg, 0.58 mmol).

R_f = 0.36 (SiO₂, CH₂Cl₂/MeOH 9:1).

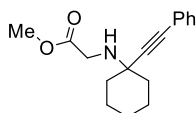
ATR-FTIR (neat) ν = 3080, 3056, 3031, 2929, 2853, 2790, 2695, 1598, 1489, 1454, 1290, 1158, 1011, 866, 754, 690 cm⁻¹.

¹H NMR (500 MHz, CDCl₃) δ = 7.44 – 7.40 (m, 2H, H_{aro}), 7.28 – 7.24 (m, 3H, H_{aro}), 2.79 (bs, 4H, NCH₂), 2.52 (bs, 4H, NCH₂), 2.30 (s, 3H, NCH₃), 2.11 – 2.02 (m, 2H, 2 × NC_qCH₂), 1.77 – 1.68 (m, 2H), 1.68 – 1.57 (m, 3H), 1.50 (td, *J* = 11.8, 3.6 Hz, 2H), 1.31 – 1.19 (m, 1H) ppm.

¹³C{¹H} NMR (126 MHz, CDCl₃) δ = 131.9 (C_{aro}H), 128.2 (C_{aro}H), 127.8 (C_{aro}H), 123.7 (C_q), 90.1 (C≡), 86.7 (C≡), 58.8 (NC_q), 55.8 (NCH₂), 46.0(9) (NCH₂), 46.0(6) (NCH₃), 35.9 (CH₂), 25.8 (CH₂), 23.0 (CH₂) ppm.

MS (ESI-TOF, + mode) *m/z* (rel intensity) 283.22 (100) [M+H]⁺, 183.12 (70) [C₁₄H₁₅]⁺, 101.11 (10) [C₈H₅]⁺.

Methyl (1-(phenylethynyl)cyclohexyl)glycinate (K.1v) (CAS: 1623816-51-2)



Chemical Formula: C₁₇H₂₁NO₂
Molecular Weight: 271,3600

Following the General Procedure A, the title compound **K.1v** was isolated as a yellow oil (54 mg, 0.20 mmol). Yield 20%.

R_f = 0.38 (SiO₂, cyclohexane/EtOAc 7:3).

ATR-FTIR (neat) ν = 3321, 3056, 3021, 2996, 2930, 2854, 1741, 1598, 1489, 1437, 1351, 1214, 1136, 991, 897, 754, 690, 558 cm⁻¹.

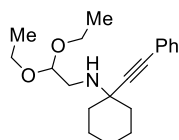
¹H NMR (500 MHz, CDCl₃) δ = 7.43 – 7.38 (m, 2H, H_{aro}), 7.32 – 7.27 (m, 3H, H_{aro}), 3.72 (s, 3H, CH₃), 3.64 (s, 2H, NCH₂), 1.96 – 1.89 (m, 2H, 2 × NC_qCH₂), 1.74 – 1.61 (m, 5H), 1.47 (td, *J* = 12.1, 4.0 Hz, 2H), 1.29 – 1.19 (m, 1H) ppm.

¹³C{¹H} NMR (126 MHz, CDCl₃) δ = 173.3 (C=O), 131.8 (C_{aro}H), 128.4 (C_{aro}H), 128.1 (C_{aro}H), 123.4 (C_q), 92.2 (C≡), 85.4 (C≡), 55.0 (NC_q), 52.1 (OCH₃), 45.5 (NCH₂), 38.2 (CH₂), 25.9 (CH₂), 23.1 (CH₂) ppm.

MS (ESI-TOF, + mode) *m/z* (rel intensity) 294.14 (60) [M+Na]⁺, 183.12 (100) [C₁₄H₁₅]⁺.

HRMS (ESI-TOF, + mode) *m/z* calcd for C₁₇H₂₁NNaO₂ 294.1464, found 294.1467 [M+Na]⁺.

N-(2,2-Diethoxyethyl)-1-(phenylethynyl)cyclohexan-1-amine (K.1w) (CAS: 2743452-53-9)



Chemical Formula: C₂₀H₂₉NO₂
Molecular Weight: 315,4570

Following the General Procedure A, the title compound **K.1w** was isolated as a yellow oil (284 mg, 0.90 mmol). Yield 90%.

R_f = 0.40 (SiO₂, cyclohexane/EtOAc 7:3).

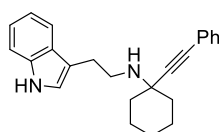
ATR-FTIR (neat) ν = 3323, 3057, 2974, 2929, 2855, 1598, 1488, 1443, 1374, 1291, 1123, 1060, 916, 754, 690 cm⁻¹.

¹H NMR (500 MHz, CDCl₃) δ = 7.42 – 7.36 (m, 2H, H_{aro}), 7.30 – 7.25 (m, 3H, H_{aro}), 4.66 (t, *J* = 5.7 Hz, 1H, O₂CH), 3.70 (dq, *J* = 9.3, 7.0 Hz, 2H, 2 × OCH₂), 3.55 (dq, *J* = 9.4, 7.0 Hz, 2H, 2 × OCH₂), 2.94 (d, *J* = 5.8 Hz, 2H, NCH₂), 1.98 – 1.88 (m, 2H, 2 × NC_qCH₂), 1.71 – 1.59 (m, 5H), 1.51 – 1.36 (m, 3H), 1.20 (t, *J* = 7.1 Hz, 6H, 2 × CH₃) ppm.

¹³C{¹H} NMR (126 MHz, CDCl₃) δ = 131.8 (C_{aro}H), 128.3 (C_{aro}H), 127.9 (C_{aro}H), 123.8 (C_q), 102.5 (CHO₂), 93.2 (C≡), 84.8 (C≡), 61.9 (OCH₂), 54.7 (NC_q), 45.6 (NCH₂), 38.4 (CH₂), 26.0 (CH₂), 23.2 (CH₂), 15.5 (CH₃) ppm.

HRMS (ESI-TOF, + mode) *m/z* calcd for C₂₀H₃₀NO₂, 316.2271, found 316.2281 [M+H]⁺.

N-(2-(1H-Indol-3-yl)ethyl)-1-(phenylethynyl)cyclohexan-1-amine (K.1x) (CAS: 2743452-55-1)



Chemical Formula: C₂₄H₂₆N₂
Molecular Weight: 342,4860

Following the General Procedure A, the title compound **K.1x** was isolated as a pale brown solid (281 mg, 0.82 mmol). Yield 82%.

R_f = 0.50 (SiO₂, CH₂Cl₂/MeOH 9:1).

ATR-FTIR (neat) ν = 3279, 3134, 3093, 3046, 3023, 2974, 2930, 2853, 2751, 2714, 1618, 1598, 1490, 1442, 1348, 1217, 1103, 910, 841,

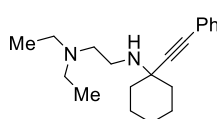
692 cm⁻¹.

¹H NMR (500 MHz, CDCl₃) δ = 7.98 (bs, 1H, NH indol), 7.66 (d, J = 7.9 Hz, 1H, H_{aro}), 7.36 (d, J = 8.2 Hz, 1H, H_{aro}), 7.33 – 7.27 (m, 5H, H_{aro}), 7.19 (t, J = 7.5 Hz, 1H, H_{aro}), 7.11 (d, J = 2.3 Hz, 1H, N_{indol}CH), 7.08 (t, J = 7.5 Hz, 1H, H_{aro}), 3.22 (t, J = 7.0 Hz, 2H, NCH₂), 3.05 (t, J = 7.0 Hz, 2H, NCH₂CH₂), 1.94 (d, J = 12.2 Hz, 2H, 2 × NC_qCH₂), 1.72 – 1.59 (m, 6H), 1.52 – 1.40 (m, 2H), 1.27 – 1.18 (m, 1H) ppm.

¹³C{¹H} NMR (126 MHz, CDCl₃) δ = 136.4 (C_q), 131.6 (C_{aro}H), 128.2 (C_{aro}H), 127.7 (C_{aro}H), 127.6 (C_q), 123.5 (C_q), 122.0 (C_{aro}H), 121.9 (C_{aro}H), 119.3 (C_{aro}H), 119.1 (C_{aro}H), 111.1 (C_{aro}H), 55.3 (CH₂NC_q) 43.1 (NCH₂), 38.1 (CH₂), 26.1 (CH₂), 25.9 (CH₂), 23.1 (CH₂) ppm. N.B.: C≡C signals were not observed in ¹³C{¹H} NMR and one C_{q-aro} is missing, perhaps due to signal overlap.

HRMS (ESI-TOF, + mode) m/z calcd for C₂₄H₂₇N₂ 343.2169, found 343.2160 [M+H]⁺.

N¹,N¹-Diethyl-N²-(1-(phenylethynyl)cyclohexyl)ethane-1,2-diamine (K.1z) (CAS: 2743452-57-3)



Chemical Formula: C₂₀H₃₀N₂
Molecular Weight: 298,4740

Following the General Procedure A, the title compound **K.1z** was isolated as a brown oil (275 mg, 0.92 mmol). Yield 92%.

R_f = 0.35 (SiO₂, CH₂Cl₂/MeOH 9:1).

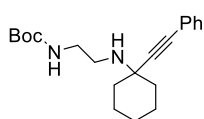
ATR-FTIR (neat) ν = 3283, 3081, 3057, 3031, 2966, 2930, 2853, 2807, 1598, 1444, 1372, 1290, 1124, 1069, 910, 754, 690 cm⁻¹.

¹H NMR (300 MHz, CDCl₃) δ = 7.44 – 7.36 (m, 2H, H_{aro}), 7.35 – 7.27 (m, 3H, H_{aro}), 2.89 (t, J = 6.1 Hz, 2H, NCH₂CH₂NEt₂), 2.66 – 2.50 (m, 6H, 2 × NCH₂CH₃ & Et₂NCH₂), 1.95 (d, J = 12.5 Hz, 2H, 2 × NC_qCH₂), 1.73 – 1.63 (m, 5H), 1.52 – 1.37 (m, 2H), 1.32 – 1.16 (m, 1H), 1.01 (t, J = 7.1 Hz, 6H, 2 × CH₃) ppm.

¹³C{¹H} NMR (126 MHz, CDCl₃) δ = 131.7 (C_{aro}H), 128.3 (C_{aro}H), 127.8 (C_{aro}H), 123.9 (C_q), 93.7 (C≡), 84.5 (C≡), 55.2 (NC_q), 52.6 (NCH₂), 46.7 (NCH₂), 40.6 (NCH₂), 38.3 (CH₂), 26.1 (CH₂), 23.3 (CH₂), 11.7 (CH₃) ppm.

HRMS (ESI-TOF, + mode) m/z calcd for C₂₀H₃₁N₂ 299.2482, found 299.2468 [M+H]⁺.

tert-Butyl 2-((1-(phenylethynyl)cyclohexyl)amino)ethylcarbamate (K.1ba) (CAS: 2743452-59-5)



Chemical Formula: C₂₁H₃₀N₂O₂
Molecular Weight: 342,4830

Following the General Procedure A, the title compound **K.1ba** was isolated as an orange viscous oil (295 mg, 0.86 mmol). Yield 86%.

R_f = 0.25 (SiO₂, cyclohexane/EtOAc 7:3).

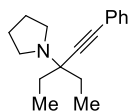
ATR-FTIR (neat) ν = 3428, 3343, 3056, 2975, 2930, 2855, 1695, 1598, 1489, 1444, 1391, 1365, 1249, 1165, 975, 860, 754, 691 cm⁻¹.

¹H NMR (500 MHz, CDCl₃) δ = 7.44 – 7.37 (m, 2H, H_{aro}), 7.32 – 7.27 (m, 3H, H_{aro}), 4.96 (bs, 1H, BocNH), 3.26 (q, J = 5.7 Hz, 2H, BocNHCH₂), 2.92 (t, J = 5.9 Hz, 2H, BocNHCH₂CH₂), 1.95 – 1.88 (m, 2H, 2 × NC_qCH₂), 1.73 – 1.59 (m, 5H), 1.49 – 1.39 (m, 12H, C(CH₃)₃ & 3H cyclohexyl), 1.29 – 1.19 (m, 1H) ppm.

¹³C{¹H} NMR (126 MHz, CDCl₃) δ = 156.3 (C=O), 131.8 (C_{aro}H), 128.4 (C_{aro}H), 128.0 (C_{aro}H), 123.6 (C_q), 93.3 (C≡), 84.7 (C≡), 79.3 (C(CH₃)₃), 54.9 (CH₂NC_q), 43.0 (NCH₂), 41.4 (NCH₂), 38.4 (CH₂), 28.6 (C(CH₃)₃), 26.0 (CH₂), 23.1 (CH₂) ppm.

HRMS (ESI-TOF, + mode) m/z calcd for C₂₁H₃₁N₂O₂ 343.2380, found 343.2397 [M+H]⁺.

1-(3-Ethyl-1-phenylpent-1-yn-3-yl)pyrrolidine (K.2a) (CAS: 1778637-35-6)^[237]



Chemical Formula: C₁₇H₂₃N
Molecular Weight: 241,3780

Following the General Procedure A, the title compound **K.2a** was obtained as a yellow oil in a hard-to-purify mixture in an estimated ¹H NMR yield of 20% using 1,3,5-trimethoxybenzene as internal standard. Following the General Procedure C, the title compound **K.2a** was isolated as a yellow oil (68 mg, 0.28 mmol). Yield 28%.

R_f = 0.25 (SiO₂, cyclohexane/EtOAc 7:3).

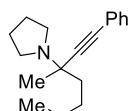
ATR-FTIR (neat) ν = 3080, 3055, 3031, 2965, 2939, 2875, 2806, 1598, 1489, 1457, 1443, 1375, 1334, 1279, 1144, 1070, 1008, 945, 912, 753, 689 cm⁻¹.

¹H NMR (500 MHz, CDCl₃) δ = 7.44 – 7.39 (m, 2H, H_{aro}), 7.31 – 7.26 (m, 3H, H_{aro}), 2.80 – 2.71 (m, 4H, 2 × NCH₂), 1.85 – 1.68 (m, 8H, 2 × NCH₂CH₂ & 2 × CH₂CH₃), 0.95 (t, *J* = 7.4 Hz, 6H, 2 × CH₃) ppm.

¹³C{¹H} NMR (126 MHz, CDCl₃) δ = 131.8 (C_{aro}H), 128.2 (C_{aro}H), 127.6 (C_{aro}H), 123.8, (C_q) 91.5 (C≡), 84.8 (C≡), 62.0 (NC_q), 47.5 (NCH₂), 28.9 (CH₂), 23.6 (CH₂), 8.2 (CH₃) ppm.

MS (ESI-TOF, + mode) *m/z* (rel intensity) 242.19 (50) [M+H]⁺, 171.12 (100) [C₁₃H₁₅]⁺.

1-(3-Methyl-1-phenylhept-1-yn-3-yl)pyrrolidine (K.2b) (CAS: 1456784-44-3)^[219]



Chemical Formula: C₁₈H₂₅N
Molecular Weight: 255,4050

Following the General Procedure A, the title compound **K.2b** was isolated as a yellow oil (138 mg, 0.54 mmol). Yield 54%.

R_f = 0.39 (SiO₂, cyclohexane/EtOAc 6:4).

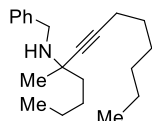
ATR-FTIR (neat) ν = 3080, 3056, 2956, 2871, 2808, 1489, 1460, 1443, 1370, 1264, 1145, 754, 690 cm⁻¹.

¹H NMR (500 MHz, CDCl₃) δ = 7.43 – 7.36 (m, 2H, H_{aro}), 7.31 – 7.22 (m, 3H, H_{aro}), 2.84 – 2.70 (m, 4H, 2 × NCH₂), 1.83 – 1.72 (m, 5H, 2 × NCH₂CH₂ & C_qCH₂), 1.65 (td, *J* = 12.6, 5.1 Hz, 1H, C_qCH₂), 1.54 – 1.27 (m, 7H), 0.92 (t, *J* = 7.2 Hz, 3H, CH₂CH₃) ppm.

¹³C{¹H} NMR (126 MHz, CDCl₃) δ = 131.9 (C_{aro}H), 128.3 (C_{aro}H), 127.8 (C_{aro}H), 123.7 (C_q), 91.6 (C≡), 84.5 (C≡), 58.1 (NC_q), 47.9 (CH₂), 41.4 (CH₂), 26.7 (C_qCH₃), 26.0 (CH₂), 23.8 (CH₂), 23.3 (CH₂), 14.3 (CH₂CH₃) ppm.

MS (ESI-TOF, + mode) *m/z* (rel intensity) 256.20 (100) [M+H]⁺, 185.13 (80) [C₁₄H₁₇]⁺.

N-Benzyl-5-methyltridec-6-yn-5-amine (K.2c) (CAS: 2743452-61-9)



Chemical Formula: C₂₁H₃₃N
Molecular Weight: 299,5020

Following the General Procedure A with a reaction temperature of 110 °C and a catalyst loading of 20 mol% (72 mg Cu^I-USY for 1.0 mmol ketone), the title compound **K.2c** was isolated as a yellow oil (159 mg, 0.53 mmol). Yield 53%.

R_f = 0.75 (SiO₂, cyclohexane/EtOAc 7:3).

ATR-FTIR (neat) ν = 3087, 3063, 3028, 2956, 2929, 2858, 1605, 1496, 1454, 1370, 1151, 1029, 728 cm⁻¹.

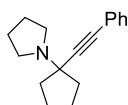
¹H NMR (500 MHz, CDCl₃) δ = 7.38 – 7.34 (m, 2H, H_{aro}), 7.34 – 7.29 (m, 2H, H_{aro}), 7.26 – 7.21 (m, 1H, H_{aro}), 3.87 (d, *J* = 11.8 Hz, 1H, NCH₂), 3.82 (d, *J* = 11.9 Hz, 1H, NCH₂), 2.23 (t, *J* = 7.0 Hz, 2H, ≡CCH₂), 1.65 – 1.49 (m, 4H), 1.47 – 1.38 (m, 4H), 1.37 – 1.25 (m, 10H), 0.95 – 0.85 (m, 6H, 2 × CH₂CH₃) ppm.

¹³C{¹H} NMR (126 MHz, CDCl₃) δ = 141.2 (C_q), 128.6 (C_{aro}H), 128.5 (C_{aro}H), 127.0 (C_{aro}H), 84.5 (C≡), 83.4 (C≡), 53.8 (NC_q), 48.8 (NCH₂), 42.3 (CH₂), 31.5 (CH₂), 29.3 (CH₂), 28.7 (CH₂), 27.5 (C_qCH₃), 26.9 (CH₂), 23.2 (CH₂), 22.8 (CH₂), 18.8 (CH₂), 14.3 (CH₂CH₃), 14.2 (CH₂CH₃) ppm.

MS (ESI-TOF, + mode) *m/z* (rel intensity) 300.27 (100) [M+H]⁺, 193.20 (10) [C₁₄H₂₅]⁺.

HRMS (ESI-TOF, + mode) m/z calcd for $C_{21}H_{34}N$ 300.2686, found 300.2690 $[M+H]^+$.

1-(1-(Phenylethynyl)cyclopentyl)pyrrolidine (K.2g) (CAS: 1542621-31-7)^[370]



Chemical Formula: $C_{17}H_{21}N$
Molecular Weight: 239,3620

Following the General Procedure A, the title compound **K.2g** was isolated as an orange oil (184 mg, 0.77 mmol). Yield 77%.

R_f = 0.66 (SiO₂, cyclohexane/EtOAc 7:3).

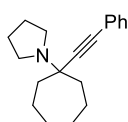
ATR-FTIR (neat) ν = 3055, 2961, 2871, 2807, 1598, 1488, 1443, 1298, 1256, 1200, 1147, 1089, 1069, 1029, 992, 911, 753, 689 cm^{-1} .

¹H NMR (300 MHz, CDCl₃) δ = 7.45 – 7.38 (m, 2H, H_{aro}), 7.33 – 7.26 (m, 3H, H_{aro}), 2.84 – 2.73 (m, 4H, 2 × NCH₂), 2.12 – 1.99 (m, 2H, 2 × NC_qCH₂), 1.91 – 1.76 (m, 10H, 2 × NCH₂CH₂ & 6H cyclopentyl) ppm.

¹³C{¹H} NMR (126 MHz, CDCl₃) δ = 131.9 (C_{aro}H), 128.3 (C_{aro}H), 127.8 (C_{aro}H), 123.8 (C_q), 91.4 (C≡), 85.0 (C≡), 65.7 (NC_q), 49.4 (NCH₂), 40.7 (CH₂), 23.8 (CH₂), 23.7 (CH₂) ppm.

MS (ESI-TOF, + mode) m/z (rel intensity) 240.18 (100) $[M+H]^+$, 169.10 (15) $[C_{13}H_{13}]^+$.

1-(1-(Phenylethynyl)cycloheptyl)pyrrolidine (K.2h) (CAS: 1542621-41-9)^[370]



Chemical Formula: $C_{19}H_{25}N$
Molecular Weight: 267,4160

Following the General Procedure A, the title compound **K.2h** was isolated in 72% yield (192 mg, 0.72 mmol). Following the General Procedure C, the title compound **K.2h** was isolated as a yellow oil (203 mg, 0.76 mmol). Yield 76%.

R_f = 0.22 (SiO₂, cyclohexane/EtOAc 7:3).

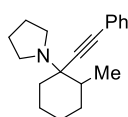
ATR-FTIR (neat) ν = 3079, 3054, 3021, 2921, 2857, 2805, 1598, 1489, 1461, 1443, 1288, 1198, 1090, 1034, 911, 724, 689 cm^{-1} .

¹H NMR (500 MHz, CDCl₃) δ = 7.45 – 7.39 (m, 2H, H_{aro}), 7.31 – 7.24 (m, 3H, H_{aro}), 2.93 – 2.62 (m, 4H, 2 × NCH₂), 2.04 (ddd, J = 14.0, 7.9, 2.4 Hz, 2H, 2 × NC_qCH₂), 1.85 (ddd, J = 14.1, 9.1, 2.4 Hz, 2H, 2 × NC_qCH₂), 1.82 – 1.75 (m, 4H, 2 × NCH₂CH₂), 1.75 – 1.52 (m, 8H) ppm.

¹³C{¹H} NMR (126 MHz, CDCl₃) δ = 131.9 (C_{aro}H), 128.3 (C_{aro}H), 127.7 (C_{aro}H), 123.9 (C_q), 92.3 (C≡), 84.7 (C≡), 62.5 (NC_q), 47.9 (CH₂), 40.3 (CH₂), 28.3 (CH₂), 23.9 (CH₂), 22.3 (CH₂) ppm.

MS (ESI-TOF, + mode) m/z (rel intensity) 268.20 (100) $[M+H]^+$, 197.13 (40) $[C_{15}H_{17}]^+$.

1-(2-Methyl-1-(phenylethynyl)cyclohexyl)pyrrolidine (K.2i) (CAS: (1R, 2S): 2320511-33-7, (1R, 2R): 2320511-51-9)^[237]



Chemical Formula: $C_{19}H_{25}N$
Molecular Weight: 267,4160

Following the General Procedure C, the title compound **K.2i** was obtained as a mixture of two diastereoisomers in a 7:3 ratio and it was isolated as a yellow oil (201 mg, 0.75 mmol). Yield 75%.

R_f = 0.71, 0.62 (SiO₂, cyclohexane/EtOAc 7:3).

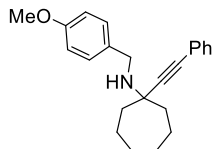
ATR-FTIR (neat) ν = 3080, 3056, 2962, 2928, 2858, 2807, 1598, 1488, 1441, 1273, 1125, 911, 753, 689 cm^{-1} .

¹H NMR (500 MHz, CDCl₃) δ = 7.46 – 7.40 (m, 3H, H_{aro}), 7.33 – 7.25 (m, 5H, H_{aro}), 2.81 – 2.66 (m, 5H, 2 × NCH₂), 2.15 – 2.07 (m, 1H), 2.07 – 1.98 (m, 1H), 1.93 – 1.85 (m, 1H), 1.83 – 1.37 (m, 16H), 1.34 – 1.24 (m, 1H), 1.15 (d, J = 6.9 Hz, 1H, CH₃, minor diastereoisomer), 1.03 (d, J = 7.1 Hz, 3H, CH₃, major diastereoisomer) ppm.

¹³C{¹H} NMR (126 MHz, CDCl₃) δ = 131.9 (C_{aro}H), 131.8 (C_{aro}H), 128.3(7) (C_{aro}H), 128.3(0) (C_{aro}H), 127.6(8) (C_{aro}H), 127.6(5) (C_{aro}H), 124.1(1) (C_q), 124.1(0) (C_q), 91.9 (C≡), 91.8 (C≡),

86.1 (C≡), 85.3 (C≡), 62.3 (NC_q), 61.6 (NC_q), 46.8 (CH₂), 46.2 (CH₂), 36.7 (CH), 31.6 (CH₂), 30.1 (CH₂), 24.0 (CH₂), 23.6(0) (CH₂), 23.5(9) (CH₂), 19.7 (CH₂), 16.9 (CH₃), 13.1 (CH₃) ppm.
MS (ESI, + mode) *m/z* 268.20 (100) [M+H]⁺, 197.13 (75) [C₁₅H₁₇]⁺.

N-(4-Methoxybenzyl)-1-(phenylethynyl)cycloheptan-1-amine (K.2k) (CAS: 1227795-22-3)^[42]



Chemical Formula: C₂₃H₂₇NO
Molecular Weight: 333,4750

Following the General Procedure A, the title compound **K.2k** was isolated as yellow oil (253 mg, 0.76 mmol). Yield 76%.

R_f = 0.48 (SiO₂, cyclohexane/EtOAc 8:2).

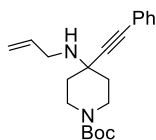
ATR-FTIR (neat) ν = 3315, 3058, 2996, 2924, 2853, 1611, 1510, 1444, 1300, 1243, 1035, 821, 754, 690 cm⁻¹.

¹H NMR (500 MHz, CDCl₃) δ = 7.49 – 7.42 (m, 2H, H_{aro}), 7.34 – 7.28 (m, 5H, H_{aro}), 6.89 – 6.83 (m, 2H, 2 × OC_qCH_{aro}), 3.88 (s, 2H, NCH₂), 3.80 (s, 3H, CH₃), 2.07 – 1.96 (m, 2H, 2 × NC_qCH₂), 1.82 – 1.55 (m, 11H) ppm.

¹³C{¹H} NMR (126 MHz, CDCl₃) δ = 158.7 (CH₃OC_q), 133.4 (C_q), 131.8 (C_{aro}H), 129.8 (C_{aro}H), 128.4 (C_{aro}H), 127.9 (C_{aro}H), 123.9 (C_q), 114.0 (C_{aro}H), 94.9 (C≡), 83.9 (C≡), 58.4 (NC_q), 55.4 (CH₂), 48.2 (CH₂), 40.9 (CH₂), 28.4 (CH₂), 22.8 (CH₂) ppm.

MS (ESI-TOF, + mode) *m/z* (rel intensity) 334.22 (40) [M+H]⁺, 197.14 (100) [C₁₅H₁₈]⁺, 121.07 (35) [C₈H₉O]⁺.

tert-Butyl 4-(allylamino)-4-(phenylethynyl)piperidine-1-carboxylate (K.2n) (CAS: 2414088-82-5)



Chemical Formula: C₂₁H₂₈N₂O₂
Molecular Weight: 340,4670

Following the General Procedure A, the title compound **K.2n** was isolated as an orange oil (272 mg). Yield 80%.

R_f = 0.28 (SiO₂, cyclohexane/EtOAc 7:3).

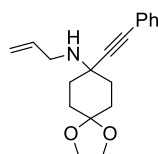
ATR-FTIR (neat) ν = 3079, 3060, 3004, 2974, 2927, 2866, 1687, 1598, 1489, 1443, 1418, 1392, 1364, 1278, 1244, 1144, 1070, 994, 864, 690 cm⁻¹.

¹H NMR (500 MHz, CDCl₃) δ = 7.45 – 7.39 (m, 2H, H_{aro}), 7.34 – 7.28 (m, 3H, H_{aro}), 5.98 (ddt, *J* = 16.5, 10.2, 6.0 Hz, 1H, CH=CH₂), 5.24 (dq, *J* = 17.1, 1.7 Hz, 1H, CH=CH₂), 5.11 (dq, *J* = 10.2, 1.5 Hz, 1H, CH=CH₂), 4.09 – 3.88 (m, 2H, 2 × BocNCH₂), 3.45 (dt, *J* = 6.1, 1.5 Hz, 2H, NCH₂ allyl), 3.19 (bs, 2H, 2 × BocNCH₂), 1.91 (d, *J* = 12.6 Hz, 2H, 2 × NC_qCH₂), 1.61 (td, *J* = 12.1, 4.1 Hz, 2H, 2 × NC_qCH₂), 1.46 (s, 9H, C(CH₃)₃) ppm.

¹³C{¹H} NMR (126 MHz, CDCl₃) δ = 154.9 (C=O), 137.0 (CH), 131.8 (CH), 128.5 (CH), 128.3 (CH), 123.1 (C_q), 116.1 (CH=CH₂), 91.2 (C≡), 86.0 (C≡), 79.7 (C(CH₃)₃), 53.8 (NC_qC≡), 46.4 (CH₂), 41.0 (CH₂), 37.6 (CH₂), 28.6 (C(CH₃)₃) ppm.

HRMS (ESI-TOF, + mode) *m/z* calcd for C₂₁H₂₉N₂O₂ 341.2224, found 341.2225 [M+H]⁺.

N-Allyl-8-(phenylethynyl)-1,4-dioxaspiro[4.5]decan-8-amine (K.2o) (CAS: 2743452-63-1)



Chemical Formula: C₁₉H₂₃NO₂
Molecular Weight: 297,3980

Following the General Procedure A, the title compound **K.2o** was isolated as a yellow oil (235 mg, 0.79 mmol). Yield 79%.

R_f = 0.20 (SiO₂, cyclohexane/EtOAc 7:3).

ATR-FTIR (neat) ν = 3307, 3079, 3058, 2951, 2929, 2879, 1643, 1597, 1489, 1442, 1369, 1273, 1207, 1159, 1034, 928, 888, 754, 690 cm⁻¹.

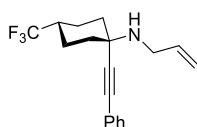
¹H NMR (500 MHz, CDCl₃) δ = 7.43 – 7.39 (m, 2H, H_{aro}), 7.32 – 7.27 (m, 3H, H_{aro}), 5.99 (ddt, *J* = 17.2, 10.2, 6.0 Hz, 1H, CH=CH₂), 5.24 (dq, *J* = 17.2, 1.6 Hz, 1H, CH=CH₂), 5.09 (dq,

$J = 10.2, 1.4$ Hz, 1H, CH=CH₂), 4.00 – 3.91 (m, 4H, 2 × OCH₂), 3.44 (dt, $J = 6.0, 1.5$ Hz, 2H, NCH₂), 2.04 – 1.87 (m, 4H), 1.85 – 1.76 (m, 4H) ppm.

¹³C{¹H} NMR (126 MHz, CDCl₃) $\delta = 137.3$ (CH), 131.7 (CH), 128.3 (CH), 127.9 (CH), 123.3 (C_q-Ph), 115.7 (CH=CH₂), 108.5 (O₂C_q), 92.2 (C≡), 84.4 (C≡), 64.4 (OCH₂), 64.2 (OCH₂), 53.9 (CH₂NC_q), 46.8 (NCH₂), 35.5 (CH₂), 31.5 (CH₂) ppm.

HRMS (ESI-TOF, + mode) m/z calcd for C₁₉H₂₄NO₂ 298.1802, found 298.1801 [M+H]⁺.

***N*-Allyl-1-(phenylethynyl)-4-(trifluoromethyl)cyclohexan-1-amine (K.2p) – *trans*-Diastereomer**



Chemical Formula: C₁₈H₂₀F₃N
Molecular Weight: 307,3602

Following the General Procedure A, the title compound **K.2p** was isolated as a yellow solid (95 mg, 0.31 mmol). Yield 41% (65% for both diastereomers combined which were obtained in a 2:1 *trans/cis* ratio in the crude product).

$R_f = 0.80$ (SiO₂, cyclohexane/EtOAc 7:3).

ATR-FTIR (neat) $\nu = 3302, 3084, 3013, 2940, 2904, 2868, 2856, 1644, 1599, 1572, 1491, 1448, 1391, 1339, 1251, 1158, 1120, 1094, 1019, 917, 824, 756, 688$ cm⁻¹.

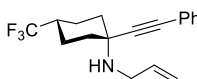
¹H NMR (300 MHz, CDCl₃) $\delta = 7.45 - 7.36$ (m, 2H, H_{aro}), 7.34 – 7.27 (m, 3H, H_{aro}), 6.00 (ddt, $J = 17.1, 10.2, 5.9$ Hz, 1H, CH=CH₂), 5.25 (dq, $J = 17.2, 1.7$ Hz, 1H, CH=CH₂), 5.09 (dq, $J = 10.2, 1.4$ Hz, 1H, CH=CH₂), 3.35 (dt, $J = 5.9, 1.5$ Hz, 2H, NCH₂), 2.17 – 1.98 (m, 3H), 1.94 – 1.67 (m, 6H) ppm.

¹⁹F{¹H} NMR (282 MHz, CDCl₃) $\delta = -72.95$ ppm.

¹³C{¹H} NMR (126 MHz, CDCl₃) $\delta = 137.4$ (CH), 131.8 (CH), 128.4 (CH), 128.1 (CH), 128.0 (q, ¹J_{C-F} = 278.3 Hz, CF₃), 123.3 (C_q), 115.7 (CH=CH₂), 94.1 (C≡), 83.0 (C≡), 51.9 (NC_q), 46.5 (NCH₂), 40.9 (q, ²J_{C-F} = 26.4 Hz, CF₃CH), 35.3 (CH₂), 19.6 (q, ³J_{C-F} = 2.7 Hz, CF₃CHCH₂) ppm.

HRMS (ESI-TOF, + mode) m/z calcd for C₁₈H₂₁F₃N 308.1621, found 308.1606 [M+H]⁺.

***N*-Allyl-1-(phenylethynyl)-4-(trifluoromethyl)cyclohexan-1-amine (K.2p) – *cis*-Diastereomer**



Chemical Formula: C₁₈H₂₀F₃N
Molecular Weight: 307,3602

Following the General Procedure A, the title compound **K.2p** was isolated as a yellow viscous oil (54 mg, 0.18 mmol). Yield 24% (65% for both diastereomers combined which were obtained in a 2:1 *trans/cis* ratio in the crude product).

$R_f = 0.35$ (SiO₂, cyclohexane/EtOAc 7:3).

ATR-FTIR (neat) $\nu = 3302, 3084, 3013, 2940, 2904, 2868, 2856, 1644, 1599, 1572, 1491, 1448, 1391, 1339, 1251, 1158, 1120, 1094, 1019, 917, 824, 756, 688$ cm⁻¹.

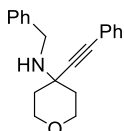
¹H NMR (300 MHz, CDCl₃) $\delta = 7.47 - 7.38$ (m, 2H, H_{aro}), 7.35 – 7.28 (m, 3H, H_{aro}), 5.99 (ddt, $J = 17.1, 10.2, 6.0$ Hz, 1H, CH=CH₂), 5.25 (dq, $J = 17.2, 1.6$ Hz, 1H, CH=CH₂), 5.12 (dq, $J = 10.3, 1.4$ Hz, 1H, CH=CH₂), 3.48 (dt, $J = 6.0, 1.5$ Hz, 2H, NCH₂), 2.15 – 1.74 (m, 7H), 1.54 – 1.40 (m, 3H) ppm.

¹⁹F{¹H} NMR (282 MHz, CDCl₃) $\delta = -73.47$ ppm.

¹³C{¹H} NMR (126 MHz, CDCl₃) $\delta = 137.0$ (CH), 131.8 (CH), 128.5 (CH), 128.3 (CH), 127.8 (q, ¹J_{C-F} = 278.5 Hz, CF₃), 123.2 (C_q), 116.2 (CH=CH₂), 91.3 (C≡), 86.3 (C≡), 54.8 (NC_q), 46.7 (NCH₂), 41.7 (q, ²J_{C-F} = 26.7 Hz, CF₃CH), 36.8 (CH₂), 22.2 (q, ³J_{C-F} = 2.6 Hz, CF₃CHCH₂) ppm.

HRMS (ESI-TOF, + mode) m/z calcd for C₁₈H₂₁F₃N 308.1621, found 308.1606 [M+H]⁺.

N-Benzyl-4-(phenylethynyl)tetrahydro-2H-pyran-4-amine (K.2t)



Chemical Formula: C₂₀H₂₁NO
Molecular Weight: 291,3940

Following the General Procedure A, the title compound **K.2t** was isolated as a yellow solid (241 mg, 0.83 mmol). Yield 83%.

R_f = 0.22 (SiO₂, cyclohexane/EtOAc 7:3).

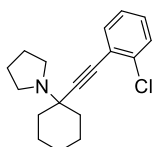
ATR-FTIR (neat) ν = 3059, 3029, 2950, 2922, 2852, 3302, 1597, 1489, 1293, 1146, 1100, 1027, 849, 753, 690 cm⁻¹.

¹H NMR (500 MHz, CDCl₃) δ = 7.49 – 7.45 (m, 2H, H_{aro}), 7.43 – 7.39 (m, 2H, H_{aro}), 7.36 – 7.31 (m, 5H, H_{aro}), 7.29 – 7.23 (m, 1H, H_{aro}), 4.02 – 3.93 (m, 4H, NCH₂ & 2 × OCH₂), 3.80 (ddd, *J* = 11.6, 10.7, 2.4 Hz, 2H, 2 × OCH₂), 1.94 (ddt, *J* = 13.1, 4.4, 2.3 Hz, 2H, 2 × NC_qCH₂), 1.82 (ddd, *J* = 13.0, 10.8, 4.2 Hz, 2H, 2 × NC_qCH₂) ppm.

¹³C{¹H} NMR (126 MHz, CDCl₃) δ = 140.8 (C_q), 131.8 (C_{aro}H), 128.6(3) (C_{aro}H), 128.6(0) (C_{aro}H), 128.5 (C_{aro}H), 128.3 (C_{aro}H), 127.2 (C_{aro}H), 123.2 (C_q), 91.9 (C≡), 85.8 (C≡), 64.9 (OCH₂), 53.2 (NC_q), 47.9 (NCH₂), 38.6(NC_qCH₂) ppm.

HRMS (ESI-TOF, + mode) *m/z* calcd for C₂₀H₂₂NO 292.1696, found 292.1682 [M+H]⁺.

1-(1-((2-Chlorophenyl)ethynyl)cyclohexyl)pyrrolidine (K.3a) (CAS: 2743452-65-3)



Chemical Formula: C₁₈H₂₂ClN
Molecular Weight: 287,8310

Following the General Procedure A, the title compound **K.3a** was isolated as a yellow oil (245 mg, 0.85 mmol). Yield 85%.

R_f = 0.32 (SiO₂, cyclohexane/EtOAc 6:4).

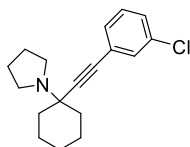
ATR-FTIR (neat) ν = 3065, 2929, 2854, 2808, 1472, 1438, 1294, 1264, 1158, 1125, 1079, 1058, 1032, 881, 750, 716, 682 cm⁻¹.

¹H NMR (500 MHz, CDCl₃) δ = 7.50 – 7.44 (m, 1H, H_{aro}), 7.41 – 7.36 (m, 1H, H_{aro}), 7.24 – 7.15 (m, 2H, H_{aro}), 2.92 – 2.75 (m, 4H, 2 × NCH₂), 2.12 – 2.02 (m, 2H, 2 × NC_qCH₂), 1.86 – 1.77 (m, 4H, 2 × NCH₂CH₂), 1.74 – 1.63 (m, 5H), 1.60 – 1.47 (m, 2H), 1.30 – 1.17 (m, 1H) ppm.

¹³C{¹H} NMR (126 MHz, CDCl₃) δ = 135.9 (C_qCl), 133.5 (C_{aro}H), 129.3 (C_{aro}H), 128.8 (C_{aro}H), 126.4 (C_{aro}H), 123.7 (C_q), 96.5 (C≡), 83.0 (C≡), 59.9 (NC_q), 47.3 (NCH₂), 38.0 (CH₂), 25.8 (CH₂), 23.7 (CH₂), 23.2 (CH₂) ppm.

HRMS (ESI-TOF, + mode) *m/z* calcd for C₁₈H₂₃ClN 288.1514, found 288.1516 [M+H]⁺.

1-(1-((3-Chlorophenyl)ethynyl)cyclohexyl)pyrrolidine (K.3b) (CAS: 2743452-67-5)



Chemical Formula: C₁₈H₂₂ClN
Molecular Weight: 287,8310

Following the General Procedure A, the title compound **K.3b** was isolated as a yellow oil (236 mg, 0.82 mmol). Yield 82%.

R_f = 0.31 (SiO₂, cyclohexane/EtOAc 6:4).

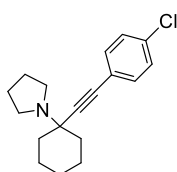
ATR-FTIR (neat) ν = 3062, 2929, 2854, 2806, 1592, 1561, 1474, 1446, 1287, 1158, 1125, 1090, 1077, 956, 877, 862, 780, 681 cm⁻¹.

¹H NMR (500 MHz, CDCl₃) δ = 7.41 (t, *J* = 1.8 Hz, 1H, C_qCHC_qCl), 7.31 (dt, *J* = 7.4, 1.6 Hz, 1H, H_{aro}), 7.28 – 7.19 (m, 2H, H_{aro}), 2.80 – 2.78 (m, 4H, 2 × NCH₂), 2.04 – 2.01 (m, 2H, 2 × NC_qCH₂), 1.85 – 1.76 (m, 4H, 2 × NCH₂CH₂), 1.74 – 1.49 (m, 8H), 1.29 – 1.18 (m, 1H) ppm.

¹³C{¹H} NMR (126 MHz, CDCl₃) δ = 134.1 (ClC_q), 131.8 (C_{aro}H), 130.0 (C_{aro}H), 129.6 (C_{aro}H), 128.1 (C_{aro}H), 125.5 (C_q), 92.1 (C≡), 85.0 (C≡), 59.6 (NC_q), 47.3 (NCH₂), 37.9 (CH₂), 25.8 (CH₂), 23.6 (CH₂), 23.2 (CH₂) ppm.

HRMS (ESI-TOF, + mode) *m/z* calcd for C₁₈H₂₃ClN 288.1514, found 288.1526 [M+H]⁺.

1-(1-((4-Chlorophenyl)ethynyl)cyclohexyl)pyrrolidine (K.3c) (CAS: 2476405-01-1)



Chemical Formula: C₁₈H₂₂ClN
Molecular Weight: 287,8310

Following the General Procedure A, the title compound **K.3c** was isolated as a yellow solid (273 mg, 0.95 mmol). Yield 95%.

R_f = 0.27 (SiO₂, cyclohexane/EtOAc 6:4).

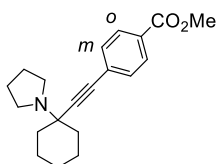
ATR-FTIR (neat) ν = 2966, 2932, 2858, 2827, 2800, 1486, 1459, 1446, 1284, 1122, 1091, 1014, 992, 880, 822, 525 cm⁻¹.

¹H NMR (500 MHz, CDCl₃) δ = 7.39 – 7.32 (m, 2H, H_{aro}), 7.28 – 7.24 (m, 2H, H_{aro}), 2.86 – 2.71 (m, 4H, 2 × NCH₂), 2.02 (d, *J* = 12.4 Hz, 2H, 2 × NC_qCH₂), 1.85 – 1.75 (m, 4H, 2 × NCH₂CH₂), 1.74 – 1.49 (m, 8H), 1.30 – 1.18 (m, 1H) ppm.

¹³C{¹H} NMR (126 MHz, CDCl₃) δ = 133.8 (ClC_q), 133.1 (C_{aro}H), 128.6 (C_{aro}H), 122.3 (C_q), 91.7 (C≡), 85.2 (C≡), 59.6 (NC_q), 47.3 (NCH₂), 37.9 (CH₂), 25.8 (CH₂), 23.6 (CH₂), 23.2 (CH₂) ppm.

HRMS (ESI-TOF, + mode) *m/z* calcd for C₁₈H₂₃ClN 288.1514, found 288.1513 [M+H]⁺.

Methyl 4-((1-(pyrrolidin-1-yl)cyclohexyl)ethynyl)benzoate (K.3e) (CAS: 2743452-78-8)



Chemical Formula: C₂₀H₂₅NO₂
Molecular Weight: 311,4250

Following the General Procedure A with toluene (1 M) as solvent, the title compound **K.3f** was isolated as a yellow solid (181 mg, 0.58 mmol). Yield 58%.

R_f = 0.25 (SiO₂, cyclohexane/EtOAc 6:4).

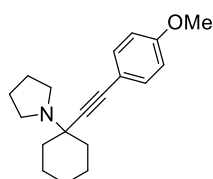
ATR-FTIR (neat) ν = 2927, 2853, 2804, 1717, 1604, 1438, 1405, 1311, 1275, 1195, 1176, 1154, 1110, 1063, 1017, 993, 960, 913, 880, 857, 825, 769, 697 cm⁻¹.

¹H NMR (500 MHz, CDCl₃) δ = 8.00 – 7.92 (m, 2H, 2 × *o*-H_{aro}), 7.51 – 7.45 (m, 2H, 2 × *m*-H_{aro}), 3.92 (s, 3H, CH₃), 2.87 – 2.70 (m, 4H, 2 × NCH₂), 2.09 – 1.99 (m, 2H, 2 × NC_qCH₂), 1.85 – 1.76 (m, 4H, 2 × NCH₂CH₂), 1.75 – 1.51 (m, 8H), 1.30 – 1.18 (m, 1H) ppm.

¹³C{¹H} NMR (126 MHz, CDCl₃) δ = 166.8 (C=O), 131.8 (C_{aro}H), 129.6 (C_{aro}H), 129.1 (C_q), 128.6 (C_q), 94.2 (C≡), 85.8 (C≡), 59.7 (NC_q), 52.4 (CH₃), 47.3 (NCH₂), 37.9 (CH₂), 25.8 (CH₂), 23.6 (CH₂), 23.2 (CH₂) ppm.

HRMS (ESI-TOF, + mode) *m/z* calcd for C₂₀H₂₆NO₂ 312.1958, found 312.1963 [M+H]⁺.

1-(1-((4-Methoxyphenyl)ethynyl)cyclohexyl)pyrrolidine (K.3f) (CAS: 1778637-36-7)



Chemical Formula: C₁₉H₂₅NO
Molecular Weight: 283,4150

Following the General Procedure A, the title compound **K.3d** was isolated as an orange solid (232 mg, 0.82 mmol). Yield 82%.

R_f = 0.16 (SiO₂, cyclohexane/EtOAc 6:4).

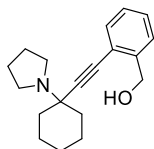
ATR-FTIR (neat) ν = 2977, 2929, 2854, 2807, 1605, 1507, 1440, 1283, 1244, 1180, 1170, 1156, 1121, 1105, 1034, 829, 807 cm⁻¹.

¹H NMR (500 MHz, CDCl₃) δ = 7.40 – 7.33 (m, 2H, H_{aro}), 6.86 – 6.78 (m, 2H, 2 × OC_qCH_{aro}), 3.81 (s, 3H, CH₃), 2.86 – 2.72 (m, 4H, 2 × NCH₂), 2.07 – 1.98 (m, 2H, 2 × NC_qCH₂), 1.84 – 1.75 (m, 4H, 2 × NCH₂CH₂), 1.73 – 1.59 (m, 5H), 1.52 (td, *J* = 11.8, 4.7 Hz, 2H), 1.28 – 1.16 (m, 1H) ppm.

¹³C{¹H} NMR (126 MHz, CDCl₃) δ = 159.3 (CH₃OC_q), 133.2 (C_{aro}H), 116.0 (≡CC_q), 113.9 (C_{aro}H), 88.8 (C≡), 86.0 (C≡), 59.5 (NC_q), 55.5 (OCH₃), 47.2 (NCH₂), 38.1 (CH₂), 25.9 (CH₂), 23.6 (CH₂), 23.3 (CH₂) ppm.

HRMS (ESI-TOF, + mode) *m/z* calcd for C₁₉H₂₆NO 284.2009, found 284.2033 [M+H]⁺.

(2-((1-(Pyrrolidin-1-yl)cyclohexyl)ethynyl)phenyl)methanol (K.3g) (CAS: 2743452-80-2)



Chemical Formula: C₁₉H₂₅NO
Molecular Weight: 283,4150

Following the General Procedure A, the title compound **K.3g** was isolated as a beige solid (235 mg, 0.83 mmol). Yield 83%.

R_f = 0.27 (SiO₂, CH₂Cl₂/MeOH 9:1).

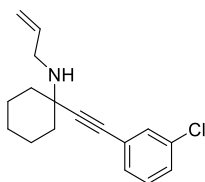
ATR-FTIR (neat) ν = 3622-3100, 3062, 3028, 2929, 2854, 1447, 1353, 1294, 1262, 1157, 1115, 1049, 1013, 946, 914, 871, 757, 723 cm⁻¹.

¹H NMR (300 MHz, CDCl₃) δ = 7.48 – 7.41 (m, 2H, H_{aro}), 7.35 – 7.28 (m, 1H, H_{aro}), 7.27 – 7.21 (m, 1H, H_{aro}), 4.84 (d, *J* = 3.8 Hz, 2H, CH₂OH), 2.90 – 2.70 (m, 4H, 2 × NCH₂), 2.17 – 1.98 (m, 3H), 1.84 – 1.77 (m, 4H, 2 × NCH₂CH₂), 1.76 – 1.51 (m, 8H), 1.32 – 1.16 (m, 1H) ppm.

¹³C{¹H} NMR (126 MHz, CDCl₃) δ = 142.4 (C_q), 132.7 (C_{aro}H), 128.3 (C_{aro}H), 127.5 (C_{aro}H), 127.2 (C_{aro}H), 121.8 (C_q), 95.9 (C≡), 83.6 (C≡), 64.4 (CH₂O), 59.8 (NC_q), 47.3 (NCH₂), 38.1 (CH₂), 25.8 (CH₂), 23.6 (CH₂), 23.3 (CH₂) ppm.

HRMS (ESI-TOF, + mode) *m/z* calcd for C₁₉H₂₆NO 284.2009, found 284.2007 [M+H]⁺.

N-Allyl-1-((3-chlorophenyl)ethynyl)cyclohexan-1-amine (K.3h)



Chemical Formula: C₁₇H₂₀ClN
Molecular Weight: 273,8040

Following the General Procedure A, the title compound **K.3h** was isolated as a yellow oil (88 mg, 0.32 mmol). Yield 64%.

R_f = 0.74 (SiO₂, cyclohexane/EtOAc 7:3).

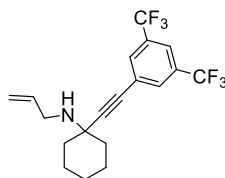
ATR-FTIR (neat) ν = 3318, 3069, 2930, 2854, 2216, 1643, 1592, 1561, 1474, 1407, 1289, 1159, 1091, 996, 917, 879, 781, 747, 681 cm⁻¹.

¹H NMR (500 MHz, CDCl₃) δ = 7.43 – 7.39 (m, 1H, H_{aro}), 7.33 – 7.20 (m, 3H, H_{aro}), 5.99 (ddt, *J* = 16.6, 10.1, 6.0 Hz, 1H, CH=CH₂), 5.24 (dq, *J* = 17.2, 1.7 Hz, 1H, CH=CH₂), 5.10 (dq, *J* = 10.2, 1.5 Hz, 1H, CH=CH₂), 3.44 (dt, *J* = 6.0, 1.5 Hz, 2H, NCH₂), 1.98 – 1.91 (m, 2H, 2 × NC_qCH₂), 1.75 – 1.58 (m, 5H), 1.46 (td, *J* = 12.1, 3.7 Hz, 2H), 1.39 (s, 1H), 1.28 – 1.18 (m, 1H) ppm.

¹³C{¹H} NMR (126 MHz, CDCl₃) δ = 137.3 (CH), 134.2 (C_q), 131.7 (CH), 129.9 (CH), 129.6 (CH), 128.2 (CH), 125.4 (C_q), 116.0 (CH₂=C), 94.7 (C≡), 83.6 (C≡), 55.1 (NC_q), 46.5 (NCH₂), 38.3 (CH₂), 29.8 (CH₂), 26.0 (CH₂), 23.2 (CH₂) ppm.

HRMS (ESI-TOF, + mode) *m/z* calcd for C₁₇H₂₁ClN 274.1357, found 274.1371 [M+H]⁺.

N-Allyl-1-((3,5-bis(trifluoromethyl)phenyl)ethynyl)cyclohexan-1-amine (K.3i) (CAS: 2743452-69-7)



Chemical Formula: C₁₉H₁₉F₆N
Molecular Weight: 375,3584

Following the General Procedure A, the title compound **K.3i** was isolated as a yellow oil (191 mg, 0.51 mmol). Yield 51%.

R_f = 0.52 (SiO₂, cyclohexane/EtOAc 7:3).

ATR-FTIR (neat) ν = 3085, 2936, 2859, 2222, 1708, 1644, 1615, 1462, 1451, 1379, 1171, 978, 895, 700, 682 cm⁻¹.

¹H NMR (300 MHz, CDCl₃) δ = 7.85 – 7.81 (m, 2H, 2 × ≡CC_qH_{aro}), 7.80 – 7.75 (m, 1H, H_{aro}), 5.99 (ddt, *J* = 17.1, 10.2, 6.0 Hz, 1H, CH=CH₂), 5.25 (dq, *J* = 17.2, 1.7 Hz, 1H, CH=CH₂), 5.12 (dq, *J* = 10.2, 1.4 Hz, 1H, CH=CH₂), 3.44 (dt, *J* = 6.0, 1.5 Hz, 2H, NCH₂), 2.02 – 1.92 (m, 2H, 2 × NC_qCH₂), 1.81 – 1.40 (m, 6H), 1.36 – 1.18 (m, 1H) ppm.

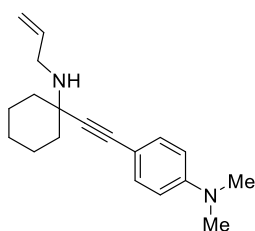
¹⁹F{¹H} NMR (282 MHz, CDCl₃) δ = -63.09 ppm.

¹³C{¹H} NMR (126 MHz, CDCl₃) δ = 137.1 (CH=CH₂), 132.0 (q, ²*J*_{C-F} = 33.6 Hz, CF₃C_{q-aro}), 131.8 – 131.6 (m, CF₃CCH), 126.0 (≡CC_{q-aro}), 123.1 (q, ¹*J*_{C-F} = 272.8 Hz, CF₃), 121.3 (sept,

$^3J_{C-F} = 4.0$ Hz, CF_3CCH), 116.1 (CH=CH₂), 97.4 (C≡), 82.2 (C≡), 55.2 (NC_q), 46.5 (NCH₂), 38.1 (CH₂), 25.9 (CH₂), 23.1 (CH₂) ppm.

HRMS (ESI-TOF, + mode) m/z calcd for C₁₉H₂₀F₆N 376.1494, found 376.1481 [M+H]⁺.

4-((1-(Allylamino)cyclohexyl)ethynyl)-N,N-dimethylaniline (K.3j)



Chemical Formula: C₁₉H₂₆N₂
Molecular Weight: 282.4310

Following the General Procedure A, the title compound **K.3j** was isolated as a yellow solid (72 mg, 0.25 mmol). Yield 51%.

R_f = 0.26 (SiO₂, cyclohexane/EtOAc 7:3).

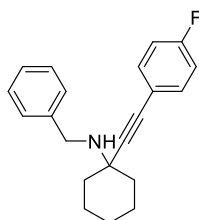
ATR-FTIR (neat) $\nu = 3090, 2928, 2853, 2981, 3037, 2797, 2205, 1643, 1609, 1519, 1444, 1358, 1292, 1224, 1188, 1156, 1116, 1063, 946, 910, 815, 748$ cm⁻¹.

¹H NMR (500 MHz, CDCl₃) $\delta = 7.32 - 7.28$ (m, 2H, H_{aro}), 6.65 - 6.60 (m, 2H, 2 × NC_qCH_{aro}), 6.00 (ddt, $J = 17.2, 10.2, 6.1$ Hz, 1H, CH=CH₂), 5.22 (dq, $J = 17.1, 1.7$ Hz, 1H, CH=CH₂), 5.08 (dq, $J = 10.2, 1.4$ Hz, 1H, CH=CH₂), 3.46 (dt, $J = 6.1, 1.4$ Hz, 2H, NCH₂), 2.96 (s, 6H, N(CH₃)₂), 1.98 - 1.90 (m, 2H, 2 × NC_qCH₂), 1.73 - 1.62 (m, 5H), 1.49 - 1.38 (m, 3H), 1.24 - 1.17 (m, 1H) ppm.

¹³C{¹H} NMR (126 MHz, CDCl₃) $\delta = 150.0$ (C_q), 137.6 (CH), 132.7 (CH), 115.8 (CH₂=C), 112.0 (CH), 110.8 (C_q), 90.6 (C≡), 85.6 (C≡), 55.2 (NC_q), 46.5 (NCH₂), 40.5 (CH₃), 38.5 (CH₂), 26.1 (CH₂), 23.3 (CH₂) ppm.

HRMS (ESI-TOF, + mode) m/z calcd for C₁₉H₂₇N₂ 283.2169, found 283.2158 [M+H]⁺.

N-Benzyl-1-((4-fluorophenyl)ethynyl)cyclohexan-1-amine (K.3k)



Chemical Formula: C₂₁H₂₂FN
Molecular Weight: 307.4124

Following the General Procedure A, the title compound **K.3k** was isolated as a yellow oil (701 mg, 2.28 mmol). Yield 76%.

R_f = 0.27 (SiO₂, cyclohexane/EtOAc 9:1).

ATR-FTIR (neat) $\nu = 3300, 3104, 3086, 3061, 3027, 2938, 2925, 2859, 2801, 1598, 1462, 1287, 1217, 1154, 1115, 1030, 947, 836, 734, 696$ cm⁻¹.

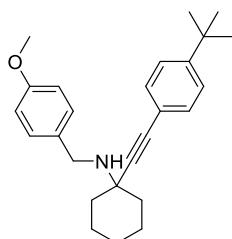
¹H NMR (500 MHz, CDCl₃) $\delta = 7.46 - 7.41$ (m, 2H, H_{aro}), 7.41 - 7.37 (m, 2H, H_{aro}), 7.35 - 7.30 (m, 2H, H_{aro}), 7.27 - 7.22 (m, 1H, H_{aro}), 7.05 - 6.98 (m, 2H, H_{aro}), 3.97 (s, 2H, NCH₂), 2.02 - 1.92 (m, 2H, 2 × NC_qCH₂), 1.78 - 1.61 (m, 5H), 1.58 - 1.44 (m, 2H), 1.33 - 1.22 (m, 1H) ppm.

¹⁹F{¹H} NMR (471 MHz, CDCl₃) $\delta = -111.90$ ppm.

¹³C{¹H} NMR (126 MHz, CDCl₃) $\delta = 162.4$ (d, $^1J_{C-F} = 248.6$ Hz, FC_q), 141.2 (C_q-Ph), 133.6 (d, $^3J_{C-F} = 8.2$ Hz, FC_qCHCH), 128.6 (C_{aro}H), 127.0 (C_{aro}H), 119.9 (d, $^4J_{C-F} = 3.4$ Hz, ≡CC_q-aro), 115.6 (d, $^2J_{C-F} = 22.0$ Hz, FC_qCH), 93.4 (d, $^5J_{C-F} = 1.3$ Hz, C_q-aroC≡), 83.8 (≡CC_qN), 55.4 (NC_q), 48.2 (NCH₂), 38.3 (CH₂), 26.0 (CH₂), 23.1 (CH₂) ppm. N.B.: one C_{aro}H missing.

HRMS (ESI-TOF, + mode) m/z calcd for C₂₁H₂₃FN 308.1809, found 308.1808 [M+H]⁺.

1-((4-(tert-Butyl)phenyl)ethynyl)-N-(4-methoxybenzyl)cyclohexan-1-amine (K.3l)



Chemical Formula: C₂₆H₃₃NO
Molecular Weight: 375.5560

Following the General Procedure A, the title compound **K.3l** was isolated as a viscous yellow oil (591 mg, 1.58 mmol). Yield 63%.

R_f = 0.32 (SiO₂, cyclohexane/EtOAc 8:2).

ATR-FTIR (neat) $\nu = 3033, 2931, 2854, 1612, 1511, 1461, 1363, 1245, 1172, 1107, 1036, 832, 737, 695$ cm⁻¹.

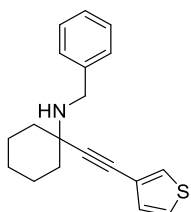
¹H NMR (500 MHz, CDCl₃) $\delta = 7.43 - 7.38$ (m, 2H, H_{aro}), 7.36 - 7.33 (m, 2H, H_{aro}), 7.32 - 7.29 (m, 2H, H_{aro}), 6.89 - 6.83 (m, 2H,

2 × OC_qCH), 3.91 (s, 2H, NCH₂), 3.80 (s, 3H, OCH₃), 2.01 – 1.92 (m, 2H, 2 × NC_qCH₂), 1.75 – 1.61 (m, 5H), 1.55 – 1.47 (m, 2H), 1.32 (s, 9H, C(CH₃)₃), 1.29 – 1.22 (m, 1H) ppm.

¹³C{¹H} NMR (126 MHz, CDCl₃) δ = 158.7 (CH₃OC_q), 151.1 (C_q), 133.5 (C_q), 131.5 (C_{aro}H), 129.8 (C_{aro}H), 125.4 (C_{aro}H), 120.9 (C_q), 114.0 (C_{aro}H), 93.1 (C≡), 84.8 (C≡), 55.5 (NC_q), 55.4 (OCH₃), 47.6 (NCH₂), 38.4 (CH₂), 34.9 (C(CH₃)₃), 31.4 (C(CH₃)₃), 26.1 (CH₂), 23.2 (CH₂) ppm.

HRMS (ESI-TOF, + mode) *m/z* calcd for C₂₆H₃₄NO 376.2635, found 376.2650 [M+H]⁺.

N-Benzyl-1-(thiophen-3-ylethynyl)cyclohexan-1-amine (K.3m)



Chemical Formula: C₁₉H₂₁NS
Molecular Weight: 295,4440

Following the General Procedure A, the title compound **K.3m** was isolated as a yellow oil (251 mg, 0.85 mmol). Yield 85%.

R_f = 0.75 (SiO₂, cyclohexane/EtOAc 7:3).

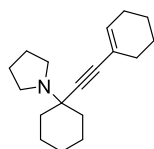
ATR-FTIR (neat) ν = 3313, 3107, 3085, 3061, 3027, 2929, 2852, 1604, 1449, 1355, 1282, 1114, 975, 867, 777, 696 cm⁻¹.

¹H NMR (500 MHz, CDCl₃) δ = 7.43 – 7.37 (m, 3H, H_{aro}), 7.35 – 7.30 (m, 2H, H_{aro}), 7.29 – 7.22 (m, 2H, H_{aro}), 7.13 (dd, *J* = 5.0, 1.3 Hz, 1H, H_{aro}), 3.96 (s, 2H, NCH₂), 2.01 – 1.93 (m, 2H, 2 × NC_qCH₂), 1.76 – 1.62 (m, 5H), 1.53 (td, *J* = 11.9, 4.0 Hz, 2H), 1.44 (s, 1H), 1.33 – 1.22 (m, 1H) ppm.

¹³C{¹H} NMR (126 MHz, CDCl₃) δ = 141.2 (C_q), 130.3 (C_{aro}H), 128.6(1) (C_{aro}H), 128.6(0) (C_{aro}H), 128.0 (C_{aro}H), 127.0 (C_{aro}H), 125.3 (C_{aro}H), 122.8 (C_q), 93.2 (C≡), 79.7 (C≡), 55.5 (NC_q), 48.2 (NCH₂), 38.3 (CH₂), 26.1 (CH₂), 23.1 (CH₂) ppm.

HRMS (ESI-TOF, + mode) *m/z* calcd for C₁₉H₂₂NS 296.1467, found 296.1470 [M+H]⁺.

1-(1-(Cyclohex-1-en-1-ylethynyl)cyclohexyl)pyrrolidine (K.3n) (CAS: 2743452-71-1)



Chemical Formula: C₁₈H₂₇N
Molecular Weight: 257,4210

Following the General Procedure A, the title compound **K.3n** was isolated as a yellow oil (206 mg, 0.78 mmol). Yield 78%.

R_f = 0.15 (SiO₂, cyclohexane/EtOAc 7:3).

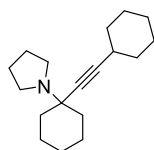
ATR-FTIR (neat) ν = 3025, 2927, 2854, 2807, 1633, 1446, 1347, 1284, 1125, 916, 883, 840, 733 cm⁻¹.

¹H NMR (400 MHz, CDCl₃) δ = 6.04 (tt, *J* = 3.8, 1.8 Hz, 1H, C=CH), 2.77 – 2.64 (m, 4H, 2 × NCH₂), 2.17 – 2.03 (m, 4H), 1.96 – 1.87 (m, 2H, 2 × NC_qCH₂), 1.80 – 1.68 (m, 4H, 2 × NCH₂CH₂), 1.68 – 1.50 (m, 9H), 1.45 (td, *J* = 11.7, 4.0 Hz, 2H, C=CH₂), 1.26 – 1.10 (m, 1H) ppm.

¹³C{¹H} NMR (126 MHz, CDCl₃) δ = 133.5 (C_q=CH), 120.9 (C_q=CH), 88.0 (C≡), 87.4 (C≡), 59.3 (NC_q), 47.1 (NCH₂), 38.2 (CH₂), 30.1 (CH₂), 25.9 (CH₂), 25.7 (CH₂), 23.6 (CH₂), 23.2 (CH₂), 22.5 (CH₂), 21.7 (CH₂) ppm.

HRMS (ESI-TOF, + mode) *m/z* calcd for C₁₈H₂₈N 258.2216, found 258.2219 [M+H]⁺.

1-(1-(Cyclohexylethynyl)cyclohexyl)pyrrolidine (K.3o) (CAS: 2743452-73-3)



Chemical Formula: C₁₈H₂₉N
Molecular Weight: 259,4370

Following the General Procedure A, the title compound **K.3o** was isolated as a yellow oil (176 mg, 0.68 mmol). Yield 68%.

R_f = 0.40 – 0.20 (SiO₂, cyclohexane/EtOAc 7:3).

ATR-FTIR (neat) ν = 2925, 2852, 2806, 2229, 1656, 1446, 1348, 1281, 1126, 1013, 886 cm⁻¹.

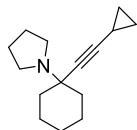
¹H NMR (400 MHz, CDCl₃) δ = 2.75 – 2.64 (m, 4H, 2 × NCH₂), 2.45 (tt, *J* = 8.3, 3.6 Hz, 1H, ≡CCH), 1.92 – 1.83 (m, 2H, 2 × NC_qCH₂), 1.80 – 1.66 (m, 8H), 1.64 – 1.54 (m, 5H), 1.51 – 1.26 (m, 8H), 1.23 – 1.10 (m, 1H) ppm.

$^{13}\text{C}\{^1\text{H}\}$ NMR (126 MHz, CDCl_3) δ = 90.4 ($\text{C}\equiv$), 80.1 ($\text{C}\equiv$), 59.0 (NC_q), 47.0 (NCH_2), 38.3 (CH_2), 33.5 (CH_2), 29.0 ($\equiv\text{CCH}$), 26.2 (CH_2), 25.9 (CH_2), 24.7 (CH_2), 23.6 (CH_2), 23.3 (CH_2) ppm.

MS (ESI-TOF, + mode) m/z (rel intensity) 260.23 (100) $[\text{M}+\text{H}]^+$, 189.16 (10) $[\text{C}_{14}\text{H}_{21}]^+$.

HRMS (ESI-TOF, + mode) m/z calcd for $\text{C}_{18}\text{H}_{30}\text{N}$ 260.2373, found 260.2367 $[\text{M}+\text{H}]^+$.

1-(1-(Cyclopropylethynyl)cyclohexyl)pyrrolidine (K.3p) (CAS: 2743452-74-4)



Chemical Formula: $\text{C}_{15}\text{H}_{23}\text{N}$
Molecular Weight: 217,3560

Following the General Procedure A, the title compound **K.3p** was isolated as a yellow oil (139 mg, 0.64 mmol). Yield 64%.

R_f = 0.30 – 0.20 (SiO_2 , cyclohexane/EtOAc 7:3).

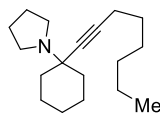
ATR-FTIR (neat) ν = 3091, 3010, 2925, 2854, 2807, 2227, 1446, 1353, 1281, 1124, 1026, 912, 883, 733 cm^{-1} .

^1H NMR (400 MHz, CDCl_3) δ = 2.73 – 2.62 (m, 4H, $2 \times \text{NCH}_2$), 1.90 – 1.80 (m, 2H, $2 \times \text{NC}_q\text{CH}_2$), 1.80 – 1.70 (m, 4H, $2 \times \text{NCH}_2\text{CH}_2$), 1.66 – 1.47 (m, 5H), 1.40 (td, J = 11.8, 3.7 Hz, 2H), 1.29 – 1.09 (m, 2H), 0.79 – 0.71 (m, 2H, $2 \times \text{CHCH}_2$), 0.64 – 0.57 (m, 2H, $2 \times \text{CHCH}_2$) ppm.

$^{13}\text{C}\{^1\text{H}\}$ NMR (126 MHz, CDCl_3) δ = 89.4 ($\text{C}\equiv$), 75.4 ($\text{C}\equiv$), 58.9 (NC_q), 47.0 (NCH_2), 38.2 (CH_2), 25.9 (CH_2), 23.6 (CH_2), 23.2 (CH_2), 8.9 (CHCH_2), -0.4 (CH) ppm.

HRMS (ESI-TOF, + mode) m/z calcd for $\text{C}_{15}\text{H}_{24}\text{N}$ 218.1903, found 218.1908 $[\text{M}+\text{H}]^+$.

1-(1-(Oct-1-yn-1-yl)cyclohexyl)pyrrolidine (K.3q) (CAS: 1404592-43-3)^[371]



Chemical Formula: $\text{C}_{18}\text{H}_{31}\text{N}$
Molecular Weight: 261,4530

Following the General Procedure A, the title compound **K.3q** was isolated as a yellow oil (175 mg, 0.67 mmol). Yield 67%.

R_f = 0.35 (SiO_2 , cyclohexane/EtOAc 7:3).

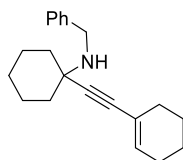
ATR-FTIR (neat) ν = 2925, 2854, 2808, 1446, 1282, 1126, 1014, 883, 724 cm^{-1} .

^1H NMR (400 MHz, CDCl_3) δ = 2.75 – 2.62 (m, 4H, $2 \times \text{NCH}_2$), 2.21 (t, J = 6.8 Hz, 2H, $\equiv\text{CCH}_2$), 1.87 (d, J = 12.1 Hz, 2H, $2 \times \text{NC}_q\text{CH}_2$), 1.79 – 1.69 (m, 4H, $2 \times \text{NCH}_2\text{CH}_2$), 1.66 – 1.35 (m, 11H), 1.35 – 1.23 (m, 4H), 1.22 – 1.10 (m, 1H), 0.88 (t, J = 6.8 Hz, 3H, CH_3) ppm.

$^{13}\text{C}\{^1\text{H}\}$ NMR (126 MHz, CDCl_3) δ = 85.6 ($\text{C}\equiv$), 80.2 ($\text{C}\equiv$), 59.0 (NC_q), 47.0 (NCH_2), 38.3 (CH_2), 31.5 (CH_2), 29.4 (CH_2), 28.6 (CH_2), 25.9 (CH_2), 23.6 (CH_2), 23.2 (CH_2), 22.7 (CH_2), 18.8 (CH_2), 14.2 (CH_3) ppm.

MS (ESI-TOF, + mode) m/z (rel intensity) 262.25 (100) $[\text{M}+\text{H}]^+$.

N-Benzyl-1-(cyclohex-1-en-1-ylethynyl)cyclohexan-1-amine (K.3r)



Chemical Formula: $\text{C}_{21}\text{H}_{27}\text{N}$
Molecular Weight: 293,4540

Following the General Procedure A, the title compound **K.3r** was isolated as a yellow oil (853 mg, 2.907 mmol). Yield 97%.

R_f = 0.83 (SiO_2 , cyclohexane/EtOAc 7:3).

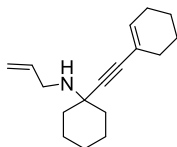
ATR-FTIR (neat) ν = 3299, 3084, 3061, 3025, 2922, 2859, 1712, 1604, 1495, 1463, 1447, 1345, 1281, 1190, 1117, 1030, 919, 853, 776, 736, 697 cm^{-1} .

^1H NMR (500 MHz, CDCl_3) δ = 7.40 – 7.35 (m, 2H, H_{aro}), 7.34 – 7.29 (m, 2H, H_{aro}), 7.26 – 7.21 (m, 1H, H_{aro}), 6.10 (tt, J = 3.9, 1.8 Hz, 1H, $\text{C}=\text{CH}$), 3.90 (s, 2H, NCH_2), 2.18 (tq, J = 6.2, 2.3 Hz, 2H, $\text{C}_q=\text{CHCH}_2$), 2.14 – 2.08 (m, 2H, $\equiv\text{CC}_q\text{CH}_2$), 1.91 – 1.85 (m, 2H, $2 \times \text{NC}_q\text{CH}_2$), 1.72 – 1.55 (m, 9H), 1.46 (td, J = 11.8, 3.8 Hz, 2H), 1.28 – 1.18 (m, 1H) ppm.

$^{13}\text{C}\{^1\text{H}\}$ NMR (126 MHz, CDCl_3) δ = 141.4 (C_q), 133.7 ($\text{C}=\text{CH}$), 128.6 (C_{aroH}), 128.5 (C_{aroH}), 126.9 (C_{aroH}), 121.0 (C_q), 90.8 ($\text{C}\equiv$), 86.6 ($\text{C}\equiv$), 55.3 (NC_q), 48.1 (NCH_2), 38.5 (NC_qCH_2), 30.0 (CHCH_2), 26.1 (CH_2), 25.7 ($\equiv\text{CC}_q\text{CH}_2$), 23.2 (CH_2), 22.5 (CH_2), 21.7 (CH_2) ppm.

HRMS (ESI-TOF, + mode) m/z calcd for $\text{C}_{21}\text{H}_{28}\text{N}$ 294.2216, found 294.2200 $[\text{M}+\text{H}]^+$.

***N*-Allyl-1-(cyclohex-1-en-1-ylethynyl)cyclohexan-1-amine (K.3s) (CAS: 1404592-43-3)**^[371]



Chemical Formula: $\text{C}_{17}\text{H}_{25}\text{N}$
Molecular Weight: 243,3940

Following the General Procedure A, the title compound **K.3s** was isolated as a yellow oil (243 mg, 0.83 mmol). Yield 83%.

R_f = 0.48 (SiO_2 , cyclohexane/EtOAc 7:3).

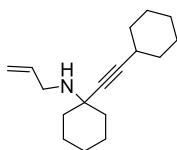
ATR-FTIR (neat) ν = 3077, 3024, 3008, 2927, 2855, 1643, 1447, 1343, 1286, 1116, 916, 841, 746 cm^{-1} .

^1H NMR (500 MHz, CDCl_3) δ = 6.05 (td, J = 4.1, 2.0 Hz, 1H, $\text{C}_q=\text{CH}$), 5.97 (ddt, J = 16.5, 11.3, 6.0 Hz, 1H, NCH_2CH), 5.21 (d, J = 17.0 Hz, 1H, $\text{CH}=\text{CH}_2$), 5.07 (d, J = 10.2 Hz, 1H, $\text{CH}=\text{CH}_2$), 3.38 (bs, 2H, NCH_2), 2.17 – 2.04 (m, 4H), 1.85 (d, J = 12.0 Hz, 2H, $2 \times \text{NC}_q\text{CH}_2$), 1.69 – 1.53 (m, 9H), 1.43 – 1.34 (m, 2H), 1.27 – 1.12 (m, 1H) ppm.

$^{13}\text{C}\{^1\text{H}\}$ NMR (126 MHz, CDCl_3) δ = 137.5 ($\text{CH}=\text{CH}_2$), 133.8 ($\text{CH}=\text{C}_q$), 120.9 ($\text{CH}=\text{C}_q$), 115.8 ($\text{CH}=\text{CH}_2$), 90.3 ($\text{C}\equiv$), 86.8 ($\text{C}\equiv$), 55.0 (NC_q), 46.4 (NCH_2), 38.5 (CH_2), 29.9 (CH_2), 26.0 (CH_2), 25.7 (CH_2), 23.2 (CH_2), 22.5 (CH_2), 21.7 (CH_2) ppm.

HRMS (ESI-TOF, + mode) m/z calcd for $\text{C}_{17}\text{H}_{26}\text{N}$ 244.2060, found 244.2062 $[\text{M}+\text{H}]^+$.

***N*-Allyl-1-(cyclohexylethynyl)cyclohexan-1-amine (K.3t) (CAS: 2743452-76-6)**



Chemical Formula: $\text{C}_{17}\text{H}_{27}\text{N}$
Molecular Weight: 245,4100

Following the General Procedure A, the title compound **K.3t** was isolated as a yellow oil (187 mg, 0.76 mmol). Yield 76%.

R_f = 0.55 (SiO_2 , cyclohexane/EtOAc 7:3).

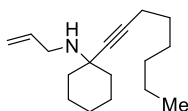
ATR-FTIR (neat) ν = 3309, 3077, 3008, 2932, 2852, 2662, 1643, 1447, 1346, 1282, 1117, 994, 914, 747 cm^{-1} .

^1H NMR (600 MHz, CDCl_3) δ = 5.97 (ddt, J = 17.2, 10.2, 6.1 Hz, 1H, $\text{CH}=\text{CH}_2$), 5.20 (dq, J = 17.1, 1.7 Hz, 1H, $\text{CH}=\text{CH}_2$), 5.07 (dq, J = 10.2, 1.4 Hz, 1H, $\text{CH}=\text{CH}_2$), 3.37 (dt, J = 6.1, 1.5 Hz, 2H, NCH_2), 2.46 – 2.40 (m, 1H, $\equiv\text{CCH}$), 1.84 – 1.74 (m, 4H), 1.73 – 1.67 (m, 2H), 1.66 – 1.54 (m, 5H), 1.53 – 1.42 (m, 2H), 1.39 – 1.28 (m, 6H), 1.22 – 1.12 (m, 1H), 1.03 (bs, 1H) ppm.

$^{13}\text{C}\{^1\text{H}\}$ NMR (126 MHz, CDCl_3) δ = 137.8 ($\text{CH}=\text{CH}_2$), 115.6 ($\text{CH}=\text{CH}_2$), 89.2 ($\text{C}\equiv$), 83.5 ($\text{C}\equiv$), 54.6 (NC_q), 46.4 (NCH_2), 38.7 (CH_2), 33.2 (CH_2), 29.1 ($\equiv\text{CCH}$), 26.2 (CH_2), 26.1 (CH_2), 24.8 (CH_2), 23.3 (CH_2) ppm.

HRMS (ESI-TOF, + mode) m/z calcd for $\text{C}_{17}\text{H}_{28}\text{N}$ 246.2216, found 246.2204 $[\text{M}+\text{H}]^+$.

***N*-Allyl-1-(oct-1-yn-1-yl)cyclohexan-1-amine (K.3u) (CAS: 2743452-77-7)**



Chemical Formula: $\text{C}_{17}\text{H}_{29}\text{N}$
Molecular Weight: 247,4260

Following the General Procedure A, the title compound **K.3u** was isolated as an orange oil (208 mg, 0.84 mmol). Yield 84%.

R_f = 0.55 (SiO_2 , cyclohexane/EtOAc 7:3).

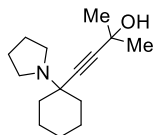
ATR-FTIR (neat) ν = 3078, 2920, 2855, 1644, 1459, 1343, 1283, 1117, 995, 915, 726 cm^{-1} .

^1H NMR (500 MHz, CDCl_3) δ = 5.97 (ddt, J = 16.5, 10.2, 6.1 Hz, 1H, $\text{CH}=\text{CH}_2$), 5.19 (dq, J = 17.2, 1.7 Hz, 1H, $\text{CH}=\text{CH}_2$), 5.07 (dq, J = 10.2, 1.5 Hz, 1H, $\text{CH}=\text{CH}_2$), 3.36 (dt, J = 6.1, 1.5 Hz, 2H, NCH_2), 2.21 (dt, J = 7.0, 1.4 Hz, 2H, $\equiv\text{CCH}_2$), 1.86 – 1.76 (m, 2H, $2 \times \text{NC}_q\text{CH}_2$), 1.68 – 1.45 (m, 7H), 1.45 – 1.24 (m, 7H), 1.23 – 1.11 (m, 1H), 0.89 (t, J = 7.0 Hz, 3H, CH_3) ppm.

$^{13}\text{C}\{^1\text{H}\}$ NMR (126 MHz, CDCl_3) δ = 137.7 ($\text{CH}=\text{CH}_2$), 115.6 ($\text{CH}=\text{CH}_2$), 84.8 ($\text{C}\equiv$), 83.6 ($\text{C}\equiv$), 54.7 (NC_q), 46.4 (NCH_2), 38.6 (CH_2), 31.5 (CH_2), 29.3 (CH_2), 28.6 (CH_2), 26.1 (CH_2), 23.2 (CH_2), 22.7 (CH_2), 18.8 (CH_2), 14.2 (CH_3) ppm.

HRMS (ESI-TOF, + mode) m/z calcd for $\text{C}_{17}\text{H}_{30}\text{N}$ 248.2373, found 248.2365 $[\text{M}+\text{H}]^+$.

2-Methyl-4-(1-(pyrrolidin-1-yl)cyclohexyl)but-3-yn-2-ol (K.3v) (CAS: 2743452-81-3)



Chemical Formula: $\text{C}_{15}\text{H}_{25}\text{NO}$
Molecular Weight: 235,3710

Following the General Procedure A, the title compound **K.3v** was isolated as brown waxy solid (167 mg, 0.71 mmol). Yield 71%.

R_f = 0.20 (SiO_2 , $\text{CH}_2\text{Cl}_2/\text{MeOH}$ 9:1).

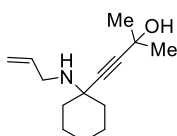
ATR-FTIR (neat) ν = 3608 – 3348, 3052, 2969, 2930, 2856, 2673, 2552, 2471, 1447, 1358, 1222, 1166, 950, 882 cm^{-1} .

^1H NMR (500 MHz, CDCl_3) δ = 2.79 (bs, 4H, $2 \times \text{NCH}_2$), 1.93 – 1.87 (m, 2H, $2 \times \text{NC}_q\text{CH}_2$), 1.80 (bs, 4H, $2 \times \text{NCH}_2\text{CH}_2$), 1.68 – 1.49 (m, 13H, $2 \times \text{CH}_3$ & 7H cyclohexyl), 1.25 – 1.13 (m, 1H) ppm.

$^{13}\text{C}\{^1\text{H}\}$ NMR (126 MHz, CDCl_3) δ = 91.8 ($\text{C}\equiv$), 80.9 ($\text{C}\equiv$), 71.2 (C_qO), 65.0 (NC_q), 47.1 (NCH_2), 37.0 (CH_2), 31.9 (CH_3), 25.2 (CH_2), 23.4 (CH_2), 22.9 (CH_2) ppm.

HRMS (ESI-TOF, + mode) m/z calcd for $\text{C}_{15}\text{H}_{26}\text{NO}$ 236.2009, found 236.2013 $[\text{M}+\text{H}]^+$.

4-(1-(Allylamino)cyclohexyl)-2-methylbut-3-yn-2-ol (K.3w) (CAS: 2743452-83-5)



Chemical Formula: $\text{C}_{14}\text{H}_{23}\text{NO}$
Molecular Weight: 221,3440

Following the General Procedure A, the title compound **K.3w** was isolated as a brown resin (77 mg, 0.35 mmol). Yield 35%.

R_f = 0.28 (SiO_2 , $\text{CH}_2\text{Cl}_2/\text{MeOH}$ 9:1).

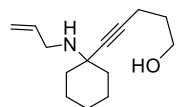
ATR-FTIR (neat) ν = 3582 – 3248, 3086, 2974, 2928, 2851, 1644, 1491, 1449, 1370, 1226, 1169, 1101, 911, 671 cm^{-1} .

^1H NMR (300 MHz, CDCl_3) δ = 5.96 (ddt, J = 17.1, 10.2, 6.1 Hz, 1H, $\text{CH}=\text{CH}_2$), 5.19 (dq, J = 17.1, 1.7 Hz, 1H, $\text{CH}=\text{CH}_2$), 5.07 (ddt, J = 10.2, 1.8, 1.3 Hz, 1H, $\text{CH}=\text{CH}_2$), 3.34 (dt, J = 6.1, 1.5 Hz, 2H, NCH_2), 1.87 – 1.77 (m, 2H, $2 \times \text{NC}_q\text{CH}_2$), 1.75 – 1.45 (m, 10H, $2 \times \text{CH}_3$ & 4H cyclohexyl), 1.42 – 1.30 (m, 2H), 1.28 – 1.11 (m, 1H) ppm.

$^{13}\text{C}\{^1\text{H}\}$ NMR (126 MHz, CDCl_3) δ = 137.4 ($\text{CH}=\text{CH}_2$), 115.9 ($\text{CH}=\text{CH}_2$), 89.8 ($\text{C}\equiv$), 85.5 ($\text{C}\equiv$), 65.4 (C_qO), 54.4 (NC_q), 46.3 (NCH_2), 38.2 (CH_2), 32.0 (CH_3), 25.9 (CH_2), 23.1 (CH_2), 22.9 (CH_2) ppm.

HRMS (ESI-TOF, + mode) m/z calcd for $\text{C}_{14}\text{H}_{24}\text{NO}$ 222.1852, found 222.1860 $[\text{M}+\text{H}]^+$.

5-(1-(Allylamino)cyclohexyl)pent-4-yn-1-ol (K.3x) (CAS: 2743452-85-7)



Chemical Formula: $\text{C}_{14}\text{H}_{23}\text{NO}$
Molecular Weight: 221,3440

Following the General Procedure A, the title compound **K.3x** was isolated as a brown oil (93 mg, 0.42 mmol). Yield 42%.

R_f = 0.10 (SiO_2 , $\text{CH}_2\text{Cl}_2/\text{MeOH}$ 8:2).

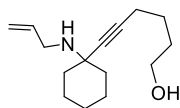
ATR-FTIR (neat) ν = 3572 – 3030, 3244, 3083, 2930, 2853, 1644, 1444, 1418, 1346, 1293, 1174, 1066, 993, 906, 603 cm^{-1} .

^1H NMR (400 MHz, CDCl_3) δ = 5.96 (ddt, J = 16.4, 10.2, 6.1 Hz, 1H, $\text{CH}=\text{CH}_2$), 5.19 (dq, J = 17.1, 1.7 Hz, 1H, $\text{CH}=\text{CH}_2$), 5.07 (dq, J = 10.3, 1.4 Hz, 1H, $\text{CH}=\text{CH}_2$), 3.77 (t, J = 6.2 Hz, 2H, CH_2OH), 3.35 (dt, J = 6.0, 1.5 Hz, 2H, NCH_2), 2.35 (t, J = 6.9 Hz, 2H, $\equiv\text{CCH}_2$), 1.84 – 1.72 (m, 5H), 1.68 – 1.47 (m, 4H), 1.34 (td, J = 12.1, 3.7 Hz, 2H), 1.27 – 1.11 (m, 1H) ppm.

$^{13}\text{C}\{^1\text{H}\}$ NMR (126 MHz, CDCl_3) δ = 137.5 ($\text{CH}=\text{CH}_2$), 115.7 ($\text{CH}=\text{CH}_2$), 84.3 ($\text{C}\equiv$), 83.8 ($\text{C}\equiv$), 62.0 (CH_2O), 54.6 (NC_q), 46.3 (NCH_2), 38.5 (CH_2), 31.9 (CH_2), 26.0 (CH_2), 23.2 (CH_2), 15.5 (CH_2) ppm.

HRMS (ESI-TOF, + mode) m/z calcd for $\text{C}_{14}\text{H}_{24}\text{NO}$ 222.1852, found 222.1858 $[\text{M}+\text{H}]^+$.

6-(1-(Allylamino)cyclohexyl)hex-5-yn-1-ol (K.3y) (CAS: 2743452-87-9)



Chemical Formula: C₁₅H₂₅NO
Molecular Weight: 235,3710

Following the General Procedure A, the title compound **K.3y** was isolated as a brown oil (195 mg, 0.83 mmol). Yield 83%.

R_f = 0.50 (SiO₂, CH₂Cl₂/MeOH 8:2).

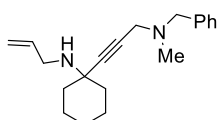
ATR-FTIR (neat) ν = 3568 – 3104, 3080, 2932, 2855, 1644, 1448, 1330, 1285, 1175, 1060, 994, 915, 831, 748, 606 cm⁻¹.

¹H NMR (300 MHz, CDCl₃) δ = 5.96 (ddt, *J* = 17.3, 10.2, 6.1 Hz, 1H, CH=CH₂), 5.19 (dq, *J* = 17.2, 1.7 Hz, 1H, CH=CH₂), 5.06 (dq, *J* = 10.2, 1.4 Hz, 1H, CH=CH₂), 3.67 (t, *J* = 6.1 Hz, 2H, CH₂OH), 3.35 (dt, *J* = 6.1, 1.5 Hz, 2H, NCH₂), 2.26 (t, *J* = 6.7 Hz, 2H, ≡CCH₂), 1.85 – 1.75 (m, 3H), 1.74 – 1.08 (m, 11H) ppm.

¹³C{¹H} NMR (126 MHz, CDCl₃) δ = 137.5 (CH=CH₂), 115.7 (CH=CH₂), 84.3 (C≡), 83.9 (C≡), 62.5 (CH₂O), 54.7 (NC_q), 46.3 (NCH₂), 38.5 (CH₂), 32.0 (CH₂), 26.0 (CH₂), 25.6 (CH₂), 23.2 (CH₂), 18.6 (CH₂) ppm.

HRMS (ESI-TOF, + mode) *m/z* calcd for C₁₅H₂₆NO 236.2009, found 236.2006 [M+H]⁺.

N-Allyl-1-(3-(benzyl(methyl)amino)prop-1-yn-1-yl)cyclohexan-1-amine (K.3ba) (CAS: 2743453-02-1)



Chemical Formula: C₂₀H₂₈N₂
Molecular Weight: 296,4580

Following the General Procedure A, the title compound **K.3ba** was isolated as an orange oil (86 mg, 0.29 mmol). Yield 29%.

R_f = 0.55 (SiO₂, CH₂Cl₂/MeOH 9:1).

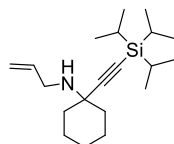
ATR-FTIR (neat) ν = 3063, 3027, 2931, 2853, 2791, 1643, 1452, 1325, 1121, 1025, 915, 737, 698 cm⁻¹.

¹H NMR (500 MHz, CDCl₃) δ = 7.26 – 7.15 (m, 5H, H_{aro}), 5.91 (ddt, *J* = 16.5, 10.3, 6.1 Hz, 1H, CH=CH₂), 5.15 (d, *J* = 17.3 Hz, 1H, CH=CH₂), 5.02 (d, *J* = 10.1 Hz, 1H, CH=CH₂), 3.51 (s, 2H, ≡CCH₂), 3.39 – 3.31 (m, 2H, NCH₂ allyl), 3.29 (s, 2H, NCH₂ benzyl), 2.27 (s, 3H, NCH₃), 1.85 – 1.78 (m, 2H, 2 × NC_qCH₂), 1.66 – 1.51 (m, 5H), 1.38 – 1.28 (m, 2H), 1.20 – 1.10 (m, 1H) ppm.

¹³C{¹H} NMR (126 MHz, CDCl₃) δ = 138.6 (C_q), 137.4 (CH=CH₂), 129.4 (C_{aro}H), 128.5 (C_{aro}H), 127.3 (C_{aro}H), 115.9 (CH=CH₂), 89.2 (C≡), 78.6 (C≡), 60.1 (NCH₂Ph), 54.9 (NC_q), 46.5 (NCH₂), 45.2 (NCH₂), 42.1 (CH₃), 38.5 (CH₂), 26.0 (CH₂), 23.2 (CH₂) ppm.

HRMS (ESI-TOF, + mode) *m/z* calcd for C₂₀H₂₉N₂ 297.2325, found 297.2321 [M+H]⁺.

N-Allyl-1-((triisopropylsilyl)ethynyl)cyclohexan-1-amine (K.3bb) (CAS: 2743452-90-4)



Chemical Formula: C₂₀H₃₇NSi
Molecular Weight: 319,6080

Following the General Procedure A, the title compound **K.3bb** was isolated as a yellow oil (67 mg, 0.21 mmol). Yield 21%.

R_f = 0.55 (SiO₂, cyclohexane/EtOAc 7:3).

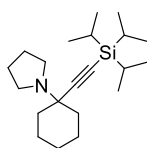
ATR-FTIR (neat) ν = 3079, 2933, 2892, 2863, 2154, 1644, 1461, 1279, 1153, 995, 882, 673 cm⁻¹.

¹H NMR (600 MHz, CDCl₃) δ = 5.97 (ddt, *J* = 17.2, 10.2, 6.2 Hz, 1H, CH=CH₂), 5.19 (dq, *J* = 17.1, 1.6 Hz, 1H, CH=CH₂), 5.07 (ddt, *J* = 10.2, 1.9, 1.2 Hz, 1H, CH=CH₂), 3.41 (dt, *J* = 6.2, 1.4 Hz, 2H, NCH₂ allyl), 1.88 – 1.83 (m, 2H, 2 × NC_qCH₂), 1.69 – 1.60 (m, 5H), 1.39 – 1.32 (m, 2H), 1.22 – 1.12 (m, 1H), 1.10 – 1.02 (m, 21H, Si(CH(CH₃)₂)₃) ppm.

¹³C{¹H} NMR (126 MHz, CDCl₃) δ = 137.5 (CH=CH₂), 116.0 (CH=CH₂), 112.0 (C≡), 84.3 (C≡), 55.5 (NC_q), 46.6 (NCH₂), 38.4 (CH₂), 26.0 (CH₂), 23.2(CH₂), 18.8 (SiCH), 11.4 (CH₃) ppm.

HRMS (ESI-TOF, + mode) m/z calcd for $C_{20}H_{38}NSi$ 320.2768, found 320.2786 $[M+H]^+$.

1-(1-((Triisopropylsilyl)ethynyl)cyclohexyl)pyrrolidine (K.3bc) (CAS: 2743452-92-6)



Chemical Formula: $C_{21}H_{39}NSi$
Molecular Weight: 333,6350

Following the General Procedure A, the title compound **K.3bc** was isolated as a yellow oil (300 mg, 0.90 mmol). Yield 90%.

R_f = 0.39 (SiO₂, cyclohexane/EtOAc 7:3).

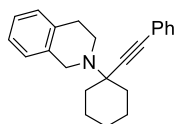
ATR-FTIR (neat) ν = 2930, 2863, 2808, 2152, 1462, 1447, 1279, 1162, 1014, 882, 658 cm^{-1} .

¹H NMR (500 MHz, CDCl₃) δ = 2.80 – 2.71 (m, 4H, 2 × NCH₂), 1.99 – 1.91 (m, 2H, 2 × NC_qCH₂), 1.77 (m, 4H, 2 × NCH₂CH₂), 1.68 – 1.58 (m, 5H), 1.46 – 1.37 (m, 2H), 1.21 – 1.13 (m, 1H), 1.11 – 1.00 (m, 21H, Si(CH(CH₃)₂)₃) ppm.

¹³C{¹H} NMR (126 MHz, CDCl₃) δ = 108.9 (C≡), 85.2 (C≡), 59.9 (NC_q), 47.2 (NCH₂), 38.2 (CH₂), 25.9 (CH₂), 23.7 (CH₂), 23.3 (CH₂), 18.9 (SiCH), 11.4 (CH₃) ppm.

HRMS (ESI-TOF, + mode) m/z calcd for $C_{21}H_{40}NSi$ 334.2925, found 334.2929 $[M+H]^+$.

2-(1-(Phenylethynyl)cyclohexyl)-1,2,3,4-tetrahydroisoquinoline (K.4b) (CAS: 2743453-08-7)



Chemical Formula: $C_{23}H_{25}N$
Molecular Weight: 315,4600

Following the General Procedure C, the title compound **K.4b** was isolated as a yellow oil (233 mg, 0.74 mmol). Yield 74%.

R_f = 0.72 (SiO₂, cyclohexane/EtOAc 8:2).

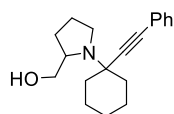
ATR-FTIR (neat) ν = 3062, 3022, 2927, 2854, 2806, 1597, 1489, 1444, 1262, 1088, 933, 742, 691 cm^{-1} .

¹H NMR (500 MHz, CDCl₃) δ = 7.47 – 7.42 (m, 2H, H_{aro}), 7.33 – 7.27 (m, 3H, H_{aro}), 7.18 – 7.06 (m, 4H, H_{aro}), 3.98 (s, 2H, NCH₂C_{q-aro}), 3.03 – 2.93 (m, 4H, NCH₂CH₂), 2.27 – 2.17 (m, 2H, 2 × NC_qCH₂), 1.84 – 1.77 (m, 2H), 1.76 – 1.62 (m, 5H), 1.38 – 1.27 (m, 1H) ppm.

¹³C{¹H} NMR (126 MHz, CDCl₃) δ = 135.7 (C_q), 134.8 (C_q), 131.8 (C_{aroH}), 128.6 (C_{aroH}), 128.3 (C_{aroH}), 127.9 (C_{aroH}), 127.1 (C_{aroH}), 126.0 (C_{aroH}), 125.6 (C_{aroH}), 123.6 (C_q), 90.1 (C≡), 86.2 (C≡), 59.2 (NC_q), 49.6 (NCH₂), 44.3 (NCH₂), 36.2 (CH₂), 30.3 (CH₂), 25.9 (CH₂), 23.0 (CH₂) ppm.

HRMS (ESI-TOF, + mode) m/z calcd for $C_{23}H_{26}N$ 316.2060, found 316.2045 $[M+H]^+$.

1-(1-(Phenylethynyl)cyclohexyl)pyrrolidin-2-yl)methanol (K.4c) (CAS: 2743453-10-1)



Chemical Formula: $C_{19}H_{25}NO$
Molecular Weight: 283,4150

Following the General Procedure C, the title compound **K.4c** was isolated as a viscous orange oil (71 mg, 0.25 mmol). Yield 25%.

R_f = 0.30 (SiO₂, CH₂Cl₂/MeOH 9:1).

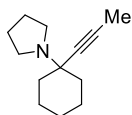
ATR-FTIR (neat) ν = 3570 – 3369, 3115, 3056, 2929, 2855, 1597, 1489, 1443, 1290, 1104, 1029, 907, 754, 690 cm^{-1} .

¹H NMR (500 MHz, CDCl₃) δ = 7.45 – 7.39 (m, 2H, H_{aro}), 7.34 – 7.27 (m, 3H, H_{aro}), 3.59 – 3.32 (m, 3H), 3.09 (bs, 1H), 2.95 (dd, J = 8.9, 8.3 Hz, 1H), 2.08 – 1.97 (m, 2H, 2 × NC_qCH₂), 1.96 – 1.38 (m, 12H), 1.29 – 1.15 (m, 1H) ppm.

¹³C{¹H} NMR (126 MHz, CDCl₃) δ = 131.8 (C_{aroH}), 128.4 (C_{aroH}), 128.0 (C_{aroH}), 123.6 (C_q), 91.5 (C≡), 85.0 (C≡), 67.0 (CH₂O), 60.7 (NC_q), 59.4 (NCH), 50.2 (NCH₂), 39.1 (CH₂), 38.0 (CH₂), 31.0 (CH₂), 25.6 (CH₂), 25.1 (CH₂), 23.3 (CH₂) ppm.

HRMS (ESI-TOF, + mode) m/z calcd for $C_{19}H_{26}NO$ 284.2009, found 284.2018 $[M+H]^+$.

1-(1-(Prop-1-yn-1-yl)cyclohexyl)pyrrolidine (K.4d) (CAS: 2743453-12-3)



Chemical Formula: C₁₃H₂₁N
Molecular Weight: 191,3180

Following the General Procedure C, the title compound **K.4d** was isolated as a yellow oil (183 mg, 0.95 mmol). Yield 95%.

$R_f = 0.30$ (SiO₂, cyclohexane/EtOAc 7:3).

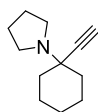
ATR-FTIR (neat) $\nu = 2929, 2854, 2809, 1445, 1282, 1263, 1165, 1125, 999, 914, 885, 833, 614 \text{ cm}^{-1}$.

¹H NMR (500 MHz, CDCl₃) $\delta = 2.73 - 2.64$ (m, 4H, 2 × NCH₂), 1.92 – 1.83 (m, 5H, 2 × NC_qCH₂ & CH₃), 1.79 – 1.72 (m, 4H, 2 × NCH₂CH₂), 1.65 – 1.51 (m, 5H), 1.41 (td, $J = 11.9, 3.9 \text{ Hz}$, 2H), 1.22 – 1.11 (m, 1H) ppm.

¹³C{¹H} NMR (126 MHz, CDCl₃) $\delta = 81.0$ (C≡), 79.4 (C≡), 58.9 (NC_q), 47.0 (NCH₂), 38.2 (CH₂), 25.9 (CH₂), 23.5 (CH₂), 23.1 (CH₂), 3.6 (CH₃) ppm.

HRMS (ESI-TOF, + mode) m/z calcd for C₁₃H₂₂N 192.1747, found 192.1736 [M+H]⁺.

1-(1-Ethynylcyclohexyl)pyrrolidine (K.4e) (CAS: 91552-94-2)^[372]



Chemical Formula: C₁₂H₁₉N
Molecular Weight: 177,2910

Following the General Procedure A, the title compound **K.4e** was obtained from propiolic acid in 22% yield. Following the General Procedure C, compound **K.4e** was obtained from propiolic acid in 4% yield.

Following a desilylative approach described below, compound **K.4e** was obtained in 58% yield (183 mg, 0.58 mmol). Cyclohexanone (1.0 mmol, 1.0 eq.), trimethylsilyl acetylene (1.5 mmol, 1.5 eq.) and Cu^I-USY (36 mg) were stirred in a sealed tube at room temperature for 15 min before addition of pyrrolidine (1.0 mmol, 1.0 eq.). The reaction mixture was heated to 40 °C in 15 min and then stirred for 60 h. The reaction mixture was treated as for General Procedure A. After column chromatography, compound **K.4e** was isolated as a colourless solid.

$R_f = 0.50 - 0.25$ (SiO₂, cyclohexane/EtOAc 7:3).

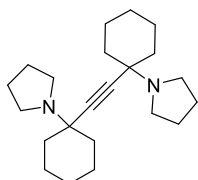
ATR-FTIR (neat) $\nu = 3130, 2964, 2926, 2877, 2857, 2812, 2076, 1444, 1364, 1280, 1121, 955, 882, 746, 553 \text{ cm}^{-1}$.

¹H NMR (300 MHz, CDCl₃) $\delta = 2.77 - 2.65$ (m, 4H, 2 × NCH₂), 2.28 (s, 1H, ≡CH), 1.99 – 1.89 (m, 2H, 2 × NC_qCH₂), 1.83 – 1.72 (m, 4H, 2 × NCH₂CH₂), 1.71 – 1.55 (m, 5H), 1.54 – 1.40 (m, 2H), 1.29 – 1.11 (m, 1H) ppm.

¹³C{¹H} NMR (126 MHz, CDCl₃) $\delta = 84.7$ (C≡), 73.2 (C≡), 58.8 (NC_q), 47.0 (NCH₂), 37.9 (CH₂), 25.7 (CH₂), 23.5 (CH₂), 22.9 (CH₂) ppm. *N.B.*: C≡C cannot be precisely assigned because both carbons are detected in DEPT135 NMR in CDCl₃.

MS (ESI-TOF, + mode) m/z 178.16 (30) [M+H]⁺.

1,2-Bis(1-(pyrrolidin-1-yl)cyclohexyl)ethyne (K.4e') (CAS: 2743452-98-2)



Chemical Formula: C₂₂H₃₆N₂
Molecular Weight: 328,5440

Following the General Procedure C, the title compound **K.4e'** was isolated as a colourless solid (237 mg) from cyclohexanone (3.0 mmol, 3.0 eq.), pyrrolidine (2.0 mmol, 2.0 eq.) and acetylenedicarboxylic acid (1.0 mmol, 1.0 eq.). Yield 72%.

$R_f = 0.15$ (SiO₂, CH₂Cl₂/MeOH 9:1).

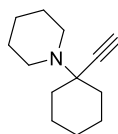
ATR-FTIR (neat) $\nu = 2925, 2852, 2808, 1441, 1281, 1169, 1124, 993, 881 \text{ cm}^{-1}$.

¹H NMR (500 MHz, CDCl₃) $\delta = 2.81 - 2.67$ (m, 8H, 4 × NCH₂), 1.92 (d, $J = 12.4 \text{ Hz}$, 4H, 4 × NC_qCH₂), 1.81 – 1.70 (m, 8H, 4 × NCH₂CH₂), 1.70 – 1.55 (m, 10H), 1.42 (td, $J = 12.1, 4.4 \text{ Hz}$, 4H), 1.23 – 1.11 (m, 2H) ppm.

$^{13}\text{C}\{^1\text{H}\}$ NMR (126 MHz, CDCl_3) δ = 85.7 ($\text{C}\equiv$), 59.4 (NC_q), 47.2 (NCH_2), 38.5 (CH_2), 25.9 (CH_2), 23.8 (CH_2), 23.4 (CH_2) ppm.

HRMS (ESI-TOF, + mode) m/z calcd for $\text{C}_{22}\text{H}_{37}\text{N}_2$ 329.2951, found 329.2956 $[\text{M}+\text{H}]^+$.

1-(1-Ethynylcyclohexyl)piperidine (K.4f) (CAS: 51165-02-7)



Chemical Formula: $\text{C}_{13}\text{H}_{21}\text{N}$
Molecular Weight: 191,3180

Following General Procedure C, compound **K.4f** was obtained from acetylene dicarboxylic acid as a colourless solid (31 mg, 0.16 mmol). Yield 16%.

R_f = 0.45 (SiO_2 , cyclohexane/EtOAc 7:3).

ATR-FTIR (neat) ν = 3153, 2983, 2962, 2851, 2795, 2078, 1444, 1275, 1150, 1091, 1019, 960, 875, 745, 686 cm^{-1} .

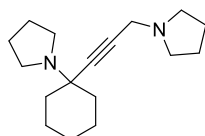
^1H NMR (500 MHz, CDCl_3) δ = 2.58 (bs, 4H, $2 \times \text{NCH}_2$), 2.31 (s, 1H, $\equiv\text{CH}$), 2.05 – 1.93 (m, 2H, $2 \times \text{NC}_q\text{CH}_2$), 1.72 – 1.38 (m, 13H), 1.29 – 1.15 (m, 1H) ppm.

$^{13}\text{C}\{^1\text{H}\}$ NMR (126 MHz, CDCl_3) δ = 84.9 ($\text{C}\equiv$), 73.1 ($\text{C}\equiv$), 58.7 (NC_q), 47.0 (NCH_2), 35.9 (CH_2), 26.7 (CH_2), 25.8 (CH_2), 24.8 (CH_2), 22.9 (CH_2) ppm. *N.B.*: $\text{C}\equiv\text{C}$ cannot be precisely assigned because both carbons are detected in DEPT135 NMR in CDCl_3 .

MS (ESI-TOF, + mode) m/z 192.17 (100) $[\text{M}+\text{H}]^+$.

HRMS (ESI-TOF, + mode) m/z calcd for $\text{C}_{13}\text{H}_{22}\text{N}$ 192.1747, found 192.1750 $[\text{M}+\text{H}]^+$.

1-(3-(1-(Pyrrolidin-1-yl)cyclohexyl)prop-2-yn-1-yl)pyrrolidine (K.4h) (CAS: 2743453-00-9)



Chemical Formula: $\text{C}_{17}\text{H}_{28}\text{N}_2$
Molecular Weight: 260,4250

Cyclohexanone (1.0 mmol, 1.0 eq.), trimethylsilylacetylene (1.5 mmol, 1.5 eq.) and Cu^{I} -USY (36 mg, 10 mol%) were successively added to a Teflon screw cap tube (10 mL) and stirred at room temperature and 500 rpm for 15 min. Then, pyrrolidine (1.0 mmol, 1.0 eq.) was added, and the mixture was flushed with argon before being progressively heated to 40 °C within 15 min and left to stir at 40 °C for 60 h. Next, paraformaldehyde (1.0 mmol, 1.0 eq.) and pyrrolidine (1.0 mmol, 1.0 eq.) were added, and the mixture was progressively heated to 80 °C within 45 min. After stirring at 80 °C and 500 rpm for 23 h, the reaction mixture was treated as in General Procedure A. Column chromatography on silica gel afforded compound **K.4h** as a yellow oil (130 mg, 0.50 mmol). Yield 50%.

R_f = 0.35 (SiO_2 , $\text{CH}_2\text{Cl}_2/\text{MeOH}$ 8:2).

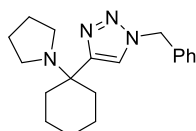
ATR-FTIR (neat) ν = 2927, 2873, 2854, 2801, 1446, 1371, 1346, 1323, 1281, 1164, 1125, 1017, 879 cm^{-1} .

^1H NMR (300 MHz, CDCl_3) δ = 3.49 (s, 2H, $\equiv\text{CCH}_2$), 2.74 – 2.69 (m, 4H, $2 \times \text{NCH}_2$), 2.67 – 2.59 (m, 4H, $2 \times \text{NCH}_2$), 1.97 – 1.87 (m, 2H, $2 \times \text{NC}_q\text{CH}_2$), 1.84 – 1.72 (m, 6H), 1.69 – 1.37 (m, 9H), 1.15 – 1.14 (m, 1H) ppm.

$^{13}\text{C}\{^1\text{H}\}$ NMR (126 MHz, CDCl_3) δ = 84.3 ($\text{C}\equiv$), 81.1 ($\text{C}\equiv$), 59.3 (NC_q), 52.5 (NCH_2), 47.1 (NCH_2), 43.4 (NCH_2), 38.0 (CH_2), 25.7 (CH_2), 24.0 (CH_2), 23.6 (CH_2), 23.2 (CH_2) ppm.

HRMS (ESI-TOF, + mode) m/z calcd for $\text{C}_{17}\text{H}_{29}\text{N}_2$ 261.2325, found 261.2328 $[\text{M}+\text{H}]^+$.

1-Benzyl-4-(1-(pyrrolidin-1-yl)cyclohexyl)-1H-1,2,3-triazole (K.4l) (CAS: 2743453-04-3)



Chemical Formula: $\text{C}_{19}\text{H}_{26}\text{N}_4$
Molecular Weight: 310,4450

Cyclohexanone (1.0 mmol, 1.0 eq.), trimethylsilylacetylene (1.5 mmol, 1.5 eq.) and Cu^{I} -USY (36 mg, 10 mol%) were successively added to a Teflon screw capped tube (10 mL) and stirred at room temperature and 500 rpm for 15 min. Then, pyrrolidine (1.0 mmol, 1.0 eq.) was added, and the mixture was flushed with argon before being progressively

heated to 80 °C within 45 min and left to stir at 80 °C for 18 h. Once cooled to room temperature, H₂O (2 mL) was added to the reaction mixture, which was degassed under argon during five minutes. Next, NaN₃ (1.1 mmol, 1.0 eq.) and benzyl bromide (1.0 mmol, 1.0 eq.) were added under argon. The sealed tube was placed into a pre-heated oil bath at 90 °C and 500 rpm and stirred for 16 h. The obtained suspension was filtered over celite at room temperature and washed with H₂O (15 mL) and EtOAc (15 mL). The aq. phase was extracted with EtOAc (3 × 5 mL) and the combined org. layers were dried over Na₂SO₄. The crude product was purified by column chromatography over silica and compound **K.4l** was isolated as a pale orange solid (109 mg, 0.35 mmol). Yield 35%.

R_f = 0.70 (SiO₂, CH₂Cl₂/MeOH 8:2).

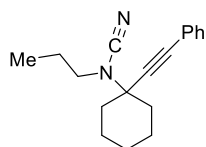
ATR-FTIR (neat) ν = 3121, 2969, 2939, 2927, 2917, 2862, 2825, 2804, 1497, 1445, 1331, 1217, 1159, 1129, 1055, 889, 831, 709, 588 cm⁻¹.

¹H NMR (300 MHz, CDCl₃) δ = 7.42 – 7.33 (m, 3H, H_{aro}), 7.25 – 7.18 (m, 3H, H_{aro}), 5.55 (s, 2H, NCH₂ benzyl), 2.58 – 2.45 (m, 4H, 2 × NCH₂), 2.31 – 2.18 (m, 2H, 2 × NC_qCH₂), 1.85 (ddd, *J* = 13.3, 10.3, 3.6 Hz, 2H), 1.70 – 1.62 (m, 2H), 1.62 – 1.54 (m, 4H, 2 × NCH₂CH₂), 1.47 – 1.14 (m, 4H) ppm.

¹³C{¹H} NMR (126 MHz, CDCl₃) δ = 147.4 (=CH), 135.1 (C_q), 129.1 (C_{aro}H), 128.6 (C_{aro}H), 127.7 (C_{aro}H), 121.9 (C_q), 57.1 (NC_q), 54.0 (PhNCH₂), 45.3 (C_qNCH₂), 35.5 (CH₂), 25.9 (CH₂), 23.2 (CH₂), 22.5 (CH₂) ppm.

HRMS (ESI-TOF, + mode) *m/z* calcd for C₁₉H₂₇N₄ 311.2230, found 311.2245 [M+H]⁺.

N-(1-(Phenylethynyl)cyclohexyl)-N-propylcyanamide (K.4m) (CAS: 2743453-06-5)



Chemical Formula: C₁₈H₂₂N₂
Molecular Weight: 266,3880

The KA² reaction was performed following the General Procedure A from cyclohexanone (4.0 mmol, 1.0 eq.), phenylacetylene (4.0 mmol, 1.0 eq.), Cu^I-USY (144 mg, 10 mol %) and *n*-propylamine (4.0 mmol, 1.0 eq.) in a tubular Schlenk tube (100 mL) equipped with a stirring bar. After 18 h the reaction was allowed to cool to room temperature. Next, AIBN (6.0 mmol, 1.5 eq.), K₂CO₃ (8.0 mmol, 2.0 eq.), and acetonitrile (60 mL) were added to the reaction mixture, which was placed into a pre-heated oil bath at 75 °C and stirred for 4 h under reflux. Upon completion, the cooled suspension was filtered over celite and washed with CH₂Cl₂ (3 × 25 mL). The solvent was evaporated and the crude resin was purified on column chromatography over silica to obtain compound **K.4m** as a yellow oil (682 mg, 2.56 mmol). Yield 64%.

R_f = 0.67 (SiO₂, cyclohexane/EtOAc 7:3).

ATR-FTIR (neat) ν = 3058, 2934, 2858, 2202, 1702, 1598, 1489, 1444, 1350, 1303, 1263, 1184, 1142, 1063, 913, 755, 690 cm⁻¹.

¹H NMR (500 MHz, CDCl₃) δ = 7.47 – 7.39 (m, 2H, H_{aro}), 7.38 – 7.28 (m, 3H, H_{aro}), 3.16 (t, *J* = 7.3 Hz, 2H, NCH₂), 2.16 – 2.08 (m, 2H, 2 × NC_qCH₂), 1.83 – 1.61 (m, 9H), 1.31 – 1.23 (m, 1H), 1.01 (t, *J* = 7.4 Hz, 3H, CH₃) ppm.

¹³C{¹H} NMR (126 MHz, CDCl₃) δ = 131.8 (C_{aro}H), 128.7 (C_{aro}H), 128.5 (C_{aro}H), 122.4 (C_q), 115.7 (C_q), 88.1 (C≡), 86.8 (C≡), 58.9 (NC_q), 48.6 (NCH₂), 36.7 (CH₂), 25.1 (CH₂), 23.1 (CH₂), 21.8 (CH₂), 11.4 (CH₃) ppm.

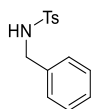
HRMS (ESI-TOF, + mode) *m/z* calcd for C₁₈H₂₂N₂Na 289.1675, found 289.1682 [M+Na]⁺.

Analytical Data of Compounds from Chapter IV

Precursors of Terminal Ynamides

Sulfonamides

N-Benzyl-4-methylbenzenesulfonamide (N.1) (CAS: 1576-37-0)^[373]



Chemical Formula: C₁₄H₁₅NO₂S
Molecular Weight: 261,34

Following the General Procedure D, the title compound was obtained as an off-white solid (2.51 g, 9.60 mmol) and used without further purification. Yield 99%.

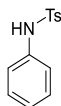
R_f = 0.13 (SiO₂, cyclohexane/EtOAc 9:1).

ATR-FTIR (neat) ν = 3267, 3033, 2914, 1597, 1495, 1453, 1421, 1321, 1287, 1160, 1093, 1082, 1058, 1028, 874, 805, 740, 682 cm⁻¹.

¹H NMR (600 MHz, CDCl₃) δ = 7.78 – 7.75 (m, 2H, H_{aro}), 7.33 – 7.24 (m, 5H, H_{aro}), 7.22 – 7.18 (m, 2H, H_{aro}), 4.62 (t, *J* = 6.1 Hz, 1H, NH), 4.13 (d, *J* = 6.1 Hz, 2H, NCH₂), 2.44 (s, 3H, CH₃) ppm.

¹³C{¹H} NMR (126 MHz, CDCl₃) δ = 143.7 (C_q), 136.9 (C_q), 136.4 (C_q), 129.9 (C_{aro}H), 128.9 (C_{aro}H), 128.1 (C_{aro}H), 128.0 (C_{aro}H), 127.3 (C_{aro}H), 47.4 (CH₂), 21.7 (CH₃) ppm.

4-Methyl-N-phenylbenzenesulfonamide (N.2) (CAS: 68-34-8)^[374]



Chemical Formula: C₁₃H₁₃NO₂S
Molecular Weight: 247,3120

Following the General Procedure D, the title compound was obtained as an off-white solid (1.21 g, 4.90 mmol) and used without further purification. Yield 98%.

R_f = 0.50 (SiO₂, cyclohexane/EtOAc 7:3).

ATR-FTIR (neat) ν = 3234, 3103, 3028, 2970, 2897, 1597, 1481, 1414, 1335, 1153, 1090, 908, 817, 753, 693 cm⁻¹.

¹H NMR (300 MHz, CDCl₃) δ = 7.67 – 7.61 (m, 2H, H_{aro}), 7.27 – 7.19 (m, 4H, H_{aro}), 7.15 – 7.08 (m, 1H, H_{aro}), 7.07 – 7.03 (m, 2H, H_{aro}), 6.42 (bs, 1H, NH), 2.38 (s, 3H, CH₃) ppm.

¹³C{¹H} NMR (126 MHz, CDCl₃) δ = 144.0 (C_q), 136.5 (C_q), 136.2 (C_q), 129.8 (C_{aro}H), 129.5 (C_{aro}H), 127.4 (C_{aro}H), 125.6 (C_{aro}H), 121.9 (C_{aro}H), 21.7 (CH₃) ppm.

N-Allyl-4-methylbenzenesulfonamide (N.3) (CAS: 50487-71-3)^[375]



Chemical Formula: C₁₀H₁₃NO₂S
Molecular Weight: 211,2790

Following the General Procedure D, the title compound was obtained as a colourless solid (2.07 g, 9.80 mmol). Yield 98%.

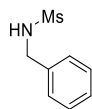
R_f = 0.43 (SiO₂, cyclohexane/EtOAc 7:3).

ATR-FTIR (neat) ν = 3245, 2927, 2853, 2105, 1747, 1648, 1595, 1493, 1422, 1373, 1318, 1157, 1092, 1062, 935, 810, 664 cm⁻¹.

¹H NMR (300 MHz, CDCl₃) δ = 7.78 – 7.73 (m, 2H, H_{aro}), 7.35 – 7.29 (m, 2H, H_{aro}), 5.73 (ddt, *J* = 17.1, 10.2, 5.8 Hz, 1H, CH=CH₂), 5.17 (dq, *J* = 17.1, 1.5 Hz, 1H, CH=CH₂), 5.10 (dq, *J* = 10.2, 1.3 Hz, 1H, CH=CH₂), 4.39 (t, *J* = 5.9 Hz, 1H, NH), 3.59 (tt, *J* = 6.0, 1.5 Hz, 2H, NCH₂), 2.43 (s, 3H, CH₃) ppm.

¹³C{¹H} NMR (126 MHz, CDCl₃) δ = 143.7 (C_q), 137.1 (C_q), 133.1 (CH), 129.9 (CH), 127.3 (CH), 117.9 (=CH₂), 45.9 (NCH₂), 21.7 (CH₃) ppm.

N-Benzylmethanesulfonamide (N.4) (CAS: 3989-45-5)^[376]



Chemical Formula: C₈H₁₁NO₂S
Molecular Weight: 185,2410

Following the General Procedure D, the title compound was obtained as a colourless solid (3.31 g, 11.32 mmol) and used without further purification. Yield 99%.

R_f = 0.21 (SiO₂, cyclohexane/EtOAc 7:3).

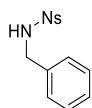
ATR-FTIR (neat) ν = 3224, 3062, 3034, 2016, 2934, 2864, 1605, 1493, 1455, 1293, 1160, 1081, 973, 874, 736 cm⁻¹.

¹H NMR (300 MHz, CDCl₃) δ = 7.42 – 7.28 (m, 5H, H_{aro}), 4.57 (bs, 1H, NH), 4.33 (d, *J* = 6.1 Hz, 2H, CH₂), 2.88 (s, 3H, CH₃) ppm.

¹³C{¹H} NMR (126 MHz, CDCl₃) δ = 136.7 (C_q-Ph), 129.1 (C_{aro}H), 128.3 (C_{aro}H), 128.0 (C_{aro}H), 47.4 (NCH₂), 41.3 (CH₃) ppm.

MS (ESI-TOF, + mode) *m/z* (rel intensity) 208.04 (100) [M+Na]⁺.

N-Benzyl-4-nitrobenzenesulfonamide (N.5) (CAS: 52374-25-1)^[376]



Chemical Formula: C₁₃H₁₂N₂O₄S
Molecular Weight: 292,3090

Following the General Procedure D, the title compound was obtained as a yellow solid (5.44 g, 18.61 mmol) and used without further purification. Yield 98%.

R_f = 0.28 (SiO₂, cyclohexane/EtOAc 8:2).

ATR-FTIR (neat) ν = 3286, 3098, 3067, 2955, 2866, 2165, 1606, 1521, 1347, 1154, 1056, 856, 735 cm⁻¹.

¹H NMR (500 MHz, CDCl₃) δ = 8.40 – 8.25 (m, 2H, H_{aro}-Ns), 8.06 – 7.89 (m, 2H, H_{aro}-Ns), 7.30 – 7.25 (m, 3H, H_{aro}), 7.20 – 7.15 (m, 2H, H_{aro}), 4.89 (t, *J* = 6.0 Hz, 1H, NH), 4.24 (d, *J* = 6.1 Hz, 2H, CH₂) ppm.

¹³C{¹H} NMR (126 MHz, CDCl₃) δ = 150.1 (C_q), 146.1 (C_q), 135.5 (C_q), 129.0 (C_{aro}H), 128.4(5) (C_{aro}H), 128.4(4) (C_{aro}H), 128.0 (C_{aro}H), 124.5 (C_{aro}H), 53.6 (CH₂) ppm.

MS (ESI-TOF, + mode) *m/z* (rel intensity) 315.04 (100) [M+Na]⁺.

4-Methyl-N-(prop-2-yn-1-yl)benzenesulfonamide (N.9) (CAS: 55022-46-3)^[377]



Chemical Formula: C₁₀H₁₁NO₂S
Molecular Weight: 209,2630

Following the General Procedure D, the title compound was isolated as a beige solid (2.69 g, 12.85 mmol) after recrystallisation in hot petrol ether and CH₂Cl₂, followed by filtration of the residue over a silica plug washing with EtOAc. Yield 67%.

R_f = 0.37 (SiO₂, cyclohexane/EtOAc 7:3).

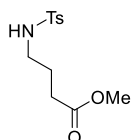
ATR-FTIR (neat) ν = 3265, 3023, 2935, 2860, 1596, 1493, 1436, 1291, 1157, 1062, 870, 696 cm⁻¹.

¹H NMR (300 MHz, CDCl₃) δ = 7.97 – 7.59 (m, 2H, H_{aro}), 7.44 – 7.16 (m, 2H, H_{aro}), 4.60 (t, *J* = 5.9 Hz, 1H, NH), 3.83 (dd, *J* = 6.1, 2.5 Hz, 2H, NCH₂), 2.43 (s, 3H, CH₃), 2.11 (t, *J* = 2.5 Hz, 1H, ≡CH) ppm.

¹³C{¹H} NMR (126 MHz, CDCl₃) δ = 144.0 (C_q), 136.6 (C_q), 129.9 (C_{aro}H), 127.5 (C_{aro}H), 78.0 (C≡), 73.2 (C≡), 33.0 (CH₂), 21.7 (CH₃) ppm. N.B.: C≡C could not be assigned as both signals appeared in DEPT135 experiment.

MS (ESI-TOF, + mode) *m/z* (rel intensity) 232.04 (100) [M+Na]⁺.

Methyl 4-((4-methylphenyl)sulfonamido)butanoate (N.10) (CAS: 118429-43-9)^[378]



Chemical Formula: C₁₂H₁₇NO₄S
Molecular Weight: 271.3310

N-Tosylpyrrolidin-2-one (19.8 g, 82.75 mmol, 1.0 eq.) was added portionwise to a stirred solution of NaOMe (5.37 g, 99.30 mmol, 1.2 eq.) in MeOH (160 mL) at room temperature. Next, the mixture was heated at reflux for 30 min. The solvent was removed under reduced pressure and the residue was dissolved in EtOAc (250 mL). This org. phase was washed with H₂O (3 × 100 mL). The combined aq. phases were back-extracted with EtOAc (100 mL) and the combined org. phases were washed with brine (150 mL), dried over MgSO₄ and the solvent was removed under reduced pressure to yield a colourless solid (19.45 g, 71.68 mmol). Yield 87%.

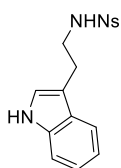
R_f = 0.30 (SiO₂, cyclohexane/EtOAc 6:4).

ATR-FTIR (neat) ν = 3270, 2959, 2892, 2848, 1720, 1595, 1429, 1330, 1268, 1202, 1158, 1080, 1050, 977, 869, 819, 673 cm⁻¹.

¹H NMR (500 MHz, CDCl₃) δ = 7.77 – 7.70 (m, 2H, H_{aro}), 7.30 (d, *J* = 8.0 Hz, 2H, H_{aro}), 4.68 (t, *J* = 6.3 Hz, 1H, NH), 3.65 (s, 3H, OCH₃), 2.99 (q, *J* = 6.6 Hz, 2H, NCH₂), 2.42 (s, 3H, CH₃ tosyl), 2.35 (t, *J* = 7.1 Hz, 2H, CH₂C=O), 1.79 (quint, *J* = 6.9 Hz, 2H, NCH₂CH₂) ppm.

¹³C{¹H} NMR (126 MHz, CDCl₃) δ = 173.7 (C=O), 143.6 (C_q), 136.9 (C_q), 129.9 (C_{aro}H), 127.2 (C_{aro}H), 51.9 (OCH₃), 42.7 (NCH₂), 31.1 (CH₂), 24.8 (CH₂), 21.7 (CCH₃) ppm.

***N*-(2-(1*H*-Indol-3-yl)ethyl)-4-nitrobenzenesulfonamide (CAS: 33284-09-2)^[379]**



Chemical Formula: C₁₆H₁₅N₃O₄S
Molecular Weight: 345.3730

Following the General Procedure D, the title compound was obtained as a yellow solid (4.30 g, 12.45 mmol) and used without further purification.

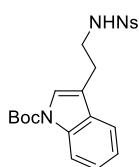
R_f = 0.75 (SiO₂, CH₂Cl₂/MeOH 9:1).

ATR-FTIR (neat) ν = 3410, 3242, 3109, 3086, 3071, 3049, 3039, 2986, 2958, 2909, 2895, 2856, 1610, 1529, 1436, 1346, 1305, 1149, 1069, 912, 854, 739 cm⁻¹.

¹H NMR (500 MHz, CDCl₃) δ = 8.14 – 8.07 (m, 2H), 8.01 (bs, 1H), 7.80 – 7.73 (m, 2H), 7.35 – 7.29 (m, 2H), 7.21 – 7.13 (m, 1H), 7.06 – 6.96 (m, 2H), 4.45 (t, *J* = 5.8 Hz, 1H, N_sNH), 3.36 (q, *J* = 6.2 Hz, 2H, NCH₂), 2.97 (t, *J* = 6.3 Hz, 2H, C_qCH₂) ppm.

¹³C{¹H} NMR (126 MHz, CDCl₃) δ = 149.8 (C_q), 145.4 (C_q), 136.5 (C_q), 128.0 (C_{aro}H), 126.6 (C_q), 124.1 (C_{aro}H), 122.7(8) (C_{aro}H), 122.7(6) (C_{aro}H), 119.9 (C_{aro}H), 118.4 (C_{aro}H), 111.5 (C_{aro}H), 111.3 (C_q), 43.1 (CH₂), 25.6 (CH₂) ppm.

***tert*-Butyl 3-(2-((4-nitrophenyl)sulfonamido)ethyl)-1*H*-indole-1-carboxylate (N.11) (CAS: 1627199-33-0)^[380]**



Chemical Formula: C₂₁H₂₃N₃O₆S
Molecular Weight: 445.4900

The title compound was prepared as described in the literature^[380] and was isolated as a yellow foam (1.28 g, 2.87 mmol) after column chromatography (EtOAc/CH₂Cl₂/cyclohexane 1:1:8) on only a fraction of the crude mixture.

R_f = 0.48 (SiO₂, cyclohexane/EtOAc 7:3).

ATR-FTIR (neat) ν = 3396, 3103, 3068, 3039, 2977, 2934, 2909, 2852, 1711, 1607, 1531, 1457, 1343, 1293, 1140, 1082, 1010, 912, 842, 736, 642 cm⁻¹.

¹H NMR (500 MHz, CDCl₃) δ = 8.28 – 8.22 (m, 2H), 8.02 (bs, 1H), 7.99 – 7.94 (m, 2H), 7.69 (d, *J* = 7.9 Hz, 1H), 7.38 (d, *J* = 8.1 Hz, 1H), 7.22 (t, *J* = 7.5 Hz, 1H), 7.13 (t, *J* = 7.4 Hz, 1H), 7.06 (d, *J* = 2.4 Hz, 1H), 4.17 – 4.09 (m, 2H, NCH₂), 3.27 – 3.19 (m, 2H, C_qCH₂), 1.32 (s, 9H, C(CH₃)₃) ppm.

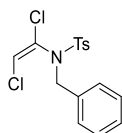
$^{13}\text{C}\{^1\text{H}\}$ NMR (126 MHz, CDCl_3) δ = 150.7 (C_q), 150.2 (C_q), 145.7 (C_q), 136.3 (C_q), 129.4 (C_{aroH}), 127.5 (C_q), 123.9 (C_{aroH}), 122.7 (C_{aroH}), 122.5 (C_{aroH}), 119.8 (C_{aroH}), 118.9 (C_{aroH}), 112.2 (C_q), 111.3 (C_{aroH}), 85.2 ($\text{C}(\text{CH}_3)_3$), 48.2 (NCH_2), 27.9 ($\text{C}(\text{CH}_3)_3$), 26.2 (CH_2) ppm.

MS (ESI-TOF, + mode) m/z (rel intensity) 484.09 (50) $[\text{M}+\text{K}]^+$.

1,2-Dichloroenamides

1,2-Dichloroenamides were prepared following a reported procedure.^[261]

(E)-N-Benzyl-N-(1,2-dichlorovinyl)-4-methylbenzenesulfonamide (C.1) (CAS: 1637778-11-0)



Chemical Formula: $\text{C}_{16}\text{H}_{15}\text{Cl}_2\text{NO}_2\text{S}$
Molecular Weight: 356,2610

Following the General Procedure E, the title compound was obtained as a colourless solid (6.52 g, 18.31 mmol) and used without further purification. Yield 94%.

R_f = 0.73 (SiO_2 , cyclohexane/EtOAc 7:3).

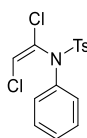
ATR-FTIR (neat) ν = 3079, 3035, 2973, 2922, 2876, 1595, 1496, 1457, 1356, 1168, 1085, 1029, 952, 814, 693 cm^{-1} .

^1H NMR (300 MHz, CDCl_3) δ = 7.91 – 7.81 (m, 2H, H_{aro}), 7.41 – 7.27 (m, 7H, H_{aro}), 6.27 (s, 1H, CHCl), 4.40 (bs, 2H, CH_2), 2.47 (s, 3H, CH_3) ppm.

$^{13}\text{C}\{^1\text{H}\}$ NMR (126 MHz, CDCl_3) δ = 144.9 (NCCl), 135.2 (C_q), 133.5 (C_q), 129.9 (CH), 129.5(2) (CH), 129.5(0) (C_q), 128.6(1) (CH), 128.6(0) (CH), 128.5 (CH), 121.9 (CH), 51.9 (NCH_2), 21.9 (CH_3) ppm.

MS (ESI-TOF, + mode) m/z (rel intensity) 393.98 (100) $[\text{M}+\text{K}]^+$.

(E)-N-(1,2-dichlorovinyl)-4-methyl-N-phenylbenzenesulfonamide (C.2) (CAS: 1198340-49-6)



Chemical Formula: $\text{C}_{15}\text{H}_{13}\text{Cl}_2\text{NO}_2\text{S}$
Molecular Weight: 342,2340

Following the General Procedure E, the title compound was isolated as a colourless solid (1.16 g, 3.38 mmol) after column chromatography over silica gel (SiO_2 , cyclohexane/EtOAc). Yield 83%. –

R_f = 0.42 (SiO_2 , cyclohexane/EtOAc 9:1).

ATR-FTIR (neat) ν = 3076, 3034, 2954, 2920, 2853, 1592, 1487, 1360, 1288, 1163, 1087, 944, 801, 698 cm^{-1} .

^1H NMR (300 MHz, CDCl_3) δ = 7.68 – 7.61 (m, 2H, H_{aro}), 7.40 – 7.29 (m, 5H, H_{aro}), 7.27 – 7.21 (m, 2H, H_{aro}), 6.46 (s, 1H, CHCl), 2.43 (s, 3H, CH_3) ppm.

$^{13}\text{C}\{^1\text{H}\}$ NMR (126 MHz, CDCl_3) δ = 144.7 (NCCl), 137.8 (C_q), 135.6 (C_q), 130.7 (C_q), 129.5(4) (CH), 129.5(0) (CH), 129.2 (CH), 128.9 (CH), 128.7 (CH), 120.7 (CH), 21.8 (CH_3) ppm.

MS (ESI-TOF, + mode) m/z (rel intensity) 379.96 (100) $[\text{M}+\text{K}]^+$.

(E)-N-Allyl-N-(1,2-dichlorovinyl)-4-methylbenzenesulfonamide (C.3) (CAS: 2820061-24-1)



Chemical Formula: $\text{C}_{12}\text{H}_{13}\text{Cl}_2\text{NO}_2\text{S}$
Molecular Weight: 306,2010

Following the General Procedure E, the title compound was obtained as a light brown waxy solid (2.76 g, 9.01 mmol) and used without further purification. Yield 95%.

R_f = 0.65 (SiO_2 , cyclohexane/EtOAc 7:3).

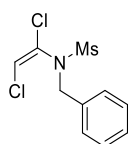
ATR-FTIR (neat) ν = 3088, 2983, 2923, 2870, 1597, 1495, 1446, 1358, 1291, 1163, 1088, 1041, 936, 804, 661 cm^{-1} .

¹H NMR (500 MHz, CDCl₃) δ = 7.80 (m, 2H, H_{aro}), 7.33 (m, 2H, H_{aro}), 6.46 (s, 1H, CHCl), 5.76 (ddt, *J* = 16.9, 10.1, 6.8 Hz, 1H, CH=CH₂), 5.31 – 5.15 (m, 2H, CH=CH₂), 3.87 (bs, 2H, CH₂), 2.44 (s, 3H, CH₃) ppm.

¹³C{¹H} NMR (126 MHz, CDCl₃) δ = 144.8 (NCCl), 135.2 (C_q), 130.8 (CH), 129.8 (CH), 129.6 (C_q), 128.5 (CH), 121.7 (CH), 120.8 (C=CH₂), 51.1 (NCH₂), 21.8 (CH₃) ppm.

HRMS (ESI-TOF, + mode) *m/z* calcd for C₁₂H₁₃Cl₂NNaO₂S 327.9936, found 327.9925 [M+Na]⁺.

(E)-N-Benzyl-N-(1,2-dichlorovinyl)methanesulfonamide (C.4) (CAS: 2794256-80-5)



Chemical Formula: C₁₀H₁₁Cl₂NO₂S
Molecular Weight: 280,1630

Following the General Procedure E, the title compound was obtained as pale brown solid (1.91 g, 6.82 mmol) and used without further purification. Yield 70%.

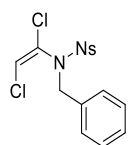
R_f = 0.50 (SiO₂, cyclohexane/EtOAc 7:3).

ATR-FTIR (neat) ν = 3087, 3065, 3032, 2931, 1671, 1344, 1152, 1027, 961, 799, 699 cm⁻¹.

¹H NMR (500 MHz, CDCl₃) δ = 7.39 – 7.27 (m, 5H, H_{aro}), 6.31 (s, 1H, CHCl), 4.59 (bs, 2H, CH₂), 3.05 (s, 3H, CH₃) ppm.

¹³C{¹H} NMR (126 MHz, CDCl₃) δ = 151.9 (C_q), 133.6 (C_q), 129.7 (CH), 128.7 (CH), 121.5 (CH), 102.3 (CH), 52.6 (CH₂), 44.2 (CH₃) ppm.

(E)-N-Benzyl-N-(1,2-dichlorovinyl)-4-nitrobenzenesulfonamide (C.5) (CAS: 1637778-31-4)



Chemical Formula: C₁₅H₁₂Cl₂N₂O₄S
Molecular Weight: 387,2310

Following the General Procedure E, the title compound was obtained as yellow solid (1.46 g, 3.77 mmol) and used without further purification. Yield 39%.

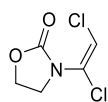
R_f = 0.71 (SiO₂, CH₂Cl₂/MeOH 9:1).

ATR-FTIR (neat) ν = 3095, 3076, 3033, 2986, 2919, 2873, 1603, 1528, 1495, 1455, 1369, 1346, 1307, 1176, 1132, 1084, 1044, 954, 862, 799, 734, 707 cm⁻¹.

¹H NMR (300 MHz, CDCl₃) δ = 8.45 – 8.34 (m, 2H, H_{aro-Ns}), 8.18 – 8.07 (m, 2H, H_{aro-Ns}), 7.35 – 7.30 (m, 5H, H_{aro}), 6.35 (s, 1H, CHCl), 4.46 (bs, 2H, CH₂) ppm.

¹³C{¹H} NMR (126 MHz, CDCl₃) δ = 150.7 (C_q), 144.1 (C_q), 132.6 (C_q), 129.8 (CH), 129.7 (CH), 129.0 (CH), 128.7 (CH), 128.6 (C_q), 124.5 (CH), 122.8 (CH), 52.6 (NCH₂) ppm.

(E)-3-(1,2-dichlorovinyl)oxazolidin-2-one (C.6) (CAS: 1637778-29-0)



Chemical Formula: C₅H₅Cl₂NO₂
Molecular Weight: 182,0000

Following the General Procedure E, the title compound was obtained as a pale brown solid (1.50 g, 8.24 mmol) and used without further purification. Yield 72%.

R_f = 0.58 (SiO₂, CH₂Cl₂/MeOH 9:1).

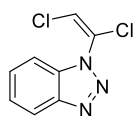
ATR-FTIR (neat) ν = 3092, 2986, 2913, 1758, 1621, 1480, 1394, 1193, 1031, 891, 822, 746 cm⁻¹.

¹H NMR (300 MHz, CDCl₃) δ = 6.36 (s, 1H, CHCl), 4.56 – 4.45 (m, 2H, OCH₂), 3.91 – 3.79 (m, 2H, NCH₂) ppm.

¹³C{¹H} NMR (126 MHz, CDCl₃) δ = 153.9 (C=O), 127.3 (NCCl), 117.1 (CHCl), 62.9 (OCH₂), 44.2 (NCH₂) ppm.

MS (ESI-TOF, + mode) *m/z* (rel intensity) 203.96 (100) [M+Na]⁺.

(E)-1-(1,2-Dichlorovinyl)-1H-benzo[d][1,2,3]triazole (C.7) (CAS: 1637778-28-9)



Chemical Formula: C₈H₅Cl₂N₃
Molecular Weight: 214,0490

Following the General Procedure E, the title compound was obtained as an orange oil (2.09 g) and purified over silica gel (petroleum ether₅₀₋₆₀/Et₂O 9:1) to give a colourless oil (1.20 g, 5.61 mmol). Yield 56%.

R_f = 0.25 (petroleum ether₅₀₋₆₀/Et₂O 9:1).

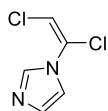
ATR-FTIR (neat) ν = 3085, 3065, 1622, 1487, 1450, 1382, 1287, 1154, 1033, 934, 836, 744 cm⁻¹.

¹H NMR (300 MHz, CDCl₃) δ = 8.15 (dt, *J* = 8.3, 1.0 Hz, 1H, H_{aro}), 7.63 (ddd, *J* = 8.3, 6.7, 1.0 Hz, 1H, H_{aro}), 7.56 (ddd, *J* = 8.3, 1.3, 0.9 Hz, 1H, H_{aro}), 7.48 (ddd, *J* = 8.1, 6.7, 1.3 Hz, 1H, H_{aro}), 6.83 (s, 1H, CHCl) ppm.

¹³C{¹H} NMR (126 MHz, CDCl₃) δ = 145.4 (C_q), 132.1 (C_q), 129.3 (CH), 125.1 (CH), 124.7 (C_q), 120.8 (CH), 118.2 (CH), 110.4 (CH) ppm.

MS (ESI-TOF, + mode) *m/z* (rel intensity) 215.99 (80) [M+H]⁺.

(E)-1-(1,2-Dichlorovinyl)-1H-imidazole (C.8) (CAS: 82754-86-7)



Chemical Formula: C₅H₄Cl₂N₂
Molecular Weight: 163,0010

Following the General Procedure E, the title compound was obtained as a yellow oil (1.08 g, 6.63 mmol) and used without further purification. Yield 66%.

R_f = 0.25 (SiO₂, cyclohexane/EtOAc 7:3).

ATR-FTIR (neat) ν = 3410, 3091, 1625, 1476, 1370, 1304, 1204, 1072, 898, 829, 729, 651 cm⁻¹.

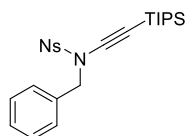
¹H NMR (500 MHz, CDCl₃) δ = 7.83 (s, 1H, N=CHN), 7.20 (s, 1H, H_{aro}), 7.14 (s, 1H, H_{aro}), 6.38 (s, 1H, CHCl) ppm.

¹³C{¹H} NMR (126 MHz, CDCl₃) δ = 137.4 (N=CHN), 130.0 (CH), 125.3 (C_qCl), 119.0 (CH), 111.5 (CH) ppm.

TIPS-Protected Ynamides

N-Benzyl-4-nitro-N-((triisopropylsilyl)ethynyl)benzenesulfonamide (H.1) (CAS: 945536-25-4)^[381]

Following the General Procedure F using K₂CO₃ and Cu^I-USY at 90 °C for two days, the title compound was isolated as a colourless solid (1.16 g, 2.45 mmol). Yield 80%.



Chemical Formula: C₂₄H₃₂N₂O₄SSi
Molecular Weight: 472,6750

R_f = 0.73 (SiO₂, cyclohexane/EtOAc 7:3).

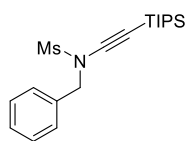
ATR-FTIR (neat) ν = 3107, 2954, 2939, 2890, 2863, 2165, 1608, 1530, 1462, 1378, 1348, 1311, 1173, 1087, 1011, 941, 857, 781, 673 cm⁻¹.

¹H NMR (500 MHz, CDCl₃) δ = 8.28 – 8.22 (m, 2H, H_{aro-Ns}), 7.96 – 7.89 (m, 2H, H_{aro-Ns}), 7.31 – 7.21 (m, 5H, H_{aro}), 4.58 (bs, 2H, CH₂), 0.96 (bs, 21H, Si(CH(CH₃)₂)₃) ppm.

¹³C{¹H} NMR (126 MHz, CDCl₃) δ = 150.5 (C_q), 143.1 (C_q), 133.8 (C_q), 129.1 (C_{aro}H), 129.0 (C_{aro}H), 128.8 (C_{aro}H), 128.7 (C_{aro}H), 124.1 (C_{aro}H), 95.5 (C≡), 71.4 (C≡), 56.3 (NCH₂), 18.6 (CH), 11.3 (CH₃) ppm.

HRMS (ESI-TOF, + mode) *m/z* calcd for C₂₄H₃₂N₂NaO₄SSi 495.1744, found 495.1773 [M+Na]⁺.

N-Benzyl-N-((triisopropylsilyl)ethynyl)methanesulfonamide (H.2) (CAS: 1160723-59-0)^[382]



Chemical Formula: C₁₉H₃₁NO₂SSi
Molecular Weight: 365,6070

Following the General Procedure F using K₂CO₃ and Cu^I-USY at 60 °C for 18 h, the title compound was isolated as a yellow oil (1.72 g, 4.70 mmol). Yield 95%.

R_f = 0.80 (SiO₂, cyclohexane/EtOAc 7:3).

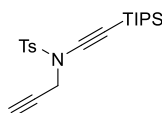
ATR-FTIR (neat) ν = 3091, 3066, 3034, 2942, 2891, 2864, 2726, 2162, 1459, 1360, 1162, 1016, 961, 882, 781, 675 cm⁻¹.

¹H NMR (500 MHz, CDCl₃) δ = 7.47 – 7.42 (m, 2H, H_{aro}), 7.39 – 7.34 (m, 3H, H_{aro}), 4.61 (s, 2H, CH₂), 2.87 (s, 3H, CH₃), 1.02 (s, 21H, Si(CH(CH₃)₂)₃) ppm.

¹³C{¹H} NMR (126 MHz, CDCl₃) δ = 134.5 (C_q-Ph), 129.2 (C_{aro}H), 128.9 (C_{aro}H), 128.8(6) (C_{aro}H), 96.2 (C \equiv), 71.0 (C \equiv), 55.8 (NCH₂), 38.6 (SCH₃), 18.7 (CH), 11.4 (CHCH₃) ppm.

MS (ESI-TOF, + mode) m/z (rel intensity) 405.15 (80) [M+K]⁺.

4-Methyl-N-(prop-2-yn-1-yl)-N-((triisopropylsilyl)ethynyl)benzenesulfonamide (H.3) (CAS: 898827-45-7)^[255]



Chemical Formula: C₂₁H₃₁NO₂SSi
Molecular Weight: 389,6290

Following the General Procedure F using K₂CO₃ and Cu^I-USY at 65 °C for 21 h, the title compound was isolated as an orange oil (636 mg, 1.63 mmol). Yield 80%.

R_f = 0.70 (SiO₂, cyclohexane/EtOAc 7:3).

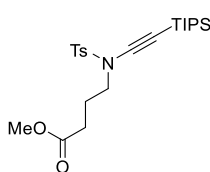
ATR-FTIR (neat) ν = 3277, 2943, 2865, 2168, 1598, 1463, 1537, 1259, 1163, 1088, 1031, 881, 729, 663 cm⁻¹.

¹H NMR (500 MHz, CDCl₃) δ = 7.83 (m, 2H, H_{aro}), 7.31 (m, 2H, H_{aro}), 4.26 (d, J = 2.6 Hz, 2H, CH₂), 2.45 (s, 3H, CH₃), 2.16 (t, J = 2.5 Hz, 1H, \equiv CH), 1.03 (s, 21H, Si(CH(CH₃)₂)₃) ppm.

¹³C{¹H} NMR (126 MHz, CDCl₃) δ = 145.0 (C_q), 134.1 (C_q), 129.6 (C_{aro}H), 128.4 (C_{aro}H), 95.4 (C \equiv), 75.9 (C \equiv), 74.7 (C \equiv), 70.5 (C \equiv), 41.8 (CH₂), 21.8 (CH₃ tosyl), 18.7 (CH), 11.4 (CHCH₃) ppm.

MS (ESI-TOF, + mode) m/z (rel intensity) 412.17 (100) [M+Na]⁺.

Methyl 4-((4-methyl-N-((triisopropylsilyl)ethynyl)phenyl)sulfonamido)butanoate (H.4) (CAS: 2820061-25-2)



Chemical Formula: C₂₃H₃₇NO₄SSi
Molecular Weight: 451,6970

Following the General Procedure F using K₂CO₃ and CuSO₄•5H₂O at 65 °C for 18 h, the title compound was isolated as a pale yellow viscous oil (201 mg, 445 μ mol). Yield 89%.

R_f = 0.44 (SiO₂, cyclohexane/EtOAc 8:2).

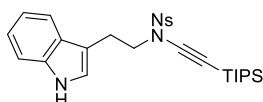
ATR-FTIR (neat) ν = 2942, 2892, 2863, 2158, 1743, 1596, 1435, 1365, 1167, 1089, 1002, 945, 881, 816, 658 cm⁻¹.

¹H NMR (500 MHz, CDCl₃) δ = 7.82 – 7.76 (m, 2H, H_{aro}), 7.32 (m, 2H, H_{aro}), 3.67 (s, 3H, OCH₃), 3.38 (t, J = 6.6 Hz, 2H, NCH₂), 2.44 (s, 3H, CH₃ tosyl), 2.41 (t, J = 7.3 Hz, 2H, CH₂C=O), 1.98 (quint, J = 7.0 Hz, 2H, NCH₂CH₂), 1.04 (s, 21H, Si(CH(CH₃)₂)₃) ppm.

¹³C{¹H} NMR (126 MHz, CDCl₃) δ = 173.2 (C=O), 144.8 (C_q), 134.5 (C_q), 129.8 (C_{aro}), 127.8 (C_{aro}), 96.0 (NC \equiv C), 69.8 (NC \equiv C), 51.8 (OCH₃), 50.6 (TsNCH₂), 30.5 (CH₂CO₂Me), 23.1 (TsCH₂CH₂), 21.8 (CH₃ tosyl), 18.7 (CH), 11.5 (CHCH₃) ppm.

HRMS (ESI-TOF, + mode) m/z calcd for C₂₃H₃₇NNaO₄SSi 474.2105, found 474.2112 [M+Na]⁺.

N-(2-(1H-Indol-3-yl)ethyl)-4-nitro-N-((triisopropylsilyl)ethynyl)benzenesulfonamide (H.5) (CAS: 2820061-26-3)



Chemical Formula: C₂₇H₃₅N₃O₄SSi
Molecular Weight: 525,7390

Following the General Procedure F using K₂CO₃ and CuSO₄•5H₂O at 85 – 95 °C for 13 days, the title compound was isolated as a brown resin (118 mg, 225 μmol) from *tert*-butyl 3-(2-((4-nitrophenyl)sulfonamido)ethyl)-1H-indole-1-carboxylate. * Yield 45%.

R_f = 0.61 (SiO₂, cyclohexane/EtOAc 7:3).

ATR-FTIR (neat) ν = 3291, 3104, 2941, 2890, 2863, 2169, 1650, 1529, 1458, 1159, 919, 792, 735 cm⁻¹.

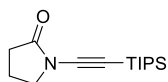
¹H NMR (500 MHz, CDCl₃) δ = 8.14 – 8.09 (m, 2H, H_{aro-Ns}), 7.82 – 7.77 (m, 2H, H_{aro-Ns}), 7.42 (d, *J* = 8.1 Hz, 1H, H_{aro}), 7.34 – 7.27 (m, 2H, H_{aro}), 7.15 – 7.10 (m, 1H, H_{aro}), 7.00 (s, 1H, NC_{sp2}H), 4.67 (s, 1H, NH), 3.37 (q, *J* = 5.6 Hz, 2H, NCH₂), 2.91 (t, *J* = 6.4 Hz, 2H, C_qCH₂), 1.21 – 1.15 (m, 21H, Si(CH(CH₃)₂)₃) ppm.

¹³C{¹H} NMR (126 MHz, CDCl₃) δ = 149.8 (C_q), 145.4 (C_q), 138.7 (C_q), 128.0 (C_{aro}H), 127.0 (C_{aro}H), 126.6 (C_q), 124.3 (C_{aro}H), 124.1 (C_{aro}H), 122.1 (C_{aro}H), 118.8 (C_{aro}H), 114.0 (C_q), 111.8 (C_{aro}H), 93.9 (NC≡C), 69.5 (NC≡C), 42.8 (NCH₂), 25.6 (CH₃ tosyl), 18.9 (CH), 11.5 (CHCH₃) ppm.

HRMS (ESI-TOF, + mode) *m/z* calcd for C₂₇H₃₅KN₃O₄SSi 564.1749, found 564.1733 [M+K]⁺.

*N.B.: Boc-deprotection occurred under the above stated reaction conditions and was not performed as an additional step.

1-((Triisopropylsilyl)ethynyl)pyrrolidin-2-one (H.6) (CAS: 1007597-70-7)^[383]



Chemical Formula: C₁₅H₂₇NOSi
Molecular Weight: 265,4720

Following the General Procedure F using K₂CO₃ and Cu^I-USY at 105 °C, the title compound was isolated as a colourless solid (138 mg, 520 μmol). Yield 43%.

R_f = 0.43 (SiO₂, cyclohexane/EtOAc 7:3).

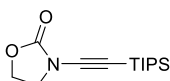
ATR-FTIR (neat) ν = 2940, 2892, 2863, 2725, 2168, 1719, 1460, 1381, 1460, 1381, 1191, 882, 672, 501 cm⁻¹.

¹H NMR (300 MHz, CDCl₃) δ = 3.75 – 3.66 (m, 2H, NCH₂), 2.46 – 2.38 (m, 2H, CH₂C=O), 2.18 – 2.05 (m, 2H, NCH₂CH₂), 1.12 – 1.06 (m, 21H, Si(CH(CH₃)₂)₃) ppm.

¹³C{¹H} NMR (126 MHz, CDCl₃) δ = 175.8 (C=O), 94.7 (NC≡C), 70.8 (NC≡C), 50.1 (NCH₂), 29.7 (CH₂), 18.8 (CH₂), 18.6 (CH), 11.3 (CH₃) ppm.

MS (ESI-TOF, + mode) *m/z* (rel intensity) 288.18 (100) [M+Na]⁺.

3-((Triisopropylsilyl)ethynyl)oxazolidin-2-one (H.7) (CAS: 1007597-70-7)^[383]



Chemical Formula: C₁₄H₂₅NO₂Si
Molecular Weight: 267,4440

Following the General Procedure F using K₂CO₃ and Cu^I-USY at 110 °C for 21 h, the title compound was isolated as a colourless solid (110 mg, 411 μmol). Yield 82%.

R_f = 0.43 (SiO₂, cyclohexane/EtOAc 7:3).

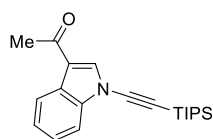
ATR-FTIR (neat) ν = 2960, 2942, 2889, 2864, 2177, 1758, 1478, 1463, 1397, 1296, 1197, 1104, 1034, 992, 881, 809, 751, 707 cm⁻¹.

¹H NMR (500 MHz, CDCl₃) δ = 4.47 – 4.39 (m, 2H, OCH₂), 3.98 – 3.90 (m, 2H, NCH₂), 1.08 (s, 21H, Si(CH(CH₃)₂)₃) ppm.

¹³C{¹H} NMR (126 MHz, CDCl₃) δ = 155.9 (C=O), 93.1 (NC≡C), 70.2 (NC≡C), 62.9 (OCH₂), 47.1 (NCH₂), 18.7 (CH), 11.3 (CH₃) ppm.

MS (ESI-TOF, + mode) m/z (rel intensity) 290.15 (60) $[M+Na]^+$.

1-(1-((Triisopropylsilyl)ethynyl)-1H-indol-3-yl)ethan-1-one (H.8) (CAS: 1007597-74-1)^[383]



Chemical Formula: $C_{21}H_{29}NO_2Si$
Molecular Weight: 339,5540

Following the General Procedure F using K_2CO_3 and Cu^I -USY at $90\text{ }^\circ\text{C}$ for two days, the title compound was isolated as an orange solid (932 mg, 2.75 mmol). Yield 87%

$R_f = 0.53$ (SiO_2 , cyclohexane/EtOAc 7:3).

ATR-FTIR (neat) $\nu = 3116, 3055, 2942, 2891, 2864, 2379, 2177, 1738, 1633, 1613, 1533, 1456, 1205, 882, 670\text{ cm}^{-1}$.

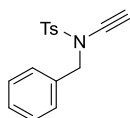
1H NMR (500 MHz, $CDCl_3$) $\delta = 8.36$ (d, $J = 7.7$ Hz, 1H, H_{aro}), 7.87 (s, 1H, $NC_{sp^2}H$), 7.54 (d, $J = 8.0$ Hz, 1H, H_{aro}), $7.44 - 7.34$ (m, 2H, H_{aro}), 2.56 (s, 3H, CH_3), $1.20 - 1.14$ (m, 21H, $Si(CH_2CH_3)_3$) ppm.

$^{13}C\{^1H\}$ NMR (126 MHz, $CDCl_3$) $\delta = 193.1$ (C=O), 138.8 (C_q), 135.5 ($C_{aro}H$), 125.2 ($C_{aro}H$), 125.1 (C_q), 124.4 ($C_{aro}H$), 123.1 ($C_{aro}H$), 119.6 (C_q), 111.5 ($C_{aro}H$), 92.8 ($NC\equiv C$), 71.2 ($NC\equiv C$), 27.9 (O=CCH $_3$), 18.8 (CH), 11.4 (CHCH $_3$) ppm.

MS (ESI-TOF, + mode) m/z (rel intensity) 362.19 (100) $[M+Na]^+$.

Terminal Ynamides

N-Benzyl-N-ethynyl-4-methylbenzenesulfonamide (Y.1) (CAS: 205885-39-8)^[384]



Chemical Formula: $C_{16}H_{15}NO_2S$
Molecular Weight: 285,3610

Following the General Procedure G, the title compound **3** was isolated as a colourless solid (4.0 g, 14.02 mmol). Yield 93%.

$R_f = 0.55$ (SiO_2 , cyclohexane/EtOAc 9:1).

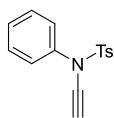
ATR-FTIR (neat) $\nu = 3275, 3062, 2963, 2929, 2132, 1596, 1495, 1431, 1356, 1164, 1087, 1026, 930, 798, 689\text{ cm}^{-1}$.

1H NMR (400 MHz, $CDCl_3$) $\delta = 7.78 - 7.74$ (m, 2H, H_{aro}), $7.34 - 7.27$ (m, 7H, H_{aro}), 4.50 (s, 2H, NCH_2), 2.67 (s, 1H, $\equiv CH$), 2.45 (s, 3H, CH_3) ppm.

$^{13}C\{^1H\}$ NMR (126 MHz, $CDCl_3$) $\delta = 144.9$ (C_q), 134.8 (C_q), 134.4 (C_q), 129.9 ($C_{aro}H$), 128.8 ($C_{aro}H$), 128.7 ($C_{aro}H$), 128.5 ($C_{aro}H$), 127.9 ($C_{aro}H$), 76.4 ($NC\equiv$), 59.8 ($\equiv CH$), 55.4 (NCH_2), 21.8 (CH_3) ppm.

MS (ESI-TOF, + mode) m/z (rel intensity) 324.05 (100) $[M+K]^+$, 155.02 (25) $[C_7H_7O_2S]^+$.

N-Ethynyl-4-methyl-N-phenylbenzenesulfonamide (Y.2) (CAS: 312329-87-6)^[261]



Chemical Formula: $C_{15}H_{13}NO_2S$
Molecular Weight: 271,3340

Following the general procedure D, the title compound was isolated as a colourless solid (554 mg, 2.04 mmol) after recrystallization in refluxed Et_2O . Yield 68%.

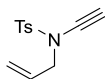
$R_f = 0.54$ (SiO_2 , cyclohexane/EtOAc 8:2)

ATR-FTIR (neat) $\nu = 3293, 3065, 3042, 2955, 2924, 2130, 1697, 1595, 1556, 1488, 1371, 1293, 1173, 1089, 925, 813, 761, 673\text{ cm}^{-1}$.

1H NMR (500 MHz, $CDCl_3$) $\delta = 7.62 - 7.57$ (m, 2H, H_{aro}), $7.37 - 7.24$ (m, 7H, H_{aro}), 2.85 (s, 1H, $\equiv CH$), 2.46 (s, 3H, CH_3) ppm.

$^{13}C\{^1H\}$ NMR (126 MHz, $CDCl_3$) $\delta = 145.2$ (C_q), 138.4 (C_q), 133.0 (C_q), 129.7 ($C_{aro}H$), 129.3 ($C_{aro}H$), 128.6 ($C_{aro}H$), 128.4 ($C_{aro}H$), 126.4 ($C_{aro}H$), 76.7 ($NC\equiv$), 59.0 ($\equiv CH$), 21.9 (CH_3) ppm.

N-Allyl-N-ethynyl-4-methylbenzenesulfonamide (Y.3) (CAS: 312329-85-4)^[381]



Chemical Formula: C₁₂H₁₃NO₂S
Molecular Weight: 235,3010

Following the General Procedure G, the title compound was isolated as pale yellow solid (167 mg, 710 μmol). Yield 71%.

R_f = 0.60 (SiO₂, cyclohexane/EtOAc 7:3).

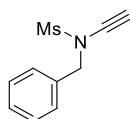
ATR-FTIR (neat) ν = 3270, 2925, 2137, 1647, 1594, 1490, 1429, 1352, 1294, 1159, 1118, 1086, 1032, 991, 921, 899, 814, 739, 709, 659 cm⁻¹.

¹H NMR (500 MHz, CDCl₃) δ = 7.84 – 7.78 (m, 2H, H_{aro}), 7.35 (m, 2H, H_{aro}), 5.72 (ddt, J = 16.6, 10.1, 6.3 Hz, 1H, CH=CH₂), 5.29 – 5.19 (m, 2H, CH=CH₂), 3.96 (dt, J = 6.4, 1.3 Hz, 2H, NCH₂), 2.73 (s, 1H, ≡CH), 2.46 (s, 3H, CH₃) ppm.

¹³C{¹H} NMR (126 MHz, CDCl₃) δ = 145.0 (C_q), 134.8 (C_q), 130.7 (CH), 129.9 (CH), 127.9 (CH), 120.3 (CH=CH₂), 76.0 (NC≡), 59.4 (≡CH), 54.1 (NCH₂), 21.8 (CH₃) ppm.

MS (ESI-TOF, + mode) m/z (rel intensity) 258.05 (20) [M+Na]⁺.

N-Benzyl-N-ethynylmethanesulfonamide (Y.4) (CAS: 737004-80-7)^[385]



Chemical Formula: C₁₀H₁₁NO₂S
Molecular Weight: 209,2630

Following the General Procedure H, the title compound was isolated as an off-white solid (85 mg, 406 μmol). Yield 81%.

R_f = 0.44 (SiO₂, cyclohexane/EtOAc 7:3).

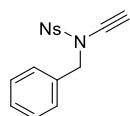
ATR-FTIR (neat) ν = 3273, 3065, 3033, 3015, 2930, 2852, 2494, 2293, 2133, 2063, 1496, 1456, 1341, 1154, 1020, 924, 784, 698 cm⁻¹.

¹H NMR (500 MHz, CDCl₃) δ = 7.47 – 7.43 (m, 2H, H_{aro}), 7.42 – 7.34 (m, 3H, H_{aro}), 4.63 (s, 2H, NCH₂), 2.89 (s, 3H, ≡CH), 2.84 (s, 1H, CH₃) ppm.

¹³C{¹H} NMR (126 MHz, CDCl₃) δ = 134.4 (C_{q-Ph}), 129.0 (C_{aroH}), 128.9(9) (C_{aroH}), 128.9(6) (C_{aroH}), 76.0 (NC≡), 60.3 (≡CH), 55.5 (CH₂), 39.0 (CH₃) ppm.

MS (ESI-TOF, + mode) m/z (rel intensity) 232.04 (100) [M+Na]⁺.

N-Benzyl-N-ethynyl-4-nitrobenzenesulfonamide (Y.5) (CAS: 329354-15-6)^[381]



Chemical Formula: C₁₅H₁₂N₂O₄S
Molecular Weight: 316,3310

Following the General Procedure H, the title compound was isolated as an off-white solid (49 mg, 155 μmol). Yield 84%.

R_f = 0.90 (SiO₂, cyclohexane/EtOAc 7:3).

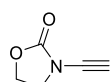
ATR-FTIR (neat) ν = 3279, 3126, 3106, 3068, 3031, 2998, 2956, 2923, 2854, 2133, 1524, 1344, 1303, 1175, 1087, 1024, 852, 686 cm⁻¹.

¹H NMR (500 MHz, CDCl₃) δ = 8.32 – 8.26 (m, 2H, H_{aro-Ns}), 7.98 – 7.91 (m, 2H, H_{aro-Ns}), 7.34 – 7.27 (m, 5H, H_{aro}), 4.60 (s, 2H, NCH₂), 2.78 (s, 1H, ≡CH) ppm.

¹³C{¹H} NMR (126 MHz, CDCl₃) δ = 150.6 (C_q), 143.1 (C_q), 133.7 (C_q), 129.0 (C_{aroH}), 128.9(6) (C_{aroH}), 128.9(0) (C_{aroH}), 128.8 (C_{aroH}), 124.3 (C_{aroH}), 75.6 (NC≡), 60.5 (≡CH), 56.1 (NCH₂) ppm.

MS (ESI-TOF, + mode) m/z (rel intensity) 317.06 (30) [M+H]⁺.

3-Ethynyloxazolidin-2-one (Y.6) (CAS: 660866-29-5)^[386]



Chemical Formula: C₅H₅NO₂
Molecular Weight: 111,1000

Following the General Procedure H, the title compound was isolated as an orange solid (37 mg, 333 μmol). Yield 88%.

R_f = 0.15 (SiO₂, cyclohexane/EtOAc 7:3).

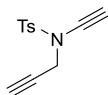
ATR-FTIR (neat) ν = 3281, 2989, 2920, 2865, 2152, 1755, 1478, 1401, 1272, 1089, 1028, 970, 748, 688, 632 cm⁻¹.

¹H NMR (300 MHz, CDCl₃) δ = 4.49 – 4.42 (m, 2H, OCH₂), 3.98 – 3.90 (m, 2H, NCH₂), 2.86 (s, 1H, ≡CH) ppm.

$^{13}\text{C}\{^1\text{H}\}$ NMR (126 MHz, CDCl_3) δ = 156.3 (C=O), 72.7 (NC \equiv), 63.2 (OCH $_2$), 60.0 (\equiv CH), 46.6 (NCH $_2$) ppm.

MS (ESI-TOF, + mode) m/z (rel intensity) 134.02 (100) [M+Na] $^+$.

N-Ethynyl-4-methyl-N-(prop-2-yn-1-yl)benzenesulfonamide (Y.9) (CAS: 2445280-24-8)^[387]



Chemical Formula: $\text{C}_{12}\text{H}_{11}\text{NO}_2\text{S}$
Molecular Weight: 233,2850

Following the General Procedure H, the title compound was isolated as yellow oil (93 mg, 399 μmol). Yield 52%.

R_f = 0.70 (SiO_2 , cyclohexane/EtOAc 7:3).

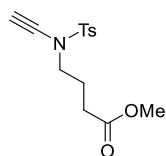
ATR-FTIR (neat) ν = 3286, 2985, 2921, 2853, 2168, 1594, 1426, 1534, 1160, 1045, 599, 812, 705, 654 cm^{-1} .

^1H NMR (500 MHz, CDCl_3) δ = 7.87 – 7.83 (m, 2H, H_{aro}), 7.35 (m, 2H, H_{aro}), 4.27 (d, J = 2.5 Hz, 2H, NCH $_2$), 2.80 (s, 1H, NC \equiv CH), 2.46 (s, 3H, CH $_3$), 2.20 (t, J = 2.5 Hz, 1H, CH $_2$ C \equiv CH) ppm.

$^{13}\text{C}\{^1\text{H}\}$ NMR (126 MHz, CDCl_3) δ = 145.3 (C_q), 134.1 (C_q), 129.8 (C_{aroH}), 128.3 (C_{aroH}), 75.6 (C \equiv), 75.3 (C \equiv), 74.8 (C \equiv), 60.0 (NC \equiv CH), 41.5 (NCH $_2$), 21.9 (CH $_3$) ppm.

HRMS (ESI-TOF, + mode) m/z calcd for $\text{C}_{12}\text{H}_{11}\text{NO}_2\text{SNa}$ 256.0403, found 256.0411 [M+Na] $^+$.

Methyl 4-((N-ethynyl-4-methylphenyl)sulfonamido)butanoate (Y.10) (CAS: 2820061-27-4)



Chemical Formula:
 $\text{C}_{14}\text{H}_{17}\text{NO}_4\text{S}$
Molecular Weight: 295,3530

Following the General Procedure H, the title compound was isolated as an off-white solid (119 mg, 263 μmol). Yield 62%.

R_f = 0.43 (SiO_2 , cyclohexane/EtOAc 7:3).

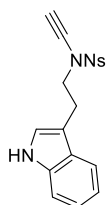
ATR-FTIR (neat) ν = 3264, 3054, 3000, 2955, 2925, 2852, 2135, 1738, 1598, 1438, 1355, 1167, 1099, 968, 808, 708, 652 cm^{-1} .

^1H NMR (500 MHz, CDCl_3) δ = 7.83 – 7.75 (m, 2H, H_{aro}), 7.35 (m, 2H, H_{aro}), 3.68 (s, 3H, OCH $_3$), 3.37 (t, J = 6.8 Hz, 2H, NCH $_2$), 2.74 (s, 1H, \equiv CH), 2.45 (s, 3H, CH $_3$ tosyl), 2.40 (t, J = 7.3 Hz, 2H, CH $_2$ C=O), 1.98 (quint, J = 7.0 Hz, 2H, NCH $_2$ CH $_2$) ppm.

$^{13}\text{C}\{^1\text{H}\}$ NMR (126 MHz, CDCl_3) δ = 173.2 (C=O), 145.0 (C_q), 134.5 (C_q), 130.0 (C_{aroH}), 127.8 (C_{aroH}), 75.8 (NC \equiv), 59.5 (\equiv CH), 51.9 (OCH $_3$), 50.5 (TsNCH $_2$), 30.4 (O=CCH $_2$), 23.0 (NCH $_2$ CH $_2$), 21.8 (CH $_3$ tosyl) ppm.

HRMS (ESI-TOF, + mode) m/z calcd for $\text{C}_{14}\text{H}_{17}\text{NNaO}_4\text{S}$ 318.0770, found 318.0783 [M+Na] $^+$.

N-(2-(1H-Indol-3-yl)ethyl)-N-ethynyl-4-nitrobenzenesulfonamide (Y.11) (CAS: 2820061-28-5)



Chemical Formula: $\text{C}_{18}\text{H}_{15}\text{N}_3\text{O}_4\text{S}$
Molecular Weight: 369,40

Following the General Procedure H, the title compound was isolated as an orange sticky solid (58 mg, 157 μmol). Yield 87%.

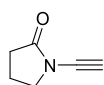
R_f = 0.38 (SiO_2 , cyclohexane/EtOAc 7:3).

ATR-FTIR (neat) ν = 3273, 3104, 2937, 2890, 2855, 2147, 1607, 1523, 1457, 1346, 1311, 1226, 1152, 1090, 1011, 914, 851, 735, 682 cm^{-1} .

^1H NMR (500 MHz, CDCl_3) δ = 8.11 – 8.04 (m, 2H, $\text{H}_{\text{aro-Ns}}$), 7.76 – 7.69 (m, 2H, $\text{H}_{\text{aro-Ns}}$), 7.41 (d, J = 8.2 Hz, 1H, H_{aro}), 7.32 (d, J = 7.8 Hz, 1H, H_{aro}), 7.28 (t, J = 7.7 Hz, 1H, H_{aro}), 7.13 (t, J = 7.5 Hz, 1H, H_{aro}), 6.90 (s, 1H, NC $_{\text{sp}^2}$ H), 4.94 – 4.35 (m, 1H, NH), 3.38 (t, J = 6.3 Hz, 2H, NCH $_2$), 3.12 (s, 1H, \equiv CH), 2.88 (t, J = 6.3 Hz, 2H, C_q CH $_2$) ppm.

$^{13}\text{C}\{^1\text{H}\}$ NMR (126 MHz, CDCl_3) δ = 149.8 (C_q), 145.5 (C_q), 138.6 (C_q), 127.9 (C_{aroH}), 126.8 (C_q), 126.7 (C_{aroH}), 124.4 (C_{aroH}), 124.1 (C_{aroH}), 122.2 (C_{aroH}), 118.9 (C_{aroH}), 114.5 (C_q), 111.7 (C_{aroH}), 73.7 ($\text{NC}\equiv$), 59.5 ($\equiv\text{CH}$), 42.9 (NCH_2), 25.5 (C_qCH_2) ppm.

1-Ethynylpyrrolidin-2-one (Y.12) (CAS: 1312921-13-3)^[388]



Chemical Formula: $\text{C}_6\text{H}_7\text{NO}$
Molecular Weight: 109,1280

Following the General Procedure H, the title compound was isolated as a colourless solid (36 mg, 330 μmol). Yield 27%.

R_f = 0.19 (SiO_2 , cyclohexane/EtOAc 7:3).

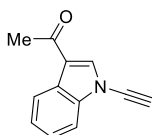
ATR-FTIR (neat) ν = 3399, 3216, 2962, 2924, 2901, 2854, 2771, 2136, 1704, 1456, 1261, 1193, 1022, 929, 802, 635 cm^{-1} .

^1H NMR (500 MHz, CDCl_3) δ = 3.71 (t, J = 7.2 Hz, 2H, NCH_2), 2.92 (s, 1H, $\equiv\text{CH}$), 2.45 (t, J = 8.1 Hz, 2H, $\text{CH}_2\text{C}=\text{O}$), 2.19 – 2.10 (m, 2H, NCH_2CH_2) ppm.

$^{13}\text{C}\{^1\text{H}\}$ NMR (126 MHz, CDCl_3) δ = 176.7 ($\text{C}=\text{O}$), 74.0 ($\text{NC}\equiv$), 61.0 ($\equiv\text{CH}$), 49.6 (NCH_2), 29.6 ($\text{O}=\text{CCH}_2$), 19.0 (NCH_2CH_2) ppm.

MS (ESI-TOF, + mode) m/z (rel intensity) 132.04 (50) $[\text{M}+\text{Na}]^+$.

1-(1-Ethynyl-1H-indol-3-yl)ethan-1-one (Y.13) (CAS: 1574275-58-3)



Chemical Formula: $\text{C}_{12}\text{H}_9\text{NO}$
Molecular Weight: 183,2100

Following the General Procedure H, the title compound was isolated as an off-white solid (110 mg, 600 μmol). Yield 60%.

R_f = 0.48 (SiO_2 , cyclohexane/EtOAc 7:3).

ATR-FTIR (neat) ν = 3308, 3105, 3049, 2924, 2853, 2470, 1735, 1642, 1453, 1218, 930, 738 cm^{-1} .

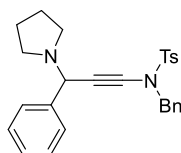
^1H NMR (500 MHz, CDCl_3) δ = 8.37 (d, J = 7.7 Hz, 1H, H_{aro}), 7.85 (s, 1H, NCH), 7.57 (d, J = 7.9 Hz, 1H, H_{aro}), 7.44 – 7.33 (m, 2H, H_{aro}), 3.20 (s, 1H, $\equiv\text{CH}$), 2.54 (s, 3H, CH_3) ppm.

$^{13}\text{C}\{^1\text{H}\}$ NMR (126 MHz, CDCl_3) δ = 193.0 ($\text{C}=\text{O}$), 138.6 (C_q), 135.2 (C_{aroH}), 125.2 (C_{aroH}), 125.0 (C_q), 124.5 (C_{aroH}), 123.1 (C_{aroH}), 120.0 (C_q), 111.3 (C_{aroH}), 72.8 ($\text{NC}\equiv$), 60.5 ($\equiv\text{CH}$), 27.8 (CH_3) ppm.

HRMS (ESI-TOF, + mode) m/z calcd for $\text{C}_{12}\text{H}_{10}\text{NO}$ 184.0757, found 184.0776 $[\text{M}+\text{H}]^+$.

γ -Amino-Ynamides

N-Benzyl-4-methyl-N-(3-phenyl-3-(pyrrolidin-1-yl)prop-1-yn-1-yl)benzenesulfonamide (G.1) (CAS: 2820060-87-3)



Chemical Formula: $\text{C}_{27}\text{H}_{28}\text{N}_2\text{O}_2\text{S}$
Molecular Weight: 444,5930

Following the General Procedure I, the title compound **G.1** was isolated as a colourless resin (196 mg, 441 μmol). Yield 88%.

R_f = 0.30 (SiO_2 , cyclohexane/EtOAc 7:3).

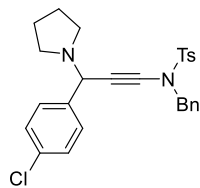
ATR-FTIR (neat) ν = 3062, 3031, 2965, 2930, 2873, 2816, 2239, 1597, 1494, 1366, 1169, 1090, 1027, 877, 814, 719, 700 cm^{-1} .

^1H NMR (400 MHz, CDCl_3) δ = 7.72 (m, 2H, H_{aro}), 7.27 – 7.15 (m, 12H, H_{aro}), 4.67 (s, 1H, $\text{CHC}\equiv$), 4.52 (d, J = 13.7 Hz, 1H, NCH_2 benzyl), 4.46 (d, J = 13.7 Hz, 1H, NCH_2 benzyl), 2.39 (s, 3H, CH_3), 2.38 – 2.22 (m, 4H, $2 \times \text{NCH}_2\text{CH}_2$), 1.62 – 1.54 (m, 4H, $2 \times \text{NCH}_2\text{CH}_2$) ppm.

$^{13}\text{C}\{^1\text{H}\}$ NMR (126 MHz, CDCl_3) δ = 144.7 (C_q), 139.5 (C_q), 134.6(1) (C_q), 134.6(0) (C_q), 129.8 (C_{aroH}), 129.0 (C_{aroH}), 128.6 (C_{aroH}), 128.4 (C_{aroH}), 128.2 (C_{aroH}), 128.1 (C_{aroH}), 127.9 (C_{aroH}), 127.4 (C_{aroH}), 79.9 ($\text{NC}\equiv\text{C}$), 68.0 ($\text{NC}\equiv\text{C}$), 58.4 (NCH), 55.6 (TsNCH_2), 49.6 (NCH_2CH_2), 23.4 (NCH_2CH_2), 21.8 (CH_3) ppm.

HRMS (ESI-TOF, + mode) m/z calcd for $C_{27}H_{29}N_2O_2S$ 445.1944, found 445.1929 $[M+H]^+$.

***N*-Benzyl-*N*-(3-(4-chlorophenyl)-3-(pyrrolidin-1-yl)prop-1-yn-1-yl)-4-methylbenzenesulfonamide (G.2) (CAS: 2820060-88-4)**



Chemical Formula: $C_{27}H_{27}ClN_2O_2S$
Molecular Weight: 479,0350

Following the General Procedure I, the title compound **G.2** was isolated as a pale yellow viscous oil (206 mg, 430 μ mol). Yield 86%.
R_f = 0.48 (SiO₂, cyclohexane/EtOAc 7:3).

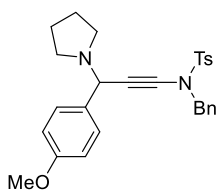
ATR-FTIR (neat) ν = 2964, 2911, 2874, 2821, 2241, 1597, 1485, 1443, 1368, 1184, 1168, 1086, 1016, 893, 811, 735, 693 cm^{-1} .

¹H NMR (500 MHz, CDCl₃) δ = 7.77 (m, 2H, H_{aro}), 7.35 – 7.26 (m, 7H, H_{aro}), 7.19 (s, 4H, H_{aro}), 4.69 (s, 1H, CHC \equiv), 4.56 (d, J = 13.7 Hz, 1H, NCH₂ benzyl), 4.49 (d, J = 13.6 Hz, 1H, NCH₂ benzyl), 2.45 (s, 3H, CH₃), 2.40 – 2.23 (m, 4H, 2 \times NCH₂CH₂), 1.68 – 1.56 (m, 4H, 2 \times NCH₂CH₂) ppm.

¹³C{¹H} NMR (126 MHz, CDCl₃) δ = 144.8 (C_q), 138.2 (C_q), 134.6 (C_q), 134.5 (C_q), 133.1 (C_q), 129.9 (C_{aro}H), 129.5 (C_{aro}H), 129.1 (C_{aro}H), 128.7 (C_{aro}H), 128.5 (C_{aro}H), 128.2 (C_{aro}H), 127.9 (C_{aro}H), 80.2 (NC \equiv C), 67.6 (NC \equiv C), 57.7 (NCH), 55.5 (TsNCH₂), 49.5 (NCH₂CH₂), 23.5 (NCH₂CH₂), 21.8 (CH₃) ppm.

HRMS (ESI-TOF, + mode) m/z calcd for $C_{27}H_{28}ClN_2O_2S$ 479.1555, found 479.1562 $[M+H]^+$.

***N*-Benzyl-*N*-(3-(4-methoxyphenyl)-3-(pyrrolidin-1-yl)prop-1-yn-1-yl)-4-methylbenzenesulfonamide (G.3) (CAS: 2820060-89-5)**



Chemical Formula: $C_{28}H_{30}N_2O_3S$
Molecular Weight: 474,6190

Following the General Procedure I, the title compound **G.3** was isolated as an orange viscous oil (209 mg, 440 μ mol). Yield 88%.
R_f = 0.19 (SiO₂, cyclohexane/EtOAc 7:3).

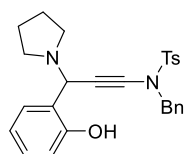
ATR-FTIR (neat) ν = 3063, 3032, 2960, 2930, 2873, 2833, 2814, 2237, 1610, 1509, 1456, 1362, 1302, 1244, 1166, 1089, 1029, 874, 837, 812, 717, 695 cm^{-1} .

¹H NMR (500 MHz, CDCl₃) δ = 7.79 – 7.73 (m, 2H, H_{aro}), 7.33 – 7.27 (m, 7H, H_{aro}), 7.22 – 7.16 (m, 2H, H_{aro}), 6.80 – 6.74 (m, 2H, 2 \times OC_qCH_{aro}), 4.65 (s, 1H, CHC \equiv), 4.55 (d, J = 13.7 Hz, 1H, NCH₂ benzyl), 4.49 (d, J = 13.7 Hz, 1H, NCH₂ benzyl), 3.79 (s, 3H, OCH₃), 2.44 (s, 3H, CCH₃), 2.41 – 2.25 (m, 4H, 2 \times NCH₂CH₂), 1.67 – 1.55 (m, 4H, 2 \times NCH₂CH₂) ppm.

¹³C{¹H} NMR (126 MHz, CDCl₃) δ = 158.9 (CH₃OC_q), 144.7 (C_q), 134.7(3) (C_q), 134.7(0) (C_q), 131.9 (C_q), 129.8, (C_{aro}H) 129.3 (C_{aro}H), 129.1 (C_{aro}H), 128.7 (C_{aro}H), 128.4 (C_{aro}H), 128.0 (C_{aro}H), 113.5 (CH₃OCCH), 79.7 (NC \equiv C), 68.4 (NC \equiv C), 57.8 (NCH), 55.6 (TsNCH₂), 55.4 (OCH₃), 49.6 (NCH₂CH₂), 23.5 (NCH₂CH₂), 21.8 (CCH₃) ppm.

HRMS (ESI-TOF, + mode) m/z calcd for $C_{28}H_{31}N_2O_3S$ 475.2050, found 475.2072 $[M+H]^+$.

***N*-Benzyl-*N*-(3-(2-hydroxyphenyl)-3-(pyrrolidin-1-yl)prop-1-yn-1-yl)-4-methylbenzenesulfonamide (G.4) (CAS: 2820060-90-8)**



Chemical Formula: $C_{27}H_{28}N_2O_3S$
Molecular Weight: 460,5920

Following the General Procedure I, the title compound **G.4** was isolated as a highly viscous red oil (195 mg, 423 μ mol). Yield 85%.
R_f = 0.35 (SiO₂, cyclohexane/EtOAc 7:3).

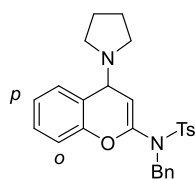
ATR-FTIR (neat) ν = 3063, 3032, 2962, 2929, 2875, 2849, 2243, 1591, 1457, 1364, 1246, 1166, 1090, 1025, 881, 812, 755, 695 cm^{-1} .

¹H NMR (500 MHz, CD₃CN) δ = 7.84 – 7.80 (m, 2H, H_{aro}), 7.46 – 7.42 (m, 2H, H_{aro}), 7.38 – 7.30 (m, 5H, H_{aro}), 7.14 (tdd, J = 8.2, 1.7, 0.7 Hz, 1H, H_{aro}), 6.99 – 6.93 (m, 1H, H_{aro}), 6.71 – 6.66 (m, 2H, H_{aro}), 5.02 (s, 1H, CHC \equiv), 4.63 (d, J = 13.9 Hz, 1H, NCH₂ benzyl), 4.55 (d, J = 13.8 Hz, 1H, NCH₂ benzyl), 2.50 – 2.44 (m, 5H, CH₃ & 2 \times NCH₂CH₂), 2.35 – 2.28 (m, 2H, 2 \times NCH₂CH₂), 1.69 – 1.59 (m, 4H, 2 \times NCH₂CH₂) ppm.

¹³C{¹H} NMR (126 MHz, CD₃CN) δ = 158.5 (C_qOH), 146.6 (C_q), 135.7 (C_q), 135.1 (C_q), 131.0 (C_{aro}H), 130.1 (C_{aro}H), 130.0 (C_{aro}H), 129.6 (C_{aro}H), 129.4 (C_{aro}H), 128.7 (C_{aro}H), 128.6 (C_{aro}H), 123.3 (C_q), 119.6 (C_{aro}H), 116.7 (C_{aro}H), 82.3 (NC \equiv C), 66.3 (NC \equiv C), 57.2 (NCH), 56.2 (TsNCH₂), 49.3 (NCH₂CH₂), 24.3 (NCH₂CH₂), 21.6 (CH₃) ppm.

HRMS (ESI-TOF, + mode) m/z calcd for C₂₇H₂₈N₂NaO₃S 483.1713, found 483.1710 [M+Na]⁺.

N-Benzyl-4-methyl-N-(4-(pyrrolidin-1-yl)-4H-chromen-2-yl)benzenesulfonamide (G.4')



Chemical Formula: C₂₇H₂₈N₂O₃S
Molecular Weight: 460,5920

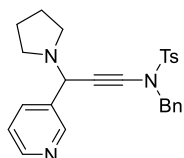
N.B.: The title compound **G.4'** could not be isolated due to degradation on NEt₃-treated silica gel.

R_f = 0.47 (SiO₂, cyclohexane/EtOAc 7:3).

¹H NMR (300 MHz, CDCl₃) δ = 7.80 – 7.74 (m, 2H), 7.34 – 7.13 (m, 9H), 7.05 (td, J = 7.4, 1.3 Hz, 1H, *p*-H_{aro}), 6.70 (dd, J = 8.2, 1.3 Hz, 1H, *o*-H_{aro}), 5.12 (d, J = 4.7 Hz, 1H, C=CH), 4.65 (d, J = 13.8 Hz, 1H, NCH₂ benzyl), 4.57 – 4.46 (m, 2H, NCH₂ benzyl &

NCH), 2.46 (s, 3H, CH₃), 2.27 – 2.09 (m, 4H, 2 \times NCH₂CH₂), 1.55 – 1.48 (m, 4H, 2 \times NCH₂CH₂) ppm.

N-Benzyl-4-methyl-N-(3-(pyridin-3-yl)-3-(pyrrolidin-1-yl)prop-1-yn-1-yl)benzenesulfonamide (G.6) (CAS: 2820060-91-9)



Chemical Formula: C₂₆H₂₇N₃O₂S
Molecular Weight: 445,5810

Following the General Procedure I, the title compound **G.6** was isolated as a pale red solid (186 mg, 417 μ mol). Yield 83%.

R_f = 0.20 (SiO₂, CH₂Cl₂/MeOH 9:1).

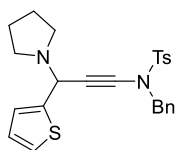
ATR-FTIR (neat) ν = 3063, 3051, 3031, 2962, 2928, 2874, 2810, 2239, 1595, 1577, 1495, 1421, 1362, 1292, 1166, 1088, 979, 812, 766, 698 cm⁻¹.

¹H NMR (500 MHz, CDCl₃) δ = 8.56 (d, J = 2.3 Hz, 1H, H_{aro}), 8.48 (dd, J = 4.8, 1.7 Hz, 1H, H_{aro}), 7.80 – 7.75 (m, 2H, H_{aro}), 7.57 (dt, J = 8.0, 2.1 Hz, 1H, H_{aro}), 7.34 – 7.29 (m, 7H, H_{aro}), 7.17 (ddd, J = 7.8, 4.8, 0.9 Hz, 1H, H_{aro}), 4.77 (s, 1H, CHC \equiv), 4.56 (d, J = 13.7 Hz, 1H, NCH₂ benzyl), 4.51 (d, J = 13.6 Hz, 1H, NCH₂ benzyl), 2.46 (s, 3H, CH₃), 2.43 – 2.24 (m, 4H, 2 \times NCH₂CH₂), 1.68 – 1.57 (m, 4H, 2 \times NCH₂CH₂) ppm.

¹³C{¹H} NMR (126 MHz, CDCl₃) δ = 149.8 (C_{aro}H), 148.7 (C_{aro}H), 144.9 (C_q), 135.6 (C_{aro}H), 135.2 (C_q), 134.6 (C_q), 134.4 (C_q), 129.9 (C_{aro}H), 129.0 (C_{aro}H), 128.7 (C_{aro}H), 128.5 (C_{aro}H), 127.8 (C_{aro}H), 123.1 (C_{aro}H), 80.5 (NC \equiv C), 66.9 (NC \equiv C), 56.2 (NCH), 55.5 (TsNCH₂), 49.5 (NCH₂CH₂), 23.5 (NCH₂CH₂), 21.7 (CH₃) ppm.

HRMS (ESI-TOF, + mode) m/z calcd for C₂₆H₂₈N₃O₂S 446.1897, found 446.1897 [M+H]⁺.

N-Benzyl-4-methyl-N-(3-(pyrrolidin-1-yl)-3-(thiophen-2-yl)prop-1-yn-1-yl)benzenesulfonamide (G.7) (CAS: 2820060-92-0)



Chemical Formula: $C_{25}H_{26}N_2O_2S_2$
Molecular Weight: 450,6150

Following the General Procedure I, the title compound **G.7** was isolated as a pale red solid (218 mg, 484 μ mol). Yield 97%.

R_f = 0.43 (SiO₂, cyclohexane/EtOAc 7:3).

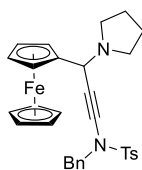
ATR-FTIR (neat) ν = 2961, 2923, 2874, 2856, 2810, 2237, 1596, 1494, 1455, 1360, 1286, 1260, 1230, 1168, 1128, 1087, 1041, 978, 877, 754, 655 cm^{-1} .

¹H NMR (500 MHz, CDCl₃) δ = 7.77 – 7.71 (m, 2H, H_{aro}), 7.29 – 7.24 (m, 7H, H_{aro}), 7.15 (dd, J = 4.9, 1.3 Hz, 1H, H_{aro}), 6.84 – 6.76 (m, 2H, H_{aro}), 4.94 (d, J = 1.2 Hz, 1H, CHC \equiv), 4.52 (d, J = 13.7 Hz, 1H, NCH₂ benzyl), 4.46 (d, J = 13.7 Hz, 1H, NCH₂ benzyl), 2.41 (s, 3H, CH₃), 2.40 – 2.31 (m, 4H, 2 \times NCH₂CH₂), 1.64 – 1.53 (m, 4H, 2 \times NCH₂CH₂) ppm.

¹³C{¹H} NMR (126 MHz, CDCl₃) δ = 144.8 (C_q), 144.6 (C_q), 134.8 (C_q), 134.6 (C_q), 129.9 (C_{aro}H), 129.1 (C_{aro}H), 128.7 (C_{aro}H), 128.4 (C_{aro}H), 128.0 (C_{aro}H), 126.2 (C_{aro}H), 125.4 (C_{aro}H), 125.2 (C_{aro}H), 79.4 (NC \equiv C), 67.5 (NC \equiv C), 55.6 (TsNCH₂), 54.0 (NCH), 49.3 (NCH₂CH₂), 23.6 (NCH₂CH₂), 21.8 (CH₃) ppm.

HRMS (ESI-TOF, + mode) m/z calcd for C₂₅H₂₇N₂O₂S₂ 451.1508, found 451.1507 [M+H]⁺.

N-Benzyl-4-methyl-N-(3-ferrocenyl-3-(pyrrolidin-1-yl)prop-1-yn-1-yl)benzenesulfonamide (G.8) (CAS: 2820064-35-3)



Chemical Formula: $C_{31}H_{32}FeN_2O_2S$
Molecular Weight: 552,5140

Following the General Procedure I, the title compound **G.8** was isolated as an orange solid (116 mg, 210 μ mol). Yield 84%.

R_f = 0.14 (SiO₂, cyclohexane/EtOAc 7:3).

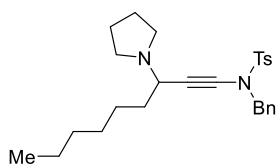
ATR-FTIR (neat) ν = 3104, 3062, 3038, 2965, 2925, 2869, 2814, 2251, 1596, 1496, 1455, 1356, 1267, 1162, 1091, 928, 810, 756, 694 cm^{-1} .

¹H NMR (500 MHz, CDCl₃) δ = 7.90 – 7.83 (m, 2H, H_{aro}), 7.40 – 7.28 (m, 7H, H_{aro}), 4.59 (s, 2H, NCH₂ benzyl), 4.56 (s, 1H, CHC \equiv), 4.17 (dt, J = 2.6, 1.4 Hz, 1H), 4.07 (dt, J = 2.6, 1.4 Hz, 1H), 4.05 – 4.01 (m, 2H), 3.99 (s, 5H), 2.46 (s, 3H, CH₃), 2.37 – 2.23 (m, 4H, 2 \times NCH₂CH₂), 1.60 – 1.53 (m, 4H, 2 \times NCH₂CH₂) ppm.

¹³C{¹H} NMR (126 MHz, CDCl₃) δ = 144.8 (C_q), 135.1 (C_q), 134.9 (C_q), 129.9 (C_{aro}H), 128.8(0) (C_{aro}H), 128.7(7) (C_{aro}H), 128.5 (C_{aro}H), 127.9 (C_{aro}H), 86.8 (C_q), 78.0 (C_q), 69.1 (CH), 68.7 (CH), 68.4 (CH), 68.2 (C_q), 68.1 (CH), 67.5 (CH), 55.7 (TsNCH₂), 54.4 (CH), 49.2 (NCH₂CH₂), 23.3 (NCH₂CH₂), 21.8 (CH₃) ppm.

HRMS (ESI-TOF, + mode) m/z calcd for C₃₁H₃₂FeN₂O₂S 552.1529, found 552.1508 [M].

N-Benzyl-4-methyl-N-(3-(pyrrolidin-1-yl)non-1-yn-1-yl)benzenesulfonamide (G.10) (CAS: 2820060-93-1)



Chemical Formula: $C_{27}H_{36}N_2O_2S$
Molecular Weight: 452,6570

Following the General Procedure I, the title compound **G.10** was isolated as a yellow viscous oil (90 mg, 199 μ mol). Yield 80%.

R_f = 0.10 (SiO₂, cyclohexane/EtOAc 7:3).

ATR-FTIR (neat) ν = 3064, 3032, 2954, 2926, 2857, 2816, 2240, 1597, 1495, 1366, 1292, 1167, 1090, 1025, 812, 697 cm^{-1} .

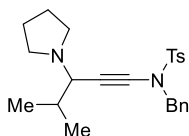
¹H NMR (500 MHz, CDCl₃) δ = 7.79 – 7.73 (m, 2H, H_{aro}), 7.34 – 7.27 (m, 7H, H_{aro}), 4.52 (d, J = 13.7 Hz, 1H, NCH₂ benzyl), 4.43 (d, J = 13.6 Hz, 1H, NCH₂ benzyl), 3.46 (dd, J = 9.9, 5.0 Hz, 1H, CHC \equiv), 2.45 (s, 3H, CH₃ tosyl), 2.41 – 2.33 (m, 4H,

2 × NCH₂CH₂), 1.65 – 1.58 (m, 4H, 2 × NCH₂CH₂), 1.57 – 1.35 (m, 2H), 1.29 – 1.19 (m, 8H), 0.88 (t, *J* = 7.1 Hz, 3H, CH₂CH₃) ppm.

¹³C{¹H} NMR (126 MHz, CDCl₃) δ = 144.6 (C_q), 134.7 (C_q), 129.7 (C_{aro}H), 129.0 (C_{aro}H), 128.5 (C_{aro}H), 128.3 (C_{aro}H), 127.9 (C_{aro}H), 78.0 (NC≡C), 69.5 (NC≡C), 55.6 (TsNCH₂), 54.6 (NCH), 49.3 (NCH₂CH₂), 35.3 (CH₂), 31.9 (CH₂), 29.2 (CH₂), 26.7 (CH₂), 23.4 (CH₂), 22.8 (CH₂), 21.8 (CH₃ tosyl), 14.3 (CH₂CH₃) ppm.

HRMS (ESI-TOF, + mode) *m/z* calcd for C₂₇H₃₇N₂O₂S 453.2570, found 453.2572 [M+H]⁺.

N-Benzyl-4-methyl-N-(4-methyl-3-(pyrrolidin-1-yl)pent-1-yn-1-yl)benzenesulfonamide (G.11) (CAS: 2820060-94-2)



Chemical Formula: C₂₄H₃₀N₂O₂S
Molecular Weight: 410,5760

Following the General Procedure I, the title compound **G.11** was isolated as a colourless solid (83 mg, 202 μmol). Yield 81%.

R_f = 0.20 (SiO₂, cyclohexane/EtOAc 7:3).

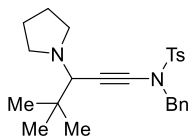
ATR-FTIR (neat) ν = 3061, 3032, 2962, 2930, 2905, 2870, 2835, 2796, 2241, 1596, 1495, 1358, 1293, 1211, 1166, 1044, 996, 861, 728, 694 cm⁻¹.

¹H NMR (500 MHz, CDCl₃) δ = 7.79 – 7.74 (m, 2H, H_{aro}), 7.34 – 7.26 (m, 7H, H_{aro}), 4.52 (d, *J* = 13.6 Hz, 1H, NCH₂ benzyl), 4.43 (d, *J* = 13.7 Hz, 1H, NCH₂ benzyl), 3.03 (d, *J* = 8.4 Hz, 1H, CHC≡), 2.45 (s, 3H, CH₃ tosyl), 2.39 – 2.26 (m, 4H, 2 × NCH₂CH₂), 1.68 – 1.55 (m, 5H, 2 × NCH₂CH₂ & CH(CH₃)₂), 0.86 (d, *J* = 6.7 Hz, 3H, 1 × CH(CH₃)₂), 0.82 (d, *J* = 6.6 Hz, 3H, 1 × CH(CH₃)₂) ppm.

¹³C{¹H} NMR (126 MHz, CDCl₃) δ = 144.6 (C_q), 134.7(6) (C_q), 134.7(5) (C_q), 129.7 (C_{aro}H), 129.0 (C_{aro}H), 128.5 (C_{aro}H), 128.3 (C_{aro}H), 127.9 (C_{aro}H), 78.0 (NC≡C), 69.0 (NC≡C), 61.9 (NCH), 55.6 (TsNCH₂), 49.8 (NCH₂CH₂), 32.1 (CH(CH₃)₂), 23.5 (NCH₂CH₂), 21.8 (CH₃), 20.2 (CH₃), 19.7 (CH₃) ppm.

HRMS (ESI-TOF, + mode) *m/z* calcd for C₂₄H₃₁N₂O₂S 411.2101, found 411.2102 [M+H]⁺.

N-Benzyl-N-(4,4-dimethyl-3-(pyrrolidin-1-yl)pent-1-yn-1-yl)-4-methylbenzenesulfonamide (G.12) (CAS: 2820060-95-3)



Chemical Formula: C₂₅H₃₂N₂O₂S
Molecular Weight: 424,6030

Following the General Procedure I, the title compound **G.12** was isolated as a pale yellow solid (85 mg, 200 μmol). Yield 80%.

R_f = 0.50 (SiO₂, cyclohexane/EtOAc 7:3).

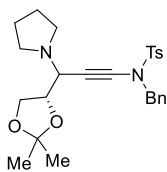
ATR-FTIR (neat) ν = 3085, 3064, 2958, 2872, 2812, 2239, 1599, 1495, 1455, 1356, 1292, 1168, 1091, 1045, 914, 812, 692 cm⁻¹.

¹H NMR (500 MHz, CDCl₃) δ = 7.80 – 7.75 (m, 2H, H_{aro}), 7.33 – 7.27 (m, 7H, H_{aro}), 4.53 (d, *J* = 13.7 Hz, 1H, NCH₂ benzyl), 4.45 (d, *J* = 13.7 Hz, 1H, NCH₂ benzyl), 3.23 (s, 1H, CHC≡), 2.45 (s, 3H, CH₃ tosyl), 2.43 – 2.37 (m, 4H, 2 × NCH₂CH₂), 1.58 – 1.48 (m, 4H, 2 × NCH₂CH₂), 0.83 (s, 9H, C(CH₃)₃) ppm.

¹³C{¹H} NMR (126 MHz, CDCl₃) δ = 144.5 (C_q), 134.8(0) (C_q), 134.7(9) (C_q), 129.7 (C_{aro}H), 129.0 (C_{aro}H), 128.6 (C_{aro}H), 128.3 (C_{aro}H), 127.9 (C_{aro}H), 79.2 (NC≡C), 68.0 (NC≡C), 64.8 (NCH), 55.7 (TsNCH₂), 51.3 (NCH₂CH₂), 36.0 (C(CH₃)₃), 27.8 (C(CH₃)₃), 24.1 (NCH₂CH₂), 21.8 (CH₃ tosyl) ppm.

HRMS (ESI-TOF, + mode) *m/z* calcd for C₂₅H₃₃N₂O₂S 425.2257, found 425.2256 [M+H]⁺.

N-Benzyl-N-(3-((S)-2,2-dimethyl-1,3-dioxolan-4-yl)-3-(pyrrolidin-1-yl)prop-1-yn-1-yl)-4-methylbenzenesulfonamide (G.12) (CAS: 2820060-97-5)



Chemical Formula: C₂₆H₃₂N₂O₄S
Molecular Weight: 468,6120

Following the General Procedure I, the title compound **G.12** was isolated as a colourless oil (84 mg, 179 μmol) in a diastereomeric ratio of 9:1. Yield 70% (both diastereoisomers combined).

R_f = 0.10 (SiO₂, cyclohexane/EtOAc 8:2).

ATR-FTIR (neat) ν = 3409, 3239, 3066, 3033, 2981, 2962, 2932, 2875, 2814, 2238, 1597, 1544, 1496, 1456, 1366, 1186, 1069, 844,

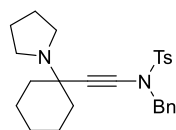
656 cm⁻¹.

¹H NMR (500 MHz, CDCl₃) (*major diastereomer*) δ = 7.76 (d, *J* = 8.3 Hz, 2H, H_{aro}), 7.38 – 7.28 (m, 5H, H_{aro}), 7.26 – 7.22 (m, 2H, H_{aro}), 4.49 (d, *J* = 13.6 Hz, 1H, NCH₂ benzyl), 4.44 (d, *J* = 13.6 Hz, 1H, NCH₂ benzyl), 3.96 (ddd, *J* = 8.6, 7.5, 6.1 Hz, 1H, CHO), 3.73 (dd, *J* = 8.5, 6.2 Hz, 1H, CH₂O), 3.65 (d, *J* = 8.6 Hz, 1H, CHC≡), 3.50 (dd, *J* = 8.4, 7.5 Hz, 1H, CH₂O), 2.46 (s, 3H, CH₃ tosyl), 2.46 – 2.38 (m, 4H, 2 × NCH₂CH₂), 1.68 – 1.60 (m, 4H, 2 × NCH₂CH₂), 1.36 (s, 3H, 1 × C(CH₃)₂), 1.32 (s, 3H, 1 × C(CH₃)₂) ppm.

¹³C{¹H} NMR (126 MHz, CDCl₃) δ = 144.9 (C_q), 134.6 (C_q), 134.4 (C_q), 129.9 (C_{aro}H), 129.0 (C_{aro}H), 128.7 (C_{aro}H), 128.6 (C_{aro}H), 127.8 (C_{aro}H), 110.2 (O₂C_q), 79.5 (NC≡C), 76.6 (CHO), 67.9 (CH₂O), 65.7 (NC≡C), 58.3 (NCH), 55.4 (TsNCH₂), 49.4 (NCH₂CH₂), 25.8 (C(CH₃)₂), 23.5 (NCH₂CH₂), 21.8 (CH₃ tosyl) ppm.

HRMS (ESI-TOF, + mode) *m/z* calcd for C₂₆H₃₃N₂O₄S 469.2156, found 469.2131 [M+H]⁺.

N-Benzyl-4-methyl-N-((1-(pyrrolidin-1-yl)cyclohexyl)ethynyl)benzenesulfonamide (G.13) (CAS: 2820060-98-6)



Chemical Formula: C₂₆H₃₂N₂O₂S
Molecular Weight: 436,6140

Following the General Procedure I, the title compound **G.13** was isolated as an off-white solid (87 mg, 199 μmol). Yield 80%.

R_f = 0.26 (SiO₂, CH₂Cl₂/MeOH 9:1).

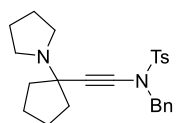
ATR-FTIR (neat) ν = 3029, 2955, 2929, 2854, 2825, 2233, 1597, 1495, 1447, 1361, 1258, 1122, 1045, 971, 809, 735, 694 cm⁻¹.

¹H NMR (500 MHz, CDCl₃) δ = 7.80 – 7.75 (m, 2H, H_{aro}), 7.35 – 7.26 (m, 7H, H_{aro}), 4.48 (s, 2H, NCH₂ benzyl), 2.46 (s, 3H, CH₃), 2.45 – 2.38 (m, 4H, 2 × NCH₂CH₂), 1.78 – 1.71 (m, 2H, 2 × NC_qCH₂), 1.64 – 1.55 (m, 4H, 2 × NCH₂CH₂), 1.55 – 1.43 (m, 2H), 1.38 – 1.18 (m, 5H), 1.13 – 1.01 (m, 1H) ppm.

¹³C{¹H} NMR (126 MHz, CDCl₃) δ = 144.6 (C_q), 134.7(0) (C_q), 134.6(5) (C_q), 129.7 (C_{aro}H), 129.1 (C_{aro}H), 128.5 (C_{aro}H), 128.3 (C_{aro}H), 127.9 (C_{aro}H), 78.8 (NC≡C), 71.3 (NC≡C), 59.3 (NC_qCH₂), 55.6 (TsNCH₂), 46.9 (NCH₂CH₂), 38.0 (CH₂), 25.6 (CH₂), 23.3 (CH₂), 22.9 (CH₂), 21.8 (CH₃) ppm.

HRMS (ESI-TOF, + mode) *m/z* calcd for C₂₆H₃₃N₂O₂S 437.2257, found 437.2250 [M+H]⁺.

N-Benzyl-4-methyl-N-((1-(pyrrolidin-1-yl)cyclopentyl)ethynyl)benzenesulfonamide (G.14) (CAS: 2820060-99-7)



Chemical Formula: C₂₅H₃₀N₂O₂S
Molecular Weight: 422,5870

Following the General Procedure I, the title compound **G.14** was isolated as a yellow solid (150 mg, 355 μmol). Yield 71%.

R_f = 0.37 (SiO₂, CH₂Cl₂/MeOH 9:1).

ATR-FTIR (neat) ν = 3268, 3060, 3031, 2961, 2929, 2869, 2808, 2232, 1597, 1495, 1454, 1423, 1365, 1323, 1309, 1292, 1188, 1165,

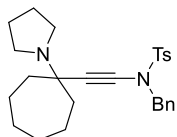
1090, 1059, 1012, 940, 912, 875, 816, 801, 781, 741, 700, 662 cm⁻¹.

¹H NMR (500 MHz, CDCl₃) δ = 7.76 (d, J = 8.3 Hz, 2H, H_{aro}), 7.33 – 7.26 (m, 7H, H_{aro}), 4.47 (s, 2H, NCH₂ benzyl), 2.46 (s, 3H, CH₃), 2.42 – 2.37 (m, 4H, 2 × NCH₂CH₂), 1.77 – 1.71 (m, 2H), 1.70 – 1.47 (m, 9H, 2 × NCH₂CH₂ & 5H cyclopentyl) ppm.

¹³C{¹H} NMR (126 MHz, CDCl₃) δ = 144.7 (C_q), 134.8(3) (C_q), 134.8(0) (C_q), 129.8 (C_{aro}H), 129.3 (C_{aro}H), 128.6 (C_{aro}H), 128.4 (C_{aro}H), 128.0 (C_{aro}H), 78.1 (NC≡C), 72.4 (NC≡C), 65.6 (NCC≡C), 55.7 (TsNCH₂), 49.2 (NCH₂CH₂), 40.7 (CH₂), 23.7 (CH₂), 23.4 (CH₂), 21.9 (CH₃) ppm.

HRMS (ESI-TOF, + mode) m/z calcd for C₂₅H₃₁N₂O₂S 423.2101, found 423.2112 [M+H]⁺.

N-Benzyl-4-methyl-N-((1-(pyrrolidin-1-yl)cycloheptyl)ethynyl)benzenesulfonamide (G.15) (CAS: 2820061-00-3)



Chemical Formula: C₂₇H₃₄N₂O₂S
Molecular Weight: 450,6410

Following the General Procedure I, the title compound **G.15** was isolated as a yellow solid (189 mg, 419 μ mol). Yield 84%.

R_f = 0.54 (SiO₂, CH₂Cl₂/MeOH 9:1).

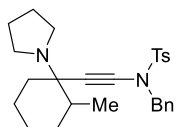
ATR-FTIR (neat) ν = 3104, 3062, 3038, 2965, 2925, 2869, 2814, 2251, 1596, 1496, 1455, 1356, 1267, 1162, 1129, 1091, 1025, 928, 905, 881, 756, 694 cm⁻¹.

¹H NMR (500 MHz, CDCl₃) δ = 7.77 (m, 2H, H_{aro}), 7.31 (m, 2H, H_{aro}), 7.30 – 7.26 (m, 4H, H_{aro}), 4.47 (s, 2H, NCH₂ benzyl), 2.45 (s, 3H, CH₃), 2.44 – 2.38 (m, 4H, 2 × NCH₂CH₂), 1.78 – 1.69 (m, 2H, 2 × NC_qCH₂), 1.65 – 1.44 (m, 12H, 2 × NCH₂CH₂ & 8H cycloheptyl), 1.42 – 1.31 (m, 2H) ppm.

¹³C{¹H} NMR (126 MHz, CDCl₃) δ = 144.5 (C_q), 134.7(9) (C_q), 134.7(6) (C_q), 129.7 (C_{aro}H), 129.1 (C_{aro}H), 128.5 (C_{aro}H), 128.3 (C_{aro}H), 128.0 (C_{aro}H), 77.6 (NC≡C), 73.1 (NC≡C), 62.5 (NC_qCH₂), 55.7 (TsNCH₂), 47.6 (NCH₂CH₂), 40.3 (CH₂), 28.1 (CH₂), 23.6 (CH₂), 22.0 (CH₂), 21.8 (CH₃) ppm.

HRMS (ESI-TOF, + mode) m/z calcd for C₂₇H₃₅N₂O₂S 451.2414, found 451.2431 [M+H]⁺.

N-Benzyl-4-methyl-N-((2-methyl-1-(pyrrolidin-1-yl)cyclohexyl)ethynyl)benzenesulfonamide (G.16) (CAS for cis: 2820061-02-5, for trans: 2820061-01-4)



Chemical Formula: C₂₇H₃₄N₂O₂S
Molecular Weight: 450,6410

Following the General Procedure I, the title compound **G.16** was isolated as a colourless viscous oil (30 mg, 68 μ mol) as a mixture of both diastereoisomers in a 1:1 ratio. Yield 27%.

R_f = 0.10 (SiO₂, cyclohexane/EtOAc 7:3).

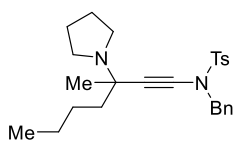
ATR-FTIR (neat) ν = 3065, 3032, 2928, 2859, 2816, 2234, 1598, 1496, 2455, 1364, 1090, 812, 657 cm⁻¹.

¹H NMR (500 MHz, CDCl₃) (both diastereoisomers, proportion 1:1) δ = 7.78 – 7.70 (m, 4H, H_{aro}), 7.32 – 7.22 (m, 14H, H_{aro}), 4.49 – 4.39 (m, 4H, TsNCH₂), 2.46 – 2.37 (m, 10H), 2.36 – 2.27 (m, 4H), 1.80 – 1.33 (m, 19H), 1.30 – 1.12 (m, 7H), 1.11 – 1.02 (m, 1H), 0.86 (d, J = 11.7 Hz, 3H, CHCH₃), 0.84 (d, J = 11.6 Hz, 3H, CHCH₃) ppm.

¹³C{¹H} NMR (126 MHz, CDCl₃) δ = 144.5 (C_q), 144.4 (C_q), 134.8(2) (C_q), 134.8(0) (C_q), 134.7 (C_q), 129.7(1) (C_{aro}H), 129.7(0) (C_{aro}H), 129.0 (C_{aro}H), 128.5(2) (C_{aro}H), 128.5(0) (C_{aro}H), 128.3 (C_{aro}H), 128.2 (C_{aro}H), 127.9(3) (C_{aro}H), 127.9(1) (C_{aro}H), 78.5 (NC≡C), 77.9 (NC≡C), 72.6 (NC≡C), 72.4 (NC≡C), 62.0 (NC_q), 61.3 (NC_q), 55.7 (TsNCH₂), 55.6(6) (TsNCH₂), 46.4 (NCH₂CH₂), 46.0 (NCH₂CH₂), 37.0 (CHCH₃) 36.5 (CHCH₃), 31.5 (CH₂), 29.6 (CH₂), 23.9 (CH₂), 23.3 (CH₂), 23.1 (CH₂), 21.8(3) (CH₂), 21.8(0) (CH₃ tosyl), 21.7(6) (CH₃ tosyl), 19.5 (CH₂), 16.6 (CHCH₃), 13.0 (CHCH₃) ppm.

HRMS (ESI-TOF, + mode) m/z calcd for C₂₇H₃₅N₂O₂S 451.2414, found 451.2407 [M+H]⁺.

N-Benzyl-4-methyl-N-(3-methyl-3-(pyrrolidin-1-yl)hept-1-yn-1-yl)benzenesulfonamide (G.18) (CAS: 2820061-03-6)



Chemical Formula: C₂₆H₃₄N₂O₂S
Molecular Weight: 438,6300

Following the General Procedure I, the title compound **G.18** was isolated as a colourless solid (68 mg, 203 μmol). Yield 79%.

R_f = 0.12 (SiO₂, cyclohexane/EtOAc 7:3).

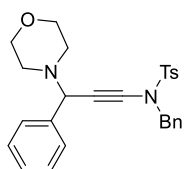
ATR-FTIR (neat) ν = 3065, 3032, 2955, 2935, 2870, 2816, 2235, 1597, 1495, 1455, 1364, 1306, 1166, 1089, 960, 898, 776, 697 cm⁻¹.

¹H NMR (500 MHz, CDCl₃) δ = 7.76 – 7.70 (m, 2H, H_{aro}), 7.31 – 7.21 (m, 6H, H_{aro}), 4.46 (d, *J* = 13.6 Hz, 1H, NCH₂ benzyl), 4.42 (d, *J* = 13.5 Hz, 1H, NCH₂ benzyl), 2.43 (s, 3H, CH₃ tosyl), 2.41 – 2.37 (m, 4H, 2 × NCH₂CH₂), 1.61 – 1.54 (m, 4H, 2 × NCH₂CH₂), 1.50 – 1.35 (m, 2H), 1.25 – 1.10 (m, 7H, C_qCH₃ & 4H *n*-butyl), 0.85 – 0.80 (m, 3H, CH₂CH₃) ppm.

¹³C{¹H} NMR (126 MHz, CDCl₃) δ = 144.5 (C_q), 134.7 (C_q), 134.6 (C_q), 129.7 (C_{aro}H), 129.1 (C_{aro}H), 128.5 (C_{aro}H), 128.3 (C_{aro}H), 128.0 (C_{aro}H), 72.4 (NC≡C), 59.8 (C_q), 58.0 (C_q), 55.6 (TsNCH₂), 47.6 (NCH₂CH₂), 41.4 (CH₂), 26.6 (CH₂), 26.0 (NC_qCH₃), 23.5 (CH₂), 23.2 (CH₂), 21.8 (CH₃ tosyl), 14.2 (CH₂CH₃) ppm.

HRMS (ESI-TOF, + mode) *m/z* calcd for C₂₆H₃₅N₂O₂S 439.2414, found 439.2436 [M+H]⁺.

N-Benzyl-4-methyl-N-(3-morpholino-3-phenylprop-1-yn-1-yl)benzenesulfonamide (G.20) (CAS: 2820061-05-8)



Chemical Formula: C₂₇H₂₈N₂O₃S
Molecular Weight: 460,5920

Following the General Procedure I, the title compound **G.20** was isolated as a colourless solid (98 mg, 213 μmol). Yield 85%.

R_f = 0.20 (SiO₂, cyclohexane/EtOAc 7:3).

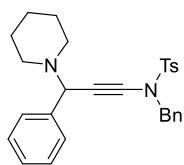
ATR-FTIR (neat) ν = 3268, 3064, 3048, 3029, 2965, 2925, 2860, 2834, 2247, 1596, 1493, 1449, 1371, 1321, 1249, 1167, 1111, 1002, 892, 804, 740, 695 cm⁻¹.

¹H NMR (300 MHz, CDCl₃) δ = 7.83 – 7.73 (m, 2H, H_{aro}), 7.34 – 7.26 (m, 9H, H_{aro}), 7.26 – 7.22 (m, 3H, H_{aro}), 4.59 (d, *J* = 13.7 Hz, 1H, NCH₂ benzyl), 4.54 – 4.47 (m, 2H, CHC≡ & NCH₂ benzyl), 3.64 – 3.50 (m, 4H, 2 × OCH₂), 2.45 (s, 3H, CH₃), 2.28 – 2.20 (m, 4H, 2 × NCH₂) ppm.

¹³C{¹H} NMR (126 MHz, CDCl₃) δ = 144.9 (C_q), 137.9 (C_q), 134.6 (C_q), 134.5 (C_q), 129.9 (C_{aro}H), 129.1 (C_{aro}H), 128.7 (C_{aro}H), 128.6 (C_{aro}H), 128.5 (C_{aro}H), 128.2 (C_{aro}H), 128.0 (C_{aro}H), 127.7 (C_{aro}H), 81.1 (NC≡C), 67.1 (OCH₂), 66.9 (NC≡C), 61.6 (NCH), 55.6 (TsNCH₂), 49.4 (NCH₂CH₂), 21.8 (CH₃) ppm.

HRMS (ESI-TOF, + mode) *m/z* calcd for C₂₇H₂₈N₂NaO₃S 483.1713, found 483.1705 [M+Na]⁺.

N-Benzyl-4-methyl-N-(3-phenyl-3-(piperidin-1-yl)prop-1-yn-1-yl)benzenesulfonamide (G.21) (CAS: 2820061-04-7)



Chemical Formula: C₂₈H₃₀N₂O₂S
Molecular Weight: 458,6200

Following the General Procedure I, the title compound **G.21** was isolated as a yellow solid (214 mg, 467 μmol). Yield 93%.

R_f = 0.43 (SiO₂, cyclohexane/EtOAc 8:2).

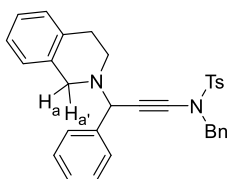
ATR-FTIR (neat) ν = 3056, 3029, 2938, 2917, 2856, 2800, 2753, 2238, 1596, 1491, 1452, 1357, 1300, 1167, 1087, 986, 811, 768, 698 cm⁻¹.

¹H NMR (300 MHz, CDCl₃) δ = 7.83 – 7.75 (m, 2H, H_{aro}), 7.35 – 7.27 (m, 8H, H_{aro}), 7.25 – 7.19 (m, 2H, H_{aro}), 4.59 (d, J = 13.7 Hz, 1H, NCH₂ benzyl), 4.55 (s, 1H, CHC \equiv), 4.51 (d, J = 13.7 Hz, 1H, NCH₂ benzyl), 2.45 (s, 3H, CH₃), 2.22 – 2.12 (m, 4H), 1.51 – 1.38 (m, 3H), 1.35 – 1.24 (m, 2H) ppm.

¹³C{¹H} NMR (126 MHz, CDCl₃) δ = 144.7 (C_q), 138.8 (C_q), 134.7 (C_q), 134.7 (C_q), 129.8 (C_{aro}H), 129.1 (C_{aro}H), 128.7 (C_{aro}H), 128.5 (C_{aro}H), 128.4 (C_{aro}H), 128.0 (C_{aro}H), 128.0 (C_{aro}H), 127.3 (C_{aro}H), 80.6 (NC \equiv C), 67.5 (NC \equiv C), 61.9 (NCH), 55.7 (TsNCH₂), 50.3 (NCH₂CH₂), 26.2 (CH₂), 24.4 (CH₂), 21.8 (CH₃) ppm.

HRMS (ESI-TOF, + mode) m/z calcd for C₂₈H₃₁N₂O₂S 459.2101, found 459.2095 [M+H]⁺.

N-Benzyl-N-(3-(3,4-dihydroisoquinolin-2(1H)-yl)-3-phenylprop-1-yn-1-yl)-4-methylbenzenesulfonamide (G.22) (CAS: 2820061-06-9)



Chemical Formula: C₃₂H₃₀N₂O₂S
Molecular Weight: 506,6640

Following the General Procedure I, the title compound **G.22** was isolated as a yellow resin (107 mg, 211 μ mol). Yield 84%.

R_f = 0.57 (SiO₂, cyclohexane/EtOAc 7:3).

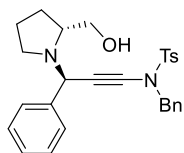
ATR-FTIR (neat) ν = 3062, 3028, 2923, 2892, 2830, 2785, 2244, 1736, 1637, 1597, 1494, 1453, 1255, 1088, 1039, 985, 886, 816, 722, 656 cm⁻¹.

¹H NMR (500 MHz, CDCl₃) δ = 7.79 (m, 2H, H_{aro}), 7.41 – 7.36 (m, 2H, H_{aro}), 7.34 – 7.21 (m, 10H, H_{aro}), 7.14 – 7.05 (m, 3H, H_{aro}), 6.94 – 6.89 (m, 1H, H_{aro}), 4.82 (s, 1H, CHC \equiv), 4.60 (d, J = 13.5 Hz, 1H, TsNCH₂), 4.52 (d, J = 13.4 Hz, 1H, TsNCH₂), 3.48 (d, J = 14.9 Hz, 1H, H_a), 3.41 (d, J = 14.8 Hz, 1H, H_{a'}), 2.76 (qt, J = 16.0, 5.8 Hz, 2H, NCH₂CH₂), 2.50 – 2.40 (m, 2H, NCH₂CH₂), 2.39 (s, 3H, CH₃) ppm.

¹³C{¹H} NMR (126 MHz, CDCl₃) δ = 144.8 (C_q), 138.3 (C_q), 135.3 (C_q), 134.5 (C_q), 134.4(1) (C_q), 134.4(0) (C_q), 129.8 (C_{aro}H), 129.1 (C_{aro}H), 128.6(8) (C_{aro}H), 128.6(7) (C_{aro}H), 128.5 (C_{aro}H), 128.4 (C_{aro}H), 128.1 (C_{aro}H), 127.9 (C_{aro}H), 127.6 (C_{aro}H), 126.8 (C_{aro}H), 125.9 (C_{aro}H), 125.5 (C_{aro}H), 81.1 (NC \equiv C), 66.8 (NC \equiv C), 61.2 (NCH), 55.6 (NCH₂), 51.8 (NCH₂), 46.7 (NCH₂), 29.6 (CH₂), 21.7 (CH₃) ppm.

HRMS (ESI-TOF, + mode) m/z calcd for C₃₂H₃₁N₂O₂S 507.2101, found 507.2076 [M+H]⁺.

N-Benzyl-N-((R)-3-((R)-2-(hydroxymethyl)pyrrolidin-1-yl)-3-phenylprop-1-yn-1-yl)-4-methylbenzenesulfonamide (G.23) (CAS for (R),(S): 2820061-08-1, for (R),(R): 2820061-07-0)



Chemical Formula: C₂₈H₃₀N₂O₃S
Molecular Weight: 474,6190

Following the General Procedure I, the title compound **G.23** was isolated as a pale yellow solid (105 mg, 221 μ mol) in a diastereomeric ratio of 92:8. Yield 88%.

R_f = 0.13 (SiO₂, cyclohexane/EtOAc 7:3).

ATR-FTIR (neat) ν = 3476, 3059, 3031, 2961, 2923, 2874, 2820, 2243, 1595, 1493, 1448, 1402, 1354, 1249, 1166, 1085, 1001, 882,

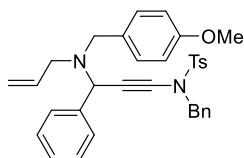
814, 768, 695 cm⁻¹.

¹H NMR (500 MHz, CDCl₃) (major diastereomer) δ = 7.84 – 7.78 (m, 2H, H_{aro}), 7.37 – 7.30 (m, 8H, H_{aro}), 7.27 – 7.23 (m, 5H, H_{aro}), 4.86 (s, 1H, CHC \equiv), 4.61 (d, J = 13.5 Hz, 1H, NCH₂ benzyl), 4.52 (d, J = 13.6 Hz, 1H, NCH₂ benzyl), 3.65 (dd, J = 10.9, 3.4 Hz, 1H, CH₂O), 3.39 (dd, J = 11.0, 2.3 Hz, 1H, CH₂O), 2.77 – 2.70 (m, 1H), 2.61 – 2.51 (m, 1H), 2.47 (s, 3H, CH₃), 2.36 – 2.28 (m, 2H), 1.75 – 1.62 (m, 2H), 1.55 – 1.46 (m, 2H) ppm.

$^{13}\text{C}\{^1\text{H}\}$ NMR (126 MHz, CDCl_3) δ = 144.9 (C_q), 139.1 (C_q), 134.6 (C_q), 134.5 (C_q), 129.9 (C_{aroH}), 129.1 (C_{aroH}), 128.7 (C_{aroH}), 128.5 (C_{aroH}), 128.3 (C_{aroH}), 128.1 (C_{aroH}), 127.9 (C_{aroH}), 127.5 (C_{aroH}), 80.3 ($\text{NC}\equiv\text{C}$), 67.2 ($\text{NC}\equiv\text{C}$), 61.7 (OCH_2), 61.5 (NCH), 55.8 (CHCH_2OH), 55.5 (TsNCH_2), 47.5 (NCH_2CH_2), 27.8 (CH_2), 23.4 (CH_2), 21.8 (CH_3) ppm.

HRMS (ESI-TOF, + mode) m/z calcd for $\text{C}_{28}\text{H}_{31}\text{N}_2\text{O}_3\text{S}$ 475.2050, found 475.2067 [$\text{M}+\text{H}$] $^+$.

N-(3-(Allyl(4-methoxybenzyl)amino)-3-phenylprop-1-yn-1-yl)-N-benzyl-4-methylbenzenesulfonamide (G.25)



Chemical Formula: $\text{C}_{34}\text{H}_{34}\text{N}_2\text{O}_3\text{S}$
Molecular Weight: 550,7170

Following the General Procedure I, the title compound **G.25** was isolated as a colourless resin (100 mg, 182 μmol). Yield 67%.

R_f = 0.57 (SiO_2 , cyclohexane/EtOAc 7:3).

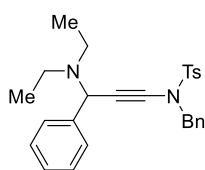
ATR-FTIR (neat) ν = 3062, 3031, 3001, 2929, 2833, 2240, 1611, 1511, 1450, 1365, 1301, 1247, 1167, 1090, 1034, 919, 870, 831, 740, 697 cm^{-1} .

^1H NMR (500 MHz, CDCl_3) δ = 7.77 (m, 2H, H_{aro}), 7.33 – 7.23 (m, 9H, H_{aro}), 7.19 – 7.09 (m, 3H, H_{aro}), 7.04 (m, 2H, H_{aro}), 6.77 – 6.68 (m, 2H, $2 \times \text{OC}_q\text{CH}_{\text{aro}}$), 5.63 (dddd, J = 16.9, 9.9, 8.5, 3.9 Hz, 1H, $\text{CH}=\text{CH}_2$), 5.03 (dt, J = 17.1, 2.2 Hz, 1H, $\text{CH}=\text{CH}_2$), 4.97 (dt, J = 10.1, 2.0 Hz, 1H, $\text{CH}=\text{CH}_2$), 4.63 (s, 1H, $\text{CHC}\equiv$), 4.55 (d, J = 13.6 Hz, 1H, TsNCH_2), 4.51 (d, J = 13.7 Hz, 1H, TsNCH_{2z}), 3.69 (s, 3H, OCH_3), 3.41 (d, J = 13.3 Hz, 1H, NCH_2 PMB), 2.83 (dt, J = 13.4, 4.0 Hz 2H, NCH_2 allyl), 2.48 (dd, J = 14.1, 8.6 Hz, 1H, NCH_2 PMB), 2.37 (s, 3H, CCH_3) ppm.

$^{13}\text{C}\{^1\text{H}\}$ NMR (126 MHz, CDCl_3) δ = 158.7 (CH_3OC_q), 144.8 (C_q), 139.4 (C_q), 136.8 (CH), 134.6 (C_q), 131.6 (C_q), 130.0 (CH), 129.9 (CH), 129.1 (CH), 128.8 (CH), 128.5 (CH), 128.2 (CH), 128.0(1) (CH), 128.0(0) (CH), 127.3 (CH), 117.2 ($\text{CH}=\text{CH}_2$), 113.6 (CH), 80.7 ($\text{NC}\equiv\text{C}$), 66.8 ($\text{NC}\equiv\text{C}$), 55.8 (CH or CH_3), 55.6 (CH_2), 55.4 (CH or CH_3), 53.8 (CH_2), 53.1 (CH_2), 21.8 (CH_3) ppm. N.B.: one aromatic C_q is missing, perhaps due to signal overlap.

HRMS (ESI-TOF, + mode) m/z calcd for $\text{C}_{34}\text{H}_{34}\text{N}_2\text{NaO}_3\text{S}$ 573.2182, found 573.2183 [$\text{M}+\text{Na}$] $^+$.

N-Benzyl-N-(3-(diethylamino)-3-phenylprop-1-yn-1-yl)-4-methylbenzenesulfonamide (G.26) (CAS: 2820061-10-5)



Chemical Formula: $\text{C}_{27}\text{H}_{30}\text{N}_2\text{O}_2\text{S}$
Molecular Weight: 446,6090

Following the General Procedure I, the title compound **G.26** was isolated as a colourless oil (59 mg, 133 μmol). Yield 53% (69% based on recovered ynamide starting material).

R_f = 0.31 (SiO_2 , cyclohexane/EtOAc 8:2).

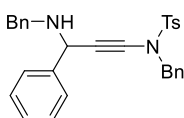
ATR-FTIR (neat) ν = 3087, 3062, 3030, 2968, 2931, 2872, 2820, 2237, 1597, 1493, 1449, 1364, 1166, 1089, 1026, 868, 812, 717, 695 cm^{-1} .

^1H NMR (500 MHz, CDCl_3) δ = 7.77 – 7.71 (m, 2H, H_{aro}), 7.30 – 7.23 (m, 7H, H_{aro}), 7.22 – 7.14 (m, 5H, H_{aro}), 4.73 (s, 1H, $\text{CHC}\equiv$), 4.51 (d, J = 13.6 Hz, 1H, NCH_2 benzyl), 4.46 (d, J = 13.6 Hz, 1H, NCH_2 benzyl), 2.40 (s, 3H, CH_3 tosyl), 2.29 (dq, J = 12.7, 7.4 Hz, 2H, $2 \times \text{CH}_2\text{CH}_3$), 2.03 (dq, J = 13.6, 6.9 Hz, 2H, $2 \times \text{CH}_2\text{CH}_3$), 0.85 (t, J = 7.1 Hz, 6H, $2 \times \text{CH}_2\text{CH}_3$) ppm.

$^{13}\text{C}\{^1\text{H}\}$ NMR (126 MHz, CDCl_3) δ = 144.7 (C_q), 140.0 (C_q), 134.7 (C_q), 134.6 (C_q), 129.8 (C_{aroH}), 129.1 (C_{aroH}), 128.7 (C_{aroH}), 128.4(3) (C_{aroH}), 128.4(0) (C_{aroH}), 128.0 (C_{aroH}), 127.9(6) (C_{aroH}), 127.1 (C_{aroH}), 80.0 ($\text{NC}\equiv\text{C}$), 67.5 ($\text{NC}\equiv\text{C}$), 56.6 (NCH), 55.6 (TsNCH_2), 44.4 (NCH_2CH_3), 21.8 (CH_3 tosyl), 13.6 (CH_2CH_3) ppm.

HRMS (ESI-TOF, + mode) m/z calcd for $\text{C}_{27}\text{H}_{31}\text{N}_2\text{O}_2\text{S}$ 447.2101, found 447.2133 [$\text{M}+\text{H}$] $^+$.

N-Benzyl-N-(3-(benzylamino)-3-phenylprop-1-yn-1-yl)-4-methylbenzenesulfonamide (G.30) (CAS: 2820061-11-6)



Chemical Formula: C₃₀H₂₈N₂O₂S
Molecular Weight: 480,6260

Ti(OEt)₄ (20.0 μL, 64 μmol, 1.0 eq.) was added to a suspension of *N*-benzylbenzaldimine (**L.62**, 25.0 mg, 128 μmol, 2.0 eq.), *N*-Benzyl-*N*-ethynyl-4-methylbenzenesulfonamide (**Y.1**, 18.5 mg, 64 μmol, 1.0 eq.) and Cu^I-USY (2.9 mg, 8 mol%) in EtOAc (1 mL) at room temperature. The vial was flushed with argon and capped.

The mixture was stirred at 30 °C for six days. Then, the mixture was dissolved in EtOAc, filtered over celite and concentrated. The crude was purified by column chromatography on silica gel (SiO₂, cyclohexane/EtOAc/Et₃N 99:0:1 to 89:10:1). The title compound **G.30** was isolated as a yellow oil (5.3 mg, 11 μmol). Yield 17%.

R_f = 0.45 (SiO₂, cyclohexane/EtOAc 7:3).

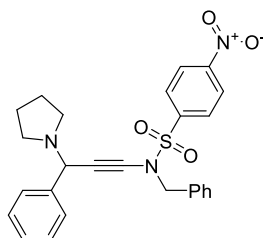
ATR-FTIR (neat) ν = 3320, 3086, 3061, 3029, 2922, 2852, 2241, 1597, 1494, 1360, 1166, 1089, 813, 695 cm⁻¹.

¹H NMR (500 MHz, CDCl₃) δ = 7.77 – 7.73 (m, 2H, H_{aro}), 7.35 – 7.21 (m, 17H, H_{aro}), 4.56 (d, *J* = 13.7 Hz, 1H TsNCH₂), 4.55 (s, 1H, CHC≡), 4.51 (d, *J* = 13.7 Hz, 1H, TsNCH₂), 3.72 (d, *J* = 13.0 Hz, 1H, NHCH₂), 3.65 (d, *J* = 13.0 Hz, 1H, NHCH₂), 2.42 (s, 3H, CH₃) ppm.

¹³C{¹H} NMR (126 MHz, CDCl₃) δ = 144.8 (C_q), 140.3 (C_q), 139.9 (C_q), 134.6(1) (C_q), 134.6(0) (C_q), 129.9 (C_{aro}H), 129.1 (C_{aro}H), 128.7 (C_{aro}H), 128.5(3) (C_{aro}H), 128.5(1) (C_{aro}H), 128.4 (C_{aro}H), 128.4 (C_{aro}H), 127.9 (C_{aro}H), 127.7 (C_{aro}H), 127.6 (C_{aro}H), 127.1 (C_{aro}H), 78.9 (NC≡C), 71.1 (NC≡C), 55.6 (NCH₂), 53.1 (NCH), 50.9 (NCH₂), 21.8 (CH₃) ppm.

HRMS (ESI-TOF, + mode) *m/z* calcd for C₃₀H₂₈N₂NaO₂S 503.1764, found 503.1727 [M+Na]⁺.

N-Benzyl-4-nitro-N-(3-phenyl-3-(pyrrolidin-1-yl)prop-1-yn-1-yl)benzenesulfonamide (G.32) (CAS: 2820061-12-7)



Chemical Formula: C₂₆H₂₅N₃O₄S
Molecular Weight: 475,5630

Following the General Procedure I, the title compound **G.32** was isolated as an orange solid (83 mg, 175 μmol). Yield 70%.

R_f = 0.36 (SiO₂, cyclohexane/EtOAc 7:3).

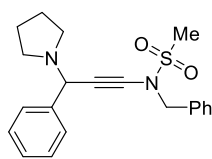
ATR-FTIR (neat) ν = 3104, 3063, 3026, 2959, 2925, 2870, 2848, 2241, 1604, 1529, 1450, 1368, 1307, 1171, 1088, 1006, 898, 854, 740, 700 cm⁻¹.

¹H NMR (500 MHz, CDCl₃) δ = 8.26 – 8.22 (m, 2H, H_{aro-Ns}), 7.96 – 7.90 (m, 2H, H_{aro-Ns}), 7.35 – 7.27 (m, 10H, H_{aro}), 4.67 (s, 1H, CHC≡), 4.62 (d, *J* = 13.9 Hz, 1H, NCH₂ benzyl), 4.58 (d, *J* = 13.9 Hz, 1H, NCH₂ benzyl), 2.46 – 2.30 (m, 4H, 2 × NCH₂CH₂), 1.73 – 1.57 (m, 4H, 2 × NCH₂CH₂) ppm.

¹³C{¹H} NMR (126 MHz, CDCl₃) δ = 150.5 (C_q), 143.0 (C_q), 139.3 (C_q), 133.9 (C_q), 129.1 (C_{aro}H), 128.9, (C_{aro}H) 128.8 (C_{aro}H), 128.4 (C_{aro}H), 128.1 (C_{aro}H), 127.8 (C_{aro}H), 124.3 (C_{aro}H), 78.8 (NC≡C), 69.4 (NC≡C), 58.7 (NCH), 56.2 (TsNCH₂), 50.1 (NCH₂CH₂), 23.5 (NCH₂CH₂) ppm. N.B.: one C_{aro}H is missing, perhaps due to signal overlap.

HRMS (ESI-TOF, + mode) *m/z* calcd for C₂₆H₂₆N₃O₄S 476.1639, found 476.1630 [M+H]⁺.

N-Benzyl-N-(3-phenyl-3-(pyrrolidin-1-yl)prop-1-yn-1-yl)methanesulfonamide (G.33)
(CAS: 2820061-13-8)



Chemical Formula: C₂₁H₂₄N₂O₂S
Molecular Weight: 368,4950

Following the General Procedure I, the title compound **G.33** was isolated as a pale yellow oil (66 mg, 179 μmol). Yield 71%.

R_f = 0.53 (SiO₂, cyclohexane/EtOAc 1:1).

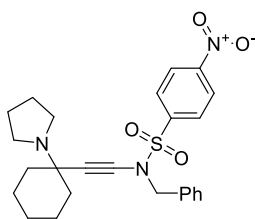
ATR-FTIR (neat) ν = 3086, 3060, 3030, 3012, 2959, 2931, 2873, 2814, 2240, 1624, 1602, 1587, 1493, 1450, 1346, 1154, 959, 906, 780, 698 cm⁻¹.

¹H NMR (500 MHz, CDCl₃) δ = 7.46 – 7.42 (m, 2H, H_{aro}), 7.41 – 7.35 (m, 5H, H_{aro}), 7.33 – 7.22 (m, 3H, H_{aro}), 4.79 (s, 1H, CHC≡), 4.66 (d, *J* = 14.2 Hz, 1H, NCH₂ benzyl), 4.62 (d, *J* = 14.2 Hz, 1H, NCH₂ benzyl), 2.94 (s, 3H, CH₃), 2.54 – 2.40 (m, 4H, 2 × NCH₂CH₂), 1.76 – 1.64 (m, 4H, 2 × NCH₂CH₂) ppm.

¹³C{¹H} NMR (126 MHz, CDCl₃) δ = 139.5 (C_q), 134.6 (C_q), 129.2 (C_{aro}H), 128.9 (C_{aro}H), 128.8 (C_{aro}H), 128.3 (C_{aro}H), 128.2 (C_{aro}H), 127.6 (C_{aro}H), 79.5 (NC≡C), 68.8 (NC≡C), 58.6 (NCH), 55.7 (TsNCH₂), 50.0 (NCH₂CH₂), 38.7 (CH₃), 23.5 (NCH₂CH₂) ppm.

HRMS (ESI-TOF, + mode) *m/z* calcd for C₂₁H₂₅N₂O₂S 369.1631, found 369.1648 [M+H]⁺.

N-Benzyl-4-nitro-N-((1-(pyrrolidin-1-yl)cyclohexyl)ethynyl)benzenesulfonamide (G.34)
(CAS: 2820061-14-9)



Chemical Formula: C₂₅H₂₉N₃O₄S
Molecular Weight: 467,5840

Following the General Procedure I, the title compound **G.34** was isolated as a pale yellow solid (96 mg, 205 μmol). Yield 82%.

R_f = 0.60 (SiO₂, CH₂Cl₂/MeOH 9:1).

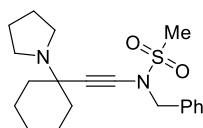
ATR-FTIR (neat) ν = 3100, 3072, 3032, 2928, 2855, 2822, 2230, 1604, 1527, 1454, 1376, 1346, 1251, 1172, 1123, 1086, 1018, 903, 785, 740, 684 cm⁻¹.

¹H NMR (500 MHz, CDCl₃) δ = 8.36 – 8.29 (m, 2H, H_{aro-Ns}), 8.03 – 7.96 (m, 2H, H_{aro-Ns}), 7.34 – 7.27 (m, 5H, H_{aro}), 4.57 (s, 2H, NCH₂ benzyl), 2.53 – 2.40 (m, 4H, 2 × NCH₂CH₂), 1.80 – 1.74 (m, 2H, 2 × NC_qCH₂), 1.67 – 1.59 (m, 4H, 2 × NCH₂CH₂), 1.58 – 1.46 (m, 3H), 1.37 (td, *J* = 12.3, 3.3 Hz, 2H), 1.31 – 1.21 (m, 3H), 1.17 – 1.07 (m, 1H) ppm.

¹³C{¹H} NMR (126 MHz, CDCl₃) δ = 150.5 (C_q), 143.2 (C_q), 134.0 (C_q), 129.0(5) (C_{aro}H), 129.0(3) (C_{aro}H), 128.8 (C_{aro}H), 128.7 (C_{aro}H), 124.2 (C_{aro}H), 77.9 (NC≡C), 72.4 (NC≡C), 59.3 (NC_qCH₂), 56.3 (TsNCH₂), 47.0 (NCH₂CH₂), 37.9 (CH₂), 25.6 (CH₂), 23.4 (CH₂), 22.9 (CH₂) ppm.

HRMS (ESI-TOF, + mode) *m/z* calcd for C₂₅H₂₉N₃NaO₄S 490.1771, found 490.1753 [M+Na]⁺.

N-Benzyl-N-((1-(pyrrolidin-1-yl)cyclohexyl)ethynyl)methanesulfonamide (G.35)
(CAS: 2820061-15-0)



Chemical Formula: C₂₀H₂₈N₂O₂S
Molecular Weight: 360,5160

Following the General Procedure I, the title compound **G.35** was isolated as a colourless solid (49 mg, 136 μmol). Yield 54%.

R_f = 0.42 (SiO₂, CH₂Cl₂/MeOH 9:1).

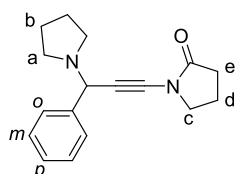
ATR-FTIR (neat) ν = 3069, 3025, 2950, 2930, 2858, 2812, 2232, 1495, 1354, 1161, 956, 787, 695 cm⁻¹.

¹H NMR (500 MHz, CDCl₃) δ = 7.44 – 7.31 (m, 5H, H_{aro}), 4.58 (s, 2H, NCH₂ benzyl), 2.92 (s, 3H, CH₃), 2.61 – 2.48 (m, 4H, 2 × NCH₂CH₂), 1.89 – 1.80 (m, 2H, 2 × NC_qCH₂), 1.71 – 1.64 (m, 4H, 2 × NCH₂CH₂), 1.64 – 1.49 (m, 3H), 1.45 – 1.34 (m, 4H), 1.18 – 1.08 (m, 1H) ppm.

$^{13}\text{C}\{^1\text{H}\}$ NMR (126 MHz, CDCl_3) δ = 134.6 ($\text{C}_{\text{q-Ph}}$), 129.2 (C_{aroH}), 128.7(4) (C_{aroH}), 128.7(0) (C_{aroH}), 78.5 ($\text{NC}\equiv\text{C}$), 72.0 ($\text{NC}\equiv\text{C}$), 59.3 (NC_qCH_2), 55.7 (TsNCH_2), 47.0 (NCH_2CH_2), 38.2 (CH_3), 38.0 (CH_2), 25.6 (CH_2), 23.4 (CH_2), 23.1 (CH_2) ppm.

HRMS (ESI-TOF, + mode) m/z calcd for $\text{C}_{20}\text{H}_{29}\text{N}_2\text{O}_2\text{S}$ 361.1944, found 361.1929 [$\text{M}+\text{H}$] $^+$.

1-(3-Phenyl-3-(pyrrolidin-1-yl)prop-1-yn-1-yl)pyrrolidin-2-one (G.36) (CAS: 2820061-16-1)



Chemical Formula: $\text{C}_{17}\text{H}_{20}\text{N}_2\text{O}$
Molecular Weight: 268,3600

Following the General Procedure I, the title compound **G.36** was isolated as a pale orange solid (18 mg, 68 μmol). Yield 27%.

R_f = 0.42 (SiO_2 , $\text{CH}_2\text{Cl}_2/\text{MeOH}$ 9:1).

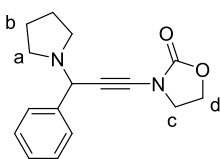
ATR-FTIR (neat) ν = 3084, 3060, 3028, 2962, 2932, 2875, 2807, 2704, 2246, 1716, 1627, 1602, 1392, 1262, 1194, 1028, 700 cm^{-1} .

^1H NMR (500 MHz, CDCl_3) δ = 7.51 – 7.43 (m, 2H, $m\text{-H}_{\text{aro}}$), 7.26 (t, J = 7.5 Hz, 2H, $m\text{-H}_{\text{aro}}$), 7.22 – 7.17 (m, 1H $p\text{-H}_{\text{aro}}$), 4.77 (s, 1H, $\text{CHC}\equiv$), 3.68 – 3.62 (m, 2H, H_c), 2.59 – 2.48 (m, 4H, H_a), 2.38 (t, J = 8.1 Hz, 2H, H_e), 2.07 (quint, J = 7.6 Hz, 2H, H_d), 1.75 – 1.63 (m, 4H, $2 \times \text{H}_b$) ppm.

$^{13}\text{C}\{^1\text{H}\}$ NMR (126 MHz, CDCl_3) δ = 176.2 ($\text{C}=\text{O}$), 139.6 ($\text{C}_{\text{q-Ph}}$), 128.3(322) (C_{aroH}), 128.3(30) (C_{aroH}), 127.6 (C_{aroH}), 77.9 ($\text{NC}\equiv\text{C}$), 69.4 ($\text{NC}\equiv\text{C}$), 58.8 (NCH), 50.3 (CH_2), 50.2 (CH_2), 29.8 ($\text{O}=\text{CCH}_2$), 23.5 (CH_2), 18.9 (CH_2) ppm.

HRMS (ESI-TOF, + mode) m/z calcd for $\text{C}_{17}\text{H}_{21}\text{N}_2\text{O}$ 269.1648, found 269.1639 [$\text{M}+\text{H}$] $^+$.

3-(3-Phenyl-3-(pyrrolidin-1-yl)prop-1-yn-1-yl)oxazolidin-2-one (G.37) (CAS: 820061-17-2)



Chemical Formula: $\text{C}_{16}\text{H}_{18}\text{N}_2\text{O}_2$
Molecular Weight: 270,3320

Following the General Procedure I, the title compound **G.37** was isolated as a pale red solid (77 mg, 285 μmol). Yield 90%.

R_f = 0.52 (SiO_2 , $\text{CH}_2\text{Cl}_2/\text{MeOH}$ 9:1).

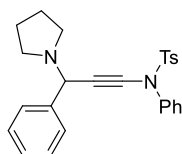
ATR-FTIR (neat) ν = 3058, 3032, 2964, 2915, 2873, 2805, 2246, 1752, 1475, 1418, 1218, 1199, 1110, 1028, 865, 748, 702 cm^{-1} .

^1H NMR (500 MHz, CDCl_3) δ = 7.56 – 7.49 (m, 2H, H_{aro}), 7.37 – 7.31 (m, 2H, H_{aro}), 7.30 – 7.26 (m, 1H, H_{aro}), 4.80 (s, 1H, $\text{CHC}\equiv$), 4.49 – 4.40 (m, 2H, H_d), 3.98 – 3.89 (m, 2H, H_c), 2.67 – 2.54 (m, 4H, H_a), 1.83 – 1.71 (m, 4H, H_b). ppm.

$^{13}\text{C}\{^1\text{H}\}$ NMR (126 MHz, CDCl_3) δ = 156.4 ($\text{C}=\text{O}$), 139.4 ($\text{C}_{\text{q-Ph}}$), 128.4 (C_{aroH}), 128.3 (C_{aroH}), 127.7 (C_{aroH}), 76.5 ($\text{NC}\equiv\text{C}$), 68.3 ($\text{NC}\equiv\text{C}$), 63.0 (OCH_2), 58.8 (NCH), 50.4 (CH_2), 47.1 (CH_2), 23.5 (NCH_2CH_2) ppm.

HRMS (ESI-TOF, + mode) m/z calcd for $\text{C}_{16}\text{H}_{18}\text{N}_2\text{NaO}_2$ 293.1260, found 293.1251 [$\text{M}+\text{Na}$] $^+$.

4-Methyl-N-phenyl-N-(3-phenyl-3-(pyrrolidin-1-yl)prop-1-yn-1-yl)benzenesulfonamide (G.39) (CAS: 2820061-18-3)



Chemical Formula: $\text{C}_{26}\text{H}_{26}\text{N}_2\text{O}_2\text{S}$
Molecular Weight: 430,5660

Following the General Procedure I, the title compound **G.39** was isolated as a yellow solid (181 mg, 420 μmol). Yield 84%.

R_f = 0.39 (SiO_2 , cyclohexane/ EtOAc 7:3).

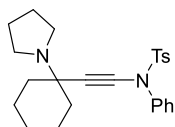
ATR-FTIR (neat) ν = 3059, 3028, 2958, 2924, 2874, 2853, 2814, 2244, 1685, 1595, 1542, 1489, 1446, 1370, 1257, 1156, 1088, 1028, 922, 888, 812, 755, 691 cm^{-1} .

^1H NMR (500 MHz, CDCl_3) δ = 7.56 – 7.52 (m, 2H, H_{aro}), 7.53 – 7.47 (m, 2H, H_{aro}), 7.36 – 7.27 (m, 8H, H_{aro}), 7.22 (m, 2H, H_{aro}), 4.84 (s, 1H, $\text{CHC}\equiv$), 2.65 – 2.52 (m, 4H, $2 \times \text{NCH}_2\text{CH}_2$), 2.42 (s, 3H, CH_3), 1.80 – 1.71 (m, 4H, $2 \times \text{NCH}_2\text{CH}_2$) ppm.

$^{13}\text{C}\{^1\text{H}\}$ NMR (126 MHz, CDCl_3) δ = 145.0 (C_q), 139.7 (C_q), 139.2 (C_q), 133.1 (C_q), 129.5 (C_{aroH}), 129.2 (C_{aroH}), 128.4 (C_{aroH}), 128.3(1) (C_{aroH}), 128.3(0) (C_{aroH}), 128.2 (C_{aroH}), 127.6 (C_{aroH}), 126.2 (C_{aroH}), 80.4 ($\text{NC}\equiv\text{C}$), 67.6 ($\text{NC}\equiv\text{C}$), 58.7 (NCH), 50.1 (NCH_2CH_2), 23.6 (NCH_2CH_2), 21.8 (CH_3) ppm.

HRMS (ESI-TOF, + mode) m/z calcd for $\text{C}_{26}\text{H}_{26}\text{N}_2\text{NaO}_2\text{S}$ 453.1607, found 453.1592 $[\text{M}+\text{Na}]^+$.

4-Methyl-N-phenyl-N-((1-(pyrrolidin-1-yl)cyclohexyl)ethynyl)benzenesulfonamide (G.40) (CAS: 2820061-19-4)



Chemical Formula: $\text{C}_{25}\text{H}_{30}\text{N}_2\text{O}_2\text{S}$
Molecular Weight: 422.5870

Following the General Procedure I, the title compound **G.40** was isolated as an orange solid (165 mg, 390 μmol). Yield 78%.

R_f = 0.45 (SiO_2 , $\text{CH}_2\text{Cl}_2/\text{MeOH}$ 9:1).

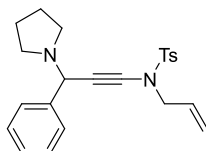
ATR-FTIR (neat) ν = 3061, 2955, 2934, 2856, 2818, 2226, 1592, 1487, 1365, 1242, 1165, 1087, 926, 812, 768, 690 cm^{-1} .

^1H NMR (300 MHz, CDCl_3) δ = 7.59 – 7.50 (m, 2H, H_{aro}), 7.40 – 7.20 (m, 7H, H_{aro}), 2.74 – 2.60 (m, 4H, 2 \times NCH_2CH_2), 2.43 (s, 3H, CH_3), 1.98 – 1.88 (m, 2H, 2 \times NC_qCH_2), 1.79 – 1.68 (m, 4H, 2 \times NCH_2CH_2), 1.68 – 1.38 (m, 7H), 1.24 – 1.10 (m, 1H) ppm.

$^{13}\text{C}\{^1\text{H}\}$ NMR (126 MHz, CDCl_3) δ = 144.9 (C_q), 139.6 (C_q), 132.9 (C_q), 129.4 (C_{aroH}), 129.1 (C_{aroH}), 128.4 (C_{aroH}), 128.0 (C_{aroH}), 126.1 (C_{aroH}), 79.5 ($\text{NC}\equiv\text{C}$), 71.0 ($\text{NC}\equiv\text{C}$), 59.4 (NC_qCH_2), 47.2 (NCH_2CH_2), 38.1 (CH_2), 25.7 (CH_2), 23.5 (CH_2), 23.1 (CH_2), 21.8 (CH_3) ppm.

HRMS (ESI-TOF, + mode) m/z calcd for $\text{C}_{25}\text{H}_{31}\text{N}_2\text{O}_2\text{S}$ 423.2101, found 423.2128 $[\text{M}+\text{H}]^+$.

N-Allyl-4-methyl-N-(3-phenyl-3-(pyrrolidin-1-yl)prop-1-yn-1-yl)benzenesulfonamide (G.41) (CAS: 2820061-20-7)



Chemical Formula: $\text{C}_{23}\text{H}_{26}\text{N}_2\text{O}_2\text{S}$
Molecular Weight: 394.5330

Following the General Procedure I, the title compound **G.41** was isolated as an off-white viscous oil (77 mg, 195 μmol). Yield 80%.

R_f = 0.20 (SiO_2 , cyclohexane/ EtOAc 7:3).

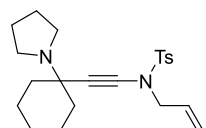
ATR-FTIR (neat) ν = 3084, 3061, 3028, 2963, 2928, 2874, 2810, 2237, 1646, 1597, 1493, 1449, 1363, 1291, 1166, 1089, 1028, 928, 862, 758, 660 cm^{-1} .

^1H NMR (500 MHz, CDCl_3) δ = 7.79 – 7.75 (m, 2H, H_{aro}), 7.46 (dd, J = 7.1, 1.8 Hz, 2H, H_{aro}), 7.34 – 7.27 (m, 5H, H_{aro}), 5.77 (ddt, J = 16.6, 10.1, 6.3 Hz, 1H, $\text{CH}=\text{CH}_2$), 5.26 (dd, J = 17.1, 1.4 Hz, 1H, $\text{CH}=\text{CH}_2$), 5.22 (dd, J = 10.2, 1.2 Hz, 1H, $\text{CH}=\text{CH}_2$), 4.79 (s, 1H, $\text{CHC}\equiv$), 4.01 (dq, J = 6.4, 1.4 Hz, 2H, TsNCH_2), 2.58 – 2.46 (m, 4H, 2 \times NCH_2CH_2), 2.44 (s, 3H, CH_3), 1.75 – 1.69 (m, 4H, 2 \times NCH_2CH_2) ppm.

$^{13}\text{C}\{^1\text{H}\}$ NMR (126 MHz, CDCl_3) δ = 144.7 (C_q), 139.7 (C_q), 134.7 (C_q), 131.2 (CH), 129.8 (CH), 128.3 (CH), 128.2 (CH), 128.0 (CH), 127.6 (CH), 120.2 ($\text{CH}=\text{CH}_2$), 79.7 ($\text{NC}\equiv\text{C}$), 67.5 ($\text{NC}\equiv\text{C}$), 58.6 (NCH), 54.4 (TsNCH_2), 50.0 (NCH_2CH_2), 23.5 (NCH_2CH_2), 21.8 (CH_3) ppm.

HRMS (ESI-TOF, + mode) m/z calcd for $\text{C}_{23}\text{H}_{27}\text{N}_2\text{O}_2\text{S}$ 395.1788, found 395.1784 $[\text{M}+\text{H}]^+$.

N-Allyl-4-methyl-N-((1-(pyrrolidin-1-yl)cyclohexyl)ethynyl)benzenesulfonamide (G.42) (CAS: 2820061-21-8)



Chemical Formula: $\text{C}_{22}\text{H}_{30}\text{N}_2\text{O}_2\text{S}$
Molecular Weight: 386.5540

Following the General Procedure I, the title compound **G.42** was isolated as an off-white viscous oil (76 mg, 197 μmol). Yield 79%.

R_f = 0.36 (SiO_2 , $\text{CH}_2\text{Cl}_2/\text{MeOH}$ 9:1).

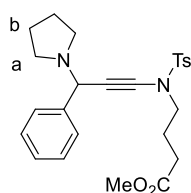
ATR-FTIR (neat) ν = 3070, 2929, 2854, 2812, 2232, 1645, 1597, 1494, 1364, 1167, 1123, 1090, 1034, 925, 812, 760, 660 cm^{-1} .

¹H NMR (500 MHz, CDCl₃) δ = 7.81 – 7.77 (m, 2H, H_{aro}), 7.33 (m, 2H, H_{aro}), 5.73 (ddt, J = 16.6, 10.1, 6.3 Hz, 1H, CH=CH₂), 5.26 – 5.18 (m, 2H, CH=CH₂), 3.97 (dt, J = 6.3, 1.3 Hz, 2H, TsNCH₂), 2.65 – 2.57 (m, 4H, 2 × NCH₂CH₂), 2.45 (s, 3H, CH₃), 1.90 – 1.83 (m, 2H, 2 × NC_qCH₂), 1.73 – 1.68 (m, 4H, 2 × NCH₂CH₂), 1.62 – 1.52 (m, 3H), 1.50 – 1.36 (m, 4H), 1.19 – 1.09 (m, 1H) ppm.

¹³C{¹H} NMR (126 MHz, CDCl₃) δ = 144.6 (C_q), 134.7 (C_q), 131.3 (CH), 129.7 (CH), 128.0 (CH), 120.0 (CH=CH₂), 78.7 (NC≡C), 70.7 (NC≡C), 59.4 (NC_qCH₂), 54.6 (TsNCH₂), 47.1 (NCH₂CH₂), 38.1 (CH₂), 25.7 (CH₂), 23.5 (CH₂), 23.1 (CH₂), 21.8 (CH₃) ppm.

HRMS (ESI-TOF, + mode) m/z calcd for C₂₂H₃₁N₂O₂S 387.2101, found 387.2127 [M+H]⁺.

Methyl 4-((4-methyl-N-(3-phenyl-3-(pyrrolidin-1-yl)prop-1-yn-1-yl)phenyl)sulfonamido)-butanoate (G.45) (CAS: 2820061-22-9)



Chemical Formula: C₂₅H₃₀N₂O₄S
Molecular Weight: 454,5850

Following the General Procedure I, the title compound **G.45** was isolated as a yellow viscous oil (110 mg, 242 μ mol). Yield 97%.

R_f = 0.15 (SiO₂, cyclohexane/EtOAc 7:3).

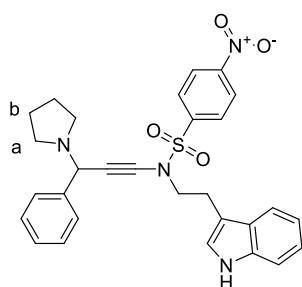
ATR-FTIR (neat) ν = 3062, 3029, 2954, 2875, 2807, 2236, 1735, 1627, 1597, 1493, 1448, 1363, 1166, 1090, 1029, 900, 814, 701, 668 cm⁻¹.

¹H NMR (500 MHz, CDCl₃) δ = 7.78 – 7.73 (m, 2H, H_{aro}), 7.49 – 7.44 (m, 2H, H_{aro}), 7.35 – 7.26 (m, 5H, H_{aro}), 4.78 (s, 1H, CHC≡), 3.67 (s, 3H, OCH₃), 3.47 – 3.35 (m, 2H, TsNCH₂), 2.58 – 2.48 (m, 4H, H_a), 2.45 – 2.40 (m, 5H, CH₃ tosyl & CH₂CO₂Me), 2.00 (quint, J = 7.0 Hz, 2H, TsNCH₂CH₂), 1.78 – 1.68 (m, 4H, H_b) ppm.

¹³C{¹H} NMR (126 MHz, CDCl₃) δ = 173.2 (C=O), 144.7 (C_q), 139.7 (C_q), 134.5 (C_q), 129.9 (C_{aro}H), 128.3(2) (C_{aro}H), 128.3(0) (C_{aro}H), 127.8 (C_{aro}H), 127.6 (C_{aro}H), 79.4 (NC≡C), 67.7 (NC≡C), 58.7 (NCH), 51.8 (OCH₃), 50.7 (NCH₂), 50.1 (NCH₂), 30.5 (CH₂), 23.6 (CH₂), 23.2 (CH₂), 21.8 (CCH₃) ppm.

HRMS (ESI-TOF, + mode) m/z calcd for C₂₅H₃₀N₂NaO₄S 477.1818, found 477.1835 [M+Na]⁺.

N-(2-(1H-Indol-3-yl)ethyl)-4-nitro-N-(3-phenyl-3-(pyrrolidin-1-yl)prop-1-yn-1-yl)benzenesulfonamide (G.46) (CAS: 2820061-23-0)



Chemical Formula: C₂₉H₂₈N₄O₄S
Molecular Weight: 528,6270

Following the General Procedure I, the title compound **G.46** was isolated as an orange foam (55 mg, 104 μ mol). Yield 77%.

R_f = 0.14 (SiO₂, cyclohexane/EtOAc 7:3).

ATR-FTIR (neat) ν = 3285, 3102, 3060, 3033, 2961, 2929, 2873, 2808, 2249, 1607, 1527, 1461, 1346, 1308, 1230, 1158, 1093, 925, 853, 735, 606 cm⁻¹.

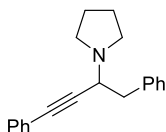
¹H NMR (500 MHz, CDCl₃) δ = 8.12 – 8.05 (m, 2H, H_{aro-Ns}), 7.82 – 7.76 (m, 2H, H_{aro-Ns}), 7.67 – 7.60 (m, 2H), 7.45 – 7.26 (m, 6H), 7.13 (t, J = 7.5 Hz, 1H), 6.99 (s, 1H), 4.98 (s, 1H, CHC≡), 3.38 (t, J = 6.4 Hz, 2H, NsNCH₂), 2.91 (t, J = 6.4 Hz, 2H, NsNCH₂CH₂), 2.77 – 2.66 (m, 4H, H_a), 1.87 – 1.78 (m, 4H, 2 × H_b) ppm.

¹³C{¹H} NMR (126 MHz, CDCl₃) δ = 149.7 (C_q), 145.4 (C_q), 139.6 (C_q), 138.7 (C_q), 128.5 (C_{aro}H), 128.0 (C_{aro}H), 128.3 (C_{aro}H), 127.9 (C_{aro}H), 127.1 (C_{aro}H), 126.7 (C_q), 124.2 (C_{aro}H), 124.1 (C_{aro}H), 121.9 (C_{aro}H), 118.9 (C_{aro}H), 114.0 (C_q), 111.7 (C_{aro}H), 77.5 (NC≡C), 67.8 (NC≡C), 59.0 (NCH), 50.5 (CH₂), 42.9 (CH₂), 25.5 (CH₂), 23.6 (CH₂) ppm.

HRMS (ESI-TOF, + mode) m/z calcd for C₂₉H₂₉N₄O₄S 529.1904, found 529.1905 [M+H]⁺.

Analytical Data of Compounds from Chapter V

1-(1,4-Diphenylbut-3-yn-2-yl)pyrrolidine (P.1a) (CAS: 1171093-13-2)



Chemical Formula: C₂₀H₂₁N
Molecular Weight: 275,3950

Following the General Procedure J (pyridine, T = 80 °C for 24 h), the title compound **P.1a** was obtained in an 82:18 ratio with its regioisomer **M.1a** according to the crude ¹H NMR spectrum. **P.1a** was isolated as a red-brown oil (204 mg, 741 μmol) by column chromatography. Yield 74% (combined 87% yield for **P.1a**+**M.1a**).

R_f = 0.30 (SiO₂, cyclohexane/EtOAc 7:3).

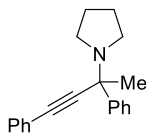
ATR-FTIR (neat) ν = 3082, 3061, 3028, 2961, 2930, 2909, 2874, 2805, 1948, 1876, 1801, 1748, 1682, 1598, 1489, 1453, 1443, 1347, 1313, 1247, 1202, 1119, 1070, 1029, 911, 754, 722, 690 cm⁻¹.

¹H NMR (300 MHz, CDCl₃) δ = 7.39 – 7.21 (m, 10H, H_{aro}), 3.95 (dd, *J* = 10.2, 4.9 Hz, 1H, NCH), 3.14 (dd, *J* = 12.9, 4.9 Hz, 1H, CHCH₂), 2.97 (dd, *J* = 12.9, 10.2 Hz, 1H, CHCH₂), 2.92 – 2.72 (m, 4H, 2 × NCH₂), 1.93 – 1.78 (m, 4H, 2 × NCH₂CH₂) ppm.

¹³C NMR (126 MHz, CDCl₃) δ = 138.9 (C_{q-aro}), 131.8 (C_{aroH}), 129.7 (C_{aroH}), 128.3(3) (C_{aroH}), 128.3(0) (C_{aroH}), 128.0 (C_{aroH}), 126.6 (C_{aroH}), 123.5 (C_{q-aro}), 87.4 (≡C), 86.6 (≡C), 57.3 (NCH), 49.9 (NCH₂), 41.9 (NCHCH₂), 23.7 (NCH₂CH₂) ppm.

MS (ESI-TOF, + mode) *m/z* (rel intensity) 276.17 (100) [M+H]⁺, 205.10 (20) [C₁₆H₁₃]⁺.

1-(2,4-Diphenylbut-3-yn-2-yl)pyrrolidine (M.1a) (CAS: 1456784-60-3)



Chemical Formula: C₂₀H₂₁N
Molecular Weight: 275,3950

Following the General Procedure J (pyridine, T = 80 °C for 24 h), the title compound **M.1a** was obtained in an 82:18 ratio with its regioisomer **P.1a** according to the crude ¹H NMR spectrum. **M.1a** was isolated as a yellow oil (37 mg, 134 μmol) by column chromatography. Yield 13% (combined 87% yield for **P.1a**+**M.1a**).

R_f = 0.75 (SiO₂, cyclohexane/EtOAc 7:3).

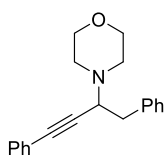
ATR-FTIR (neat) ν = 3080, 3058, 3024, 2964, 2932, 2873, 2810, 1951, 1884, 1809, 1683, 1598, 1489, 1445, 1365, 1262, 1221, 1135, 1071, 1027, 1000, 913, 754, 698 cm⁻¹.

¹H NMR (300 MHz, CDCl₃) δ = 7.83 – 7.73 (m, 2H, H_{aro}), 7.56 – 7.49 (m, 2H, H_{aro}), 7.38 – 7.30 (m, 5H, H_{aro}), 7.29 – 7.22 (m, 1H, H_{aro}), 2.84 – 2.54 (m, 4H, 2 × NCH₂), 1.82 – 1.75 (m, 4H, 2 × NCH₂CH₂), 1.74 (s, 3H, CH₃) ppm.

¹³C NMR (126 MHz, CDCl₃) δ = 145.7 (C_{q-aro}), 131.9 (C_{aroH}), 128.3 (C_{aroH}), 128.1 (C_{aroH}), 128.0 (C_{aroH}), 127.1 (C_{aroH}), 126.5 (C_{aroH}), 123.4 (C_{q-aro}), 89.4 (≡C), 87.2 (≡C), 62.6 (NC_q), 48.5 (NCH₂), 32.4 (CH₃), 23.9 (NCH₂CH₂) ppm.

MS (ESI-TOF, + mode) *m/z* (rel intensity) 276.18 (10) [M+H]⁺, 205.10 (100) [C₁₆H₁₃]⁺.

4-(1,4-Diphenylbut-3-yn-2-yl)morpholine (P.1r) (CAS: 211934-93-9)



Chemical Formula: C₂₀H₂₁NO
Molecular Weight: 291,3940

Following the General Procedure J (pyridine, T = 80 °C for 24 h), the title compound **P.1r** was obtained in a 98:2 ratio with its regioisomer **M.1r** according to the crude ¹H NMR spectrum. **P.1r** was isolated as a yellow viscous oil (166 mg, 572 μmol) by column chromatography. Yield 57%.

R_f = 0.23 (SiO₂, cyclohexane/EtOAc 7:3).

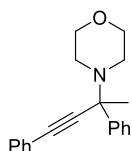
ATR-FTIR (neat) ν = 3057, 3026, 2961, 2935, 2894, 2855, 2818, 1677, 1595, 1497, 1453, 1327, 1281, 1253, 1113, 1070, 1009, 920, 863, 756, 726, 692 cm⁻¹.

¹H NMR (500 MHz, CDCl₃) δ = 7.43 – 7.38 (m, 2H, H_{aro}), 7.38 – 7.33 (m, 4H, H_{aro}), 7.33 – 7.29 (m, 3H, H_{aro}), 7.29 – 7.25 (m, 1H, H_{aro}), 3.86 – 3.72 (m, 5H, 2 × OCH₂ & NCH), 3.09 (dd, J = 13.0, 5.4 Hz, 1H, CHCH₂), 3.01 (dd, J = 13.0, 9.6 Hz, 1H, CHCH₂), 2.85 (ddd, J = 11.4, 6.3, 3.2 Hz, 2H, 2 × NCH₂), 2.68 (ddd, J = 11.3, 6.2, 3.2 Hz, 2H, 2 × NCH₂) ppm.

¹³C NMR (126 MHz, CDCl₃) δ = 138.6 (C_{q-aro}), 131.7 (C_{aroH}), 129.6 (C_{aroH}), 128.3(5) (C_{aroH}), 128.3(3) (C_{aroH}), 128.2 (C_{aroH}), 126.6 (C_{aroH}), 123.2 (C_{q-aro}), 87.5 (\equiv C), 86.4 (\equiv C), 67.2 (OCH₂), 60.3 (NCH), 50.0 (NCH₂), 39.7 (NCHCH₂) ppm.

MS (ESI-TOF, + mode) m/z (rel intensity) 292.17 (100) [M+H]⁺, 205.10 (40) [C₁₆H₁₃]⁺.

4-(2,4-Diphenylbut-3-yn-2-yl)morpholine (M.1r) (CAS: 859823-93-1)



Chemical Formula: C₂₀H₂₁NO
Molecular Weight: 291,3940

Following the General Procedure J (no pyridine, T = 70 °C for 24 h), the title compound **M.1r** was obtained in a 73:27 ratio with its regioisomer **P.1r** according to the crude ¹H NMR spectrum. **M.1r** was isolated as an orange solid (33 mg, 113 μ mol) by column chromatography. Yield 11%.

R_f = 0.63 (SiO₂, cyclohexane/EtOAc 7:3).

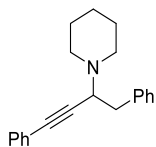
ATR-FTIR (neat) ν = 3080, 3058, 3023, 2984, 2957, 2912, 2891, 2850, 2820, 2760, 2737, 2688, 1598, 1489, 1444, 1390, 1361, 1268, 1116, 1071, 1026, 960, 927, 861, 755, 690 cm⁻¹.

¹H NMR (500 MHz, CDCl₃) δ = 7.81 – 7.75 (m, 2H, H_{aro}), 7.58 – 7.53 (m, 2H, H_{aro}), 7.38 – 7.33 (m, 5H, H_{aro}), 7.30 – 7.26 (m, 1H, H_{aro}), 3.79 – 3.71 (m, 4H, 2 × OCH₂), 2.82 – 2.69 (m, 2H, 2 × NCH₂), 2.57 – 2.44 (m, 2H, 2 × NCH₂), 1.69 (s, 3H, CH₃) ppm.

¹³C NMR (126 MHz, CDCl₃) δ = 144.9 (C_{q-aro}), 132.0 (C_{aroH}), 128.4(5) (C_{aroH}), 128.4(0) (C_{aroH}), 128.3 (C_{aroH}), 127.4 (C_{aroH}), 126.7 (C_{aroH}), 123.3 (C_{q-aro}), 88.4 (\equiv C), 88.3 (\equiv C), 67.6 (OCH₂), 63.5 (NC_q), 48.2 (NCH₂), 30.6 (CH₃) ppm.

MS (ESI-TOF, + mode) m/z (rel intensity) 292.17 (2) [M+H]⁺, 205.10 (100) [C₁₆H₁₃]⁺.

1-(1,4-Diphenylbut-3-yn-2-yl)piperidine (P.1q) (CAS: 24907-33-3)



Chemical Formula: C₂₁H₂₃N
Molecular Weight: 289,4220

Following the General Procedure J (pyridine, T = 80 °C for 24 h), the title compound **P.1q** was obtained in a 92:8 ratio with its regioisomer **M.1q** according to the crude ¹H NMR spectrum. **P.1q** was isolated as an orange resin (211 mg, 731 μ mol) by column chromatography. Yield 70% (**M.1q** was not isolated in pure form).

R_f = 0.55 (SiO₂, cyclohexane/EtOAc 7:3).

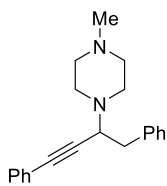
ATR-FTIR (neat) ν = 3083, 3061, 3028, 2931, 2852, 2803, 2750, 1598, 1489, 1442, 1331, 1155, 1098, 1032, 912, 754, 691 cm⁻¹.

¹H NMR (500 MHz, CDCl₃) δ = 7.40 – 7.27 (m, 9H, H_{aro}), 7.25 – 7.21 (m, 1H, H_{aro}), 3.73 (dd, J = 10.2, 4.8 Hz, 1H, NCH), 3.08 (dd, J = 12.8, 4.8 Hz, 1H, CHCH₂), 2.99 (dd, J = 12.8, 10.2 Hz, 1H, CHCH₂), 2.82 – 2.73 (m, 2H, NCH₂), 2.65 – 2.54 (m, 2H, NCH₂), 1.74 – 1.59 (m, 4H, 2 × NCH₂CH₂), 1.49 (quint, J = 6.0 Hz, 2H, NCH₂CH₂CH₂) ppm.

¹³C NMR (126 MHz, CDCl₃) δ = 139.1 (C_{q-aro}), 131.8 (C_{aroH}), 129.7 (C_{aroH}), 128.3(3) (C_{aroH}), 128.3(0) (C_{aroH}), 128.0 (C_{aroH}), 126.5 (C_{aroH}), 123.5 (C_{q-aro}), 87.2 (\equiv C), 87.0 (\equiv C), 60.9 (NCH), 50.8 (NCH₂), 40.1 (CHCH₂), 26.2 (CH₂), 24.6 (CH₂) ppm.

MS (ESI-TOF, + mode) m/z (rel intensity) 290.19 (100) [M+H]⁺.

1-(1,4-Diphenylbut-3-yn-2-yl)-4-methylpiperazine (P.1s) (CAS: 2743452-96-0)



Chemical Formula: C₂₁H₂₄N₂
Molecular Weight: 304,4370

Following the General Procedure J (no pyridine, T = 70 °C for 24 h), the title compound **P.1s** was obtained in a 91:9 ratio with its regioisomer **M.1s** according to the crude ¹H NMR spectrum. **P.1s** was isolated as a dark orange oil (232 mg, 763 μmol) by column chromatography. Yield 76% (**M.1s** was not isolated in pure form).

R_f = 0.43 (SiO₂, CH₂Cl₂/MeOH 9:1).

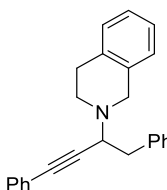
ATR-FTIR (neat) ν = 3081, 3059, 3028, 2934, 2882, 2793, 1679, 1598, 1489, 1454, 1375, 1284, 1158, 1071, 1009, 755, 691 cm⁻¹.

¹H NMR (500 MHz, CDCl₃) δ = 7.37 – 7.21 (m, 10H, H_{aro}), 3.76 (dd, J = 9.9, 5.1 Hz, 1H, NCH), 3.06 (dd, J = 12.9, 5.2 Hz, 1H, CHCH₂), 2.98 (dd, J = 13.0, 9.9 Hz, 1H, CHCH₂), 2.92 – 2.85 (m, 2H, CH₂-piperazine), 2.74 – 2.68 (m, 2H, CH₂-piperazine), 2.55 (bs, 4H, CH₂-piperazine), 2.33 (s, 3H, CH₃) ppm.

¹³C NMR (126 MHz, CDCl₃) δ = 138.8 (C_{q-aro}), 131.8 (C_{aroH}), 129.7 (C_{aroH}), 128.3 (C_{aroH}), 128.3 (C_{aroH}), 128.0 (C_{aroH}), 126.6 (C_{aroH}), 123.3 (C_{q-aro}), 87.4 (≡C), 86.6 (≡C), 60.0 (NCH), 55.3 (CH₂), 46.1 (CH₃), 40.1 (CH₂) ppm.

HRMS (ESI-TOF, + mode) m/z calcd for C₂₁H₂₅N₂ 305.2012, found 305.2011 [M+H]⁺.

2-(1,4-Diphenylbut-3-yn-2-yl)-1,2,3,4-tetrahydroisoquinoline (P.4b)



Chemical Formula: C₂₅H₂₃N
Molecular Weight: 337,4660

Following the General Procedure J (pyridine, T = 80 °C for 48 h), the title compound **P.4b** was obtained in a 93:7 ratio with its regioisomer **M.4b** according to the crude ¹H NMR spectrum. **P.4b** was isolated as a yellow oil (177 mg, 524 μmol) by column chromatography. Yield 75% (**M.4b** was not isolated in pure form).

R_f = 0.73 (SiO₂, cyclohexane/EtOAc 7:3).

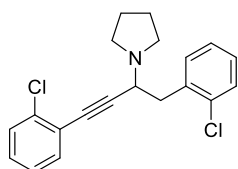
ATR-FTIR (neat) ν = 3082, 3061, 3024, 2921, 2807, 2749, 1683, 1597, 1489, 1453, 1327, 1126, 1090, 1029, 935, 739, 690 cm⁻¹.

¹H NMR (500 MHz, CDCl₃) δ = 7.38 – 7.20 (m, 10H, H_{aro}), 7.15 – 7.04 (m, 4H, H_{aro}), 3.99 (d, J = 14.7 Hz, 1H, NCH₂C_{q-aro}), 3.94 (dd, J = 9.7, 5.3 Hz, 1H, NCH), 3.85 (d, J = 14.7 Hz, 1H, NCH₂C_{q-aro}), 3.19 – 3.05 (m, 3H), 3.03 – 2.89 (m, 2H), 2.87 – 2.80 (m, 1H) ppm.

¹³C NMR (126 MHz, CDCl₃) δ = 138.8 (C_{q-aro}), 135.2 (C_{q-aro}), 134.4 (C_{q-aro}), 131.8 (C_{aroH}), 129.7 (C_{aroH}), 128.8 (C_{aroH}), 128.3(8) (C_{aroH}), 128.3(5) (C_{aroH}), 128.1 (C_{aroH}), 126.9 (C_{aroH}), 126.6 (C_{aroH}), 126.2 (C_{aroH}), 125.8 (C_{aroH}), 123.2 (C_{q-aro}), 87.3 (≡C), 86.5 (≡C), 60.2 (NCH), 52.3 (NCH₂), 47.7 (NCH₂), 40.4 (CH₂), 29.7 (CH₂) ppm.

HRMS (ESI-TOF, + mode) m/z calcd for C₂₅H₂₄N 338.1903, found 338.1895 [M+H]⁺.

1-(1,4-Bis(2-chlorophenyl)but-3-yn-2-yl)pyrrolidine (P.3a)



Chemical Formula: C₂₀H₁₉Cl₂N
Molecular Weight: 344,2790

Following the General Procedure J (pyridine, T = 80 °C for 31 h, on 350 μmol pyrrolidine scale), the title compound **P.3a** was isolated as an orange oil (83 mg, n = 241 μmol) by column chromatography. Yield 69%.

R_f = 0.45 (SiO₂, cyclohexane/EtOAc 7:3).

ATR-FTIR (neat) ν = 3061, 2962, 2933, 2874, 2809, 1572, 1472, 1438, 1316, 1127, 1034, 745, 679 cm⁻¹.

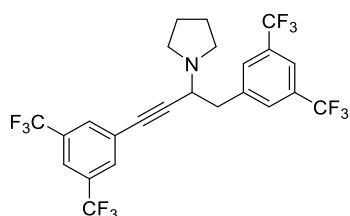
¹H NMR (500 MHz, CDCl₃) δ = 7.45 – 7.42 (m, 1H, H_{aro}), 7.38 – 7.32 (m, 3H, H_{aro}), 7.22 – 7.13 (m, 4H, H_{aro}), 4.16 (dd, J = 10.4, 5.1 Hz, 1H, NCH), 3.36 (dd, J = 13.0, 5.1 Hz, 1H,

CHCH₂), 3.07 (dd, *J* = 13.1, 10.4 Hz, 1H, CHCH₂), 2.96 – 2.83 (m, 4H, 2 × NCH₂), 1.91 – 1.81 (m, 4H, 2 × NCH₂CH₂) ppm.

¹³C NMR (126 MHz, CDCl₃) δ = 136.1 (C_{q-aro}), 135.8 (C_{q-aro}), 134.5 (C_{q-aro}), 133.5 (C_{aroH}), 132.3 (C_{aroH}), 129.5 (C_{aroH}), 129.3 (C_{aroH}), 129.0 (C_{aroH}), 128.1 (C_{aroH}), 126.6 (C_{aroH}), 126.4 (C_{aroH}), 123.3 (C_{q-aro}), 92.9 (≡C), 83.1 (≡C), 55.2 (NCH), 49.9 (NCH₂), 39.0 (CHCH₂), 23.8 (NCH₂CH₂) ppm.

HRMS (ESI-TOF, + mode) *m/z* calcd for C₂₀H₂₀Cl₂N 344.0967, found 344.0950 [M+H]⁺.

1-(1,4-Bis(3,5-bis(trifluoromethyl)phenyl)but-3-yn-2-yl)pyrrolidine (P.3i)



Chemical Formula: C₂₄H₁₇F₁₂N
Molecular Weight: 547,3878

Following the General Procedure J (pyridine, T = 80 °C for 23 h, on 350 μmol pyrrolidine scale), the title compound **P.3i** was isolated as a dark orange oil (170 mg, 311 μmol) by column chromatography. Yield 89%.

R_f = 0.24 (SiO₂, cyclohexane/EtOAc 7:3).

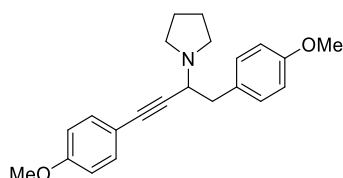
ATR-FTIR (neat) ν = 2968, 2917, 2881, 2815, 1622, 1463, 1378, 1274, 1169, 1123, 999, 895, 845, 700, 682 cm⁻¹.

¹H NMR (500 MHz, CDCl₃) δ = 7.85 – 7.72 (m, 6H, H_{aro}), 3.97 (dd, *J* = 9.8, 5.5 Hz, 1H, NCH), 3.25 (dd, *J* = 13.2, 5.5 Hz, 1H, CHCH₂), 3.09 (dd, *J* = 13.2, 9.8 Hz, 1H, CHCH₂), 2.88 – 2.71 (m, 4H, 2 × NCH₂), 1.94 – 1.82 (m, 4H, 2 × NCH₂CH₂) ppm.

¹³C NMR (126 MHz, CDCl₃) δ = 140.8 (C_{q-aro}), 132.1 (q, ²*J*_{C-F} = 33.6 Hz, CF₃C_{q-aro}), 131.6 (q, ²*J*_{C-F} = 33.0 Hz, CF₃C_{q-aro}), 131.7 – 131.5 (m, CF₃C_{q-aro}H), 130.1 – 129.5 (m, CF₃C_{q-aro}H), 125.0, 123.5 (q, ¹*J*_{C-F} = 271.9 Hz, CF₃), 123.0 (q, ¹*J*_{C-F} = 273.8 Hz, CF₃), 122.0 – 121.7 (m, CF₃C_{q-aro}H), 121.0 – 120.9 (m, CF₃C_{q-aro}H), 90.1 (≡C), 84.9 (≡C), 56.6 (NCH), 50.0 (NCH₂), 40.9 (CHCH₂), 23.6 (NCH₂CH₂) ppm.

HRMS (ESI-TOF, + mode) *m/z* calcd for C₂₄H₁₈F₁₂N 548.1242, found 548.1241 [M+H]⁺.

1-(1,4-Bis(4-methoxyphenyl)but-3-yn-2-yl)pyrrolidine (P.3f)



Chemical Formula: C₂₂H₂₅NO₂
Molecular Weight: 335,4470

Following the General Procedure J (pyridine, T = 80 °C for 54 h, on 350 μmol pyrrolidine scale), the title compound **P.3f** was obtained in a 1:1 ratio with its regioisomer **M.3f** according to the crude ¹H NMR spectrum. **P.3f** was isolated as an orange oil (143 mg, 425 μmol) by column chromatography. Yield 42.5% (combined 85% yield for **P.3f**+**M.3f**).

R_f = 0.25 (SiO₂, cyclohexane/EtOAc 1:1).

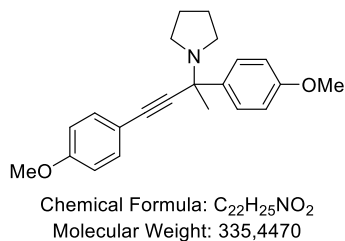
ATR-FTIR (neat) ν = 2959, 2932, 2873, 2834, 2810, 1606, 1505, 1462, 1440, 1290, 1242, 1170, 1152, 1135, 1097, 1031, 1001, 829 cm⁻¹.

¹H NMR (300 MHz, CDCl₃) δ = 7.34 – 7.28 (m, 2H, H_{aro}), 7.28 – 7.23 (m, 2H, H_{aro}), 6.89 – 6.83 (m, 2H, 2 × OC_qCH_{aro}), 6.82 – 6.74 (m, 2H, 2 × OC_qCH_{aro}), 3.86 (dd, *J* = 10.2, 4.8 Hz, 1H, NCH), 3.80 (s, 3H, CH₃), 3.79 (s, 3H, CH₃), 3.06 (dd, *J* = 13.0, 4.8 Hz, 1H, CHCH₂), 2.95 – 2.70 (m, 5H, 2 × NCH₂ & CHCH₂), 1.88 – 1.78 (m, 4H, 2 × NCH₂CH₂) ppm.

¹³C NMR (126 MHz, CDCl₃) δ = 159.4 (OC_{q-aro}), 158.3 (OC_{q-aro}), 133.1 (C_{aroH}), 131.1 (C_{q-aro}), 130.6 (C_{aroH}), 115.7 (C_{q-aro}), 113.9 (C_{aroH}), 113.7 (C_{aroH}), 86.4 (≡C), 85.9 (≡C), 57.6 (NCH), 55.4 (OCH₃), 55.4 (OCH₃), 49.9 (NCH₂), 41.0 (CHCH₂), 23.7 (NCH₂CH₂) ppm.

HRMS (ESI-TOF, + mode) *m/z* calcd for C₂₂H₂₆NO₂ 336.1958, found 336.1963 [M+H]⁺.

1-(2,4-Bis(4-methoxyphenyl)but-3-yn-2-yl)pyrrolidine (M.3f)



Following the General Procedure J (pyridine, T = 80 °C for 54 h, on 350 μmol pyrrolidine scale), the title compound **M.3f** was obtained in a 1:1 ratio with its regioisomer **P.3f** according to the crude ¹H NMR spectrum. **M.3f** was isolated as a yellow oil (143 mg, 425 μmol) by column chromatography. Yield 85% (combined 85% yield for **P.3f**+**M.3f**).

R_f = 0.60 (SiO₂, cyclohexane/EtOAc 1:1).

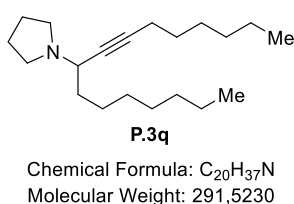
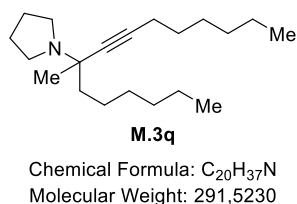
ATR-FTIR (neat) ν = 2955, 2932, 2834, 2807, 1605, 1507, 1462, 1441, 1288, 1242, 1172, 1120, 1106, 1030, 986, 829, 789, 760 cm⁻¹.

¹H NMR (300 MHz, CDCl₃) δ = 7.73 – 7.64 (m, 2H, H_{aro}), 7.50 – 7.41 (m, 2H, H_{aro}), 6.91 – 6.82 (m, 4H, 4 × OC_qCH_{aro}), 3.83 (s, 3H, OCH₃), 3.81 (s, 3H, OCH₃), 2.78 – 2.70 (m, 2H, 2 × NCH₂), 2.63 – 2.53 (m, 2H, 2 × NCH₂), 1.85 – 1.74 (m, 4H, 2 × NCH₂CH₂), 1.70 (s, 3H, CCH₃) ppm.

¹³C NMR (126 MHz, CDCl₃) δ = 159.5 (OC_{q-aro}), 158.7 (OC_{q-aro}), 138.3 (C_{q-aro}), 133.3 (C_{aroH}), 127.7 (C_{aroH}), 115.8 (C_{q-aro}), 114.0 (C_{aroH}), 113.4 (C_{aroH}), 88.1 (≡C), 87.0 (≡C), 62.1 (NC_q), 55.5 (OCH₃), 55.4 (OCH₃), 48.6 (NCH₂), 32.5 (C_qCH₃), 24.0 (NCH₂CH₂) ppm.

HRMS (ESI-TOF, + mode) m/z calcd for C₂₂H₂₆NO₂ 336.1958, found 336.1953 [M+H]⁺.

1-(7-Methylpentadec-8-yn-7-yl)pyrrolidine (M.3q) and 1-(hexadec-9-yn-8-yl)pyrrolidine (P.3q)



Following the General Procedure J (no pyridine, T = 100 °C for 31 h), the title compound **M.3q** was obtained in an approximate 9:1 ratio with its regioisomer **P.3q** according to the crude ¹H NMR spectrum. **M.3q** and **P.3q** could not be

separated by column chromatography and were isolated as a mixture appearing as a yellow oil (265 mg, 910 μmol). Yield 91%.

R_f = 0.25 (SiO₂, cyclohexane/EtOAc 8:2).

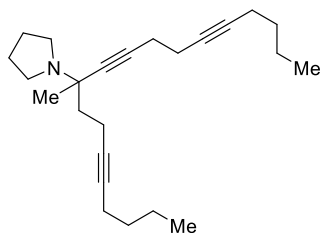
ATR-FTIR (neat) ν = 2955, 2927, 2857, 2809, 1464, 1369, 1328, 1217, 1192, 1173, 1148, 1108, 1009, 870, 725 cm⁻¹.

¹H NMR (500 MHz, CDCl₃) δ = 3.44 – 3.34 (m, 1H, NCH from **P.3q**), 2.78 – 2.54 (m, 4H, NCH₂), 2.19 (t, 2H, ≡CCH₂), 1.84 – 1.68 (m, 5H, NCH₂CH₂), 1.62 (td, J = 12.4, 4.5 Hz, 1H), 1.56 – 1.24 (m, 21H, C_qCH₃), 0.93 – 0.83 (m, 6H, CH₃) ppm.

¹³C NMR (126 MHz, CDCl₃) δ = 85.3 (≡C), 84.2 (≡C), 81.5 (≡C), 78.5 (≡C), 57.6 (NC_q), 54.9 (NCH), 49.8 (NCH₂), 47.7 (NCH₂), 42.0 (CH₂), 35.5 (CH₂), 31.9(9) (CH₂), 31.9(7) (CH₂), 31.5 (CH₂), 30.0 (CH₂), 29.6 (CH₂), 29.3(9) (CH₂), 29.3(6) (CH₂), 29.2 (CH₂), 28.6(3) (CH₂), 28.6(0) (CH₂), 26.9 (CH₂), 26.3 (CH₃), 24.5 (CH₂), 23.7 (CH₂), 23.6 (CH₂), 22.8 (CH₂), 22.7 (CH₂), 18.8 (CH₂), 18.7 (CH₂), 14.3 (CH₃), 14.2 (CH₃) ppm.

HRMS (ESI-TOF, + mode) m/z calcd for C₂₀H₃₈N 292.2999, found 292.3008 [M+H]⁺.

1-(9-Methylnonadeca-5,10,14-triyn-9-yl)pyrrolidine (M.3be)



Chemical Formula: C₂₄H₃₇N
Molecular Weight: 339,5670

Following the General Procedure J (no pyridine, T = 80 °C for 31 h, on 846 μmol pyrrolidine scale), the title compound **M.3be** was obtained in an 83:17 ratio with its regioisomer **P.3be** according to the crude ¹H NMR spectrum. **M.3be** was isolated as a yellow oil (103 mg, 303 μmol) by column chromatography. Yield 36% (combined 43% yield for **P.3be**+**M.3be**).

R_f = 0.48 (SiO₂, cyclohexane/EtOAc 8:2).

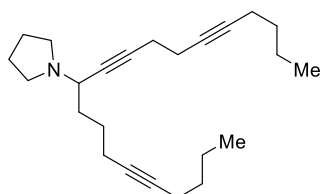
ATR-FTIR (neat) ν = 2957; 2930; 2872; 2812, 1460, 1433, 1371, 1354, 1338, 1298, 1270, 1256, 1230, 1191, 1171, 1125, 1009 cm⁻¹.

¹H NMR (300 MHz, CDCl₃) δ = 2.81 – 2.57 (m, 4H, 2 × NCH₂), 2.39 – 2.23 (m, 6H), 2.19 – 2.09 (m, 4H), 1.96 – 1.79 (m, 2H), 1.79 – 1.70 (m, 4H, 2 × NCH₂CH₂), 1.54 – 1.32 (m, 8H), 1.32 (s, 3H, C_qCH₃), 0.90 (td, J = 7.1, 2.4 Hz, 6H, 2 × CH₂CH₃) ppm.

¹³C NMR (126 MHz, CDCl₃) δ = 83.6 (≡C), 81.3 (≡C), 80.3 (≡C), 80.2 (≡C), 78.7 (≡C), 57.2 (NC_q), 47.7 (NCH₂), 41.1 (CH₂), 31.4 (CH₂), 31.3 (CH₂), 25.8 (C_qCH₃), 23.8 (CH₂), 22.1 (2 × CH₂), 19.8 (2 × CH₂), 19.5 (CH₂), 18.6 (CH₂), 18.5 (CH₂), 14.3 (CH₂), 13.8 (2 × CH₃) ppm.

HRMS (ESI-TOF, + mode) m/z calcd for C₂₄H₃₈N 340.2999, found 340.3009 [M+H]⁺.

1-(Icosa-5,11,15-triyn-10-yl)pyrrolidine (P.3be)



Chemical Formula: C₂₄H₃₇N
Molecular Weight: 339,5670

Following the General Procedure J (no pyridine, T = 80 °C for 31 h, on 846 μmol pyrrolidine scale), the title compound **P.3be** was obtained in an 83:17 ratio with its regioisomer **M.3be** according to the crude ¹H NMR spectrum. **P.3be** was isolated as a brown oil (20 mg, 59 μmol) by column chromatography. Yield 7% (combined 43% yield for **P.3be**+**M.3be**).

R_f = 0.26 (SiO₂, cyclohexane/EtOAc 8:2).

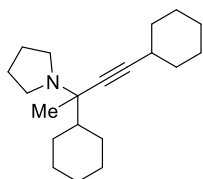
ATR-FTIR (neat) ν = 2956, 2929, 2871, 2811, 1711, 1625, 1531, 1458, 1433, 1378, 1363, 1337, 1294, 1256, 1198, 1122, 1034, 961, 930, 901, 876, 801, 750, 729 cm⁻¹.

¹H NMR (500 MHz, CDCl₃) δ = 3.49 – 3.38 (m, 1H, NCH), 2.79 – 2.54 (m, 4H, 2 × NCH₂), 2.44 – 2.29 (m, 4H), 2.23 – 2.07 (m, 6H), 1.80 – 1.75 (m, 4H, 2 × NCH₂CH₂), 1.75 – 1.57 (m, 4H), 1.49 – 1.34 (m, 8H), 0.90 (td, J = 7.2, 0.8 Hz, 6H, 2 × CH₃) ppm.

¹³C NMR (126 MHz, CDCl₃) δ = 84.2 (≡C), 81.3 (≡C), 80.7 (≡C), 79.9 (≡C), 78.9 (≡C), 78.7 (≡C), 54.5 (NCH), 49.8 (NCH₂), 34.4 (CH₂), 31.4 (CH₂), 31.3 (CH₂), 26.4 (CH₂), 23.6 (CH₂), 22.10 (CH₂), 22.08 (CH₂), 19.7 (CH₂), 19.6 (CH₂), 18.8 (CH₂), 18.61 (CH₂), 18.55 (CH₂), 13.8 (2 × CH₃) ppm.

HRMS (ESI-TOF, + mode) m/z calcd for C₂₄H₃₈N 340.2999, found 340.3004 [M+H]⁺.

1-(2,4-Dicyclohexylbut-3-yn-2-yl)pyrrolidine (M.3o)



Chemical Formula: C₂₀H₃₃N
Molecular Weight: 287,4910

Following the General Procedure J (no pyridine, T = 100 °C for 24 h, on 1.01 mmol pyrrolidine scale), the title compound **M.3o** was obtained in a 72:28 ratio with its regioisomer **P.3o** according to the crude ¹H NMR spectrum. **M.3o** was isolated as a colourless oil (164 mg, 570 μmol) by column chromatography. Yield 56% (combined 78% yield for **P.3o**+**M.3o**).

R_f = 0.50 (SiO₂, cyclohexane/EtOAc 8:2).

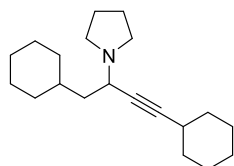
ATR-FTIR (neat) $\nu = 2987, 2924, 2851, 2806, 1447, 1370, 1314, 1199, 1170, 1149, 1115, 989, 888, 861, 844 \text{ cm}^{-1}$.

^1H NMR (300 MHz, CDCl_3) $\delta = 2.73 - 2.55$ (m, 4H, $2 \times \text{NCH}_2$), $2.45 - 2.35$ (m, 1H, $\text{CH}_{\text{cyclohexyl}}$), $2.05 - 1.93$ (m, 1H, $\text{CH}_{\text{cyclohexyl}}$), $1.91 - 1.58$ (m, 12H, $2 \times \text{NCH}_2\text{CH}_2$), $1.56 - 1.17$ (m, 9H), 1.16 (s, 3H, CH_3), $1.13 - 0.89$ (m, 3H) ppm.

^{13}C NMR (126 MHz, CDCl_3) $\delta = 88.7$ ($\equiv\text{C}$), 81.5 ($\equiv\text{C}$), 61.0 (NC_q), 47.3 (NCH_2), 46.3 (NC_qCH), 33.5 (CH_2), 29.6 (CH_2), 29.0 ($\equiv\text{CCH}$), 27.4 (CH_2), 27.2 (CH_2), 27.0 (CH_2), 26.4 (CH_2), 26.2 (CH_2), 24.8 (CH_2), 23.8 (CH_2), 21.5 (CH_3) ppm.

HRMS (ESI-TOF, + mode) m/z calcd for $\text{C}_{20}\text{H}_{34}\text{N}$ 288.2686, found 288.2694 $[\text{M}+\text{H}]^+$.

1-(1,4-Dicyclohexylbut-3-yn-2-yl)pyrrolidine (P.3o)



Chemical Formula: $\text{C}_{20}\text{H}_{33}\text{N}$
Molecular Weight: 287.4910

Following the General Procedure J (no pyridine, $T = 100 \text{ }^\circ\text{C}$ for 24 h, on 1.01 mmol pyrrolidine scale), the title compound **P.3o** was obtained in a 72:28 ratio with its regioisomer **M.3o** according to the crude ^1H NMR spectrum. **P.3o** was isolated as an orange oil (66 mg, 230 μmol) by column chromatography. Yield 22% (combined 78% yield for **P.3o**+**M.3o**). $R_f = 0.25$ (SiO_2 , cyclohexane/EtOAc 8:2).

ATR-FTIR (neat) $\nu = 2921, 2850, 2806, 1699, 1447, 1348, 1315, 1295, 1234, 1197, 1128, 1080, 1027, 1013, 986, 966, 941, 889, 871, 862, 844 \text{ cm}^{-1}$.

^1H NMR (500 MHz, CDCl_3) $\delta = 3.62$ (m, 1H, NCH), $2.75 - 2.59$ (m, 4H, $2 \times \text{NCH}_2$), $2.45 - 2.37$ (m, 1H, $\text{CH}_{\text{cyclohexyl}}$), $1.84 - 1.73$ (m, 6H, $2 \times \text{NCH}_2\text{CH}_2$), $1.72 - 1.60$ (m, 6H), $1.59 - 1.38$ (m, 6H), $1.37 - 1.08$ (m, 7H), $1.03 - 0.81$ (m, 2H) ppm.

^{13}C NMR (126 MHz, CDCl_3) $\delta = 90.0$ ($\equiv\text{C}$), 77.8 ($\equiv\text{C}$), 52.4 (NCH), 49.4 (NCH_2), 42.8 (NCHCH_2), 35.0 ($\text{CH}_{\text{cyclohexyl}}$), 34.2 (CH_2), 33.22 (CH_2), 33.19 (CH_2), 32.5 (CH_2), 29.1 ($\text{CH}_{\text{cyclohexyl}}$), 26.8 (CH_2), 26.5 (CH_2), 26.3 (CH_2), 26.1 (CH_2), 24.8 (CH_2), 23.7 (CH_2) ppm.

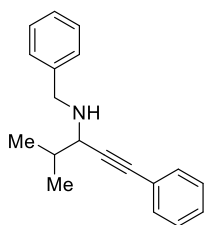
HRMS (ESI-TOF, + mode) m/z calcd for $\text{C}_{20}\text{H}_{34}\text{N}$ 288.2686, found 288.2696 $[\text{M}+\text{H}]^+$.

Analytical Data of Compounds from Chapter VI

Propargylamines

Additional propargylamines prepared according to the indicated procedures.

N-Benzyl-4-methyl-1-phenylpent-1-yn-3-amine (K.5a) (CAS: 73508-14-2)



Chemical Formula: $\text{C}_{19}\text{H}_{21}\text{N}$
Molecular Weight: 263.3840

The title compound was prepared following the general procedure reported by VAN DER EYCKEN and co-workers.^[208] Analytical data were in accordance with the literature. The title compound **K.5a** was isolated as a yellow oil (223.9 mg, 850 μmol). Yield 85%.

$R_f = 0.64$ (SiO_2 , cyclohexane/EtOAc 7:3).

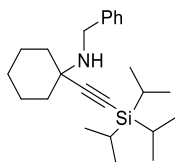
ATR-FTIR (neat) $\nu = 3327, 3082, 3062, 3028, 2958, 2927, 2870, 2841, 1598, 1489, 1453, 1365, 1101, 1070, 1028, 913, 754, 689 \text{ cm}^{-1}$.

^1H NMR (500 MHz, CDCl_3) $\delta = 7.49 - 7.44$ (m, 2H, H_{aro}), $7.43 - 7.39$ (m, 2H, H_{aro}), $7.37 - 7.29$ (m, 5H, H_{aro}), $7.29 - 7.24$ (m, 1H, H_{aro}), 4.11 (d, $J = 13.1 \text{ Hz}$, 1H, NCH_2), 3.90 (d, $J = 13.1 \text{ Hz}$, 1H, NCH_2), 3.41 (d, $J = 5.5 \text{ Hz}$, 1H, NCH), 1.96 (quintd, $J = 6.8, 5.5 \text{ Hz}$, 1H, $\text{CH}(\text{CH}_3)_2$), 1.08 (dd, $J = 6.7, 1.7 \text{ Hz}$, 6H, $\text{CH}(\text{CH}_3)_2$) ppm.

$^{13}\text{C}\{^1\text{H}\}$ NMR (126 MHz, CDCl_3) δ = 140.4 (C_q), 131.8 (C_{aroH}), 128.5(3) (C_{aroH}), 128.5(0) (C_{aroH}), 128.4 (C_{aroH}), 128.0 (C_{aroH}), 127.1 (C_{aroH}), 123.7 (C_q), 89.9 ($\text{C}\equiv$), 84.8 ($\text{C}\equiv$), 56.4 (NCH), 51.9 (NCH_2), 33.1 ($\text{CH}(\text{CH}_3)_2$), 19.9 ($1 \times \text{CH}(\text{CH}_3)_2$), 18.2($1 \times \text{CH}(\text{CH}_3)_2$) ppm.

MS (ESI-TOF, + mode) m/z (rel intensity) 264.17 (100) $[\text{M}+\text{H}]^+$, 157.10 (95) $[\text{C}_{12}\text{H}_{13}]^+$.

N-Benzyl-1-((triisopropylsilyl)ethynyl)cyclohexan-1-amine (CAS: 1651825-41-0)



Chemical Formula: $\text{C}_{24}\text{H}_{39}\text{NSi}$
Molecular Weight: 369,6680

The title compound was prepared following the procedure reported by LARSEN and co-workers.^[234] The title compound was isolated as a pale yellow oil (64 mg, 173 μmol). Yield 35%.

R_f = 0.55 (SiO_2 , cyclohexane/EtOAc 7:3).

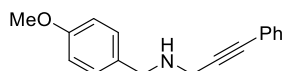
ATR-FTIR (neat) ν = 3029, 2940, 2860, 2155, 1599, 1450, 1321, 1248, 1140, 1110, 960, 886, 793, 725, 689 cm^{-1} .

^1H NMR (500 MHz, CDCl_3) δ = 7.39 – 7.34 (m, 2H, H_{aro}), 7.34 – 7.29 (m, 2H, H_{aro}), 7.27 – 7.22 (m, 1H, H_{aro}), 3.93 (s, 2H, NCH_2), 1.94 – 1.85 (m, 2H, $2 \times \text{NC}_q\text{CH}_2$), 1.73 – 1.61 (m, 5H), 1.47 – 1.39 (m, 2H), 1.31 – 1.17 (m, 2H), 1.15 – 1.03 (m, 20H, $(\text{CH}(\text{CH}_3)_2)_3$) ppm.

$^{13}\text{C}\{^1\text{H}\}$ NMR (126 MHz, CDCl_3) δ = 141.3 (C_q), 128.8 (C_{aroH}), 128.6 (C_{aroH}), 127.0 (C_{aroH}), 112.4 ($\text{C}\equiv$), 84.3 ($\text{C}\equiv$), 55.9 (NC_q), 48.3 (NCH_2), 38.4 (CH_2), 26.1 (CH_2), 23.2 (CH_2), 18.9 (CH), 11.5 (CH_3) ppm.

MS (ESI-TOF, + mode) m/z (rel intensity) 370.29 (100) $[\text{M}+\text{H}]^+$.

N-(4-Methoxybenzyl)-3-phenylprop-2-yn-1-amine (CAS: 892595-64-1)



Chemical Formula: $\text{C}_{17}\text{H}_{17}\text{NO}$
Molecular Weight: 251,3290

The title compound was prepared following the general procedure reported by YAMADA and co-workers.^[24] To a degassed solution of $\text{PdCl}_2(\text{PPh}_3)_2$ (14.0 mg, 0.02 mmol, 2 mol%), CuI (7.6 mg, 0.04 mmol, 4 mol%), distilled Et_3N (278.8 μL , 2 mmol, 2.0 eq.) and iodobenzene (122.6 μL , 1.1 mmol, 1.1 eq.) in anhydrous THF (2 mL), *N*-(4-methoxybenzyl)prop-2-yn-1-amine (175.2 mg, 1 mmol, 1.0 eq.) was added dropwise as a solution in anhydrous THF (0.3 mL) and the mixture was stirred at room temperature. Upon completion (17 h), the reaction mixture was quenched with aq. sat. NH_4Cl (5 mL) and extracted with Et_2O (3 \times 5 mL). The combined org. layers dried over Na_2SO_4 and the solvent was removed under reduced pressure. The residue was purified by column chromatography over silica gel ($\text{CH}_2\text{Cl}_2 \rightarrow \text{CH}_2\text{Cl}_2/\text{MeOH}$ 98:2) to give the title compound as an orange oil (203 mg, 808 μmol). Analytical data were in accordance with the literature.^[389] Yield 81%.

R_f = 0.16 (SiO_2 , cyclohexane/EtOAc 7:3).

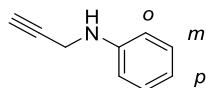
ATR-FTIR (neat) ν = 3324, 3057, 3032, 2997, 2952, 2931, 2907, 2833, 1610, 1510, 1441, 1242, 1173, 1031, 754, 690 cm^{-1} .

^1H NMR (500 MHz, CDCl_3) δ = 7.48 – 7.40 (m, 2H, H_{aro}), 7.35 – 7.26 (m, 5H, H_{aro}), 6.93 – 6.83 (m, 2H, $2 \times \text{OC}_q\text{CH}_{\text{aro}}$), 3.89 (s, 2H, $\text{NCH}_2\text{C}_{\text{aro}}$), 3.81 (s, 3H, CH_3), 3.64 (s, 2H, $\text{NCH}_2\text{C}\equiv$) ppm.

$^{13}\text{C}\{^1\text{H}\}$ NMR (126 MHz, CDCl_3) δ = 158.9 (CH_3OC_q), 131.8 ($\times 2$) (C_{aroH}), 129.8 (C_{aroH}), 128.4 (C_{aroH}), 128.2 (C_{aroH}), 123.4 (C_q), 114.0 (C_{aroH}), 87.8 ($\text{C}\equiv$), 83.8 ($\text{C}\equiv$), 55.4 (CH_3), 52.0 ($\text{NCH}_2\text{C}_{\text{aro}}$), 38.2 ($\text{CH}_2\text{C}\equiv$) ppm.

MS (ESI-TOF, + mode) m/z (rel intensity) 252.14 (55) $[\text{M}+\text{H}]^+$, 121.06 (100) $[\text{C}_8\text{H}_9\text{O}]^+$.

N-(Prop-2-yn-1-yl)aniline (CAS: 14465-74-8)



Chemical Formula: C₉H₉N
Molecular Weight: 131,1780

A solution of propargyl bromide (384 μL, 5.0 mmol, 1.0 eq., 98% stabilised with MgO) in anhydrous THF (5 mL) was added dropwise to a cooled suspension of aniline (685 μL, 7.5 mmol, 1.5 eq.) and K₂CO₃ (1.38 g, 10.0 mmol, 2.0 eq.) in anhydrous THF (10 mL) at 0 °C. The reaction mixture was allowed to warm to room temperature and stirred for 16 h. Next, the suspension was filtered over celite and washed with EtOAc. The solvent was removed under reduced pressure to give an orange crude oil. Only a fraction of the crude product was purified *via* column chromatography over silica gel (cyclohexane/EtOAc) to yield the title compound as a yellow oil. Analytical data is in accordance with the literature.^[390]

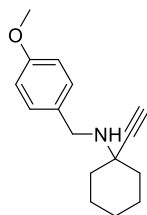
R_f = 0.57 (SiO₂, cyclohexane/EtOAc 7:3).

ATR-FTIR (neat) ν = 3402, 3285, 3085, 3052, 3022, 2924, 2847, 1601, 1502, 1439, 1313, 1252, 1181, 1096, 909, 874, 749, 690 cm⁻¹.

¹H NMR (300 MHz, CDCl₃) δ = 7.26 – 7.18 (m, 2H, *m*-H_{aro}), 6.84 – 6.75 (m, 1H, *p*-H_{aro}), 6.74 – 6.66 (m, 2H, 2 × *p*-H_{aro}), 3.95 (d, *J* = 2.5 Hz, 2H, NCH₂), 3.87 (bs, 1H, NH), 2.22 (t, *J* = 2.3 Hz, 1H, ≡CH) ppm.

¹³C{¹H} NMR (126 MHz, CDCl₃) δ = 147.0 (C_q-Ph), 129.4 (C_{aro}H), 118.8 (C_{aro}H), 113.6 (C_{aro}H), 81.1 (C≡), 71.4 (C≡), 33.8 (CH₂) ppm.

1-Ethynyl-N-(4-methoxybenzyl)cyclohexan-1-amine (CAS: 1330527-40-6)



Chemical Formula: C₁₆H₂₁NO
Molecular Weight: 243,3500

The title compound was prepared following the general procedure reported by DUAN and co-workers.^[391] Propargylamine was isolated as a pale yellow solid (192 mg, 789 μmol). Yield 79%.

R_f = 0.50 (SiO₂, cyclohexane/EtOAc 7:3).

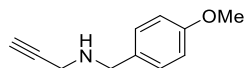
ATR-FTIR (neat) ν = 3293, 3034, 2998, 2931, 2854, 1612, 1512, 1451, 1300, 1245, 1172, 1115, 1036, 940, 824, 746, 634 cm⁻¹.

¹H NMR (500 MHz, CDCl₃) δ = 7.32 – 7.27 (m, 2H, H_{aro}), 6.89 – 6.83 (m, 2H, 2 × OC_qCH_{aro}), 3.83 (s, 2H, NCH₂), 3.80 (s, 3H, CH₃), 2.41 (s, 1H, ≡CH), 1.92 – 1.84 (m, 2H, 2 × NC_qCH₂), 1.74 – 1.55 (m, 5H), 1.45 (td, *J* = 11.9, 3.8 Hz, 2H), 1.29 – 1.19 (m, 1H) ppm.

¹³C{¹H} NMR (126 MHz, CDCl₃) δ = 158.7 (CH₃OC_q), 133.2 (NCH₂C_q), 129.8 (C_{aro}H), 113.9 (C_{aro}H), 88.2 (C≡), 72.0 (C≡), 55.4 (CH₃), 54.8 (NC_q), 47.3 (NCH₂), 38.1 (CH₂), 25.9 (CH₂), 22.9 (CH₂) ppm. N.B.: C≡C could not be assigned as both signals appeared in DEPT135 experiment.

HRMS (ESI-TOF, + mode) *m/z* calcd for C₁₆H₂₂NO 244.1696, found 244.1698 [M+H]⁺.

N-(4-Methoxybenzyl)prop-2-yn-1-amine (CAS: 98729-72-7)



Chemical Formula: C₁₁H₁₃NO
Molecular Weight: 175,2310

The title compound was prepared following the general procedure reported by DUAN and co-workers.^[391] The title compound was isolated as a pale yellow oil (793 mg, 4.527 mmol). Yield 90%.

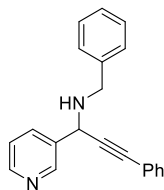
R_f = 0.15 (SiO₂, cyclohexane/EtOAc 7:3).

ATR-FTIR (neat) ν = 3288, 3062, 3033, 2999, 2954, 2933, 2911, 2835, 1611, 1511, 1455, 1300, 1242, 1173, 1101, 1032, 906, 812, 636 cm⁻¹.

¹H NMR (500 MHz, CDCl₃) δ = 7.29 – 7.24 (m, 2H, H_{aro}), 6.89 – 6.84 (m, 2H, 2 × OC_qCH_{aro}), 3.82 (s, 2H, NCH₂C_{aro}), 3.80 (s, 3H, CH₃), 3.42 (d, *J* = 2.4 Hz, 2H, NCH₂C≡), 2.26 (t, *J* = 2.4 Hz, 1H, ≡CH) ppm.

$^{13}\text{C}\{^1\text{H}\}$ NMR (126 MHz, CDCl_3) δ = 159.0 (CH_3OC_q), 131.7 ($\text{C}_{q\text{-aro}}$), 129.9 (C_{aroH}), 114.0 (C_{aroH}), 82.4 ($\text{C}\equiv$), 71.7 ($\text{C}\equiv$), 55.5 (CH_3), 51.9 (NCH_2C_q), 37.4 ($\text{NCH}_2\text{C}\equiv$) ppm.

N-Benzyl-3-phenyl-1-(pyridin-3-yl)prop-2-yn-1-amine



Chemical Formula: $\text{C}_{21}\text{H}_{18}\text{N}_2$
Molecular Weight: 298,3890

Following the General Procedure A, the title compound was isolated as an orange viscous oil (88 mg, 295 μmol). Yield 30%.

R_f = 0.54 (SiO_2 , $\text{CH}_2\text{Cl}_2/\text{MeOH}$ 9:1).

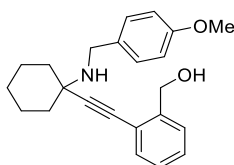
ATR-FTIR (neat) ν = 3303, 3254, 3082, 3057, 3028, 2923, 2844, 1957, 1880, 1791, 1644, 1576, 1489, 1421, 1295, 1095, 1026, 754, 690 cm^{-1} .

^1H NMR (500 MHz, CDCl_3) δ = 8.87 (d, J = 2.4 Hz, 1H, H_{aro}), 8.56 (d, J = 2.5 Hz, 1H, H_{aro}), 7.97 (dt, J = 8.0, 2.0 Hz, 1H, H_{aro}), 7.53 – 7.48 (m, 2H, H_{aro}), 7.43 – 7.39 (m, 2H, H_{aro}), 7.37 – 7.27 (m, 8H, H_{aro}), 4.85 (s, 1H, NCH), 4.01 (s, 2H, NCH_2) ppm.

$^{13}\text{C}\{^1\text{H}\}$ NMR (126 MHz, CDCl_3) δ = 149.6 (C_{aroH}), 149.3 (C_{aroH}), 139.6 ($\text{C}_{q\text{-aro}}$), 135.4 (C_{aroH}), 131.9 (C_{aroH}), 128.7 (C_{aroH}), 128.6(2) (C_{aroH}), 128.6(0) (C_{aroH}), 128.5 (C_{aroH}), 127.4 (C_{aroH}), 123.5 (C_{aroH}), 122.8 ($\text{C}_{q\text{-aro}}$), 88.0 ($\text{C}\equiv$), 86.7 ($\text{C}\equiv$), 51.6 (CH), 51.2 (CH_2) ppm.

HRMS (ESI-TOF, + mode) m/z calcd for $\text{C}_{21}\text{H}_{19}\text{N}_2$ 299.1543, found 299.1536 [$\text{M}+\text{H}$] $^+$.

(2-((1-((4-Methoxybenzyl)amino)cyclohexyl)ethynyl)phenyl)methanol



Chemical Formula: $\text{C}_{23}\text{H}_{27}\text{NO}_2$
Molecular Weight: 349,4740

Following the General Procedure A at 65 $^\circ\text{C}$ for 80 h, the title compound was isolated as an orange resin (569 mg, 1.63 mmol). Yield 41%.

R_f = 0.35 (SiO_2 , $\text{CH}_2\text{Cl}_2/\text{MeOH}$ 95:5).

ATR-FTIR (neat) ν = 3296, 3062, 3030, 2997, 2929, 2853, 1611, 1512, 1448, 1299, 1245, 1176, 1104, 1034, 820, 757, 713 cm^{-1} .

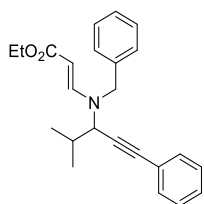
^1H NMR (500 MHz, CDCl_3) δ = 7.50 – 7.43 (m, 2H, H_{aro}), 7.37 – 7.24 (m, 4H, H_{aro}), 6.89 – 6.83 (m, 2H, 2 \times $\text{OC}_q\text{CH}_{\text{aro}}$), 4.86 (s, 2H, OCH_2), 3.91 (s, 2H, NCH_2), 3.79 (s, 3H, CH_3), 2.03 – 1.96 (m, 2H, 2 \times NC_qCH_2), 1.78 – 1.71 (m, 2H), 1.71 – 1.61 (m, 3H), 1.54 (td, J = 12.0, 3.7 Hz, 2H), 1.33 – 1.22 (m, 1H) ppm.

$^{13}\text{C}\{^1\text{H}\}$ NMR (126 MHz, CDCl_3) δ = 158.7 (CH_3OC_q), 142.5 ($\text{C}_{q\text{-aro}}$), 133.0 ($\text{C}_{q\text{-aro}}$), 132.5 (C_{aroH}), 129.8 (C_{aroH}), 128.4, (C_{aroH}) 127.5 (C_{aroH}), 127.2 (C_{aroH}), 121.7 (C_q), 114.0 (C_{aroH}), 98.8 ($\text{C}\equiv$), 82.2 ($\text{C}\equiv$), 64.2 (OCH_2), 55.7 (NC_q), 55.4 (CH_3), 47.6 (NCH_2), 38.3 (CH_2), 26.0 (CH_2), 23.2 (CH_2) ppm.

HRMS (ESI-TOF, + mode) m/z calcd for $\text{C}_{23}\text{H}_{28}\text{NO}_2$ 350.2115, found 350.2132 [$\text{M}+\text{H}$] $^+$.

Enynes

Ethyl (E)-3-(benzyl(4-methyl-1-phenylpent-1-yn-3-yl)amino)acrylate (E.3)



Chemical Formula: $\text{C}_{24}\text{H}_{27}\text{NO}_2$
Molecular Weight: 361,4850

Following the General Procedure K in EtOAc at 100 $^\circ\text{C}$ for 16 h, the title compound **E.3** was obtained as an orange resin (81 mg) and used without further purification.

R_f = 0.58 (Al_2O_3 neutral, cyclohexane/EtOAc 8:2).

ATR-FTIR (neat) ν = 3084, 3062, 3030, 2966, 2931, 2901, 2872, 1720, 1687, 1606, 1490, 1453, 1368, 1242, 1136, 1045, 968, 793, 756, 691 cm^{-1} .

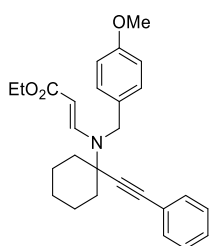
^1H NMR (500 MHz, CDCl_3) δ = 7.77 (d, J = 13.2 Hz, 1H, $\text{NCH}=\text{CH}$), 7.35 – 7.27 (m, 10H, H_{aro}), 4.66 (d, J = 13.2 Hz, 1H, $\text{NCH}=\text{CH}$), 4.60 (d, J = 16.3 Hz, 1H, NCH_2), 4.34 (d, J = 16.2 Hz, 1H, NCH_2), 4.10 (q, J = 7.0 Hz, 2H, OCH_2), 4.05 (d, J = 8.1 Hz, 1H, NCH), 2.12

(h, $J = 6.8$ Hz, 1H, $\text{CH}(\text{CH}_3)_2$), 1.23 (t, $J = 7.1$ Hz, 3H, OCH_2CH_3), 1.11 (d, $J = 6.6$ Hz, 3H, $1 \times \text{CH}(\text{CH}_3)_2$), 0.99 (d, $J = 6.7$ Hz, 3H, $1 \times \text{CH}(\text{CH}_3)_2$) ppm.

$^{13}\text{C}\{^1\text{H}\}$ NMR (126 MHz, CDCl_3) $\delta = 169.7$ (C=O), 150.8 (NCH=), 136.5 (C_q), 131.7 (CH), 128.7 (CH), 128.6 (CH), 128.4 (CH), 127.4 (CH), 127.1 (CH), 122.5 (C_q), 87.4 (C \equiv), 87.2 (NCH=CH), 85.5 (C \equiv), 59.2 (OCH_2), 52.2 (NCHC \equiv) 33.3 ($\text{CH}(\text{CH}_3)_2$), 19.8 ($1 \times \text{CH}(\text{CH}_3)_2$), 19.1 ($1 \times \text{CH}(\text{CH}_3)_2$), 14.7 (CH_2CH_3) ppm.

HRMS (ESI-TOF, + mode) m/z calcd for $\text{C}_{24}\text{H}_{28}\text{NO}_2$ 362.2115, found 362.2100 $[\text{M}+\text{H}]^+$.

Ethyl (E)-3-((4-methoxybenzyl)(1-(phenylethynyl)cyclohexyl)amino)acrylate (E.4)



Chemical Formula: $\text{C}_{27}\text{H}_{31}\text{NO}_3$
Molecular Weight: 417,5490

Following the General Procedure K in EtOAc at 100 °C for 21 h, the title compound **E.4** was obtained as an orange resin (511 mg) and used without further purification.

$R_f = 0.56$ (Al_2O_3 neutral, cyclohexane/EtOAc 8:2).

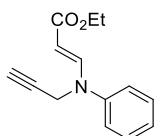
ATR-FTIR (neat) $\nu = 3059, 2933, 2858, 2836, 1685, 1597, 1511, 1443, 1328, 1242, 1139, 1099, 1033, 961, 911, 792, 755, 691$ cm^{-1} .

^1H NMR (500 MHz, CDCl_3) $\delta = 8.20$ (d, $J = 12.9$ Hz, 1H, NCH=CH), 7.36 – 7.27 (m, 5H, H_{aro}), 7.19 – 7.12 (m, 2H, H_{aro}), 6.86 – 6.82 (m, 2H, $2 \times \text{OC}_q\text{CH}_{\text{aro}}$), 4.59 (d, $J = 13.0$ Hz, 1H, NCH=CH), 4.57 (s, 2H, NCH $_2$), 4.09 (q, $J = 7.1$ Hz, 2H, OCH_2), 3.79 (s, 3H, OCH_3), 2.15 – 2.09 (m, 2H, $2 \times \text{NC}_q\text{CH}_2$), 1.83 – 1.68 (m, 7H), 1.22 (t, $J = 7.1$ Hz, 3H, OCH_2CH_3), 1.19 – 1.12 (m, 1H) ppm.

$^{13}\text{C}\{^1\text{H}\}$ NMR (126 MHz, CDCl_3) $\delta = 170.0$ (C=O), 158.5 (CH_3OC_q), 147.7 (NCH), 131.7 (CH), 129.4 (C_q), 128.6 (CH), 128.4 (CH), 127.5 (CH), 122.6 (C_q), 114.0 (CH), 89.2 (C \equiv), 88.1 (C \equiv), 87.7 (NCH=CH), 63.0 (NC_q), 59.1 (OCH_2), 55.4 (OCH_3), 50.0 (NCH $_2$), 37.6 (CH_2), 25.2 (CH_2), 23.9 (CH_2), 14.7 (CH_2CH_3) ppm.

HRMS (ESI-TOF, + mode) m/z calcd for $\text{C}_{27}\text{H}_{31}\text{NNaO}_3$ 440.2196, found 440.2193 $[\text{M}+\text{Na}]^+$.

Ethyl (E)-3-(phenyl(prop-2-yn-1-yl)amino)acrylate (E.5)



Chemical Formula: $\text{C}_{14}\text{H}_{15}\text{NO}_2$
Molecular Weight: 229,2790

Following the General Procedure L in EtOH at 100 °C for 5 h, the title compound **E.5** was obtained as an orange viscous oil (44 mg) and used without further purification.

$R_f = 0.50$ (Al_2O_3 neutral, cyclohexane/EtOAc 9:1).

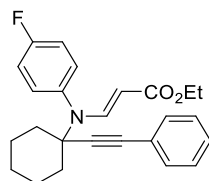
ATR-FTIR (neat) $\nu = 3290, 3246, 3091, 3064, 3043, 2979, 2932, 2904, 2872, 2119, 1688, 1614, 1584, 1496, 1444, 1325, 1275, 1210, 1142, 1050, 965, 918, 802, 757, 694$ cm^{-1} .

^1H NMR (300 MHz, CDCl_3) $\delta = 7.84$ (d, $J = 13.4$ Hz, 1H, NCH=CH), 7.42 – 7.33 (m, 2H, H_{aro}), 7.25 – 7.13 (m, 3H, H_{aro}), 5.10 (d, $J = 13.4$ Hz, 1H, NCH=CH), 4.33 (d, $J = 2.5$ Hz, 2H, NCH $_2$), 4.18 (q, $J = 7.1$ Hz, 2H, OCH_2), 2.34 (t, $J = 2.5$ Hz, 1H, $\equiv\text{CH}$), 1.29 (t, $J = 7.1$ Hz, 3H, CH_3) ppm.

$^{13}\text{C}\{^1\text{H}\}$ NMR (126 MHz, CDCl_3) $\delta = 169.0$ (C=O), 147.1 (CH), 145.5 ($\text{C}_{q-\text{Ph}}$), 129.7 (CH), 125.1 (CH), 120.6 (CH), 92.3, 77.6, 73.5, 59.7 (OCH_2), 39.9 (NCH $_2$), 14.7 (CH_3) ppm. N.B.: $2 \times$ (C \equiv) and (NCH=CH) could not be assigned as all three signals appeared in DEPT135 experiment.

HRMS (ESI-TOF, + mode) m/z calcd for $\text{C}_{14}\text{H}_{15}\text{NNaO}_2$ 252.0995, found 252.1007 $[\text{M}+\text{Na}]^+$.

Ethyl (E)-3-((4-fluorophenyl)(1-(phenylethynyl)cyclohexyl)amino)acrylate (E.6)



Chemical Formula: C₂₅H₂₆FNO₂
Molecular Weight: 391,4864

Following the General Procedure L in EtOH at 100 °C for 18, the title compound **E.6** was isolated as a brown resin (90 mg) and used without further purification.

R_f = 0.60 (Al₂O₃ neutral, cyclohexane/EtOAc 8:2).

ATR-FTIR (neat) ν = 3081, 2977, 2933, 2858, 1688, 1609, 1590, 1504, 1330, 1223, 1132, 1066, 803, 755, 691 cm⁻¹.

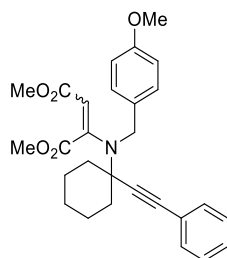
¹H NMR (500 MHz, CDCl₃) δ = 8.35 (d, J = 13.0 Hz, 1H, NCH=CH), 7.49 – 7.40 (m, 2H, H_{aro}), 7.36 – 7.29 (m, 3H, H_{aro}), 7.24 – 7.18 (m, 2H, H_{aro}), 7.14 – 7.07 (m, 2H, H_{aro}), 4.18 (d, J = 12.9 Hz, 1H, NCH=CH), 4.09 (q, J = 7.1 Hz, 2H, OCH₂), 2.13 – 2.04 (m, 2H, 2 × NC_qCH₂), 1.81 – 1.63 (m, 6H), 1.56 (m, 2H), 1.21 (t, J = 7.1 Hz, 3H, CH₃), 1.15 – 1.05 (m, 1H) ppm.

¹⁹F{¹H} NMR (282 MHz, CDCl₃) δ = -113.11 ppm.

¹³C{¹H} NMR (126 MHz, CDCl₃) δ = 169.4 (C=O), 162.2 (d, ¹J_{C-F} = 248.1 Hz, FC_q), 149.8 (NCH), 136.3 (d, ⁴J_{C-F} = 3.4 Hz, NC_{q-aro}), 132.0 (d, ³J_{C-F} = 8.6 Hz, FC_qCHCH), 131.8 (CH), 128.6 (CH), 128.5 (CH), 122.6 (C_q), 116.5 (d, ²J_{C-F} = 22.4 Hz, FC_qCH), 90.2 (NCH=CH), 90.0 (C≡), 88.1 (C≡), 61.7 (NC_q), 59.2 (OCH₂), 38.5 (CH₂), 25.0 (CH₂), 23.7 (CH₂), 14.7 (CH₃) ppm.

HRMS (ESI-TOF, + mode) m/z calcd for C₂₅H₂₆FNNaO₂ 414.1840, found 414.1853 [M+Na]⁺.

Dimethyl 2-((4-methoxybenzyl)(1-(phenylethynyl)cyclohexyl)amino)maleate (E.8)



Chemical Formula: C₂₈H₃₁NO₅
Molecular Weight: 461,5580

Following the General Procedure L in EtOH at 100 °C for 5 min, the title compound **E.8** was isolated as a yellow viscous oil (75 mg, 162 μmol) after column chromatography over silica gel. Yield 86%.

R_f = 0.30 (SiO₂, cyclohexane/EtOAc 8:2).

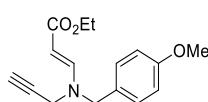
ATR-FTIR (neat) ν = 3063, 2992, 2935, 2858, 1738, 1698, 1566, 1512, 1435, 1353, 1246, 1139, 1035, 941, 799, 756, 691 cm⁻¹.

¹H NMR (500 MHz, CDCl₃) δ = 7.38 – 7.24 (m, 7H, H_{aro}), 6.88 – 6.79 (m, 2H, 2 × OC_qCH_{aro}), 5.68 (s, 1H, CHC=O), 4.47 (s, 2H, NCH₂), 3.78 (s, 3H, OCH₃), 3.77 (s, 3H, OCH₃), 3.65 (s, 3H, OCH₃), 2.46 – 2.34 (m, 2H, 2 × NC_qCH₂), 1.78 – 1.56 (m, 7H), 1.20 – 1.08 (m, 1H) ppm.

¹³C{¹H} NMR (126 MHz, CDCl₃) δ = 167.9 (C=O), 167.1 (C=O), 158.8 (CH₃OC_q), 153.0 (C_q), 131.7 (CH), 130.6 (C_q), 128.4 (CH), 128.3 (CH), 128.3 (CH), 122.9 (C_q), 113.9 (CH), 94.3 (NCH=CH), 89.2 (C≡), 88.8 (C≡), 60.2 (NC_q), 55.3 (OCH₃), 53.0 (OCH₃), 51.4 (NCH₂), 51.1 (OCH₃), 35.6 (CH₂), 25.3 (CH₂), 23.5 (CH₂) ppm.

HRMS (ESI-TOF, + mode) m/z calcd for C₂₈H₃₁NNaO₅ 484.2094, found 484.2104 [M+Na]⁺.

Ethyl (E)-3-((4-methoxybenzyl)(prop-2-yn-1-yl)amino)acrylate (E.15)



Chemical Formula: C₁₆H₁₉NO₃
Molecular Weight: 273,3320

Following the General Procedure K in EtOAc at 100 °C for 1 h, the title compound **E.15** was obtained as an orange resin (82 mg) and used without further purification.

R_f = 0.37 (Al₂O₃ neutral, cyclohexane/EtOAc 8:2).

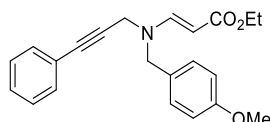
ATR-FTIR (neat) ν = 3286, 3246, 3033, 2977, 2934, 2904, 2837, 2116, 1683, 1604, 1511, 1442, 1366, 1300, 1245, 1137, 1033, 972, 793, 639 cm⁻¹.

¹H NMR (500 MHz, CDCl₃) δ = 7.57 (d, J = 13.1 Hz, 1H, NCH=CH), 7.19 – 7.14 (m, 2H, H_{aro}), 6.90 – 6.84 (m, 2H, 2 × OC_qCH_{aro}), 4.83 (d, J = 13.2 Hz, 1H, NCH=CH), 4.34 (s, 2H, NCH₂C_{aro}), 4.15 (q, J = 7.1 Hz, 2H, OCH₂), 3.80 (s, 3H, OCH₃), 3.77 (d, J = 2.4 Hz, 2H, NCH₂C≡), 2.28 (t, J = 2.5 Hz, 1H, ≡CH), 1.27 (t, J = 7.1 Hz, 3H, CH₂CH₃) ppm.

¹³C{¹H} NMR (126 MHz, CDCl₃) δ = 169.6 (C=O), 159.5 (CH₃OC_q), 151.3 (NCH), 129.3 (CH), 127.6 (CH₂C_{q-aro}), 114.3 (CH), 87.5 (NCH=CH), 73.5 (C≡), 59.4 (OCH₂), 55.4 (OCH₃), 14.7 (CH₂CH₃) ppm. N.B.: some C signals are missing because they were not observed in the ¹³C NMR spectrum.

HRMS (ESI-TOF, + mode) m/z calcd for C₁₆H₂₀NO₃ 274.1438, found 274.1439 [M+H]⁺.

Ethyl (E)-3-((4-methoxybenzyl)(3-phenylprop-2-yn-1-yl)amino)acrylate (E.16)



Chemical Formula: C₂₂H₂₃NO₃
Molecular Weight: 349,4300

Following the General Procedure L in EtOH at 100 °C for 10 min, the title compound **E.16** was isolated as an orange resin (38 mg) and used without further purification.

R_f = 0.50 (SiO₂, cyclohexane/EtOAc 7:3).

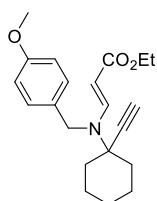
ATR-FTIR (neat) ν = 3059, 3034, 2977, 2955, 2931, 2905, 2836, 1686, 1606, 1511, 1442, 1366, 1246, 1138, 1032, 973, 792, 756, 691 cm⁻¹.

¹H NMR (300 MHz, CDCl₃) δ = 7.64 (d, J = 13.2 Hz, 1H, NCH=CH), 7.42 – 7.34 (m, 2H, H_{aro}), 7.34 – 7.27 (m, 3H, H_{aro}), 7.24 – 7.17 (m, 2H, H_{aro}), 6.91 – 6.85 (m, 2H, 2 × OC_qCH_{aro}), 4.86 (d, J = 13.1 Hz, 1H, NCH=CH), 4.41 (s, 2H, NCH₂C_{aro}), 4.15 (q, J = 7.1 Hz, 2H, OCH₂), 4.01 (s, 2H, NCH₂C≡), 3.80 (s, 3H, OCH₃), 1.27 (t, J = 7.1 Hz, 3H, CH₂CH₃) ppm.

¹³C{¹H} NMR (126 MHz, CDCl₃) δ = 169.7 (C=O), 159.5 (CH₃OC_q), 151.5 (NCH), 131.9 (CH), 129.3 (CH), 128.7 (CH), 128.4 (CH), 127.9 (C_q), 122.5 (C_q), 114.3 (CH), 87.2 (NCH=CH), 85.3 (C≡), 82.9 (C≡), 59.3 (OCH₂), 55.5 (OCH₃), 14.7 (CH₂CH₃) ppm. N.B.: The NCH₂C≡ was not observed in the ¹³C and DEPT135 NMR spectra.

HRMS (ESI-TOF, + mode) m/z calcd for C₂₂H₂₄NO₃ 350.1751, found 350.1735 [M+H]⁺.

Ethyl (E)-3-((1-ethynylcyclohexyl)(4-methoxybenzyl)amino)acrylate (E.17)



Chemical Formula: C₂₁H₂₇NO₃
Molecular Weight: 341,4510

Following the General Procedure L in EtOH at 100 °C for 10 min, the title compound **E.17** was obtained as a colourless resin (44 mg) and used without further purification.

R_f = 0.55 (Al₂O₃ neutral, cyclohexane/EtOAc 8:2).

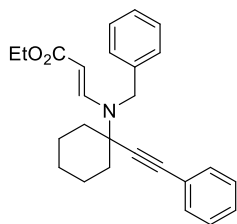
ATR-FTIR (neat) ν = 3286, 3229, 2935, 2860, 2836, 1683, 1598, 1511, 1447, 1329, 1243, 1142, 1102, 1035, 971, 909, 794, 730, 645 cm⁻¹.

¹H NMR (300 MHz, CDCl₃) δ = 8.11 (d, J = 13.0 Hz, 1H, NCH=CH), 7.15 – 7.07 (m, 2H, H_{aro}), 6.87 – 6.80 (m, 2H, 2 × OC_qCH_{aro}), 4.58 (d, J = 13.0 Hz, 1H, NCH=CH), 4.50 (s, 2H, NCH₂), 4.08 (q, J = 7.1 Hz, 2H, OCH₂), 3.78 (s, 3H, OCH₃), 2.56 (s, 1H, ≡CH), 2.10 – 1.99 (m, 2H, 2 × NC_qCH₂), 1.81 – 1.56 (m, 7H), 1.21 (t, J = 7.1 Hz, 3H, CH₂CH₃), 1.16 – 1.04 (m, 1H) ppm.

¹³C{¹H} NMR (126 MHz, CDCl₃) δ = 169.9 (C=O), 158.5 (CH₃OC_q), 147.6 (NCH), 129.3 (C_{q-aro}), 127.4 (C_{aro}H), 114.0 (C_{aro}H), 88.1, 83.9, 75.9, 62.2 (NC_q), 59.1 (OCH₂), 55.4 (OCH₃), 49.8 (NCH₂), 37.3 (CH₂), 25.0 (CH₂), 23.6 (CH₂), 14.7 (CH₂CH₃) ppm. N.B.: C=C and NCH=CH could not be assigned as all three signals appeared in DEPT135 experiment.

HRMS (ESI-TOF, + mode) m/z calcd for C₂₁H₂₈NO₃ 342.2064, found 342.2055 [M+H]⁺.

Ethyl (E)-3-(benzyl(1-(phenylethynyl)cyclohexyl)amino)acrylate



Chemical Formula: C₂₆H₂₉NO₂
Molecular Weight: 387,5230

Following the General Procedure K in EtOAc at 100 °C for 20 h, the title compound was obtained as a brown solid (109 mg) and used without further purification.

R_f = 0.72 (Al₂O₃ neutral, cyclohexane/EtOAc 8:2).

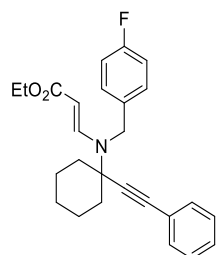
ATR-FTIR (neat) ν = 3057, 2977, 2933, 2855, 1679, 1596, 1452, 1329, 1288, 1148, 1013, 905, 797, 755, 692 cm⁻¹.

¹H NMR (500 MHz, CDCl₃) δ = 8.22 (d, *J* = 13.0 Hz, 1H, NCH=CH), 7.34 – 7.27 (m, 7H, H_{aro}), 7.25 – 7.21 (m, 3H, H_{aro}), 4.63 (s, 2H, NCH₂), 4.58 (d, *J* = 13.0 Hz, 1H, NCH=CH), 4.09 (q, *J* = 7.1 Hz, 2H, OCH₂), 2.17 – 2.09 (m, 2H, 2 × NC_qCH₂), 1.84 – 1.68 (m, 7H), 1.22 (t, *J* = 7.1 Hz, 3H, CH₃), 1.20 – 1.12 (m, 1H) ppm.

¹³C{¹H} NMR (126 MHz, CDCl₃) δ = 169.9 (C=O), 147.7 (NCH), 137.4 (C_q), 131.7 (CH), 128.6(1) (CH), 128.6(0) (CH), 128.4 (CH), 126.9 (CH), 126.3 (CH), 122.6 (C_q), 89.1 (C≡), 88.1 (C≡), 87.8 (NCH=CH), 63.0 (NC_q), 59.1 (OCH₂), 50.5 (NCH₂), 37.6 (CH₂), 25.2 (CH₂), 23.9 (CH₂), 14.7 (CH₃). ppm.

HRMS (ESI-TOF, + mode) *m/z* calcd for C₂₆H₂₉NNaO₂ 410.2090, found 410.2107 [M+Na]⁺.

Ethyl (E)-3-((4-fluorobenzyl)(1-(phenylethynyl)cyclohexyl)amino)acrylate



Chemical Formula: C₂₆H₂₈FNO₂
Molecular Weight: 405,5134

Following the General Procedure K in EtOAc at 100 °C for 18 h, the title compound was obtained as an orange resin (102 mg) and used without further purification.

R_f = 60 (Al₂O₃ neutral, cyclohexane/EtOAc 8:2).

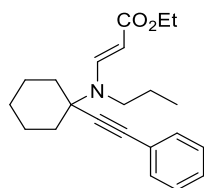
ATR-FTIR (neat) ν = 3057, 2933, 2858, 1686, 1595, 1508, 1444, 1328, 1222, 1141, 1108, 962, 793, 755, 691 cm⁻¹.

¹H NMR (500 MHz, CDCl₃) δ = 8.18 (d, *J* = 13.0 Hz, 1H, NCH=CH), 7.34 – 7.28 (m, 5H, H_{aro}), 7.23 – 7.17 (m, 2H, H_{aro}), 7.03 – 6.96 (m, 2H, H_{aro}), 4.59 (s, 2H, NCH₂), 4.55 (d, *J* = 13.0 Hz, 1H, NCH=CH), 4.10 (q, *J* = 7.1 Hz, 2H, OCH₂), 2.15 – 2.08 (m, 2H, 2 × NC_qCH₂), 1.84 – 1.70 (m, 7H), 1.22 (t, *J* = 7.1 Hz, 3H, CH₃), 1.20 – 1.16 (m, 1H) ppm.

¹³C{¹H} NMR (126 MHz, CDCl₃) δ = 169.8 (C=O), 161.9 (d, ¹*J*_{C-F} = 244.7 Hz, FC_q), 147.4 (NCH), 133.0 (d, ⁴*J*_{C-F} = 3.1 Hz, NCH₂C_q), 131.7 (CH), 128.7 (CH), 128.5 (CH), 127.9 (d, ³*J*_{C-F} = 7.9 Hz, FC_qCHCH), 122.4 (C_q), 115.5 (d, ²*J*_{C-F} = 21.5 Hz, FC_qCH), 89.0 (C≡), 88.2 (C≡), 88.0 (NCH=CH), 63.0 (NC_q), 59.2 (OCH₂), 50.0 (NCH₂), 37.7 (CH₂), 25.2 (CH₂), 23.9 (CH₂), 14.7(CH₃) ppm.

HRMS (ESI-TOF, + mode) *m/z* calcd for C₂₆H₂₈FNNaO₂ 428.1996, found 428.1989 [M+Na]⁺.

Ethyl (E)-3-((1-(phenylethynyl)cyclohexyl)(propyl)amino)acrylate



Chemical Formula: C₂₂H₂₉NO₂
Molecular Weight: 339,4790

Following the General Procedure K in EtOAc at 100 °C for 3 h, the title compound was obtained as an orange resin (87 mg) and used without further purification.

R_f = 0.60 (SiO₂, cyclohexane/EtOAc 7:3).

ATR-FTIR (neat) ν = 3059, 2933, 2859, 1686, 1593, 1490, 1444, 1329, 1253, 1172, 1137, 1071, 963, 790, 755, 690 cm⁻¹.

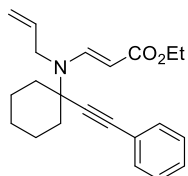
¹H NMR (500 MHz, CDCl₃) δ = 8.02 (d, *J* = 13.0 Hz, 1H, NCH=CH), 7.47 – 7.41 (m, 2H, H_{aro}), 7.36 – 7.29 (m, 3H, H_{aro}), 4.64 (d, *J* = 13.0 Hz, 1H, NCH=CH), 4.14 (q, *J* = 7.1 Hz, 2H, OCH₂), 3.30 – 3.22 (m, 2H, NCH₂), 2.10 – 2.03 (m, 2H,

2 × NC_qCH₂), 1.82 – 1.65 (m, 9H), 1.27 (t, *J* = 7.1 Hz, 3H, OCH₂CH₃), 1.22 – 1.13 (m, 1H), 0.91 (t, *J* = 7.4 Hz, 3H, NCH₂CH₂CH₃) ppm.

¹³C{¹H} NMR (126 MHz, CDCl₃) δ = 170.2 (C=O), 147.2 (NCH), 131.7 (CH), 128.6 (CH), 128.5 (CH), 122.7 (C_q-aro), 89.2 (C≡), 87.8 (C≡), 85.3 (NCH=CH), 62.3 (NC_q), 59.1 (OCH₂), 48.6 (NCH₂), 37.5 (CH₂), 25.2 (CH₂), 23.8 (CH₂), 20.9 (CH₂), 14.8 (CH₃), 11.6 (CH₃) ppm.

HRMS (ESI-TOF, + mode) *m/z* calcd for C₂₂H₂₉NNaO₂ 362.2090, found 362.2099 [M+Na]⁺.

Ethyl (E)-3-(allyl(1-(phenylethynyl)cyclohexyl)amino)acrylate



Chemical Formula: C₂₂H₂₇NO₂
Molecular Weight: 337,4630

Following the General Procedure L in EtOH at 100 °C for 45 min, the title compound was obtained as a yellow-orange resin (58 mg) and used without further purification.

R_f = 0.55 (SiO₂, cyclohexane/EtOAc 7:3).

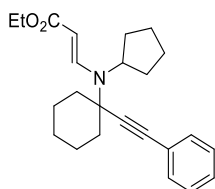
ATR-FTIR (neat) ν = 3081, 3061, 2976, 2933, 2858, 1687, 1596, 1444, 1328, 1241, 1141, 1050, 962, 792, 756, 691 cm⁻¹.

¹H NMR (400 MHz, CDCl₃) δ = 8.08 (d, *J* = 12.9 Hz, 1H, NCH=CH), 7.47 – 7.40 (m, 2H, H_{aro}), 7.35 – 7.27 (m, 3H, H_{aro}), 5.81 (ddt, *J* = 17.3, 10.2, 5.0 Hz, 1H, CH=CH₂), 5.24 – 5.14 (m, 2H, CH=CH₂), 4.68 (d, *J* = 12.9 Hz, 1H, NCH=CH), 4.13 (q, *J* = 7.1 Hz, 2H, OCH₂), 4.01 (dt, *J* = 5.0, 1.9 Hz, 2H, NCH₂), 2.15 – 2.04 (m, 2H, 2 × NC_qCH₂), 1.84 – 1.66 (m, 7H), 1.26 (t, *J* = 7.1 Hz, 3H, CH₃), 1.23 – 1.12 (m, 1H) ppm.

¹³C{¹H} NMR (126 MHz, CDCl₃) δ = 170.0 (C=O), 147.2 (NCH), 133.2 (CH), 131.8 (CH), 128.6 (CH), 128.5 (CH), 122.7 (≡C_{aro}), 116.8 (CH=CH₂), 89.1 (C≡), 87.9 (C≡), 86.7 (NCH=CH), 62.5 (NC_q), 59.1 (OCH₂), 49.0 (NCH₂), 37.5 (CH₂), 25.2 (CH₂), 23.8 (CH₂), 14.8 (CH₃) ppm.

HRMS (ESI-TOF, + mode) *m/z* calcd for C₂₂H₂₈NO₂ 338.2115, found 338.2131 [M+H]⁺.

Ethyl (E)-3-(cyclopentyl(1-(phenylethynyl)cyclohexyl)amino)acrylate



Chemical Formula: C₂₄H₃₁NO₂
Molecular Weight: 365,5170

Following the General Procedure K in EtOAc at 100 °C for 24 h, the title compound was obtained as a brown viscous oil (95 mg) and used without further purification.

R_f = 0.68 (Al₂O₃ neutral, cyclohexane/EtOAc 8:2).

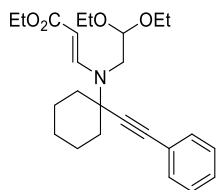
ATR-FTIR (neat) ν = 3059, 2936, 2862, 1720, 1686, 1591, 1490, 1478, 1444, 1332, 1240, 1178, 1135, 1093, 1048, 794, 756, 691 cm⁻¹.

¹H NMR (500 MHz, CDCl₃) δ = 7.87 (d, *J* = 13.7 Hz, 1H, NCH=CH), 7.45 – 7.41 (m, 2H, H_{aro}), 7.35 – 7.30 (m, 3H, H_{aro}), 4.61 (d, *J* = 13.6 Hz, 1H, NCH=CH), 4.25 – 4.19 (m, 1H, NCH cyclopentyl), 4.14 (q, *J* = 7.1 Hz, 2H, OCH₂), 2.28 – 2.19 (m, 2H), 2.16 – 2.09 (m, 2H, 2 × NC_qCH₂), 1.90 – 1.55 (m, 13H), 1.26 (t, *J* = 7.1 Hz, 3H, CH₃), 1.23 – 1.13 (m, 1H) ppm.

¹³C{¹H} NMR (126 MHz, CDCl₃) δ = 170.1 (C=O), 143.6 (NCH=), 131.7 (CH), 128.5(3) (CH), 128.5(1) (CH), 122.8 (C_q), 89.6 (C≡), 87.2 (C≡), 85.7 (NCH=CH), 63.6 (NC_q), 59.4 (NCHCH₂), 59.0 (OCH₂), 37.5 (CH₂), 26.3 (CH₂), 25.4 (CH₂), 25.3 (CH₂), 24.0 (CH₂), 14.9 (CH₂) ppm.

HRMS (ESI-TOF, + mode) *m/z* calcd for C₂₄H₃₁NNaO₂ 388.2247, found 388.2245 [M+Na]⁺.

Ethyl (E)-3-((2,2-diethoxyethyl)(1-(phenylethynyl)cyclohexyl)amino)acrylate



Chemical Formula: C₂₅H₃₅NO₄
Molecular Weight: 413,5580

Following the General Procedure K in EtOAc at 100 °C for 24 h, the title compound was obtained as a brown viscous oil (80 mg) and used without further purification.

R_f = 0.62 (Al₂O₃ neutral, cyclohexane/EtOAc 8:2).

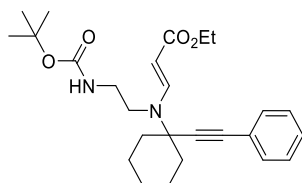
ATR-FTIR (neat) ν = 3057, 2975, 2932, 2861, 1722, 1689, 1598, 1444, 1365, 1331, 1240, 1140, 1042, 795, 756, 691 cm⁻¹.

¹H NMR (500 MHz, CDCl₃) δ = 8.16 (d, *J* = 13.1 Hz, 1H, NCH=CH), 7.49 – 7.42 (m, 2H, H_{aro}), 7.35 – 7.28 (m, 3H, H_{aro}), 4.83 (d, *J* = 13.1 Hz, 1H, NCH=CH), 4.71 (t, *J* = 5.0 Hz, 1H, O₂CH), 4.14 (q, *J* = 7.1 Hz, 2H, CO₂CH₂), 3.71 (dq, *J* = 9.2, 7.0 Hz, 2H, CH(OCH₂CH₃)₂), 3.53 (dq, *J* = 9.2, 7.0 Hz, 2H, CH(OCH₂CH₃)₂), 3.48 (d, *J* = 5.0 Hz, 2H, NCH₂), 2.10 – 2.03 (m, 2H, 2 × NC_qCH₂), 1.83 – 1.65 (m, 7H), 1.26 (t, *J* = 7.1 Hz, 3H, CO₂CH₂CH₃), 1.20 (t, *J* = 7.0 Hz, 6H, CH(OCH₂CH₃)₂) ppm.

¹³C{¹H} NMR (126 MHz, CDCl₃) δ = 169.9 (C=O), 148.8 (NCH), 131.8 (CH), 128.5 (CH), 128.4 (CH), 122.8 (C_{q-aro}), 100.2 (CHO₂), 89.6 (C≡), 88.2 (C≡), 87.3 (NCH=CH), 63.8 (OCH₂), 62.6 (NC_q), 59.2 (OCH₂), 50.0 (NCH₂), 37.7 (CH₂), 25.2 (CH₂), 24.0 (CH₂), 15.5 (CH₃), 14.8 (CH₃) ppm.

HRMS (ESI-TOF, + mode) *m/z* calcd for C₂₅H₃₅NNaO₄ 436.2458, found 436.2464 [M+Na]⁺.

Ethyl (E)-3-((2-((tert-butoxycarbonyl)amino)ethyl)(1-(phenylethynyl)cyclohexyl)amino)acrylate



Chemical Formula: C₂₆H₃₆N₂O₄
Molecular Weight: 440,5840

Following the General Procedure K in EtOAc at 100 °C for 8.5 h, the title compound was obtained as an orange resin (44 mg) and used without further purification.

R_f = 0.30 (Al₂O₃ neutral, cyclohexane/EtOAc 8:2).

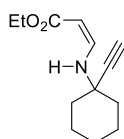
ATR-FTIR (neat) ν = 3347, 3061, 2976, 2934, 2860, 2247, 1690, 1593, 1512, 1444, 1331, 1246, 1142, 1064, 963, 909, 756, 691 cm⁻¹.

¹H NMR (500 MHz, CDCl₃) δ = 8.08 (d, *J* = 13.1 Hz, 1H, NCH=CH), 7.50 – 7.42 (m, 2H, H_{aro}), 7.36 – 7.28 (m, 3H, H_{aro}), 4.83 – 4.72 (m, 2H, 1 × NCH=CH & NH), 4.14 (q, *J* = 7.1 Hz, 2H, OCH₂), 3.51 – 3.41 (m, 2H, BocNHCH₂CH₂), 3.33 (q, *J* = 6.8 Hz, 2H, BocNHCH₂), 2.10 – 2.03 (m, 2H, 2 × NC_qCH₂), 1.84 – 1.63 (m, 7H), 1.43 (s, 9H, C(CH₃)₃), 1.26 (t, *J* = 7.1 Hz, 3H, CH₂CH₃), 1.22 – 1.12 (m, 1H) ppm.

¹³C{¹H} NMR (126 MHz, CDCl₃) δ = 169.9 (CHC=O), 156.1 (NC=O), 147.5 (NCH), 131.8 (CH), 128.7 (CH), 128.5 (CH), 122.5 (C_{q-aro}), 89.0 (C≡), 88.3 (C≡), 86.8 (NCH=CH), 79.6 (C(CH₃)₃), 62.3 (NC_q), 59.2 (OCH₂), 45.7 (CH₂), 38.0 (CH₂), 37.4 (CH₂), 28.5 (C(CH₃)₃), 25.1 (CH₂), 23.8 (CH₂), 14.8 (CH₂CH₃) ppm.

HRMS (ESI-TOF, + mode) *m/z* calcd for C₂₆H₃₇N₂O₄ 441.2748, found 441.2765 [M+H]⁺.

Ethyl (Z)-3-((1-ethynylcyclohexyl)amino)acrylate



Chemical Formula: C₁₃H₁₉NO₂
Molecular Weight: 221,3000

Following the General Procedure L in EtOH at 55 °C for 2 h, the title compound was obtained as a yellow oil (36 mg) and used without further purification.

R_f = 0.70 (SiO₂, cyclohexane/EtOAc 7:3).

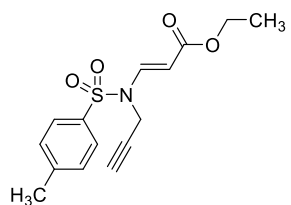
ATR-FTIR (neat) ν = 3294, 2978, 2933, 2858, 1661, 1612, 1470, 1301, 1150, 1035, 784, 634 cm⁻¹.

¹H NMR (500 MHz, CDCl₃) δ = 8.11 (d, J = 12.1 Hz, 1H, NH), 7.08 (dd, J = 13.0, 8.2 Hz, 1H, NCH=CH), 4.59 (d, J = 8.2 Hz, 1H, NCH=CH), 4.11 (q, J = 7.1 Hz, 2H, OCH₂), 2.46 (s, 1H, \equiv CH), 1.98 – 1.91 (m, 2H, 2 \times NC_qCH₂), 1.71 – 1.52 (m, 8H), 1.26 (t, J = 7.1 Hz, 3H, CH₃) ppm.

¹³C{¹H} NMR (126 MHz, CDCl₃) δ = 170.9 (C=O), 148.2 (NCH), 85.2 (C \equiv), 83.7 (NCH=CH), 73.8 (C \equiv), 58.9 (OCH₂), 54.3 (NC_q), 39.5 (CH₂), 25.1 (CH₂), 22.7 (CH₂), 14.7 (CH₃) ppm.

HRMS (ESI-TOF, + mode) m/z calcd for C₁₃H₂₀NO₂ 222.1489, found 222.1487 [M+H]⁺.

Ethyl (E)-3-((4-methyl-N-(prop-2-yn-1-yl)phenyl)sulfonamido)acrylate



Chemical Formula: C₁₅H₁₇NO₄S
Molecular Weight: 307,3640

Ethyl propiolate (153 μ L, 1.5 mmol, 1.5 eq.) was added at room temperature to a solution of propargylamine (209 mg, 1.0 mmol, 1.0 eq.) in MeCN (5 mL, 0.2 M) in a Teflon screw cap tube (3 mL) equipped with a stirrer. Next, *N*-methylmorpholine (110 μ L, 1.0 mmol, 1.0 eq.) was added and the reaction flask was briefly flushed with argon (10 s) before sealing. After 5 h, the reaction mixture was filtered over a silica pad and washed with cyclohexane/EtOAc 7:3 (150 mL). All volatiles were removed under reduced to give a dark yellow crude oil. The crude product was next purified over silica gel (cyclohexane/EtOAc 98:2 \rightarrow 85:15) to give the title compound as a yellow oil (113 mg, 368 μ mol). Yield 37%. N.B.: the (*Z*)-diastereoisomer was isolated in 12% yield.

R_f = 0.51 (SiO₂, cyclohexane/EtOAc 7:3).

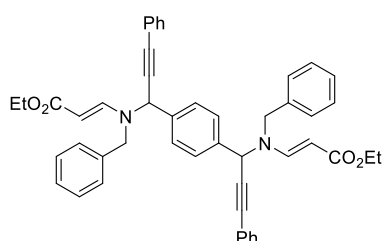
ATR-FTIR (neat) ν = 3289, 3092, 3066, 2981, 2932, 1703, 1623, 1364, 1259, 1152, 1056, 910, 814, 659 cm⁻¹.

¹H NMR (500 MHz, CDCl₃) δ = 7.97 (d, J = 14.0 Hz, 1H, NCH=CH), 7.74 – 7.67 (m, 2H, H_{aro}), 7.34 – 7.28 (m, 2H, H_{aro}), 5.28 (d, J = 14.0 Hz, 1H, NCH=CH), 4.29 (d, J = 2.5 Hz, 2H, NCH₂), 4.16 (q, J = 7.2 Hz, 2H, OCH₂), 2.40 (s, 3H, CH₃ tosyl), 2.06 (t, J = 2.5 Hz, 1H, \equiv CH), 1.25 (t, J = 7.1 Hz, 3H, CH₂CH₃) ppm.

¹³C{¹H} NMR (126 MHz, CDCl₃) δ = 166.8 (C_q), 145.1 (CH), 140.3 (CH), 135.1 (C_q), 130.1 (CH), 127.5 (CH), 100.3 (CH), 75.0, 74.3, 60.3 (OCH₂), 35.4 (NCH₂), 21.7 (CH₃ tosyl), 14.4 (CH₂CH₃) ppm. N.B.: C \equiv C could not be assigned as both signals appear in DEPT135 and in the same phase.

HRMS (ESI-TOF, + mode) m/z calcd for C₁₅H₁₈NO₄S 308.0951, found 308.0952 [M+H]⁺.

Diethyl 3,3'-((1,4-phenylenebis(3-phenylprop-2-yne-1,1-diyl))bis(benzylazanediy))-(2E,2'E)-diacrylate



Chemical Formula: C₄₈H₄₄N₂O₄
Molecular Weight: 712,8900

Following the General Procedure L in EtOH at 100 °C for 20 min with ethyl propiolate (2.1 eq.), the title compound was obtained as a yellow foam (151 mg) and used without further purification.

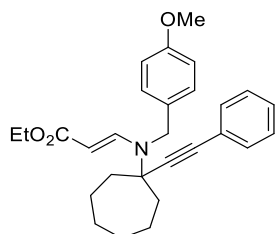
R_f = 0.40 (Al₂O₃ neutral, cyclohexane/EtOAc 9:1).

ATR-FTIR (neat) ν = 3082, 3058, 3030, 2977, 2932, 2899, 1683, 1602, 1490, 1443, 1367, 1239, 1143, 1029, 966, 869, 795, 755, 690 cm⁻¹.

¹H NMR (500 MHz, CDCl₃) δ = 7.69 (d, J = 13.3 Hz, 2H, 2 \times NCH=CH), 7.16 – 6.93 (m, 22H, H_{aro}), 5.37 (s, 2H, 2 \times \equiv CCH), 4.56 (d, J = 13.2 Hz, 2H, 2 \times NCH=CH), 4.15 (d, J = 16.0 Hz, 2H, 2 \times NCH₂), 3.99 (d, J = 16.1 Hz, 2H, 2 \times NCH₂), 3.87 (q, J = 7.1 Hz, 4H, 2 \times OCH₂), 0.99 (t, J = 7.1 Hz, 6H, 2 \times CH₃) ppm.

$^{13}\text{C}\{^1\text{H}\}$ NMR (126 MHz, CDCl_3) δ = 169.5 (C=O), 150.4 (NCH=), 137.5 (C_q), 136.1 (C_q), 131.8 (CH), 129.0 (CH), 128.7 (CH), 128.4 (CH), 128.1(3) (CH), 128.1(2) (CH), 127.5 (CH), 127.3 (CH), 122.0 (C_q), 88.9 ($\text{C}\equiv$), 88.7 (NCH=CH), 84.4 ($\text{C}\equiv$), 59.3 (OCH_2), 14.6 (CH_3) ppm.
HRMS (ESI-TOF, + mode) m/z calcd for $\text{C}_{48}\text{H}_{44}\text{N}_2\text{NaO}_4$ 735.3193, found 735.3212 [$\text{M}+\text{Na}$] $^+$.

Ethyl (E)-3-((4-methoxybenzyl)(1-(phenylethynyl)cycloheptyl)amino)acrylate



Chemical Formula: $\text{C}_{28}\text{H}_{33}\text{NO}_3$
 Molecular Weight: 431,5760

Following the General Procedure K in EtOAc at 100 °C for 21 h, the title compound was obtained as an orange viscous oil (109 mg) and used without further purification.

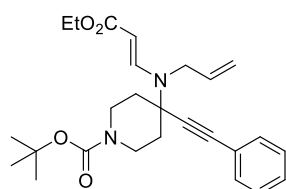
R_f = 0.63 (Al_2O_3 neutral, cyclohexane/EtOAc 8:2).

ATR-FTIR (neat) ν = 3060, 2928, 2858, 1685, 1597, 1511, 1443, 1329, 1242, 1143, 1035, 968, 755, 691 cm^{-1} .

^1H NMR (500 MHz, CDCl_3) δ = 8.19 (d, J = 13.0 Hz, 1H, NCH=CH), 7.32 – 7.27 (m, 5H, H_{aro}), 7.19 – 7.14 (m, 2H, H_{aro}), 6.87 – 6.82 (m, 2H, 2 \times $\text{OC}_q\text{CH}_{\text{aro}}$), 4.58 – 4.52 (m, 3H, 1 \times NCH=CH & NCH₂), 4.09 (q, J = 7.1 Hz, 2H, OCH_2), 3.79 (s, 3H, OCH_3), 2.21 – 2.14 (m, 2H), 2.04 (ddd, J = 13.6, 10.3, 2.8 Hz, 2H), 1.86 – 1.67 (m, 6H), 1.64 – 1.54 (m, 2H), 1.22 (t, J = 7.1 Hz, 3H, CH_2CH_3) ppm.
 $^{13}\text{C}\{^1\text{H}\}$ NMR (126 MHz, CDCl_3) δ = 169.9 (C=O), 158.6 (CH_3OC_q), 148.1 (NCH), 131.7 (CH), 129.5 (C_q), 128.6 (CH), 128.4 (CH), 127.5 (CH), 122.6 (C_q), 114.0 (CH), 90.0 ($\text{C}\equiv$), 87.9 (NCH=CH), 87.7 ($\text{C}\equiv$), 66.3 (NC_q), 59.1 (OCH_2), 55.4 (OCH_3), 50.6 (NCH₂), 40.8 (CH_2), 27.4 (CH_2), 23.4 (CH_2), 14.7 (CH_2CH_3) ppm.

HRMS (ESI-TOF, + mode) m/z calcd for $\text{C}_{28}\text{H}_{34}\text{NO}_3$ 432.2533, found 432.2540 [$\text{M}+\text{H}$] $^+$.

tert-Butyl (E)-4-(allyl(3-ethoxy-3-oxoprop-1-en-1-yl)amino)-4-(phenylethynyl)piperidine-1-carboxylate



Chemical Formula: $\text{C}_{26}\text{H}_{34}\text{N}_2\text{O}_4$
 Molecular Weight: 438,5680

Following the General Procedure K in EtOAc at 100 °C for 24 h, the title compound was isolated as a red-brown viscous oil (75 mg) and used without further purification.

R_f = 0.48 (Al_2O_3 neutral, cyclohexane/EtOAc 8:2).

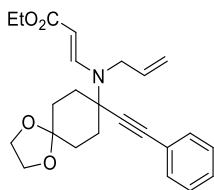
ATR-FTIR (neat) ν = 3083, 3062, 2975, 2931, 2869, 1687, 1597, 1419, 1364, 1330, 1245, 1139, 1023, 962, 864, 794, 756, 691 cm^{-1} .

^1H NMR (500 MHz, CDCl_3) δ = 8.02 (d, J = 13.0 Hz, 1H, NCH=CH), 7.45 – 7.42 (m, 2H, H_{aro}), 7.38 – 7.30 (m, 3H, H_{aro}), 5.79 (ddt, J = 17.6, 9.9, 4.8 Hz, 1H, $\text{CH}=\text{CH}_2$), 5.20 (m, 2H, $\text{CH}=\text{CH}_2$), 4.72 (d, J = 13.0 Hz, 1H, NCH=CH), 4.33 – 4.07 (m, 4H, 2 \times BocNCH₂ & OCH_2), 3.99 (dd, J = 4.6, 2.3 Hz, 2H, NCH₂ allyl), 3.16 (bs, 2H, 2 \times BocNCH₂), 2.08 – 1.99 (m, 2H, 2 \times NC_qCH_2), 1.87 (td, J = 12.3, 4.3 Hz, 2H, 2 \times NC_qCH_2), 1.47 (s, 9H, $\text{C}(\text{CH}_3)_3$), 1.26 (t, J = 7.1 Hz, 3H, CH_2CH_3) ppm.

$^{13}\text{C}\{^1\text{H}\}$ NMR (126 MHz, CDCl_3) δ = 169.8 ($\text{CHC}=\text{O}$), 154.6 ($\text{NC}=\text{O}$), 146.7 (NCH), 132.7 (CH), 131.8 (CH), 129.0 (CH), 128.6 (CH), 121.9 (C_q), 117.1 ($\text{CH}=\text{CH}_2$), 89.1 ($\text{C}\equiv$), 87.8 (NCH=CH), 87.1 ($\text{C}\equiv$), 80.2 ($\text{C}(\text{CH}_3)_3$), 61.1 (NC_q), 59.3 (OCH_2), 48.9 ($=\text{CHNCH}_2$), 41.8 (CH_2), 40.9 (CH_2), 36.7 (CH_2), 28.5 ($\text{C}(\text{CH}_3)_3$), 14.8 (CH_2CH_3) ppm.

HRMS (ESI-TOF, + mode) m/z calcd for $\text{C}_{26}\text{H}_{34}\text{N}_2\text{NaO}_4$ 461.2411, found 461.2405 [$\text{M}+\text{Na}$] $^+$.

Ethyl (E)-3-(allyl(8-(phenylethynyl)-1,4-dioxaspiro[4.5]decan-8-yl)amino)acrylate



Chemical Formula: C₂₄H₂₉NO₄
Molecular Weight: 395,4990

Following the General Procedure K in EtOAc at 100 °C for 24 h, the title compound was isolated as a brown viscous oil (100 mg) and used without further purification.

R_f = 0.38 (Al₂O₃ neutral, cyclohexane/EtOAc 8:2).

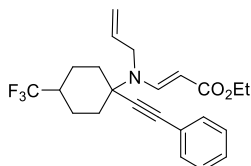
ATR-FTIR (neat) ν = 3081, 3060, 2955, 2932, 2885, 2244, 1717, 1686, 1597, 1490, 1443, 1367, 1329, 1242, 1144, 1106, 1033, 954, 793, 757, 691 cm⁻¹.

¹H NMR (500 MHz, CDCl₃) δ = 8.11 (d, *J* = 13.0 Hz, 1H, NCH=CH), 7.46 – 7.41 (m, 2H, H_{aro}), 7.36 – 7.29 (m, 3H, H_{aro}), 5.79 (ddt, *J* = 17.2, 10.1, 4.9 Hz, 1H, CH=CH₂), 5.25 – 5.14 (m, 2H, CH=CH₂), 4.68 (d, *J* = 13.0 Hz, 1H, NCH=CH), 4.13 (q, *J* = 7.1 Hz, 2H, O=COCH₂), 4.02 – 3.92 (m, 6H, NCH₂ & OCH₂CH₂O), 2.13 – 2.03 (m, 5H), 1.85 – 1.76 (m, 2H), 1.25 (t, *J* = 7.1 Hz, 4H, OCH₂CH₃ & 1H cyclohexyl) ppm.

¹³C{¹H} NMR (126 MHz, CDCl₃) δ = 169.9 (C=O), 147.3 (NCH), 132.9 (CH), 131.8 (CH), 128.8 (CH), 128.5 (CH), 122.3 (CH), 116.9 (CH=CH₂), 107.5 (C_q), 88.1 (C≡), 87.7 (C≡), 87.2 (NCH=CH), 64.7 (C_qOCH₂), 64.4 (C_qOCH₂), 61.5 (NC_q), 59.1 (CO₂CH₂), 49.0 (NCH₂), 34.6 (CH₂), 32.4 (CH₂), 14.8 (CH₃) ppm.

HRMS (ESI-TOF, + mode) *m/z* calcd for C₂₄H₂₉NNaO₄ 418.1989, found 418.1992 [M+Na]⁺.

Ethyl (E)-3-(allyl(1-(phenylethynyl)-4-(trifluoromethyl)cyclohexyl)amino)acrylate



Chemical Formula: C₂₃H₂₆F₃NO₂
Molecular Weight: 405,4612

Following the General Procedure L in EtOH at 100 °C for 1 h, the title compound was obtained as a yellow resin (72 mg) and used without further purification.

R_f = 0.40 (Al₂O₃ neutral, cyclohexane/EtOAc 9:1).

ATR-FTIR (neat) ν = 3084, 3032, 3010, 2940, 2901, 2866, 2856, 1689, 1644, 1599, 1570, 1491, 1446, 1391, 1339, 1250, 1158, 1120, 1093, 1019, 919, 824, 756, 687 cm⁻¹.

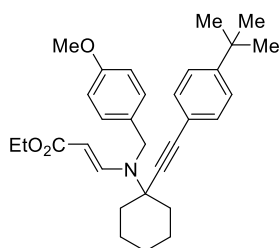
¹H NMR (500 MHz, CDCl₃) δ = 7.96 (d, *J* = 13.0 Hz, 1H, NCH=CH), 7.45 – 7.28 (m, 5H, H_{aro}), 5.84 (ddt, *J* = 17.2, 10.4, 5.2 Hz, 1H, CH=CH₂), 5.29 – 5.16 (m, 2H, CH=CH₂), 4.79 (d, *J* = 13.0 Hz, 1H, NCH=CH), 4.14 (q, *J* = 7.1 Hz, 2H, OCH₂), 4.00 – 3.87 (m, 2H, NCH₂), 2.38 – 2.21 (m, 3H), 2.02 – 1.89 (m, 4H), 1.87 – 1.77 (m, 2H), 1.26 (t, *J* = 7.1 Hz, 3H, CH₃) ppm.

¹⁹F{¹H} NMR (282 MHz, CDCl₃) δ = -70.54 ppm

¹³C{¹H} NMR (126 MHz, CDCl₃) δ = 169.7 (C=O), 147.5 (NCH), 132.8 (CH), 131.8 (CH), 128.8 (CH), 128.5 (CH), 127.9 (q, ¹*J*_{C-F} = 279.7 Hz, CF₃), 122.2 (C_q), 117.3 (CH=CH₂), 89.6 (C≡), 88.7 (NCH=CH), 85.8 (C≡), 59.4 (NC_q), 59.3 (OCH₂), 49.2 (NCH₂), 38.3 (q, ²*J*_{C-F} = 24.1 Hz, F₃CCH), 33.7 (CH₂), 20.9 (q, ³*J*_{C-F} = 2.4 Hz, F₃CCHCH₂), 14.7 (CH₃) ppm.

HRMS (ESI-TOF, + mode) *m/z* calcd for C₂₃H₂₆F₃NNaO₂ 428.1808, found 428.1797 [M+Na]⁺.

Ethyl (E)-3-((1-((4-(tert-butyl)phenyl)ethynyl)cyclohexyl)(4-methoxybenzyl)amino)acrylate



Chemical Formula: $C_{31}H_{39}NO_3$
Molecular Weight: 473,6570

Following the General Procedure L in EtOH at 100 °C for 1 h, the title compound was obtained as a yellow resin (108 mg) and used without further purification.

R_f = 0.36 (SiO₂, cyclohexane/EtOAc 8:2).

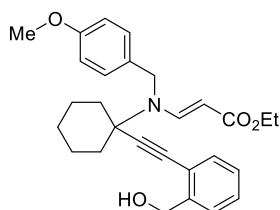
ATR-FTIR (neat) ν = 3036, 2930, 2857, 1688, 1599, 1511, 1460, 1328, 1244, 1139, 1101, 1037, 962, 834, 792 cm⁻¹.

¹H NMR (500 MHz, CDCl₃) δ = 8.19 (d, J = 12.9 Hz, 1H, NCH=CH), 7.34 – 7.27 (m, 4H, H_{aro}), 7.18 – 7.14 (m, 2H, H_{aro}), 6.87 – 6.82 (m, 2H, 2 × OC_qCH_{aro}), 4.59 (d, J = 12.9 Hz, 1H, NCH=CH), 4.56 (s, 2H, NCH₂), 4.09 (q, J = 7.2 Hz, 2H, OCH₂), 3.79 (s, 3H, OCH₃), 2.15 – 2.06 (m, 2H, 2 × NC_qCH₂), 1.83 – 1.68 (m, 7H), 1.30 (s, 9H, C(CH₃)₃), 1.22 (t, J = 7.1 Hz, 3H, CH₂CH₃), 1.18 – 1.12 (m, 1H) ppm.

¹³C{¹H} NMR (126 MHz, CDCl₃) δ = 170.0 (C=O), 158.6 (CH₃OC_q), 151.9 (C_q), 147.7 (NCH), 131.5 (CH), 129.5 (C_q), 127.5 (CH), 125.4 (CH), 119.6 (C_q), 114.0 (CH), 88.5 (C≡), 88.3 (C≡), 87.6 (NCH=CH), 63.0 (NC_q), 59.1 (OCH₂), 55.4 (OCH₃), 50.0 (NCH₂), 37.7 (CH₂), 34.9 (C(CH₃)₃), 31.3 (C(CH₃)₃), 25.2 (CH₂), 23.9 (CH₂), 14.7 (CH₂CH₃) ppm.

HRMS (ESI-TOF, + mode) m/z calcd for C₃₁H₄₀NO₃ 474.3003, found 474.3016 [M+H]⁺.

Ethyl (E)-3-((1-((2-(hydroxymethyl)phenyl)ethynyl)cyclohexyl)(4-methoxybenzyl)amino)acrylate



Chemical Formula: $C_{28}H_{33}NO_4$
Molecular Weight: 447,5750

Following the General Procedure L in EtOH at 100 °C for 20 min, the title compound was isolated as an orange-red sticky foam (335 mg) and used without further purification.

R_f = 0.78 (SiO₂, CH₂Cl₂/MeOH 9:1).

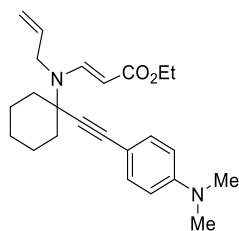
ATR-FTIR (neat) ν = 3405, 3062, 2932, 2857, 1667, 1583, 1511, 1446, 1329, 1243, 1143, 1098, 1034, 962, 908, 793, 757 cm⁻¹.

¹H NMR (500 MHz, CDCl₃) δ = 8.45 (d, J = 13.1 Hz, 1H, NCH=CH), 7.48 – 7.39 (m, 2H, H_{aro}), 7.34 (td, J = 7.6, 1.4 Hz, 1H, H_{aro}), 7.28 – 7.22 (m, 1H, H_{aro}), 7.14 (s, 2H, H_{aro}), 6.89 – 6.80 (m, 2H, 2 × OC_qCH_{aro}), 4.80 (s, 2H, CH₂OH), 4.61 (d, J = 13.0 Hz, 1H, NCH=CH), 4.52 (s, 2H, NCH₂), 4.10 (q, J = 7.1 Hz, 2H, CO₂CH₂), 3.79 (s, 3H, OCH₃), 3.27 (bs, 1H, OH), 2.11 – 2.03 (m, 2H, 2 × NC_qCH₂), 1.84 – 1.70 (m, 7H), 1.21 (t, J = 7.1 Hz, 3H, CH₂CH₃), 1.19 – 1.09 (m, 1H) ppm.

¹³C{¹H} NMR (126 MHz, CDCl₃) δ = 170.6 (C=O), 158.7 (CH₃OC_q), 149.2 (NCH), 142.4 (C_q), 132.5 (CH), 129.1 (C_q), 129.0 (CH), 128.3 (CH), 127.6 (CH), 127.4 (CH), 121.4 (C_q), 114.1 (CH), 93.2 (C≡), 87.4 (NCH=CH), 87.0 (C≡), 63.9 (CH₂OH), 63.6 (NC_q), 59.4 (CO₂CH₂), 55.4 (OCH₃), 49.0 (NCH₂), 37.4 (CH₂), 25.1 (CH₂), 24.0 (CH₂), 14.7 (CH₂CH₃) ppm.

HRMS (ESI-TOF, + mode) m/z calcd for C₂₈H₃₃NNaO₄ 470.2302, found 470.2293 [M+Na]⁺.

Ethyl (E)-3-(allyl(1-((4-(dimethylamino)phenyl)ethynyl)cyclohexyl)amino)acrylate



Chemical Formula: $C_{24}H_{32}N_2O_2$
Molecular Weight: 380,5320

Following the General Procedure K in EtOAc at 100 °C for 20 h, the title compound was obtained as orange resin (43 mg) and used without further purification.

R_f = 0.38 (Al₂O₃ neutral, cyclohexane/EtOAc 9:1).

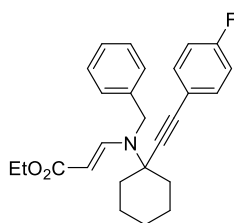
ATR-FTIR (neat) ν = 3073, 2977, 2933, 2858, 2808, 2212, 1687, 1600, 1521, 1445, 1360, 1329, 1237, 1142, 1110, 946, 816, 792 cm⁻¹.

¹H NMR (500 MHz, CDCl₃) δ = 8.08 (d, J = 12.9 Hz, 1H, NCH=CH), 7.35 – 7.27 (m, 2H, H_{aro}), 6.65 – 6.58 (m, 2H, 2 × NC_{q-aro}CH), 5.79 (ddt, J = 17.2, 10.2, 5.0 Hz, 1H, CH=CH₂), 5.24 – 5.14 (m, 2H, CH=CH₂), 4.65 (d, J = 13.0 Hz, 1H, NCH=CH), 4.13 (q, J = 7.1 Hz, 2H, OCH₂), 4.01 (dt, J = 5.2, 1.9 Hz, 2H, NCH₂), 2.97 (s, 6H, N(CH₃)₂), 2.10 – 2.02 (m, 2H, 2 × NC_qCH₂), 1.84 – 1.61 (m, 7H), 1.26 (t, J = 7.1 Hz, 3H, CH₂CH₃), 1.20 – 1.11 (m, 1H) ppm.

¹³C{¹H} NMR (126 MHz, CDCl₃) δ = 170.1 (C=O), 150.3 (NC_{q-aro}), 147.3 (NCH), 133.4 (CH), 132.8 (CH), 116.7 (CH=CH₂), 111.9 (CH), 109.5 (C_{q-aro}), 88.8 (C≡), 86.6 (C≡), 86.1 (NCH=CH), 62.8 (NC_q), 59.0 (OCH₂), 49.1 (NCH₂), 40.4 (N(CH₃)₂), 37.7 (CH₂), 25.3 (CH₂), 23.9 (CH₂), 14.8 (CH₂CH₃) ppm.

HRMS (ESI-TOF, + mode) m/z calcd for C₂₄H₃₂N₂NaO₂, 403.2356, found 403.2353 [M+Na]⁺.

Ethyl (E)-3-(benzyl(1-((4-fluorophenyl)ethynyl)cyclohexyl)amino)acrylate



Chemical Formula: $C_{26}H_{28}FNO_2$
Molecular Weight: 405,5134

Following the General Procedure L in EtOH at 100 °C for 1 h, the title compound was obtained as a pale yellow resin and used without further purification (99.8 mg)

R_f = 0.24 (SiO₂, cyclohexane/EtOAc 9:1).

ATR-FTIR (neat) ν = 3064, 3029, 2933, 2858, 1686, 1598, 1506, 1452, 1329, 1234, 1141, 1108, 961, 836, 794, 729, 695 cm⁻¹.

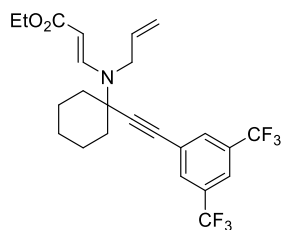
¹H NMR (500 MHz, CDCl₃) δ = 8.21 (d, J = 13.0 Hz, 1H, NCH=CH), 7.33 – 7.20 (m, 7H, H_{aro}), 7.01 – 6.93 (m, 2H, H_{aro}), 4.61 (s, 2H, NCH₂), 4.58 (d, J = 12.9 Hz, 1H, NCH=CH), 4.09 (q, J = 7.1 Hz, 2H, OCH₂), 2.18 – 2.06 (m, 2H, 2 × NC_qCH₂), 1.86 – 1.68 (m, 7H), 1.24 – 1.12 (m, 4H, CH₃ & 1H cyclohexyl) ppm.

¹⁹F{¹H} NMR (471 MHz, CDCl₃) δ = -110.6 ppm.

¹³C{¹H} NMR (126 MHz, CDCl₃) δ = 169.9 (C=O), 162.7 (d, ¹J_{C-F} = 249.9 Hz, FC_q), 147.7 (NCH), 137.4 (C_q), 133.6 (d, ³J_{C-F} = 8.4 Hz, FC_qCHCH), 128.6 (CH), 126.9 (CH), 126.3 (CH), 118.6 (d, ⁴J_{C-F} = 3.6 Hz, ≡CC_{q-aro}), 115.7 (d, ²J_{C-F} = 22.0 Hz, FC_qCH), 88.9 (d, ⁵J_{C-F} = 1.5 Hz, ≡CC_{q-aro}), 87.9 (NCH=CH), 87.1 (NC_qC≡), 62.9 (NC_q), 59.2 (OCH₂), 50.5 (NCH₂), 37.6 (CH₂), 25.2 (CH₂), 23.9 (CH₂), 14.7 (CH₃) ppm.

HRMS (ESI-TOF, + mode) m/z calcd for C₂₆H₂₉FNO₂ 406.2177, found 406.2178 [M+H]⁺.

Ethyl (E)-3-(allyl(1-((3,5-bis(trifluoromethyl)phenyl)ethynyl)cyclohexyl)amino)acrylate



Chemical Formula: $C_{24}H_{25}F_6NO_2$
Molecular Weight: 473,4594

Following the General Procedure K in EtOAc at 100 °C for 22 h, the title compound was obtained as an orange resin (57 mg) and used without further purification.

R_f = 0.70 (Al₂O₃ neutral, cyclohexane/EtOAc 8:2).

ATR-FTIR (neat) ν = 3086, 2980, 2937, 2862, 1689, 1600, 1449, 1380, 1329, 1276, 1130, 897, 795, 683 cm⁻¹.

¹H NMR (500 MHz, CDCl₃) δ = 8.01 (d, J = 12.9 Hz, 1H, NCH=CH), 7.84 (bs, 2H, 2 × ≡CC_qCH_{aro}), 7.82 (bs, 1H, H_{aro}), 5.80

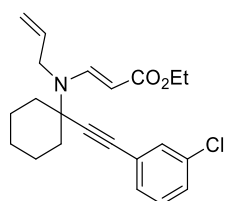
(ddt, $J = 17.4, 10.0, 4.9$ Hz, 1H, $\text{CH}=\text{CH}_2$), 5.22 (dq, $J = 4.9, 1.6$ Hz, 1H, $\text{CH}=\text{CH}_2$), 5.19 (dq, $J = 2.7, 1.6$ Hz, 1H, $\text{CH}=\text{CH}_2$), 4.72 (d, $J = 13.0$ Hz, 1H, $\text{NCH}=\text{CH}$), 4.14 (q, $J = 7.1$ Hz, 2H, OCH_2), 3.99 (dt, $J = 4.9, 1.9$ Hz, 2H, NCH_2), 2.19 – 2.13 (m, 2H, $2 \times \text{NC}_q\text{CH}_2$), 1.90 – 1.66 (m, 7H), 1.25 (t, $J = 7.1$ Hz, 3H, CH_3), 1.23 – 1.17 (m, 1H) ppm.

$^{19}\text{F}\{^1\text{H}\}$ NMR (471 MHz, CDCl_3) $\delta = -63.1$ ppm.

$^{13}\text{C}\{^1\text{H}\}$ NMR (126 MHz, CDCl_3) $\delta = 169.8$ (C=O), 146.8 (NCH), 133.0 (CH), 132.2 (q, $^2J_{\text{C-F}} = 33.7$ Hz, $\text{CF}_3\text{C}_{q\text{-aro}}$), 131.8 – 131.6 (m, CH, CF_3CCH), 124.9 ($\equiv\text{CC}_{q\text{-aro}}$), 123.0 (q, $^1J_{\text{C-F}} = 272.8$ Hz, CF_3), 122.1 (h, $^3J_{\text{C-F}} = 4.3$ Hz, CF_3CCH), 117.0 ($\text{CH}=\text{CH}_2$), 93.2 (C \equiv), 87.7 (NCH=CH), 84.5 (C \equiv), 62.2 (NC_q), 59.2 (OCH_2), 49.1 (NCH_2), 37.3 (CH_2), 25.1 (CH_2), 23.8 (CH_2), 14.8 (CH_3) ppm.

HRMS (ESI-TOF, + mode) m/z calcd for $\text{C}_{24}\text{H}_{26}\text{F}_6\text{NO}_2$ 474.1862, found 474.1857 $[\text{M}+\text{H}]^+$.

Ethyl (E)-3-(allyl(1-((3-chlorophenyl)ethynyl)cyclohexyl)amino)acrylate



Chemical Formula: $\text{C}_{22}\text{H}_{26}\text{ClNO}_2$
Molecular Weight: 371,9050

Following the General Procedure L in EtOH at 100 °C for 20 min, the title compound was isolated as a brown viscous oil (38 mg) and used without further purification.

$R_f = 0.68$ (Al_2O_3 neutral, cyclohexane/EtOAc 8:2).

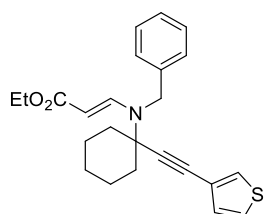
ATR-FTIR (neat) $\nu = 3066, 2976, 2933, 2858, 1686, 1594, 1446, 1327, 1240, 1141, 1091, 1049, 963, 925, 873, 784, 681$ cm^{-1} .

^1H NMR (500 MHz, CDCl_3) $\delta = 8.04$ (d, $J = 13.0$ Hz, 1H, $\text{NCH}=\text{CH}$), 7.41 (t, $J = 1.7$ Hz, 1H, H_{aro}), 7.34 – 7.29 (m, 2H, H_{aro}), 7.28 – 7.23 (m, 1H, H_{aro}), 5.79 (ddt, $J = 17.3, 10.1, 4.9$ Hz, 1H, $\text{CH}=\text{CH}_2$), 5.23 – 5.19 (m, 1H, $\text{CH}=\text{CH}_2$), 5.18 (t, $J = 1.8$ Hz, 1H, $\text{CH}=\text{CH}_2$), 4.68 (d, $J = 13.0$ Hz, 1H, $\text{NCH}=\text{CH}$), 4.13 (q, $J = 7.1$ Hz, 2H, OCH_2), 4.01 – 3.95 (m, 2H, NCH_2), 2.13 – 2.06 (m, 2H, $2 \times \text{NC}_q\text{CH}_2$), 1.84 – 1.67 (m, 7H), 1.26 (t, $J = 7.1$ Hz, 3H, CH_3), 1.22 – 1.13 (m, 1H) ppm.

$^{13}\text{C}\{^1\text{H}\}$ NMR (126 MHz, CDCl_3) $\delta = 170.0$ (C=O), 147.0 (NCH), 134.3 (C_q), 133.1 (CH), 131.6 (CH), 129.9 (CH), 129.7 (CH), 128.9 (CH), 124.3 (C_q), 116.9 ($\text{CH}=\text{CH}_2$), 90.5 (C \equiv), 87.0 (NCH=CH), 86.4 (C \equiv), 62.4 (NC_q), 59.2 (OCH_2), 49.0 (NCH_2), 37.4 (CH_2), 25.1 (CH_2), 23.8 (CH_2), 14.8 (CH_3) ppm.

HRMS (ESI-TOF, + mode) m/z calcd for $\text{C}_{22}\text{H}_{27}\text{ClNO}_2$ 372.1725, found 372.1722 $[\text{M}+\text{H}]^+$.

Ethyl (E)-3-(benzyl(1-(thiophen-3-ylethynyl)cyclohexyl)amino)acrylate



Chemical Formula: $\text{C}_{24}\text{H}_{27}\text{NO}_2\text{S}$
Molecular Weight: 393,5450

Following the General Procedure K in EtOAc at 100 °C for 45 h, the title compound was obtained as an orange resin (85 mg) and used without further purification.

$R_f = 0.70$ (Al_2O_3 neutral, cyclohexane/EtOAc 7:3).

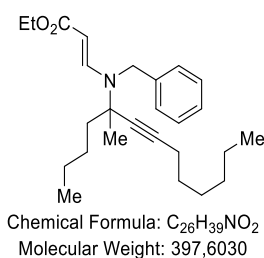
ATR-FTIR (neat) $\nu = 3105, 3088, 3062, 3028, 2976, 2932, 2857, 2234, 1683, 1596, 1451, 1327, 1241, 1139, 963, 782, 727, 694$ cm^{-1} .

^1H NMR (500 MHz, CDCl_3) $\delta = 8.20$ (d, $J = 12.9$ Hz, 1H, $\text{NCH}=\text{CH}$), 7.33 – 7.27 (m, 3H, H_{aro}), 7.25 – 7.20 (m, 4H, H_{aro}), 6.98 (dd, $J = 5.0, 1.3$ Hz, 1H, H_{aro}), 4.61 (s, 2H, NCH_2), 4.57 (d, $J = 13.0$ Hz, 1H, $\text{NCH}=\text{CH}$), 4.09 (q, $J = 7.2$ Hz, 2H, OCH_2), 2.17 – 2.09 (m, 2H, $2 \times \text{NC}_q\text{CH}_2$), 1.84 – 1.68 (m, 8H), 1.21 (t, $J = 7.1$ Hz, 3H, CH_3), 1.19 – 1.12 (m, 1H) ppm.

$^{13}\text{C}\{^1\text{H}\}$ NMR (126 MHz, CDCl_3) $\delta = 170.0$ (C=O), 147.7 (NCH), 137.4 (C_q), 129.9 (CH), 129.0 (CH), 128.6 (CH), 126.9 (CH), 126.3 (CH), 125.5 (CH), 121.5 (C_q), 88.7 (C \equiv), 87.7 (NCH=CH), 83.1 (C \equiv), 63.0 (NC_q), 59.1 (OCH_2), 50.5 (NCH_2), 37.6 (CH_2), 25.2 (CH_2), 23.9 (CH_2), 14.7 (CH_3) ppm.

HRMS (ESI-TOF, + mode) m/z calcd for $C_{24}H_{28}NO_2S$ 394.1835, found 394.1836 $[M+H]^+$.

Ethyl (E)-3-(benzyl(5-methyltridec-6-yn-5-yl)amino)acrylate



Following the General Procedure K in EtOAc at 100 °C for 24 h, the title compound was isolated as an orange viscous oil (55 mg) and used without further purification.

R_f = 0.72 (Al_2O_3 neutral, cyclohexane/EtOAc 8:2).

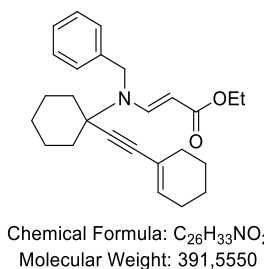
ATR-FTIR (neat) ν = 3087, 3063, 3029, 2956, 2931, 2860, 2248, 1720, 1690, 1601, 1454, 1330, 1296, 1239, 1136, 1094, 964, 794, 728, 696 cm^{-1} .

1H NMR (500 MHz, $CDCl_3$) δ = 8.10 (d, J = 13.0 Hz, 1H, $NCH=CH$), 7.31 – 7.27 (m, 2H, H_{aro}), 7.23 – 7.17 (m, 3H, H_{aro}), 4.55 – 4.42 (m, 3H, 1 \times $NCH=CH$ & NCH_2), 4.07 (q, J = 7.1 Hz, 2H, OCH_2), 2.14 (t, J = 7.0 Hz, 2H), 1.85 – 1.79 (m, 1H), 1.74 – 1.66 (m, 1H), 1.47 – 1.17 (m, 18H, OCH_2CH_3 & C_qCH_3 & 12H aliphatic), 0.90 (t, J = 7.1 Hz, 3H, CH_2CH_3), 0.87 (t, J = 7.0 Hz, 3H, CH_2CH_3) ppm.

$^{13}C\{^1H\}$ NMR (126 MHz, $CDCl_3$) δ = 169.9 (C=O), 148.5 (NCH), 137.5 (C_q-Ph), 128.5 (CH), 126.9 (CH), 126.4 (CH), 87.4 (C \equiv), 87.2 (NCH=CH), 81.0 (C \equiv), 61.4 (NC_q), 59.0 (OCH_2), 50.4 (NCH_2), 41.8 (CH_2), 31.4 (CH_2), 28.6 (CH_2), 28.5(5) (CH_2), 28.5(0) (NC_qCH_3), 27.2 (CH_2), 22.8 (CH_2), 22.7 (CH_2), 18.7 (CH_2), 14.7 (CH_3), 14.2 (CH_3), 14.1(6) (CH_3) ppm.

HRMS (ESI-TOF, + mode) m/z calcd for $C_{26}H_{39}NNO_2$ 420.2873, found 420.2873 $[M+Na]^+$.

Ethyl (E)-3-(benzyl(1-(cyclohex-1-en-1-ylethynyl)cyclohexyl)amino)acrylate



Following the General Procedure L in EtOH at 100 °C for 50 min, the title compound was obtained as a yellow resin (42.5 mg) and used without further purification.

R_f = 0.46 (SiO_2 , cyclohexane/EtOAc 8:2).

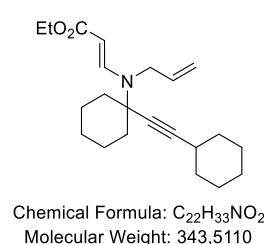
ATR-FTIR (neat) ν = 3084, 3061, 3030, 2931, 2857, 1687, 1599, 1451, 1328, 1240, 1137, 1105, 965, 794, 727, 695 cm^{-1} .

1H NMR (500 MHz, $CDCl_3$) δ = 8.18 (d, J = 12.9 Hz, 1H, $NCH=CH$), 7.31 – 7.27 (m, 2H, H_{aro}), 7.22 – 7.17 (m, 3H, H_{aro}), 6.01 (tt, J = 3.8, 1.6 Hz, 1H, $C_q=CH$), 4.55 (s, 2H, NCH_2), 4.53 (d, J = 13.0 Hz, 1H, $NCH=CH$), 4.08 (q, J = 7.1 Hz, 2H, OCH_2), 2.09 – 1.96 (m, 6H), 1.78 – 1.52 (m, 11H), 1.21 (t, J = 7.1 Hz, 3H, CH_3), 1.12 (s, 1H) ppm.

$^{13}C\{^1H\}$ NMR (126 MHz, $CDCl_3$) δ = 170.0 (C=O), 147.9 (NCH), 137.5 (C_q), 135.1 (CH), 128.5 (CH), 126.8 (CH), 126.4 (CH), 120.2 (C_q), 90.2 (C \equiv), 87.5 (NCH=CH), 86.2 (C \equiv), 63.0 (NC_q), 59.1 (OCH_2), 50.3 (NCH_2), 37.7 (CH_2), 29.2 (CH_2), 25.7 (CH_2), 25.2 (CH_2), 23.9 (CH_2), 22.3 (CH_2), 21.6 (CH_2), 14.7 (CH_3) ppm.

HRMS (ESI-TOF, + mode) m/z calcd for $C_{26}H_{34}NO_2$ 392.2584, found 392.2596 $[M+H]^+$.

Ethyl (E)-3-(allyl(1-(cyclohexylethynyl)cyclohexyl)amino)acrylate



Following the General Procedure K in EtOAc at 100 °C for 24 h, the title compound was obtained as a brown resin (69 mg) and used without further purification.

R_f = 0.56 (Al_2O_3 neutral, cyclohexane/EtOAc 9:1).

ATR-FTIR (neat) ν = 3082, 2976, 2928, 2854, 2233, 1729, 1688, 1598, 1447, 1328, 1238, 1141, 1050, 966, 790 cm^{-1} .

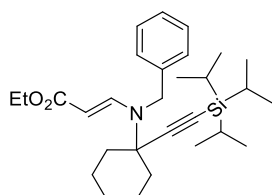
1H NMR (300 MHz, $CDCl_3$) δ = 8.07 (d, J = 13.0 Hz, 1H, $NCH=CH$), 5.82 – 5.68 (m, 1H, $CH=CH_2$), 5.18 (dq, J = 6.3, 1.7 Hz, 1H, $CH=CH_2$), 5.13 (t, J = 1.8 Hz, 1H, $CH=CH_2$), 4.61

(d, $J = 12.9$ Hz, 1H, NCH=CH), 4.12 (q, $J = 7.1$ Hz, 2H, OCH₂), 3.92 (dt, $J = 5.0, 1.9$ Hz, 2H, NCH₂), 2.53 – 2.39 (m, 1H, ≡CCH), 1.94 – 1.86 (m, 2H, 2 × NC_qCH₂), 1.84 – 1.57 (m, 14H), 1.53 – 1.29 (m, 8H), 1.25 (t, $J = 7.1$ Hz, 3H, CH₃), 1.18 – 1.01 (m, 1H) ppm.

¹³C{¹H} NMR (126 MHz, CDCl₃) $\delta = 170.1$ (C=O), 147.6 (NCH), 133.4 (CH=CH₂), 116.6 (CH=CH₂), 93.0 (C≡), 85.9 (NCH=CH), 79.8 (C≡), 62.3 (NC_q), 59.0 (OCH₂), 48.6 (NCH₂), 37.6 (CH₂), 32.7 (CH₂), 29.1 (≡CCH), 26.0 (CH₂), 25.2 (CH₂), 24.8 (CH₂), 23.8 (CH₂), 14.8 (CH₃) ppm.

HRMS (ESI-TOF, + mode) m/z calcd for C₂₂H₃₄NO₂ 344.2584, found 344.2603 [M+H]⁺.

Ethyl (E)-3-(benzyl(1-((triisopropylsilyl)ethynyl)cyclohexyl)amino)acrylate



Chemical Formula: C₂₉H₄₅NO₂Si
Molecular Weight: 467,7690

Following the General Procedure K in EtOAc at 100 °C for 90 h, the title compound was obtained as a brown resin (60 mg) and used without further purification.

R_f = 0.39 (SiO₂, cyclohexane/EtOAc 9:1).

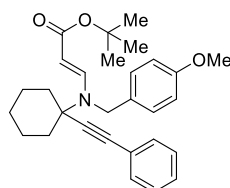
ATR-FTIR (neat) $\nu = 3087, 3063, 3029, 2936, 2863, 2166, 1692, 1601, 1453, 1328, 1241, 1142, 1110, 963, 882, 795, 727, 676$ cm⁻¹.

¹H NMR (500 MHz, CDCl₃) $\delta = 8.10$ (d, $J = 13.0$ Hz, 1H, NCH=CH), 7.31 – 7.26 (m, 2H, H_{aro}), 7.22 – 7.15 (m, 3H, H_{aro}), 4.60 (s, 2H, NCH₂), 4.51 (d, $J = 13.0$ Hz, 1H, NCH=CH), 4.07 (q, $J = 7.1$ Hz, 2H, OCH₂), 2.10 – 1.99 (m, 2H, 2 × NC_qCH₂), 1.81 – 1.73 (m, 4H), 1.73 – 1.63 (m, 3H), 1.20 (t, $J = 7.1$ Hz, 3H, CH₂CH₃), 1.17 – 1.12 (m, 1H), 1.10 – 0.93 (m, 21H, Si(CH(CH₃)₂)₃) ppm.

¹³C{¹H} NMR (126 MHz, CDCl₃) $\delta = 169.8$ (C=O), 147.4 (NCH), 137.2 (C_{q-Ph}), 128.5 (CH), 126.8 (CH), 126.2 (CH), 107.2 (C≡), 89.0 (C≡), 88.1 (NCH=CH), 63.1 (NC_q), 59.1 (OCH₂), 50.6 (NCH₂), 37.7 (CH₂), 25.2 (CH₂), 23.9 (CH₂), 18.7 (CH(CH₃)₂), 14.7 (CH₂CH₃), 11.2 (CH(CH₃)₂) ppm.

HRMS (ESI-TOF, + mode) m/z calcd for C₂₉H₄₅NNaO₂Si 490.3112, found 490.3109 [M+Na]⁺.

tert-Butyl (E)-3-((4-methoxybenzyl)(1-(phenylethynyl)cyclohexyl)amino)acrylate



Chemical Formula: C₂₉H₃₅NO₃
Molecular Weight: 445,6030

Following the General Procedure L in EtOH at 100 °C for 1.5 h, the title compound was obtained as a yellow foam (89 mg, 200 μ mol) and used without further purification.

R_f = 0.57 (SiO₂, cyclohexane/EtOAc 7:3).

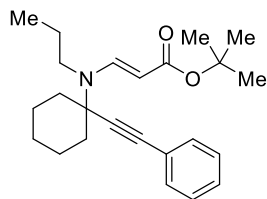
ATR-FTIR (neat) $\nu = 3061, 2932, 2858, 1682, 1596, 1511, 1443, 1328, 1244, 1129, 1033, 979, 912, 793, 755, 691$ cm⁻¹.

¹H NMR (500 MHz, CDCl₃) $\delta = 8.10$ (d, $J = 12.9$ Hz, 1H, NCH=CH), 7.35 – 7.27 (m, 5H, H_{aro}), 7.19 – 7.13 (m, 2H, H_{aro}), 6.88 – 6.81 (m, 2H, 2 × OC_qCH_{aro}), 4.59 – 4.50 (m, 3H, 1 × NCH=CH & NCH₂), 3.79 (s, 3H, OCH₃), 2.17 – 2.06 (m, 2H, 2 × NC_qCH₂), 1.81 – 1.67 (m, 7H), 1.43 (s, 9H, C(CH₃)₃), 1.22 – 1.10 (m, 1H) ppm.

¹³C{¹H} NMR (126 MHz, CDCl₃) $\delta = 169.8$ (C=O), 158.5 (CH₃OC_q), 147.1 (NCH), 131.8 (CH), 129.8 (C_q), 128.5 (CH), 128.4 (CH), 127.5 (CH), 122.7 (C_q), 114.0 (CH), 89.4 (C≡), 89.3 (NCH=CH), 87.8 (C≡), 78.4 (C(CH₃)₃), 62.8 (NC_q), 55.4 (OCH₃), 50.1 (NCH₂), 37.7 (CH₂), 28.7 (C(CH₃)₃), 25.2 (CH₂), 23.9 (CH₂) ppm.

HRMS (ESI-TOF, + mode) m/z calcd for C₂₉H₃₅NNaO₃ 468.2509, found 468.2521 [M+Na]⁺.

tert-Butyl (E)-3-((1-(phenylethynyl)cyclohexyl)(propyl)amino)acrylate



Chemical Formula: C₂₄H₃₃NO₂
Molecular Weight: 367,5330

Following the General Procedure L in EtOH at 100 °C for 2.5 h, the title compound was obtained as a yellow resin (111 mg) and used without further purification.

R_f = 0.64 (SiO₂, cyclohexane/EtOAc 7:3).

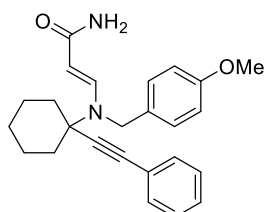
ATR-FTIR (neat) ν = 3082, 3058, 2964, 2932, 2860, 1683, 1593, 1452, 1363, 1329, 1254, 1127, 1070, 981, 886, 792, 755, 690 cm⁻¹.

¹H NMR (300 MHz, CDCl₃) δ = 7.91 (d, *J* = 13.0 Hz, 1H, NCH=CH), 7.48 – 7.38 (m, 2H, H_{aro}), 7.36 – 7.27 (m, 3H, H_{aro}), 4.58 (d, *J* = 13.0 Hz, 1H, NCH=CH), 3.33 – 3.18 (m, 2H, NCH₂), 2.12 – 2.00 (m, 2H, 2 × NC_qCH₂), 1.83 – 1.60 (m, 9H), 1.48 (s, 9H, C(CH₃)₃), 1.24 – 1.09 (m, 1H), 0.91 (t, *J* = 7.4 Hz, 3H, CH₂CH₃) ppm.

¹³C{¹H} NMR (126 MHz, CDCl₃) δ = 170.0 (C=O), 146.5 (NCH), 131.7 (CH), 128.5(2) (CH), 128.5(0) (CH), 122.8 (C_{q-Ph}), 89.4 (C≡), 87.5 (C≡), 87.0 (NCH=CH), 78.2 (C(CH₃)₃), 62.1 (NC_q), 48.8 (NCH₂), 37.6 (CH₂), 28.8 (C(CH₃)₃), 25.2 (CH₂), 23.8 (CH₂), 20.9 (CH₂), 11.6 (CH₂CH₃) ppm.

HRMS (ESI-TOF, + mode) *m/z* calcd for C₂₄H₃₄NO₂ 368.2584, found 368.2603 [M+H]⁺.

(E)-3-((4-Methoxybenzyl)(1-(phenylethynyl)cyclohexyl)amino)acrylamide



Chemical Formula: C₂₅H₂₈N₂O₂
Molecular Weight: 388,5110

Following the General Procedure L in EtOH at 120 °C for 48 h, the title compound was obtained as a yellow sticky solid (40 mg) and used without further purification.

R_f = 0.50 (SiO₂, CH₂Cl₂/MeOH 9:1).

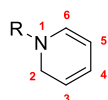
ATR-FTIR (neat) ν = 3323, 3166, 2989, 2931, 2856, 2154, 1698, 1646, 1566, 1511, 1393, 1329, 1243, 1104, 980, 806, 756, 691 cm⁻¹.

¹H NMR (500 MHz, CDCl₃) δ = 8.14 (d, *J* = 12.6 Hz, 1H, NCH=CH), 7.34 – 7.26 (m, 5H, H_{aro}), 7.19 – 7.14 (m, 2H, H_{aro}), 6.89 – 6.82 (m, 2H, 2 × OC_qCH_{aro}), 4.87 (s, 2H, NH₂), 4.58 (s, 2H, NCH₂), 4.55 (d, *J* = 12.6 Hz, 1H, NCH=CH), 3.79 (s, 3H, OCH₃), 2.18 – 2.10 (m, 2H, 2 × NC_qCH₂), 1.84 – 1.66 (m, 7H), 1.22 – 1.11 (m, 1H) ppm.

¹³C{¹H} NMR (126 MHz, CDCl₃) δ = 170.9 (C=O), 158.5 (CH₃OC_q), 146.1 (NCH), 131.7 (CH), 129.7 (C_q), 128.5 (CH), 128.4 (CH), 127.5 (CH), 122.7 (C_q), 114.0 (CH), 89.5 (C≡), 89.0 (NCH=CH), 87.6 (C≡), 62.8 (NC_q), 55.4 (OCH₃), 50.4 (NCH₂), 37.7 (CH₂), 25.2 (CH₂), 23.9 (CH₂) ppm.

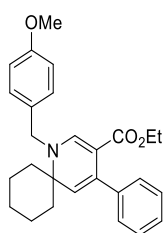
HRMS (ESI-TOF, + mode) *m/z* calcd for C₂₅H₂₈N₂NaO₂ 411.2043, found 411.2050 [M+Na]⁺.

Dihydropyridines



Hydrogen and carbon atoms of the 1,2-dihydropyridine core were described indicating their respective position.

Ethyl 1-(4-methoxybenzyl)-4-phenyl-1-azaspiro[5.5]undeca-2,4-diene-3-carboxylate (D.1a)



Chemical Formula: C₂₇H₃₁NO₃
Molecular Weight: 417,5490

Following the General Procedure M (stirring for 26 h), the title compound **D.1a** was isolated as an orange solid (86 mg, 206 μmol). Yield 94%.

R_f = 0.30 (Al₂O₃ neutral, cyclohexane/EtOAc 9:1).

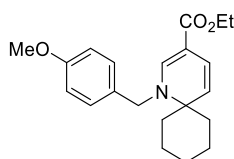
ATR-FTIR (neat) ν = 2931, 2978, 3008, 3029, 3055, 2850, 1662, 1606, 1545, 1511, 1456, 1357, 1287, 1251, 1195, 1129, 1032, 954, 832, 753, 702 cm⁻¹.

¹H NMR (500 MHz, CDCl₃) δ = 7.63 (s, 1H, H₆), 7.32 – 7.22 (m, 5H, H_{aro}), 7.21 – 7.15 (m, 2H, H_{aro}), 6.90 – 6.83 (m, 2H, 2 × OC_qCH_{aro}), 5.08 (s, 1H, H₃), 4.50 (s, 2H, NCH₂), 3.95 (q, *J* = 7.1 Hz, 2H, OCH₂), 3.80 (s, 3H, OCH₃), 2.00 – 1.93 (m, 2H, 2 × NC_qCH₂), 1.69 – 1.62 (m, 1H), 1.60 – 1.51 (m, 4H), 1.46 (td, *J* = 12.0, 5.3 Hz, 2H), 1.15 – 1.04 (m, 1H), 0.94 (t, *J* = 7.1 Hz, 3H, CH₂CH₃) ppm.

¹³C{¹H} NMR (126 MHz, CDCl₃) δ = 166.8 (C=O), 159.1 (CH₃OC_q), 150.2 (C₆), 142.0 (C_q), 136.1 (C_q), 131.0 (C_q), 128.0 (CH), 127.9 (CH), 127.5 (CH), 126.7 (CH), 116.3 (CH), 114.2 (CH), 99.8 (C₅), 60.8 (C₂), 59.0 (OCH₂), 55.4 (OCH₃), 53.1 (NCH₂), 34.3 (CH₂), 25.6 (CH₂), 21.8 (CH₂), 14.2 (CH₂CH₃) ppm.

HRMS (ESI-TOF, + mode) *m/z* calcd for C₂₇H₃₁NNaO₃ 440.2196, found 440.2179 [M+Na]⁺.

Ethyl 1-(4-methoxybenzyl)-1-azaspiro[5.5]undeca-2,4-diene-3-carboxylate (D.1g)



Chemical Formula: C₂₁H₂₇NO₃
Molecular Weight: 341,4510

Following the General Procedure M (stirring for 42 h at 78 °C), the title compound **D.1g** was isolated as a yellow resin (39 mg, 114 μmol). Yield 87%.

R_f = 0.60 (Al₂O₃ neutral, cyclohexane/EtOAc 8:2).

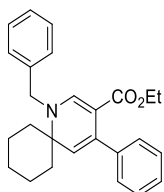
ATR-FTIR (neat) ν = 3058, 2930, 2858, 1726, 1679, 1612, 1561, 1512, 1452, 1364, 1296, 1246, 1214, 1173, 1134, 1085, 1032, 959, 821, 728 cm⁻¹.

¹H NMR (500 MHz, CDCl₃) δ = 7.36 (s, 1H, H₆), 7.17 – 7.13 (m, 2H, H_{aro}), 6.89 – 6.83 (m, 2H, 2 × OC_qCH_{aro}), 6.50 – 6.43 (m, 1H, H₄), 5.26 (d, *J* = 9.9 Hz, 1H, H₃), 4.42 (s, 2H, NCH₂), 4.15 (q, *J* = 7.1 Hz, 2H, OCH₂), 3.79 (s, 3H, OCH₃), 1.91 – 1.85 (m, 2H, 2 × NC_qCH₂), 1.75 – 1.60 (m, 2H), 1.54 – 1.43 (m, 5H), 1.26 (t, *J* = 7.0 Hz, 3H, CH₂CH₃), 1.11 – 1.02 (m, 1H) ppm.

¹³C{¹H} NMR (126 MHz, CDCl₃) δ = 166.9 (C=O), 159.0 (CH₃OC_q), 148.3 (C₆), 131.2 (C_q), 127.9 (CH), 121.1 (CH), 115.1 (CH), 114.2 (CH), 98.6 (C₅), 60.4 (C₂), 59.3 (OCH₂), 55.4 (OCH₃), 52.9 (NCH₂), 35.2 (CH₂), 25.5 (CH₂), 21.4 (CH₂), 14.8 (CH₃) ppm.

HRMS (ESI-TOF, + mode) *m/z* calcd for C₂₁H₂₈NO₃ 342.2064, found 342.2041 [M+H]⁺.

Ethyl 1-benzyl-4-phenyl-1-azaspiro[5.5]undeca-2,4-diene-3-carboxylate (D.2a)



Chemical Formula: C₂₆H₂₉NO₂
Molecular Weight: 387,5230

Following the General Procedure M (stirring for 23 h), the title compound **D.2a** was isolated as a yellow solid (79 mg, 204 μmol). Yield 87%.

R_f = 0.47 (Al₂O₃ neutral, cyclohexane/EtOAc 9:1).

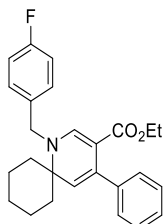
ATR-FTIR (neat) ν = 3050, 3032, 2975, 2935, 2919, 2852, 1677, 1661, 1609, 1546, 1494, 1444, 1362, 1293, 1216, 1135, 1086, 1032, 951, 806, 753, 728, 695 cm⁻¹.

¹H NMR (500 MHz, CDCl₃) δ = 7.64 (s, 1H, H₆), 7.36 – 7.23 (m, 10H, H_{aro}), 5.10 (s, 1H, H₃), 4.57 (s, 2H, NCH₂), 3.96 (q, J = 7.1 Hz, 2H, OCH₂), 2.00 – 1.94 (m, 2H, 2 × NC_qCH₂), 1.69 – 1.63 (m, 1H), 1.57 – 1.51 (m, 4H), 1.46 (td, J = 12.0, 5.0 Hz, 2H), 1.15 – 1.04 (m, 1H), 0.95 (t, J = 7.1 Hz, 3H, CH₃) ppm.

¹³C{¹H} NMR (126 MHz, CDCl₃) δ = 166.7 (C=O), 150.4 (C₆), 142.0 (C_q), 139.3 (C_q), 136.1 (C_q), 128.9 (CH), 127.9 (CH), 127.6 (CH), 127.5 (CH), 126.7 (CH), 126.6 (CH), 116.5 (CH), 100.0 (C₅), 60.8 (C₂), 59.1 (OCH₂), 53.6 (NCH₂), 34.3 (CH₂), 25.6 (CH₂), 21.7 (CH₂), 14.2 (CH₃) ppm.

HRMS (ESI-TOF, + mode) m/z calcd for C₂₆H₃₀NO₂ 388.2271, found 388.2295 [M+H]⁺.

Ethyl 1-(4-fluorobenzyl)-4-phenyl-1-azaspiro[5.5]undeca-2,4-diene-3-carboxylate (D.2b)



Chemical Formula: C₂₆H₂₈FNO₂
Molecular Weight: 405,5134

Following the General Procedure M (stirring for 19 h), the title compound **D.2b** was isolated as a yellow resin (74 mg, 182 μ mol). Yield 73%.

R_f = 0.63 (Al₂O₃ neutral, cyclohexane/EtOAc 8:2).

ATR-FTIR (neat) ν = 3053, 3024, 2976, 2928, 2855, 1678, 1616, 1551, 1508, 1445, 1362, 1292, 1207, 1137, 1070, 1042, 971, 908, 819, 757, 698 cm⁻¹.

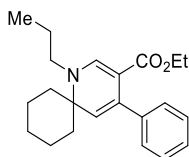
¹H NMR (500 MHz, CDCl₃) δ = 7.61 (s, 1H, H₆), 7.35 – 7.19 (m, 7H, H_{aro}), 7.06 – 6.99 (m, 2H, H_{aro}), 5.10 (s, 1H, H₃), 4.53 (s, 2H, NCH₂), 3.96 (q, J = 7.2 Hz, 2H, OCH₂), 1.99 – 1.92 (m, 2H, 2 × NC_qCH₂), 1.69 – 1.63 (m, 1H), 1.60 – 1.52 (m, 4H), 1.48 – 1.39 (m, 2H), 1.16 – 1.03 (m, 1H), 0.94 (t, J = 7.1 Hz, 3H, CH₃) ppm.

¹⁹F{¹H} NMR (282 MHz, CDCl₃) δ = -115.1 ppm.

¹³C{¹H} NMR (126 MHz, CDCl₃) δ = 166.7 (C=O), 162.2 (d, ¹ J_{C-F} = 245.9 Hz, FC_q), 150.1 (C₆), 141.9 (C_q), 136.1 (C_q), 135.0 (d, ⁴ J_{C-F} = 3.2 Hz, NCH₂C_q), 128.3 (d, ³ J_{C-F} = 8.1 Hz, FC_qCHCH), 127.9, (CH), 127.6 (CH), 126.8 (CH), 116.6 (CH), 115.8 (d, ² J_{C-F} = 21.6 Hz, FC_qCH), 100.4 (C₅), 60.8 (C₂), 59.1 (OCH₂), 53.0 (NCH₂), 34.3 (CH₂), 25.6 (CH₂), 21.7 (CH₂), 14.1 (CH₃) ppm.

HRMS (ESI-TOF, + mode) m/z calcd for C₂₆H₂₈FKNO₂ 444.1736, found 444.1749 [M+K]⁺.

Ethyl 4-phenyl-1-propyl-1-azaspiro[5.5]undeca-2,4-diene-3-carboxylate (D.2c)



Chemical Formula: C₂₂H₂₉NO₂
Molecular Weight: 339,4790

Following the General Procedure M (stirring for 22 h), the title compound **D.2c** was isolated as a yellow resin (72 mg, 212 μ mol). Yield 84%.

R_f = 0.75 (Al₂O₃ neutral, cyclohexane/EtOAc 8:2).

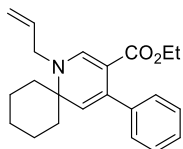
ATR-FTIR (neat) ν = 3078, 3053, 3024, 2929, 2857, 1677, 1615, 1551, 1446, 1362, 1287, 1225, 1146, 1068, 969, 755, 697 cm⁻¹.

¹H NMR (500 MHz, CDCl₃) δ = 7.56 (s, 1H, H₆), 7.30 – 7.20 (m, 6H, H_{aro}), 5.02 (s, 1H, H₃), 3.95 (q, J = 7.1 Hz, 2H, OCH₂), 3.28 – 3.19 (m, 2H, NCH₂), 2.08 – 1.99 (m, 2H, 2 × NC_qCH₂), 1.73 – 1.57 (m, 7H), 1.53 – 1.43 (m, 2H), 1.20 – 1.09 (m, 1H), 0.94(3) (t, J = 7.3 Hz, 3H, CH₃), 0.93(7) (t, J = 7.2 Hz, 3H, CH₃) ppm.

¹³C{¹H} NMR (126 MHz, CDCl₃) δ = 166.9 (C=O), 149.9 (C₆), 142.1 (C_q), 136.0 (C_q), 127.9 (CH), 127.4 (CH), 126.6 (CH), 115.7 (CH), 98.7 (C₅), 60.4 (C₂), 58.9 (OCH₂), 51.7 (NCH₂), 34.4 (CH₂), 25.6 (CH₂), 25.5 (CH₂), 21.8 (CH₂), 14.2 (OCH₂CH₃), 11.3 (N(CH₂)₂CH₃) ppm.

HRMS (ESI-TOF, + mode) m/z calcd for C₂₂H₃₀NO₂ 340.23, found 340.2271 [M+H]⁺.

Ethyl 1-allyl-4-phenyl-1-azaspiro[5.5]undeca-2,4-diene-3-carboxylate (D.2d)



Chemical Formula: C₂₂H₂₇NO₂
Molecular Weight: 337,4630

Following the General Procedure M (stirring for 23 h), the title compound **D.2d** was isolated as a yellow resin (86 mg, 255 μmol). Yield 85%.

R_f = 0.61 (SiO₂, cyclohexane/EtOAc 7:3).

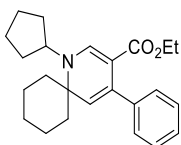
ATR-FTIR (neat) ν = 3078, 3054, 3023, 2977, 2929, 2856, 1679, 1615, 1551, 1445, 1362, 1287, 1202, 1136, 1070, 924, 756, 698 cm⁻¹.

¹H NMR (500 MHz, CDCl₃) δ = 7.56 (s, 1H, H₆), 7.33 – 7.22 (m, 5H, H_{aro}), 5.92 (ddt, J = 17.1, 10.6, 5.4 Hz, 1H, CH=CH₂), 5.28 (dq, J = 17.1, 1.6 Hz, 1H, CH=CH₂), 5.23 (dq, J = 10.2, 1.5 Hz, 1H, CH=CH₂), 5.09 (s, 1H, H₃), 4.02 – 3.91 (m, 4H, OCH₂ & NCH₂), 2.11 – 2.02 (m, 2H, 2 × NC_qCH₂), 1.76 – 1.68 (m, 1H), 1.66 – 1.58 (m, 4H), 1.57 – 1.47 (m, 2H), 1.22 – 1.09 (m, 1H), 0.97 (t, J = 7.1 Hz, 3H, CH₃) ppm.

¹³C{¹H} NMR (126 MHz, CDCl₃) δ = 166.7 (C=O), 149.5 (C₆), 142.1 (C_q), 135.9 (C_q), 135.7 (CH), 127.9 (CH), 127.5 (CH), 126.6 (CH), 117.5 (CH=CH₂), 116.1 (CH), 99.6 (C₅), 60.5 (C₂), 59.0 (OCH₂), 52.1 (NCH₂), 34.3 (CH₂), 25.6 (CH₂), 21.7 (CH₂), 14.2 (CH₃) ppm.

HRMS (ESI-TOF, + mode) m/z calcd for C₂₂H₂₈NO₂ 338.2115, found 338.2129 [M+H]⁺.

Ethyl 1-cyclopentyl-4-phenyl-1-azaspiro[5.5]undeca-2,4-diene-3-carboxylate (D.2e)



Chemical Formula: C₂₄H₃₁NO₂
Molecular Weight: 365,5170

Following the General Procedure M (stirring for 24 h), the title compound **D.2e** was isolated as a yellow resin (65 mg, 178 μmol). Yield 83%.

R_f = 0.80 (Al₂O₃ neutral, cyclohexane/EtOAc 8:2).

ATR-FTIR (neat) ν = 3056, 3024, 2927, 2857, 1721, 1675, 1621, 1555, 1445, 1370, 1285, 1251, 1235, 1188, 1125, 1069, 1024, 929, 759,

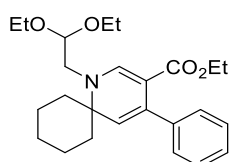
700 cm⁻¹.

¹H NMR (500 MHz, CDCl₃) δ = 7.72 (s, 1H, H₆), 7.29 – 7.19 (m, 5H, H_{aro}), 5.03 (s, 1H, H₃), 3.93 (q, J = 7.1 Hz, 2H, OCH₂), 3.86 (quint, J = 8.1 Hz, 1H, CH cyclopentyl), 2.05 – 1.94 (m, 4H), 1.88 – 1.79 (m, 2H), 1.74 – 1.54 (m, 11H), 1.21 – 1.08 (m, 1H), 0.91 (t, J = 7.1 Hz, 3H, CH₃) ppm.

¹³C{¹H} NMR (126 MHz, CDCl₃) δ = 166.9 (C=O), 145.5 (C₆), 142.4 (C_q), 135.3 (C_q), 127.8 (CH), 127.4 (CH), 126.5 (CH), 115.8 (CH), 98.3 (C₅), 61.2 (C₂), 58.9 (OCH₂), 56.9 (NCHCH₂), 35.3 (CH₂), 34.7 (CH₂), 25.6 (CH₂), 24.3 (CH₂), 21.7 (CH₂), 14.1 (CH₃) ppm.

HRMS (ESI-TOF, + mode) m/z calcd for C₂₄H₃₂NO₂ 366.2428, found 366.2412 [M+H]⁺.

Ethyl 1-(2,2-diethoxyethyl)-4-phenyl-1-azaspiro[5.5]undeca-2,4-diene-3-carboxylate (D.2f)



Chemical Formula: C₂₅H₃₅NO₄
Molecular Weight: 413,5580

Following the General Procedure M (stirring for 24 h), the title compound **D.2f** was isolated as an orange resin (58 mg, 140 μmol). Yield 76%.

R_f = 0.61 (Al₂O₃ neutral, cyclohexane/EtOAc 8:2).

ATR-FTIR (neat) ν = 3078, 3055, 3023, 2975, 2928, 2858, 1682, 1618, 1553, 1445, 1361, 1290, 1124, 1054, 925, 756, 697 cm⁻¹.

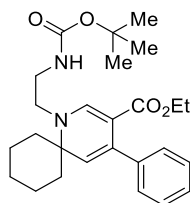
¹H NMR (500 MHz, CDCl₃) δ = 7.60 (s, 1H, H₆), 7.31 – 7.18 (m, 5H, H_{aro}), 5.05 (s, 1H, H₃), 4.41 (t, J = 5.3 Hz, 1H, NCH₂CH), 3.97 (q, J = 7.1 Hz, 2H, O=COCH₂), 3.75 (dq, J = 9.2, 7.0 Hz, 2H, CH(OCH₂CH₃)₂), 3.52 (dq, J = 9.2, 7.0 Hz, 2H, CH(OCH₂CH₃)₂), 3.39 (d, J = 5.4 Hz, 2H, NCH₂), 2.08 – 1.99 (m, 2H, 2 × NC_qCH₂), 1.73 – 1.66 (m, 1H), 1.64 – 1.58

(m, 4H), 1.52 – 1.43 (m, 2H), 1.23 (t, $J = 7.0$ Hz, 6H, $2 \times \text{CH}_3$), 1.20 – 1.08 (m, 1H), 0.99 (t, $J = 7.1$ Hz, 3H, CH_3) ppm.

$^{13}\text{C}\{^1\text{H}\}$ NMR (126 MHz, CDCl_3) $\delta = 166.5$ (C=O), 150.8 (C_6), 142.0 (C_q), 136.1 (C_q), 127.8 (CH), 127.5 (CH), 126.7 (CH), 116.2 (CH), 103.2 (CH), 99.8 (C_5), 64.4 ($\text{CH}(\text{OCH}_2)_2$), 60.2 (C_2), 58.9 (OCH_2), 52.5 (NCH_2), 34.6 (CH_2), 25.6 (CH_2), 21.8 (CH_2), 15.4 (CH_3), 14.3 (CH_3) ppm.

HRMS (ESI-TOF, + mode) m/z calcd for $\text{C}_{25}\text{H}_{35}\text{KNO}_4$ 452.2198, found 452.2204 $[\text{M}+\text{K}]^+$.

Ethyl 1-(2-((tert-butoxycarbonyl)amino)ethyl)-4-phenyl-1-azaspiro[5.5]undeca-2,4-diene-3-carboxylate (D.2g)



Chemical Formula: $\text{C}_{26}\text{H}_{36}\text{N}_2\text{O}_4$
Molecular Weight: 440,5840

Following the General Procedure M (stirring for 24 h), the title compound **D.2g** was isolated as an off-white solid (35 mg, 79 μmol). Yield 81%.

$R_f = 0.25$ (Al_2O_3 neutral, cyclohexane/EtOAc 8:2).

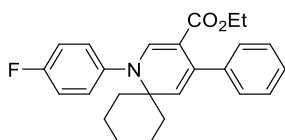
ATR-FTIR (neat) $\nu = 3368, 3084, 3058, 2970, 2921, 2855, 1704, 1672, 1628, 1557, 1497, 1422, 1363, 1292, 1248, 1220, 1168, 1129, 1097, 1066, 1000, 932, 856, 763, 763, 696$ cm^{-1} .

^1H NMR (500 MHz, CDCl_3) $\delta = 7.48$ (s, 1H, H_6), 7.30 – 7.20 (m, 5H, H_{aro}), 5.08 (s, 1H, H_3), 4.78 (t, $J = 6.3$ Hz, 1H, BocNH), 3.95 (q, $J = 7.1$ Hz, 2H, OCH_2), 3.42 (t, $J = 6.5$ Hz, 2H, NCH_2CH_2), 3.25 (q, $J = 6.5$ Hz, 2H, BocNHCH_2), 2.07 – 1.99 (m, 2H, $2 \times \text{NC}_q\text{CH}_2$), 1.73 – 1.65 (m, 1H), 1.64 – 1.54 (m, 4H), 1.51 – 1.42 (m, 11H, $\text{C}(\text{CH}_3)_3$), 1.20 – 1.10 (m, 1H), 0.96 (t, $J = 7.1$ Hz, 3H, CH_2CH_3) ppm.

$^{13}\text{C}\{^1\text{H}\}$ NMR (126 MHz, CDCl_3) $\delta = 166.5$ ($\text{C}_5\text{C}=\text{O}$), 156.0 ($\text{NC}=\text{O}$), 149.8 (C_6), 141.8 ($\text{C}_{q\text{-aro}}$), 135.8 ($\text{C}_{q\text{-aro}}$), 127.8 (CH), 127.5 (CH), 126.7 (CH), 116.5 (CH), 100.1 (C_5), 79.8 ($\text{C}(\text{CH}_3)_3$), 60.3 (C_2), 59.0 (OCH_2), 48.8 (CH_2), 42.2 (CH_2), 34.4 (CH_2), 28.5 ($\text{C}(\text{CH}_3)_3$), 25.5 (CH_2), 21.7 (CH_2), 14.2 (CH_2CH_3) ppm.

HRMS (ESI-TOF, + mode) m/z calcd for $\text{C}_{26}\text{H}_{36}\text{N}_2\text{NaO}_4$ 463.2567, found 463.2568 $[\text{M}+\text{Na}]^+$.

Ethyl 1-(4-fluorophenyl)-4-phenyl-1-azaspiro[5.5]undeca-2,4-diene-3-carboxylate (D.2h)



Chemical Formula: $\text{C}_{25}\text{H}_{26}\text{FNO}_2$
Molecular Weight: 391,4864

Following the General Procedure M (stirring for 54 h), the title compound **D.2h** was isolated as a yellow resin (49 mg, 125 μmol). Yield 61%.

$R_f = 0.25$ (SiO_2 , cyclohexane/EtOAc 9:1).

ATR-FTIR (neat) $\nu = 3077, 3055, 3026, 2978, 2930, 2857, 1686, 1618, 1550, 1505, 1446, 1235, 1214, 1094, 911, 846, 757, 699$ cm^{-1} .

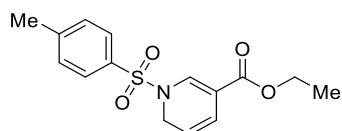
^1H NMR (300 MHz, CDCl_3) $\delta = 7.56$ (s, 1H, H_6), 7.35 – 7.20 (m, 7H, H_{aro}), 7.13 – 7.04 (m, 2H, H_{aro}), 5.22 (s, 1H, H_3), 3.97 (q, $J = 7.1$ Hz, 2H, OCH_2), 2.17 – 2.06 (m, 2H, $2 \times \text{NC}_q\text{CH}_2$), 1.71 – 1.50 (m, 5H), 1.39 – 1.27 (m, 2H), 1.09 – 0.99 (m, 1H), 0.96 (t, $J = 7.1$ Hz, 3H, CH_3) ppm.

$^{19}\text{F}\{^1\text{H}\}$ NMR (282 MHz, CDCl_3) $\delta = -113.37$ ppm.

$^{13}\text{C}\{^1\text{H}\}$ NMR (126 MHz, CDCl_3) $\delta = 166.7$ (C=O), 162.0 (d, $^1J = 248.0$ Hz, FC_q), 148.3 (C_6), 141.8 (C_q), 138.8 (d, $^4J = 3.3$ Hz, $\text{NC}_{q\text{-aro}}$), 136.0 (C_q), 131.5 (d, $^3J = 8.6$ Hz, FC_qCHCH), 127.9 (CH), 127.6 (CH), 126.9 (CH), 117.3 (CH), 116.0 (d, $^2J = 22.6$ Hz, FC_qCH), 101.5 (C_5), 61.4 (C_2), 59.2 (OCH_2), 35.2 (CH_2), 25.5 (CH_2), 21.8 (CH_2), 14.2 (CH_3) ppm.

HRMS (ESI-TOF, + mode) m/z calcd for $\text{C}_{25}\text{H}_{26}\text{FNNaO}_2$ 414.1840, found 414.1825 $[\text{M}+\text{Na}]^+$.

Ethyl 1-tosyl-1,6-dihydropyridine-3-carboxylate D.3b



Chemical Formula: C₁₅H₁₇NO₄S
Molecular Weight: 307,3640

Following the General Procedure M (stirring for 16 h at 120 °C), the title compound **D.3b** was obtained as a yellow oil (17 mg). Yield 87% crude. N.B.: product unstable under air. Yield and analytical data correspond to crude product.

R_f unknown as product degrades on TLC (Al₂O₃ neutral, cyclohexane/EtOAc 8:2 + 1% Et₃N).

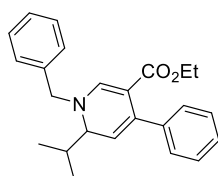
ATR-FTIR (neat) ν = 3092, 3066, 2981, 2929, 2873, 1701, 1626, 1593, 1364, 1293, 1242, 1165, 1165, 1088, 1025, 911, 814, 657 cm⁻¹.

¹H NMR (400 MHz, CDCl₃) δ = 7.77 (t, J = 1.3 Hz, 1H, H₆), 7.74 – 7.69 (m, 2H, H_{aro}), 7.37 (s, 2H, H_{aro}), 6.29 (dq, J = 10.1, 1.8 Hz, 1H, H₄), 5.39 – 5.30 (m, 1H, H₃), 4.25 – 4.16 (m, 4H, OCH₂ & H₂), 2.45 (s, 3H, CH₃ tosyl), 1.30 (t, J = 7.1 Hz, 3H, CH₂CH₃) ppm.

¹³C{¹H} NMR (126 MHz, CDCl₃) δ = 165.3 (C=O), 145.2 (C_q), 135.7 (CH), 133.7 (C_q), 130.3 (CH), 127.7 (CH), 121.2 (CH), 115.5 (CH), 108.8 (C₅), 60.5 (OCH₂), 44.3 (C₂), 21.8 (CH₃ tosyl), 14.5 (CH₂CH₃) ppm.

MS (ESI-TOF, positive mode) m/z (rel intensity) 330.08 (30) [M+Na]⁺.

Ethyl 1-benzyl-6-isopropyl-4-phenyl-1,6-dihydropyridine-3-carboxylate (D.3c)



Chemical Formula: C₂₄H₂₇NO₂
Molecular Weight: 361,4850

Following the General Procedure M (stirring for 21 h), the title compound **D.3c** was isolated as a yellow resin (70 mg, 194 μ mol). Yield 90%.

R_f = 0.58 (Al₂O₃ neutral, cyclohexane/EtOAc 8:2).

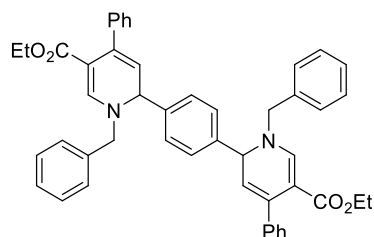
ATR-FTIR (neat) ν = 3057, 3028, 2960, 2928, 2870, 1736, 1678, 1620, 1562, 1444, 1364, 1240, 1148, 1074, 921, 756, 697 cm⁻¹.

¹H NMR (500 MHz, CDCl₃) δ = 7.61 (d, J = 1.4 Hz, 1H, H₆), 7.32 – 7.12 (m, 10H, H_{aro}), 4.74 (d, J = 5.7 Hz, 1H, H₃), 4.46 (d, J = 15.5 Hz, 1H, NCH₂), 4.43 (d, J = 15.4 Hz, 1H, NCH₂), 3.94 – 3.77 (m, 3H, OCH₂ & H₂), 2.02 (heptd, J = 6.9, 5.3 Hz, 1H, CH(CH₃)₂), 0.99 (d, J = 6.7 Hz, 3H, 1 \times CH(CH₃)₂), 0.87 (t, J = 7.1 Hz, 3H, CH₂CH₃), 0.84 (d, J = 6.9 Hz, 3H, 1 \times CH(CH₃)₂) ppm.

¹³C{¹H} NMR (126 MHz, CDCl₃) δ = 166.7 (C=O), 149.3 (C₆), 142.2 (C_q), 138.2 (C_q), 136.6 (C_q), 129.1 (CH), 128.1 (CH), 127.8 (CH), 127.4(04) (CH), 127.4(00) (CH), 126.6 (CH), 110.9 (CH), 99.3 (C₅), 62.8 (NCH), 58.9 (CH₂), 58.5 (CH₂), 32.3 (CH(CH₃)₂), 18.0 (CH(CH₃)₂), 16.7 (CH(CH₃)₂), 14.2 (CH₂CH₃) ppm.

HRMS (ESI-TOF, + mode) m/z calcd for C₂₄H₂₇NNaO₂ 384.1934, found 384.1962 [M+Na]⁺.

Diethyl 6,6'-(1,4-phenylene)bis(1-(4-methoxybenzyl)-4-phenyl-1,6-dihydropyridine-3-carboxylate) (D.3d)



Chemical Formula: C₄₈H₄₄N₂O₄
Molecular Weight: 712,8900

Following the General Procedure M (stirring for 4 d), the title compound **D.3d** was isolated as a yellow solid (137 mg, 177 μ mol). Yield 76%.

R_f = 0.60 (Al₂O₃ neutral, cyclohexane/EtOAc 7:3).

ATR-FTIR (neat) ν = 3058, 3029, 2979, 2931, 2902, 1724, 1689, 1636, 1569, 1494, 1440, 1359, 1288, 1207, 1143, 1049, 910, 842, 725, 695 cm⁻¹.

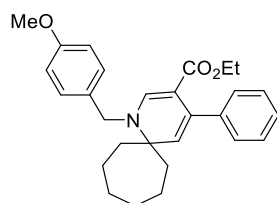
¹H NMR (300 MHz, CDCl₃) δ = 7.74 (s, 2H, 2 \times H₆), 7.45 – 7.20 (m, 24H, H_{aro}), 5.13 (d, J = 5.1 Hz, 2H, NCH or H₂), 4.98 (d, J = 5.1 Hz, 2H, NCH or H₂),

4.39 (d, $J = 15.1$ Hz, 2H, $2 \times \text{NCH}_2$), 4.25 (d, $J = 15.1$ Hz, 2H, $2 \times \text{NCH}_2$), 4.07 – 3.89 (m, 4H, $2 \times \text{OCH}_2$), 0.99 (t, $J = 7.1$ Hz, 6H, $2 \times \text{CH}_3$) ppm.

$^{13}\text{C}\{^1\text{H}\}$ NMR (126 MHz, CDCl_3) $\delta = 166.6$ (C=O), 148.9 (C_6), 141.9 (C_q), 141.5 (C_q), 135.5 (C_q), 135.4 (C_q), 129.1 (CH), 128.4 (CH), 128.1 (CH), 128.0 (CH), 127.6 (CH), 127.4 (CH), 126.7 (CH), 115.4 (CH), 97.6 (C_5), 61.0 (C_2), 59.2 (CH_2), 57.7 (CH_2), 45.6 (CH_2), 14.2 (CH_3) ppm.

HRMS (ESI-TOF, + mode) m/z calcd for $\text{C}_{48}\text{H}_{43}\text{N}_2\text{O}_4$ 711.3217, found 711.3223 $[\text{M}-\text{H}]^+$.
N.B.: the title compound is not stable.

Ethyl 1-(4-methoxybenzyl)-4-phenyl-1-azaspiro[5.6]dodeca-2,4-diene-3-carboxylate (D.3e)



Chemical Formula: $\text{C}_{28}\text{H}_{33}\text{NO}_3$
Molecular Weight: 431,5760

Following the General Procedure M (stirring for 19 h), the title compound **D.3e** was isolated as a yellow resin (92 mg, 213 μmol). Yield 85%.

$R_f = 0.63$ (Al_2O_3 neutral, cyclohexane/EtOAc 8:2).

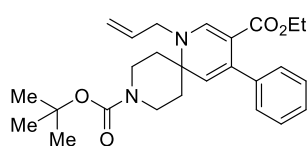
ATR-FTIR (neat) $\nu = 3077, 3054, 3024, 2974, 2924, 2852, 1679, 1612, 1553, 1511, 1443, 1361, 1285, 1246, 1213, 1149, 1072, 1033, 922, 814, 757, 698$ cm^{-1} .

^1H NMR (500 MHz, CDCl_3) $\delta = 7.52$ (s, 1H, H_6), 7.31 – 7.22 (m, 5H, H_{aro}), 7.21 – 7.16 (m, 2H, H_{aro}), 6.92 – 6.87 (m, 2H, $2 \times \text{OC}_q\text{CH}_{\text{aro}}$), 4.95 (s, 1H, H_3), 4.51 (s, 2H, NCH_2), 3.93 (q, $J = 7.1$ Hz, 2H, OCH_2), 3.81 (s, 3H, OCH_3), 2.03 – 1.86 (m, 4H), 0.93 (t, $J = 7.1$ Hz, 3H, CH_2CH_3) ppm.

$^{13}\text{C}\{^1\text{H}\}$ NMR (126 MHz, CDCl_3) $\delta = 166.6$ (C=O), 159.1 (CH_3OC_q), 149.3 (C_6), 141.9 (C_q), 135.5 (C_q), 130.7 (C_q), 128.2 (CH), 127.9 (CH), 127.5 (CH), 126.6 (CH), 119.8 (CH), 114.3 (CH), 99.5 (C_5), 63.7 (C_2), 59.0 (OCH_2), 55.4 (OCH_3), 53.0 (NCH_2), 38.9 (CH_2), 29.6 (CH_2), 22.3 (CH_2), 14.1 (CH_2CH_3) ppm.

HRMS (ESI-TOF, + mode) m/z calcd for $\text{C}_{28}\text{H}_{34}\text{NO}_3$ 432.2533, found 432.2531 $[\text{M}+\text{H}]^+$.

9-(tert-Butyl) 3-ethyl 1-allyl-4-phenyl-1,9-diazaspiro[5.5]undeca-2,4-diene-3,9-dicarboxylate (D.3f)



Chemical Formula: $\text{C}_{26}\text{H}_{34}\text{N}_2\text{O}_4$
Molecular Weight: 438,5680

Following the General Procedure M (stirring for 21 h), the title compound **D.3f** was isolated as a yellow resin (59 mg, 135 μmol). Yield 75%.

$R_f = 0.40$ (Al_2O_3 neutral, cyclohexane/EtOAc 8:2).

ATR-FTIR (neat) $\nu = 3080, 3055, 2975, 2929, 2868, 1683, 1615, 1551, 1418, 1363, 1287, 1243, 1209, 1140, 1079, 1043, 980, 862,$

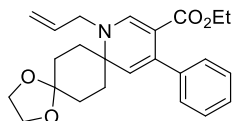
$756, 698$ cm^{-1} .

^1H NMR (500 MHz, CDCl_3) $\delta = 7.49$ (s, 1H, H_6), 7.24 – 7.18 (m, 3H, H_{aro}), 7.16 – 7.13 (m, 2H, H_{aro}), 5.81 (ddt, $J = 17.0, 10.4, 5.3$ Hz, 1H, $\text{CH}=\text{CH}_2$), 5.19 (dq, $J = 17.0, 1.5$ Hz, 1H, $\text{CH}=\text{CH}_2$), 5.15 (dq, $J = 10.2, 1.3$ Hz, 1H, $\text{CH}=\text{CH}_2$), 4.96 (s, 1H, H_3), 4.10 – 3.83 (m, 6H, OCH_2 & $\text{NCH}_2\text{CH}=\text{}$ & BocNCH_2), 2.95 (bs, 2H, $2 \times \text{NC}_q\text{CH}_2$), 1.94 – 1.86 (m, 2H, $2 \times \text{NC}_q\text{CH}_2$), 1.70 – 1.59 (m, 2H), 1.40 (s, 9H, $\text{C}(\text{CH}_3)_3$), 0.87 (t, $J = 7.1$ Hz, 3H, CH_2CH_3) ppm.

$^{13}\text{C}\{^1\text{H}\}$ NMR (126 MHz, CDCl_3) $\delta = 166.5$ ($\text{C}_5\text{C}=\text{O}$), 154.9 ($\text{NC}=\text{O}$), 149.3 (C_6), 141.5 (C_q), 137.7 (C_q), 135.2 (CH), 127.9 (CH), 127.6 (CH), 127.0 (CH), 117.8 ($\text{CH}=\text{CH}_2$), 113.5 (CH), 100.5 (C_5), 80.0 ($\text{C}(\text{CH}_3)_3$), 59.2 (OCH_2), 58.8 (C_2), 52.2 ($\text{NCH}_2\text{CH}=\text{}$), 39.6 (CH_2), 33.6 (CH_2), 28.6 ($\text{C}(\text{CH}_3)_3$), 14.1 (CH_2CH_3) ppm.

HRMS (ESI-TOF, + mode) m/z calcd for $C_{26}H_{34}KN_2O_4$ 477.2150, found 477.2147 $[M+K]^+$.

Ethyl 9-allyl-12-phenyl-1,4-dioxo-9-azadispiro[4.2.5⁸.2⁵]pentadeca-10,12-diene-11-carboxylate (D.3g)



Chemical Formula: $C_{24}H_{26}NO_4$
Molecular Weight: 395,4990

Following the General Procedure M (stirring for 24 h), the title compound **D.3g** was isolated as a yellow resin (56 mg, 142 μ mol). Yield 71%.

R_f = 0.40 (Al₂O₃ neutral, cyclohexane/EtOAc 8:2).

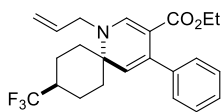
ATR-FTIR (neat) ν = 3079, 3056, 3023, 2933, 2887, 1678, 1616, 1552, 1444, 1364, 1286, 1208, 1100, 1032, 912, 729, 698 cm^{-1} .

¹H NMR (500 MHz, CDCl₃) δ = 7.54 (s, 1H, H₆), 7.30 – 7.19 (m, 5H, H_{aro}), 5.88 (ddt, J = 17.3, 10.4, 5.2 Hz, 1H, CH=CH₂), 5.28 – 5.18 (m, 2H, CH=CH₂), 5.09 (s, 1H, H₃), 3.98 – 3.92 (m, 8H, O=COCH₂ & OCH₂CH₂O), 2.06 – 1.99 (m, 2H, 2 \times NC_qCH₂), 1.96 – 1.82 (m, 4H), 1.66 – 1.63 (m, 1H), 0.94 (t, J = 7.1 Hz, 3H, CH₃) ppm.

¹³C{¹H} NMR (126 MHz, CDCl₃) δ = 166.6 (C=O), 149.7 (C₆), 141.7 (C_q), 137.0 (C_q), 135.3 (CH), 127.8 (CH), 127.5 (CH), 126.8 (CH), 117.6 (CH=CH₂), 114.5 (CH), 107.8 (C_q), 99.8 (C₅), 64.5 (C_qOCH₂), 64.4 (C_qOCH₂), 59.5 (C₂), 59.1 (CO₂CH₂), 52.1 (NCH₂), 31.2 (CH₂), 30.3 (CH₂), 14.1 (CH₃) ppm.

HRMS (ESI-TOF, + mode) m/z calcd for $C_{24}H_{30}NO_4$ 396.2169, found 396.2178 $[M+H]^+$.

Ethyl 1-allyl-4-phenyl-9-(trifluoromethyl)-1-azaspiro[5.5]undeca-2,4-diene-3-carboxylate (D.3h)



Chemical Formula: $C_{23}H_{26}F_3NO_2$
Molecular Weight: 405,4612

Following the General Procedure M (stirring for 48 h), the title compound **D.3h** was isolated as an orange solid (53 mg, 131 μ mol). Yield 72%.

R_f = 0.43 (SiO₂, cyclohexane/EtOAc 7:3).

ATR-FTIR (neat) ν = 3075, 3025, 3000, 2953, 2938, 2892, 2862, 1665, 1609, 1549, 1465, 1366, 1292, 1219, 1171, 1091, 997, 911, 825, 757, 700 cm^{-1} .

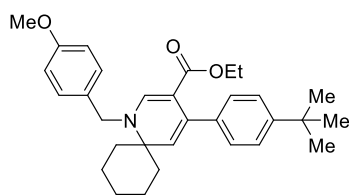
¹H NMR (500 MHz, CDCl₃) δ = 7.55 (s, 1H, H₆), 7.34 – 7.26 (m, 3H, H_{aro}), 7.24 – 7.18 (m, 2H, H_{aro}), 5.89 (ddt, J = 17.1, 10.5, 5.3 Hz, 1H, CH=CH₂), 5.31 – 5.18 (m, 2H, CH=CH₂), 4.98 (s, 1H, H₃), 3.99 – 3.89 (m, 4H, OCH₂ & NCH₂), 2.17 (d, J = 12.3 Hz, 2H), 2.07 – 1.94 (m, 1H), 1.87 – 1.79 (m, 2H), 1.69 (qd, J = 13.3, 3.2 Hz, 2H), 1.62 – 1.52 (m, 2H), 0.94 (t, J = 7.1 Hz, 3H, CH₃) ppm.

¹⁹F{¹H} NMR (282 MHz, CDCl₃) δ = -73.49 ppm.

¹³C{¹H} NMR (126 MHz, CDCl₃) δ = 166.6 (C=O), 149.4 (C₆), 141.5 (C_q), 137.0 (C_q), 135.4 (CH), 127.8 (CH), 127.6 (CH), 127.5 (q, $^1J_{C-F}$ = 277.4 Hz, CF₃), 126.9 (CH), 117.8 (CH=CH₂), 114.3 (CH), 100.3 (C₅), 59.4 (C₂), 59.2 (OCH₂), 52.3 (NCH₂), 41.3 (q, $^2J_{C-F}$ = 26.9 Hz, F₃CCH), 32.4 (CH₂), 20.5 (q, $^3J_{C-F}$ = 2.6 Hz, F₃CCHCH₂), 14.1 (CH₃) ppm.

HRMS (ESI-TOF, + mode) m/z calcd for $C_{23}H_{26}F_3NNaO_2$ 428.1808, found 428.1795 $[M+Na]^+$.

Ethyl 4-(4-(*tert*-butyl)phenyl)-1-(4-methoxybenzyl)-1-azaspiro[5.5]undeca-2,4-diene-3-carboxylate (D.4a)



Chemical Formula: C₃₁H₃₉NO₃
Molecular Weight: 473,6570

Following the General Procedure M (stirring for 27 h), the title compound **D.4a** was isolated as a yellow solid (95.1 mg, 201 μmol). Yield 89%.

R_f = 0.70 (Al₂O₃ neutral, cyclohexane/EtOAc 8:2).

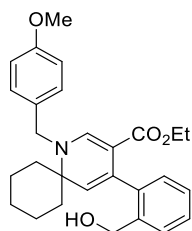
ATR-FTIR (neat) ν = 3036, 3036, 2940, 2860, 1670, 1619, 1552, 1511, 1454, 1363, 1291, 1210, 1131, 1033, 970, 828, 757 cm⁻¹.

¹H NMR (500 MHz, CDCl₃) δ = 7.62 (s, 1H, H₆), 7.34 – 7.28 (m, 2H, H_{aro}), 7.22 – 7.19 (m, 2H, H_{aro}), 7.19 – 7.14 (m, 2H, H_{aro}), 6.88 – 6.84 (m, 2H, 2 × OC_qCH_{aro}), 5.08 (s, 1H, H₃), 4.49 (s, 2H, NCH₂), 3.96 (q, *J* = 7.1 Hz, 2H, OCH₂), 3.80 (s, 3H, OCH₃), 2.00 – 1.92 (m, 2H, 2 × NC_qCH₂), 1.69 – 1.62 (m, 1H), 1.60 – 1.51 (m, 4H), 1.46 (td, *J* = 12.2, 4.8 Hz, 2H), 1.33 (s, 9H, (C(CH₃)₃)), 1.15 – 1.03 (m, 1H), 0.92 (t, *J* = 7.1 Hz, 3H, CH₂CH₃) ppm.

¹³C{¹H} NMR (126 MHz, CDCl₃) δ = 166.9 (C=O), 159.1 (CH₃OC_q), 150.2 (C₆), 149.5 (C_q), 139.0 (C_q), 135.8 (C_q), 131.1 (C_q), 128.0 (CH), 127.6 (CH), 124.4 (CH), 116.1 (CH), 114.2 (CH), 99.9 (C₅), 60.8 (C₂), 59.0 (OCH₂), 55.4 (OCH₃), 53.1 (NCH₂), 34.6 (C(CH₃)₃), 34.3 (CH₂), 31.6 (C(CH₃)₃), 25.6 (CH₂), 21.8 (CH₂), 14.0 (OCH₂CH₃) ppm.

HRMS (ESI-TOF, + mode) *m/z* calcd for C₃₁H₄₀NO₃ 474.3003, found 474.2993 [M+H]⁺.

Ethyl 4-(2-(hydroxymethyl)phenyl)-1-(4-methoxybenzyl)-1-azaspiro[5.5]undeca-2,4-diene-3-carboxylate (D.4b)



Chemical Formula: C₂₈H₃₃NO₄
Molecular Weight: 447,5750

Following the General Procedure M (stirring for 28 h), the title compound **D.4b** was isolated as a yellow solid (171 mg, 382 μmol). Yield 89%.

R_f = 0.46 (SiO₂, cyclohexane/EtOAc 7:3).

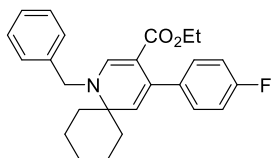
ATR-FTIR (neat) ν = 3398, 3071, 3029, 2927, 2853, 2244, 1678, 1582, 1511, 1456, 1363, 1294, 1246, 1143, 1073, 1030, 964, 909, 760, 724 cm⁻¹.

¹H NMR (500 MHz, CDCl₃) δ = 7.69 (s, 1H, H₆), 7.25 – 7.16 (m, 5H, H_{aro}), 7.02 – 6.96 (m, 1H, H_{aro}), 6.92 – 6.86 (m, 2H, 2 × OC_qCH_{aro}), 5.23 (d, *J* = 11.9 Hz, 1H, CH₂O), 5.13 (d, *J* = 11.9 Hz, 1H, CH₂O), 4.56 (d, *J* = 16.1 Hz, 1H, NCH₂), 4.34 (d, *J* = 16.0 Hz, 1H, NCH₂), 3.90 – 3.72 (m, 5H, CO₂CH₂ & OCH₃), 2.74 (d, *J* = 14.5 Hz, 1H), 2.62 – 2.54 (m, 1H), 1.76 – 1.47 (m, 7H), 1.43 – 1.28 (m, 2H), 1.16 – 1.05 (m, 1H), 0.77 (t, *J* = 7.1 Hz, 3H, CH₂CH₃) ppm. N.B.: H₃ is not observed in ¹H NMR spectrum.

¹³C{¹H} NMR (126 MHz, CDCl₃) δ = 167.9 (C=O), 159.0 (CH₃OC_q), 150.4 (C₆), 146.4 (C_q), 139.9 (C_q), 131.4 (C_q), 128.1 (CH), 127.1 (CH), 126.9 (CH), 120.8 (CH), 120.5 (CH), 114.2 (CH), 98.7 (C_q), 84.1 (C_q), 71.9 (CH₂OH), 58.9 (C₂), 58.7 (OCH₂), 55.4 (OCH₃), 52.8 (NCH₂), 44.7 (CH₂), 36.7 (CH₂), 29.9 (CH₂), 25.6 (CH₂), 23.0 (CH₂), 22.7 (CH₂), 13.9 (CH₂CH₃) ppm. N.B.: one C_{sp2}H signal is not observed in ¹³C, nor DEPT 135 NMR.

HRMS (ESI-TOF, + mode) *m/z* calcd for C₂₈H₃₃NNaO₄ 470.2302, found 470.2283 [M+Na]⁺.

Ethyl 1-benzyl-4-(4-fluorophenyl)-1-azaspiro[5.5]undeca-2,4-diene-3-carboxylate (D.4d)



Chemical Formula: C₂₆H₂₈FNO₂
Molecular Weight: 405.5134

Following the General Procedure M (stirring for 30 h), the title compound **D.4d** was isolated as an off-white foam (78.3 mg, 193 μmol). Yield 78%.

R_f = 0.43 (SiO₂, cyclohexane/EtOAc 8:2).

ATR-FTIR (neat) ν = 3062, 3031, 2977, 2929, 2855, 1680, 1616, 1550, 1507, 1451, 1361, 1290, 1208, 1136, 1069, 1028, 971, 842, 796, 726, 695 cm⁻¹.

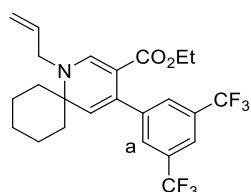
¹H NMR (500 MHz, CDCl₃) δ = 7.64 (s, 1H, H₆), 7.37 – 7.31 (m, 2H, H_{aro}), 7.30 – 7.21 (m, 5H, H_{aro}), 7.02 – 6.96 (m, 2H, H_{aro}), 5.06 (s, 1H, H₃), 4.57 (s, 2H, NCH₂), 3.98 (q, *J* = 7.1 Hz, 2H, OCH₂), 2.01 – 1.94 (m, 2H, 2 × NC_qCH₂), 1.70 – 1.62 (m, 1H), 1.59 – 1.52 (m, 4H), 1.52 – 1.42 (m, 2H), 1.15 – 1.05 (m, 1H), 1.01 (t, *J* = 7.1 Hz, 3H, CH₃) ppm.

¹⁹F{¹H} NMR (282 MHz, CDCl₃) δ = -116.63 ppm.

¹³C{¹H} NMR (126 MHz, CDCl₃) δ = 166.5 (C=O), 162.1 (d, ¹*J*_{C-F} = 244.5 Hz, FC_q), 150.4 (C₆), 139.1 (C_q), 137.9 (d, ⁴*J*_{C-F} = 3.2 Hz, ≡CC_{q-aro}), 135.2 (C_q), 129.4 (d, ³*J*_{C-F} = 7.8 Hz, FC_qCHCH), 128.9 (CH), 127.6 (CH), 126.7 (CH), 116.4 (d, *J* = 1.0 Hz, CH), 114.3 (d, ²*J*_{C-F} = 21.3 Hz, FC_qCH), 99.8 (C₅), 60.8 (C₂), 59.1 (OCH₂), 53.6 (NCH₂), 34.3 (CH₂), 25.5 (CH₂), 21.7 (CH₂), 14.3 (CH₃) ppm.

HRMS (ESI-TOF, + mode) *m/z* calcd for C₂₆H₂₉FNO₂ 406.2177, found 406.2173 [M+H]⁺.

Ethyl 1-allyl-4-(3,5-bis(trifluoromethyl)phenyl)-1-azaspiro[5.5]undeca-2,4-diene-3-carboxylate (D.4e)



Chemical Formula: C₂₄H₂₅F₆NO₂
Molecular Weight: 473.4594

Following the General Procedure M (stirring for 54 h), the title compound **D.4e** was isolated as yellow resin (45 mg, 95 μmol). Yield 76%.

R_f = 0.75 (Al₂O₃ neutral, cyclohexane/EtOAc 8:2).

ATR-FTIR (neat) ν = 3086, 2981, 2933, 2859, 1682, 1624, 1612, 1554, 1371, 1275, 1168, 1126, 1046, 895, 765, 684 cm⁻¹.

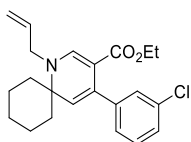
¹H NMR (500 MHz, CDCl₃) δ = 7.75 (s, 1H), 7.64 (s, 2H, H_a), 7.60 (s, 1H), 5.89 (ddt, *J* = 17.1, 10.6, 5.5 Hz, 1H, CH=CH₂), 5.29 – 5.21 (m, 2H, CH=CH₂), 5.06 (s, 1H, H₃), 3.96 (dt, *J* = 5.5, 1.7 Hz, 2H, NCH₂), 3.92 (q, *J* = 7.1 Hz, 2H, OCH₂), 2.08 – 2.01 (m, 2H, 2 × NC_qCH₂), 1.77 – 1.69 (m, 1H), 1.66 – 1.51 (m, 6H), 1.21 – 1.10 (m, 1H), 0.90 (t, *J* = 7.2 Hz, 3H, CH₃) ppm.

¹⁹F{¹H} NMR (282 MHz, CDCl₃) δ = -62.65 ppm.

¹³C{¹H} NMR (126 MHz, CDCl₃) δ = 166.2 (C=O), 150.3 (C₆), 144.3 (C_q), 135.2 (CH), 134.1 (C_q), 130.6 (q, ²*J*_{C-F} = 33.0 Hz, CF₃C_{q-aro}), 128.2 – 128.1 (m, CH, CF₃CCH), 123.7 (d, ¹*J*_{C-F} = 272.5 Hz, CF₃), 120.3 (h, ³*J*_{C-F} = 3.8 Hz, CF₃CCH), 118.0 (CH), 117.5 (CH=CH₂), 98.4 (C₅), 60.8 (C₂), 59.2 (OCH₂), 52.2 (NCH₂), 34.3 (CH₂), 25.5 (CH₂), 21.7 (CH₂), 14.0 (CH₃) ppm.

HRMS (ESI-TOF, + mode) *m/z* calcd for C₂₄H₂₅F₆NNaO₂ 496.1682, found 496.1679 [M+Na]⁺.

Ethyl 1-allyl-4-(3-chlorophenyl)-1-azaspiro[5.5]undeca-2,4-diene-3-carboxylate (D.4f)



Chemical Formula: C₂₂H₂₆ClNO₂
Molecular Weight: 371,9050

Following the General Procedure M (stirring for 72 h), the title compound **D.4f** was isolated as a yellow viscous oil (32 mg, 85 μmol). Yield 85%.

R_f = 0.37 (Al₂O₃ neutral, cyclohexane/EtOAc 9:1).

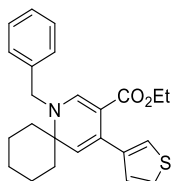
ATR-FTIR (neat) ν = 3063, 2978, 2930, 2856, 1680, 1616, 1594, 1552, 1449, 1417, 1362, 1288, 1202, 1136, 1079, 984, 924, 780, 692 cm⁻¹.

¹H NMR (500 MHz, CDCl₃) δ = 7.54 (s, 1H, H₆), 7.25 – 7.17 (m, 3H, H_{aro}), 7.14 – 7.08 (m, 1H, H_{aro}), 5.88 (ddt, *J* = 17.1, 10.6, 5.4 Hz, 1H, CH=CH₂), 5.28 – 5.19 (m, 2H, CH=CH₂), 5.05 (s, 1H, H₃), 4.00 – 3.91 (m, 4H, OCH₂ & NCH₂), 2.08 – 1.99 (m, 2H, 2 × NC_qCH₂), 1.73 – 1.66 (m, 1H), 1.64 – 1.46 (m, 6H), 1.19 – 1.08 (m, 1H), 0.97 (t, *J* = 7.1 Hz, 3H, CH₃) ppm.

¹³C{¹H} NMR (126 MHz, CDCl₃) δ = 166.5 (C=O), 149.8 (C₆), 144.0 (C_q), 135.5 (CH), 134.9 (C_q), 133.2 (C_q), 128.6 (CH), 128.0 (CH), 126.7 (CH), 126.2 (CH), 117.7 (CH=CH₂), 116.5 (CH), 99.1 (C₅), 60.6 (C₂), 59.1 (OCH₂), 52.1 (NCH₂), 34.3 (CH₂), 25.6 (CH₂), 21.7 (CH₂), 14.2 (CH₃) ppm.

HRMS (ESI-TOF, + mode) *m/z* calcd for C₂₂H₂₆ClNNO₂ 394.1544, found 394.1542 [M+Na]⁺.

Ethyl 1-benzyl-4-(thiophen-3-yl)-1-azaspiro[5.5]undeca-2,4-diene-3-carboxylate (D.4g)



Chemical Formula: C₂₄H₂₇NO₂S
Molecular Weight: 393,5450

Following the General Procedure M (stirring for 5 d), the title compound **D.4g** was isolated as a yellow resin (60 mg, 152 μmol). Yield 83%.

R_f = 0.59 (Al₂O₃ neutral, cyclohexane/EtOAc 7:3).

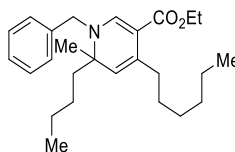
ATR-FTIR (neat) ν = 3105, 3087, 3061, 3029, 2927, 2854, 1675, 1612, 1551, 1495, 1451, 1361, 1289, 1210, 1136, 1070, 1029, 908, 732, 697 cm⁻¹.

¹H NMR (500 MHz, CDCl₃) δ = 7.62 (s, 1H, H₆), 7.37 – 7.31 (m, 2H, H_{aro}), 7.29 – 7.23 (m, 3H, H_{aro}), 7.21 (dd, *J* = 5.0, 3.0 Hz, 1H, H_{aro}), 7.15 (dd, *J* = 3.0, 1.3 Hz, 1H, H_{aro}), 7.01 (dd, *J* = 4.9, 1.3 Hz, 1H, H_{aro}), 5.20 (s, 1H, H₃), 4.56 (s, 2H, NCH₂), 4.02 (q, *J* = 7.1 Hz, 2H, OCH₂), 1.99 – 1.92 (m, 2, 2 × NC_qCH₂H), 1.69 – 1.62 (m, 1H), 1.57 – 1.51 (m, 4H), 1.49 – 1.41 (m, 2H), 1.15 – 1.09 (m, 1H), 1.06 (t, *J* = 7.1 Hz, 3H, CH₃) ppm.

¹³C{¹H} NMR (126 MHz, CDCl₃) δ = 166.6 (C=O), 150.3 (C₆), 142.5 (C_q), 139.2 (C_q), 130.7 (C_q), 128.9 (CH), 128.7 (CH), 127.6 (CH), 126.6 (CH), 123.7 (CH), 121.0 (CH), 116.0 (CH), 99.8 (C₅), 60.6 (C₂), 59.2 (OCH₂), 53.7 (NCH₂), 34.3 (CH₂), 25.5 (CH₂), 21.7 (CH₂), 14.3 (CH₃) ppm.

HRMS (ESI-TOF, + mode) *m/z* calcd for C₂₄H₂₈NO₂S 394.1835, found 394.1824 [M+H]⁺.

Ethyl 1-benzyl-6-butyl-4-hexyl-6-methyl-1,6-dihydropyridine-3-carboxylate (D.4h)



Chemical Formula: C₂₆H₃₉NO₂
Molecular Weight: 397,6030

Following the General Procedure M (stirring for 24 h), the title compound **D.4h** was isolated as an impure fraction representing a yellow resin (52 mg). Yield 48% (60 μmol, estimated *via* ¹H NMR using 1,3,5-trimethoxybenzene as internal standard).

R_f = 0.85 (Al₂O₃ neutral, cyclohexane/EtOAc 8:2).

ATR-FTIR (neat) ν = 3088, 3063, 3030, 2956, 2927, 2857, 1721, 1682, 1568, 1454, 1364, 1288, 1224, 1166, 1110, 1062, 973, 868, 763, 728, 697 cm⁻¹.

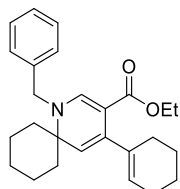
¹H NMR (500 MHz, CDCl₃) some characteristic signals δ = 7.45 (s, 1H, H₆), 4.08 (q, *J* = 7.1 Hz, 2H, OCH₂), 1.21 (s, 3H, C_qCH₃) ppm.

$^{13}\text{C}\{^1\text{H}\}$ NMR (126 MHz, CDCl_3) some characteristic signals $\delta = 166.9$ (C=O), 150.2 (C_6), 97.2 (C_5), 61.5 (C_2), 58.9 (OCH_2), 52.7 (NCH_2) ppm.

MS (ESI-TOF, + mode) m/z (rel intensity) 398.31 (100) $[\text{M}+\text{H}]^+$, 340.24 (40) $[\text{C}_{22}\text{H}_{30}\text{NO}_2]^+$.

HRMS (ESI-TOF, + mode) m/z calcd for $\text{C}_{26}\text{H}_{39}\text{NNaO}_2$ 420.2873, found 420.2878 $[\text{M}+\text{Na}]^+$.

Ethyl 1-benzyl-4-(cyclohex-1-en-1-yl)-1-azaspiro[5.5]undeca-2,4-diene-3-carboxylate (D.4i)



Chemical Formula: $\text{C}_{26}\text{H}_{33}\text{NO}_2$
Molecular Weight: 391,5550

Following the General Procedure M (stirring for 30 h), the title compound **D.4i** was isolated as a yellow resin (32.0 mg). Yield 75%.

$R_f = 0.92$ (Al_2O_3 neutral, cyclohexane/EtOAc 8:2).

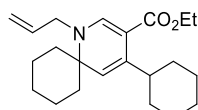
ATR-FTIR (neat) $\nu = 3059, 3028, 2927, 2855, 1681, 1610, 1550, 1495, 1451, 1361, 1288, 1204, 1132, 1070, 983, 844, 729, 696$ cm^{-1} .

^1H NMR (500 MHz, CDCl_3) $\delta = 7.50$ (s, 1H, H_6), 7.35 – 7.30 (m, 2H, H_{aro}), 7.28 – 7.19 (m, 3H, H_{aro}), 5.61 (tt, $J = 3.6, 1.6$ Hz, 1H, $\text{C}_q=\text{CH}$), 4.98 (s, 1H, H_3), 4.50 (s, 2H, NCH_2), 4.13 (q, $J = 7.1$ Hz, 2H, OCH_2), 2.16 – 2.03 (m, 4H), 1.92 – 1.82 (m, 2H, $2 \times \text{NC}_q\text{CH}_2$), 1.73 – 1.45 (m, 9H), 1.39 (td, $J = 12.3, 4.7$ Hz, 2H), 1.25 (t, $J = 7.1$ Hz, 3H, CH_3), 1.11 – 1.00 (m, 1H) ppm.

$^{13}\text{C}\{^1\text{H}\}$ NMR (126 MHz, CDCl_3) $\delta = 166.7$ (C=O), 150.1 (C_6), 140.6 (C_q), 139.5 (C_q), 138.4 (C_q), 128.8 (C_{aroH}), 127.5 (C_{aroH}), 126.6 (C_{aroH}), 122.5 ($\text{C}_q=\text{CHCH}_2$), 113.5 (C_3), 99.7 (C_5), 60.2 (C_2), 59.2 (OCH_2), 53.5 (NCH_2), 34.4 (CH_2), 29.1 (CH_2), 25.7 (CH_2), 25.6 (CH_2), 23.2 (CH_2), 22.5 (CH_2), 21.7 (CH_2), 14.7 (CH_3) ppm.

HRMS (ESI-TOF, + mode) m/z calcd for $\text{C}_{26}\text{H}_{34}\text{NO}_2$ 392.2584, found 392.2591 $[\text{M}+\text{H}]^+$.

Ethyl 1-allyl-4-cyclohexyl-1-azaspiro[5.5]undeca-2,4-diene-3-carboxylate (D.4j)



Chemical Formula: $\text{C}_{22}\text{H}_{33}\text{NO}_2$
Molecular Weight: 343,5110

Au(JohnPhos)NTf₂ (4.4 mg, 5 mol%) was added to a solution of crude enyne (113 μmol , 1.0 eq.) in 1,2-dichloroethane (0.12 mL, 1 M) in a Teflon screw cap tube (10 mL) equipped with a stirrer. The reaction flask was briefly flushed with argon (10 s) before sealing. Next, the mixture was placed into a pre-heated aluminium block set to 100 $^\circ\text{C}$ and 500 rpm and stirred until completion of enyne. Once cooled to rt,

the mixture was filtered through a short pad of Al_2O_3 and washed several times with EtOAc. Finally, the solvent was removed under reduced pressure and the crude product was purified *via* column chromatography over silica gel using 0.5% triethylamine in cyclohexane. The title compound **D.4j** was isolated as a yellow resin (30 mg, 87 μmol). Yield 77%.

$R_f = 0.70$ (Al_2O_3 neutral, cyclohexane/EtOAc 8:2).

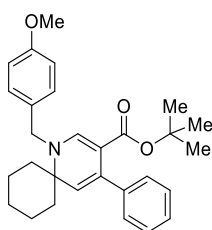
ATR-FTIR (neat) $\nu = 3079, 2924, 2851, 1726, 1682, 1631, 1555, 1448, 1365, 1284, 1221, 1136, 1071, 988, 921, 765$ cm^{-1} .

^1H NMR (500 Hz, CDCl_3) $\delta = 7.41$ (s, 1H, H_6), 5.84 (ddt, $J = 17.1, 10.5, 5.4$ Hz, 1H, $\text{CH}=\text{CH}_2$), 5.23 – 5.12 (m, 2H, $\text{CH}=\text{CH}_2$), 4.97 (d, $J = 0.6$ Hz, 1H, H_3), 4.17 – 4.08 (m, 2H, OCH_2), 3.84 (dt, $J = 5.4, 1.7$ Hz, 2H, NCH_2), 3.04 – 2.94 (m, 1H), 1.93 – 1.80 (m, 4H), 1.79 – 1.59 (m, 6H), 1.56 – 1.32 (m, 8H), 1.27 (t, $J = 7.1$ Hz, 3H, CH_3), 1.14 – 1.03 (m, 2H) ppm.

$^{13}\text{C}\{^1\text{H}\}$ NMR (126 MHz, CDCl_3) $\delta = 167.0$ (C=O), 149.7 (C_6), 139.8 (C_q), 136.0 (CH), 117.2 ($\text{CH}=\text{CH}_2$), 110.3 (CH), 98.8 (C_5), 59.6 (C_2), 58.9 (OCH_2), 51.8 (NCH_2), 38.8 (CHCH_2), 34.7 (CH_2), 33.8 (CH_2), 27.2 (CH_2), 26.9 (CH_2), 25.7 (CH_2), 21.7 (CH_2), 14.8 (CH_3) ppm.

HRMS (ESI-TOF, + mode) m/z calcd for $\text{C}_{22}\text{H}_{34}\text{NO}_2$ 344.2584, found 344.2576 $[\text{M}+\text{H}]^+$.

tert-Butyl 1-(4-methoxybenzyl)-4-phenyl-1-azaspiro[5.5]undeca-2,4-diene-3-carboxylate (D.5a)



Chemical Formula: C₂₉H₃₅NO₃
Molecular Weight: 445,6030

Following the General Procedure M (stirring for 72 h), the title compound **D.5a** was isolated as an off-white solid (51 mg, 114 μmol). Yield 57%.

R_f = 0.68 (Al₂O₃ neutral, cyclohexane/EtOAc 8:2).

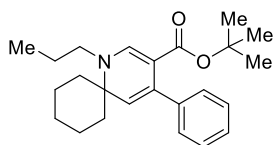
ATR-FTIR (neat) ν = 3055, 3024, 3001, 2925, 2858, 2235, 1655, 1619, 1555, 1511, 1444, 1363, 1301, 1222, 1136, 1036, 913, 803, 734, 698 cm⁻¹.

¹H NMR (300 MHz, CDCl₃) δ = 7.56 (s, 1H, H₆), 7.34 – 7.20 (m, 6H, H_{aro}), 7.20 – 7.14 (m, 2H, H_{aro}), 6.89 – 6.83 (m, 2H, 2 × OC_qCH_{aro}), 5.01 (s, 1H, H₃), 4.47 (s, 2H, NCH₂), 3.80 (s, 3H, OCH₃), 2.02 – 1.92 (m, 2H, 2 × NC_qCH₂), 1.74 – 1.38 (m, 7H), 1.16 (s, 9H), 1.12 – 1.04 (m, 1H) ppm.

¹³C{¹H} NMR (126 MHz, CDCl₃) δ = 166.7 (C=O), 159.0 (CH₃OC_q), 149.9 (C₆), 142.7 (C_q), 136.4 (C_q), 131.2 (C_q), 128.1 (CH), 128.0 (CH), 127.5 (CH), 126.5 (CH), 116.0 (CH), 114.2 (CH), 101.4 (C₅), 78.6 (C(CH₃)₃), 60.7 (C₂), 55.4 (OCH₃), 53.0 (NCH₂), 34.2 (CH₂), 28.1 (C(CH₃)₃), 25.7 (CH₂), 21.8 (CH₂) ppm.

HRMS (ESI-TOF, + mode) m/z calcd for C₂₉H₃₅NNaO₃ 468.2509, found 468.2508 [M+Na]⁺.

tert-Butyl 4-phenyl-1-propyl-1-azaspiro[5.5]undeca-2,4-diene-3-carboxylate (D.5b)



Chemical Formula: C₂₄H₃₃NO₂
Molecular Weight: 367,5330

Following the General Procedure M (stirring for 24 h), the title compound **D.5b** was obtained as a brown resin (111 mg, 302 μmol). Yield 100% crude.

R_f = 0.65 (SiO₂, cyclohexane/EtOAc 7:3).

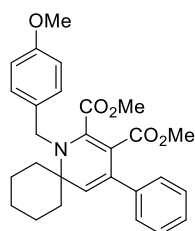
ATR-FTIR (neat) ν = 3051, 2964, 2928, 2858, 1672, 1615, 1551, 1449, 1363, 1297, 1226, 1139, 1069, 970, 759, 698 cm⁻¹.

¹H NMR (500 MHz, CDCl₃) δ = 7.49 (s, 1H, H₆), 7.30 – 7.17 (m, 5H, H_{aro}), 4.95 (s, 1H, H₃), 3.25 – 3.16 (m, 2H, NCH₂), 2.07 – 2.00 (m, 2H, 2 × NC_qCH₂), 1.74 – 1.56 (m, 8H), 1.51 – 1.42 (m, 2H), 1.14 (s, 9H, (C(CH₃)₃)), 0.93 (t, J = 7.3 Hz, 3H, CH₂CH₃) ppm.

¹³C{¹H} NMR (126 MHz, CDCl₃) δ = 166.9 (C=O), 149.6 (C₆), 142.9 (C_q), 136.3 (C_q), 128.0 (CH), 127.4 (CH), 126.4 (CH), 115.4 (CH), 100.4 (C₅), 78.5 (C(CH₃)₃), 60.3 (C₂), 51.5 (NCH₂), 34.3 (CH₂), 28.1 (C(CH₃)₃), 25.7 (CH₂), 25.5 (CH₂), 21.8 (CH₂), 11.3 (CH₂CH₃) ppm.

HRMS (ESI-TOF, + mode) m/z calcd for C₂₄H₃₄NO₂ 368.2584, found 368.2587 [M+H]⁺.

Dimethyl 1-(4-methoxybenzyl)-4-phenyl-1-azaspiro[5.5]undeca-2,4-diene-2,3-dicarboxylate (D.5c)



Chemical Formula: C₂₈H₃₁NO₅
Molecular Weight: 461,5580

Following the General Procedure M (stirring for 24 h), the title compound **D.5c** was isolated as a yellow sticky solid (33 mg, 71 μmol). Yield 45%.

R_f = 0.50 (Al₂O₃ neutral, cyclohexane/EtOAc 8:2).

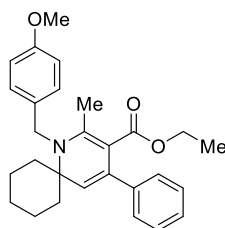
ATR-FTIR (neat) ν = 3056, 3024, 2997, 2926, 2854, 1736, 1688, 1611, 1511, 1433, 1353, 1292, 1245, 1174, 1109, 1032, 956, 805, 729, 699 cm⁻¹.

¹H NMR (500 MHz, CDCl₃) δ = 7.35 – 7.26 (m, 5H, H_{aro}), 7.18 – 7.13 (m, 2H, H_{aro}), 6.84 – 6.79 (m, 2H, 2 × OC_qCH_{aro}), 5.11 (s, 1H, H₃), 4.45 (s, 2H, NCH₂), 3.84 (s, 3H, OCH₃), 3.77 (s, 3H, OCH₃), 3.40 (s, 3H, OCH₃), 2.03 – 1.95 (m, 2H, 2 × NC_qCH₂), 1.68 – 1.63 (m, 1H), 1.61 – 1.44 (m, 6H), 1.15 – 1.06 (m, 1H) ppm.

$^{13}\text{C}\{^1\text{H}\}$ NMR (126 MHz, CDCl_3) δ = 166.9 (C=O), 166.6 (C=O), 158.9 (CH_3OC_q), 150.5 (C_q), 141.7 (C_q), 135.8 (C_q), 131.2 (C_q), 127.8 (CH), 127.6(0) (CH), 127.5(6) (CH), 126.9 (CH), 118.0 (CH), 114.1 (CH), 101.2 (C_5), 61.5 (C_2), 55.4 (CH_3), 53.0 (CH_3), 50.8 (CH_3), 49.9 (NCH_2), 33.4 (CH_2), 25.6 (CH_2), 22.1 (CH_2) ppm.

HRMS (ESI-TOF, + mode) m/z calcd for $\text{C}_{28}\text{H}_{31}\text{NNaO}_5$ 484.2094, found 484.2080 $[\text{M}+\text{Na}]^+$.

Ethyl 1-(4-methoxybenzyl)-2-methyl-4-phenyl-1-azaspiro[5.5]undeca-2,4-diene-3-carboxylate (D.5e)



Chemical Formula: $\text{C}_{28}\text{H}_{33}\text{NO}_3$
Molecular Weight: 431,5760

Ethyl buta-2,3-dienoate (**J.10**, 23.5 mg, 210 μmol , 1.05 eq.) was added to a solution of propargylamine **K.1g** (63.9 mg, 200 μmol , 1.0 eq.) in *t*-AmOH (0.20 mL, 1 M) in a Teflon screw cap tube equipped with a magnetic stirrer. The reactor was flushed with argon for 15 s before sealing and then placed into a pre-heated aluminium block at 90 °C and stirred for 4 h at 500 rpm. Then, the reaction mixture was filtered over celite, washed with EtOAc and the solvent was removed under reduced pressure. The crude was purified over silica gel (cyclohexane/EtOAc/Et₃N

98.5:1.5:1) to give the title compound **D.5e** as yellow solid (73.4 mg, 170 μmol). Yield 85%.

R_f = 0.48 (SiO_2 , cyclohexane/EtOAc 8:2).

ATR-FTIR (neat) ν = 3051, 3033, 2972, 2933, 2851, 1715, 1672, 1613, 1510, 1462, 1445, 1410, 1360, 1235, 1178, 1111, 1059, 1005, 906, 818, 756, 705 cm^{-1} .

^1H NMR (400 MHz, CDCl_3) δ = 7.35 – 7.18 (m, 5H, H_{aro}), 7.09 – 7.03 (m, 2H, H_{aro}), 6.85 – 6.80 (m, 2H, 2 \times $\text{OC}_q\text{CH}_{\text{aro}}$), 5.11 (s, 1H, H_3), 4.66 (s, 2H, NCH_2), 3.80 – 3.72 (m, 5H, OCH_2 & OCH_3), 2.52 (s, 3H, C_6CH_3), 2.09 – 2.01 (m, 2H, 2 \times NC_qCH_2), 1.72 – 1.52 (m, 5H), 1.43 (td, J = 12.1, 4.3 Hz, 2H), 1.17 – 1.07 (m, 1H), 0.62 (t, J = 7.1 Hz, 3H, CH_2CH_3) ppm.

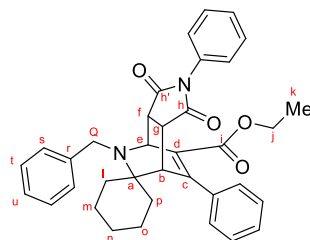
$^{13}\text{C}\{^1\text{H}\}$ NMR (126 MHz, CDCl_3) δ = 168.7 (C=O), 158.7 (CH_3OC_q), 154.8 (C_q), 143.9 (C_q), 137.5 (C_q), 131.8 (C_q), 127.8 (CH), 127.2 (CH), 127.0 (CH), 126.4 (CH), 115.8 (CH), 114.2 (CH), 103.1 (C_5), 60.4 (C_2), 59.0 (OCH_2), 55.4 (OCH_3), 47.4 (NCH_2), 34.0 (CH_2), 25.8 (CH_2), 22.6 (CH_2), 17.9 (C_6CH_3), 13.5 (CH_2CH_3) ppm.

HRMS (ESI-TOF, + mode) m/z calcd for $\text{C}_{28}\text{H}_{34}\text{NO}_3$ 432.2533, found 432.2534 $[\text{M}+\text{H}]^+$.

Synthetic Applications

Uncatalysed cycloaddition reactions were performed as reported by ELLMAN and BERGMAN.^[361]

Ethyl 9'-benzyl-1',3'-dioxo-2',6'-diphenyl-2',3',3a',4',7',7a'-hexahydro-1'H-spiro[cyclohexane-1,8'-[4,7](epiminomethano)isoindole]-5'-carboxylate (Q.7)



Chemical Formula: $\text{C}_{36}\text{H}_{36}\text{N}_2\text{O}_4$
Molecular Weight: 560,6940

Dihydropyridine **D.2a** (58.0 mg, 150 μmol , 1.00 eq.) was dissolved in dry CH_2Cl_2 (0.30 mL, 0.5 M) in a Teflon screw cap tube (10 mL) equipped with a stirrer. Next, *N*-phenylmaleimide (27.4 mg, 158 μmol , 1.05 eq.) was added, the mixture was flushed with argon (15 s) before sealing and placed into a pre-heated oil bath at 50 °C and 500 rpm. After 22 h, temperature was risen to 100 °C leading to full conversion of dihydropyridine **D.2a** after 14 d at 100 °C. The solvent was removed under reduced pressure and the residue was purified by column chromatography on silica gel using cyclohexane/EtOAc 1:0 \rightarrow 9:1. The title compound **Q.7** was isolated as a colourless solid (79 mg, 141 μmol). Yield 94%.

R_f = 0.54 (SiO_2 , cyclohexane/EtOAc 7:3).

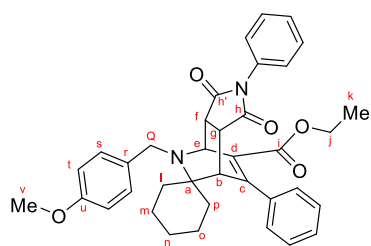
ATR-FTIR (neat) $\nu = 3060, 3028, 2924, 2851, 1777, 1707, 1599, 1495, 1453, 1382, 1263, 1184, 1126, 1070, 1028, 976, 905, 756, 730, 697 \text{ cm}^{-1}$.

^1H NMR (500 MHz, CDCl_3) $\delta = 7.51 - 7.43$ (m, 2H, H_{aro}), $7.40 - 7.26$ (m, 11H, H_{aro}), $7.03 - 6.96$ (m, 2H, H_{aro}), 4.25 (d, $J = 4.0$ Hz, 1H, H_{e}), $4.10 - 3.97$ (m, 4H, $1 \times \text{H}_{\text{Q}}$ & $2 \times \text{H}_{\text{j}}$ & H_{b}), 3.73 (d, $J = 13.4$ Hz, 1H, $1 \times \text{H}_{\text{Q}}$), 3.44 (dd, $J = 8.1, 2.9$ Hz, 1H, H_{g}), 3.38 (dd, $J = 8.1, 4.1$ Hz, 1H, H_{f}), $1.91 - 1.84$ (m, 1H), $1.81 - 1.52$ (m, 6H), $1.50 - 1.40$ (m, 2H), $1.16 - 1.05$ (m, 1H), 1.01 (t, $J = 7.1$ Hz, 3H, H_{k}) ppm.

$^{13}\text{C}\{^1\text{H}\}$ NMR (126 MHz, CDCl_3) $\delta = 179.0$ ($\text{C}_{\text{h/h}'}$), 175.7 ($\text{C}_{\text{h/h}'}$), 166.8 (C_{i}), 149.2 (C_{c}), $140.8, 137.9$ (C_{q}), 132.0 (C_{q}), 131.5 (C_{d}), 129.3 (C_{aroH}), 129.0 (C_{aroH}), 128.8 (C_{aroH}), $128.5(9)$ (C_{aroH}), $128.5(8)$ (C_{aroH}), $128.5(5)$ (C_{aroH}), 127.9 (C_{aroH}), 127.3 (C_{aroH}), 127.1 (C_{aroH}), 61.5 (C_{a}), 60.9 (C_{a}), 54.8 (C_{e}), 51.8 (C_{Q}), 46.8 (C_{f}), 43.6 (C_{b}), 38.0 (C_{g}), 35.7 (CH_2), 32.3 (CH_2), 25.7 (CH_2), 23.4 (CH_2), 22.7 (CH_2), 13.9 (C_{k}) ppm.

HRMS (ESI-TOF, + mode) m/z calcd for $\text{C}_{36}\text{H}_{37}\text{N}_2\text{O}_4$ 561.2748, found 561.2763 $[\text{M}+\text{H}]^+$.

Ethyl 9'-(4-methoxybenzyl)-1',3'-dioxo-2',6'-diphenyl-2',3',3a',4',7',7a'-hexahydro-1'H-spiro[cyclohexane-1,8']-[4,7](epiminomethano)isoindole]-5'-carboxylate (Q.8)



Chemical Formula: $\text{C}_{37}\text{H}_{38}\text{N}_2\text{O}_5$
Molecular Weight: 590,7200

Dihydropyridine **D.1a** (25.1 mg, 60 μmol , 1.00 eq.) was dissolved in dry CH_2Cl_2 (0.30 mL, 0.2 M) in a Teflon screw cap tube (10 mL) equipped with a stirrer. Next, *N*-phenylmaleimide (10.9 mg, 63 μmol , 1.05 eq.) and Cu^{I} -USY (2.2 mg, 0.1 eq. copper) were added, the mixture was flushed with argon (15 s) before sealing and placed into a pre-heated oil bath at 100 $^\circ\text{C}$ and 500 rpm. After 48 h, dihydropyridine **D.1a** was fully converted. The mixture was filtered through a short celite pad and washed

with CH_2Cl_2 (3×5 mL). The solvent was removed under reduced pressure and the residue was purified by column chromatography on silica gel using cyclohexane/EtOAc 95:5. The title compound **Q.8** was isolated as a colourless solid (32 mg, 54 μmol). Yield 90%.

$R_f = 0.38$ (SiO_2 , cyclohexane/EtOAc 7:3).

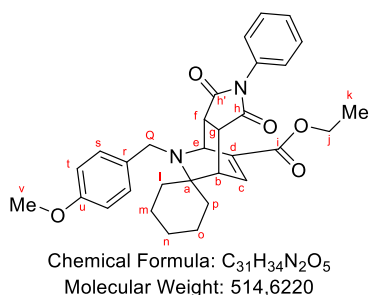
ATR-FTIR (neat) $\nu = 3061, 2924, 2854, 1707, 1597, 1510, 1456, 1380, 1240, 1150, 1030, 909, 822, 727, 691 \text{ cm}^{-1}$.

^1H NMR (500 MHz, CDCl_3) $\delta = 7.40 - 7.29$ (m, 10H, H_{aro}), $7.02 - 6.98$ (m, 2H, H_{aro}), $6.92 - 6.88$ (m, 2H, H_{i}), 4.26 (d, $J = 4.1$ Hz, 1H, H_{e}), $4.11 - 3.98$ (m, 3H, $2 \times \text{H}_{\text{j}}$ & H_{b}), 3.93 (d, $J = 13.2$ Hz, 1H, $1 \times \text{H}_{\text{Q}}$), 3.84 (s, 3H, H_{v}), 3.65 (d, $J = 13.1$ Hz, 1H, $1 \times \text{H}_{\text{Q}}$), 3.43 (dd, $J = 8.1, 3.0$ Hz, 1H, H_{g}), 3.34 (dd, $J = 8.2, 4.1$ Hz, 1H, H_{f}), $1.89 - 1.82$ (m, 1H), $1.79 - 1.53$ (m, 7H), 1.46 (td, $J = 13.3, 4.0$ Hz, 1H), $1.14 - 1.05$ (m, 1H), 1.01 (t, $J = 7.1$ Hz, 3H, H_{k}) ppm.

$^{13}\text{C}\{^1\text{H}\}$ NMR (126 MHz, CDCl_3) $\delta = 179.1$ (C_{h}), 175.7 ($\text{C}_{\text{h}'}$), 166.9 (C_{i}), 158.9 (C_{u}), 149.2 ($\text{C}_{\text{q-aro}}$), 138.0 ($\text{C}_{\text{q-aro}}$), 132.7 ($\text{C}_{\text{q-aro}}$), 132.0 ($\text{C}_{\text{q-aro}}$), 131.6 ($\text{C}_{\text{q-aro}}$), 130.0 (C_{aroH}), 129.3 (C_{aroH}), 129.0 (C_{aroH}), 128.6 (C_{aroH}), 127.9 (C_{aroH}), 127.2 (C_{aroH}), 114.0 (C_{aroH}), 61.5 (C_{a}), 60.9 (C_{j}), 55.5 (CH_3 or CH), 54.5 (CH_3 or CH), 51.1 (C_{Q}), 46.9 (CH), 43.6 (CH), 38.0 (CH), 35.7 (CH_2), 32.2 (CH_2), 25.7 (CH_2), 23.4 (CH_2), 22.7 (CH_2), 13.9 (C_{k}) ppm.

HRMS (ESI-TOF, + mode) m/z calcd for $\text{C}_{37}\text{H}_{39}\text{N}_2\text{O}_5$ 591.2853, found 591.2853 $[\text{M}+\text{H}]^+$.

Ethyl 9'-(4-methoxybenzyl)-1',3'-dioxo-2'-phenyl-2',3',3a',4',7',7a'-hexahydro-1'H-spiro[cyclohexane-1,8'-[4,7](epiminomethano)isoindole]-5'-carboxylate (Q.9)



Dihydropyridine **D.1g** (36.0 mg, 108 μ mol, 1.00 eq.) was dissolved in dry CH₂Cl₂ (0.20 mL, 0.5 M) in a Teflon screw cap tube (10 mL) equipped with a stirrer. Next, *N*-phenylmaleimide (19.8 mg, 114 μ mol, 1.05 eq.) was added, the mixture was flushed with argon (15 s) before sealing and placed into a preheated oil bath at 100 °C and 500 rpm. After 24 h, dihydropyridine **D.1g** was fully converted. The solvent was removed under reduced pressure and the residue was purified by column

chromatography on silica gel using cyclohexane/EtOAc 1:0 \rightarrow 9:1. The title compound **Q.9** was isolated as a pale yellow, waxy solid (36 mg, 70 μ mol). Yield 65%.

R_f = 0.46 (cyclohexane/EtOAc 7:3).

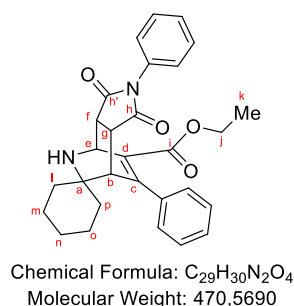
ATR-FTIR (neat) ν = 3065, 2928, 2857, 1777, 1707, 1611, 1510, 1456, 1377, 1249, 1168, 1086, 1031, 970, 908, 823, 750, 729, 708 cm⁻¹.

¹H NMR (500 MHz, CDCl₃) δ = 7.42 – 7.37 (m, 2H, H_{aro}), 7.36 – 7.32 (m, 1H, H_{aro}), 7.31 (dd, J = 6.7, 1.9 Hz, 1H, H_c), 7.29 – 7.26 (m, 2H, H_s), 7.05 – 7.01 (m, 2H, H_{aro}), 6.90 – 6.85 (m, 2H, H_t), 4.33 (dd, J = 3.5, 1.9 Hz, 1H, H_f), 4.26 (dq, J = 10.9, 7.1 Hz, 1H, 1 \times H_j), 4.16 (dq, J = 10.8, 7.1 Hz, 1H, 1 \times H_j), 3.93 – 3.89 (m, 1H, H_b), 3.87 (d, J = 13.4 Hz, 1H, 1 \times H_q), 3.83 (s, 3H, H_v), 3.43 (d, J = 13.3 Hz, 1H, 1 \times H_q), 3.34 – 3.28 (m, 2H, H_e & H_g), 1.83 – 1.37 (m, 9H), 1.27 (t, J = 7.1 Hz, 3H, H_k), 1.22 – 1.12 (m, 1H) ppm.

¹³C NMR (12z6 MHz, CDCl₃) δ = 178.2 (C_{h/h'}), 175.4 (C_{h/h'}), 163.8 (C_i), 158.9 (C_q), 142.2 (C_c), 137.9 (C_d), 132.5 (C_q), 131.9 (C_q), 129.8 (C_{aroH}), 129.3 (C_{aroH}), 128.8 (C_{aroH}), 126.7 (C_{aroH}), 114.0 (C_{aroH}), 61.0 (C_j), 60.4 (C_a), 55.4 (C_v), 51.6 (C_f), 51.1 (C_q), 45.6 (C_e), 38.2 (C_b), 37.6 (C_g), 35.4 (CH₂), 32.6 (CH₂), 25.8 (CH₂), 23.4(4) (CH₂), 23.4(0) (CH₂), 14.4 (C_k) ppm.

HRMS (ESI-TOF, + mode) m/z calcd for C₃₁H₃₅N₂O₅ 515.2540, found 515.2556 [M+H]⁺.

Ethyl 1',3'-dioxo-2',6'-diphenyl-2',3',3a',4',7',7a'-hexahydro-1'H-spiro[cyclohexane-1,8'-[4,7](epiminomethano)isoindole]-5'-carboxylate (Q.11)



Isoquinuclidine **Q.7** (72.0 mg, 128 μ mol, 1.0 eq.) was suspended in EtOH (1.2 mL, 0.1 M) in an oven-dried microwave vial (8 mL) equipped with a stirrer under argon. The suspension was degassed with argon prior to the addition of 10% Pd/C (7.0 mg, 5 mol%, CAUTION! readily causes ignition of flammable solvents in the presence of air). The argon atmosphere was replaced by hydrogen and the reaction mixture was stirred under a hydrogen atmosphere (ambient pressure) for 4 days at 500 rpm. Next, the catalyst was filtered off using a celite pad and the residue was washed with EtOAc. The solvent was removed

under reduced pressure. Purification over silica gel (CH₂Cl₂/MeOH 99:1) afforded the title compound **Q.11** as a yellow resin (45.4 mg, 96 μ mol). Yield 75%.

R_f = 0.75 (SiO₂, CH₂Cl₂/MeOH 9:1) and **R_f** = 0.07 (SiO₂, cyclohexane/EtOAc 7:3).

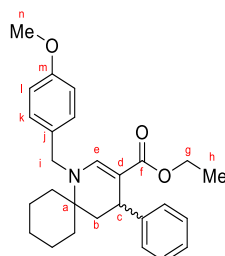
ATR-FTIR (neat) ν = 3321, 3057, 2926, 2853, 1775, 1704, 1497, 1372, 1183, 1095, 756, 691 cm⁻¹.

¹H NMR (500 MHz, CDCl₃) δ = 7.39 – 7.27 (m, 8H, H_{aro}), 7.07 – 7.01 (m, 2H, H_{aro}), 4.65 (d, J = 3.6 Hz, 1H, H_b), 4.08 – 3.97 (m, 2H, H_j), 3.56 – 3.45 (m, 3H, H_e & H_f & H_g), 1.71 – 1.60 (m, 3H), 1.57 – 1.49 (m, 1H), 1.49 – 1.42 (m, 1H), 1.34 – 1.16 (m, 5H), 0.97 (t, J = 7.1 Hz, 3H, H_k) ppm.

$^{13}\text{C}\{^1\text{H}\}$ NMR (126 MHz, CDCl_3) δ = 178.5 ($\text{C}_{\text{h/h}'}$), 175.7 ($\text{C}_{\text{h/h}'}$), 166.5 (C_i), 149.1 (C_q), 138.3 (C_q), 131.9 (C_q), 129.3 (C_{aroH}), 128.9 (C_{aroH}), 128.7 (C_{aroH}), 128.5 (C_{aroH}), 128.1 (C_{aroH}), 127.0 (C_{aroH}), 60.9 (C_j), 56.6 (C_a), 52.6 (CH), 47.6 (CH), 45.6 (CH), 38.4 (CH), 38.0 (CH_2), 37.6 (CH_2), 25.2 (CH_2), 23.0 (CH_2), 22.0 (CH_2), 13.8 (C_k) ppm.

HRMS (ESI-TOF, + mode) m/z calcd for $\text{C}_{29}\text{H}_{31}\text{N}_2\text{O}_4$ 471.2278, found 471.2283 $[\text{M}+\text{H}]^+$.

Ethyl 1-(4-methoxybenzyl)-4-phenyl-1-azaspiro[5.5]undec-2-ene-3-carboxylate ((±)-D.13)



Chemical Formula: $\text{C}_{27}\text{H}_{33}\text{NO}_3$
Molecular Weight: 419,5650

Dihydropyridine **D.1a** (105.6 mg, 253 μmol , 1.0 eq.) was suspended in MeOH/EtOH (2:1, 6 mL, 0.04 M) in an oven-dried two-neck round bottom flask (25 mL) equipped with a stirrer under argon. The suspension was degassed with argon prior to the addition of 10% Pd/C (13.9 mg, 5 mol%), CAUTION! readily causes ignition of flammable solvents in the presence of air). The argon atmosphere was replaced by hydrogen and the reaction mixture was stirred under a hydrogen atmosphere (ambient pressure) for 18 h at 400 rpm. Next, the catalyst was filtered off using a celite pad and the residue was washed with EtOAc. The solvent was removed under reduced pressure to afford the title compound ((±)-**D.13** as a colourless resin (106 mg, 253 μmol). Yield 100% crude.

R_f = 0.46 (SiO_2 , cyclohexane/EtOAc 7:3, colours pink in ninhydrin TLC stain).

R_f = 0.46 (SiO_2 , cyclohexane/EtOAc 7:3, colours pink in ninhydrin TLC stain).

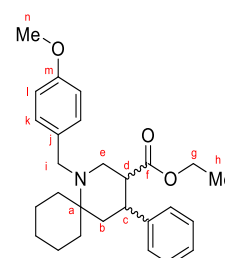
ATR-FTIR (neat) ν = 3060, 3024, 2972, 2928, 2859, 1680, 1598, 1511, 1454, 1361, 1295, 1246, 1209, 1171, 1137, 1094, 1031, 986, 909, 822, 761, 700 cm^{-1} .

^1H NMR (500 MHz, CDCl_3) δ = 7.63 (d, J = 1.0 Hz, 1H, H_e), 7.27 (m, 4H, $\text{H}_{\text{aro-Ph}}$), 7.23 – 7.18 (m, 2H, H_k), 7.18 – 7.13 (m, 1H, $\text{H}_{\text{aro-Ph}}$), 6.94 – 6.85 (m, 2H, 2 \times H_i), 4.49 (d, J = 16.2 Hz, 1H, 1 \times H_i), 4.28 (d, J = 16.1 Hz, 1H, 1 \times H_i), 3.98 (dq, J = 10.8, 7.1 Hz, 1H, 1 \times H_g), 3.90 – 3.79 (m, 4H, 1 \times H_g & H_n), 3.74 (dd, J = 10.2, 6.1 Hz, 1H, H_c), 2.42 (dd, J = 13.9, 6.1 Hz, 1H, 1 \times H_b), 1.90 – 1.81 (m, 1H), 1.73 (dd, J = 13.8, 10.4 Hz, 1H, 1 \times H_b), 1.65 – 1.55 (m, 3H), 1.52 – 1.34 (m, 3H), 1.33 – 1.19 (m, 2H), 1.13 – 1.01 (m, 1H), 0.91 (t, J = 7.1 Hz, 3H, H_h) ppm.

$^{13}\text{C}\{^1\text{H}\}$ NMR (126 MHz, CDCl_3) δ = 168.5 (C_f), 158.9 (C_m), 149.1 (C_e), 147.0 (C_q), 132.0 (C_q), 128.2 (C_{aroH}), 128.0 (C_k), 127.2 (C_{aroH}), 125.7 (C_{aroH}), 114.1 (C_l), 97.8 (C_d), 58.8 (C_g), 58.5 (C_a), 55.4 (C_n), 52.5 (C_i), 40.6 (C_b), 36.5 (C_c), 34.8 (CH_2), 31.8 (CH_2), 25.6 (CH_2), 22.3 (CH_2), 22.0 (CH_2), 14.3 (C_h) ppm.

HRMS (ESI-TOF, + mode) m/z calcd for $\text{C}_{27}\text{H}_{34}\text{NO}_3$ 420.2533, found 420.2546 $[\text{M}+\text{H}]^+$.

Ethyl 1-(4-methoxybenzyl)-4-phenyl-1-azaspiro[5.5]undecane-3-carboxylate (D.14)



Chemical Formula: $\text{C}_{27}\text{H}_{35}\text{NO}_3$
Molecular Weight: 421,5810

In an oven-dried two-neck round bottom flask (25 mL) equipped with a stirrer, tetrahydropyridine **D.13** (100.0 mg, 238 μmol , 1.0 eq.) was dissolved in glacial acetic acid (1.19 mL) and dry MeOH (1.0 mL) under argon. The resulting solution was cooled to 0 $^\circ\text{C}$. Next, a solution of NaBH_3CN (29.9 mg, 476 μmol , 2.0 eq.) in dry MeOH (2.0 mL, 0.24 M) was added dropwise at 0 $^\circ\text{C}$ under vigorous stirring over 5 min. The reaction mixture was left to warm to rt progressively without removing the ice bath. After 3.5 h the mixture was concentrated under high vacuum for 1 h and the concentrate was poured onto ice. Progressive basification

with aq. NH_3 (30%) to pH 9 resulted in precipitation of a colourless solid. CH_2Cl_2 (15 mL) was added, and the mixture was given into a separatory funnel. The aq. phase was extracted with CH_2Cl_2 (4 \times 10 mL) and the combined org. layers were dried over Na_2SO_4 and concentrated under reduced pressure to give a colourless oil. The latter was washed over a short pipette silica

pad and with CH₂Cl₂ to give the title compound **D.14** as a colourless resin (72 mg, 171 μmol) as a mixture of two diastereoisomers (*dr* = 8:2). Yield 72% (combined yield).

ATR-FTIR (neat) ν = 3062, 3029, 2926, 2854, 1726, 1611, 1585, 1510, 1454, 1367, 1300, 1240, 1168, 1032, 967, 821, 760, 698 cm⁻¹.

HRMS (ESI-TOF, + mode) *m/z* calcd for C₂₇H₃₆NO₃ 422.2690, found 422.2720 [M+H]⁺.

Purification over silica gel (cyclohexane → cyclohexane/EtOAc 98:2) afforded a pure fraction of the major diastereoisomer.

Major diastereoisomer

R_f = 0.62 (SiO₂, cyclohexane/EtOAc 7:3).

¹H NMR (500 MHz, CDCl₃) δ = 7.33 – 7.17 (m, 7H, H_k & H_{aro-Ph}), 6.91 – 6.82 (m, 2H, H_l), 4.01 (d, *J* = 14.0 Hz, 1H, 1 × H_i), 3.89 – 3.74 (m, 5H, H_n & H_g), 3.34 (d, *J* = 14.0 Hz, 1H, 1 × H_i), 3.09 (ddd, *J* = 13.5, 10.9, 3.6 Hz, 1H, H_c), 2.91 – 2.75 (m, 3H, H_d & H_e), 2.06 (dd, *J* = 13.6, 3.7 Hz, 1H, 1 × H_b), 1.99 – 1.92 (m, 1H), 1.87 (ddd, *J* = 13.5, 10.4, 3.7 Hz, 1H), 1.79 – 1.71 (m, 1H), 1.71 – 1.24 (m, 8H, 1 × H_b), 0.89 (t, *J* = 7.1 Hz, 3H, H_h) ppm.

¹³C{¹H} NMR (126 MHz, CDCl₃) δ = 174.1 (C_f), 158.5 (C_m), 144.3 (C_{q-Ph}), 133.3 (C_j), 129.4 (C_k), 128.5 (C_{aroH}), 127.5 (C_{aroH}), 126.6 (C_{aroH}), 113.7 (C_l), 60.0 (C_g), 56.0 (C_a), 55.4 (C_n), 50.7 (C_e), 47.8 (C_i), 47.3 (C_d), 40.9 (C_c), 39.6 (C_b), 37.6 (CH₂), 27.0 (CH₂), 26.6 (CH₂), 22.3 (CH₂), 22.2 (CH₂), 14.0 (C_h) ppm.

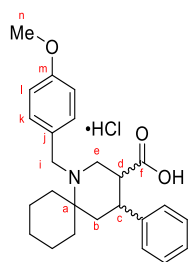
Minor diastereoisomer

R_f = 0.58 (SiO₂, cyclohexane/EtOAc 7:3).

¹H NMR (300 MHz, CDCl₃) some characteristic signals δ = 6.86 – 6.76 (m, 2H, H_l), 4.09 (d, *J* = 14.3 Hz, 1H, 1 × H_i), 2.96 (t, *J* = 4.0 Hz, 2H), 2.42 (t, *J* = 13.3 Hz, 1H), 2.27 (ddd, *J* = 13.2, 3.6, 1.0 Hz, 1H), 0.86 (t, *J* = 7.2 Hz, 3H, H_h) ppm.

¹³C{¹H} NMR (126 MHz, CDCl₃) δ = 172.3 (C_f), 158.4 (C_m), 144.0 (C_{q-Ph}), 133.9 (C_j), 129.2 (C_k), 128.1 (C_{aroH}), 128.0 (C_{aroH}), 126.2 (C_{aroH}), 113.5 (C_l), 59.7 (C_g), 56.2 (C_a), 55.4 (C_n), 51.4 (CH₂), 49.0 (CH₂), 46.4 (CH), 37.9 (CH), 37.4 (CH₂), 31.9 (CH₂), 24.2 (CH₂), 22.9 (CH₂), 22.6 (CH₂), 13.9 (C_h) ppm.

1-(4-Methoxybenzyl)-4-phenyl-1-azaspiro[5.5]undecane-3-carboxylic acid hydrochloride (D.15)



Chemical Formula: C₂₅H₃₂ClNO₃
Molecular Weight: 429,9850

Aq. 2 M KOH (165 μL, 330 μmol, 6.0 eq.) was added to a solution of ester **D.14** (23.0 mg, 55 μmol, 1.0 eq.) in MeOH/2-MeTHF (1:1, 2 mL) in a round bottom flask (25 mL) equipped with a magnetic stirrer. The reaction mixture was stirred at rt for 6.5 h, followed by another addition of 2 M KOH (330 μL, 660 μmol, 12.0 eq.). After stirring at rt for 17 h, the reaction was equipped with a reflux condenser and was set to 65 °C for 15 h. After completion as determined by TLC (cyclohexane/EtOAc 7:3), the mixture was acidified to pH 3 with 5% aq. HCl. The aq. phase was completely evaporated under vacuum to give a colourless solid residue. The latter was triturated with

CH₂Cl₂/MeOH (9:1, 10 × 15 mL) and the combined org. phases were dried over Na₂SO₄. Evaporation of the solvent under reduced pressure afforded carboxylic acid **D.15** as a colourless solid (23.1 mg, 54 μmol). Yield 98%.

R_f = 0.30 (SiO₂, CH₂Cl₂/MeOH 9:1).

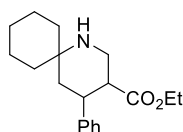
ATR-FTIR (neat) ν = 3662, 3313, 2932, 2866, 2833, 2605, 2219, 2053, 1732, 1611, 1587, 1514, 1461, 1246, 1181, 1162, 1030, 903, 826, 761, 700 cm⁻¹.

¹H NMR (300 MHz, CD₂Cl₂/CD₃OD 9:1) δ = 7.65 – 7.47 (m, 2H, H_{aro-Ph}), 7.35 – 7.18 (m, 5H, H_k & H_{aro-Ph}), 7.04 – 6.86 (m, 2H, H_l), 4.68 (d, J = 12.8 Hz, 1H, 1 \times H_l), 3.97 – 3.77 (m, 4H, 1 \times H_l & H_n), 3.75 – 3.55 (m, 4H), 3.44 (t, J = 11.7 Hz, 1H, NH), 3.24 (dd, J = 12.9, 4.3 Hz, 1H, H_e), 3.19 – 3.00 (m, 2H, H_c & 1 \times H_e), 2.54 – 2.32 (m, 3H, H_b & H_d), 2.31 – 2.20 (m, 1H), 2.12 (td, J = 12.4, 4.2 Hz, 1H), 1.95 – 1.67 (m, 4H), 1.62 – 1.40 (m, 2H), 1.38 – 1.14 (m, 1H) ppm.

¹³C{¹H} NMR (126 MHz, CD₂Cl₂/CD₃OD 9:1) δ = 172.8 (C_f), 161.3 (C_m), 141.7 (C_q), 133.6 (C_i), 129.1 (C_{aroH}), 127.9 (C_{aroH}), 127.8 (C_{aroH}), 120.7 (C_q), 114.9 (C_{aroH}), 67.7 (C_a), 55.7 (C_n), 52.4 (C_i), 46.8 (C_e), 46.1 (C_d), 39.2 (C_c), 35.8 (C_b), 34.0 (CH₂), 25.3 (CH₂), 22.2 (CH₂), 22.0 (CH₂) ppm.

HRMS (ESI-TOF, + mode) m/z calcd for C₂₅H₃₂NO₃ 394.2377, found 394.2394 [M+H]⁺ (corresponds to mass of amino acid without HCl).

Ethyl 4-phenyl-1-azaspiro[5.5]undecane-3-carboxylate ((+)-D.16) (FSc721)



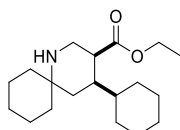
Chemical Formula: C₁₉H₂₇NO₂
Molecular Weight: 301,4300

With H₂ degassed EtOH (5 mL) was added to a mixture of dihydropyridine **D.1a** (106 mg, 254 μ mol, 1.0 eq.) and Pd/C (54 mg, 20 mol%), CAUTION! readily causes ignition of flammable solvents in the presence of air) in a pressure-resistant rolled rim glass vial under air. The latter was rapidly given into a cell disruption vessel and sealed. The air atmosphere was first replaced by argon, then three evacuation-filling cycles with H₂ were performed. The reaction mixture was stirred at room temperature for 22 h at 300 rpm and 20 bar. As incomplete conversion was observed *via* TLC, the reaction mixture was heated to 60 °C and stirred for 28 h at 300 rpm and 30 bar. Next, the catalyst was filtered off using a celite pad and the residue was washed with EtOAc. The solvent was removed under reduced pressure to afford the title compound (\pm)-**D.16** as a pale yellow viscous crude oil (74 mg).

R_f = 0.43 and 0.33 (SiO₂, CH₂Cl₂/MeOH 9:1).

¹H NMR (400 MHz, CDCl₃) δ = 7.31 – 7.24 (m, 2H), 7.23 – 7.15 (m, 3H), 3.95 – 3.80 (m, 2H), 3.26 – 3.03 (m, 3H), 2.74 – 2.61 (m, 1H), 1.92 – 1.18 (m, 16H), 0.97 – 0.89 (m, 3H), 0.87 – 0.76 (m, 1H) ppm.

Ethyl 4-cyclohexyl-1-azaspiro[5.5]undecane-3-carboxylate (D.17)



Chemical Formula: C₁₉H₃₃NO₂
Molecular Weight: 307,4780

PtO₂ (20.0 mg, 88 μ mol, 1.1 eq.) was added to an argon degassed solution of dihydropyridine **D.1a** (33.6 mg, 80 μ mol, 1.0 eq.) in AcOH/TFA (1:1, 0.8 mL). The argon atmosphere was replaced by hydrogen and the reaction mixture was stirred under a hydrogen atmosphere (ambient pressure) for 18 h at 500 rpm. Next, the catalyst was filtered off using a celite pad and the residue was washed with CH₂Cl₂. After evaporation of volatiles, the residue was dissolved in CH₂Cl₂ (10 mL) and washed with sat. aq. NaHCO₃ (15 mL), H₂O (15 mL) and brine (15 mL). After drying over Na₂SO₄, the solvent was removed under reduced pressure to afford a pale yellow crude oil (26.4 mg). Purification over silica gel afforded the title compound **D.17** as a mixture of two diastereomers (dr = 8:2) and as a colourless oil (20.2 mg, max. 66 μ mol) but the sample is still contaminated with small amounts of an unidentified by-product. Yield < 83%. Analytical data below are given for the mixture of diastereomers and by-product.

R_f = 0.05 (SiO₂, CH₂Cl₂/MeOH 9:1).

ATR-FTIR (neat) ν = 2924, 2852, 1728, 1560, 1448, 1399, 1248, 1173, 1029 cm⁻¹.

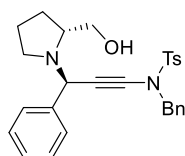
¹H NMR (500 MHz, CDCl₃) δ = 4.16 (dq, J = 10.5, 7.1 Hz, 1H, OCH₂), 4.07 (dq, J = 10.8, 7.1 Hz, 1H, OCH₂), 3.13 – 2.90 (m, 2H), 2.70 – 2.45 (m, 1H), 1.98 – 0.99 (m, 26H), 0.96 – 0.72 (m, 2H) ppm.

¹³C{¹H} NMR (126 MHz, CDCl₃) δ = 174.5 (C=O), 174.3 (C=O), 60.4 (OCH₂), 60.2 (OCH₂), 53.1 (NC_q), 52.4 (NC_q), 46.4 (CH), 43.1 (CH₂), 42.7 (CH₂), 41.2 (CH₂), 40.5(5) (CH), 40.5(0) (CH), 40.4 (CH₂), 40.3 (CH), 38.9 (CH), 38.4 (CH), 34.4 (CH₂), 33.9 (CH₂), 32.1 (CH₂), 31.1 (CH₂), 30.9 (CH₂), 30.6 (CH₂), 30.5 (CH₂), 30.4 (CH₂), 29.8 (CH₂), 29.5 (CH₂), 27.1 (CH₂), 27.0 (CH₂), 26.9 (CH₂), 26.8 (CH₂), 26.7 (CH₂), 26.3 (CH₂), 26.1 (CH₂), 22.8 (CH₂), 21.8 (CH₂), 21.7 (CH₂), 21.6(5) (CH₂), 21.6(0) (CH₂), 14.4(5) (CH₃), 14.4(2) (CH₃), 14.3 (CH₃) ppm.

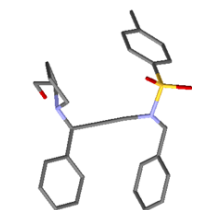
HRMS (ESI-TOF, + mode) m/z calcd for C₁₉H₃₄NO₂ 308.2584, found 308.2590 [M+H]⁺.

Crystallographic Data

Crystal data for compound G.23



G.23



ORTEP view of G.23

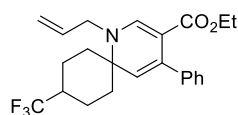
Table S2. Sample and crystal data for Compound G.23.

Identification code	PPFS210322	
Chemical formula	C ₂₈ H ₃₀ N ₂ O ₃ S	
Formula weight	474.60 g/mol	
Temperature	120(2) K	
Wavelength	1.54178 Å	
Crystal size	0.100 x 0.200 x 0.200 mm	
Crystal system	orthorhombic	
Space group	P 21 21 21	
Unit cell dimensions	a = 10.6469(3) Å	α = 90°
	b = 15.8266(4) Å	β = 90°
	c = 28.9384(7) Å	γ = 90°
Volume	4876.2(2) Å ³	
Z	8	
Density (calculated)	1.293 g/cm ³	
Absorption coefficient	1.438 mm ⁻¹	
F(000)	2016	

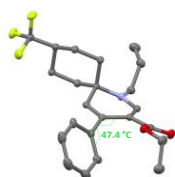
Table S3. Data collection and structure refinement for Compound G.23.

Theta range for data collection	3.05 to 66.56°
Index ranges	-12<=h<=12, -18<=k<=18, -34<=l<=34
Reflections collected	52110
Independent reflections	8605 [R(int) = 0.0496]
Max. and min. transmission	0.7528 and 0.6327
Structure solution technique	direct methods
Structure solution program	SHELXT 2014/5 (Sheldrick, 2014)
Refinement method	Full-matrix least-squares on F ²
Refinement program	SHELXL-2018/3 (Sheldrick, 2018)
Function minimized	$\Sigma w(F_o^2 - F_c^2)^2$
Data/restraints/parameters	8605 / 0 / 617
Goodness-of-fit on F²	1.043
Δ/σ_{\max}	0.001
Final R indices	8115 data; I>2 σ (I) R1 = 0.0327, wR2 = 0.0886 all data R1 = 0.0356, wR2 = 0.0907
Weighting scheme	$w=1/[\sigma^2(F_o^2)+(0.0504P)^2+1.3595P]$ where $P=(F_o^2+2F_c^2)/3$
Absolute structure parameter	0.009(6)
Largest diff. peak and hole	0.298 and -0.306 eÅ ⁻³
R.M.S. deviation from mean	0.039 eÅ ⁻³

Crystal data for compound D.3h



D.3h



ORTEP view of D.3h

Table S4. Sample and crystal data for Compound D.3h.

Identification code	eppfsa	
Chemical formula	C ₂₃ H ₂₆ F ₃ NO ₂	
Formula weight	405.45 g/mol	
Temperature	120(2) K	
Wavelength	0.71073 Å	
Crystal size	0.120 x 0.120 x 0.100 mm	
Crystal system	monoclinic	
Space group	P 21/c	
Unit cell dimensions	a = 11.3608(4) Å	α = 90°
	b = 21.0436(7) Å	β = 99.2140(10)°
	c = 8.5705(3) Å	γ = 90°
Volume	2022.53(12) Å ³	
Z	4	
Density (calculated)	1.332 g/cm ³	
Absorption coefficient	0.103 mm ⁻¹	
F(000)	856	

Table S5. Data collection and structure refinement for Compound D.3h.

Theta range for data collection	1.935 to 27.933°	
Index ranges	-14<=h<=14, -27<=k<=27, -11<=l<=11	
Reflections collected	37298	
Independent reflections	4828 [R(int) = 0.0471]	
Max. and min. transmission	0.7456 and 0.7069	
Structure solution technique	direct methods	
Structure solution program	SHELXT 2014/5 (Sheldrick, 2014)	
Refinement method	Full-matrix least-squares on F ²	
Refinement program	SHELXL-2018/3 (Sheldrick, 2018)	
Function minimized	Σ w(F _o ² - F _c ²) ²	
Data/restraints/parameters	4828/0/263	
Goodness-of-fit on F ²	1.029	
Δ/σ _{max}	0.001	
Final R indices	I>2σ(I)	R1 = 0.0401, wR2 = 0.0915
	all data	R1 = 0.0572, wR2 = 0.1024
Absolute structure parameter	0.009(6)	
Largest diff. peak and hole	0.312 and -0.273 eÅ ⁻³	

References

- [1] P. T. Anastas, J. C. Warner, *Green Chemistry: Theory and Practice*, Oxford University Press, Oxford, **1998**.
- [2] P. T. Anastas, M. M. Kirchhoff, T. C. Williamson, *Appl. Catal., A* **2001**, *221*, 3–13.
- [3] S. Hübner, J. G. de Vries, V. Farina, *Adv. Synth. Catal.* **2016**, *358*, 3–25.
- [4] F. Rascón, R. Wischert, C. Copéret, *Chem. Sci.* **2011**, *2*, 1449–1456.
- [5] A. Bahuguna, A. Kumar, V. Krishnan, *Asian J. Org. Chem.* **2019**, *8*, 1263–1305.
- [6] A. Corma, H. Garcia, *Adv. Synth. Catal.* **2006**, *348*, 1391–1412.
- [7] J. Lu, P. H. Toy, *Chem. Rev.* **2009**, *109*, 815–838.
- [8] S. Chassaing, V. Beneteau, B. Louis, P. Pale, *Curr. Org. Chem.* **2017**, *21*, 779–793.
- [9] V. Pascanu, G. González Miera, A. K. Inge, B. Martín-Matute, *J. Am. Chem. Soc.* **2019**, *141*, 7223–7234.
- [10] J. Dong, X. Han, Y. Liu, H. Li, Y. Cui, *Angew. Chem., Int. Ed.* **2020**, *59*, 13722–13733.
- [11] J. N. Armor, in *Catalysis by Unique Metal Ion Structures in Solid Matrices: From Science to Application* (Eds.: G. Centi, B. Wichterlová, A.T. Bell), Springer Netherlands, Dordrecht, **2001**, pp. 21–29.
- [12] K. Lauder, A. Toscani, N. Scalacci, D. Castagnolo, *Chem. Rev.* **2017**, *117*, 14091–14200.
- [13] M. Duan, G. Hou, Y. Zhao, C. Zhu, C. Song, *J. Org. Chem.* **2022**, *87*, 11222–11225.
- [14] Bhawna, A. Kumar, M. Bhatia, A. Kapoor, P. Kumar, S. Kumar, *Eur. J. Med. Chem.* **2022**, *242*, 114655.
- [15] A. Albrecht, I. Vovk, J. Mavri, J. Marco-Contelles, R. R. Ramsay, *Front. Chem.* **2018**, *6*, 169.
- [16] Y. Xu, H. Wang, X. Li, S. Dong, W. Liu, Q. Gong, T. Wang, Y. Tang, J. Zhu, J. Li, H. Zhang, F. Mao, *Eur. J. Med. Chem.* **2018**, *143*, 33–47.
- [17] C. Yao, X. Jiang, R. Zhao, Z. Zhong, J. Ge, J. Zhu, X.-Y. Ye, Y. Xie, Z. Liu, T. Xie, R. Bai, *Bioorg. Chem.* **2022**, *122*, 105724.
- [18] I. E. Kopka, Z. A. Fataftah, M. W. Rathke, *J. Org. Chem.* **1980**, *45*, 4616–4622.
- [19] F. Mao, J. Li, H. Wei, L. Huang, X. Li, *J. Enzyme Inhib. Med. Chem.* **2015**, *30*, 995–1001.
- [20] V. Vaněk, J. Pícha, B. Fabre, M. Buděšínský, M. Lepšík, J. Jiráček, *Eur. J. Org. Chem.* **2015**, *2015*, 3689–3701.
- [21] P. B. Huleatt, M. L. Khoo, Y. Y. Chua, T. W. Tan, R. S. Liew, B. Balogh, R. Deme, F. Göllöncsér, K. Magyar, D. P. Sheela, H. K. Ho, B. Sperlágh, P. Mátyus, C. L. L. Chai, *J. Med. Chem.* **2015**, *58*, 1400–1419.
- [22] M. L. Schmitt, A.-T. Hauser, L. Carlino, M. Pippel, J. Schulz-Fincke, E. Metzger, D. Willmann, T. Yiu, M. Barton, R. Schüle, W. Sippl, M. Jung, *J. Med. Chem.* **2013**, *56*, 7334–7342.
- [23] A. F. Abdel-Magid, K. G. Carson, B. D. Harris, C. A. Maryanoff, R. D. Shah, *J. Org. Chem.* **1996**, *61*, 3849–3862.
- [24] K. Sekine, R. Kobayashi, T. Yamada, *Chem. Lett.* **2015**, *44*, 1407–1409.
- [25] G. A. Aleku, S. P. France, H. Man, J. Mangas-Sanchez, S. L. Montgomery, M. Sharma, F. Leipold, S. Hussain, G. Grogan, N. J. Turner, *Nat. Chem.* **2017**, *9*, 961–969.
- [26] Z. Zhan, Z. Xu, S. Yu, J. Feng, F. Liu, P. Yao, Q. Wu, D. Zhu, *Adv. Synth. Catal.* **2022**, *364*, 2380–2386.
- [27] L. Zani, C. Bolm, *Chem. Commun.* **2006**, 4263–4275.
- [28] C.-J. Li, *Acc. Chem. Res.* **2010**, *43*, 581–590.
- [29] I. A. Bidusenko, E. Yu. Schmidt, I. A. Ushakov, B. A. Trofimov, *Eur. J. Org. Chem.* **2018**, *2018*, 4845–4849.
- [30] C. Cimarelli, F. Navazio, F. V. Rossi, F. D. Bello, E. Marcantoni, *Synthesis* **2019**, *51*, 2387–2396.
- [31] J.-X. Ji, T. T.-L. Au-Yeung, J. Wu, C. W. Yip, A. S. C. Chan, *Adv. Synth. Catal.* **2004**, *346*, 42–44.

- [32] S. A. Shehzadi, A. Saeed, F. Lemièrre, B. U. W. Maes, K. A. Tehrani, *Eur. J. Org. Chem.* **2018**, 2018, 78–88.
- [33] S. A. Shehzadi, K. Kushwaha, H. Sterckx, K. Abbaspour Tehrani, *Adv. Synth. Catal.* **2018**, 360, 4393–4401.
- [34] L. Rubio-Pérez, M. Iglesias, J. Munárriz, V. Polo, P. J. S. Miguel, J. J. Pérez-Torrente, L. A. Oro, *Chem. Commun.* **2015**, 51, 9860–9863.
- [35] C. Pfeffer, P. Probst, N. Wannemacher, W. Frey, R. Peters, *Angew. Chem., Int. Ed.* **2022**, 61, e202206835.
- [36] J. P. Guermont, *Bull. Soc. Chim. Fr.* **1953**, 386–390.
- [37] B. Karlen, B. Lindeke, S. Lindgren, K. G. Svensson, R. Dahlbom, D. J. Jenden, J. E. Giering, *J. Med. Chem.* **1970**, 13, 651–657.
- [38] J. J. McNally, M. A. Youngman, S. L. Dax, *Tetrahedron Lett.* **1998**, 39, 967–970.
- [39] A. B. Dyatkin, R. A. Rivero, *Tetrahedron Lett.* **1998**, 39, 3647–3650.
- [40] S. Ghosh, K. Biswas, S. Bhattacharya, P. Ghosh, B. Basu, *Beilstein J. Org. Chem.* **2017**, 13, 552–557.
- [41] B. Udaykumar, M. Periasamy, *ACS Omega* **2019**, 4, 21587–21595.
- [42] O. P. Pereshivko, V. A. Peshkov, E. V. Van der Eycken, *Org. Lett.* **2010**, 12, 2638–2641.
- [43] Z. Li, C.-J. Li, *J. Am. Chem. Soc.* **2004**, 126, 11810–11811.
- [44] F. Alonso, A. Arroyo, I. Martín-García, Y. Moglie, *Adv. Synth. Catal.* **2015**, 357, 3549–3561.
- [45] T. Dang-Bao, C. Pradel, I. Favier, M. Gómez, *Adv. Synth. Catal.* **2017**, 359, 2832–2846.
- [46] H. Yang, Z. Sun, H. Chen, F. Mao, X. Li, X. Xu, *Tetrahedron Lett.* **2022**, 109, 154136.
- [47] C. Gardner, V. Kerrigan, J. D. Rose, B. C. L. Weedon, *J. Chem. Soc.* **1949**, 780–782.
- [48] C. W. Kruse, R. F. Kleinschmidt, *J. Am. Chem. Soc.* **1961**, 83, 216–220.
- [49] F. Zhao, S. Kim, D. Castagnolo, in *Methodologies in Amine Synthesis* (Eds.: A. Ricci, L. Bernardi), Wiley, **2021**, pp. 103–154.
- [50] V. A. Peshkov, O. P. Pereshivko, A. A. Nechaev, A. A. Peshkov, E. V. Van der Eycken, *Chem. Soc. Rev.* **2018**, 47, 3861–3898.
- [51] A. R. Pandey, D. K. Tiwari, A. Prakhar, D. P. Mishra, S. K. Sharma, *Monatsh. Chem.* **2022**, 153, 383–407.
- [52] X. Sheng, K. Chen, C. Shi, D. Huang, *Synthesis* **2020**, 52, 1–20.
- [53] P. Crabbé, H. Fillion, D. André, J.-L. Luche, *J. Chem. Soc., Chem. Commun.* **1979**, 859–860.
- [54] X. Huang, S. Ma, *Acc. Chem. Res.* **2019**, 52, 1301–1312.
- [55] X. Zhang, *Asian J. Org. Chem.* **2014**, 3, 309–313.
- [56] Z. L. Palchak, P. T. Nguyen, C. H. Larsen, *Beilstein J. Org. Chem.* **2015**, 11, 1425–1433.
- [57] A. W. Patterson, W. J. L. Wood, M. Hornsby, S. Lesley, G. Spraggon, J. A. Ellman, *J. Med. Chem.* **2006**, 49, 6298–6307.
- [58] K. Brak, P. S. Doyle, J. H. McKerrow, J. A. Ellman, *J. Am. Chem. Soc.* **2008**, 130, 6404–6410.
- [59] S. Qiu, W. Chen, D. Li, Y. Chen, Y. Niu, Y. Wu, Y. Lei, L. Wu, W. He, *Synthesis* **2022**, 9, 2175–2184.
- [60] R. Kumar, R. K. Arigela, S. Samala, B. Kundu, *Chem. - Eur. J.* **2015**, 21, 18828–18833.
- [61] Z. Jiang, P. Lu, Y. Wang, *Org. Lett.* **2012**, 14, 6266–6269.
- [62] P. García-Domínguez, L. Fehr, G. Rusconi, C. Nevado, *Chem. Sci.* **2016**, 7, 3914–3918.
- [63] S.-F. Cai, L.-Q. Qiu, W.-B. Huang, H.-R. Li, L.-N. He, *Chem. Commun.* **2022**, 58, 6332–6335.
- [64] P. D. G. Greenwood, J. Waser, *Eur. J. Org. Chem.* **2019**, 2019, 5183–5186.
- [65] S. Ghosh, R. Ali Molla, U. Kayal, A. Bhaumik, S. Manirul Islam, *Dalton Trans.* **2019**, 48, 4657–4666.
- [66] J. Wu, R. He, S. Cheng, L. Han, H. Hong, N. Zhu, *ACS Sustainable Chem. Eng.* **2022**, 3, 1214–1219.
- [67] G. Cheng, Y. Weng, X. Yang, X. Cui, *Org. Lett.* **2015**, 17, 3790–3793.

- [68] F. P. Byrne, S. Jin, G. Paggiola, T. H. M. Petchey, J. H. Clark, T. J. Farmer, A. J. Hunt, C. Robert McElroy, J. Sherwood, *Sustain. Chem. Process.* **2016**, *4*, 7.
- [69] S. Undeela, S. Thadkapally, J. B. Nanubolu, K. K. Singarapu, R. S. Menon, *Chem. Commun.* **2015**, *51*, 13748–13751.
- [70] B. K. Das, S. Pradhan, T. Punniyamurthy, *Org. Lett.* **2018**, *20*, 4444–4448.
- [71] C. Sheng, Z. Ling, T. Ahmad, F. Xie, W. Zhang, *Chem. - Eur. J.* **2022**, *28*, e202200128.
- [72] Cronsted, Axel Frederik, *Akad. Handl. Stockholm* **1756**, *18*, 120–130.
- [73] L. B. McCusker, F. Liebau, G. Engelhardt, *Microporous Mesoporous Mater.* **2003**, *58*, 3–13.
- [74] W. Loewenstein, *Am. Mineral.* **1954**, *39*, 92–96.
- [75] A. D. McNaught, A. Wilkinson, International Union of Pure and Applied Chemistry, Eds. , *Compendium of Chemical Terminology: IUPAC Recommendations*, Blackwell Science, Oxford, England ; Malden, MA, USA, **1997**.
- [76] S. Lopez-Orozco, A. Inayat, A. Schwab, T. Selvam, W. Schwieger, *Adv. Mater.* **2011**, *23*, 2602–2615.
- [77] W. Schwieger, A. Gonche Machoke, T. Weissenberger, A. Inayat, T. Selvam, M. Klumpp, A. Inayat, *Chem. Soc. Rev.* **2016**, *45*, 3353–3376.
- [78] D. Verboekend, J. Pérez-Ramírez, *Catal. Sci. Technol.* **2011**, *1*, 879–890.
- [79] K. P. de Jong, J. Zečević, H. Friedrich, P. E. de Jongh, M. Bulut, S. van Donk, R. Kenmogne, A. Finiels, V. Hulea, F. Fajula, *Angew. Chem., Int. Ed.* **2010**, *49*, 10074–10078.
- [80] M. Milina, S. Mitchell, P. Crivelli, D. Cooke, J. Pérez-Ramírez, *Nat. Commun.* **2014**, *5*, 1–10.
- [81] Y. Li, J. N. Armor, *Appl. Catal., A* **1999**, *188*, 211–217.
- [82] I. Yamane, T. Nakazawa, *Pure Appl. Chem.* **1986**, *58*, 1397–1404.
- [83] S. Wang, Y. Peng, *Chem. Eng. J.* **2010**, *156*, 11–24.
- [84] B. Smit, T. L. M. Maesen, *Nature* **2008**, *451*, 671–678.
- [85] A. Corma, *J. Catal.* **2003**, *216*, 298–312.
- [86] N. Y. Chen, W. W. Kaeding, F. G. Dwyer, *J. Am. Chem. Soc.* **1979**, *101*, 6783–6784.
- [87] V. Komvokis, L. X. L. Tan, M. Clough, S. S. Pan, B. Yilmaz, in *Zeolites in Sustainable Chemistry: Synthesis, Characterization and Catalytic Applications* (Eds.: F.-S. Xiao, X. Meng), Springer, Berlin, Heidelberg, **2016**, pp. 271–297.
- [88] S. Soltanian, C. L. Lee, S. S. Lam, *Biofuel Res. J.* **2020**, *7*, 1217–1234.
- [89] R. Pophale, P. A. Cheeseman, M. W. Deem, *Phys. Chem. Chem. Phys.* **2011**, *13*, 12407–12412.
- [90] Sainte-Claire Deville, H. C. R., *Acad. Sci.* **1862**, *54*, 324–327.
- [91] Barrer, Richard M., *J. Chem. Soc.* **1948**, 127–132.
- [92] D. W. Breck, W. G. Eversole, R. M. Milton, T. B. Reed, T. L. Thomas, *J. Am. Chem. Soc.* **1956**, *78*, 5963–5972.
- [93] R. M. Milton, *Molecular Sieve Adsorbents*, **1959**, US2882243A.
- [94] R. M. Milton, *Molecular Sieve Adsorbents*, **1959**, US2882244A.
- [95] L. Broussard, D. P. Shoemaker, *J. Am. Chem. Soc.* **1960**, *82*, 1041–1051.
- [96] D. W. Breck, *Crystalline Zeolite Y*, **1964**, US3130007.
- [97] Barrer, Richard M. Denny, P. J., *J. Chem. Soc.* **1961**, 971–982.
- [98] R. L. Wadlinger, G. T. Kerr, E. J. Rosinski, *Catalytic Composition of a Crystalline Zeolite*, **1967**, US3308069A.
- [99] R. J. Argauer, G. R. Landolt, *Crystalline Zeolite ZSM-5 and Method of Preparing the Same*, **1972**, US3702886A.
- [100] J. Čejka, A. Corma, S. Zones, *Zeolites and Catalysis: Synthesis, Reactions and Applications*, John Wiley & Sons, **2010**.
- [101] E. M. Flanigen, R. L. Patton, *Silica Polymorph and Process for Preparing Same*, **1978**, US4073865A.
- [102] S. Shimizu, H. Hamada, *Angew. Chem., Int. Ed.* **1999**, *38*, 2725–2727.

- [103] J.-M. Woo, J. Y. Seo, H. Kim, D.-H. Lee, Y. C. Park, C.-K. Yi, Y. S. Park, J.-H. Moon, *Ultrason. Sonochem.* **2018**, *44*, 146–151.
- [104] C. Chizallet, P. Raybaud, *Angew. Chem., Int. Ed.* **2009**, *48*, 2891–2893.
- [105] W. J. Mortier, *J. Catal.* **1978**, *55*, 138–145.
- [106] G. Sastre, A. Corma, *J. Mol. Catal. A: Chem.* **2009**, *305*, 3–7.
- [107] F. Leydier, C. Chizallet, D. Costa, P. Raybaud, *J. Catal.* **2015**, *325*, 35–47.
- [108] J. F. Haw, *Phys. Chem. Chem. Phys.* **2002**, *4*, 5431–5441.
- [109] Z. Li, K. Xie, R. C. T. Slade, *Appl. Catal., A* **2001**, *209*, 107–115.
- [110] Y. Li, L. Li, J. Yu, *Chem* **2017**, *3*, 928–949.
- [111] H. Yousefzadeh, S. E. Bozbag, C. Erkey, *J. Supercrit. Fluids* **2022**, *179*, 105417.
- [112] P. Li, G. Liu, H. Wu, Y. Liu, J. Jiang, P. Wu, *J. Phys. Chem. C* **2011**, *115*, 3663–3670.
- [113] T. Kusakari, T. Sasaki, Y. Iwasawa, *Chem. Commun.* **2004**, 992–993.
- [114] N. Rane, M. Kersbulck, R. A. van Santen, E. J. M. Hensen, *Microporous Mesoporous Mater.* **2008**, *110*, 279–291.
- [115] J. Zhang, R. Tu, T. Goto, *J. Ceram. Soc. Jpn.* **2013**, *121*, 226–229.
- [116] S. M. T. Almutairi, B. Mezari, P. C. M. M. Magusin, E. A. Pidko, E. J. M. Hensen, *ACS Catal.* **2012**, *2*, 71–83.
- [117] P. Serna, D. Yardimci, J. D. Kistler, B. C. Gates, *Phys. Chem. Chem. Phys.* **2013**, *16*, 1262–1270.
- [118] J. Lu, C. Aydin, N. D. Browning, L. Wang, B. C. Gates, *Catal. Lett.* **2012**, *142*, 1445–1451.
- [119] J. D. Kistler, N. Chotigkrai, P. Xu, B. Enderle, P. Praserthdam, C.-Y. Chen, N. D. Browning, B. C. Gates, *Angew. Chem., Int. Ed.* **2014**, *53*, 8904–8907.
- [120] C. Martinez-Macias, P. Xu, S.-J. Hwang, J. Lu, C.-Y. Chen, N. D. Browning, B. C. Gates, *ACS Catal.* **2014**, *4*, 2662–2666.
- [121] H. Wang, L. Wang, F.-S. Xiao, *ACS Cent. Sci.* **2020**, *6*, 1685–1697.
- [122] S.-M. Wu, X.-Y. Yang, C. Janiak, *Angew. Chem., Int. Ed.* **2019**, *58*, 12340–12354.
- [123] N. Wang, Q. Sun, J. Yu, *Adv. Mater.* **2019**, *31*, 1803966.
- [124] N. Kosinov, C. Liu, E. J. M. Hensen, E. A. Pidko, *Chem. Mater.* **2018**, *30*, 3177–3198.
- [125] L. Wang, S. Xu, S. He, F.-S. Xiao, *Nano Today* **2018**, *20*, 74–83.
- [126] P. Gallezot, in *Post-Synthesis Modification I*, Springer Berlin Heidelberg, Berlin, Heidelberg, **2002**, pp. 257–305.
- [127] D. Farrusseng, A. Tuel, in *Encapsulated Catalysts* (Ed.: S. Sadjadi), Academic Press, **2017**, pp. 335–386.
- [128] L. Liu, U. Díaz, R. Arenal, G. Agostini, P. Concepción, A. Corma, *Nat. Mater.* **2017**, *16*, 132–138.
- [129] I. Pala Rosas, J. L. Contreras, J. Salmones, C. Tapia, B. Zeifert, J. Navarrete, T. Vázquez, D. C. García, *Catalysts* **2017**, *7*, 73.
- [130] S. Goel, Z. Wu, S. I. Zones, E. Iglesia, *J. Am. Chem. Soc.* **2012**, *134*, 17688–17695.
- [131] N. Wang, Q. Sun, R. Bai, X. Li, G. Guo, J. Yu, *J. Am. Chem. Soc.* **2016**, *138*, 7484–7487.
- [132] M. Shamzhy, M. Opanasenko, P. Concepción, A. Martínez, *Chem. Soc. Rev.* **2019**, *48*, 1095–1149.
- [133] M. N. Rao, P. Kumar, A. P. Singh, R. S. Reddy, *Synth. Commun.* **1992**, *22*, 1299–1305.
- [134] P. Kumar, R. S. Reddy, A. P. Singh, B. Pandey, *Tetrahedron Lett.* **1992**, *33*, 825–826.
- [135] P. Kumar, R. S. Reddy, A. P. Singh, B. Pandey, *Synthesis* **1993**, *1993*, 67–69.
- [136] P. Kumar, V. R. Hegde, T. Pavan Kumar, *Tetrahedron Lett.* **1995**, *36*, 601–602.
- [137] R. Ballini, M. Bordoni, G. Bosica, R. Maggi, G. Sartori, *Tetrahedron Lett.* **1998**, *39*, 7587–7590.
- [138] C. Pereira, B. Gigante, M. J. Marcelo-Curto, H. Carreyre, G. Pérot, M. Guisnet, *Synthesis* **1995**, *1995*, 1077–1078.
- [139] J. E. Choi, G. Y. Ko, *Bull. Korean Chem. Soc.* **2001**, *22*, 1177–1178.
- [140] R. Ballini, F. Bigi, S. Carloni, R. Maggi, G. Sartori, *Tetrahedron Lett.* **1997**, *38*, 4169–4172.

- [141] V. Magné, T. Garnier, M. Danel, P. Pale, S. Chassaing, *Org. Lett.* **2015**, *17*, 4494–4497.
- [142] L. I. Pilkington, D. Barker, *Synlett* **2015**, *26*, 2425–2428.
- [143] E. Wimmer, S. Borghèse, A. Blanc, V. Bénéteau, P. Pale, *Chem. Eur. J.* **2017**, *23*, 1484–1489.
- [144] K. V. N. S. Srinivas, I. Mahender, B. Das, *Synlett* **2003**, *2003*, 2419–2421.
- [145] S. P. Chavan, R. Anand, K. Pasupathy, B. S. Rao, *Green Chem.* **2001**, *3*, 320–322.
- [146] R. K. Pandey, V. S. Kadam, R. K. Upadhyay, M. K. Dongare, P. Kumar, *Synth. Commun.* **2003**, *33*, 3017–3024.
- [147] J. R. Cabrero-Antonino, A. Leyva-Pérez, A. Corma, *Angew. Chem., Int. Ed.* **2015**, *54*, 5658–5661.
- [148] S. R. Mistry, R. S. Joshi, K. C. Maheria, *J. Chem. Sci.* **2011**, *123*, 427–432.
- [149] J. J. Gabla, S. R. Mistry, K. C. Maheria, *Catal. Sci. Technol.* **2017**, *7*, 5154–5167.
- [150] L. H. R. Alpointi, M. Picinini, E. A. Urquieta-Gonzalez, A. G. Corrêa, *J. Mol. Struct.* **2021**, *1227*, 129430.
- [151] P. Sánchez-López, Y. Kotolevich, R. I. Yocupicio-Gaxiola, J. Antúnez-García, R. K. Chowdari, V. Petranovskii, S. Fuentes-Moyado, *Front. Chem.* **2021**, *9*, 716745.
- [152] B. Tang, X.-H. Lu, D. Zhou, J. Lei, Z.-H. Niu, J. Fan, Q.-H. Xia, *Catal. Commun.* **2012**, *21*, 68–71.
- [153] A. Olmos, S. Rigolet, B. Louis, P. Pale, *J. Phys. Chem. C* **2012**, *116*, 13661–13670.
- [154] A. Olmos, A. Alix, J. Sommer, P. Pale, *Chem. - Eur. J.* **2009**, *15*, 11229–11234.
- [155] A. Olmos, J. Sommer, P. Pale, *Chem. - Eur. J.* **2011**, *17*, 1907–1914.
- [156] A. Olmos, B. Louis, P. Pale, *Chem. - Eur. J.* **2012**, *18*, 4894–4901.
- [157] M. J. Baruah, A. Dutta, S. Biswas, G. Gogoi, N. Hoque, P. K. Bhattacharyya, K. K. Bania, *ACS Appl. Nano Mater.* **2022**, *5*, 1446–1459.
- [158] K. Namitharan, K. Pitchumani, *Eur. J. Org. Chem.* **2010**, *2010*, 411–415.
- [159] R. Maggi, A. Bello, C. Oro, G. Sartori, L. Soldi, *Tetrahedron* **2008**, *64*, 1435–1439.
- [160] S. Borghèse, P. Drouhin, V. Bénéteau, B. Louis, P. Pale, *Green Chem.* **2013**, *15*, 1496–1500.
- [161] R. M. Gillard, M. A. Brimble, *Org. Biomol. Chem.* **2019**, *17*, 8272–8307.
- [162] C. S. Hampton, M. Harmata, *Adv. Synth. Catal.* **2015**, *357*, 549–552.
- [163] M. Harmata, C. Huang, *Adv. Synth. Catal.* **2008**, *350*, 972–974.
- [164] S. Mohan, P. Dinesha, S. Kumar, *Chem. Eng. J.* **2020**, *384*, 123253.
- [165] R. Trammell, K. Rajabimoghadam, I. Garcia-Bosch, *Chem. Rev.* **2019**, *119*, 2954–3031.
- [166] R. Innocenti, E. Lenci, A. Trabocchi, *Tetrahedron Lett.* **2020**, *61*, 152083.
- [167] T. D. Suja, R. S. Menon, in *Copper Catalysis in Organic Synthesis* (Eds.: G. Anilkumar, S. Saranya), Wiley, **2020**, pp. 209–237.
- [168] Y. Yamamoto, *J. Org. Chem.* **2007**, *72*, 7817–7831.
- [169] J. Ipaktschi, *Z. Naturforsch. B* **1986**, *41*, 496–498.
- [170] W. G. Dauben, H. O. Krabbenhoft, *J. Am. Chem. Soc.* **1976**, *98*, 1992–1993.
- [171] C. Langham, S. Taylor, D. Bethell, P. McMorn, P. C. B. Page, D. J. Willock, C. Sly, F. E. Hancock, F. King, G. J. Hutchings, *J. Chem. Soc., Perkin Trans. 2* **1999**, 1043–1050.
- [172] D. A. Evans, M. T. Bilodeau, M. M. Faul, *J. Am. Chem. Soc.* **1994**, *116*, 2742–2753.
- [173] R. Huisgen, G. Szeimies, L. Möbius, *Chem. Ber.* **1967**, *100*, 2494–2507.
- [174] V. V. Rostovtsev, L. G. Green, V. V. Fokin, K. B. Sharpless, *Angew. Chem., Int. Ed.* **2002**, *41*, 2596–2599.
- [175] C. W. Tornøe, C. Christensen, M. Meldal, *J. Org. Chem.* **2002**, *67*, 3057–3064.
- [176] S. Chassaing, M. Kumarraja, A. Sani Souna Sido, P. Pale, J. Sommer, *Org. Lett.* **2007**, *9*, 883–886.
- [177] S. Chassaing, A. Sani Souna Sido, A. Alix, M. Kumarraja, P. Pale, J. Sommer, *Chem. Eur. J.* **2008**, *14*, 6713–6721.
- [178] A. Alix, S. Chassaing, P. Pale, J. Sommer, *Tetrahedron* **2008**, *64*, 8922–8929.
- [179] V. Bénéteau, A. Olmos, T. Boningari, J. Sommer, P. Pale, *Tetrahedron Lett.* **2010**, *51*, 3673–3677.

- [180] T. Boningari, A. Olmos, B. M. Reddy, J. Sommer, P. Pale, *Eur. J. Org. Chem.* **2010**, 2010, 6338–6347.
- [181] B. Sarmah, B. Satpati, R. Srivastava, *RSC Adv.* **2016**, 6, 87066–87081.
- [182] E. R. Costa, F. C. D. Andrade, D. Y. de Albuquerque, L. E. M. Ferreira, T. M. Lima, C. G. S. Lima, D. S. A. Silva, E. A. Urquieta-González, M. W. Paixão, R. S. Schwab, *New J. Chem.* **2020**, 44, 15046–15053.
- [183] F. Ullmann, *Ber. Dtsch. Chem. Ges.* **1903**, 36, 2382–2384.
- [184] F. Ullmann, P. Sponagel, *Ber. Dtsch. Chem. Ges.* **1905**, 38, 2211–2212.
- [185] I. Goldberg, *Ber. Dtsch. Chem. Ges.* **1906**, 39, 1691–1692.
- [186] T. Garnier, M. Danel, V. Magné, A. Pujol, V. Bénéteau, P. Pale, S. Chassaing, *J. Org. Chem.* **2018**, 83, 6408–6422.
- [187] T. Garnier, R. Sakly, M. Danel, S. Chassaing, P. Pale, *Synthesis* **2017**, 49, 1223–1230.
- [188] P. Y. S. Lam, C. G. Clark, S. Saubern, J. Adams, M. P. Winters, D. M. T. Chan, A. Combs, *Tetrahedron Lett.* **1998**, 39, 2941–2944.
- [189] A. Clerc, V. Bénéteau, P. Pale, S. Chassaing, *ChemCatChem* **2020**, 12, 2060–2065.
- [190] M. O. Frederick, J. A. Mulder, M. R. Tracey, R. P. Hsung, J. Huang, K. C. M. Kurtz, L. Shen, C. J. Douglas, *J. Am. Chem. Soc.* **2003**, 125, 2368–2369.
- [191] Y. Zhang, R. P. Hsung, M. R. Tracey, K. C. M. Kurtz, E. L. Vera, *Org. Lett.* **2004**, 6, 1151–1154.
- [192] H. Harkat, S. Borghèse, M. D. Nigris, S. Kiselev, V. Bénéteau, P. Pale, *Adv. Synth. Catal.* **2014**, 356, 3842–3848.
- [193] P. Saha, H. Jeon, P. K. Mishra, H.-W. Rhee, J. H. Kwak, *J. Mol. Catal. A: Chem.* **2016**, 417, 10–18.
- [194] K. Tishinov, N. Fei, D. Gillingham, *Chem. Sci.* **2013**, 4, 4401–4406.
- [195] M. Henrion, S. Smolders, D. E. D. Vos, *Catal. Sci. Technol.* **2020**, 10, 940–943.
- [196] F. G. Cirujano, A. Dhakshinamoorthy, *New J. Chem.* **2022**, 46, 1469–1482.
- [197] V. A. Peshkov, O. P. Pereshivko, E. V. Van der Eycken, *Chem. Soc. Rev.* **2012**, 41, 3790–3807.
- [198] I. Jesin, G. C. Nandi, *Eur. J. Org. Chem.* **2019**, 2019, 2704–2720.
- [199] J. Farhi, I. N. Lykakis, G. E. Kostakis, *Catalysts* **2022**, 12, 660.
- [200] B. V. Rokade, J. Barker, P. J. Guiry, *Chem. Soc. Rev.* **2019**, 48, 4766–4790.
- [201] R. Innocenti, E. Lenci, L. Baldini, C. Faggi, G. Menchi, A. Trabocchi, *Eur. J. Org. Chem.* **2019**, 2019, 6203–6210.
- [202] Y. Volkova, S. Baranin, I. Zavarzin, *Adv. Synth. Catal.* **2021**, 363, 40–61.
- [203] L. P. Zorba, G. C. Vougioukalakis, *Coord. Chem. Rev.* **2021**, 429, 213603.
- [204] C.-J. Li, C. Wei, *Chem. Commun.* **2002**, 268–269.
- [205] C. Wei, C.-J. Li, *J. Am. Chem. Soc.* **2003**, 125, 9584–9585.
- [206] C. Wei, Z. Li, C.-J. Li, *Org. Lett.* **2003**, 5, 4473–4475.
- [207] L. Shi, Y.-Q. Tu, M. Wang, F.-M. Zhang, C.-A. Fan, *Org. Lett.* **2004**, 6, 1001–1003.
- [208] J. B. Bariwal, D. S. Ermolat'ev, E. V. Van der Eycken, *Chem. - Eur. J.* **2010**, 16, 3281–3284.
- [209] T. T. T. Trang, D. S. Ermolat'ev, E. V. Van der Eycken, *RSC Adv.* **2015**, 5, 28921–28924.
- [210] M.-T. Chen, O. Navarro, *Synlett* **2013**, 24, 1190–1192.
- [211] M. K. Patil, M. Keller, B. M. Reddy, P. Pale, J. Sommer, *Eur. J. Org. Chem.* **2008**, 2008, 4440–4445.
- [212] R. Yi, Z.-J. Wang, Z. Liang, M. Xiao, X. Xu, N. Li, *Appl. Organomet. Chem.* **2019**, 33, e4917.
- [213] F. Li, J.-L. Kan, B.-J. Yao, Y.-B. Dong, *Angew. Chem., Int. Ed.* **2022**, 61, e202115044.
- [214] L. Chaabane, M. H. V. Baouab, E. Beyou, *Appl. Organomet. Chem.* **2022**, 36, e6625.
- [215] K. M. Ahmed, K. Amani, *Appl. Organomet. Chem.* **2022**, 36, e6630.
- [216] Y.-D. Wu, K. N. Houk, M. N. Paddon-Row, *Angew. Chem., Int. Ed.* **1992**, 31, 1019–1021.

- [217] Z. Li, H. Jangra, Q. Chen, P. Mayer, A. R. Ofial, H. Zipse, H. Mayr, *J. Am. Chem. Soc.* **2018**, *140*, 5500–5515.
- [218] C. J. Pierce, M. Nguyen, C. H. Larsen, *Angew. Chem., Int. Ed.* **2012**, *51*, 12289–12292.
- [219] X. Tang, J. Kuang, S. Ma, *Chem. Commun.* **2013**, *49*, 8976–8978.
- [220] Y. Cai, X. Tang, S. Ma, *Chem. - Eur. J.* **2016**, *22*, 2266–2269.
- [221] A. Elhampour, F. Nemati, *J. Chin. Chem. Soc.* **2016**, *63*, 653–659.
- [222] P. C. Perumgani, S. Keesara, S. Parvathaneni, M. R. Mandapati, *New J. Chem.* **2016**, *40*, 5113–5120.
- [223] A. Elhampour, M. Malmir, E. Kowsari, F. B. Ajdari, F. Nemati, *RSC Adv.* **2016**, *6*, 96623–96634.
- [224] G. Fernández, L. Bernardo, A. Villanueva, R. Pleixats, *New J. Chem.* **2020**, *44*, 6130–6141.
- [225] M. J. Aliaga, D. J. Ramón, M. Yus, *Org. Biomol. Chem.* **2010**, *8*, 43–46.
- [226] S. Yan, S. Pan, T. Osako, Y. Uozumi, *ACS Sustainable Chem. Eng.* **2019**, *7*, 9097–9102.
- [227] G. Purohit, D. S. Rawat, *ACS Sustainable Chem. Eng.* **2019**, *7*, 19235–19245.
- [228] W. E. Van Beek, J. Van Stappen, P. Franck, K. Abbaspour Tehrani, *Org. Lett.* **2016**, *18*, 4782–4785.
- [229] W. E. Van Beek, K. Gadde, K. A. Tehrani, *Chem. - Eur. J.* **2018**, *24*, 16645–16651.
- [230] P. Kuhn, P. Pale, J. Sommer, B. Louis, *J. Phys. Chem. C* **2009**, *113*, 2903–2910.
- [231] M. Keller, A. Sani Souna Sido, P. Pale, J. Sommer, *Chem. - Eur. J.* **2009**, *15*, 2810–2817.
- [232] F. Brotzel, Y. C. Chu, H. Mayr, *J. Org. Chem.* **2007**, *72*, 3679–3688.
- [233] T. Kanzian, T. A. Nigst, A. Maier, S. Pichl, H. Mayr, *Eur. J. Org. Chem.* **2009**, *2009*, 6379–6385.
- [234] Z. L. Palchak, D. J. Lussier, C. J. Pierce, C. H. Larsen, *Green Chem.* **2015**, *17*, 1802–1810.
- [235] S. Dhanasekaran, Vinod. K. Kannaujiya, R. G. Biswas, V. K. Singh, *J. Org. Chem.* **2019**, *84*, 3275–3292.
- [236] S. I. Sampani, V. Zdorichenko, J. Devonport, G. Rossini, M. C. Leech, K. Lam, B. Cox, A. Abdul-Sada, A. Vargas, G. E. Kostakis, *Chem. - Eur. J.* **2021**, *27*, 4394–4400.
- [237] N. V. Tzouras, S. P. Neofotistos, G. C. Vougioukalakis, *ACS Omega* **2019**, *4*, 10279–10292.
- [238] S. P. Neofotistos, N. V. Tzouras, M. Pauze, E. Gómez-Bengoa, G. C. Vougioukalakis, *Adv. Synth. Catal.* **2020**, *362*, 3872–3885.
- [239] G. Abbiati, A. Arcadi, G. Bianchi, S. Di Giuseppe, F. Marinelli, E. Rossi, *J. Org. Chem.* **2003**, *68*, 6959–6966.
- [240] N. Sharma, U. K. Sharma, N. M. Mishra, E. V. Van der Eycken, *Adv. Synth. Catal.* **2014**, *356*, 1029–1037.
- [241] L. Zhou, D. S. Bohle, H.-F. Jiang, C.-J. Li, *Synlett* **2009**, *2009*, 937–940.
- [242] U. C. Rajesh, U. Gulati, D. Rawat, *ACS Sustainable Chem. Eng.* **2016**, *4*, 3409–3419.
- [243] U. Gulati, U. C. Rajesh, D. S. Rawat, *Tetrahedron Lett.* **2016**, *57*, 4468–4472.
- [244] M. A. Idris, S. Lee, *Synthesis* **2020**, *52*, 2277–2298.
- [245] N. Sakai, N. Uchida, T. Konakahara, *Synlett* **2008**, *2008*, 1515–1519.
- [246] I. M. de Oliveira, D. C. Pimenta, J. Zukerman-Schpector, H. A. Stefani, F. Manarin, *New J. Chem.* **2018**, *42*, 10118–10123.
- [247] N. Li, S. Xu, X. Wang, L. Xu, J. Qiao, Z. Liang, X. Xu, *Chin. Chem. Lett.* **2021**, *32*, 3993–3997.
- [248] Z. Lin, D. Yu, Y. N. Sum, Y. Zhang, *ChemSusChem* **2012**, *5*, 625–628.
- [249] P. Zhao, H. Feng, H. Pan, Z. Sun, M. Tong, *Org. Chem. Front.* **2017**, *4*, 37–41.
- [250] H. Feng, P. Zhao, L. Huang, Z. Sun, M. Tong, *Asian J. Org. Chem.* **2017**, *6*, 161–164.
- [251] F. Teng, J.-T. Yu, Z. Zhou, H. Chu, J. Cheng, *J. Org. Chem.* **2015**, *80*, 2822–2826.
- [252] M.-H. Larraufie, G. Maestri, M. Malacria, C. Ollivier, L. Fensterbank, E. Lacôte, *Synthesis* **2012**, *44*, 1279–1292.
- [253] M. R. R. Prabhath, L. Williams, S. V. Bhat, P. Sharma, *Molecules* **2017**, *22*, 615.

- [254] H. A. Laub, G. Evano, H. Mayr, *Angew. Chem., Int. Ed.* **2014**, *53*, 4968–4971.
- [255] X. Zhang, Y. Zhang, J. Huang, R. P. Hsung, K. C. M. Kurtz, J. Oppenheimer, M. E. Petersen, I. K. Sagamanova, L. Shen, M. R. Tracey, *J. Org. Chem.* **2006**, *71*, 4170–4177.
- [256] D. Rodríguez, M. F. Martínez-Esperón, L. Castedo, C. Saá, *Synlett* **2007**, *2007*, 1963–1965.
- [257] R. Qi, X.-N. Wang, K. A. DeKorver, Y. Tang, C.-C. Wang, Q. Li, H. Li, M.-C. Lv, Q. Yu, R. P. Hsung, *Synthesis* **2013**, *45*, 1749–1758.
- [258] X.-N. Wang, R. P. Hsung, R. Qi, S. K. Fox, M.-C. Lv, *Org. Lett.* **2013**, *15*, 2514–2517.
- [259] X.-N. Wang, R. P. Hsung, S. K. Fox, M.-C. Lv, R. Qi, *Heterocycles* **2014**, *88*, 1233–1254.
- [260] C. Verrier, S. Carret, J.-F. Poisson, *Org. Lett.* **2012**, *14*, 5122–5125.
- [261] S. J. Mansfield, C. D. Campbell, M. W. Jones, E. A. Anderson, *Chem. Commun.* **2015**, *51*, 3316–3319.
- [262] P. Zhang, A. M. Cook, Y. Liu, C. Wolf, *J. Org. Chem.* **2014**, *79*, 4167–4173.
- [263] K. A. DeKorver, R. P. Hsung, W.-Z. Song, X.-N. Wang, M. C. Walton, *Org. Lett.* **2012**, *14*, 3214–3217.
- [264] A. M. Cook, C. Wolf, *Tetrahedron Lett.* **2015**, *56*, 2377–2392.
- [265] A. K. Nadipuram, W. M. David, D. Kumar, S. M. Kerwin, *Org. Lett.* **2002**, *4*, 4543–4546.
- [266] B. Darses, A. Milet, C. Philouze, A. E. Greene, J.-F. Poisson, *Org. Lett.* **2008**, *10*, 4445–4447.
- [267] F. Schlimpen, C. Plaçais, E. Starck, V. Bénétteau, P. Pale, S. Chassaing, *J. Org. Chem.* **2021**, *86*, 16593–16613.
- [268] M. K. Sahoo, S. Pradhan, D. Kim, J.-W. Park, S. Chang, *Organometallics* **2022**, *41*, 900–905.
- [269] M. Hourtoule, L. Miesch, *Org. Lett.* **2022**, *24*, 3896–3900.
- [270] R. Appel, H. Mayr, *J. Am. Chem. Soc.* **2011**, *133*, 8240–8251.
- [271] O. Cortezano-Arellano, M. A. Hernández-Gasca, D. Ángeles-Beltrán, G. E. Negrón-Silva, R. Santillan, *Tetrahedron Lett.* **2018**, *59*, 2403–2406.
- [272] M. Z. C. Hatit, J. C. Sadler, L. A. McLean, B. C. Whitehurst, C. P. Seath, L. D. Humphreys, R. J. Young, A. J. B. Watson, G. A. Burley, *Org. Lett.* **2016**, *18*, 1694–1697.
- [273] C. P. Seath, G. A. Burley, A. J. B. Watson, *Angew. Chem., Int. Ed.* **2017**, *56*, 3314–3318.
- [274] M. Patel, R. K. Saunthwal, A. K. Verma, *Acc. Chem. Res.* **2017**, *50*, 240–254.
- [275] R. Severin, S. Doye, *Chem. Soc. Rev.* **2007**, *36*, 1407–1420.
- [276] T. E. Müller, K. C. Hultsch, M. Yus, F. Foubelo, M. Tada, *Chem. Rev.* **2008**, *108*, 3795–3892.
- [277] L. Huang, M. Arndt, K. Gooßen, H. Heydt, L. J. Gooßen, *Chem. Rev.* **2015**, *115*, 2596–2697.
- [278] Z. Tashrifi, M. Mohammadi Khanaposhtani, M. Biglar, B. Larijani, M. Mahdavi, *Asian J. Org. Chem.* **2020**, *9*, 969–991.
- [279] S. M. Coman, V. I. Parvulescu, *Org. Process Res. Dev.* **2015**, *19*, 1327–1355.
- [280] S. Takano, T. Kochi, F. Kakiuchi, *Chem. Lett.* **2017**, *46*, 1620–1623.
- [281] J. Han, B. Xu, G. B. Hammond, *J. Am. Chem. Soc.* **2010**, *132*, 916–917.
- [282] J. E. Baldwin, *J. Chem. Soc., Chem. Commun.* **1976**, 734–736.
- [283] M. Biyikal, M. Porta, P. W. Roesky, S. Blechert, *Adv. Synth. Catal.* **2010**, *352*, 1870–1875.
- [284] M. Biyikal, K. Löhnwitz, N. Meyer, M. Dochnahl, P. W. Roesky, S. Blechert, *Eur. J. Inorg. Chem.* **2010**, *2010*, 1070–1081.
- [285] N. Purkait, S. Blechert, *Adv. Synth. Catal.* **2012**, *354*, 2079–2083.
- [286] Y. Luo, Z. Li, C.-J. Li, *Org. Lett.* **2005**, *7*, 2675–2678.
- [287] X.-Y. Liu, P. Ding, J.-S. Huang, C.-M. Che, *Org. Lett.* **2007**, *9*, 2645–2648.
- [288] X.-Y. Liu, C.-M. Che, *Angew. Chem., Int. Ed.* **2008**, *47*, 3805–3810.
- [289] C. J. Pierce, H. Yoo, C. H. Larsen, *Adv. Synth. Catal.* **2013**, *355*, 3586–3590.

- [290] Z. L. Palchak, D. J. Lussier, C. J. Pierce, H. Yoo, C. H. Larsen, *Adv. Synth. Catal.* **2015**, *357*, 539–548.
- [291] M. Periasamy, P. O. Reddy, I. Satyanarayana, L. Mohan, A. Edukondalu, *J. Org. Chem.* **2016**, *81*, 987–999.
- [292] W. Zheng, Y. Liu, L. Huilan, B. Wenhui, T. Yingzhi, W. Ming, T. Zilong, H. Weimin, *Chin. J. Org. Chem.* **2018**, *38*, 2639.
- [293] H. J. Kim, J. E. Lee, G. Koyyada, M. Lakavathu, J. H. Kim, *Asian J. Org. Chem.* **2022**, *11*, e202200053.
- [294] J. Datka, E. Kukulska-Zajac, W. Kobyzewa, *Catal. Today* **2005**, *101*, 123–129.
- [295] S. D. Lepore, A. Khoram, D. C. Bromfield, P. Cohn, V. Jairaj, M. A. Silvestri, *J. Org. Chem.* **2005**, *70*, 7443–7446.
- [296] Corwin. Hansch, A. Leo, R. W. Taft, *Chem. Rev.* **1991**, *91*, 165–195.
- [297] J. Bahri, Nouvelles méthodes d'hydroamination d'alcynes (p. 103-109), PhD, Ecole nationale supérieure de chimie, Montpellier, **2015**.
- [298] H. Jang, A. R. Zhugralin, Y. Lee, A. H. Hoveyda, *J. Am. Chem. Soc.* **2011**, *133*, 7859–7871.
- [299] S.-L. Shi, S. L. Buchwald, *Nat. Chem.* **2015**, *7*, 38–44.
- [300] M. Gruttadauria, F. Giacalone, R. Noto, *Green Chem.* **2013**, *15*, 2608–2618.
- [301] C. Shao, G. Cheng, D. Su, J. Xu, X. Wang, Y. Hu, *Adv. Synth. Catal.* **2010**, *352*, 1587–1592.
- [302] E. Vitaku, D. T. Smith, J. T. Njardarson, *J. Med. Chem.* **2014**, *57*, 10257–10274.
- [303] V. K. Sharma, S. K. Singh, *RSC Adv.* **2017**, *7*, 2682–2732.
- [304] A. B. Charette, M. Grenon, A. Lemire, M. Pourashraf, J. Martel, *J. Am. Chem. Soc.* **2001**, *123*, 11829–11830.
- [305] A. Lemire, A. B. Charette, *Org. Lett.* **2005**, *7*, 2747–2750.
- [306] N. Satoh, T. Akiba, S. Yokoshima, T. Fukuyama, *Angew. Chem., Int. Ed.* **2007**, *46*, 5734–5736.
- [307] E. M. P. Silva, P. A. M. M. Varandas, A. M. S. Silva, *Synthesis* **2013**, *45*, 3053–3089.
- [308] F. W. Fowler, *J. Org. Chem.* **1972**, *37*, 1321–1323.
- [309] A. Heusler, J. Fliege, T. Wagener, F. Glorius, *Angew. Chem., Int. Ed.* **2021**, *60*, 13793–13797.
- [310] J. Jia, F. Hu, Y. Xia, *Synthesis* **2022**, *54*, 92–110.
- [311] D. J. Robinson, S. P. Spurlin, J. D. Gorden, R. R. Karimov, *ACS Catal.* **2020**, *10*, 51–55.
- [312] J.-P. Wan, S.-F. Gan, G.-L. Sun, Y.-J. Pan, *J. Org. Chem.* **2009**, *74*, 2862–2865.
- [313] T.-G. Le, H.-T. Pham, J. P. Martin, I. Chataigner, J.-L. Renaud, *Synth. Commun.* **2020**, *50*, 2673–2684.
- [314] L. Shen, S. Cao, J. Wu, J. Zhang, H. Li, N. Liu, X. Qian, *Green Chem.* **2009**, *11*, 1414–1420.
- [315] G. Bosica, K. Demanuele, J. M. Padrón, A. Puerta, *Beilstein J. Org. Chem.* **2020**, *16*, 2862–2869.
- [316] A. R. De Lera, W. Reischl, W. H. Okamura, *J. Am. Chem. Soc.* **1989**, *111*, 4051–4063.
- [317] D. Tejedor, G. Méndez-Abt, F. García-Tellado, *Chem. - Eur. J.* **2010**, *16*, 428–431.
- [318] D. Tejedor, L. Cotos, G. Méndez-Abt, F. García-Tellado, *J. Org. Chem.* **2014**, *79*, 10655–10661.
- [319] B. J. Fallon, J.-B. Garsi, E. Derat, M. Amatore, C. Aubert, M. Petit, *ACS Catal.* **2015**, *5*, 7493–7497.
- [320] D. A. Colby, R. G. Bergman, J. A. Ellman, *J. Am. Chem. Soc.* **2008**, *130*, 3645–3651.
- [321] G. Yin, Y. Zhu, N. Wang, P. Lu, Y. Wang, *Tetrahedron* **2013**, *69*, 8353–8359.
- [322] Y.-W. Liu, Y.-B. Xie, D.-J. Li, L. Wang, *Russ. J. Gen. Chem.* **2015**, *85*, 2163–2166.
- [323] Y.-B. Xie, S.-P. Ye, W.-F. Chen, Y.-L. Hu, D.-J. Li, L. Wang, *Asian J. Org. Chem.* **2017**, *6*, 746–750.
- [324] A. Saito, T. Konishi, Y. Hanzawa, *Org. Lett.* **2010**, *12*, 372–374.

- [325] M. A. P. Martins, M. Rossatto, C. P. Frizzo, E. Scapin, L. Buriol, N. Zanatta, H. G. Bonacorso, *Tetrahedron Lett.* **2013**, *54*, 847–849.
- [326] X. Xin, D. Wang, F. Wu, X. Li, B. Wan, *J. Org. Chem.* **2013**, *78*, 4065–4074.
- [327] O. Alduhaish, R. Varala, S. F. Adil, M. Khan, M. R. H. Siddiqui, A. AlWarthan, M. M. Alam, *J. Chem.* **2020**, *2020*, e9139648.
- [328] J. Mikušek, P. Matouš, E. Matoušová, M. Janoušek, J. Kuneš, M. Pour, *Adv. Synth. Catal.* **2016**, *358*, 2912–2922.
- [329] B. D. Sherry, F. D. Toste, *J. Am. Chem. Soc.* **2004**, *126*, 15978–15979.
- [330] H. Menz, S. F. Kirsch, *Org. Lett.* **2006**, *8*, 4795–4797.
- [331] H. Kim, C. Lee, *J. Am. Chem. Soc.* **2006**, *128*, 6336–6337.
- [332] H. Mizoguchi, R. Watanabe, S. Minami, H. Oikawa, H. Oguri, *Org. Biomol. Chem.* **2015**, *13*, 5955–5963.
- [333] H. Tan, X.-F. Jiang, L. Jiang, C. Yuan, X. Tang, M.-F. Li, S.-W. Liu, S. Liu, H.-L. Cui, *Synlett* **2020**, *31*, 723–729.
- [334] C. Liu, G. Wang, Y. Wang, O. P. Pereshivko, V. A. Peshkov, *Eur. J. Org. Chem.* **2019**, *2019*, 1981–1985.
- [335] S. A. Shehzadi, C. M. L. V. Velde, A. Saeed, K. A. Tehrani, *Org. Biomol. Chem.* **2018**, *16*, 3241–3247.
- [336] R. F. Winter, G. Rauhut, *Chem. - Eur. J.* **2002**, *8*, 641–649.
- [337] S. Dongbang, D. N. Confair, J. A. Ellman, *Acc. Chem. Res.* **2021**, *54*, 1766–1778.
- [338] S. Duttwyler, S. Chen, M. K. Takase, K. B. Wiberg, R. G. Bergman, J. A. Ellman, *Science* **2013**, *339*, 678–682.
- [339] S. Duttwyler, C. Lu, A. L. Rheingold, R. G. Bergman, J. A. Ellman, *J. Am. Chem. Soc.* **2012**, *134*, 4064–4067.
- [340] S. Duttwyler, S. Chen, C. Lu, B. Q. Mercado, R. G. Bergman, J. A. Ellman, *Angew. Chem., Int. Ed.* **2014**, *53*, 3877–3880.
- [341] S. Chen, V. Bacauanu, T. Knecht, B. Q. Mercado, R. G. Bergman, J. A. Ellman, *J. Am. Chem. Soc.* **2016**, *138*, 12664–12670.
- [342] E. M. P. Silva, D. H. A. Rocha, A. M. S. Silva, *Synthesis* **2018**, *50*, 1773–1782.
- [343] P. Ramaraju, A. P. Pawar, E. Iype, N. A. Mir, S. Choudhary, D. K. Sharma, R. Kant, I. Kumar, *J. Org. Chem.* **2019**, *84*, 12408–12419.
- [344] H. Mizoguchi, H. Oikawa, H. Oguri, *Nat. Chem.* **2014**, *6*, 57–64.
- [345] T. Wayama, Y. Arai, H. Oguri, *J. Org. Chem.* **2022**, *87*, 5938–5951.
- [346] K. V. Zavyalov, M. S. Novikov, A. F. Khlebnikov, N. V. Rostovskii, G. L. Starova, *Russ. J. Org. Chem.* **2017**, *53*, 1214–1221.
- [347] D. Tejedor, M. C. Prieto-Ramírez, M. Ingold, M. Chicón, F. García-Tellado, *Org. Lett.* **2016**, *18*, 2770–2773.
- [348] G. Domány, J. Matúz, K. Sághy, E. Ezer, *Eur. J. Med. Chem.* **1993**, *28*, 633–636.
- [349] M. S. Al-Said, M. S. Bashandy, S. I. Al-Qasoumi, M. M. Ghorab, *Eur. J. Med. Chem.* **2011**, *46*, 137–141.
- [350] I. Salama, M. A. O. Abdel-Fattah, M. S. Hany, S. A. El-Sharif, M. A. M. El-Naggar, R. M. H. Rashied, G. A. Piazza, A. H. Abadi, *Med. Chem.* **2012**, *8*, 372–383.
- [351] G. M. Schroeder, Y. An, Z.-W. Cai, X.-T. Chen, C. Clark, L. A. M. Cornelius, J. Dai, J. Gullo-Brown, A. Gupta, B. Henley, J. T. Hunt, R. Jeyaseelan, A. Kamath, K. Kim, J. Lippy, L. J. Lombardo, V. Manne, S. Oppenheimer, J. S. Sack, R. J. Schmidt, G. Shen, K. Stefanski, J. S. Tokarski, G. L. Trainor, B. S. Wautlet, D. Wei, D. K. Williams, Y. Zhang, Y. Zhang, J. Fagnoli, R. M. Borzilleri, *J. Med. Chem.* **2009**, *52*, 1251–1254.
- [352] N. Ghassab-Abdollahi, K. Mobasser, A. Dehghani Ahmadabad, H. Nadrian, M. Mirghafourvand, *Phytother. Res.* **2021**, *35*, 4971–4987.
- [353] R. Watanabe, H. Mizoguchi, H. Oikawa, H. Ohashi, K. Watashi, H. Oguri, *Bioorg. Med. Chem.* **2017**, *25*, 2851–2855.
- [354] K. Rajkumar, T. R. Murthy, A. Zehra, P. S. Khursade, S. V. Kalivendi, A. K. Tiwari, R. S. Prakasham, B. C. Raju, *ChemistrySelect* **2018**, *3*, 13729–13735.

- [355] E. Knaus, P. Kumar, *Eur. J. Med. Chem.* **1993**, *28*, 881–885.
- [356] F. J. Fañanás, T. Arto, A. Mendoza, F. Rodríguez, *Org. Lett.* **2011**, *13*, 4184–4187.
- [357] J. Cui, D. I. Chai, C. Miller, J. Hao, C. Thomas, J. Wang, K. A. Scheidt, S. A. Kozmin, *J. Org. Chem.* **2012**, *77*, 7435–7470.
- [358] C. Laurence, S. Mansour, D. Vuluga, K. Sraïdi, J. Legros, *J. Org. Chem.* **2022**, *87*, 6273–6287.
- [359] F. Sirindil, S. P. Nolan, S. Dagorne, P. Pale, A. Blanc, P. de Frémont, *Chem. - Eur. J.* **2018**, *24*, 12630–12637.
- [360] Z. Ma, J. A. van Bokhoven, *ChemCatChem* **2012**, *4*, 2036–2044.
- [361] R. M. Martin, R. G. Bergman, J. A. Ellman, *Org. Lett.* **2013**, *15*, 444–447.
- [362] M. Zendejdel, N. Foroghi. Far, Z. Gaykani, *J. Incl. Phenom. Macrocycl. Chem.* **2005**, *53*, 47–49.
- [363] J. Zheng, R. Wen, X. Luo, G. Lin, J. Zhang, L. Xu, L. Guo, H. Jiang, *Bioorg. Med. Chem. Lett.* **2006**, *16*, 225–227.
- [364] D. A. Evans, T. C. Britton, J. A. Ellman, *Tetrahedron Lett.* **1987**, *28*, 6141–6144.
- [365] T. Mutai, Y. Abe, K. Araki, *J. Chem. Soc., Perkin Trans. 2* **1997**, 1805–1810.
- [366] P. Szcześniak, S. Buda, L. Lefevre, O. Staszewska-Krajewska, J. Mlynarski, *Eur. J. Org. Chem.* **2019**, *2019*, 6973–6982.
- [367] F. Lovering, J. Bikker, C. Humblet, *J. Med. Chem.* **2009**, *52*, 6752–6756.
- [368] S. Sadjadi, T. Hosseinejad, M. Malmir, M. M. Heravi, *New J. Chem.* **2017**, *41*, 13935–13951.
- [369] M. Cheng, Q. Zhang, X.-Y. Hu, B.-G. Li, J.-X. Ji, A. S. C. Chan, *Adv. Synth. Catal.* **2011**, *353*, 1274–1278.
- [370] M. Hosseini-Sarvari, F. Moeini, *New J. Chem.* **2014**, *38*, 624–635.
- [371] C. J. Pierce, C. H. Larsen, *Green Chem.* **2012**, *14*, 2672–2676.
- [372] R. Mataka, Y. Niwa, H. Matsubara, *Org. Lett.* **2015**, *17*, 2354–2357.
- [373] W. Huang, Q. Shen, J. Wang, X. Zhou, *J. Org. Chem.* **2008**, *73*, 1586–1589.
- [374] A. Kumar, G. Ye, Y. Ahmadibeni, K. Parang, *J. Org. Chem.* **2006**, *71*, 7915–7918.
- [375] J. D. Wilden, L. Geldeard, C. C. Lee, D. B. Judd, S. Caddick, *Chem. Commun.* **2007**, 1074–1076.
- [376] M. H. S. A. Hamid, C. L. Allen, G. W. Lamb, A. C. Maxwell, H. C. Maytum, A. J. A. Watson, J. M. J. Williams, *J. Am. Chem. Soc.* **2009**, *131*, 1766–1774.
- [377] Y. Liu, Y. Huang, H. Song, Y. Liu, Q. Wang, *Chem. - Eur. J.* **2015**, *21*, 5337–5340.
- [378] K. Miyazawa, T. Koike, M. Akita, *Adv. Synth. Catal.* **2014**, *356*, 2749–2755.
- [379] A. Becker, C. P. Grugel, B. Breit, *Org. Lett.* **2021**, *23*, 3788–3792.
- [380] Q. Cai, Q. Yin, S.-L. You, *Asian J. Org. Chem.* **2014**, *3*, 408–411.
- [381] X. Zhang, R. P. Hsung, H. Li, *Chem. Commun.* **2007**, 2420–2422.
- [382] B. Yao, Z. Liang, T. Niu, Y. Zhang, *J. Org. Chem.* **2009**, *74*, 4630–4633.
- [383] T. Hamada, X. Ye, S. S. Stahl, *J. Am. Chem. Soc.* **2008**, *130*, 833–835.
- [384] K. Dooleweerd, T. Ruhland, T. Skrydstrup, *Org. Lett.* **2009**, *11*, 221–224.
- [385] M. R. Tracey, Y. Zhang, M. O. Frederick, J. A. Mulder, R. P. Hsung, *Org. Lett.* **2004**, *6*, 2209–2212.
- [386] B. S. L. Collins, M. G. Suero, M. J. Gaunt, *Angew. Chem., Int. Ed.* **2013**, *52*, 5799–5802.
- [387] X. Li, M. Jiang, T. Zhan, W. Cao, X. Feng, *Chem. - Asian J.* **2020**, *15*, 1953–1956.
- [388] E. Romain, C. Fopp, F. Chemla, F. Ferreira, O. Jackowski, M. Oestreich, A. Perez-Luna, *Angew. Chem., Int. Ed.* **2014**, *53*, 11333–11337.
- [389] L. Buzzetti, M. Puriņš, P. D. G. Greenwood, J. Waser, *J. Am. Chem. Soc.* **2020**, *142*, 17334–17339.
- [390] V. Marsicano, A. Arcadi, M. Aschi, V. Michelet, *Org. Biomol. Chem.* **2020**, *18*, 9438–9447.
- [391] Z. Chang, X. Jing, C. He, X. Liu, C. Duan, *ACS Catal.* **2018**, *8*, 1384–1391.

Résumé en français

TABLE DES MATIERES

1. Objectifs et contexte général du travail de thèse	-i-
1.1. <i>Les propargylamines</i>	<i>-i-</i>
1.2. <i>Les zéolithes</i>	<i>-ii-</i>
2. Résultats et discussions	-iv-
2.1. <i>Synthèse de propargylamines</i>	<i>-iv-</i>
2.2. <i>Applications en synthèse des propargylamines</i>	<i>-xiii-</i>
3. Conclusion générale	-xvii-
4. Références	-xviii-

1. Objectifs et contexte général du travail de thèse

L'objectif principal de cette thèse est de développer des procédures plus vertes pour la synthèse de propargylamines et leurs dérivés à l'aide de zéolithes dopées aux métaux comme catalyseurs hétérogènes. Plusieurs approches basées sur des réactions multicomposants ont été envisagées pour la synthèse de propargylamines (*voir partie 2.1*) et leur application en synthèse a également été évaluée pour la construction d'hétérocycles d'intérêt *via* des réactions à haute économie d'atomes (*voir partie 2.2*). Pour toutes ces méthodologies catalysées par des zéolithes métallées, la recyclabilité du catalyseur a été examinée.

Avant de résumer les résultats obtenus, voici une brève présentation des propargylamines (*voir partie 1.1*) et des zéolithes (*voir partie 1.2*), qui sont les deux pierres angulaires de mon travail de thèse.

1.1. Les propargylamines

Les propargylamines, constituées d'un groupe amino en position β d'une triple liaison carbone-carbone $C\equiv C$ (**Figure 1**), sont d'un grand intérêt en chimie organique et chimie médicinale.^[1] Le motif propargylamine est effectivement présent et essentiel dans diverses molécules d'intérêt biologique. On peut notamment citer la dynémicine A (**Figure 1a**), un ènediène naturel reconnu pour son potentiel anticancéreux, mais également la pargyline, la rasagiline et la sélégiline, trois agents actifs d'origine synthétique actuellement sur le marché (**Figure 1b**). Il a été démontré que ces trois petites molécules avaient des propriétés neuroprotectrices en agissant comme analogues de substrat pour les enzymes monoamine oxydase (MAO).^[2] Par conséquent, elles sont utilisées pour traiter les maladies neurodégénératives, telles que les maladies de PARKINSON et D'ALZHEIMER.

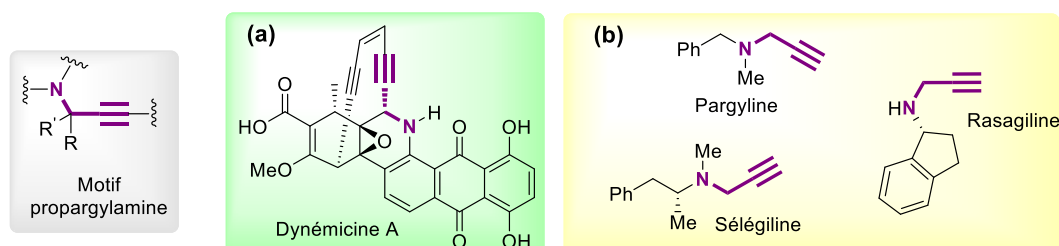


Figure 1. Le motif « propargylamine » et des exemples de molécules (A) naturelles et (B) synthétiques bioactives.

La présence simultanée du groupe amino et de la triple liaison $C\equiv C$ confère aux propargylamines une réactivité chimique unique et exploitable pour une grande variété de réactions chimiques. Les propargylamines ont ainsi été employées avec succès comme intermédiaires versatiles permettant la synthèse d'une multitude de composés de complexité moléculaire très variée, comme notamment les allènes ou divers *N*-hétérocycles (**Figure 2**). Les propargylamines représentent donc des intermédiaires clés dans la synthèse de produits naturels et thérapeutiques.

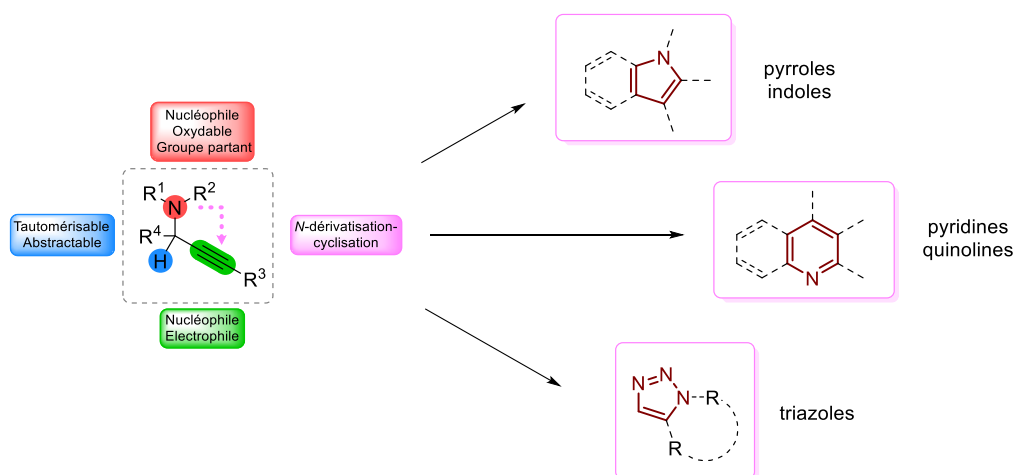
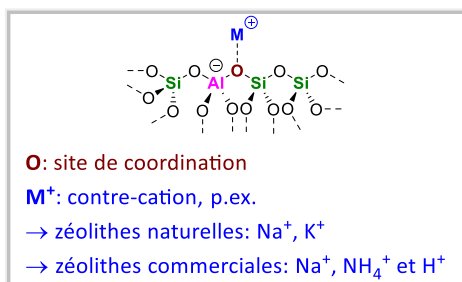


Figure 2. Réactivité des propargylamines et exemples d'applications synthétiques.

1.2. Les zéolithes

Étant donné leur grand intérêt, des procédures de synthèse durables s'inscrivant dans le contexte de la chimie verte^[3] sont nécessaires pour accéder aux propargylamines. Outre la réduction des déchets ainsi que la conception de synthèses plus courtes et à haute économie d'atomes, la catalyse joue un rôle clé dans la synthèse verte et durable.^[4] La catalyse est souvent menée par des métaux de transition qui permettent souvent la construction de structures moléculaires complexes et à haute valeur ajoutée dans des conditions douces et chimiosélectives à partir de réactifs simples.^[5,6] L'utilisation des métaux de transition comme catalyseur a ainsi permis la découverte de nouvelles réactions et la mise en lumière de nouvelles réactivités permettant la synthèse de nombreuses classes de molécules organiques, dont les propargylamines. Néanmoins, l'extraction et la purification de ces métaux sont des processus polluants et énergivores. De plus, les ressources de ces métaux de transition sont limitées ce qui est inévitablement reliée à une hausse de leur coût au fil du temps. Une stratégie visant à diminuer les impacts négatifs associés à l'exploitation des métaux en catalyse, et ainsi augmenter la durabilité des procédés, consiste à supporter les espèces métalliques catalytiquement actives sur des matériaux intrinsèquement sûrs, stables et récupérables. Les zéolithes, qui sont des aluminosilicates cristallins naturels ou synthétiques, répondent à ces critères (**Figure 3**). Jusqu'à présent, 248 structures zéolithiques distinctes ont été décrites dans la littérature avec notamment de nombreuses topologies différentes. Ces matériaux hautement microporeux présentent des grandes surfaces spécifiques (SSA, > 400 m²/g) et sont commercialement accessibles en grande quantité et à bas prix (< 1€/g).



	Les zéolithes les plus étudiées (The "Big Five")				
Nom	Mordenite	Y	beta	Ferrierite	ZSM-5
Code	MOR	FAU	BEA	FER	MFI
Topologie	Canal	Cage	Canal	Canal	Canal
Pore (Å)	6.5 × 7.0 3.4 × 3.8	7.4 × 7.4	7.6 × 6.4 5.5 × 5.5	4.2 × 5.4 3.5 × 4.8	5.1 × 5.5 5.3 × 5.6
SSA (m ² /g)	~450	~600	~700	~400	~400
Prix	0.25 €/g chez Zeolyst International®				

Figure 3. Structure simplifiée d'une zéolithe (gauche) et caractéristiques clés de zéolithes courantes (droite).
SSA : surface spécifique (SSA de l'anglais « specific surface area »).

Leurs nombreuses propriétés ajustables, comme la forme (canaux ou cages) et la taille des pores (< 20 Å), mais aussi le nombre de pores et la localisation de sites actifs, permet d'envisager la conception et l'élaboration à façon d'un catalyseur hautement performant pour une application ciblée. En vue de ces propriétés attractives, les zéolithes sont utilisées en tant que support pour immobiliser des espèces métalliques exploitables en catalyse.

L'une des stratégies les plus fréquemment utilisées pour la préparation de zéolithes métallées est l'échange de cations compensant la charge négative de la charpente aluminosilicate chargée négativement. Une distinction générale est faite entre une réaction d'échange d'ions en milieux aqueux et une réaction d'échange d'ions à l'état solide (Figure 4).^[7] Ces zéolithes métallées se sont déjà révélées être des catalyseurs polyvalents pour de nombreuses transformations de chimie organique, avec dans la plupart des cas le bénéfice associé à leur facilité de récupération et de réutilisation/recyclage.^[8]

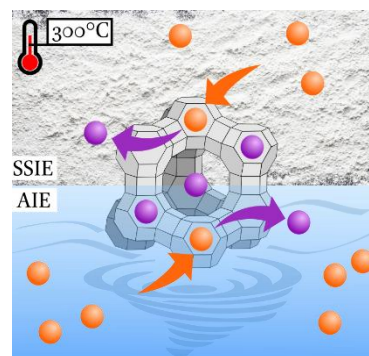


Figure 4. Représentation graphique de l'échange de cations en milieux aqueux (AIE) ou par échange solide-solide (SSIE).

Au cours de ces travaux de thèse, l'accent sera mis sur une zéolithe métallée particulière, la Cu^I-USY, qui s'est avérée particulièrement efficace en tant que catalyseur dans des transformations organiques antérieures.^[8] D'un point de vue pratique, la Cu^I-USY se prépare facilement par échange solide-solide à partir d'un mélange de H-USY et de CuCl, qui est chauffé à 350 °C pendant trois jours sous diazote (Schéma 1).^[9] La charge finale en cuivre, déterminée par ICP-AES, est d'environ 3 mmol/g, ce qui correspond à un taux d'échange d'environ 80%.

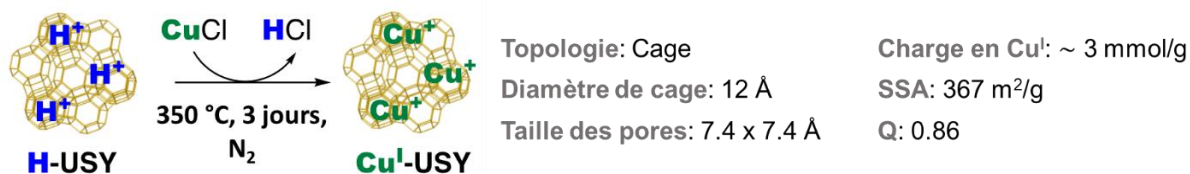


Schéma 1. Préparation par échange solide-solide et caractéristiques clés de la Cu^I-USY.

SSA: surface spécifique (660 m²/g pour H-USY). Q: cristallinité (1.0 pour H-USY).

2. Résultats et discussions

Cette partie résume dans un premier temps les résultats qui ont été obtenus concernant les différentes méthodologies étudiées pour la synthèse des propargylamines (*partie 2.1*). Dans un second temps sera présentée l'exploitation synthétique des propargylamines qui a été développée pour accéder à des molécules plus élaborées de type 1,2-dihydropyridine et isoquinuclidine (*partie 2.2*).

2.1. Synthèse de propargylamines

2.1.1. Via des réactions de couplage « carbonyle-amine-alcyne »

2.1.1.1. Couplage « cétone-amine-alcyne » catalysé par la zéolithe Cu^I-USY

Compte tenu de leur intérêt, plusieurs approches synthétiques ont vu le jour pour la préparation efficace de propargylamines.^[1] Parmi celles-ci, la réaction de couplage « carbonyl-amine-alcyne » à trois composants catalysée par les métaux de transition représente la méthode la plus simple et la plus 'verte', avec une excellente économie d'atomes et la formation d'eau comme seul sous-produit (**Schéma 2**). Dans un premier temps, la réaction de couplage « Aldéhyde-Amine-Alcyne » (A³), conduisant à la formation de propargylamines α -primaires et -secondaires (avec R² = H), est apparue.^[10,11] Le remplacement de l'aldéhyde par une cétone, donnant lieu à la réaction dite « Cétone-Amine-Alcyne » (KA² de l'anglais « Ketone-Amine-Alkyne »), est apparue comme une évolution attrayante permettant l'accès à des propargylamines α -tertiaires (R¹, R² \neq H).^[12]

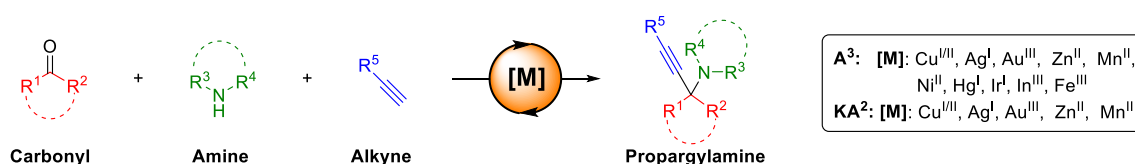


Schéma 2. La réaction de couplage « Cétone-Amine-Alcyne » (KA²) métallocatalysée.

Historiquement, KARLEN *et coll.* ont rapporté dès 1970 la préparation de propargylamines dérivées de *N*-alcynyl succinimides *via* l'utilisation de CuCl en quantité catalytique (2 mol%) en présence d'acide acétique glacial (2 équivalents) (**Figure 5**).^[13] Bien plus tard, en 1998, RIVERO *et coll.* ont également employé CuCl (10 mol%) dans ce qui est considéré comme la première réaction A³, avec comme alcynes terminaux des alcynes supportés sur des polymères organiques.^[14] Bien que de nombreux autres systèmes catalytiques aient été rapportés au cours des années suivantes, y compris des systèmes à base d'autres métaux de transition tels que l'argent(I)^[15] et l'or(III),^[16] ces systèmes présentaient tous de sévères limitations quant à l'étendue du substrat. Une procédure de couplage A³ assistée par micro-ondes, plutôt universelle et rapide, a été publiée par TU *et coll.* en 2004.^[17] La réaction a été réalisée en présence de CuI (15 mol%) comme catalyseur et avec l'eau comme solvant. Ces conditions ont permis d'accéder

à diverses propargylamines à partir d'aldéhydes et d'alcynes terminaux aromatiques et aliphatiques, ainsi que d'amines secondaires aliphatiques, de *t*-butylamine et d'aniline avec de bons à d'excellents rendements (41-93%). Dans le but d'augmenter la durabilité de cette réaction attrayante à trois composants, l'équipe de PALE a employé avec succès diverses zéolithes dopées en cations cuivreux, dont la Cu^I-USY, comme catalyseurs réutilisables en absence de solvant.^[18]

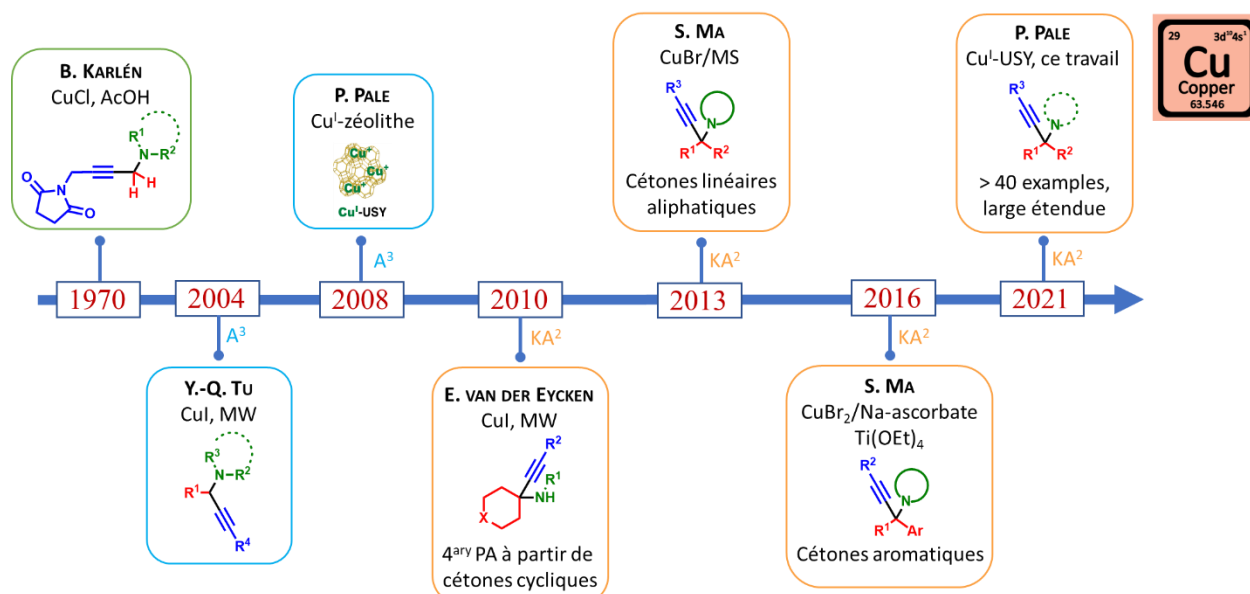


Figure 5. Une sélection chronologique de réactions de couplage entre un dérivé carbonylé, une amine et un alcyne terminal catalysées par le cuivre.

L'une des premières procédures de couplage KA², impliquant une cétone comme partenaire de couplage à la place d'un aldéhyde, a été rapportée en 2010 par l'équipe de VAN DER EYCKEN avec CuI (20 mol%) comme catalyseur et les micro-ondes comme méthode d'activation (Figure 5).^[19] Alors que la procédure de VAN DER EYCKEN a permis la formation de diverses propargylamines dérivées de cétones aliphatiques cycliques et d'amines primaires, les cétones linéaires se sont avérées être des partenaires de couplage beaucoup moins performants. Pour surmonter cette limitation, l'équipe de MA a décrit en 2013 des conditions efficaces reposant sur la combinaison de CuBr (2.5 mol%) et de tamis moléculaire ; dans ces conditions, le couplage KA² s'est montré efficace pour la formation de diverses propargylamines à partir de cétones linéaires et d'amines secondaires cycliques.^[20] L'équipe de MA s'est également intéressée au développement de conditions permettant le couplage KA² de cétones aromatiques, autres cétones dont la réactivité représente un challenge pour ce type de couplage.^[21] En 2016, ils ont ainsi montré qu'une combinaison de CuBr₂, d'ascorbate de sodium et de Ti(OEt)₄ permet d'employer les cétones aromatiques comme partenaires de couplage KA². Ces conditions originales ont d'ailleurs permis d'obtenir des produits KA² auparavant inaccessibles (21 exemples, rendement de 27-96%). Il convient néanmoins de mentionner que seules la pyrrolidine et la pipéridine ont été employées avec succès, tandis que les amines secondaires acycliques ou les amines primaires étaient incompatibles. Bien que des catalyseurs supportés aient été rapportés, la portée

du substrat est souvent très limitée, avec l'utilisation dans la plupart des cas uniquement de cétones cycliques ou d'amines cycliques secondaires.^[15,16,22,23]

Comme la Cu^I-USY s'est avéré être un catalyseur supporté performant pour la réaction de couplage A³,^[18] le champ d'application de cette réaction à trois composants a été étendu avec succès à l'utilisation de cétones (KA²) pour accéder à plus de 40 exemples de propargylamines α -tertiaires avec des rendements allant de 16 à 95%, et ceci à partir de divers types d'alcynes comme partenaires nucléophiles (**Schéma 3**). En effet, en plus des alcynes usuels que sont les alcynes aromatiques et aliphatiques terminaux, les acides alcynoïques et le triméthylsilylacétylène ont été employés avec succès dans des réactions de type KA² décarboxylante et désilylante, respectivement.

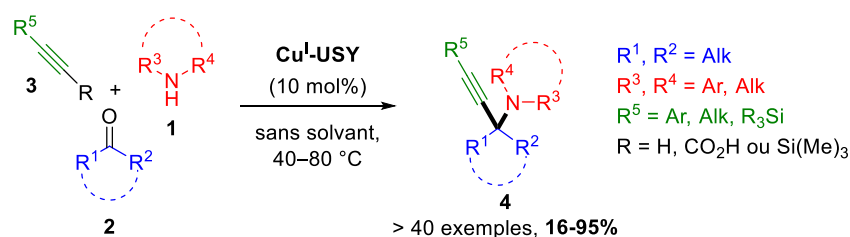


Schéma 3. Synthèse de propargylamines par réaction de couplage de type KA² entre un dérivé carbonylé, une amine et un alcyne catalysée par Cu^I-USY.^[24]

En ce qui concerne la réaction KA² classique avec des alcynes terminaux, des exemples illustratifs de l'étendue du champ d'application de la méthode sont donnés en **Figure 6**. Concernant le partenaire alcyne, plusieurs alcynes (hétéro)aromatiques (produits **4a,b**), ainsi que des alcynes aliphatiques (**4c**) ont été efficaces comme partenaires de couplage. De plus, l'emploi du (triisopropylsilyl)acétylène a conduit à la formation de la propargylamine **4d** avec un excellent rendement de 90 %. Dans le cas des amines, plusieurs amines primaires diversement fonctionnalisées ont été évaluées dont celles fournissant les propargylamines **4e** et **4f** avec d'excellents rendements. Il est à noter que bien que les anilines ont été rapportées comme partenaires performants pour les réactions de couplage A³, aucun exemple efficace n'a été rapporté jusqu'à présent dans le cas de la réaction KA², les anilines conduisant généralement à des mélanges réactionnels complexes. Nous avons ainsi appliqué nos conditions catalytiques à l'aniline, et à notre grande surprise, nous avons observé la formation de la propargylamine **4h** correspondante, avec un rendement toutefois modeste de 36%. Nous avons également soumis la 4-fluoroaniline et la 4-méthoxyaniline dans les conditions de couplage afin d'évaluer d'éventuels effets électroniques. Alors que la propargylamine **4g** a été obtenue avec la 4-fluoroaniline avec une meilleure efficacité que **4h**, la 4-méthoxyaniline a été entièrement consommée mais a conduit à un mélange complexe dans lequel aucune trace de la propargylamine **4i** désirée n'a été détectée. En bref, plus l'aniline est appauvrie en électrons (donc moins elle est nucléophile), plus le couplage KA² est efficace. En plus de la cyclohexanone, d'autres cétones cycliques ont

été évaluées avec succès, dont notamment celles ayant conduit à la formation efficace des propargylamines **4j** et **4k**. Ces deux derniers exemples mettent en avant la tolérance de nos conditions de couplage vis-à-vis de groupes protecteurs acidolabiles comme le Boc ou le 1,3-dioxolane. Comme généralement observé dans ce type de couplage, les cétones aliphatiques acycliques, ne libérant aucune contrainte énergétique au cours des réactions d'addition, se sont également révélées moins réactives dans nos conditions. Augmenter la température à 110 °C et la charge catalytique à 20 mol% a néanmoins permis de préparer la propargylamine **4l** avec un rendement tout-à-fait honorable de 53%. Les cétones aromatiques, considérées comme les cétones les moins réactives pour la réaction KA², ne se sont pas avérées plus réactives dans nos conditions, avec par exemple la propargylamine **4m** dérivée de l'acétophénone formée seulement à l'état de traces.

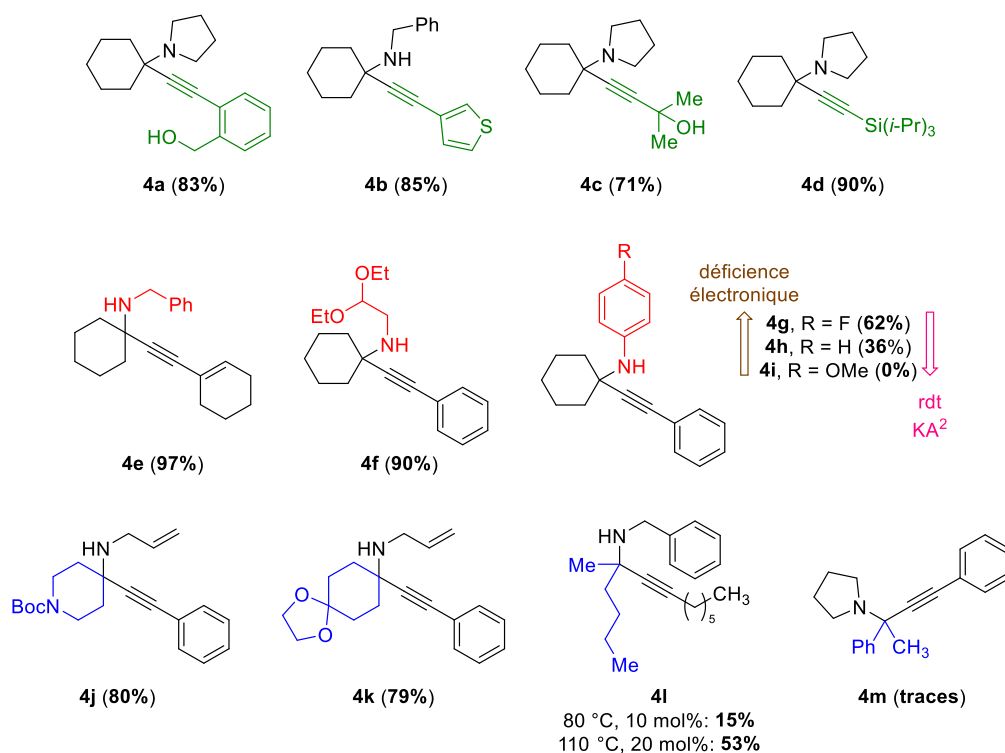


Figure 6. Sélection d'exemples de propargylamines **4** obtenues par la réaction KA² catalysée par la Cu^I-USY. Conditions réactionnelles : cétone (1.0 mmol, 1 eq.), amine (1.0 mmol, 1 eq.), alcyne (1.5 mmol, 1.5 eq.), Cu^I-USY (10 mol%), sans solvant, 80 °C, 18 h.

Une étude de recyclabilité a montré que le catalyseur zéolithique pouvait être facilement récupéré et réutilisé plusieurs fois dans la réaction KA² (**Figure 7**). Cette étude a néanmoins mis en avant une érosion progressive de l'activité catalytique du matériau, en particulier lors du Run 5 où le rendement du couplage chute à 48%. L'analyse ICP-AES du matériau récupéré après le Run 5 a ainsi révélé que la teneur en cuivre du catalyseur Cu^I-USY a diminué au fil des réactions, avec environ 60% de sa charge initiale.

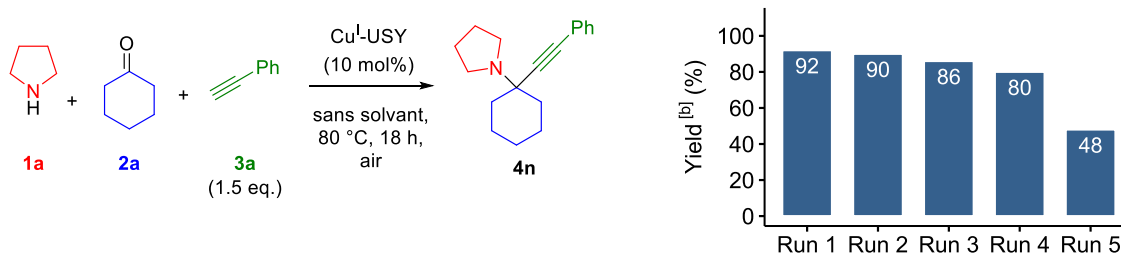


Figure 7. Étude de la recyclabilité de la Cu^I-USY dans la réaction KA².^[a]

^[a] Entre chaque réaction (« Run »), la zéolithe a été lavée avec des solvants organiques, puis séchée sous vide. La zéolithe a été réengagée sans calcination entre chaque réaction. ^[b] Rendement (« Yield ») estimé *via* RMN ¹H du brut réactionnel avec le 1,3,5-triméthoxybenzène comme étalon interne.

Nous avons également développé une version décarboxylante de la réaction KA², version dans laquelle le partenaire alcyne terminal est remplacé par le dérivé carboxylé correspondant, c'est-à-dire un alcyne alcynoïque (**Schéma 4**). En plus d'avoir amélioré la performance de certains couplages (notamment dans le cas des amines secondaires), cette version décarboxylante a également permis l'incorporation de fragments alcynes à 2 ou 3 atomes de carbone. Dans ce cas, l'acide alcynoïque joue le rôle d'équivalent liquide ou solide d'un alcyne terminal gazeux, ce qui simplifie le montage expérimental et la manipulation des matières premières. Grâce à cette version, les propargylamines **4o** et **4p** ont pu être obtenues de manière efficace, *via* l'emploi d'acide but-2-ynoïque (**3b**) et d'acide but-2-yndioïque (**3c**) comme équivalents solides du propyne et de l'acétylène gazeux respectivement.

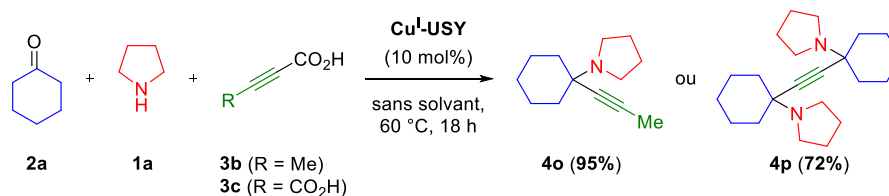


Schéma 4. Incorporation effective et efficace de fragments d'alcynes à 2 ou 3 atomes de carbones par une réaction KA² décarboxylante.

Enfin, une version désilylante, avec du triméthylsilylacétylène (**3d**) comme équivalent de l'acétylène gazeux, a été développée et a permis d'accéder à la propargylamine terminale **4q** avec un rendement intéressant de 58% (**Schéma 5**). Nous avons ensuite envisagé d'exploiter la réactivité du fragment alcyne terminal ainsi généré dans des processus 'one-pot' et de manière avantageuse, nous avons pu montrer que cette version désilylante peut être combinée à d'autres transformations catalysées par le cuivre(I). Ainsi, nous avons démontré la faisabilité de plusieurs processus 'one-pot', comme par exemple un processus KA²/A³ (→ **4r**) ainsi qu'un processus KA²/formation d'azoture/CuAAC (→ **4s**) en l'absence de solvant ou en milieu aqueux.^[25]

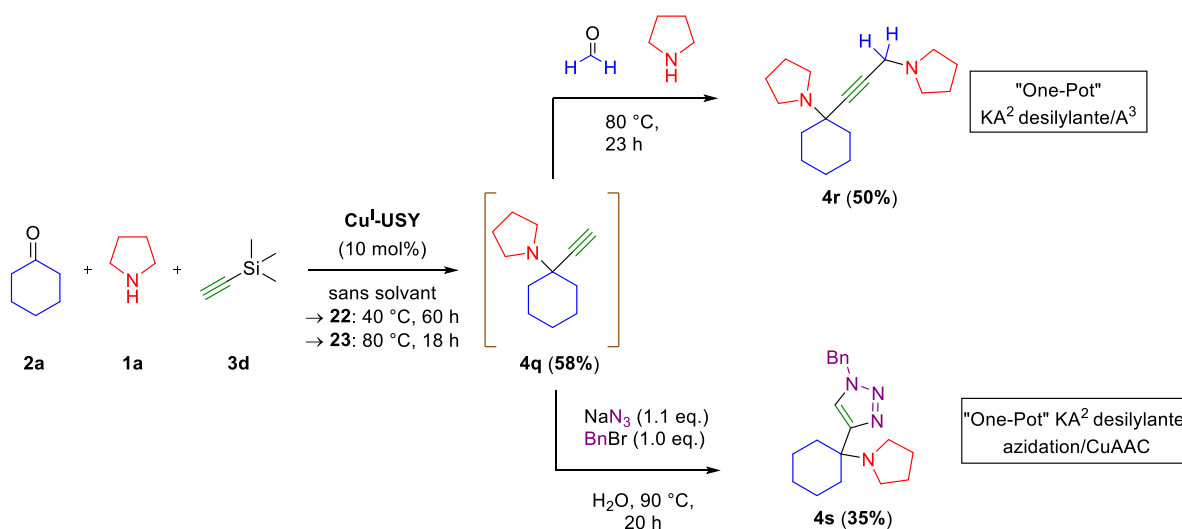


Schéma 5. Formation d'une propargylamine terminale par réaction KA² désilylante et exploitation de l'alcyne terminal résultant dans des processus 'one-pot'.

2.1.1.2. Couplage « carbonyle-ynamide-amine » catalysé par la Cu^I-USY

En 2013, l'équipe de HSUNG a rapporté une méthode de synthèse de γ -amino-ynamides qui constituent une classe de propargylamines à haut potentiel synthétique.^[26] Cependant, le potentiel synthétique de tels ynamides reste sous-exploité, sans doute car peu de méthodes faciles à mettre en œuvre sont à disposition. Alors que la méthode de HSUNG^[26] nécessite de travailler à basse température ($-50\text{ }^{\circ}\text{C}$) dans le THF avec un excès d'un des réactifs, seule une autre méthode catalytique^[27] avec un champ d'application restreint a été décrite jusque-là.

Dans ce contexte, développer une méthode simple et efficace d'accès aux γ -amino-ynamides serait donc d'intérêt. C'est pourquoi et dans la continuité de notre travail sur la réaction A³ et KA² mentionnée précédemment,^[18,24] nous avons décidé d'évaluer pour la première fois le potentiel d'ynamides terminaux comme substitués d'alcynes terminaux dans cette réaction à trois composants. Nos premiers tests ont rapidement démontré la faisabilité de cette nouvelle approche d'accès aux γ -amino-ynamides. Après optimisation des conditions réactionnelles, il est apparu que les meilleures conditions consistent en la réaction de l'ynamide terminal, du dérivé carbonylé et de l'amine dans des quantités stœchiométriques à température ambiante dans l'acétate d'éthyle comme solvant ou en l'absence de solvant (Schéma 6).^[28] Comparée aux méthodes précédemment décrites,^[26,27] cette procédure catalytique employant la Cu^I-USY est clairement plus facile à mettre en œuvre et plus économique en termes d'atomes et d'étapes, avec comme seul sous-produit l'eau.

Par rapport aux versions A³ et KA²,^[18,24] nous avons montré que cette version tolère une plus grande gamme de dérivés carbonylés, comme notamment des aldéhydes (hétéro)aromatiques et aliphatiques, ainsi que des cétones aliphatiques cycliques et linéaires. A noter que diverses amines aliphatiques secondaires se sont également avérées être des partenaires de couplage

efficaces. En revanche, les amines primaires ont conduit à des mélanges réactionnels complexes en raison de l'hydroamination et de l'oligomérisation compétitives et/ou la faible électrophilie de l'imine intermédiaire. En ce qui concerne les ynamides, nous avons principalement validé l'efficacité des ynesulfonamides mais les carbamates et lactames cycliques ont également permis d'obtenir les γ -amino-ynamides désirés.

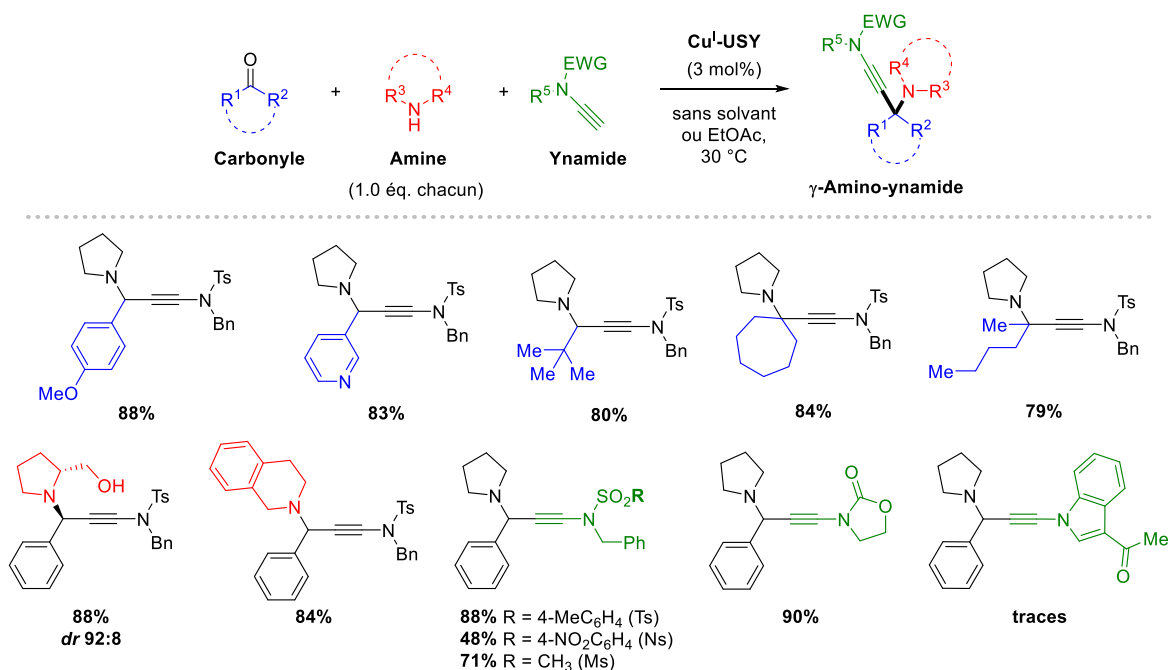


Schéma 6. Extension de la méthodologie A^3/KA^2 aux ynamides terminaux comme substitués d'alcynes.

Il est intéressant de mentionner que les halogénures de cuivre, couramment utilisés pour catalyser les versions A^3 et KA^2 usuelles, se sont avérés beaucoup moins performants avec une chimiosélectivité largement diminuée. Grâce à la haute chimiosélectivité observée, le $\text{Cu}^{\text{I}}\text{-USY}$ apparaît donc comme le catalyseur de choix pour cette nouvelle réaction à trois composants. Nous avons également effectué un test de SHELDON au cours duquel la conversion complète des partenaires du couplage a été observée après filtration du catalyseur, ceci suggérant un lessivage du cuivre dans les conditions de la réaction. Néanmoins, la zéolithe récupérée après réaction maintient une activité catalytique, mais une érosion progressive de celle-ci a été observée lors de l'étude de la recyclabilité (Figure 8).

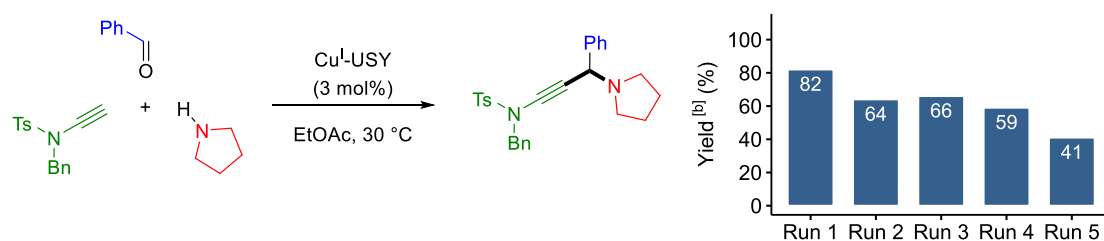


Figure 8. Étude de la recyclabilité de la $\text{Cu}^{\text{I}}\text{-USY}$ dans la réaction AYA (Aldéhyde-Ynamide-Amine).^[a]

^[a] Entre chaque réaction (« Run »), la zéolithe a été lavée à l'acétate d'éthyle et puis a été réengagée directement dans la prochaine réaction. ^[b] Rendement (« Yield ») estimé *via* RMN ^1H du brut réactionnel avec le 1,3,5-triméthoxybenzène comme étalon interne.

2.1.2. Via une séquence one-pot hydroamination/protonation/addition d'alcyne

En parallèle, nous avons également étudié une stratégie complémentaire pour accéder aux propargylamines *via* une séquence 'one-pot' hydroamination-protonation-addition d'alcyne (HPA) (Schéma 7). Plusieurs métaux ou combinaisons métalliques ont été rapportés pour catalyser de manière efficace cette séquence, avec des exemples inter- mais également intramoléculaires. D'un point de vue mécanistique, cette réaction en cascade démarre par l'hydroamination d'un alcyne terminal pour donner une énamine intermédiaire qui après protonation, conduit à la formation d'un ion aldiminium ou kétiminium intermédiaire, selon la régiosélectivité de l'hydroamination. L'intermédiaire électrophile ainsi généré subit finalement l'addition nucléophile d'un acétylure métallique pour donner la propargylamine (PA) α -tertiaire ou α -secondaire. Cette méthode peut donc être considérée comme une stratégie alternative aux réactions A³/KA² où le partenaire « carbonyle » est remplacé par un second équivalent d'alcyne.

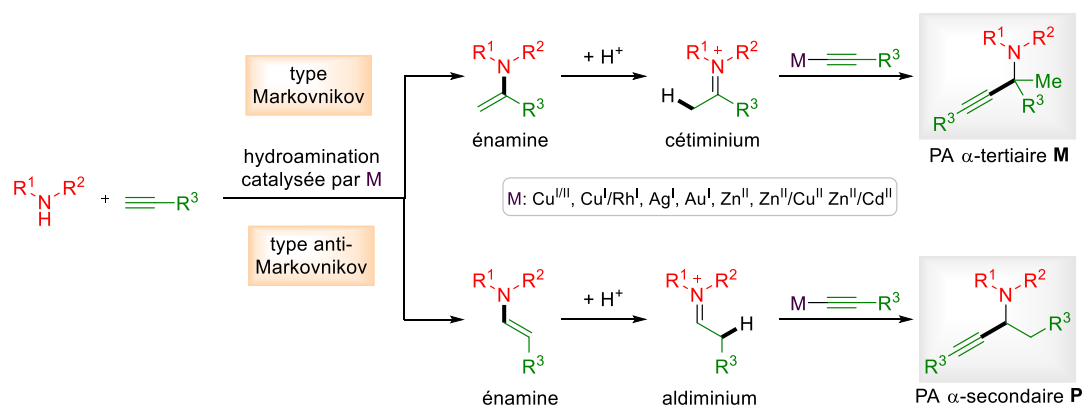


Schéma 7. Synthèse de propargylamines par réaction HPA.

Les conditions de réaction en présence de la Cu^I-USY comme catalyseur ont été optimisées à l'aide de plans d'expériences en utilisant la réaction entre la pyrrolidine et le phénylacétylène comme réaction modèle (Figure 9). Il est intéressant de noter que nous avons identifié un impact significatif de la vitesse d'agitation et du type de barreau aimanté sur le rendement global des produits HPA. De plus, la température et le nombre d'équivalents d'alcynes se sont avérés être des facteurs critiques pour la performance de la réaction en termes de rendement. Quant à la régiosélectivité, il est apparu qu'elle est principalement contrôlée par la température, avec une sélectivité décroissante pour le produit anti-MARKOVNIKOV lorsque la température augmente. Ceci met en évidence un effet opposé de la température sur le rendement HPA et l'excès du produit anti-MARKOVNIKOV.

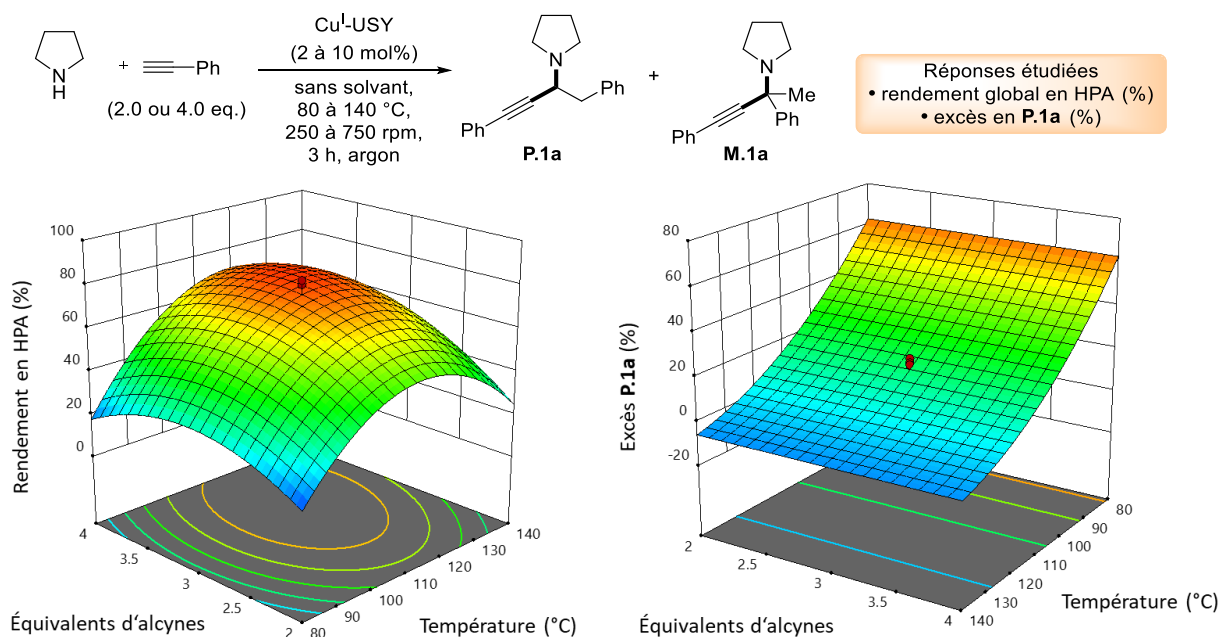


Figure 9. Gauche : surface 3D du modèle quadratique pour le rendement en produits HPA (P.1a + M.1a). Droite : surface 3D du modèle quadratique pour l'excès en P.1a.

Notre étude a démontré que les deux régioisomères **P.1a** et **M.1a** sont accessibles et que les rendements globaux avec la Cu^{I} -USY comme catalyseur sont compétitifs avec les conditions homogènes rapportées (**Schéma 8**). A notre connaissance, notre méthode représente la première version employant un catalyseur supporté. Des résultats préliminaires ont montré que la régiosélectivité est fortement influencée par la température de réaction pour les alcynes aromatiques. Ces derniers favorisent généralement la formation de propargylamines α -secondaires **P**, mais la régiosélectivité est également impactée par des effets électroniques. En effet, la présence de groupements fortement électroattracteurs permet d'accéder sélectivement aux propargylamines α -secondaires **P**, alors que des substituants de plus en plus électrodonneurs induisent une proportion croissante du régioisomère α -tertiaire **M**.

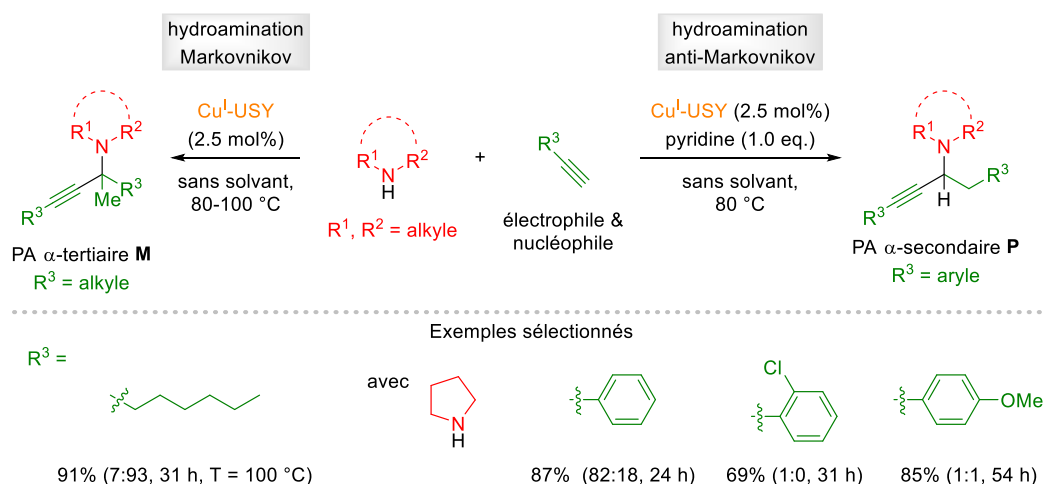


Schéma 8. Synthèse de propargylamines par hydroamination d'alcynes catalysée par la Cu^{I} -USY.
Ratio P/M estimé *via* RMN ^1H du brut réactionnel.

Un test de SHELDON a révélé que la catalyse a lieu au moins partiellement en solution car nous avons observé qu'après filtration du catalyseur à chaud (« Filtered after 7 h »), la conversion des réactifs se poursuit à un niveau comparable à celui d'une réaction non traitée (Figure 10). Néanmoins, une étude de recyclabilité a montré que la Cu^I-USY récupérée donne un rendement plus élevé à partir du deuxième Run (Figure 11). A noter enfin qu'un rendement et un rapport **P.1a/M.1a** stables ont été obtenus jusqu'au sixième Run.

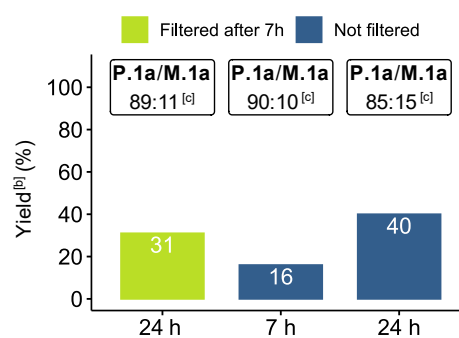


Figure 10. Test de SHELDON avec la Cu^I-USY pour la réaction HPA entre la pyrrolidine et le phénylacétylène.

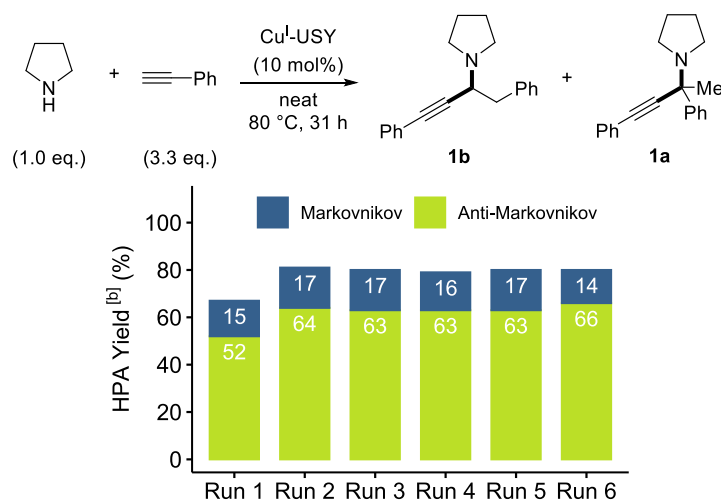


Figure 11. Etude de la recyclabilité de la Cu^I-USY dans la réaction HPA.^[a]

^[a] Entre chaque réaction (« Run »), la zéolithe a été lavée au dichlorométhane, puis séchée sous vide. La zéolithe a été réengagée sans calcination entre chaque réaction. ^[b] Rendement (« Yield ») estimé *via* RMN ¹H du brut réactionnel avec le 1,3,5-triméthoxybenzène comme étalon interne.

2.2. Applications en synthèse des propargylamines

2.2.1. Synthèse de 1,2-dihydropyridines

Dans le but de valoriser et exploiter la réactivité des propargylamines préparées par notre procédure KA² à partir d'amines primaires (voir Schéma 3 partie 2.1.1.1), nous avons décidé d'évaluer le potentiel catalytique de la Cu^I-USY dans la cycloisomérisation de 3-*aza*-1,5-énynes, facilement accessibles à partir de propargylamines (Schéma 9). Les 3-*aza*-1,5-énynes peuvent être obtenus par addition nucléophile d'une propargylamine sur un ester propynoïque *via* une réaction d'*aza*-MICHAEL (première étape du Schéma 9). Une étude de solvants a été réalisée afin d'optimiser la réaction d'*aza*-MICHAEL. Parmi les solvants évalués, l'acétate d'éthyle s'est avéré prometteur car à 100 °C, la réaction s'est généralement déroulée de manière sélective et a fourni l'ényne souhaitée avec un rendement quantitatif sans qu'il soit nécessaire de procéder à une purification. Néanmoins, les temps de réaction nécessaires pour que la

conversion soit complète étaient d'au moins 24 heures en utilisant deux équivalents de propiolate d'éthyle. Cette performance a pu être largement améliorée en réalisant la réaction dans des solvants protiques, comme l'éthanol, le butan-1-ol et l'alcool *t*-amylique. En effet, l'addition d'*aza*-MICHAEL a été largement favorisée dans ces solvants, permettant d'accéder quantitativement aux énynes en quelques minutes/heures avec un seul équivalent de propiolate d'éthyle.

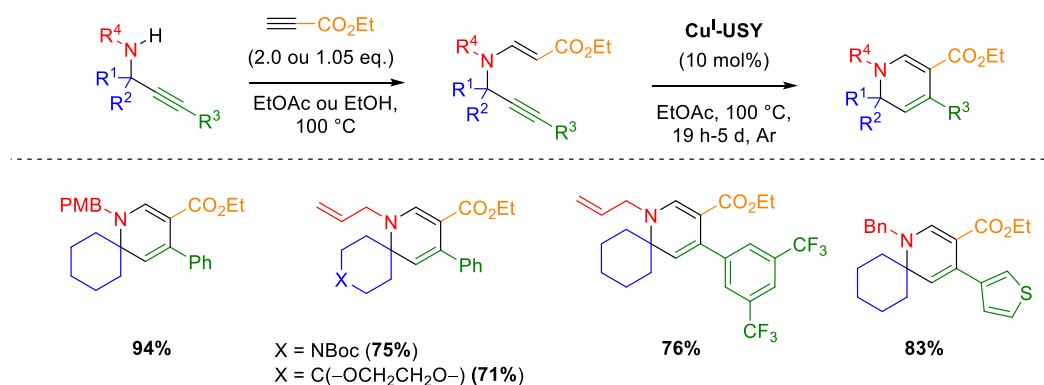


Schéma 9. Synthèse de 1,2-dihydropyridines par cycloisomérisation de 3-*aza*-1,5-énynes catalysée par la Cu^I-USY.

La réaction de cycloisomérisation a alors été examinée et les conditions optimales que nous avons identifiées consistent à réaliser la réaction dans l'acétate d'éthyle à 100 °C en présence d'une quantité catalytique de Cu^I-USY (10 mol%) (seconde étape du **Schéma 9**). Diverses énynes ont alors été soumises à ces conditions réactionnelles, ce qui a permis la synthèse efficace de nombreuses 1,2-dihydropyridines, avec en particulier des dérivés 1-azaspirocycliques comme ceux représentés sur le **Schéma 9**. A noter également que nous avons observé que les conditions de cycloisomérisation tolèrent une large gamme de groupes fonctionnels. En effet, plus d'une trentaine de 1,2-dihydropyridines diversement fonctionnalisées/substituées au niveau de l'atome d'azote, de la position propargylique mais aussi au niveau de l'alcyne dans les énynes correspondantes, ont ainsi été préparés de manière efficaces. Comme limitations, nous pouvons néanmoins mentionner que les énynes dérivés d'alcyne aliphatiques ont conduit à la formation de mélanges complexes mais aussi que certains substrats ont nécessité plusieurs jours de réaction pour cycloisomériser totalement. De plus, nous avons montré que la formation de la 1,2-dihydropyridine peut être effectuée de manière séquentielle en 'one-pot' à partir de la propargylamine sans isoler l'ényne intermédiaire. Cette séquence 'one-pot' est faisable dans l'acétate d'éthyle en utilisant un équivalent de propiolate.

Dans ce cas, le caractère hétérogène du système catalytique a été évalué avec succès par un test de SHELDON (**Figure 12**, gauche). En effet, contrairement aux applications précédentes (i.e., KA², AYA/KYA, HPA) impliquant des amines nucléophiles, la filtration du catalyseur a conduit à l'arrêt de la réaction. De plus, nous avons montré que la Cu^I-USY est recyclable quatre fois sans perte d'activité catalytique (**Figure 12**, droite).

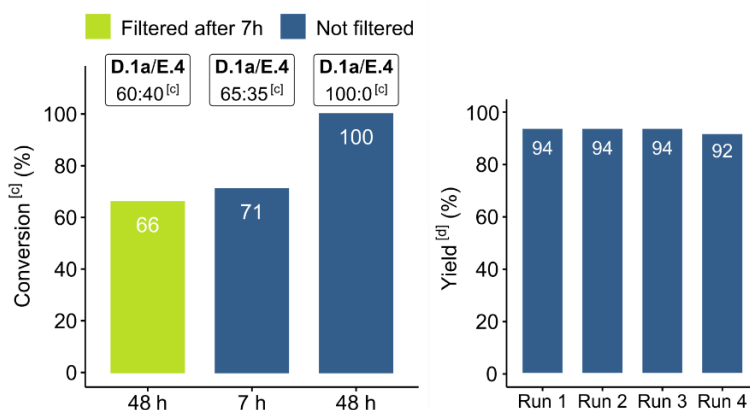
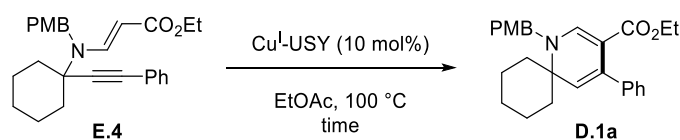


Figure 12. Test de SHELDON^[a] (gauche) et étude de la recyclabilité^[b] de la Cu^I-USY dans la cycloisomérisation de l'ényne **E.4** menant à la dihydropyridine **D.1a**.

^[a] Réactions réalisées dans EtOAc (0.3 M concentration) à 100 °C avec 10 mol% de la Cu^I-USY. ^[b] Réactions réalisées dans EtOAc (1 M) à 100 °C pendant 26 h (pour « Run » 1 à 3). Pour « Run » 4, 83% de conversion a été obtenue après 26 h et une conversion complète après 31 h. ^[c] Les conversions et les ratios **D.1a/E.4** ont été déterminés *via* RMN ¹H du brut réactionnel. ^[d] Rendement (« Yield ») estimé *via* RMN ¹H du brut réactionnel avec le 1,3,5-triméthoxybenzène comme étalon interne.

En plus de la faisabilité ‘one-pot’ de manière séquentielle, des conditions pour une version ‘one-pot’ en cascade ont été élaborées. En effet, la Cu^I-USY (10 mol%) a permis d’accéder à la 1,2-dihydropyridine **D.1a** avec une excellente chimiosélectivité dans l’alcool *t*-amylique à 100 °C en partant de quantités équimolaires de propargylamine et de propiolate d’éthyle (**Schéma 10**). La généralité de cette procédure en cascade doit encore être confirmée à l’aide d’autres exemples. Un premier exemple a d’ailleurs déjà permis de montrer qu’elle peut être étendue à des allénoates en tant qu’électrophile. La 1,2-dihydropyridine tétrasubstituée **D.5e** a ainsi été obtenue avec un rendement prometteur de 85% (**Schéma 10**). Evaluer la faisabilité de cette version en cascade à l’échelle du gramme méritera aussi d’être réalisé.

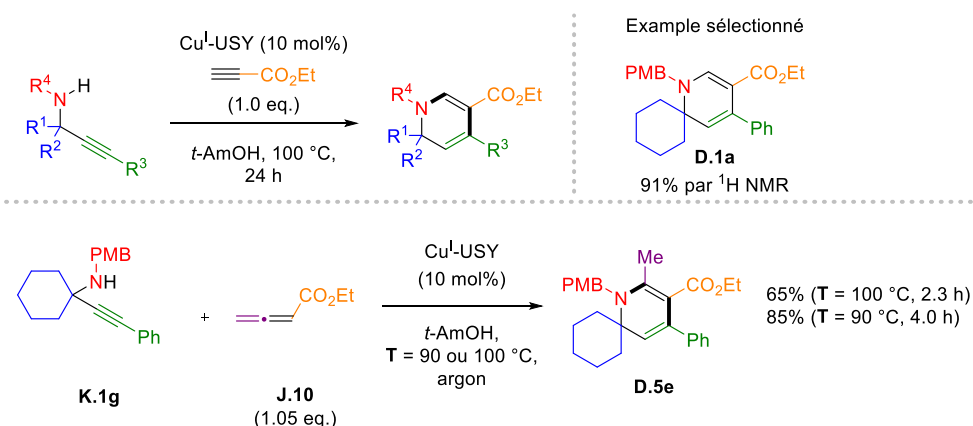


Schéma 10. Synthèse ‘one-pot’ en cascade de 1,2-dihydropyridines catalysée par la Cu^I-USY.

2.2.2. Exploitation de la réactivité des 1,2-dihydropyridines

Les 1,2-dihydropyridines présentent également un intérêt en tant qu'intermédiaire en synthèse organique. Elles servent par exemple de précurseurs pour les pyridines et les pipéridines, mais se sont également avérées être des diènes efficaces pour des cycloadditions [4+2] de DIELS-ALDER. L'utilisation de dihydropyridines *gem*-disubstituées dans de telles réactions est toutefois rare.

Nous avons ainsi montré que le motif 1,3-butadiène de dihydropyridines *gem*-disubstituées peut être exploité dans des réactions de DIELS-ALDER à demande normale avec le *N*-phénylmaléimide pour donner des isoquinuclidines spirocycliques sans précédents (Schéma 11).^[29] La cinétique de la cycloaddition est fortement influencée par la nature du substituant R² en C4. Nous avons également observé une accélération de la cycloaddition en présence de Cu^I-USY (10 mol%) mais des efforts supplémentaires pour substituer le dichlorométhane par une alternative plus verte sont en cours d'investigation. Un résultat particulièrement encourageant a été obtenu avec l'alcool *t*-amylique comme solvant vert, avec l'isoquinuclidine qui a été formée de manière très efficace avec 94% de rendement. Toutefois, une température de 150 °C a été nécessaire pour réduire le temps de réaction à sept heures. D'autres solvants/et ou catalyseurs vont être évalués afin d'accélérer cette réaction dans des conditions plus douces.

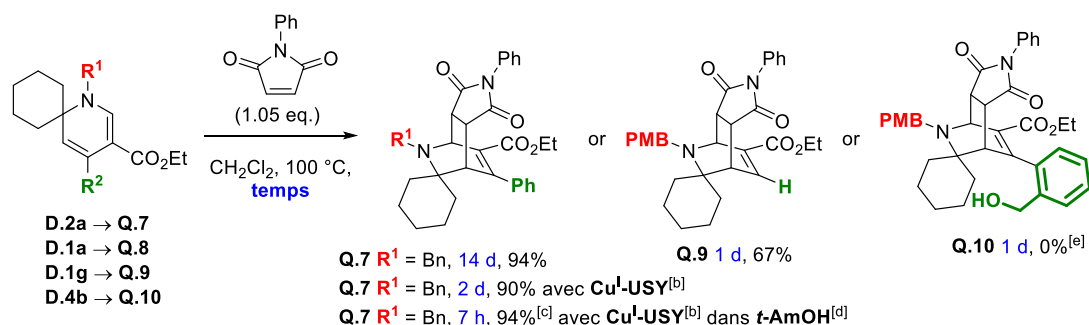


Schéma 11. Effet du substituant R² en C4 d'une 1,2-dihydropyridine spirocyclique sur leur performance dans la cycloaddition de DIELS-ALDER.^[a]

^[a] Réactions réalisées à une concentration de 0.1 M dans des tube scellés avec des rendements isolés, sauf indication contraire.

^[b] 10 mol% Cu^I-USY. ^[c] Rendement estimé *via* RMN ¹H du brut réactionnel avec le nitrométhane comme étalon interne. ^[d] Mélange réactionnel chauffé à 150 °C. ^[e] Aucune conversion observée, même à 120 °C.

3. Conclusion générale

La zéolithe Cu^I-USY s'est avérée être un catalyseur efficace, facile à manipuler et réutilisable pour la synthèse de propargylamines α -tertiaires *via* des réactions de couplage à trois composants de type KA² dans des conditions sans solvant. Cette méthodologie a été étendue avec succès à l'utilisation d'ynamides terminaux comme substitués d'alcynes classiques, représentant ainsi la première approche multicomposante catalytique vers les γ -amino-ynamides portant une amine nucléophile en position γ . En termes d'applications synthétiques, la réactivité de propargylamines porteuses d'une amine secondaire a été exploitée avec succès dans une séquence addition d'*aza*-MICHAEL/cycloisomérisation catalysée par la Cu^I-USY, cette séquence conduisant à la formation de 1,2-dihydropyridines spirocycliques tout-à-fait attrayantes. La présence du motif 1,3-butadiène dans ces 1,2-dihydropyridines a d'ailleurs permis d'accéder *via* une réaction de DIELS-ALDER à des squelettes isoquinuclidines spirocycliques totalement inédits. L'amélioration des conditions de cycloadditions et l'étude de l'étendue de la méthode représentent des perspectives intéressantes.

4. Références

- [1] K. Lauder, A. Toscani, N. Scalacci, D. Castagnolo, *Chem. Rev.* **2017**, *117*, 14091–14200.
- [2] Bhawna, A. Kumar, M. Bhatia, A. Kapoor, P. Kumar, S. Kumar, *Eur. J. Med. Chem.* **2022**, *242*, 114655.
- [3] P. T. Anastas, J. C. Warner, *Green Chemistry: Theory and Practice*, Oxford University Press, Oxford, **1998**.
- [4] P. T. Anastas, M. M. Kirchoff, T. C. Williamson, *Appl. Catal. Gen.* **2001**, *221*, 3–13.
- [5] M. Beller, C. Bolm, *Transition Metals for Organic Synthesis: Building Blocks and Fine Chemicals*, WILEY-VCH, Weinheim, **2008**.
- [6] R. Bates, *Organic Synthesis Using Transition Metals*, John Wiley & Sons, Ltd, Chichester, UK, **2012**.
- [7] J. N. Armor, in *Catal. Unique Met. Ion Struct. Solid Matrices Sci. Appl.* (Eds.: G. Centi, B. Wichterlová, A.T. Bell), Springer Netherlands, Dordrecht, **2001**, pp. 21–29.
- [8] S. Chassaing, V. Beneteau, B. Louis, P. Pale, *Curr. Org. Chem.* **2017**, *21*, 779–793.
- [9] P. Kuhn, P. Pale, J. Sommer, B. Louis, *J. Phys. Chem. C* **2009**, *113*, 2903–2910.
- [10] V. A. Peshkov, O. P. Pereshivko, E. V. Van der Eycken, *Chem. Soc. Rev.* **2012**, *41*, 3790–3807.
- [11] I. Jesin, G. C. Nandi, *Eur. J. Org. Chem.* **2019**, *2019*, 2704–2720.
- [12] L. P. Zorba, G. C. Vougioukalakis, *Coord. Chem. Rev.* **2021**, *429*, 213603.
- [13] B. Karlen, B. Lindeke, S. Lindgren, K. G. Svensson, R. Dahlbom, D. J. Jenden, J. E. Giering, *J. Med. Chem.* **1970**, *13*, 651–657.
- [14] A. B. Dyatkin, R. A. Rivero, *Tetrahedron Lett.* **1998**, *39*, 3647–3650.
- [15] A. Elhampour, M. Malmir, E. Kowsari, F. B. Ajdari, F. Nemati, *RSC Adv.* **2016**, *6*, 96623–96634.
- [16] G. Fernández, L. Bernardo, A. Villanueva, R. Pleixats, *New J. Chem.* **2020**, *44*, 6130–6141.
- [17] L. Shi, Y.-Q. Tu, M. Wang, F.-M. Zhang, C.-A. Fan, *Org. Lett.* **2004**, *6*, 1001–1003.
- [18] M. K. Patil, M. Keller, B. M. Reddy, P. Pale, J. Sommer, *Eur. J. Org. Chem.* **2008**, *2008*, 4440–4445.
- [19] O. P. Pereshivko, V. A. Peshkov, E. V. Van der Eycken, *Org. Lett.* **2010**, *12*, 2638–2641.
- [20] X. Tang, J. Kuang, S. Ma, *Chem. Commun.* **2013**, *49*, 8976–8978.
- [21] Y. Cai, X. Tang, S. Ma, *Chem. – Eur. J.* **2016**, *22*, 2266–2269.
- [22] A. Elhampour, F. Nemati, *J. Chin. Chem. Soc.* **2016**, *63*, 653–659.
- [23] P. C. Perumgani, S. Keesara, S. Parvathaneni, M. R. Mandapati, *New J. Chem.* **2016**, *40*, 5113–5120.
- [24] F. Schlimpen, C. Plaçais, E. Starck, V. Bénéteau, P. Pale, S. Chassaing, *J. Org. Chem.* **2021**, *86*, 16593–16613.
- [25] V. Bénéteau, A. Olmos, T. Boningari, J. Sommer, P. Pale, *Tetrahedron Lett.* **2010**, *51*, 3673–3677.
- [26] R. Qi, X.-N. Wang, K. A. DeKorver, Y. Tang, C.-C. Wang, Q. Li, H. Li, M.-C. Lv, Q. Yu, R. P. Hsung, *Synthesis* **2013**, *45*, 1749–1758.
- [27] P. Zhang, A. M. Cook, Y. Liu, C. Wolf, *J. Org. Chem.* **2014**, *79*, 4167–4173.
- [28] F. Schlimpen, T. Ast, V. Bénéteau, P. Pale, S. Chassaing, *Green Chem.* **2022**, *24*, 6467–6475.
- [29] R. M. Martin, R. G. Bergman, J. A. Ellman, *Org. Lett.* **2013**, *15*, 444–447.

Synthesis of Propargylamines and Derivatives through Copper Catalysis Using Modified Zeolites

Résumé

Les propargylamines sont d'un grand intérêt synthétique et thérapeutique, avec diverses applications comme intermédiaires de synthèse et dans la conception de médicaments. Au cours des dernières années, la préparation du motif propargylamine *via* des stratégies à forte économie d'atomes et d'étapes a été rendue possible grâce au développement de diverses méthodes métallocatalysées. L'utilisation d'une zéolithe dopée au cuivre comme catalyseur hétérogène, ainsi que sa recyclabilité dans la synthèse de diverses propargylamines et de dérivés, ont été étudiées. Plusieurs procédures en cascade ont été développées dans des conditions sans solvant ou dans des solvants "verts", avec des stœchiométries de réactifs responsables et à des températures les plus douces possibles.

Des propargylamines, dont des γ -amino-ynamides, ont été préparées *via* des réactions à trois composants et d'hydroamination. Des propargylamines α -tertiaires portant des amines secondaires ont été dérivées en 1,2-dihydropyridines spirocycliques. Ces dernières ont enfin été utilisées comme précurseurs d'isoquinuclidines et de pipéridines.

Mots clés : propargylamines, zéolithe, catalyse hétérogène, cuivre, chimie verte, réactions en cascade, γ -amino-ynamides, 1,2-dihydropyridines, cycloisomérisation, plans d'expériences

Résumé en anglais

Propargylamines are versatile compounds of great synthetic and therapeutic interest with diverse applications as versatile synthetic intermediates and as lead structures in drug design. In recent years, several metal-catalysed methodologies have emerged for their atom- and step-economical preparation. Aiming for improved sustainability, the use of a copper-exchanged zeolite as a heterogeneous catalyst, as well as its recyclability in the synthesis of diverse propargylamines and valuable derivatives, were investigated. Several atom- and step-economical catalytic procedures were developed under solvent-free conditions or based on "green" solvents, attractive reagent stoichiometries, and the mildest possible temperatures.

Propargylamines, including γ -amino-ynamides, were prepared *via* three-component and hydroamination reactions. α -Tertiary propargylamines carrying secondary amines were derivatised into spirocyclic 1,2-dihydropyridines. The latter were used as precursors to isoquinuclidines and piperidines.

Keywords: propargylamines, zeolite, heterogeneous catalysis, copper, green chemistry, cascade reactions, γ -amino-ynamides, 1,2-dihydropyridines, cycloisomerisation, design of experiments